Loughborough University

This item is held in Loughborough University's Institutional Repository (https://dspace.lboro.ac.uk/) and was harvested from the British Library's EThOS service (http://www.ethos.bl.uk/). It is made available under the following Creative Commons Licence conditions.

creative commons

COMMONS DEED

Attribution-NonCommercial-NoDerivs 2.5

You are free:

- to copy, distribute, display, and perform the work

Under the following conditions:

Attribution. You must attribute the work in the manner specified by the author or licensor.

Noncommercial. You may not use this work for commercial purposes.

No Derivative Works. You may not alter, transform, or build upon this work.

- For any reuse or distribution, you must make clear to others the license terms of this work.
- Any of these conditions can be waived if you get permission from the copyright holder.

Your fair use and other rights are in no way affected by the above.

This is a human-readable summary of the Legal Code (the full license).

Disclaimer

For the full text of this licence, please go to:
http://creativecommons.org/licenses/by-nc-nd/2.5/

LIME STABILISATION: CLAY-METAL-LIME INTERACTIONS

by

DAVID IAN BOARDMAN

A Doctoral Thesis

Submitted in partial fulfilment of the requirements

for the award of

Doctor of Philosophy of Loughborough University

August 1999

© DAVID BOARDMAN 1999

To my parents Mary and Allan Boardman.

Your strength, courage and love have taught me humility.

You are always in my thoughts.

ACKNOWLEDGEMENTS

I would like to thank my brother and sisters Gavin, Gina and Esther for putting up with me and my Grandmother Violet Boardman for her generosity to the end.

Dr Stephanie Glendinning and Professor Chris Rogers are thanked for their support, kindness and at times tolerance as supervisors throughout this project.

Professor Andrew Wheatley is thanked for his role as director of research and for allowing me to run riot with all his expensive laboratory equipment.

Thanks are also extended to all the supporting laboratory technical staff at Loughborough. In particular Stuart Dale for turning a blind eye to the fact that I lived in the ICP room and used far too much argon gas, and to Nina Ladner, Geoff Russell and Chris Shaw. Without their help and humour life at Loughborough would not have been quite so entertaining or sustainable. May the show go on for future generations!

Personal thanks are extended to all the staff in Rutherford Hall, Vince, Chris, Christine, Vicky and in particular Bob and Heather who welcomed me into their homes. This was truly a happy time!

Finally I would like to thank James for never failing to laugh when I fall off high rocks and Konny for her kind spirit and for introducing me to the beauty of the Alps.

ABSTRACT

The literature review identified the current scientific understanding of element and lime interactions with clay minerals and the leaching protocols used to assess contaminant mobility. This understanding formed the basis for the mechanisms postulated for clay-contaminant-lime interactions and the appropriate methods of chemically assessing time-dependent interactions.

Two refined clay minerals English China Clay (predominantly kaolinite) and Wyoming Bentonite (predominantly sodium-montmorillonite) were used to assess the time-dependent effects of mineral structural chemistry on clay-contaminant-lime interactions. The two clays, representing the extremes of structural negative charge development, were contaminated with 5000ppm of either Pb^{2+} or Fe^{3+} ions, the sources of which were $Pb(NO_3)_{2(s)}$ and $Fe(NO_3)_3.9H_2O_{(s)}$ respectively. Eighteen clay-contaminant-quicklime mixes were compacted and stored in controlled conditions.

Changes in the physico-chemistry of the samples was monitored after 7 days, 175 days and 301 days curing by performing batch leaching tests and monitoring changes in undrained shear strength and Atterberg Limits. Each batch test was performed using de-ionised water as the leachant. The variables studied in the batch tests were, solid to liquid ratio, test duration, initial particle size, and batch mixer rotation speed. The effects of changing the batch test operating parameters and increasing the curing period were assessed by measuring changes in solution pH, conductivity and by analysis of soluble Ca, Na, Al, Si, Mg, Mn, Pb and Fe fractions.

The solidification processes due to lime addition were found to be different for the two minerals. English China Clay and Wyoming Bentonite pozzolanic reactions were found to be based on Al and Si dissolution from the respective mineral. This dissolution was only detectable after 175 and 301 day's curing, suggesting that initial 7 day undrained shear strength increases and changes in Atterberg Limits were associated with ion exchange effects alone.

The difference between the dissolution of Si and Al from the two minerals had a significant impact on re-crystallisation. Pb^{2+} ions were found to enhance solidification by enhancing dissolution of Al from English China Clay, whilst Fe^{3+} ions were found to have inhibitive effects preventing interaction of Ca^{2+} ions in the formation of calcium aluminate hydrates. On re-crystallisation, the Pb^{2+} and Fe^{3+} ion-

contaminated English China Clay samples had respectively higher and lower undrained shear strengths than the uncontaminated samples. Contaminants were found to have no appreciable influence on Wyoming Bentonite re-crystallisation.

Development of the batch leaching test demonstrated that changing the operational parameters had no effects on the observed *trends* associated with the time-dependent stabilisation and solidification reactions. It was also shown that successful solidification could be monitored using simple conductivity measurements without the need for expensive, complex elemental analysis.

CONTENTS

		Page
ACKNOWLEDGEMENTS		i
ABSTRACT		ii
CONTENTS		iv
NOMENCLATURE		xi
1.0	INTRODUCTION	1
1.1	THE LEGACY OF CONTAMINATION	2
1.2	ALTERNATIVE REMEDIATION TECHNOLOGIES	3
1.3	THE NEED FOR ECONOMIC SOLUTIONS	4
1.4	THE THESIS	5
2.0	LITERATURE REVIEW	6
2.1	INTRODUCTION	7
2.2	CONTAMINATION	8
2.2.1	Introduction	8
2.2.2	Sources of contamination	8
2.2.2.1	Organic compounds	8
2.2.2.2	Inorganic compounds	11
2.2.2.3	Radioactive compounds	20
2.2.3	Conclusions	23
2.3	CLAY-ELEMENT INTERACTIONS	26
2.3.1	Introduction	26
2.3.2	Soil formation and structure	26
2.3.2.1	Smectites	30
2.3.2.2	Vermiculites	32
2.3.2.3	Illites	33
2.3.2.4	Chlorites	33
2.3.2.5	Clays from arid or glacial climates	35
2.3.2.6	Cation-permeability interactions	35
2.3.2.7	Soil organic matter	36

2.3.3 Predicting clay-ion behaviour 42
2.3.3.1 Introduction 42
2.3.3.2 The condition for equilibrium 42
2.3.3.3 Organic contaminant attenuation and organophilic clays 45
2.4 STABILISATION/SOLIDIFICATION PROCESSES 48
2.4.1 Introduction 48
2.4.2 The clay-lime reaction 50
2.4.3 Principles of chemical stabilisation of contaminants 60
2.4.4 Cement stabilisation 64
2.4.5 Lime-fly ash stabilisation 67
2.4.6 Stabilisation via sorption alone 68
2.4.7 Organophilic clay-reagent stabilisation and solidification processes 69
2.4.7.1 The origin of hydrogen ions (acids) in soil 71
2.5 METHODS OF REAGENT APPLICATION 74
2.5.1 Ex-situ methods of application 74
2.5.1.1 Plant processing methods 74
2.5.1.2 Direct mixing methods 75
2.5.1.3 Drum processing methods 76
2.5.2 In-situ methods of application 77
2.5.2.1 Surface clay-reagent mixing 77
2.5.2.2 Deep clay-reagent mixing 79
2.6 SITE APPLICATION OF TECHNOLOGIES / RECENT CASE STUDIES 82
2.6.1 Evaluation of operations 84
2.6.2 The HAZCON process 92
2.6.3 Conclusions to the pilot studies 95
2.7 CHEMICAL ANALYSIS OF CONTAMINATED MATERIALS 96
2.7.1 Introduction 96
2.7.2 Agitated batch leaching tests 98
2.7.3 Dynamic leaching tests 104
2.7.4 Leach test parameters 108
2.7.4.1 Solid to liquid ratio 108
2.7.4.2 Leachant composition 109
2.7.4.3 Sample preparation methods 110

2.7.4.4 Leaching period 111

2.7.4.5 Contact method 111

2.7.4.6 Test environmental conditions 112

2.7.4.7 Solid and leachate separation methods 112

2.7.4.8 Sample storage and sample analysis method 113

2.7.4.9 Further significant factors affecting leachate generation 113

2.8 LABORATORY LEACHING TEST RESEARCH 116

3.0 RESEARCH PHILOSOPHY 125

3.1 AIMS AND OBJECTIVES 129

4.0 EXPERIMENTAL METHODOLOGY 130

4.1 MATERIALS SPECIFICATION 131

4.1.1 Clay minerals 131

4.1.2 Lime used in laboratory investigations 133

4.1.3 Contaminating metals added during the investigations 135

4.1.4 The water quality used at different stages of the investigations 136

4.1.5 Application and quality of acids used during the investigations 138

4.2 EQUIPMENT 140

4.2.1 Sample mixing and compaction equipment 140

4.2.2 Chemical measurement 141

4.2.2.1 Batch test equipment 141

4.2.2.2 pH and conductivity measurement 142

4.2.2.3 Solution separation techniques and ICP analysis 143

4.2.3 Physical analysis equipment 143

4.3 MATERIALS CHARACTERISATION 143

4.3.1 Lime requirement 145

4.3.2 Compaction 146

4.3.3 Levels of contamination 149

4.4 LABORATORY 'FULL-SCALE' SAMPLE PREPARATION 150

4.4.1 Introduction 150

4.4.2 Contaminant preparation 150

4.4.3 Clay-contaminant-lime mix preparation 151

4.5 BATCH TESTING 154

4.5.1 Pre-batch test clay analysis via acid digestion 154
4.5.2 Batch testing methods and undrained shear strength measurements 156
4.5.3 Inductively coupled argon plasma atomic emission spectrometer analysis 161
4.5.4 Sample mix acid digestions after 301 days curing 163
4.6 ATTERBERG LIMITS 163
4.7 THE POTENTIAL FOR VARIABILITY AND EXPERIMENTAL ERROR 164
4.7.1 Introduction 164
4.7.2 Initial material characterisation 164
4.7.3 Determination of acid soluble mineral fractions and ICP analysis 165
4.7.4 Preparation of compacted samples 169
4.7.5 Batch testing 170
4.7.6 Shear strength measurements 171
4.7.7 Atterberg limit measurements 172

5.0 RESULTS 174
5.1 PRELIMINARY MATERIAL CHARACTERISATION 175
5.1.1 Particle size distribution 175
5.1.2 Acid soluble clay fractions 176
5.1.3 Initial consumption of lime tests 178
5.1.4 Preliminary dry density-moisture content investigations 179
5.2 BATCH EXTRACTION TESTS 184
5.2.1 The effects of extraction test parameters on element concentrations 184
5.2.1.1 English China Clay sample variations due to changing initial cube size 185
5.2.1.2 Wyoming Bentonite sample variations due to changing initial cube size 186
5.2.1.3 English China Clay sample variations due to changing rotation speed and test duration 191
5.2.1.4 Wyoming Bentonite sample variations due to changing rotation speed and test duration 192
5.2.1.5 English China Clay and Wyoming Bentonite sample variations due to changing solid to liquid ratio 200

5.2.2 End of test pH and conductivity variations with curing time for English China Clay and Wyoming Bentonite samples 214
5.2.3 ICP chemical analysis of end of batch test solutions 219
5.2.3.1 Gravity filtered English China Clay samples with lime added 219
5.2.3.2 Gravity filtered Wyoming Bentonite samples with lime added 220
5.2.3.3 Gravity filtered English China Clay samples with no lime added 224
5.2.3.4 Centrifuged Wyoming Bentonite samples with no lime added 226
5.2.3.5 Centrifuged Wyoming Bentonite samples with 2.5% lime added 228
5.3 PHYSICAL BEHAVIOUR 229
5.3.1 End of batch test particle size distribution and chemical analysis 229
5.3.2 Acid digestions 230
5.3.2.1 Acid digestion of particles from batch test mixtures retained on a 63μm sieve 230
5.3.2.2 Acid digestion of compacted clay-lime-contaminant mixes 234
5.3.3 Shear strength measurements 238
5.3.4 Atterberg limit test results 241
5.3.4.1 Liquid limits 241
5.3.4.2 Plastic limits 245
5.3.4.3 Plasticity index 247

6.0 DISCUSSION 249
6.1 PRELIMINARY MATERIAL CHARACTERISATION 251
6.1.1 Initial particle size and chemical characterisation 251
6.1.2 Mechanisms controlling the initial consumption of lime test (ICL) 252
6.1.3 Dry density-water content relationships 258
6.1.3.1 Clay-lime mixes 258
6.1.3.2 Clay-lime-contaminant mixes 258
6.2 CORRELATION BETWEEN CHEMICAL MEASUREMENTS AND SHEAR STRENGTH 260
6.2.1 Introduction 260
6.2.2 Measured chemical changes due to particle breakdown and time-dependent chemical reactions 261
6.2.2.1 Clay-lime mixes 261

6.2.2.2 Clay-lime-contaminant mixes 263
6.2.3 Relationships between shear strength and soluble chemistry for English China Clay 263
6.2.3.1 Clay-lime mixes 263
6.2.3.2 Clay-lime-contaminant mixes 264
6.2.3.3 Suggested mechanisms governing selective dissolution of the English China Clay structure due to pozzolanic reactions 266
6.2.4 Relationships between shear strength and soluble chemistry for Wyoming Bentonite 268
6.2.4.1 Clay-lime mixes 268
6.2.4.2 Clay-lime-contaminant mixes 268
6.2.4.3 Suggested mechanisms governing selective dissolution of the Wyoming Bentonite structure due to pozzolanic reactions 269
6.2.4.4 The influence of contaminants on pozzolanic reactions 270
6.2.4.5 Wyoming Bentonite at lime additions below the ICL value 271
6.2.4.6 Wyoming Bentonite behaviour for samples containing 0% lime 273
6.3 ACID DIGESTION OF CLAY-CONTAMINANT-LIME MIXES 274
6.3.1 Introduction 274
6.3.2 Acid digestion of clay mixes with no added lime 274
6.3.2.1 Uncontaminated clay mixes 274
6.3.2.2 Contaminated clay mixes 275
6.3.3 Acid digestion of clay mixes with added lime 276
6.3.3.1 Uncontaminated clay mixes 276
6.3.3.2 Contaminated clay mixes 277
6.3.3.3 Acid soluble constituents of material retained on 63μm sieves after batch tests 279
6.4 ATTERBERG LIMITS 283
6.4.1 English China Clay 283
6.4.1.1 Samples without lime added 283
6.4.1.2 Samples with lime added 285
6.4.2 Wyoming Bentonite 287
6.4.2.1 Samples without lime added 287
6.4.2.2 Samples with lime added 289

6.4.3 Interpretation of Atterberg Limits 289

7.0 CONCLUSIONS 295
7.1 BATCH TEST DEVELOPMENT 296
7.2 LIME-CLAY REACTION MECHANISMS 297
7.3 STABILISATION/SOLIDIFICATION OF CONTAMINANTS 300
7.3.1 Stabilisation/solidification of contaminants 300
7.3 FUTURE WORK 303
7.3.1 Author's comments 303
7.3.2 Proposals for future research 304
7.5 SUMMARY 305

REFERENCES 307

A1 APPENDIX 1 - DETAILED PRESENTATION OF THE BATCH TEST RESULTS AND THE EFFECT OF THE INITIAL OPERATING PARAMETERS ON THE SOLUTION CHEMISTRY 337
A2 APPENDIX 2 - CLAY-ION-INTERACTIONS: ENERGY MODELS
A3 APPENDIX 3 - CLAY, CONTAMINANT AND LIME MIX PREPARATION

NOMENCLATURE

Elements and Cations

Al	Aluminium
Al^{3+}	Aluminium cation
Ag	Silver
Am	Americium
As	Arsenic
B	Boron
Ba	Barium
Be	Beryllium
Bi	Bismuth
Br	Bromine
Ca	Calcium
Ca^{2+}	Calcium cation
Cd	Cadmium
Ce	Cerium
Cl	Chlorine
Cm	Curium
Co	Cobalt
Cr	Chromium
Cs	Caesium
^{137}Cs	Radioactive Caesium 137 isotope
Cu	Copper
F	Fluorine
Fe	Iron
Fe^{2+}	Iron (II) cation
Fe^{3+}	Iron (III) cation
Ga	Gallium
Ge	Germanium
H	Hydrogen
Hg	Mercury
W	Tungsten
Zr	Zirconium
I	Iodine
K	Potassium
Li	Lithium
Mg	Magnesium
Mn	Manganese
Mo	Molybdenum
Na	Sodium
Na^{+}	Sodium cation
Ni	Nickel
Np	Neptunium
O	Oxygen
P	Phosphorous
Pb	Lead
Pb^{2+}	Lead (II) cation
Po	Polonium
Pu	Plutonium
Ra	Radium
Rb	Rubidium
Ru	Ruthenium
S	Sulphur
Se	Selenium
Si	Silicon
Sn	Tin
Sr	Strontium
^{90}Sr	Radioactive Strontium 90 isotope
Ti	Titanium
Th	Thorium
U	Uranium
V	Vanadium
Zn	Zinc

Anions

Cl^-	Chloride ion
F^-	Fluoride ion
NO_3^-	Nitrate ion
OH^-	Hydroxide ion
SO_4^{2-}	Sulphate ion

Compounds

Al_2O_3	Aluminium Oxide
$CaCl_2$	Calcium Chloride
$CaCO_3$	Calcium Carbonate
CaO	Calcium Oxide
$Ca(OH)_2$	Calcium Hydroxide
$CaSO_4$	Calcium Sulphate
FeO	Iron (II) Oxide
Fe_2O_3	Iron (III) Oxide
$Fe(OH)_3$	Iron (III) Hydroxide
$Fe(OH)_2$	Iron (II) Hydroxide
$FeSO_4$	Iron (II) Sulphate
KCl	Potassium Chloride
K_2CO_3	Potassium Carbonate
K_2SO_4	Potassium Sulphate
$MgCl_2$	Magnesium Chloride
$MgCO_3$	Magnesium Carbonate
$Mg(OH)_2$	Magnesium Hydroxide
$MgSO_4$	Magnesium Sulphate
$NaCl$	Sodium Chloride
$NaNO_3$	Sodium Nitrate
Na_2SO_4	Sodium Sulphate
Na_2SO_3	Sodium Sulphite
NH_4Cl	Ammonium Chloride
H_20	Water
SiO_2	Silicon Oxide

CHAPTER 1.0

1.0 INTRODUCTION

1.1 THE LEGACY OF CONTAMINATION

Public awareness of the adverse effects of contamination on the environment has grown considerably over the last two decades, partly due to the active involvement of environmental groups. This has produced pressure upon government bodies to act urgently by introducing new legislation to control waste disposal. With increasing demands for environmental responsibility, the European Community has set strict controls on the content and quantity of waste that can be disposed of at sea or applied to land. The economic consequence of this has been greatly increased costs for industries producing toxic wastes as by-products of their production processes, and for governments or other bodies who are responsible for cleaning up contaminated sites for future development or public use (derelict industrial sites, docks, canals, etc.). Two of the major categories of material that need to be dealt with are clay-based sediments deposited under water and clays that contain inorganic contaminants, the remediation of which forms the basis of this thesis.

Major source of contamination derives from industrial processes. The composition of the contamination varies enormously from one industrial process to another. Typical sources of such contamination are copper, lead and zinc smelting industries, duplicating and photographic equipment manufacturing industries, pharmaceutical industries and sewage treatment works. Whilst industries are now closely controlled and produce waste materials that are both identifiable and are treated, this has not always been the case. By studying the waste materials (known as waste streams or sludges) produced by modern processes, good indications of the contamination of the environment caused by past industrial processes can be obtained. These contribute to the contamination of sediments in rivers, canals, lakes and reservoirs following transport via air and/or water, and to land by these routes or by direct contact. This highlights an important fundamental principle: remove one stage from the source-pathway-receptor series and there is no risk due to contamination. Although controls on material handling and disposal now in place reduce the risk of contamination to an acceptably small level

by removing the source, the degree of control until relatively recently has been minimal and much contamination has been caused. Indeed metal contamination can result from sources as apparently innocuous as fly ash and colliery spoil heaps. In Europe alone there are just under one million known or potentially contaminated sites requiring remediation. Although this thesis only deals with the contaminated environment, the technology put forward could be adapted to treat the waste sludges directly in combination with the addition of a pozzolana (Lutz & Minehan, 1986).

1.2 ALTERNATIVE REMEDIATION TECHNOLOGIES

Due to the variability of contaminant composition in clays and sediments it is difficult to find a single treatment which fulfils all the requirements to render that material 'safe' in the long-term. Prior to disposal of contaminated materials such as excavated clays and dredged sediments, assurance is necessary that toxic elements will in some way be contained permanently within the waste disposal facility boundaries, or at least that losses will be kept to a sufficiently low level that no harmful effects occur to the environment. Methods of disposal currently available and under research include spreading on land, de-watering and landfill disposal, encapsulation and burial, and stabilisation and disposal on land or in landfill sites. The main aim of these processes is either to affect the source or the pathway to inhibit future adverse effects. There are intermediate processes that can be used to increase the physical, chemical and cost effectiveness of the primary disposal methods, such as precipitating toxic metal species from the waste materials by altering the pH of the solutions. Toxic metals also tend to attenuate preferentially on small mineral particles. Thus it is possible to remove a large quantity of certain contaminants by removing specific particle sizes as a means of pre-treatment.

Stabilisation techniques generally involve mixing the contaminated material with a chemical additive such as lime or cement. The combination of a high pH and the production of cementitious compounds create a solidified mass which encapsulates contaminants chemically stabilised within the encapsulating material resulting in the reduced mobility of toxic elements in the waste. Stabilisation methods tend to cost less

than other treatments such as vitrification, organic encapsulation (e.g. thermo-setting plastic) or electro-osmosis, but their application can be limited due to the contaminant composition and the limitations of the 'fixation' processes. For example, both the solids content and the form of the toxic species present in the contaminated material influence their suitability. The environment is similarly important because, for example, if water can permeate through the contaminated deposit, some species will become mobile. In addition, the presence of some contaminants can impede or enhance the creation of the cementitious products that are associated with the solidification process.

1.3 THE NEED FOR ECONOMIC SOLUTIONS

The problems, in terms of numbers of sites and varieties of contamination, are as serious worldwide as they are in Europe. While in some European countries the government has to pay for remediation of sites if the industrial polluter cannot pay or cannot be made to pay, the USA has firmly embraced the philosophy that the polluters must pay for the clean up of contamination. In order for these industries to remain competitive with industries in countries where pollution control is not so rigorous and/or to reduce the burden on governments, there is a need to develop economical treatment and disposal techniques. Thus, any technique that is simple to operate, can deal with large amounts of contaminated soil and does not require large quantities of expensive additives is of major importance.

Chemical stabilisation using lime would satisfy these criteria. Furthermore, the addition of lime to clay soils has proved to be of great benefit in improving their engineering properties, making the material physically as well as chemically stable. Supplies of lime, more so than cement, are relatively high around the world making lime an almost universally viable option. There is consequently a need to investigate lime stabilisation of contaminated clays and clay-based sediments. In particular there is a need to understand the processes controlling physico-chemical behaviour, and therefore inherently the processes controlling ion mobility in the aqueous phase.

1.4 THE THESIS

The requirement for lime stabilisation and solidification of contaminated clays has been established along with the necessity to understand the mechanisms associated with the process. The thesis aims to investigate the physico-chemical mechanisms of clay-lime-contaminant interactions. It was important that the testing methods used to monitor these chemical mechanisms reflected the requirements for cost-effective analysis using simple inexpensive testing protocols.

Chapter 2 describes sources of both organic and inorganic contaminants as well as providing examples of sites where they can be found. In addition the fundamentals of clay mineralogy are presented from the perspective of understanding contaminant interactions. This was considered to be essential to enable engineers to appreciate some of the complex chemical interactions discussed later in the thesis. The processes relating to stabilisation are reviewed thereafter together with the chemical methods currently adopted to assess contaminant leachability.

From the information gained in the literature a research philosophy was formulated and this is presented in Chapter 3. Chapter 4 describes in detail the experimental methodology, and data collected from the resulting laboratory programme are presented in Chapter 5 and discussed in detail in Chapter 6. Finally, Chapter 7 concludes the discussion and highlights areas where further research would be beneficial in improving the understanding of stabilised and solidified contaminated clays.

CHAPTER 2.0

2.0 LITERATURE REVIEW

2.1 INTRODUCTION

Lime stabilisation is a technique used worldwide in construction to improve the engineering properties of soils prior to site development. The technique is used on a variety of clay mineral types often under environmental extremes. Alteration of properties such as plasticity, compressibility and permeability can all occur as a result of the addition of stabilising agents. However, in most cases stabilising methods are adopted to induce rapid cost-effective improvements in soil strength and stiffness, and resistance to weakening/softening by water. Many sites are directly or indirectly contaminated by organic and inorganic contaminants by society, although elevated concentrations of elements and compounds can occur from naturally occurring sources. Lime stabilisation is a chemical approach to ground improvement whereby clay soil is modified and particles are subsequently bonded together by a process of cementation. The presence of 'contamination' alters the initiation, development and final properties of the stabilising soil and potentially the rate at which improvements will develop.

This review aims to:

- identify some of the most prolific sources of contamination,
- identify how the chemical structure of clay soils and in particular mineral charge development affects the interaction of contaminants,
- explain the fundamental principles of the initial stabilisation and longer-term solidification brought about by the addition of lime,
- explain how inorganic contaminants are involved in the stabilisation and solidification process, and
- describe the fundamental characteristics of chemical leaching tests currently used to assess the quantities of contaminants present in soil.

2.2 CONTAMINATION

2.2.1 Introduction

A contaminant can be generally described as a chemical element, ion or compound that has the ability to pose an immediate or long-term threat to human health or the environment, mainly as a result of its toxic properties. Chemical contamination is prevalent in the environment, considerably complex, and predominantly heterogeneous with a diverse level of containment. Contaminants consequently pose problems to engineers seeking to reduce their bioavailability. To understand the behaviour of these contaminants within the chemistry of the natural environment, it is important to categorise contaminants.

Contaminants can be divided into two broad categories, organic and inorganic contaminants, although organic contaminants can often occur with an attached inorganic group. The structure of organic compounds is based around molecules containing carbon, whereas inorganic chemistry encompasses all elements and compounds that do not involve carbon-based chemistry.

2.2.2 Sources of contamination

2.2.2.1 Organic compounds

Many organic compounds originate from crude oil, including motor oils, lubricating oils, heating oils, plastics, detergents, paints, and antifreeze. Crude oil is the source of 70% of Britain's organic chemicals. The components of crude oil must be partially separated by distillation and if necessary modified, prior to being useful. Many types of organic contaminants can result from this process and can be found polluting the environment. They can be generally characterised as follows.

Volatile organic compounds (VOCs) such as chlorinated solvents, have been in widespread use since World War II. In their pure form at ambient temperatures, many of the VOCs are liquids, often called NAPLs (non-aqueous-phase liquids), which are sparingly soluble in water. The distribution of these contaminants in an environment such as an aquifer is quite complex (e.g. Fretwell *et al*, 1998). The petroleum hydrocarbons are referred to as LNAPLs because they are less dense than water and are often found contaminating the upper layers of aquifers. Chlorinated solvents referred to as DNAPLs are more dense than water and are often found

contaminating the lower levels of aquifers hence creating a different remediation problem to LNAPLs (Mackay, 1998; Delaney *et al*, 1998; Rivett *et al*, 1998).

Separation and modification industries such as refineries are one of the first potential sources of organic contamination (e.g. Christofi *et al*, 1998; Wallace *et al*, 1998; Pritchard, *et al*, 1991). The second source of organic contaminants is from the distribution, use, and disposal of the carbon-based products. This may be the result of leaking oil tanks (e.g. Ulfig *et al*, 1998), leaking fuel storage tanks at fuel stations (e.g. Davis, 1998), accidental spills (e.g. Muvrin *et al*, 1998), the deposition of pesticides on fields, or the placement of waste sludges in land based trenches. Broholm *et al* (1998) describes the leakage of coal tar from storage tanks at a coal carbonation plant releasing phenols, naphthalenes, mono-aromatic hydrocarbons (BTEXs) and polyaromatic hydrocarbons (PAHs) into an aquifer. Prior to improved environmental awareness, UK based gasworks were responsible for disposing of waste locally and are one source of soil and groundwater contamination by a suite of organic and inorganic compounds, including aromatic and polyaromatic hydrocarbons and ammonia (Torstensson *et al*, 1998).

It is important to exert careful control over both the disposal of potential contaminants and remediation of contaminated sites (e.g. Csizer *et al*, 1998). The current basis for safe disposal and remediation relies heavily upon risk assessment techniques. Ferguson *et al* (1998), Sowinski (1998), Wcislo (1998), Poborski (1998) and Feige-Munzig (1998) discuss such ideas. The degree of control applied to a disposal method is directly associated with the current levels of understanding, technology, cost, environmental awareness and consequently government policy.

An example illustrating the consequences of lack of understanding and awareness was the disaster at Love Canal in the United States of America (USA). In 1978, the US President declared that a major chemical emergency existed at Love Canal (Niagra Falls, New York). Officials of the Hooker Chemicals and Plastics Corporation acknowledged that from 1942 to 1953 the company disposed of some 20×10^6 kg of chemical wastes in an uncompleted canal. Adjacent land was subsequently sold to allow an elementary school to be built in 1955. By 1966, the remainder of the site was covered by a housing development. The selling of such a site by the company cannot be considered gross negligence on the part of the company since warnings about the dangers of the site were apparently communicated

to the purchaser. By 1987, approximately $100 million (US) had been spent on site remediation, resident relocation, and human health investigations. Cytogenetic assessments of 36 former residents of the Love Canal area highlighted chromosomal abnormalities and damage (Deegan, 1987A&B).

Military sites are also well known as a source of organic contaminating substances. Many USA Department of Defence (DOD) sites are contaminated with explosive waste as a result of explosives manufacturing, munitions loading, assembly and packing operations, explosives machining, casting and curing, and laboratory testing of munitions. One of the major explosive wastes of concern at DOD sites is a residue from land disposal of explosives-contaminated process water (U.S. EPA, 1993). Explosives-contaminated waters are subdivided into red water, which comes strictly from the manufacture of TNT and which ceased in the mid-1980s, and pink water, which includes any wash-water associated with military processes involving contact with TNT. Pink waters are notably derived from demilitarisation operations conducted in the 1970s, which used jets of hot water to mine the explosives out of the munitions. The residual waters were placed in settling basins so that solid explosive particles could be removed, and the remaining water was siphoned into lagoons. Contaminants often present in these lagoons and the surrounding soils are illustrated in Table 2.1. On some sites rocket and gun propellants can be found (U.S. EPA, 1993; Whittaker *et al*, 1998).

Table 2.1 shows the frequency of occurrence of various nitroaromatics and nitroamines that occur at explosives-contaminated sites (U.S. EPA, 1993). The remediation of military sites contaminated with explosives creates many unique physical handling problems as well as the potential chemical contamination problem.

The chemical behaviour and interaction within the natural environment of organic contamination generally necessitates that it is investigated independently from inorganic compounds. However, as new chemicals that combine organic and inorganic species are increasingly developed there is a need to combine treatment methods.

Table 2.1 **Nitroaromatics and Nitroamines study by US Army Cold Regions Research and Engineering Laboratory (CRREL) and the Missouri River Division (MRD) of explosives-contaminated soils from army sites (Adapted from U.S. EPA, 1993).**

Category	Contaminant	Frequency (%)	
		CRREL	MRD
Nitroaromatics	TNT	85	76
	TNB	53	38
	DNB	25	19
	2,4-DNT	41	17
	2,6-DNT	*	*
	4-Amino-DNT	6	3
	2-Amino-DNT	27	11
Nitroamines	RDX	44	28
	HMX	27	4
	Tetryl	8	14

Glossary of terms:

TNT	-	2,4,6-Trinitrotoluene
TNB	-	1,3,5-trinitrobenzene
DNB	-	1,3-dinitrobenzene
2,4-DNT	-	2,4-dinitrotoluene (2,4-dinitromethylbenzene)
2,6-DNT	-	2,6-dinitrotoluene (2,6-dinitromethylbenzene)
RDX	-	Cyclo-1,3,5-trimethylene-2,4,6-trinitroamine
HMX	-	Cyclo-1,3,5,7-tetramethylene-2,4,6,8-tetranitramine
Tetryl	-	Trinitro-2,4,6-phenylmethylnitamine

2.2.2.2 Inorganic compounds

Inorganic contamination encompasses all contaminating elements and compounds that do not involve carbon-based chemistry. Inorganic contamination does occur independently in spite of its frequent association with organic contamination. There are also situations when inorganic elements are chemically incorporated within the structure of organic molecules such as herbicides including diquat and paraquat (Mossom, 1998; McBride, 1994). Elements occur naturally as trace elements that are essential for life. However, elements within an industrialised area are present in wild herbage, particularly leaves, at very high concentrations, i.e.

those beyond the requirements for life. A trace element is defined as an element in natural materials such as the lithosphere, that is present at a level < 0.1%. If concentrations are high enough, they can be toxic to living organisms (Adriano, 1986). Trace elements include trace metals, heavy metals and micronutrients (Elejalde *et al*, 1992). Heavy metals are those elements having densities greater than 5.0 gcm^{-3}, and include As, Cd, Cr, Co, Cu, Pb, Hg and Ni (Sparks, 1995). Table 2.2 illustrates natural concentrations of some of these elements, ions and compounds in groundwater whilst Table 2.3 shows the concentrations of trace elements in soil forming rocks and other natural materials. The values stated are highly variable, inherently site specific with bioavailability also being site specific and clearly above what could be classified as guideline values. The effects, significance and occurrence of these elements in the US are further illustrated in Table 2.4. These tables clearly portray the significance and prevalence of inorganic contamination in the natural environment.

Mixtures of inorganic elements within a soil matrix create very complex chemical equilibrium environments from which removal of the contaminating elements is very expensive if indeed possible. In many respects the presence of several inorganic elements in the solid and or liquid phases mixed together with varying behavioural characteristics is a more difficult remediation problem than that of many organic contaminants, which can be susceptible to natural attenuation via biodegradation. For many forms of potential inorganic contamination, the element, ion or compound likely exists naturally in varying concentrations depending on potential sources. Assessment of the level at which an element is thought to cause pollution has far-reaching implications. Experience has shown that as research in the field of risk assessment develops the assessment of what is regarded as pollution changes. However, consideration of natural concentrations of elements in groundwater and rocks helps to create a degree of perspective.

Table 2.2 **Natural concentrations of some elements, ions, and compounds in groundwater[a,b] (Sparks, 1995)**

Element	Concentration		Element	Concentration	
	Typical value	Extreme value		Typical value	Extreme value
Major elements (mg liter^{-1})			Bi	<20	
Ca	1.0-150[c]	95,000[d]	Br	<100-2,000	
	<500[e]		Cd	<1.0	
Cl	1.0-70[c]	200,000[d]	Co	<10	
	<1,000[e]		Cr	<1.0-5.0	
F	0.1-5.0	70	Cu	<1.0-30	
		1,600[d]	Ga	<2.0	
Fe	0.01-10	>1,000[d,f]	Ge	<20-50	
K	1.0-10	25,000[d]	Hg	<1.0	
Mg	1.0-50[c]	52,000[d]	I	<1.0-1,000	48[d]
	<400[e]		Li	1.0-150	
Na	0.5-120[c]	120,000[d]	Mn	<1.0-1,000	10[b]
	<1000[e]		Mo	<1.0-30	10
NO_3	0.2-20	70	Ni	<10-50	
SiO_2	5.0-100	4,000[d]	PO_4	<100-1,000	
SO_4	3.0-150[c]	200,000[d]	Pb	<15	
	<2,000[e]		Ra	<0.1-4.0[g]	0.7[d,g]
Sr	0.1-4.0	50	Rb	<1.0	
Trace elements (mg liter^{-1})			Se	<1.0-10	
Ag	<5.0		Sn	<200	
Al	<5.0-1,000		Ti	<1.0-150	
As	<1.0-30	4	U	0.1-40	
B	20-1,000	5	V	<1.0-10	0.07
Ba	10-500		Zn	<10-2,000	
	<10		Zr	<25	

[a]From Dragun (1988).

[b]Based on an analysis of data presented in Durfer and Becker (1964), and Ebens & Schaklette (1982).

[c]In relatively humid regions.

[d]In brine.

[e]In relatively dry regions.

[f]In thermal springs and mine areas.

[g]Picocuries liter^{-1} (i.e., 0.037 disintegrations sec^{-1}).

Table 2.3 **Concentrations (mg kg^{-1}) of trace elements in some soil-forming rocks and other natural materials[a,b] (Sparks, 1995)**

Element	Ultramalic igneous	Basaltic igneous	Granitic igneous	Shales and clays	Black shales	Deep-sea clays	Limestones	Sandstones
Arsenic	**0.3-16**, 3.0	**0.2-10**, 2.0	**0.2-13.8**, 2.0	**—**, 10	**—**, —	**—**, 13	**0.1-8.1**, 1.7	**0.6-9.7**, 2
Barium	**0.2-40**, 1	**20-400**, 300	**300-1,800**, 700	**460-1,700**, 700	**70-1,000**, 300	**—**, 2,300	**10**, —	**—**, 20
Beryllium	**—**,—	**—**, 1.0	**2-3**, —	**—**, 3	**—**, —	**2.6**, —	**—**,—	**—**,—
Cadmium	**0-0.2**, 0.05	**0.006-0.6**, 0.2	**0.003-0.18**, 0.15	**0-11**, 1.4	**<0.3-8.4**, 1.0	**0.1-1**, 0.5	**—**, 0.05	**—**, 0.05
Chromium	**1,000-3,400**, 1,800	**40-600**, 200	**2-90**, 20	**30-590**, 120	**26-1,000**, 100	**—**, 90	**—**, 10	**—**, 35
Cobalt	**90-270**, 150	**24-90**, 50	**1-15**, 5	**5-25**, 20	**7-100**, 10	**—**, 74	**—**, 0.1	**—**, 0.3
Copper	**2-100**, 15	**30-160**, 90	**4-30**, 15	**18-120**, 50	**20-200**, 70	**—**, 250	**—**, 4	**—**, 2
Fluorine	**—**,—	**20-1,060**, 360	**20-2,700**, 870	**10-7,600**, 800	**—**, —	**—**,1,300	**0-1,200**, 220	**10-880**, 180
Iron	**94,000**, —	**86,000**, —	**14,000-30,000**, —	**—**, 47,200	**—**, 20,000	**—**, 65,000	**—**, 3,800	**—**, 9,800
Lead	**—**, 1	**2-18**, 6	**6-30**, 18	**16-150**, 20	**7-150**, 30	**—**, 80	**—**,9	**<1-31**, 12
Mercury	**0.004-0.5**, 0.1	**0.002-0.5**, 0.05	**0.005-0.4**, 0.06	**0.005-0.51**, 0.09	**0.03-2.8**, 0.5	**0.02-2.0**, 0.4	**0.01-0.22**, 0.04	**0.001-0.3**, 0.05
Molybdenum	**—**, 0.3	**0.9-7**, 1.5	**1-6**, 1.4	**—**, 2.5	**1-300**, 10	**—**, 27	**—**, 0.4	**—**, 0.2
Nickel	**270-3,600**, 2,000	**45-410**, 140	**2-20**, 8	**20-250**, 68	**10-500**, 50	**—**, 225	**—**, 20	**—**, 2
Selenium	**—**, 0.05	**—**, 0.05	**—**, 0.05	**—**, 0.6	**—**, —	**—**, 0.17	**—**, 0.08	**—**, 0.05
Vanadium	**17-300**, 40	**50-360**, 250	**9-90**, 60	**30-200**, 130	**50-1,000**, 150	**—**, 120	**—**, 20	**—**, 20
Zinc	**—**, 40	**48-240**, 110	**5-140**, 40	**18-180**, 90	**34-1,500**, 100	**—**, 165	**—**, 20	**2-41**, 16

[a]From Tourtelot (1971)

[b] The values in bold print are the usually reported range, the subsequent values in normal print are average values

Table 2.4 Occurrence and significance of trace elements in natural waters[a] (Sparks, 1995)

Element	Sources	Effects and Significance	U.S. Public Health Service limit (mg litre^{-1})[b]	Occurrence: % of samples, highest and mean concentrations (μg litre^{-1})[c]
Arsenic	Mining by-product, pesticides, chemical waste	Toxic, possibly carcinogenic	0.05	5.5% (above 5 μg litre^{-1}), 336, 64
Beryllium	Coal, nuclear power, and space industries	Acute and chronic toxicity, carcinogenic	Not given	Not given
Boron	Coal, detergent formulations, industrial wastes	Toxic to some plants	1.0	98% (above 1 μg litre^{-1}), 5000, 101
Cadmium	Industrial discharge, mining waste, metal plating, water pipes	Replaces zinc biochemically, causes high blood pressure and kidney damage, destroys testicular tissue and red blood cells, toxic to aquatic biota.	0.01	2.5%, Not given, 9.5
Chromium	Metal plating, cooling-tower water additive (chromate), normally found as Cr(VI) in polluted water	Essential trace element, (glucose tolerance factor), possibly carcinogenic as CR(VI)	0.05	24.5%, 112, 9.7
Copper	Metal plating, industrial and domestic wastes, mining, mineral leaching	Essential trace element, not very toxic to animals, toxic to plants and algae at moderate levels	1.0	74.4%, 280, 15
Fluorine (fluoride ion)	Natural geological sources, industrial waste, water additive	Prevents tooth decay at about 1 mg liter^{-1}, causes mottled teeth and bone damage at around 5 mg liter^{-1} in water	0.8-1.7 depending on temperature	Not given
Iodine (iodide)	Industrial waste, natural brines, seawater intrusion	Prevents goitre	Not given	Rare in fresh water

[a] From Manahan (1991).

[b] U.S. Public Health Service (1962).

[c] Kopp & Kroner (1991). The first figure is the percentage of samples showing the element; the second is the highest value found; the third is the mean value in positive samples (samples showing the presence of the metal at detectable levels).

Table 2.4 Occurrence and significance of trace elements in natural waters continued.....[a] (Sparks, 1995)

Element	Sources	Effects and Significance	U.S. Public Health Service limit (mg litre^{-1})[b]	Occurrence: % of samples, highest and mean concentrations (μg litre^{-1})[c]
Iron	Corroded metal, industrial wastes, acid mine drainage, low pE water in contact with iron minerals	Essential nutrient (component of haemoglobin), not very toxic, damages materials (bathroom fixtures and clothing)	0.05	75.6%, 4600, 52
Lead	Industry, mining, plumbing, coal, gasoline (petrol).	Toxicity (anaemia, kidney disease, nervous system), wildlife destruction	0.05	19.3% (above 2 μg litre^{-1}), 140, 23
Manganese	Mining, industrial waste, acid mine drainage, microbial action on manganese minerals at low pE	Relatively non-toxic to animals, toxic to plants at higher levels, stains materials (bathroom fixtures and clothing)	0.05	51.4% (above 0.3 μg litre^{-1}), 3230, 58
Mercury	Industrial waste, mining, pesticides, coal	Acute and chronic toxicity	Not given	Not given
Molybdenum	Industrial waste, natural sources, cooling-tower water additive	Possibly toxic to animals, essential for plants	Not given	32.7% (above 2 μg litre^{-1}), 5400, 120
Selenium	Natural geological sources, sulphur (sulphur), coal	Essential at low levels, toxic at higher levels, causes 'alkali disease' and 'blind staggers' in cattle, possibly carcinogenic	0.01	Not given
Silver	Natural geological sources, mining, electroplating, film-processing wastes, disinfection of water	Causes blue-grey discoloration of skin, mucus membranes, eyes	0.05	6.6% (above 0.1 μg litre^{-1}), 38, 2.6
Zinc	Industrial waste, metal plating, plumbing	Essential element in many metalloenzymes, aids wound healing, toxic to plants at higher levels; major component of sewage sludge, limits land disposal of sludge	5.0	76.5% (above 2 μg litre^{-1}), 1180, 64

[a]From Manahan (1991). [b] U.S. Public Health Service (1962).

[c]Kopp & Kroner (1991). The first figure is the percentage of samples showing the element; the second is the highest value found; the third is the mean value in positive samples (samples showing the presence of the metal at detectable levels).

Sources of inorganic contamination are vast and depend on the past and present industrial development of a particular country. Examples of some further possible sources are industrial sludges or by-products from for example, copper, lead, iron and zinc smelting industries (e.g. Daniels *et al*, 1998; Hadjihristova, 1998), mining operations (e.g. Ceto *et al*, 1998; Winnicki, 1998) duplicating and photographic manufacturing industries (e.g. Kucar *et al*, 1998), pharmaceutical industries, plating and electroplating works (e.g. Grabar *et al*, 1998), battery manufacturing works and both new and old military sites. Examples of some elements that may become released into the environment from these processes are given in Table 2.5.

Table 2.5 The composition of particular industrial waste streams and sludges (after Landreth, 1982)

Sludge description	Annual production (tonnes, wet)	% Solids	Density (Mg m^{-3})	pH	Constituents > 10 g kg^{-1} (dry)	Constituents 0.1-10 g kg^{-1} (dry)	Constituents 1-100 mg kg^{-1} (dry)
Electroplating sludge	50	32	1.27	7.6	Ca, Cr, Cu, Fe, SO_4, Cl, Si	Be, Cd, Pb, Mg, Mn, Ni, Zn	As, Hg
Nickel-cadmium battery sludge	100	40	1.25	12.3	Ca, Ni, Cl, Si	Cd, Cr, Cu, Fe, Pb, Mg, Zn	As, Hg
Pigment production	17 000	25	1.17	8.4	Ca, Cr, Fe, Pb, Mg, SO_4, Cl, Si	As, Cd, Cu, Mn, Ni, Zn	Hg
Chlorine production brine	3 000	59	1.57	9.5	Ca, SO_4, Cl, Si	Cu, Fe, Mg, Mn, Ni, Zn, Hg	As, Cd, Cr, Pb
Glass etching sludge	2 000	47	1.41	8.3	Ca, SO_4, Cl, Si	Cu, Fe, Pb, Mg, Mn, Ni, Zn	As, Cd, Cr, Hg

A further potential source of trace element contamination is sewage sludge, which in the past has been deposited directly into rivers, oceans and on land. Millions of tons of this type of waste are processed each year, consequently making sewage a very important potential contamination source. Table 2.6 lists some of the important trace elements found in sewage sludges from five different countries. There is variability in the concentration of particular elements between countries. For example, the UK Pb levels relative to the U.S. Pb levels may indicate sampling variability, although more likely it is indicating varying levels and types of industrial activity.

Table 2.6 Concentrations (mg kg^{-1}) of Trace Elements in Sewage Sludges[a]

Element	United States[b]		United Kingdom[c]		Sweden[d]		Canada[e] Mean	New Zealand[f] Mean
	Mean	Range	Mean	Range	Mean	Range		
Ag	---	---	32	5-150	---	---	---	---
As	14.3	3-30	---	---	---	---	---	---
B	37.0	22-90	70	15-1,000	---	---	1,950	480
Ba	621	272-1,066	1,700	150-4,000	---	---	---	580
Be	<8.5	---	5	1-30	---	---	---	---
Bi	16.8	<1-56	34	<12-100	---	---	---	---
Cd	104	7-444	<200	<60-1,500	13	2-171	38	4.5
Co	9.6	4-18	24	2-260	15	2-113	19	21
Cr	1,441	169-14,000	980	40-8,800	872	20-40,615	1,960	850
Cu	1,346	458-2,890	970	200-8,000	791	52-3,300	1,600	720
F	167	370-739	---	---	---	---	---	---
Hg	8.6	3-18	---	---	6.0	<0.1-55	---	---
Mn	194	32-527	500	150-2,500	517	73-3,861	2,660	610
Mo	14.3	1-40	7	2-30	---	---	13	8
Ni	235	36-562	510	20-5,300	121	16-2,120	380	350
Pb	1,832	136-7,627	820	120-3,000	281	52-2,914	1,700	610
Sb	10.6	2-44	---	---	---	---	---	---
Se	3.1	1-5	---	---	---	---	---	---
Sn	216	111-492	160	40-700	---	---	---	80
Ti	2,331	1,080-4,580	2,000	<1,000-4,500	---	---	---	4,700
V	40.6	15-92	75	20-400	---	---	15	80
W	20.2	1-100	---	---	---	---	---	---
Zn	2,132	560-6,890	4,100	700-49,000	2,055	705-14,700	6,140	700

[a]From Adriano (1986).

[b]Furr *et al* (1976); includes Atlanta, Chicago, Denver, Houston, Los Angeles, Miami, Milwaukee, San Francisco, Seattle, Washington, DC, and five cities in New York.

[c]Berrow & Webber (1972); includes 42 samples from different locations in England and Wales

[d]Berggren & Oden (1972); from 93 treatment plants.

[e]Oliver & Cosgrove (1975); from 10 sites in southern Ontario, Canada.

Wells & Whitton (1977).

Potential sources and pathways of contamination continually change due to the development of new industrial processes and methods of waste disposal, which demonstrates the importance of retaining records about the history and previous usage of a site. This is important because it provides information about the type and distribution of contaminants, the potential for changes in contaminant form with time due to natural environmental processes and the legal implications for the current and future owners or developers of the site.

Changes in type and level of pollution are recorded in naturally deposited submerged sediments. Research on from the Fourth Estuary by Lindsay *et al* (1998) indicate some changes in the levels and type of contamination created before, during and after the industrial revolution. Core sample contamination changes with depth indicate that the lower Forth Estuary has been affected by substantial industrial pollution in the recent past. However, lower heavy metal concentrations in the surface core samples reflect the fact that in recent years some industrial discharges have been reduced, perhaps due to pollution control legislation. Lindsay *et al* (1998) were also able to attribute the presence of radionuclides to discharges from Sellafield, Cumbria, highlighting a reduction in Cs^{137} from Sellafield since 1975. A reduction in the discharge limits of cooling water from nuclear submarines has also led to a three-fold reduction in surface sediment Cs^{60} levels since 1975. Radioactive inorganic contamination is a relatively new problem, having developed over the last 50 years and originating from energy generation facilities and military weapons testing and manufacture. Disposal of military wastes and remediation of contaminated sites has notably become an important issue in recent years especially since the end of the cold war.

Historical site information is clearly important at old military sites because there is a possibility of discovering dangerous and potentially explosive material as well as radioactive material. A long established Navy base in Portsmouth, England, highlights some of the problems associated with military sites. The 'Glory Hole' was an arm of Eastney Lake in the extreme Southeast corner of Portsea Island, Portsmouth, which was bunded off and infilled by the Royal Navy between approximately 1914 and 1955. A wide variety of naval scrap and waste materials were dumped into this muddy creek, including asbestos from boiler and armaments lagging, lead from submarine and other batteries, mercury from switchgear, zinc and cadmium plated metal objects. No records of the wastes deposited are available. The

2 ha site was covered over with topsoil onto which naval married quarters were constructed between 1955 and 1965. Some of this was leased for council tenancy during the mid-1980s. During the course of nearby excavations to construct a new marina in the late 1980s, substantial contamination was found. Typical results, highlighted in Table 2.7, demonstrated that the site was unfit for family habitation (Walton *et al*, 1998).

Table 2.7 Summary results of selected significant contaminant concentrations found in the surface soils at the Lumsden Road (Glory Hole) site (Walton *et al*, 1998)

Chemical determined	Detected range (mg kg^{-1})	Arithmetic mean (mg kg^{-1})	ICRCL (gardens) threshold trigger (mg kg^{-1})
Arsenic	<3-700	13	10
Cadmium	<1-17	1	3
Copper	<6-10 000	230	130
Lead	<20-96 000	1400	500
Mercury	<1-590	7	3
Zinc	11-11 000	440	300
PAH	<50-150	88	50
Asbestos	10-1000	36	10

This case proves the necessity to have a clear strategy to prevent contamination before and after military bases are abandoned and is the basis for further research (e.g. Barnett, 1998; Drawbaugh, 1998; Touchette *et al*, 1998; Rury *et al*, 1998).

2.2.2.3 Radioactive compounds

In the USA (as for most countries with a past or present military capability), contamination from military sites is a problem due to its extent, distribution and variation.

Several radioactive elements including uranium, radium and radon occur naturally in soil and groundwater (e.g. Strzelecki *et al,* 1998). Radioactive contamination can also result from processes associated with the production of nuclear energy and nuclear weapons, or indeed fallout from disasters or through disposal of wastes. Some of the behavioural characteristics of these radionuclides are discussed by Myasoedov (1998), Soundararajan (1998), Burmistrov *et al* (1998), and Firsova *et al,* (1998). Kisseleva *et al* (1998) also discusses the long-lasting alterations in the immune system of Chernobyl accident victims.

The Nuclear Weapons Complex (NWC) in the USA is a collection of very large factories devoted to metal fabrication, chemical separation processes, and electronic assembly associated with the production of nuclear weapons. In approximately 50 years of nuclear weapons production, these factories have released vast quantities of hazardous chemicals and radionuclides to the environment. Evidence exists that air, groundwater, surface water, sediment, and soil, as well as vegetation and wildlife, have been contaminated at most, if not all, nuclear weapons production facilities. Table 2.8 shows the types and complexity of wastes often found at NWC sites.

Most sites in non-arid locations also have surface contamination. Almost 4000 solid waste management units have been identified throughout the NWC, and many of these sites require some form of remedial action. Substantial quantities of waste have also been buried at the NWC, often with inadequate records of the burial location or composition of the waste buried (U.S. EPA, 1993).

Table 2.8 Nuclear weapons site contaminants and contaminant mixtures (Adapted from U.S. EPA, 1993)

Inorganic Contaminant			Organic Contaminants	Organic Facilitators[a]	Mixtures of Contaminants
Radionuclides	Metals	Other			
Americium-241 Cesium-134, -137 Cobalt-60 Plutonium-238,-239 Radium-224, -226 Strontium-90 Technetium-99 Thorium-228, -232 Uranium-234, -238	Chromium Copper Lead Mercury Nickel	Cyanide	Benzene Chlorinated hydrocarbons Methylethyl ketone, cyclohexanone, acetone Polychlorinated biphenyles and selected polycyclic aromatic hydrocarbons	Aliphatic acids Aromatic acids Chelating agents Solvents, diluents, and chelate radiolysis fragments	Radionuclides and metal ions. Radionuclides, metals, and organic acids. Radionuclides, metals, and natural organic Substances. Radionuclides and synthetic chelating Agents. Radionuclides and Solvents. Radionuclides, metal ions, and Organophosphates. Radionuclides, metal ions, and petroleum Hydrocarbons. Radionuclides, chlorinated solvents, and petroleum Hydrocarbons. Petroleum hydrocarbons and polychlorinated Biphenyls. Complex solvent mixtures.

[a] Facilitators are organic compounds that interact with and modify metal or radionuclide geochemical behaviour.

An extensive study of Department of Energy (DOE) sites and military bases in the USA that further illustrates pollution has recently been conducted. The sites are located around the US and were also sites for weapons production. Radioactive wastes were produced and at some military based toxic chemicals were disposed of in water supplies. Riley *et al* (1992) reports contamination of soils/sediments and groundwater at 91 waste sites on 18 DOE facilities, occupying 7280 km^2 in 48 states. It is reported that much of the wastes now contaminating the subsurface environment were disposed of on the ground surface, in ponds, pits, injection wells and landfills. Leaking subsurface storage tanks are also adding to this contamination problem. Over 100 individual chemicals and mixtures have been discovered, the most prevalent

metals being Pb, Cr, As, and Zn while the major anion found was NO_3^-. The sources of the metals and anions are associated with reactor operations (Cr and Pb), irradiated fuel processing (Cr, NO_3^- CN^-, and F^-), uranium recovery (NO_3^-), fuel fabrication (Cr, NO_3^-, and Cu), fuel production (Hg), and isotope separation (Hg) (Stenner *et al*, 1988; Rogers *et al*, 1989; Evans *et al*, 1990).

Tables 2.9a and 2.9b show the levels of contamination and 1995 approved clean-up costs for some of America's most secret military bases.

2.2.3 Conclusions

The total area of the world contaminated by organic and inorganic contamination is vast and poorly documented. Contamination of land and water resources is inherently site specific as well as historically specific. Bioavailability of many contaminants is also site specific and consequently the approach to contamination remediation must be considered in a site-specific manner. The sheer variability in the contaminated sites described shows that there can never really be a unique solution to remediating a contamination problem. Consequently, any remediation strategy will encompass a variety of processes carefully engineered to produce an environment meeting a predetermined level of risk.

Table 2.9a Contamination at U.S. Energy Department Sites and Costs of Cleanup[a] (Adapted from Sparks, 1995)

Site and location	Type of contamination	Spent to Sept. 1990 on cleanup[b]	Estimated or approved cost of cleanup[b]
1. Hanford Nuclear Reservation[c] (Richland, WA)	Plutonium and other radioactive nuclides, toxic chemicals, heavy metals, leaking radioactive waste tanks, groundwater and soil contamination, seepage into the Columbia river.	$1,000 plus	$30,000-50,000
2. McClellan Air Force Base[d] (Sacramento, CA)	Solvents, metal-plating wastes, degreasers, paints, lubricants, acids, PCBs in groundwater	61.0	170.5
3. Hunters Point Naval Air Station[e] (San Francisco, CA)	Chemical spills in soil, heavy metals, solvents	21.5	114.0
4. Lawrence Livermore National Laboratory[c] (Livermore, CA)	Chemical and radioactive contamination of buildings and soil	N.A.	1,000 plus
5. Castle Air Force Base[d] (Merced, CA)	Solvents fuels, oils, pesticides, cyanide, cadmium in soil, landfills, and disposal pits	12.7	90.0
6. Edwards Airforce Base[d] (Kern County, CA)	Oil, solvents, petroleum by-products in abandoned sites and drum storage area	21.0	53.4
7. Nevada Test Site[c] (near Las Vegas, NV)	Radioactive groundwater contamination	100 plus	1,000 plus
8. Idaho National Engineering Laboratory[c] (near Idaho Falls, ID)	Radioactive wastes, contamination of Snake River aquifer, chemical-waste lagoons	N.A.	5,000 plus
9. Tooele Army Depot[f] (Tooele County, UT)	Heavy metals, lubricants, paint primers, PCBs, plating and explosives wastes in groundwater and ponds	10.0	64.4
10. Rocky mountain Arsenal[f] (Denver, CO)	Pesticide, nerve gas, toxic solvents, and fuel oil in shallow, leaking pits	315.5	2,037.1
11. Rocky Flats Plant[c] (Golden, CO)	Plutonium, americium, chemicals, other radioactive wastes in groundwater, lagoons and dump sites	200 plus	1,000 plus
12. Los Alamos National Laboratory[c] (Los Alamos, NM)	Millions of gallons of radioactive and toxic wastes poured into ravines and canyons across hundreds of sites	N.A.	1,000 plus
13. Tinker Air Force Base[d] (Oklahoma City, OK)	Trichloroethylene and chromium in underground water	20.1	69.7

[a]From Energy Department, Air Force, Navy, General Accounting Office; New York Times, August 15, 1991.

[b]Army, Navy, and Air Force figures represent costs for committed or approved cleanup activities. Energy Department figures represent total estimated costs. **All costs are in millions of dollars.**

[c]Energy Department site.

[d]Air Force site.

[e]Navy site.

[f]Army site.

Table 2.9b Contamination at U.S. Energy Department Sites and Costs of Cleanup[a] continued...(Adapted from Sparks, 1995)

Site and location	Type of contamination	Spent to Sept. 1990 on cleanup[b]	Estimated or approved cost of cleanup[b]
14. Twin Cities Army Ammunition Plant[f] (New Brighton, MN)	Chemical by-products and solvents from ammunition manufacturing	28.0	59.9
15. Lake City Army Ammunition Plant[f] (Independence, MO)	Toxic metals and chemicals in groundwater	25.9	55.1
16.Louisiana Army Ammunition Plant[f] (Doyline, LA)	Hazardous wastes, groundwater contamination	38.0	66.9
17.Oak Ridge National Laboratory[c] (Oak Ridge, TN)	Mercury, radioactive sediments in streams, lakes, and groundwater	1,000 plus	4,000-8,000
18.Griffiss Air Force Base[d] (Rome, NY)	Heavy metals, greases, solvents, caustic cleaners, dyes in tank farms and groundwater and disposal sites	7.3	100.0
19.Letterkenny Army Depot[f] (Franklin County, PA)	Oil, pesticides, solvents, metal-plating wastes, phenolics, painting wastes in soil and water	11.9	56.2
20.Naval Weapons Station[e] (Colts Neck, NJ)	Heavy metals, lubricants, oil, corrosive acids in pits and disposal sites	1.1	33.8
21.Aberdeen Proving Ground[f] (Aberdeen, MD)	Arsenic, napalm, nitrates, and chemical warfare agents contaminating soil and groundwater	19.8	579.4
22.Camp Lejeune Military Reservation[e] (Jacksonville NC)	Lithium batteries, paints, thinners, pesticides, PCBs in soil and potentially draining into New River	3.0	59.0
23.Cherry Point Marine Air Corps Station[e] (Cherry Point, NC)	Untreated wastes soaking creek sediments with heavy metals, industrial wastes, and electroplating wastes	1.6	51.6
24.Savannah River Site[c] (Aiken, SC)	Radioactive waste burial grounds, toxic chemical pollution, contamination of groundwater	N.A.	5,000 plus
25.Mound Laboratory[c] (Miamisburg, OH)	Plutonium in soil and toxic wastes	150 plus	500 plus
26. Feed Materials Production Center[c] (Fernald, OH)	Uranium and chemicals in ponds and soil	600 plus	1,000-3000

[a]From Energy Department, Air Force, Navy, General Accounting Office; New York Times, August 15, 1991.

[b]Army, Navy, and Air Force figures represent costs for committed or approved cleanup activities. Energy Department figures represent total estimated costs. **All costs are in millions of dollars.**

[c]Energy Department site.

[d]Air Force site.

[e]Navy site.

[f]Army site.

2.3 CLAY-ELEMENT INTERACTIONS

2.3.1 Introduction

When a waste spill occurs or when a contaminant is slowly deposited on a site, the first mechanism to be considered is the interaction of the contaminant with the solids, interstitial fluids and gases in the surface 'soil' deposits. The depth, and physical and chemical nature of the surface layers and subsurface layers varies considerably and are dependent on the geological and environmental influences of the local environment developed over millions of years. Soil and subsoil layers are complex, dynamic, multicomponent and multiphasic.

Soil systems can be broadly defined as the surface layer of the lithosphere in contact with the atmosphere where the influence of the climate or the terrestrial ecosystems or human beings on the lithosphere material can be characterised. Subsurface systems are those subsurface layers of the lithosphere just below soil systems where the influence of the climate or the terrestrial ecosystems or human beings on the groundwater flows or groundwater quality can be characterised. Understanding the fundamental factors governing the formation of 'soil' deposits, their composition and subsequent interaction with contaminants is important when considering interactions with stabilisation and solidification treatments.

2.3.2 Soil formation and structure

Lithospheric materials can be defined as 'primary' or 'secondary' materials. Primary lithospheric materials include metamorphic and sedimentary rocks. The action of the climate via glacial or water action, wind, heating and cooling results in fracturing, weathering, and transport of solutes and particles subsequently structuring porous spaces. These physical processes are accompanied by the action of terrestrial ecosystems including the action of microorganisms, plant roots, water, nutrients, mineral carbon and oxygen. These large-scale changes in the natural landscape occur naturally over geological timescales but can often occur more rapidly due to the actions of humans. Once the macro structure has been physically broken down into particles of a smaller size, chemical transformations due to solubilisation, hydrolysis, hydration, carbonation, oxidation and reduction can occur much more readily forming secondary minerals such as clays.

The solubilisation effects of water on rock minerals are partly dependent on the dipole nature of water molecules. The development of slight positive charge around the hydrogen nuclei and negative charge around the oxygen nucleus due to the high electronegativity of oxygen allows the dissolution of ionic solids such a KCl.

During hydrolysis, cations are released from the soil minerals because they are exchanged by H^+ at the crystal surface. Metallic cations and silica are released into solution. This is the main process by which soluble silica enters the soil solution and is released from the soil (Jauzein, 1998). These released cations may react with the soluble silica forming new minerals or be involved in cation exchange reactions.

During hydration, minerals such as $CaSO_4$ (gypsum) absorb water often causing increases in volume. Many clays allow water between the lattice layers, causing expansion and potentially increasing the rate of decomposition.

During carbonation of Ca and Mg carbonates, soluble bicarbonates are formed as shown in Equation 2.1. Indeed Equation 2.1 is an example of carbonation and hydrolysis.

$$H_20 + CO_2 \Leftrightarrow H_2CO_3 \Leftrightarrow H^+ + HCO_3^- \qquad \textbf{Equation 2.1}$$

Atmospheric carbon dioxide	Carbonic acid	Bicarbonate ion

In aluminosilicate minerals, carbonation involves the exchange of H^+ for cations at the crystal surface with the formation of soluble metal carbonate. All soluble carbonate and bicarbonate products can be removed by leaching.

In a soil system where the availability of oxygen varies such as in a peat, the chemical environment equilibrates between reducing (under waterlogged conditions of low or zero oxygen availability) and oxidising (under aerated conditions of optimal oxygen availability) conditions. These conditions are generally termed redox conditions. Essentially redox reactions occur together and can be described in terms of electron transfers. The electron donor that loses an electron is oxidised and the electron acceptor is reduced.

Since physical and chemical transformations vary with climate and surface geological features so secondary clay mineral structure varies enormously throughout the world. Physically, clay minerals are defined as those particles in a soil system smaller than 2μm. Chemically the fundamental structure of many minerals is based

upon silicates, iron and aluminium oxides and hydroxides. In many areas of the world minerals tend to be of the layer silicate form. In glaciated or arid regions where the soil has not been subjected to intense or prolonged weathering the soil is typically of the iron and aluminium oxide or hydroxide form. Layer silicates are the most stable and persistent silicates which occur as weathered products of primary minerals and are essentially constructed of silicon bonded to oxygen in stable tetrahedral structures and aluminium bonded to oxygen in octahedral structures. These fundamental mineral building blocks are illustrated in Figure 2.1.

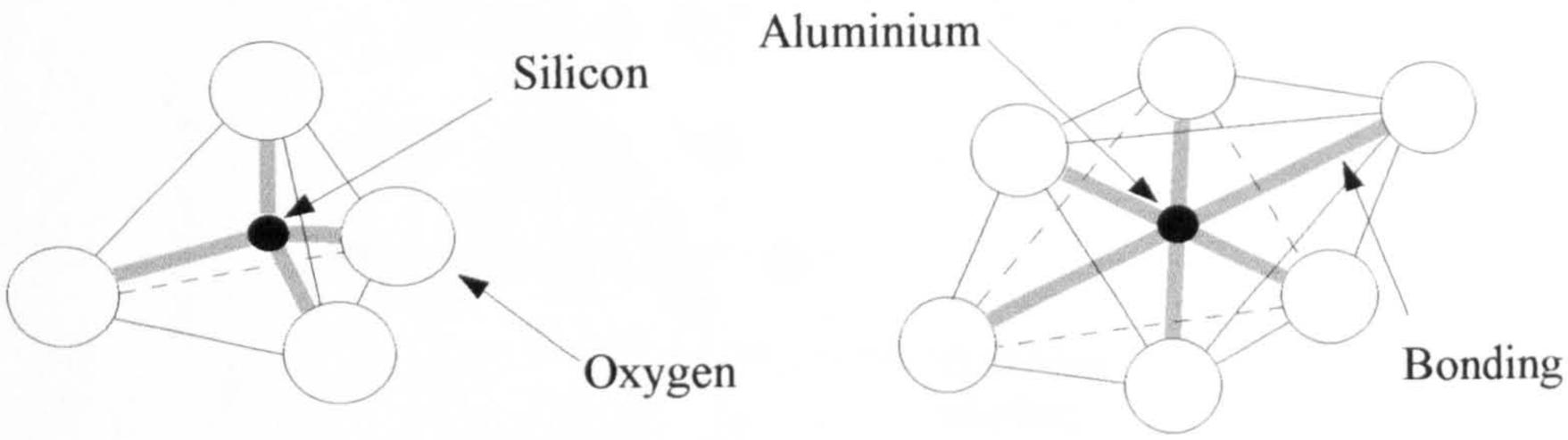

Tetrahedral Structure

Octahedral Structure

Figure 2.1 The fundamental building blocks of clay minerals

These basic tetrahedral and octahedral structures can form complex sheets when joined together. An example of an octahedral sheet is illustrated in Figure 2.2.

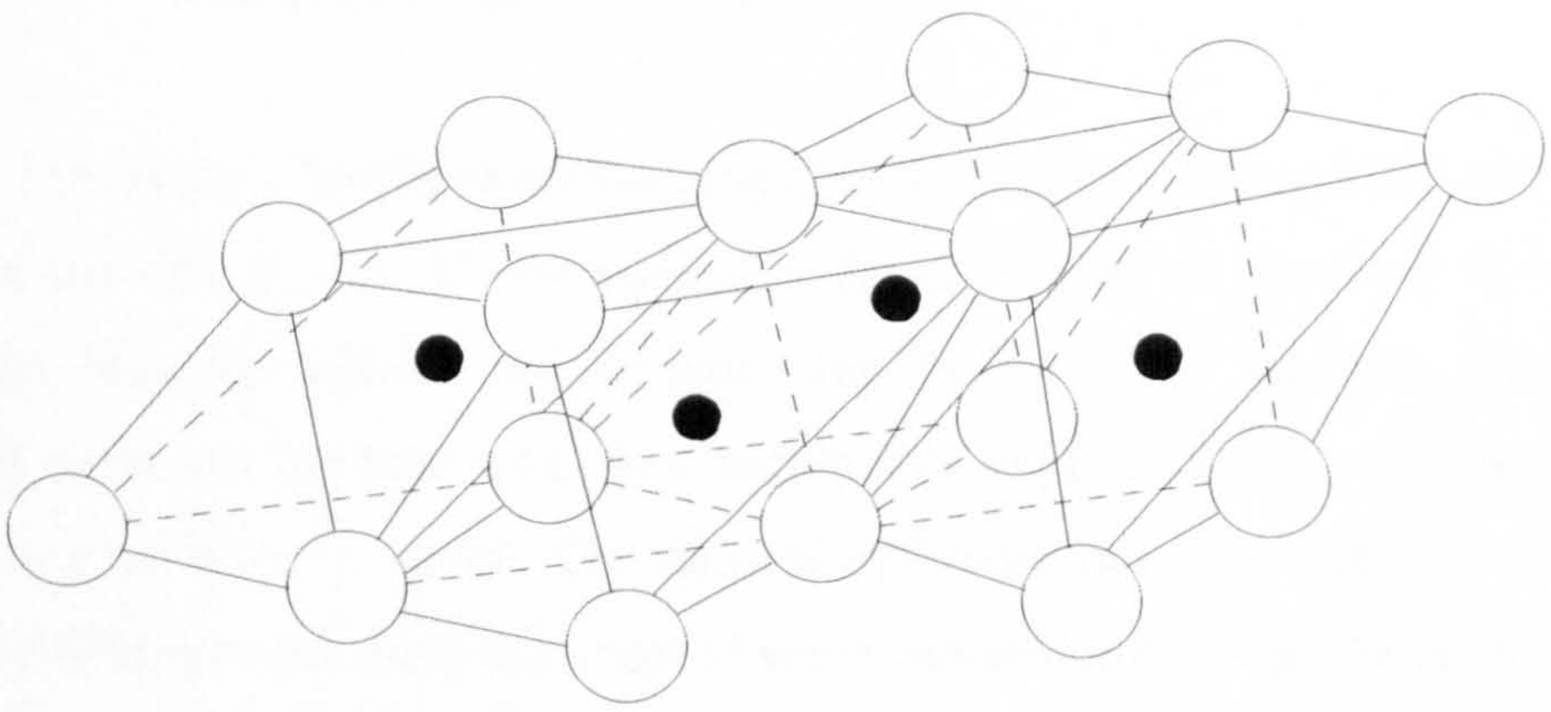

Figure 2.2 Octahedral sheet structure

Layer silicates derive their name from the tetrahedral and octahedral silicates and aluminates in their structural sheets. 1:1 layer silicates are so called because each individual layer is constructed from one tetrahedral silicate sheet and one octahedral aluminate sheet. The sheets are bonded together by the sharing of O^{2-} ions between the octahedral Al^{3+} cation and Si^{4+} cation. Each layer stacks to form a crystal of the 1:1 mineral. Layers are attracted together by a variety of bonding mechanisms, including, attraction via ions in solution and in some cases hydrogen bonding. The dioctahedral 1:1 mineral called kaolinite can be seen in Figure 2.3.

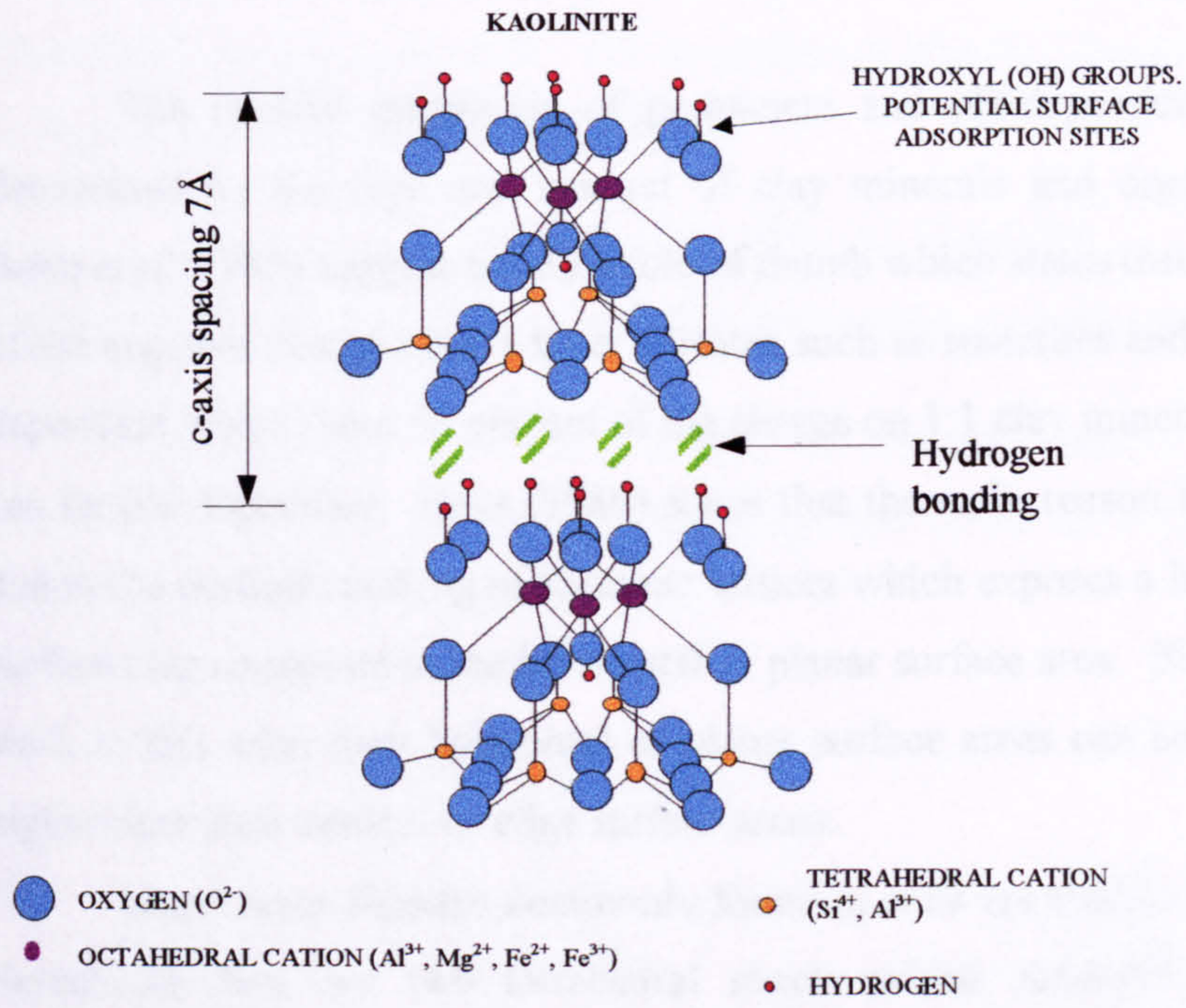

Figure 2.3 The structure of the 1:1 dioctahedral mineral kaolinite (Adapted from McBride, 1994)

The layers of kaolinite are held together by relatively strong hydrogen bonding between the OH groups of one layer and the O groups of the other layer. This interlayer bonding reduces the tendency for the layers to separate, producing a material with low surface area, low cation exchange capacity and low swelling potential when water is added. The mineral halloysite has the same 1:1 structure as kaolinite with the exception of a sheet of water molecules between the layer. Heating hallosite causes irreversible collapse to the kaolinite structure. The ideal structure of kaolinite $Si_4Al_4O_{10}(OH)_8$ has no effective charge. However this mineral has a small measurable charge deficit due to fractured edge sites, a small degree of isomorphous

substitution (see smectites) and potential for pH manipulation of charge on the hydroxyl edge sites. Dragun (1988) states that at low pH the equilibrium Equation 2.2, below, is valid, resulting in a high proportion of positive charge sites on the clay surface, attracting anions. At high pH equilibrium Equation 2.3, is valid, resulting in a high proportion of negative charge sites on the clay surface, attracting cations.

$$XOH + H^+ \Leftrightarrow XOH_2^+ \qquad \textbf{Equation 2.2}$$

$$XOH \Leftrightarrow H^+ + XO^- \qquad \textbf{Equation 2.3}$$

Where X = Mineral Structure.

The relative magnitude of permanent and pH-dependent charge in soil is determined by the type and amount of clay minerals and organic matter present. Bohn *et al* (1985) suggest a simple rule of thumb which states that about 5-10 per cent of the negative charge on 2:1 layer silicates such as smectites and vermiculites is pH-dependent while about 50 percent of the charge on 1:1 clay minerals such as kaolinite can be pH-dependent. Ross (1989) states that the main reason for this difference is due to the vertical stacking of kaolinite lattices which exposes a large vertical or edge surface area compared to the horizontal or planar surface area. Since smectites do not stack in this way, their horizontal or planar surface areas can be up to twenty times higher than their vertical or edge surface areas.

Many layer silicates commonly found in soils are similar in structure to mica. Essentially they are two tetrahedral sheets which sandwich a single sheet of octahedrally co-ordinated cations (2:1 layer silicates) and include smectite, vermiculite, illite and chlorite, each representing a clay group.

2.3.2.1 Smectites

Smectites are a group of minerals based on either the trioctahedral 2:1 talc ($Mg_3Si_4O_{10}(OH)_2$) or dioctahedral 2:1 pyrophyllite ($Al_2Si_4O_{10}(OH)_2$) structure. Smectites differ from these neutral structures due to the actions of isomorphous substitution.

During the physical and chemical weathering processes, isomorphous substitution can occur within the octahedral or tetrahedral sheets of minerals. Essentially quantities of the elements present in the mineral structure are displaced by other elements of a lower valence, or charge, including magnesium and iron (II). This

substitution (see smectites) and potential for pH manipulation of charge on the hydroxyl edge sites. Dragun (1988) states that at low pH the equilibrium Equation 2.2, below, is valid, resulting in a high proportion of positive charge sites on the clay surface, attracting anions. At high pH equilibrium Equation 2.3, is valid, resulting in a high proportion of negative charge sites on the clay surface, attracting cations.

$$XOH + H^+ \Leftrightarrow XOH_2^+ \qquad \textbf{Equation 2.2}$$

$$XOH \Leftrightarrow H^+ + XO^- \qquad \textbf{Equation 2.3}$$

Where X = Mineral Structure.

The relative magnitude of permanent and pH-dependent charge in soil is determined by the type and amount of clay minerals and organic matter present. Bohn *et al* (1985) suggest a simple rule of thumb which states that about 5-10 per cent of the negative charge on 2:1 layer silicates such as smectites and vermiculites is pH-dependent while about 50 percent of the charge on 1:1 clay minerals such as kaolinite can be pH-dependent. Ross (1989) states that the main reason for this difference is due to the vertical stacking of kaolinite lattices which exposes a large vertical or edge surface area compared to the horizontal or planar surface area. Since smectites do not stack in this way, their horizontal or planar surface areas can be up to twenty times higher than their vertical or edge surface areas.

Many layer silicates commonly found in soils are similar in structure to mica. Essentially they are two tetrahedral sheets which sandwich a single sheet of octahedrally co-ordinated cations (2:1 layer silicates) and include smectite, vermiculite, illite and chlorite, each representing a clay group.

2.3.2.1 Smectites

Smectites are a group of minerals based on either the trioctahedral 2:1 talc ($Mg_3Si_4O_{10}(OH)_2$) or dioctahedral 2:1 pyrophyllite ($Al_2Si_4O_{10}(OH)_2$) structure. Smectites differ from these neutral structures due to the actions of isomorphous substitution.

During the physical and chemical weathering processes, isomorphous substitution can occur within the octahedral or tetrahedral sheets of minerals. Essentially quantities of the elements present in the mineral structure are displaced by other elements of a lower valence, or charge, including magnesium and iron (II). This

displacement creates a measurable charge deficit within the layers of the mineral structure leading to the attraction of positively charged cations, usually in the form of positively charged metals in solution. This deficit is responsible for the majority of a clay's cation exchange capacity. Schofield (1949) found that the cation exchange capacity of a clay subsoil at Rothamsted Experimental Station in England was relatively constant between pH 2.5 and 5, but increased between pH 5 an 7. He also showed that the cation exchange capacity of montmorillonite did not vary below pH6, but increased as pH increased from 6 to 9. He ascribed the constant charge component to isomorphous substitution and the variable charge to ionisation of H from SiOH groups on the clay. The dioctahedral smectite, montmorillonite illustrated in Figure 2.4 has the general formula:

$$M^{+}_{x+y}(Al_{2-x}Mg_x)(Si_{4-y}Al_y)O_{10}(OH)_2$$

Where $x \approx 0.4$ and $x > y$, M^+ = balancing monovalent exchangeable cations.

The relatively low layer charge of smectites allows layers to separate producing a material with high surface area, high cation exchange capacity and high swelling potential when water is added.

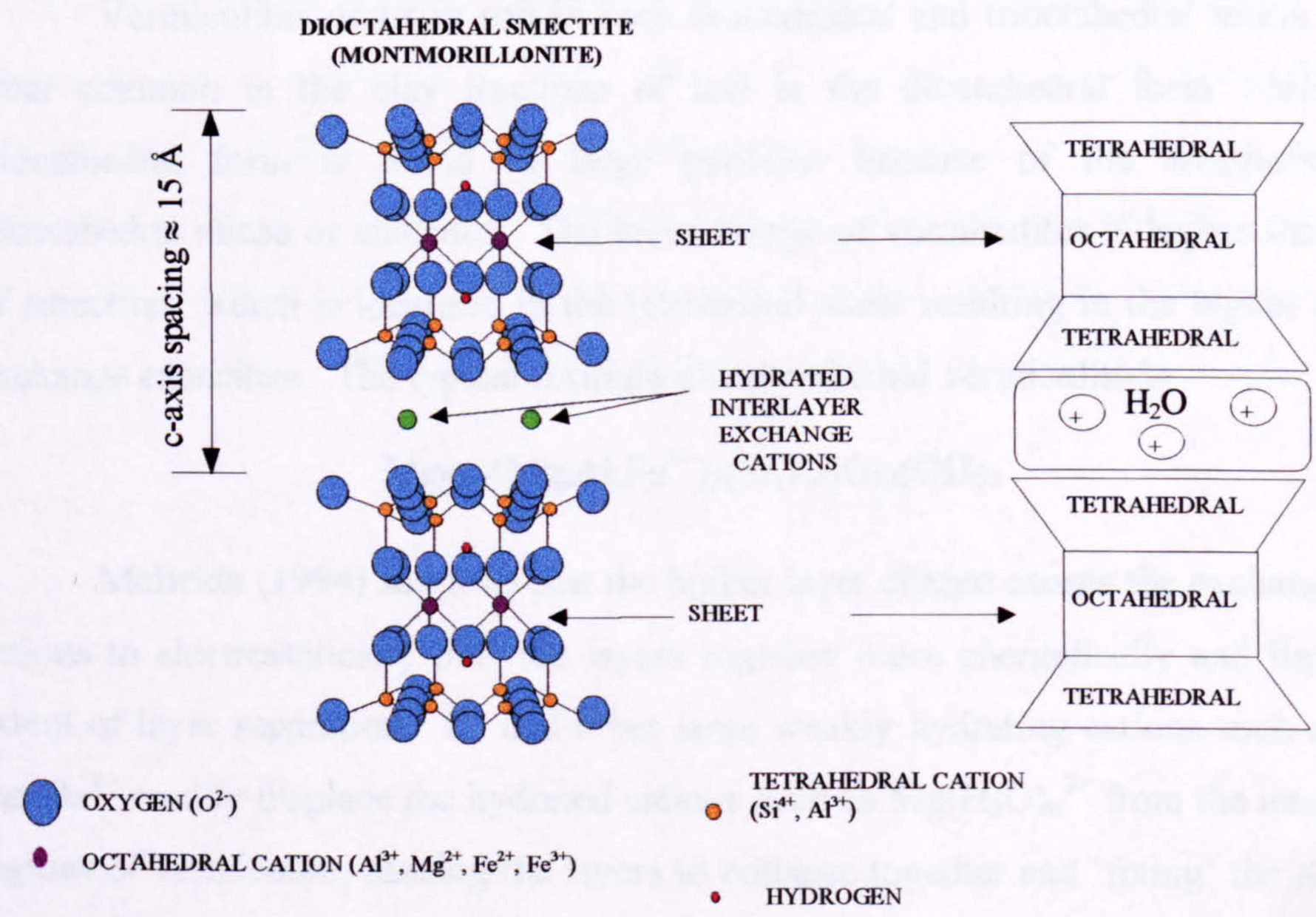

Figure 2.4 The general structure of 2:1 dioctahedral smectite

An example of the important effect of differing exchange cations on the c-axis spacing (Figure 2.4) and hence potentially physical properties of montmorillonite and vermiculite is depicted in Table 2.10.

Table 2.10 Measured c-axis spacings for common Vermiculite and Montmorillonite minerals saturated with exchangeable K^+, Na^+, and Mg^{2+} cations (After McBride 1994)

Mineral	Exchange Ion	c-Spacing (Å)		
		Air-Dry	Wet	Glycerol Added
Montmorillonite	K^+	11.6	>>20	17
	Na^+	12.4	>>20	17
	Mg^{2+}	14.7	19.5	17
Vermiculite	K^+	10.0	10.0	10.0
	Na^+	12.0	14.7	12.8
	Mg^{2+}	14.2	14.2	14.2

2.3.2.2 Vermiculites

Vermiculites occur in soil in both dioctahedral and trioctahedral forms. The most common in the clay fractions of soil is the dioctahedral form whilst the trioctahedral form is found in large particles because of the weathering of trioctahedral micas or chlorites. The layer charge of vermiculites is higher than that of smectites, which is localised in the tetrahedral sheet resulting in the higher cation exchange capacities. The typical formula of trioctahedral vermiculite is:

$$Mg_{0.33}(Mg,Al,Fe^{3+})_3(Si_3Al)O_{10}(OH)_2$$

McBride (1994) suggests that the higher layer charge causes the exchangeable cations to electrostatically pull the layers together more energetically and limit the extent of layer separation. K^+ and other large weakly hydrating cations such as Cs^+ and Ba^{2+} readily displace the hydrated cations such as $Mg(H_2O)_6^{2+}$ from the interlayer regions of vermiculite, causing the layers to collapse together and 'fixing' the K^+ into the mica like structure.

2.3.2.3 Illites

The structure of illite is very similar to that of mica although it is less crystalline, contains less K^+ and more water than mica. The K^+ is essentially fixed between silicate layers producing a material with little swelling potential, low surface area and low cation exchange capacity.

2.3.2.4 Chlorites

Similarly to vermiculite, chlorites contain tetrahedrally charged 2:1 layers with the octahedral layers being either dioctahedral or trioctahedral in nature. Similarly to vermiculite, usually the dioctahedral chlorites are found in the clay size fraction of soils. The major structural difference between chlorites and vermiculites is the presence of a positively charged metal hydroxide (brucite) sheet between the 2:1 silicate layers. The general structural formula is

$$[M^{2+},M^{3+})_3(Si,Al)_4O_{10}(OH)_2]^{x-}[(M^{2+},M^{3+})_3(OH)_6]^{x+}$$

2:1 Layer Brucite Sheet

Typically, the interlayer sheet of the primary mineral chlorite is $Mg(OH)_2$. During weathering and isomorphous substitution, the Mg^{2+} is displaced by Al^{3+} producing an excess of positive charge, which partially balances the 2:1 structure charge deficit. Particularly in acid soils, the hydroxide interlayer sheet will be predominantly $Al(OH)_3$ resembling gibbsite rather than brucite. Due to the interlayer sheets being filled by rigid interlayer sheets rather than the hydrated interlayers of vermiculite, chlorites have low surface areas, low cation exchange capacities and do not expand in water. Figure 2.5 shows diagrammatically the structural differences of some of the minerals described and Table 2.11 shows typical cation exchange capacities and surface areas for these secondary minerals.

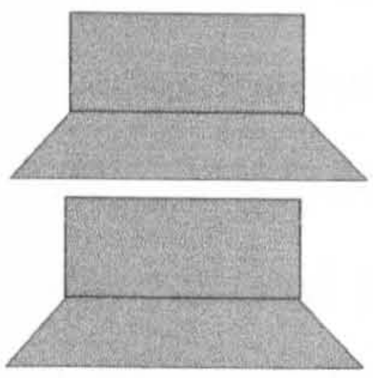

KAOLINITE

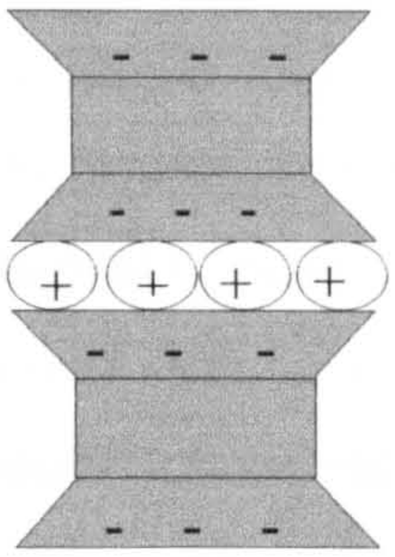

ILLITE

VERMICULITE

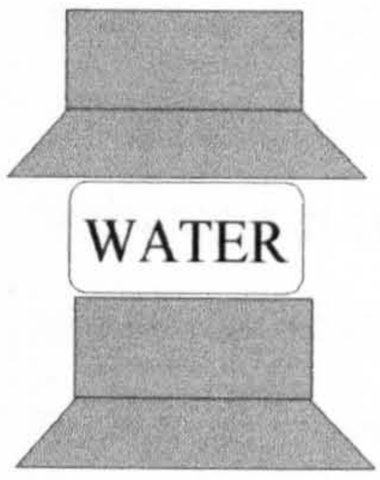

HALLOYSITE

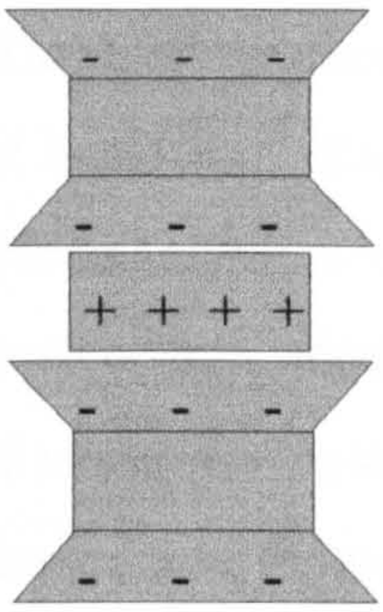

CHLORITE

SMECTITE

Figure 2.5 **Some typical layer silicate mineral structures (Adapted from McBride, 1994)**

Table 2.11 **Cation exchange capacity and surface area of secondary soil minerals (Adapted from Sparks, 1995)**

Mineral	**Specific surface area ($m^2\ g^{-1}$)**	**Cation exchange capacity ($cmol\ kg^{-1}$)**
Kaolinite	7-30	2-15
Halloysite	10-45	10-40
Talc	65-80	< 1
Montmorillonite	600-800	80-150
Dioctahedral vermiculite	50-800	10-150
Trioctahedral vermiculite	600-800	100-200
Chlorite	25-150	10-40
Allophane	100-800	5-350

2.3.2.5 Clays from arid or glacial climates

As previously mentioned clays throughout the world are not simply comprised of layer silicates. In arid or glacial regions composition will consist of oxides, hydroxides, and oxyhydroxides formed from the parent rock over millions of years. These minerals tend to be hexagonal or cubic close packed O^{2-} and / or OH^- with Fe^{3+}, Al^{3+}, Mn^{4+}, Mn^{3+} in the octahedral sites. Unlike the layer silicates, Fe and Al oxides do not tend to take part in isomorphous substitution and as such do not develop permanent structural charge. Hence, it is possible for these minerals to have very high surface area and very low cation exchange capacities (McBride, 1994). The low capacities achieved are due to limited pH-dependent surface adsorption previously described for layer silicates. Three of the most common crystalline oxides found in soils are gibbsite, geothite, and hematite. However, not all minerals are crystalline. Allophane, a non-crystalline hydrous aluminosilicate, is common in soils formed from volcanic ash and have been found in soils formed from glacial tills. McBride (1994) states that allophane consists of extremely small spherical aluminosilicate particles in which Al^{3+} occupies both octahedral and tetrahedral sites. Tetrahedral Al^{3+} would be expected to generate permanent negative charge in the structure, yet there is no indication that allophanes possess permanent charge. The cation exchange capacity of allophane is determined by the pH of the soil solution.

2.3.2.6 Cation-permeability interactions

The structure of the mineral and the proportion of specific elements present within exchange sites between the mineral structural layers affect the physical properties. Figure 2.6 illustrates the behaviour of sodium and calcium when present at exchange sites of kaolinite, illite and montmorillonite in varying proportions. Due to the structure of the minerals, kaolinite has a very low exchange capacity, illite has a low capacity due to the very stable presence of K^+, and montmorillonite has a very high exchange capacity. It is important to note, however that many salts can increase soil permeability by causing soil shrinkage to the point of causing cracking. The consequences of this may be enhanced ion movements. For example, aqueous solutions of NaCl, $CaCl_2$, $MgCl_2$, KCl, NH_4Cl, K_2CO_3, $CaSO_4$, $MgSO_4$, K_2SO_4, $NaNO_3$, $FeSO_4$, and FeO increase the permeability of Bentonite (see Table 2.12). However, aqueous solutions of $CaCO_3$, $MgCO_3$, Na_2SO_4, and Na_2SO_3 have negligible effect on Bentonite permeability (see Table 2.12).

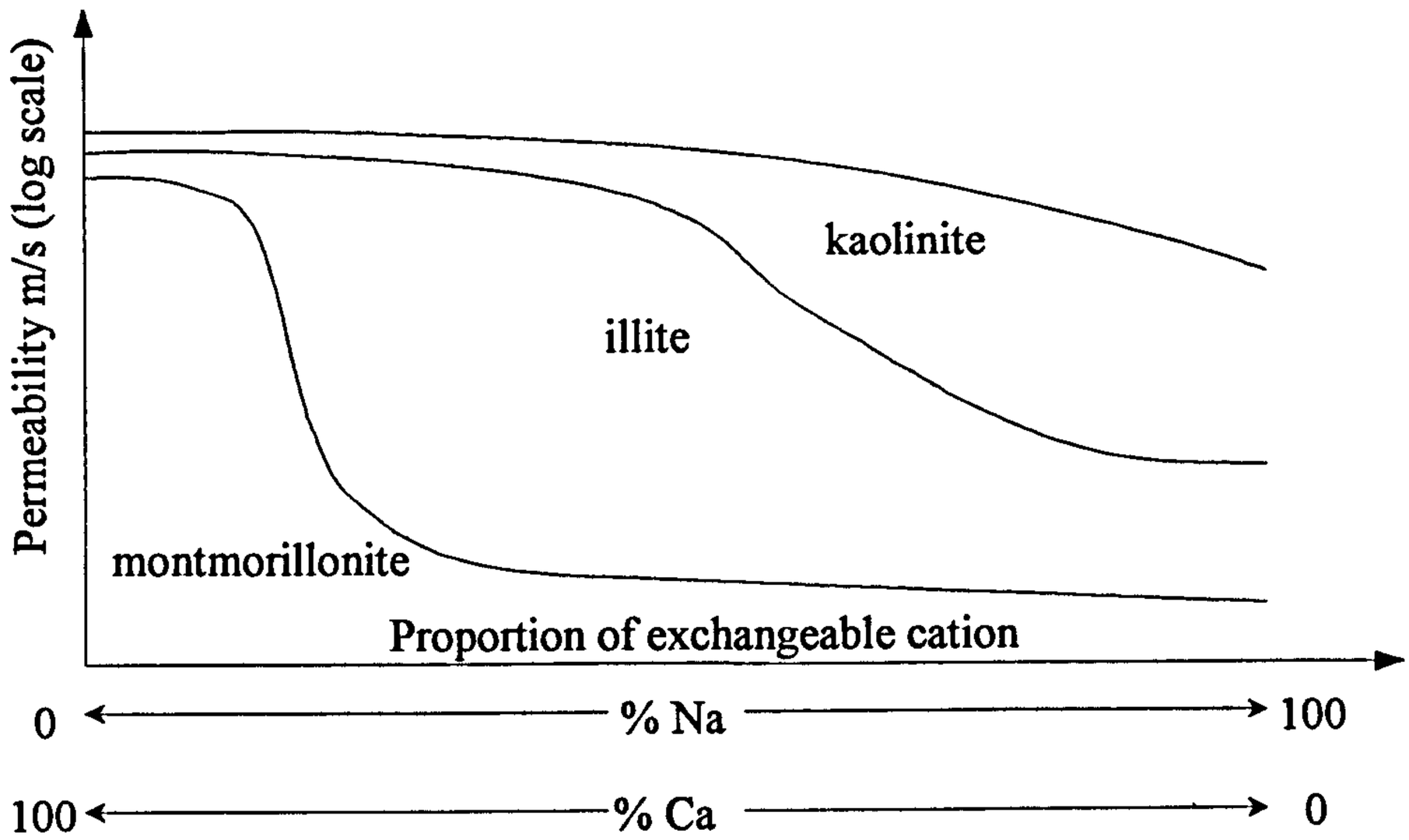

Figure 2.6 Variability of clay permeability with type and proportion of exchangeable cation (Jauzein, 1998)

Table 2.12 Effect of various salt solutions on Bentonite permeability (Alther *et al*, 1985)

Salt	Log Permeability, (cm/sec)								
	0%	0.25%	0.5%	1%	2%	3%	4%	5%	8%
NaCl	7.38	—	—	7.29	7.24	—	—	6.88	—
$CaCl_2$	7.41	6.96	6.79	6.73	6.74	—	—	6.74	—
$MgCl_2$	7.41	7.08	6.85	6.78	6.78	—	—	6.80	—
KCl	7.41	7.46	7.34	7.30	—	6.80	—	6.70	—
NH_4Cl	7.41	7.41	7.29	6.97	6.78	6.54	—	—	—
$CaCO_3$	7.41	—	—	—	7.42	7.38	7.37	7.37	7.43
$MgCO_3$	7.46	—	—	—	7.34	7.30	7.30	7.23	7.21
K_2CO_3	7.41	—	—	7.34	7.20	6.95	6.78	6.71	—
$CaSO_4$	7.46	7.16	6.97	6.96	—	7.03	—	7.01	—
$MgSO_4$	7.46	7.29	7.04	6.94	—	6.90	—	6.92	—
K_2SO_4	7.46	—	—	—	7.27	7.05	6.93	6.84	—
Na_2SO_4	7.46	—	—	—	7.37	7.40	7.40	7.37	—
Na_2SO_3	7.40	—	—	—	7.41	7.43	7.44	7.29	—
$NaNO_3$	7.40	—	—	—	7.35	7.24	7.22	7.10	—
$FeSO_4$	7.33	—	7.24	7.01	6.87	—	6.78	—	—
FeO	7.33	—	7.05	6.93	6.91	—	6.95	—	—

2.3.2.7 Soil organic matter

Soils are not simply formed by alteration of inorganic lithospheric materials, they combine with organic biospheric materials. The main difference between soils and subsoils are, soils tend to have a higher content of active organic constituents, higher

surface area with larger electric charge, more active biological and biochemical processes, greater porosity and hence more rapid fluxes of materials including changes in water content. The structure of soil with depth can be categorised as a series of profiles with horizons. Fundamentally, these consist of :

- O horizon: accumulation of organic matter overlying the soil with several layers depending on decomposition,
- A horizon: humified organic matter with mineral material,
- E horizon: characterised by loss of organic matter, Fe and Al oxides and clay minerals,
- B horizon: characterised by the accumulation of clay or the development of a distinctive structure, and
- C horizon: soil formation less affected by surface processes.

The structure of subsoils below 1 to 1.5 meters in temperate regions to about 3 meters or more in tropical regions the main modified factors are water dependent, even if roots are observed down to 5-10 meters (Jauzein, 1998). The structure of the unsaturated zone and the saturated zone are also modified mainly by wetting and drying as well as variability in the water table level creating cracks and fissures.

Considering the O, A and E horizons the organic matter has important implications to chemical behaviour. Helling *et al* (1964) found that in soils with uniform clay mineralogy, about 92 per cent of the variation in cation exchange capacity could be attributed to their clay and organic matter contents. The results of several investigations have suggested that organic matter content mainly determines soil cation exchange capacity in cultivated topsoils, with clay content mainly responsible for the cation exchange capacity of subsoils (Wright *et al*, 1972). Particle sizes within the clay fraction appear to contribute differently, with the < 0.2 μm clay fraction being the main cation exchange capacity contributor in the B horizons (Wilding *et al*, 1966). Only clay colloids can generate a positively charged surface when the soil is acidic, while both clay and organic colloids will have negatively charged surfaces when the soil 'solution' is alkaline. A simplified illustration of the constituents of soil organic matter is depicted in Figure 2.7.

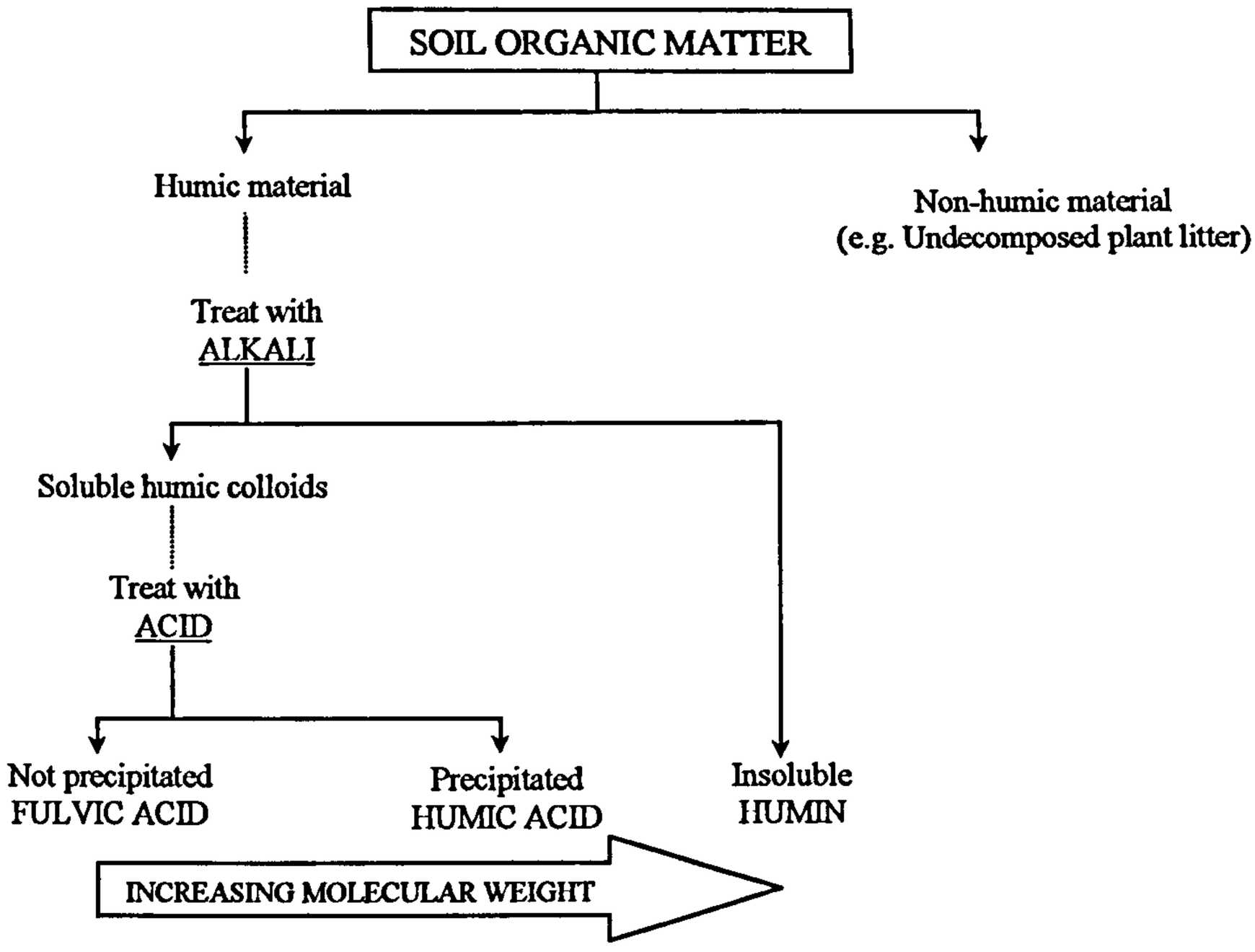

Figure 2.7 Schematic fractionation of soil organic matter (Ross, 1989)

The mechanism for the attenuation capacity of organic colloids is the same as that for layer silicates and is therefore equally important when considering lime-clay-contaminant interactions. The organic material humus is typically the substance that is involved in attenuation of cations. Humus is the relatively stable fraction of soil organic matter which remains in soils after the chemicals comprising plant and animal residues (amino acids, carbohydrates, fats, waxes, resins, and organic acid) have decomposed. Dragun (1988) describes humus as a series of relatively high molecular weight polymers. The typical humus colloid is comprised of: (i) a central unit containing primarily C and H, and (ii) a colloidal surface comprised of carboxylic (COOH) and hydroxyl (OH) functional groups. Infra red spectroscopic studies by Schnitzer *et al* (1969) identified the fulvic acid fraction (Figure 2.7) as the main organic component (87%) of the leachate from a humic surface soil. Schnitzer *et al* (1969) had also shown, by selectively blocking both acid carboxyl (COOH) groups and phenolic hydroxyl (OH) groups on their fulvic acid fraction, that both COOH and OH groups are important sites of metal bonding. These functional groups, when dissociated, possess negative charges and are depicted in Figure 2.8. These findings were further validated by Schnitzer (1977) and the complexation mechanisms of metals to humic acids by Stevenson (1977) and Livins (1991).

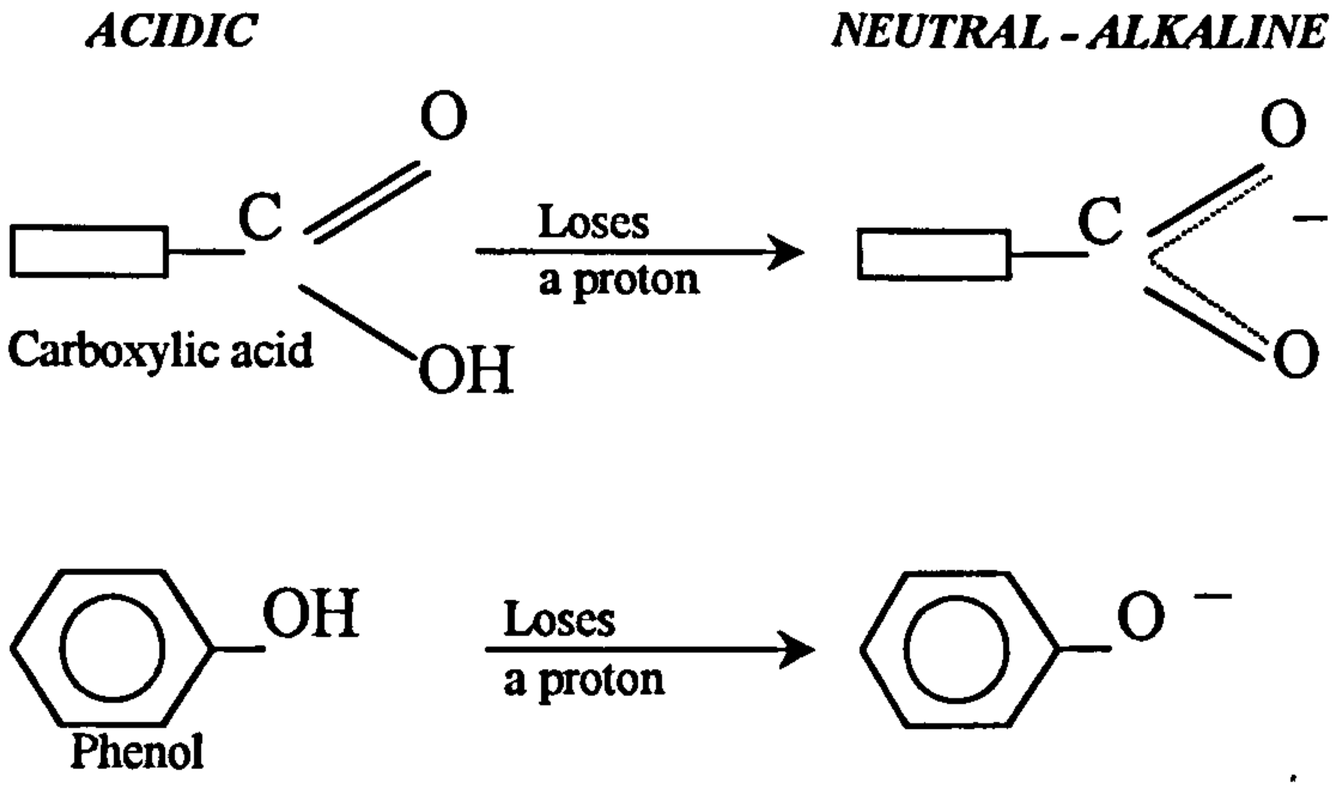

Figure 2.8 Development of pH-dependent charge in organic colloids

An empirical study of fulvic acid with an ionic strength of 0.1 and pH 3 by Schnitzer and Hansen (1970) identified an 'organic matter Lyotropic' series.

decreasing affinity ⟶

$$Fe^{3+} > Al^{3+} > Cu^{2+} > Ni^{2+} > Co^{2+} > Pb^{2+} = Ca^{2+} > Zn > Mn^{2+} > Mg^{2+}$$

According to McBride (1994) the affinity of humus for the essential macronutrients, Ca^{2+} and K^{+}, is (fortunately for plants and animals) higher than electronegativity would predict, suggesting that complexing or chelating groups in humus select for these metals on the basis of ionic size.

Perhaps the most important control of humic and fulvic acids and their metal complexes is the relative viscosity they impose on the soil 'solution'. Ross (1989) defines relative viscosity as the ratio of the solution viscosity to that of pure water. The viscosity is influenced by changes in the molecular configuration of the polymer, which can occur, by the addition of an electrolyte. The result is ionisation of the polymer and expansion of the organic molecule due to repulsive forces by similarly charged functional groups on the polymer chain (Hayes *et al*, 1978). Research by Smith *et al* (1964) concluded that increased concentration of Na and K in the soil solution would act to increase the mobility of humic substances. However, Hayes *et al* (1978) found that increasing the pH increased the dissociation of the polymer carboxyls increasing molecular expansion and solution viscosity thus reducing humic

polymer mobility. This would be an important mechanism during high pH lime treatment of contaminated surface soils. Ritchie *et al* (1982) found the solubility of humic acid-metal complexes increased when more hydrated species of complexing cations were involved. Ross (1989) suggests that these more hydrolysed ions e.g. Fe^{3+} and Al^{3+} occur at higher pH implying greater metal-humate mobility with increasing soil solution pH. Whatever the solubility of humic substances the permanent and temporary charges developed in soils due to mineral and organic fractions are of importance to natural attenuation and lime treatment processes. They are summarised schematically in Figure 2.9.

These schematic diagrams show the relative contributions of variable pH-dependent charge sites (cation exchange capacity (CEC_v)) and permanent cation exchange capacity (CEC_p) to the total soil cation exchange capacity (CEC_t). Depending on mineralogy, temperate mineral soils are likely to have measurable CEC_t at any pH due to the presence of CEC_p on 2:1 clay minerals, with additional CEC_v determined primarily by the amount of soil organic matter present. The large proportion of organic colloids in peat soils accounts for the dominance in these soils of CEC_v. The presence in highly weathered tropical soils of allophane and hydrous oxides of Fe and Al with very high isoelectric pHs (point of zero charge) may result in a net positive charge and the dominance of anion exchange in these soils at low pH (after Ross 1989).

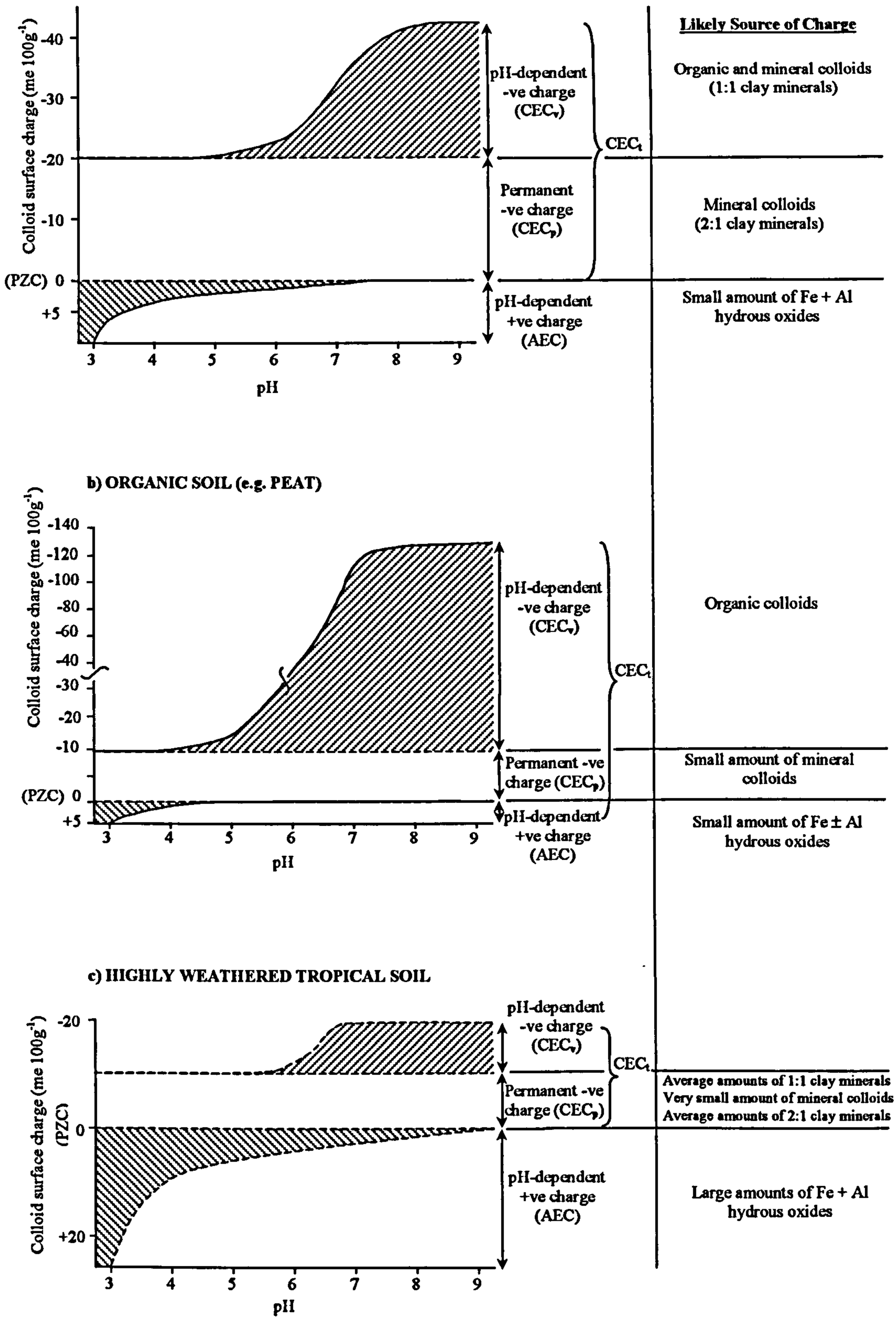

Figure 2.9 **Schematic effect of pH on surface colloidal charge for temperate mineral and organic soils and tropical soils (Ross, 1989).**

2.3.3 Predicting clay-ion behaviour

2.3.3.1 Introduction

It is apparent from the discussion of temporary and permanent charge on clay minerals that this potential for partial element containment is important. It is also important to consider that some elemental ions are contained in preference to others. Selectivity of one ion for another by cation exchange within a mineral is complex. Exchange depends on the physical and chemical behaviour of both the ion present in the mineral and the exchanging ion. Hence, selectivity depends on surface charge, ion radius and the thermodynamics of the chemical reaction. The thermodynamics and equilibrium behaviour of these reactions can be used to predict the quantities of reaction product of exchange reactions. However, where more than one exchanging ion exists, the theory becomes very complex and unpredictable and from an engineering perspective a descriptive analysis is required.

2.3.3.2 The condition for equilibrium

Cation exchange reactions are rapid, reversible and stoichiometric, where quantities of exchanged ions are chemically equivalent. Although the exchange process can be considered instantaneous, ion diffusion to or from the colloid surface is probably the rate-limiting step, especially in heterogeneous field conditions (Bohn *et al*, 1985). Cation exchange reactions may be driven in either direction by manipulating the concentrations of reactants and products. This principle is used in soil extraction techniques such that a salt solution, such as ammonium acetate, is leached through the soil sample. In this instance, the exchanging cation is the ammonium ion (NH_4^+) and the displaced ion can be measured in the solution.

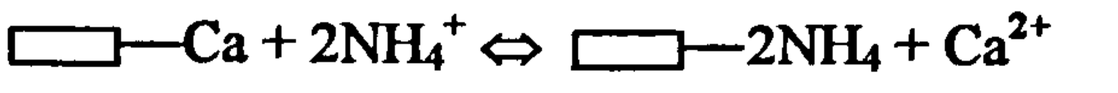

Due to the relative charge difference, two ammonium ions are required to replace one calcium ion. The reversible relationship between a cation in water with an exchangeable cation at equilibrium can be described by Equation 2.4 (after Dragun, 1988).

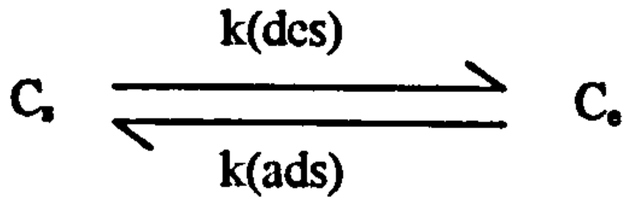

Equation 2.4

Where

C_s = concentration adsorbed on soil surfaces (μg/gram soil)

C_e = concentration in water (μg/ml)

k(des) = desorption rate

k(ads) = adsorption rate

Analysis of this equation reveals that the equilibrium distribution of a cation is governed by the two opposing rate processes. The adsorption rate is the rate at which the dissolved cation in water transfers into the adsorbed state and the desorption rate is the rate at which the cation transfers from the adsorbed state into water. The adsorption coefficient K_d is the simplest way of expressing the extent of adsorption and is defined as the ratio of C_s/C_e. Hence, the more adsorption that occurs, the greater the magnitude of K_d.

Table 2.13 identifies the K_ds for some common elements. It is evident that there is a large variation even for a single element. Since the magnitude of K_d is dependent upon the size and charge of the cation and upon the soil properties, and because the soil properties vary widely among soils, an elements K_d also varies widely among soils.

Table 2.13 Ranges for K_ds for various elements in soils and clays (Dragun, 1988)

Element	Observed Range (ml/g)	Element	Observed Range (ml/g)	Element	Observed Range (ml/g)
Ag	10-1,000	Cr(VI)	1.2-1,800	Po	196-1,063
Am	1.0-47,230	Cs	10-52,000	Pu	11-300,000
As(III)	1.0-8.3	Cu	1.4-333	Ru	48-1,00
As(V)	1.9-18	Fe	1.4-1,000	Se(IV)	1.2-8.6
Ca	1.2-9.8	K	2.0-9.0	Sr	0.2-3,300
Cd	1.3-27	Mg	1.6-13.5	Tc	0.003-0.28
Ce	58-6,000	Mn	0.2-10,000	Th	2,000-510,000
Cm	93-51,900	Mo	0.4-400	U	11-4,400
Co	0.2-3,800	Np	0.2-929	Zn	0.1-8,000
Cr(III)	470-150,000	Pb	4.5-7,640		

Dragun (1988) states if ions were point charges then no preference for ions of the same valence would exist; however, ions do have significantly different hydrated sizes. Since electrostatics are involved in the attraction of ions at a charged soil surface then it can be predicted that the ion with the smallest hydrated radius and largest charge will be preferentially accumulated. Marshall (1975), reporting the results of cation exchange research on montmorillonite clay by Schachtschabel (1940), gives the following order of cation exchange:

$$\xrightarrow{\text{Replaceability}}$$

Monovalent cations: $Li^+ > Na^+ > K^+ > Rb^+ > Cs^+$

Divalent cations: $Mg^{2+} > Ca^{2+} = Sr^{2+} > Ba^{2+}$

The order for replaceability on kaolinite is very similar as suggested by Bohn *et al* (1985):

$$\xrightarrow{\text{Replaceability}}$$

$$Li^+ \approx Na^+ > K^+ \approx NH_4^+ > Rb^+ > Cs^+ \approx Mg^{2+} > Ca^{2+} > Sr^{2+} \ldots$$

$$\ldots \approx Ba^{2+} > La^{3+} \approx H^+(Al^{3+}) > Th^{4+}$$

This order is termed the Lyotropic series and represents increasing cation replaceability, or decreasing cation attraction, with increasing radius, increasing atomic number and thus decreasing polarising power and ionic hydration. Generally, less hydrated ions with smaller hydrated radii, such as Na^+ and K^+, are more strongly attracted to charged mineral surfaces. Cation valency is the second major controlling factor on the order of exchange, with multivalent ions being more strongly retained than monovalent ions (Ross, 1989). Clearly cation exchange and selectivity on mineral surfaces are significant in helping to explain physico-chemical changes due to contaminant attenuation and indeed the early improvements induced by the addition of lime. Appendix A2 contains a brief description of some of the more fundamental mechanisms governing these ion mineral interactions, including the Eisenman energy model of cation exchange, the Stern diffuse double layer model of cation exchange, the effects of ionic potential, reaction enthalpy (are exchange processes exothermic or endothermic?) and entropy (system disorder).

The cation selectivity of organic colloids described in Section 2.3.2.7 depends on the configuration of carboxylic and phenolic groups on organic molecules because

it is this which determines the surface negative charge density. Ross (1989) suggests that two or three adjacent groups on aliphatic and aromatic compounds attract multivalent cations more selectively than when they are widely spaced (Talibudeen, 1981). Talibudeen (1981) states that the influence of one carboxyl group on the dissociation of an adjacent carboxyl group is negligible when they are separated by more than four CH groups. He specifies three general rules of organic colloid-cation selectivity: (1) multivalent cations are preferred to monovalent cations; (2) transition group metals (Fe, Mn, Cu, Zn) are preferred to strongly basic (alkali) metals (K, Na, Ca, Mg), and (3) cation selectivity increases with cation exchange capacity.

2.3.3.3 Organic contaminant attenuation and organophilic clays

There has been much interest in using clays, in particular high surface area smectites, for removal of organic pollutants from water. In the context of lime stabilisation, the removal of organics in this way is thought to remove the impeding effects of many organic molecules on the stabilisation mechanisms. Clays created in the natural environment contain exchangeable metal ions which make clay surfaces hydrophilic and ineffective at sorbing non-ionic organic compounds. There are however few ionic organic species that occur in soils as pollutants, with perhaps the exception of certain herbicides such as diquat and paraquat. The chloride salt of paraquat is shown in Figure 2.10.

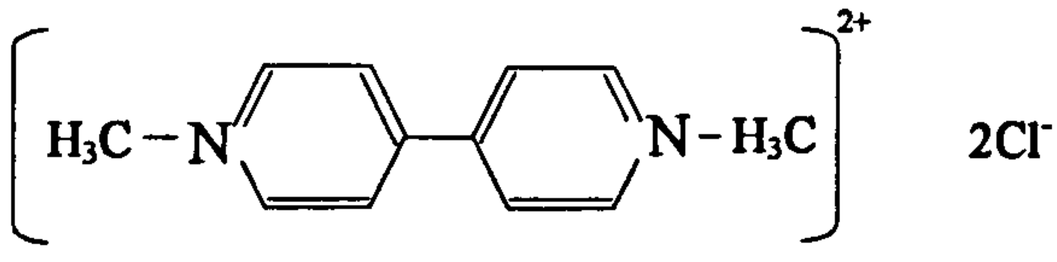

Figure 2.10 Chloride salt structure of the herbicide paraquat

McBride (1994) explains that these cations are strongly attenuated by cation exchange reactions on smectite and less strongly on vermiculites and kaolinite. He also states that the selectivity of the clay is far greater for the organic cation than the inorganic cations it displaces resulting in very little desorption even for very high concentrations of competing inorganic cations. However, these organic cations are apparently adsorbed less strongly on soil humic material especially when the pH is lowered and the H^+ ions preferentially occupy the negative carboxylic functional

groups. High molecular weight organo cations are adsorbed with higher selectivity on minerals. The order of preference for a series of ammonium cations on smectite is:

$$(CH_3CH_2CH_2)_4N^+ > (CH_3CH_2)_4N^+ > (CH_3)_4N^+$$

This order is not simply due to differences in electrostatic attraction but more to do with increasing entropy (disorder) as the molecule increases in size. This is linked to the idea that as the molecule increases in size, more water must be displaced from the exchange site to accommodate the cation. These organo cations do not possess the strong hydration forces of some inorganic cations that keep the interlayer of swelling clays expanded. This can lead to collapse of the interlayer and subsequently flocculation of the mineral. The low hydration forces associated with attenuated organo cations changes the properties of the mineral exchange surface from hydrophilic to organophilic, a property exploited in smectites to improve adsorption of non-polar organic molecules. These modified clays are referred to as organoclays and are very effective in sorbing non-ionic organic compounds (Mortland, 1970; Mortland *et al*, 1986). Zhang & Sparks (1993) found that untreated montmorillonite adsorbed little phenol but adsorption was greatly improved after the clay was modified with $HDTMA^+$ (hexadecyltri-methyl-ammonium). Zhang *et al* (1993) showed that the surfactants in the exchange sites of the clay are not easily desorbed suggesting that organoclays are stable complexes. Although currently cost may be inhibitive, organoclays clearly have a number of potential uses including use as landfill liners for improved organic leachate retention. Soundarajan *et al* (1990) also suggests the use of organoclay in wastewater treatment and spill control situations.

Generally in current in-situ conditions unmodified clays with high permanent charge, including vermiculites, do not expand significantly in water. This is insufficient space for the larger organo cations. McBride (1994) also suggests that since silicate clays with high charge localised in the tetrahedral sheet (e.g. vermiculites) hydrate more strongly than those with lower charge localised mainly in the octahedral sheet (e.g. smectites), organocations adsorb less energetically on vermiculite surfaces because of the greater energy cost in displacing the water from the adsorption site. This is illustrated diagrammatically in Figure 2.11.

It is therefore clear that unmodified clays of the appropriate mineralogy can be partially successful with specific ionic organic compounds. It is also clear that to retain non-ionic organic compounds a modified clay is necessary. Although expensive, once mixed it is possible that the attenuated organic compound may not interfere with any stabilisation and solidification reactions once a solidifying reagent has been added. This would result in the permanent binding of the compound permanently within a monolithic mass. This would be especially beneficial in situations involving mixtures of ionic organic compounds, non-ionic organic compounds and inorganic ionic compounds.

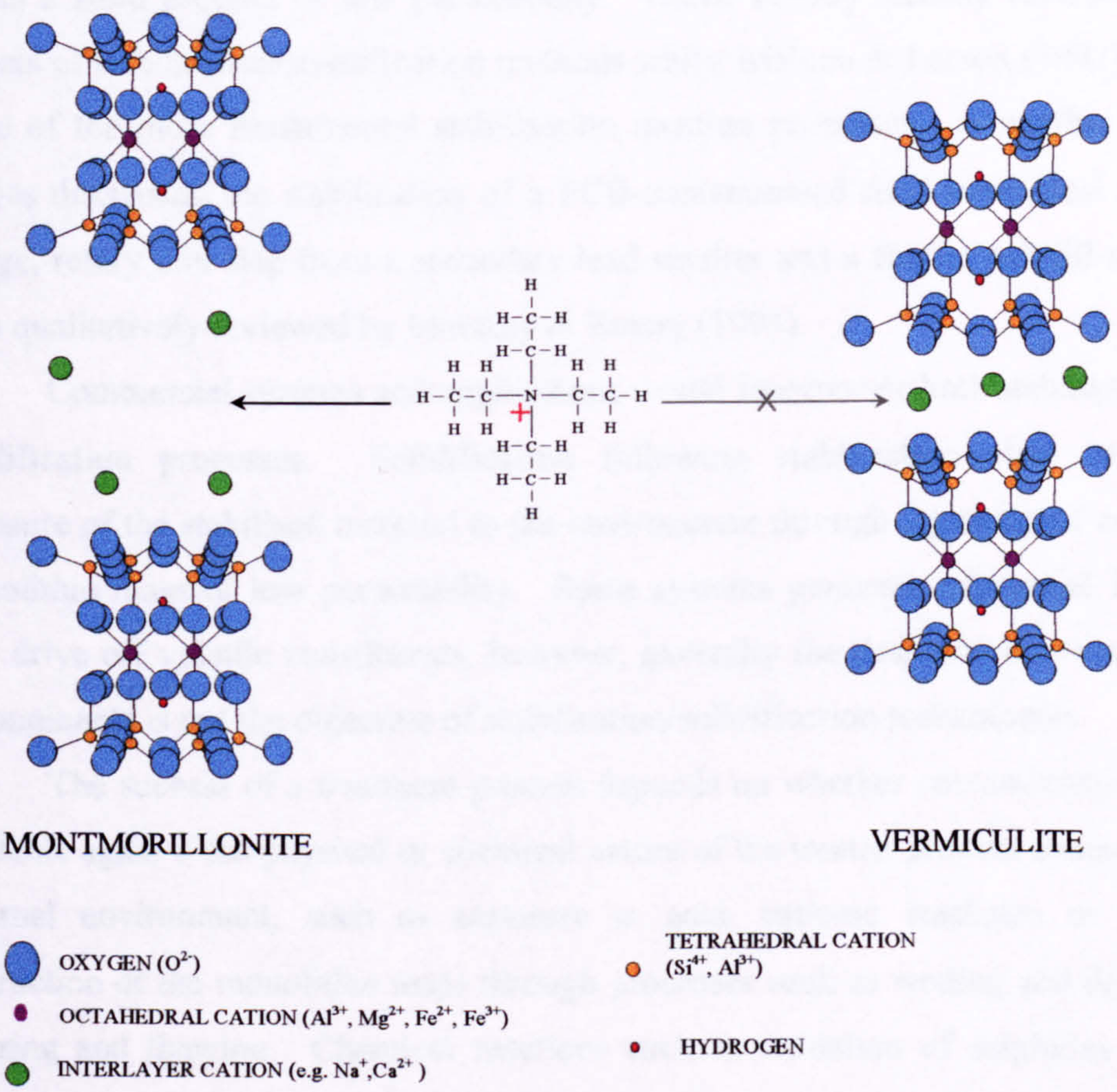

Figure 2.11 Selectivity of mineral structure cation exchange sites for large organic cations. (after McBride, 1994)

2.4 STABILISATION/SOLIDIFICATION PROCESSES

2.4.1 Introduction

In the context of treating contaminated land, stabilisation refers to the fixation of a contaminant to the chemical structure of a soil material whilst solidification refers to the cementation of the soil material due to the addition of a solidification reagent such as lime or cement thereby reducing the flow of solution through the solidified mass. Stabilisation/solidification methods, sometimes called immobilisation methods, change the physical state of a contaminated material, such as solidifying a contaminated sludge, sediment or clay. In addition, chemical stabilisation can reduce the availability of contaminants to potential sensitive targets, usually by containment within a solid product of low permeability. Harris (1995) recently reviewed some aspects of stabilisation/solidification methods whilst Malone & Larson (1983) discuss some of the more fundamental stabilisation reaction processes. A number of case studies discussing the stabilisation of a PCB-contaminated road base, steel industry sludge, rotary kiln slag from a secondary lead smelter and a former ash fill site have been qualitatively reviewed by MacKay & Emery (1993).

Commercial systems and applications would incorporate both stabilisation and solidification processes. Solidification following stabilisation aims to reduce exposure of the stabilised material to the environment through a process of creating a monolithic mass of low permeability. Some systems generate substantial heat that may drive off volatile constituents, however, generally the destruction or removal of contaminants is not the objective of stabilisation/solidification technologies.

The success of a treatment process depends on whether contaminants become available again if the physical or chemical nature of the treated product changes in the external environment, such as exposure to acid, cationic leachates or physical destruction of the monolithic mass through processes such as wetting and drying and freezing and thawing. Chemical reactions such as oxidation of sulphides forming expansive sulphates may also destroy the monolithic mass. Hence, the essential concepts for choosing a stabilisation method are therefore:

- the ability to achieve and maintain chemical stability or permanently bind contaminants, entrapping them over the long-term whilst retaining the desired physical properties, and

- the methods to be used to determine treatability including short and long-term performance.

Smith (1998) suggests that the effectiveness of stabilisation/solidification methods depend on:

- proper characterisation of the material to be treated so that the most appropriate formulation can be selected,
- effective contact between the contaminants and treatment reagents, which for many systems involves achieving a well mixed system, hence requiring appropriate mixing equipment,
- control over external factors including temperature, humidity, degree of mixing allowed after reagents have been added and begun to react, since these directly affect the setting and strength development hence potentially, the long-term durability of the finished matrix, and
- absence of chemical substances that may inhibit the stabilisation/solidification process, or addition of pre-treating agents to render such substances harmless.

Generally, stabilisation/solidification systems can be classified according to the main stabilising agent added. They can be based on cement/lime, pozzolana, silicate, thermoplastic or polymer systems. Commercially, systems available in the U.S. are proprietary in nature, relying on mixtures of those agents identified above. In many instances waste sources of reactive agents have been utilised, including, cement kiln dust, lime kiln dust and steel slag fines. Depending on the source, resources such as cement kiln dust may contain reactive lime, calcium silicates, pozzolanic clay minerals and alkali sulphates creating some potentially complex chemical reactions.

Organic binders tend be more expensive because they rely on refined materials such as asphalt, polyethylene, resins, epoxies, urea formaldehyde, polyesters and potentially organophilic clays. Indeed the employment of an organic binder in itself may not be environmentally desirable. Their application, therefore, tends to be limited to particularly hazardous wastes, such as nuclear wastes, and highly toxic industrial waste (Hinsenveld, 1993).

Stabilisation and solidification in the U.S. and Canada is regarded as an established technology for treating inorganic contaminants (U.S. EPA, 1989; U.S.EPA, 1991; Bishop, 1990). Although techniques have also been adopted in Europe, doubts exist about the physical and chemical nature of the processes, the testing and predicting performance and subsequently the long-term performance. Although many experts believe that a high proportion of stabilised contaminants will ultimately be released, the concentrations in the leachate at any one time can be low enough to pose no direct hazard to the environment. However, if the waste leaches for an extended period, the environment will become loaded with contaminants unless the contaminants are remineralised and components are incorporated into soil organic matter (Hinsenveld, 1993).

The situation is exacerbated by the fact that with the exception of thermoplastic-based methods and some propriety lime-based methods, one of the limiting factors associated with conventional systems is that very low concentrations of organic contaminants can interfere dramatically with crystallisation (setting) processes. Hence, much recent research has focussed on methods of stabilising and solidifying mixed organic and inorganic contaminated systems. One approach incorporates organophilic clays to preferentially absorb organic contaminants prior to the conventional stabilisation and solidification treatment. Other adsorbents could include ion exchange resins, activated carbon and zeolites. Although this research is in its infancy, refined adsorbents such as organophilic clays are very expensive which currently make the application of the technology inhibitive. Many stabilisation and solidification processes produce heat, which can lead to the volatilisation of VOCs. In these situations, the process should be executed in a closed system, where the VOCs can be trapped, and subsequently treated. This increases the expense and reduces the financial viability of the whole approach.

2.4.2 The clay-lime reaction

The addition of lime, either in the form of quicklime ($CaO_{(s)}$) or as hydrated or 'slaked' lime ($Ca(OH)_2$), to a soil system initiates a two-stage reaction. The reactions of cement could be considered similar because cement is 70% $CaO_{(s)}$, although it also contains significant gypsum $CaSO_{4(s)}$ to control the reaction rate. During the first stage, if added, the quicklime reacts with water in the soil system according to the following equation:

$$CaO + H_2O \Rightarrow Ca(OH)_2 + \text{heat}$$

This reaction is highly exothermic, producing approximately 17×10^9 joules per kilogram of calcium oxide. Quicklime is sometimes used purely as a de-watering agent due to the benefits of dehydration of the soil system by reaction and by steam generation. Associated with the first stage of the reaction, within minutes to hours of mixing, there is a decrease in the plasticity of the clay caused by the flocculation of the clay particles. This is accompanied by an increase in strength caused by both the dehydration and fundamental changes in the clay particle chemistry. This *modification* of the clay occurs immediately in a well mixed system and is due to the exchange of cations such as Na^+ and H^+ in the clay mineral structure for Ca^{2+}.

The second stage of the reaction process, termed *solidification*, occurs in the longer term over a period of days and weeks and is the result of pozzolanic reactions (Glendinning & Boardman, 1996). These reactions have been studied and reported in detail by many researchers including Arman & Munfakh (1970, Eades & Grim (1960) and Diamond & Kinter (1965). Sherwood (1993) defines a pozzolana as a material that is capable of reacting in the presence of water, at ordinary temperatures, to produce cementitious compounds. In simplified terms, the addition of lime to a clay in appropriate quantities (generally between 1-7%) creates a highly alkaline environment ($\approx$pH 12.4) and promotes the dissolution of silica and alumina from the clay mineral structure, particularly at the edge sites of the clay plates, permitting the formation of calcium silicate hydrate and calcium aluminate hydrate gels. These gels crystallise with time to create cementitious reaction products that are analogous to the composition of cement paste. The dissolution effects of high pH on the basic building 'blocks' of clay minerals including silicon oxides, aluminium oxides and iron oxides is evident from observation of Figure 2.12

The second-stage reaction generally results in continued reduction in a clay's plasticity as reported by Lund & Ramsey (1959), Wang *et al* (1963) and Jan & Walker (1963). However, lime affects the liquid limit in various ways. Wang *et al* (1963) and Jan & Walker (1963) reported decreases in the liquid limit, whereas Zolkov (1962) reported substantial increases. Lund & Ramsey (1959) and Taylor & Arman (1960) found increasing and decreasing liquid limits that were dependent on

the soil type. Along with changes in Atterberg Limits there is usually an increase in shear strength on addition of lime (Thompson, 1966). Thompson (1965) showed that organic matter with a high exchange capacity retarded the strength producing pozzolanic reactions, probably due to the process of Ca attenuation. However, a study by Arman and Munfakh (1970) concluded that organic soil-lime mixtures produce cementitious products similar to those reported for inorganic soil-lime reactions and that the organic matter does not appear to block the reaction that results in an increase in the soil strength. In the context of treating contaminated land, the most significant physical change is in permeability because it could either lead to an increase or decrease in soluble contaminant mobility due to leaching. In the short-term after addition of lime it is expected that the permeability will increase, the degree depending on the mixing, mellowing (the time the mixture is left before compaction), compaction and curing conditions (the environment in which the cementitious gels crystallise) during lime treatment. This increase in permeability was hypothesised by Townsend and Klym (1966) when their tests on lime-treated heavy clays exhibited slight increases in permeability. McCallister and Petry (1992) reported on research by Ranganatham (1961) who found a ten-fold increase in permeability after adding lime to expansive clays. Fossberg (1965) however, reported a reduction in permeability after treating a clay with lime. In the longer-term this tendency for increased permeability can reverse as the calcium aluminate hydrate and calcium silicate hydrate gels form and crystallise in the pore spaces between the flocs (El-Rawi *et al*, 1981). This theory is reinforced by the research of Gutschick (1978) who reported that the permeability of a lime-flyash-aggregate canal liner showed initial increases in permeability which gradually decreased to produce flow rates comparable with the natural clay.

Column leaching tests on lime-treated clays by McCallister & Petry (1992) concluded that lime dramatically increased the permeability of soil with maximum permeability occurring at the lime modification optimum. This lime modification optimum is the minimum percentage lime content required to create a significant change in material characteristics. It is determined by addition of specific quantities of lime to clay-water mixtures and determining the minimum lime content at which the pH does not increase on addition of higher lime contents. According to the research of McCallister & Petry (1992) column leachate pH increased as the lime content of the sample increased but decreased linearly during the leach cycle.

Calcium concentration in the leachate was lowest in specimens prepared at the lime modification optimum but increased as the lime content increased. Hence they concluded that there is strong evidence to suggest that calcium removal and permeability are in correlation to the complex ion interaction within the soil-lime mixture (cation exchange and solidification mechanisms) and therefore the lime modification optimum is a central parameter in determining the leaching properties of lime-treated soils.

Glendinning (1995) compiled observations of a number of researchers investigating the addition of lime and suggested reaction mechanisms to help explain changes in the physical behaviour of clays. The results of this compilation are summarised in Table 2.14a, 2.14b, 2.14c

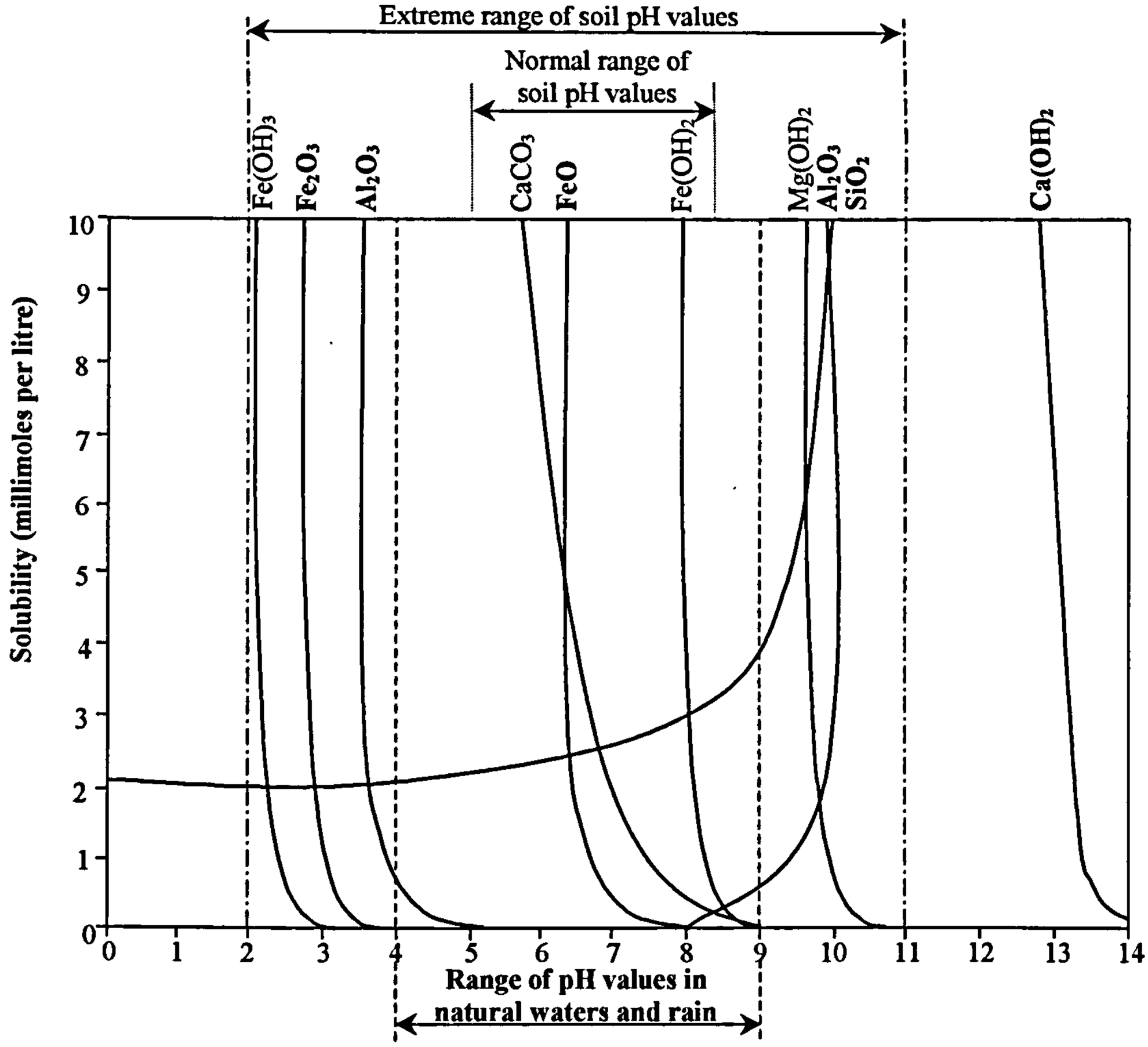

Figure 2.12 Solubility of some soil mineral species in relation to pH (Loughnan, 1969)

Table 2.14a Summary of suggested reaction mechanisms (Glendinning, 1995)

Author	Observation	Suggested Mechanism
Newman (1987).	Flocculation.	Cation exchange leading to reduction of double layer.
Diamond and Kinter (1965).	Flocculation in calcium saturated clay. Changes in plasticity, shrinkage and swelling. Increase in strength.	Formation of small amounts of cementitious material at points of contact.
Lees *et al* (1982).	Clay + 2% lime addition gives sharp increase in ϕ .	Modification by flocculation and particle rearrangement.
Hilt and Davidson (1960).	Limitation to the increase in plastic limit with addition of more lime.	Lime-fixation-crowding of cations within clay structure.
Diamond and Kinter (1965).	Limitation of lime taken out of solution, Ca in same proportion as hydroxyl ions. No overall charge change. Able to wash out. No heat given off.	Physical absorption of lime – a single molecular layer of $Ca(OH)_2$.
"	Increased adsorption. Not able to fully wash out.	Chemical reaction at contact points.
Bell (1988).	Non-linear relationship between lime % and strength gain after 2% addition for montmorillonite; 2-4% for kaolinite.	The existence of an optimum addition of lime.
Lees *at al* (1982).	Decrease in ϕ for kaolinite with increases for lime addition over 2%.	Optimum lime addition/particle rearrangement dominant stabilising factor.
"	No decrease in strength with larger additions of lime to montmorillonite.	Pozzolanic reactions dominant stabilising factor.
Bell (1988).	Decrease in maximum dry density.	Formation of cementitious compounds that form interlocking compounds.

Table 2.14b Summary of suggested reaction mechanisms (Glendinning, 1995)

Author	Observation	Suggested Mechanism
Brandl (1981). Mateos (1964).	Swelling potential/pressures reduced.	Formation of cementitious compounds that form interlocking compounds.
Eades and Grim (1966).	Formation of calcium aluminate hydrates/silicate hydrates at high pH (high lime content).	High pH induces solubility of silicates and aluminates in the clay, hence reaction able to occur.
Diamond and Kinter (1965).	"	Lime adsorption leads to reaction at clay surfaces, giving rise to precipitate reaction.
Harty and Thomson (1973).	Greater improvements with highly weathered soils.	Weathering increases clay susceptibility to dissolution of silica and alumina.
Quigley and DiNaro (1978).	Greater improvements using high lime contents on weathered soil than non-weathered.	Weathering increases smectite content that reacts via a different mechanism.
Moore and Jones (1971).	Reactivity greatly reduced with high iron content.	Iron in the form of positively charged aggregations reducing ion-exchange capacity.
Mateos (1964).	Lesser degree of improvement using illite and chlorite than montmorillonite.	Cation exchange capacity reduced.
"	Higher increases in plastic limit with increasing clay content.	Clay is the reactive clay constituent.
Bell (1988).	Kaolinite + 2% lime, liquid limit rise; kaolinite +< 2% lime liquid limit falls.	Particle surfaces modified by the action of hydroxyl ions.

Table 2.14c Summary of suggested reaction mechanisms (Glendinning, 1995)

Author	Observation	Suggested Mechanism
Bell (1988).	Higher compaction densities obtained in kaolinite than montmorillonite.	Expandable minerals have greater affinity for water due to shape and higher specific surface.
Lees *et al* (1982).	No clear optimum of moisture content-dry density compaction curve- most noticeable in montmorillonite	Initial formation of cementitious compounds affects compactibility-montmorillonite most reactive.
Bell (1988).	Dramatic immediate increase in the unconfined compressive strength with small lime addition in montmorillonite.	Expansive clays react more quickly due to greater cation exchange capacity.
Lees *et al* (1988).	Cohesion and unconfined compressive strength correlation.	Both affected by the same part of the mechanism.

Clearly due to differences in mineral structure, individual mineral chemistry will vary thus affecting the development of lime stabilised material and the final physical properties including the unconfined compressive strength, the liquid limit, the plastic limit and the cohesion and angle of friction. Glendinning (1995) summarises in Table 2.15 the effects of lime on some of these physical properties for a variety of British clay minerals.

Table 2.15 British clays: properties, mineralogy and effects of lime (Glendinning, 1995)

Formation	LL (%)	PI (%)	Clay fraction < 2μm (%)	Average undrained shear strength (kN/m^2)	Effective cohesion c' (kN/m^2)	Effective angle of friction ϕ' (degrees)	Mineralogy	Effects of lime: Author, test, effects
Palaeogene								
London clay	66-100	40-65	40-72	100-173	12-18	17-23	Mainly illite-mica with kaolinite and traces of chlorites, smectites and vermiculite. $CaCO_3$ barytes and gypsum also found	Dumbleton, 1962, mix test, 10% lime. Increase in UCS. Also 5% reduced plasticity.
Creaceous								
Gault clay	70-92	27-80	38-62	60	----	----	Usually illite-mica, poorly crystallised kaolinite and expanding chlorite/vermiculite. Mixed layer structure.	Dumbleton, 1962, mix test, 10% lime. Increase in UCS. Also 5% reduced plasticity.
Weald clay	42-82	28-32	20-74	----	----	----	Similar to above with impurities of calcite, siderite, pyrite, gypsum, ostracod and ferrous iron	Dumbleton, 1962, mix test, 10% lime. No increase in UCS in 12 weeks; affects to LL & PL
Jurassic								
Kimmeridge clay	----	24-59	57	----	14-67	14-23	Dominantly illitic	Dumbleton, 1962 mix test, 10% lime. Increase in UCS
Oxford clay	----	28-50	30-70	----	0.2	21.5-28	Dominantly illitic	Dumbleton, 1962 mix test, 10% lime. Increase in UCS. Cobbe, 1988 mix test; 2% $Ca(OH)_2$ PL and LL & PI raised 1 hour after mixing.

Notes: UCS is the Unconfined Compressive Strength; LL is the Liquid Limit; PL is the Plastic Limit; PI is the Plasticity Index (LL-PL)

Table 2.15 British clays: properties, mineralogy and effects of lime.....continued (Glendinning, 1995)

Formation	LL (%)	PI (%)	Clay fraction < 2μm (%)	Average undrained shear strength (kN/m^2)	Effective cohesion c' (kN/m^2)	Effective angle of friction ϕ' (degrees)	Mineralogy	Effects of lime: Author, test, effects
Jurassic								
Upper Lias	56-68	20-39	55-65	30-150	10-17	18-25	Kaolinite-illite with traces of chlorite. Rare mixed layers	Cobbe, 1998, mix test, 2% $Ca(OH)_2$, PI and LL raised 1 hour after mixing.
Lower Lias	56-62	32-37	50-56	---	5	27	Dominantly illitic with impurities of marcite, pyrite, glauconite, fossils; high iron content.	Dumbleton, 1962, mix test, 10% lime, UCS raised.
Triassic								
Keuper Marl	25-60	10-35	10-50	100-150	2-80	25-42	> 40% illite mica, 4-34% dolomite, gypsum, high alkalinity.	Dumbleton, 1962, mix test, 10% lime, UCS raised.

Notes: UCS is the Unconfined Compressive Strength; LL is the Liquid Limit; PL is the Plastic Limit; PI is the Plasticity Index (LL-PL)

2.4.3 Principles of chemical stabilisation of contaminants

There are several different reaction processes that combine to facilitate chemical stabilisation of inorganic contaminants in clays and hence have a large effect on the lime modification and solidification reactions. The primary aim for the benefit of the environment is to stabilise the association of the contaminants with the clays such that they are not mobile and subsequently not bio-available. The initial association between metal contaminants and clays occurs via the previously discussed cation exchange reaction. This complex reaction occurs in accordance with the Lyotropic series that varies significantly with changing humus, mineral composition and pH of a soil. However, in general (as previously stated) ions having a higher valency state substitute for ions of a lower valency on the exchange sites of the clay minerals. This 'natural' substitution causes temporary stability, but the metal ions could become disassociated by future cation exchange. In addition, the quantity of contaminant rendered immobile by cation exchange is finite and determined by the specific structure of the clay mineral present. Thus some means of both creating further association of the free metal ions and preventing disassociation needs to be sought. There are broadly three ways that such stability can be brought about.

The first is to increase the pH of the environment in order to bring about enhanced surface adsorption at the mineral edge sites. This mechanism was previously discussed in Section 2.3.2 and remains successful as long as the pH remains high, but its effectiveness is also dependent on specific mineral structure and will reduce if the pH reduces. Assurance of continued high pH is likely to pose a problem, however, because natural groundwater tends towards acidity rather than alkalinity (Figure 2.12). Therefore an artificial means of maintaining a high pH needs to be provided. In addition a further consideration must be made since the process of cation exchange inherently results in the displacement of the host cations from the clay. For example, it is probable that following penetration of metal ions through a clay barrier lining a landfill site, cation exchange would occur to a significant degree. This would in turn result in the displaced ions such as Na^+ creating a plume of pollution leading away from the site in the direction of groundwater flow. The consequences of Na^+ pollution might not prove as severe as those of the escaping metal ions, but nevertheless they could form a subsequent problem that would need to be addressed. Griffin & Shimp (1975) noted this behaviour whilst investigating the attenuation of metals from landfill leachate on kaolinite (1:1 lattice type clay mineral),

montmorillonite (2:1 expanding lattice), and illite (2:1 non-expanding lattice, mica type). During column leaching of landfill leachate through these clays, elution of soluble Ca, and to a lesser degree soluble Fe and Mn was observed. The elution of soluble Ca was attributed to Ca being the predominant exchangeable cation present on the clays. However, the elution of soluble Mn was not attributed to cation exchangeable metals. Griffin *et al.* (1976) state that Mn is three times more abundant on the surface of kaolinite than on montmorillonite and that this difference corresponds to the increased elution from kaolinite columns. Thus the potential for the elution from clays is not purely dependent on cation exchange but also on surface adsorption. However, on addition of lime to a soil system this is likely to be the main mechanism for the release of metals from the treated material.

The second mechanism is similarly pH-dependent and relies upon precipitation of salts from solution. As well as increasing the surface adsorption of ions, increasing the concentration of OH^- ions in solution can ultimately result in the formation of metal complexes and subsequently precipitation of the metal salt will occur. This mechanism is of significance when considered along with the lime solidification reaction. Griffin & Shimp (1976) considered the precipitation reactions of lead (Pb) from landfill leachate along with Pb adsorption on the surface of kaolinite. They showed that species other than Pb^{2+} were relatively insignificant at pH values less than 6. It was evident that at values above a pH of 6 adsorption of Pb coincided with the formation of hydroxyl Pb species. Precipitation was found to be an important mechanism for Pb removal and the effect is depicted in Figure 2.13. Precipitation of specific metal salts under conditions of high pH thus provides an important means of reducing the mobility of metal ions as long as the pH remains high. Reversal of precipitation would occur if the pH reduced to a lower level, although this level depends on the cation present, thus presenting the same long-term limitation as that of surface adsorption.

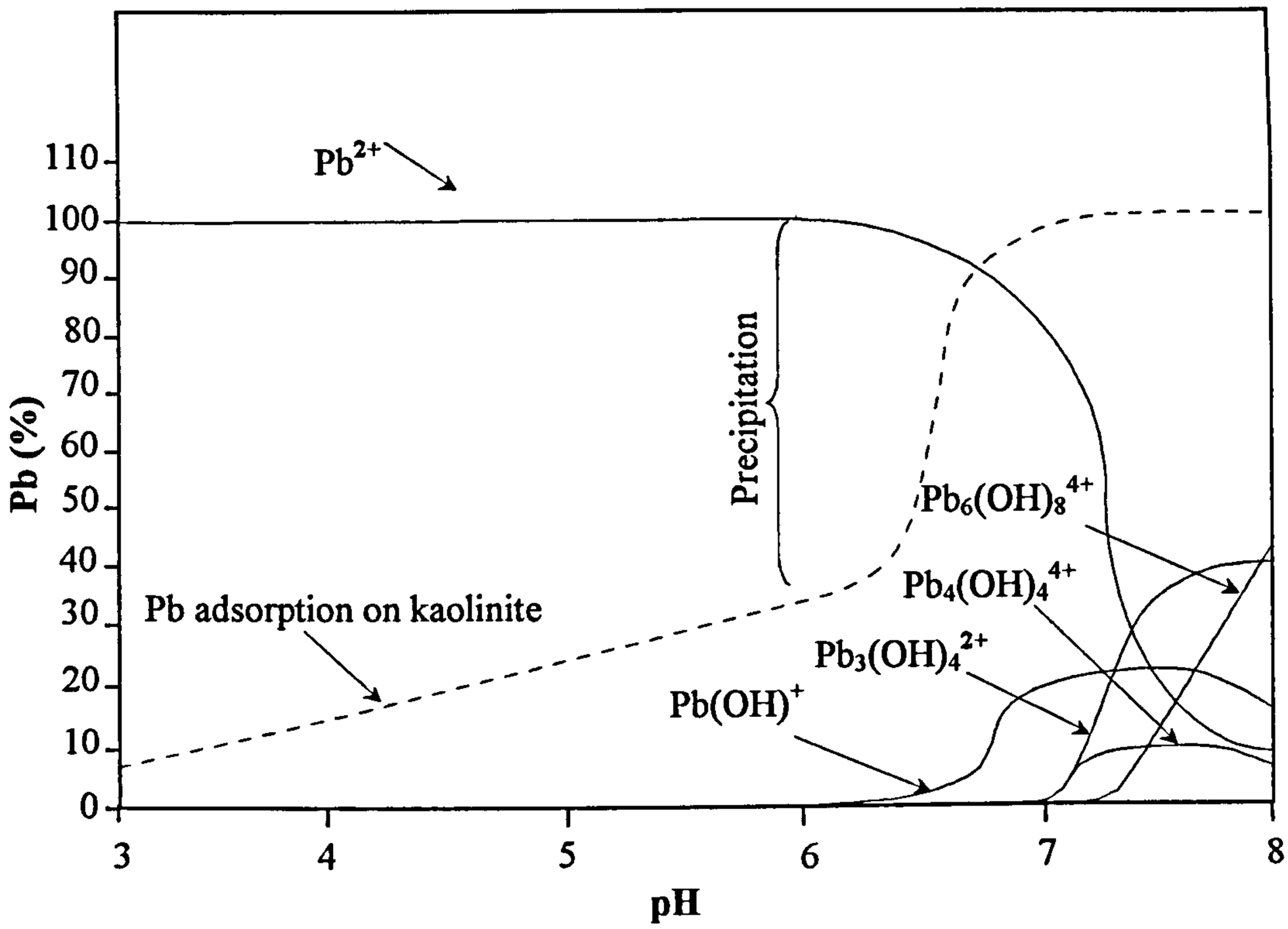

Figure 2.13 Distribution of Pb (II) species in 4×10^{-4}M $Pb(NO_3)_2$ and uptake by 0.1g kaolinite from 60ml of solution (Griffin & Shimp 1976).

An additional problem is the amphoteric nature of metals. This means that as the pH of a solution containing certain metals in solution rises from acidic pH 1 towards alkaline, between say pH 7-11, the metal precipitates due to its reduced solubility. At a higher pH, possibly pH 9 to pH 12, the metal solubility increases (MacKay & Emery, 1993). Cr and Pb are heavy metals that have amphoteric hydroxides and this behaviour is illustrated in Figure 2.14. Based upon Figure 2.14 and research undertaken by Wilk (1997) it would appear necessary that for precipitation to occur with optimum effect, the stabilising reagent should be added in such a proportion as to ensure the optimum pH. One limitation of this theory would be that if the pH is not high enough the solidification reactions would not be optimised and the pH of the material may fall rapidly due to leaching, potentially releasing the contaminant into solution. The theoretical solubility predicted by Figure 2.14 of one element in solution is also not likely occur since in the case of lime stabilisation, the porewater is likely to be highly saturated with Ca ions thus, due to

equilibrium, significantly reducing the likelihood that comparatively small quantities of contaminant would be released into solution.

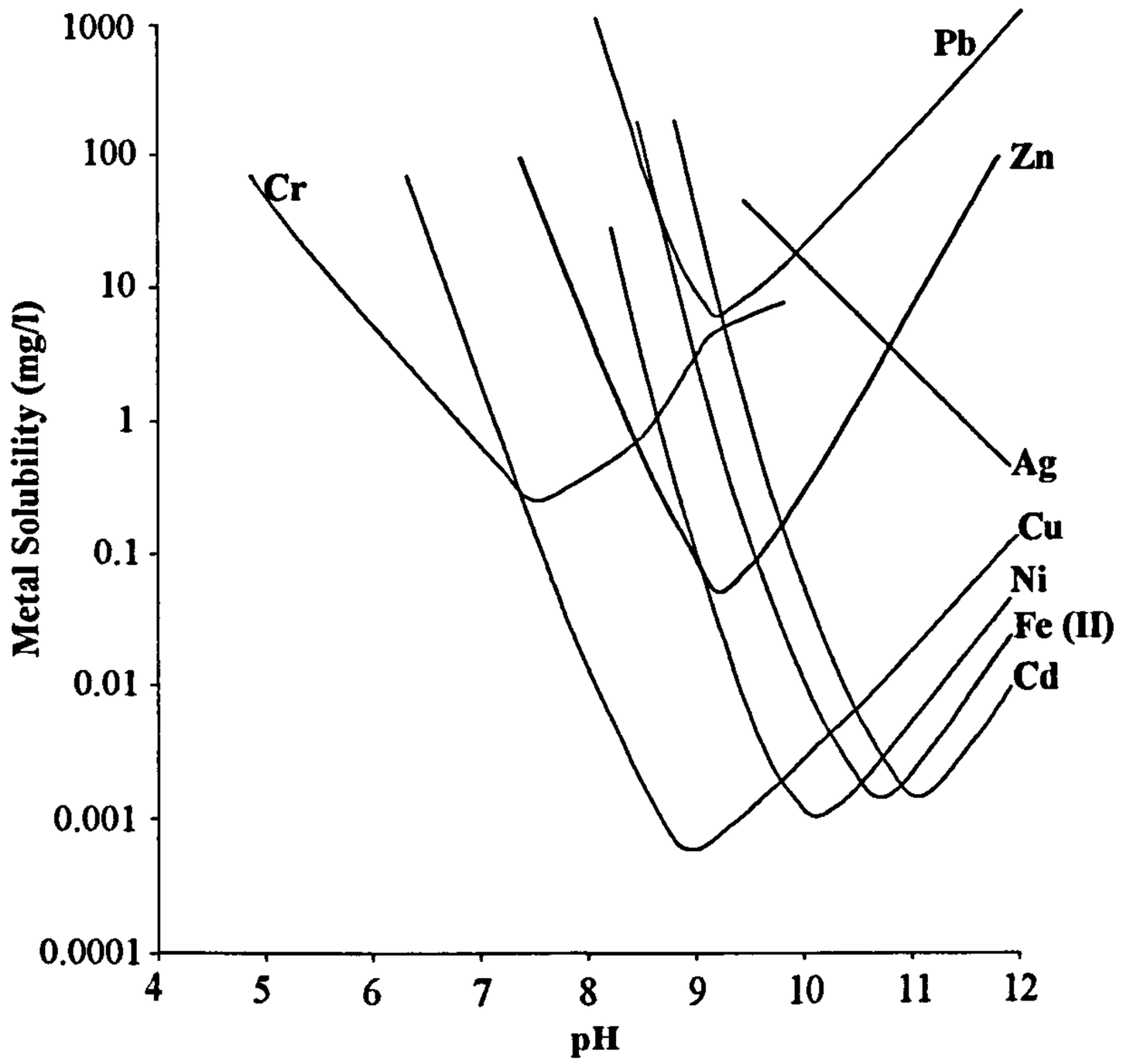

Figure 2.14 Theoretical solubilities of metal hydroxides as a function of pH (adapted from U.S. EPA, 1987 and Wilk, 1997)

The third means of improvement consequently produces the most important potential change in properties, since it provides a long-term stabilising process that acts subsequently to adsorption and metal precipitation. This reaction process is that of cementation via the clay-lime reactions described above. Dissolution of alumina and silica and subsequent crystallisation of calcium aluminate hydrate and calcium silicate hydrate gels produces a very strong and stiff, yet brittle, cemented structure. The principle of contaminant stabilisation, or fixation and encapsulation, is that contaminants become physically and chemically bound into the cemented structure. According to this principle the cemented structure of crystallised calcium silicates and calcium aluminates, which essentially binds the flocculated particles (containing the adsorbed ions) together, also incorporate the precipitated metals (held as an amorphous mass in the pore spaces between the flocs). It is unclear whether the

cementation reactions would be inhibited by the presence of the contaminant ions or metal precipitate in the soil structure, and in particular whether the gel crystallisation process would result in a continuous cemented structure being formed. This is because little published research directly concerning clay-lime-contaminant processes are available. However direct parallels have been researched in the form of cement stabilisation and lime-fly ash stabilisation of contaminated sludges (as have waste materials including cement kiln dust, waste lime tailings and clays from the manufacture of brick; see Stanczyk *et al,* 1982). Some of this research will now be presented in section 2.4.4 and 2.4.5.

2.4.4 Cement stabilisation

Betteker *et al* (1986) performed extensive research into the stabilisation/solidification of contaminated dredged material, including the addition of Type 1 Portland cement and two proprietary pozzolanic additives. The technologies were assessed for both physical and chemical stabilisation. The cement-based and pozzolanic-based additives were used to convert contaminated sediment into a solidified mass, in the manner discussed above. A polymer was added to determine its effect on the leaching of selected organic compounds, clearly different to the chemistry of inorganic fixation processes previously discussed. Physical stabilisation was assessed by measuring the changes in unconfined compressive strength, while leaching tests were used to evaluate the chemical stabilisation. Leachates were analysed for PAHs, PCBs, arsenic, zinc, cadmium and lead.

This research concluded that physical stabilisation of single contaminated dredged material is a viable option, but no single process formulation proved to be effective in providing chemical stabilisation for all contaminants as a group. Portland cement proved to be the most effective at treating arsenic, while more than half of the PCBs could not be detected in the leachate of Portland cement solidified sediment. Those PCBs that did leach were measured at less than one part per billion. Zinc, cadmium and lead were contained most effectively by the proprietary pozzolanic additive with no detectable concentrations of the metals in any of the leachates. The polymer additive was most effective at containing the PAHs, with more than half the PAHs being completely immobilised. Those PAHs that were not totally immobilised were found in concentrations four or five orders of magnitude lower in the leachates than in the untreated sediment. This indicates that some organic contaminants can be

treated by solidification processes as well as inorganic contaminants, and highlights the fact that every waste to be treated should be assessed independently to design the most appropriate stabilisation mix. Landreth (1982) carried out similar investigations, producing similar conclusions.

Cement stabilisation and solidification research was also carried out by Wilk (1997) on Pb, Cr, Cd, As and Hg. The chemistry of contaminated mature cement paste reactions was investigated by means of sequential batch leaching tests with 0.1M acetic acid as the leaching agent. The research concluded that the metal mobility as a function of pH was in general far less than would be predicted by the theoretical solubility of the corresponding metal hydroxides, particularly for lead. This was partially attributed to the incorporation of the metals into the cement hydration products, an idea reinforced by the fact that there appeared to be a correlation between increasing Pb leachability with increasing alumina leachability as well as a similar correlation between Cr and Si. Although this correlation was discussed for Pb and Cr none the other metals apparently had any correlation to Si and Al solubility. The researchers also suggested that combinations of the three metals were shown to be slightly better stabilised in a cement matrix than were the individual metals. It is a possibility that the reason there is a lower solubility in the batch tests than theory predicts and that this reduces further for addition of mixtures of elements is due to the effects of equilibrium conditions in the batch test and the effects of very high ionic concentrations of leachable Ca. Similar tests were carried on a dolomitic soil and a siliceous soil for comparison and it was determined that generally the metals were stabilised better in the dolomitic soil than in the siliceous soil due in part to pH effects. It is also possible although not mentioned in the report that organic humus improved attenuation, although no total organic carbon tests were reported to have been carried out.

Attempts were made by Wilk (1997) to improve the various mix designs by adding different types of cement with a degree of success as well as adding adsorption agents to attenuate the apparently troublesome lead due to its amphoteric nature and high solubility at high pH. The report states that this was very effective in 'certain' circumstances. The results of the various mixes are summarised in Table 2.16

Table 2.16 Qualitative guide for stabilisation of metals studied (Wilk, 1997)

Metal	Good	Better	Best
Pb	Type I cement	Type I cement with silica fume	Type V with silica fume and a little extra gypsum (ξ)
Cd	Cement with silica fume	Higher cement factor, no silica fume (ψ)	Still more cement for long-term durability
Cr	Portland cement	Portland cement with silica fume	Same, but with oxidation inhibitor to avoid hexavalent chromium
As	Portland cement with added $FeSO_4$	Portland cement with preoxidation of As to its highest oxidation state with H_2O_2 and added $FeSO_4$	Same, but with higher cement factor and higher Fe/As ratio
Hg	Portland cement	Higher cement factor	More cement to ensure strongly reduced porosity

Addition of most of the improvement agents appears to be sensible with logical effects with the exception of adding no silica fume (ψ) and a little extra gypsum (ξ). Firstly silica fume may be improving attenuation and solidification. Naturally with higher silica content and subsequent attenuation perhaps more calcium is required and generally more cement to retain a high pH to initiate solidification reactions. Figure 2.14 suggests the higher the pH and subsequently the cement content the higher solubility of Cd. Furthermore, there appears no reasonable reason for reduced performance on addition of silica fume especially as it appears to improve the behaviour of the metals in some of the other mixes. The addition of gypsum ($CaSO_4$) is also puzzling. The author acknowledges that this is intended to produce increased quantities of ettringite on hydration of the cement, and that apparently this, under 'certain' conditions, particularly at high pHs, suppressed metal leachability. Although the production of different hydration products is very important and possibly one of the reasons for improvement, the production of ettringite causes volume increases which may produce a material of lower density and perhaps higher

porosity, possibly resulting in a material more susceptible to leaching in the longer term. Alternatively perhaps the slower rate of crystallisation produces more cementitious 'gels' incorporating more Pb into the final crystalline structure. The question arises, why is this increased concentration of gypsum more successful for Pb and not required for the other metals? Perhaps the answer lies in the fact that at the higher pH most of the other metals have precipitated and remain retained as solids within the monolithic mass whereas more Pb is soluble at the high pH due to its higher amphoteric behaviour and must take part directly in the crystallisation reactions. This clearly requires more detailed investigation since its implications are potentially highly valuable.

2.4.5 Lime-fly ash stabilisation

By far the most widely researched pozzolana used in stabilisation processes has been fly ash. Weng & Huang (1994) investigated a specific fly ash with cement for treating industrial wastewaters. The chemical composition of the fly ash used was dominated by silicates (SiO_2, 44%) and aluminates (Al_2O_3, 31%), with smaller amounts of iron, calcium, magnesium, potassium and titanium oxides. The addition of cement created a high pH environment, thus resulting in the formation of calcium silicates and aluminates. As with the clay-lime reaction, this cementitious reaction bound the particles together producing a solidified matrix. Weng & Huang (1994) also stated that the high proportion of silica, alumina and iron oxide implied that the fly ash would be a good metal adsorbent, at least for Zn (II) and Cd (II). Although fly ash has a relatively low metal adsorption capacity relative to activated carbon, it can be obtained cheaply in large quantities and used as a neutralising agent in the treatment process due to its generally alkaline nature.

Landreth (1982) evaluated the containment efficiency and physical properties of four different stabilisation/solidification processes when applied to common industrial wastes. The four treatment processes included a patented lime fly ash additive. The chemical success of the treatments was monitored via column tests, whilst durability was assessed using compression, freeze-thaw, permeability and Atterberg Limit tests. Landreth (1982) stated that the lime-fly ash treatment achieved a variable degree of success, containing electroplating sludge to a relatively high degree but losing contaminants to a higher degree than the control columns for the untreated nickel-cadmium battery and glass-etching sludges. Some of these effects

could be predicted. If the principal fixation mechanism is adsorption, then generally at high pH cations are preferentially retained whereas at low pH anions are preferentially retained. Hence in the case of chlorine production sludge, it is no surprise that Cl^- and SO^-_4 ions are mobile at high pH. This prediction is possible assuming that they are not partially immobilised by retention or incorporation within the crystallising calcium silicates and aluminates. However in complex mixtures of pozzolanic material, organic and inorganic contaminants, the chemistry is not necessarily predictable due to complex chemical speciation and the potential for inhibitive effects on the crystallisation processes.

2.4.6 Stabilisation via sorption alone

Recent investigations as part of NATO/CCMS Pilot Studies (Smith, 1998) have researched the sorption and solidification of selected heavy metals and radionuclides onto unconventional sorbents. The goal of the pilot study was to develop cost-effective unconventional sorbents, preferably metallurgical waste solids. The removal capacities of heavy metals Cd, Pb, and Cu and radionuclides ^{137}Cs (half life 30 years) and ^{90}Sr (half life 28 years) and the sorption modelling of 'red muds' and fly ashes, products from the Bayer process for the manufacture of alumina, were studied. Metal uptake (sorption) and release (desorption) were investigated by batch experiments. The leaching solutions adopted for batch tests were distilled water, saturated aqueous carbonic acid (pH 4.75), and $H_2CO_3/NaHCO_3$ buffer solutions (pH 7.0) to simulate carbonated groundwater conditions. Red muds and especially fly ashes were shown to exhibit a high capacity for adsorption of heavy metals. The sorption sequence in accordance with the order of insolubility of the corresponding metal hydroxides was Cu>Pb>Cd. A statement was then made that the metals were held irreversibly and would not leach out into carbonic acid or bicarbonate-buffered solutions. This is a bold statement since although the metals may not be exchanged by hydrogen ions from a weak acid this does not mean that there would not be preferential sorption of another ion should it come into contact with the system. The report further states that bauxite wastes of alumina manufacture (red muds) are capable of removing the radionuclides ^{137}Cs and ^{90}Sr from water, but heat treatment is detrimental to the surface hydroxyl sites that are important for ion-exchange sorption of ^{90}Sr. It is argued that Caesium uptake is predominantly irreversible and dependent on the specific surface area of the sorbent. A rise in pH favours the exchange sorption

of Sr on the hydroxyl sites as would be expected by a metal on a pH sensitive hydroxyl site. The report, however, does not state how the predominantly irreversible nature of these sorption processes are measured.

Solidification of the red muds and fly ash was carried out by adding to them a mixture of cement, standard sand, and water. When metal-loaded solid waste was added (up to 20% by mass) to Portland cement-based formulations, the fixed metals did not leach out from the solidified blocks over extended periods with the exception of Cu^{2+}, which reached a concentration of 0.4mg/kg after 8 months in water of pH 8-9. In solid-waste concentrations below 20%, the compressive strengths and shear strengths of the doped concrete did not significantly differ from the control concrete suggesting that the presence of ions and precipitates did not interfere with the solidification reactions. However, it was highlighted that there is a critical weight percentage of 10-20% additives above which the strength declines dramatically.

2.4.7 Organophilic clay-reagent stabilisation and solidification processes

Recent investigations as part of other NATO/CCMS Pilot Studies (Smith, 1998) have also researched the sorption and solidification of selected organic chemicals. Conventional stabilisation and solidification methods based on purely cementitious and pozzolanic products have had limited success at treating soils contaminated with organic compounds. The 'Envirotreat' project involved developing a range of modified organophilic clays. Commercially available organophilic clays are typically made by the substitution of quaternary ammonium salts (NH_4^+) into smectite clay minerals (e.g. montmorillonite). The primary objective of the project was to modify the clays by substitution of the cations between clay layers to improve stabilisation of organic contaminants by:

- increasing the size of the interlamellar spacing within the clays to accommodate large molecules, such as PCBs and PAHs; to increase the effective surface area; and to increase the reactivity by introducing selected pillaring agents,
- optimising the polarity of the interlamellar environment to increase the absorption and adsorption of organic contaminants,
- providing a reactive environment on interlamellar clay surfaces to chemically bind contaminants permanently, and

- providing an active medium for effective treatment of heavy metals and other inorganics by cation exchange processes or interaction with pillaring molecules which can then be immobilised within the cementitious matrix following alkaline precipitation.

Laboratory trials developed a range of specific clays for treating specific non-polar organic contaminants. According to Smith, (1998) reporting on an 'Envirotreat' publication, the clay formulation used was Al^{3+} pillared and Fe^{3+} exchanged and then treated with benzyl quaternary ammonium salt. Due to commercial interests and prevent synthesis of the material this description is deliberately vague. However, the modified clay was produced as a suspension with a modified clay concentration of 20g/l. Prior to field trials the proportions of cement, fly ash and clay for the grout and the optimum grout : soil ratio was determined.

Field trials were carried out on a site occupied since the turn of the century by a variety of industrial operations, including a chemical waste 'quarantine store', chemistry laboratory, flammables store, battery bank, engine testing areas, underground storage tanks, and nucleonic laboratory. Site characterisation was very limited with specific PAH concentrations at 12mg/kg well below the current (1998) U.K. threshold value for residential development (50mg/kg for 16 U.S. EPA PAHs) and the 1000mg/kg for commercial developments. Maximum copper, lead, and zinc concentrations were 635, 3330 and 785mg/kg respectively. Likely other unconfirmed contaminants included flammable materials, solvents, concentrated sulphuric acid, oils, gasoline, and radioactive species. Grout was added to the $6m^2$ soil system to a depth of 2.5m using an auger producing 900mm diameter overlapping columns of soil mixed with reactive agents. Volume increase was reported as about 6.5%.

The effectiveness of the treatments were assessed based on :

- unconfined compressive strength (ASTM method),
- leachability using an aggressive acid leaching medium (U.S. EPA Toxicity Characteristic Leaching Procedure, TCLP), and
- Durability via freeze/thaw, wet/dry and permeability tests.

The results of testing cores taken at 44 and 57 days were judged 'satisfactory'. Unconfined compressive strength values exceeded the target value of 350kPa, which was particularly true for the mixes containing quicklime. The PAH concentrations in the leachates were all below 2µg/L. The desired target for the heavy metal concentrations were 50 times the U.K. drinking water values, however, the results for chromium, copper, lead and zinc were described only as satisfactory with no specific values reported. All samples failed the ASTM freeze-thaw test and only one sample satisfied the permeability criterion of less than 1×10^{-9}m/s, whilst this one exception was probably due to the presence of natural bentonite according to the report author. A more positive note was the fact that permeability values decreased with time as expected due to the continuing cement hydration processes.

Smith (1998) states that the largest weakness in the study was the fact that there were no control mixes not containing the modified clay. Thus, the possibility that a similar 'satisfactory' performance could have been achieved in the absence of the clay cannot be ruled out. The detailed leaching results for metals are not given in the reports, but it should be noted that the criteria applied 50 times the U.K. drinking water limits seems quite generous. Smith (1998) also states a calculation shows that the PAHs in the treated soil would be reduced to about 8.5mg/kg compared to 12mg/kg in the soil due to dilution by the other ingredients. The concentration of modified clay is about 500mg/kg. Given the low solubility of the PAHs, and the probable inefficient mixing, it seems unlikely the clay could have a profound effect on binding the PAHs.

Organophilic clay adsorption prior to stabilisation such as that demonstrated by the 'Envirotreat Process' clearly has potential but needs to be employed in better designed studies that are more likely to reveal the claimed benefits of the active ingredient.

2.4.8 The origin of hydrogen ions (acids) in soil

There are a large variety of potential sources of acids that can affect soil chemistry and stabilised soils in particular, some natural and some industrial. By natural processes, ammonium ions are produced in soils during the decomposition of plant residues and humus by micro-organisms (Hutchinson, 1980) as well as being added in large quantities as fertilisers. Some bacteria can oxidise ammonium ions to

form H^+ and NO_3^-. A variety of organic acids are also produced via direct release from organic residues (Dragun,1988). The addition of monocalcium phosphate fertiliser to agricultural soil also increases the acidity of a soil, since, the fertiliser reacts with water to produce dicalcium phosphate and phosphoric acid (Adams, 1984):

$$Ca(H_2PO_4)_2 \Rightarrow CaHPO_4 + H_3PO_4$$

Micro-organisms can break down plant residue and soil organic matter using reduced sulphur (S) or sulphate (SO_4^{2-}) from the soil system. These sources of sulphur are then oxidised by bacteria aerobically which is inevitably accompanied by the release of two H^+ ions (acid) for every oxidised S atom:

$$H_2S + 2O_2 \Rightarrow 2H^+ + SO_4^{2-}$$

$$S + 1.5O_2 + H_2O \Rightarrow 2H^+ + SO_4^{2-}$$

Dragun (1988) suggests that if plant uptake of SO_4^{2-} is occurring with plant release of OH^-, then no change in soil acidity will occur. However, if the release of OH^- is slow then SO_4^{2-} may accumulate resulting in increased acidity because the plants are not releasing OH^- to neutralise the generated H^+. CO_2 in soil water also affects acidity. When dissolved in water CO_2 reacts to form the weak acid H_2CO_3. Pure water in equilibrium with atmospheric CO_2 (0.03%) has a pH of around 5.6, mildly acidic. However, the activity of micro-organisms and subsequent aerobic biodegradation of soil organic material results in the production of CO_2 which in topsoils could result in soil air concentrations of CO_2 exceeding 1% with a pH of perhaps 4.9. This is illustrated in Figure 2.15

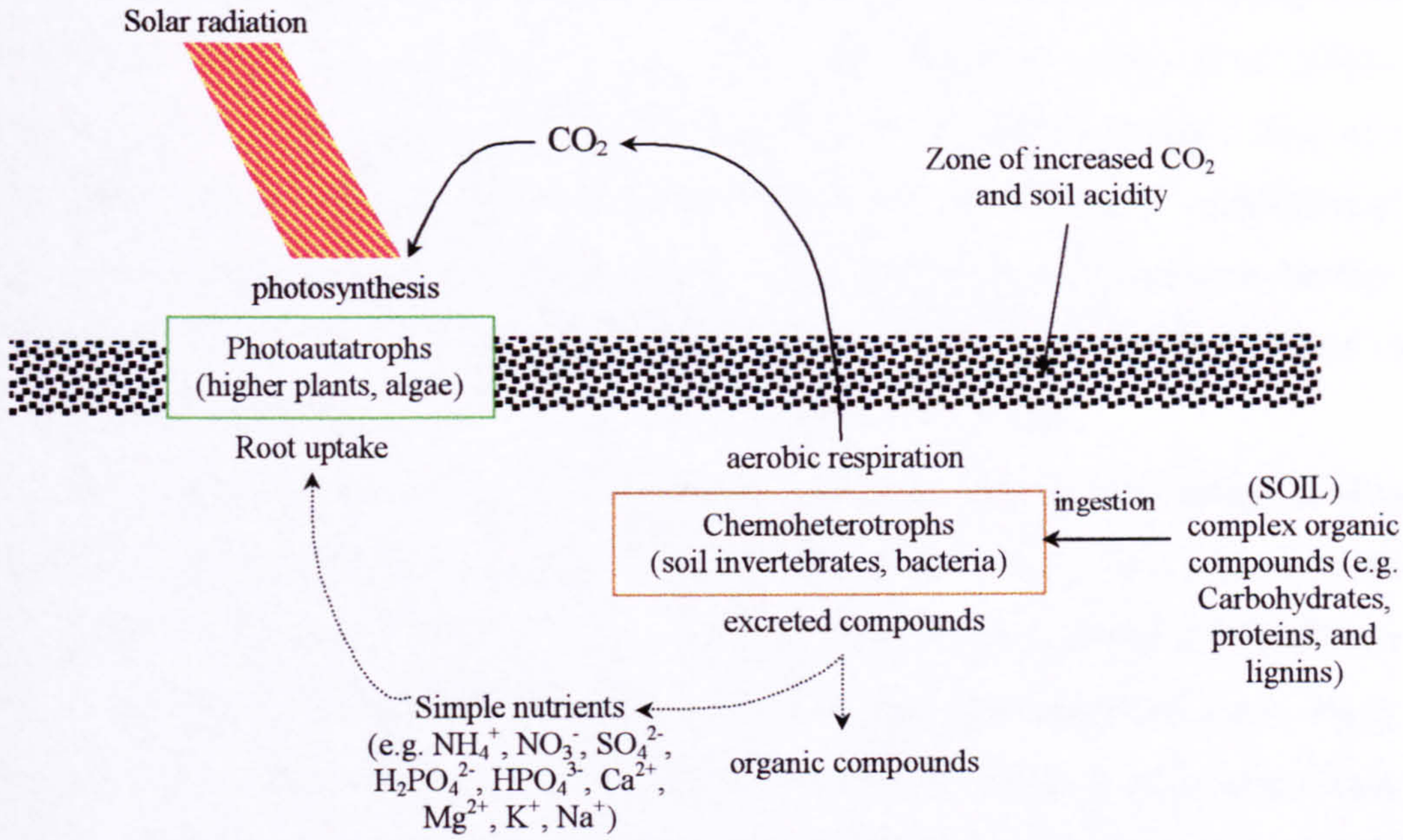

Figure 2.15 Relationships between soil chemoheterotrophs (decomposers) and photoautotrophs (plants) in the soil-plant ecosystem (adapted from Ross, 1989)

It is also known that the oxidation of pyrite (FeS_2) in mine spoils, drained tideland soils, estuarine muds affects soil pH. Oxidation of pyrite forms sulphuric acid:

$$2FeS_2 + 7H_2O + 7.5O_2 \Leftrightarrow 4H_2SO_4 + 2Fe(OH)_3$$

Mine spoils contain large amounts of pyrite and consequently pH values can be as low as 2.

A well publicised source of acidity to soil is from acid rain, snow, hail etc. Nitric oxide, sulphur dioxide and nitrogen dioxide are all responsible for formation of acidic compounds in rain water and can have a pH as low as 4.

Frink *et al* (1977) states that in the North-eastern U.S. where acid deposition is high, agricultural practice usually necessitates the addition of a few thousand pounds of limestone per acre to neutralise acidity generated by a combination of natural processes and fertiliser amendments.

Acidity neutralisation has an important role in the remediation of many sites including the Gulf Coast Lead (GCL) site in Tampa, Florida (Furman *et al*, 1985). Works at this facility involved the recovery of Pb from acid batteries. Soil and groundwater contamination resulted from the percolation of acid metal contaminated wash waters from an unlined surface pond. A subsurface acid reaction barrier, consisting of a deep trench filled with crushed limestone and oyster shells was laid to intercept and neutralise acid groundwater that migrated off the site.

Ravenfield Tip site in South Yorkshire, England also incorporated acidity neutralisation as part of a remediation strategy (Khan *et al*, 1980). This site regarded as the United Kingdoms 'Love Canal', was comprised of a group of sandstone quarries which were utilised for the disposal of acid tars, contaminated earth, slags, chromium waste, fluoride waste, nickel waste, phenolic waste and other chemicals. Waste was excavated then mixed with quicklime at ratio ranging from 1:4 to 1:10 depending on the degree of acidity, deposited, covered with 15cm to 23cm of limestone chips and subsequently covered with subsoil and soil.

Controlling acidity is an important aspect of lime based stabilisation and solidification technologies.

2.5 METHODS OF REAGENT APPLICATION

2.5.1 Ex-situ methods of application

The practical applicability of a treatment is frequently dependent on site conditions, plant access conditions and the final placement method adopted for the treated waste. Hence, with regard to stabilisation and solidification methods in-situ and ex-situ application can be considered.

Ex-situ stabilisation and solidification methods are generally applied in three ways: plant processing methods, direct mixing methods and drum processing methods.

2.5.1.1 Plant processing methods

Plant processing methods involve excavation with subsequent addition of reactive agents via a plant specifically designed for the process or adapted from concrete batching and mixing plants. Boardman & MacLean (1996) describe such a method currently used in the U.K. whilst Stanczyk *et al* (1982) illustrate how

solidification and stabilisation processes can be appropriate for rapid treatment of hazardous chemicals and in particular waste spills. Figure 2.16 illustrates a specially designed plant being used in the U.K. to add lime to sewage sludge cakes whilst Figure 2.17 depicts an adapted version of this plant being used to treat dredged contaminated canal sediment with lime. Stabilisation/solidification of contaminated dredged material is discussed in some detail by Betteker *et al* (1986).

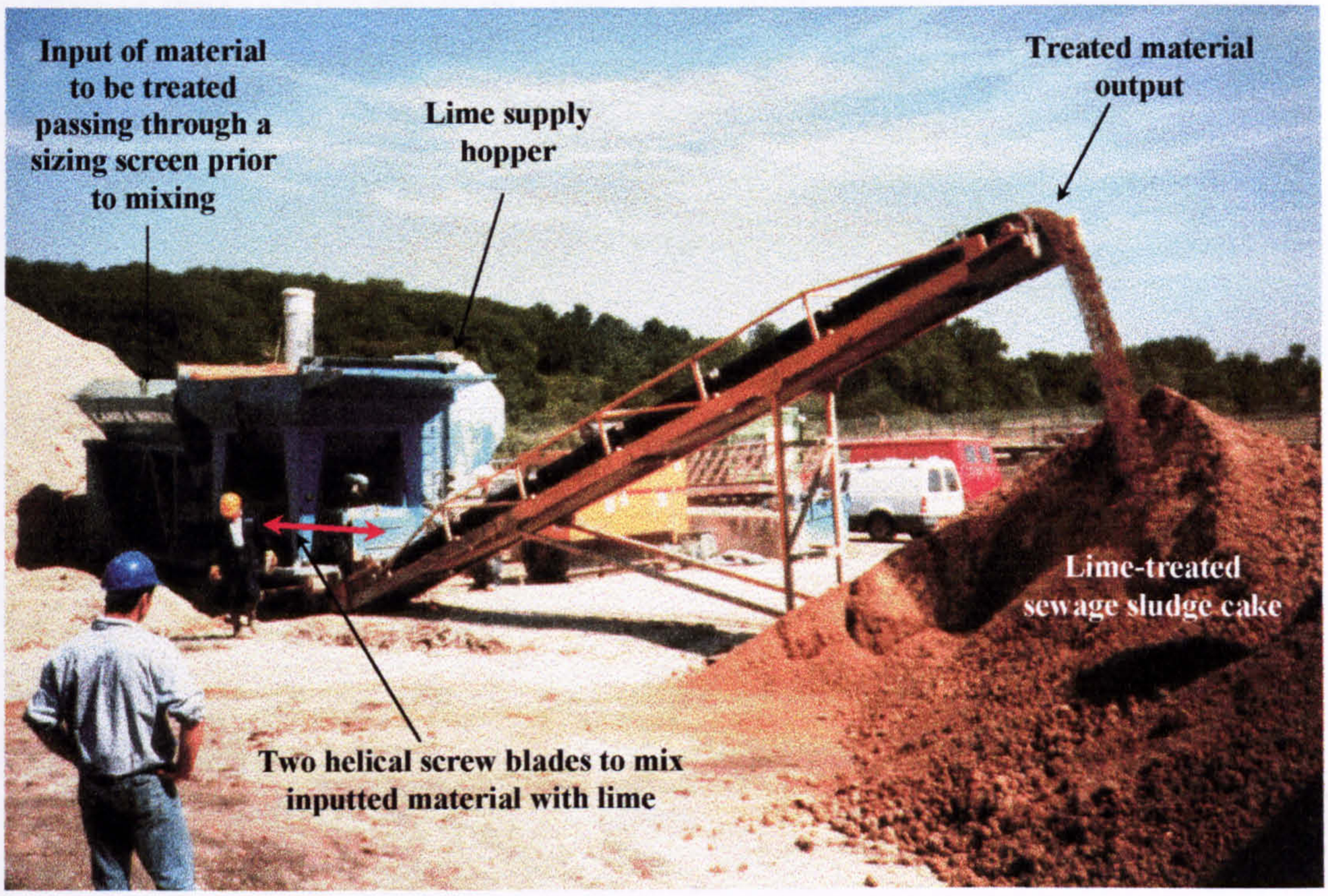

Figure 2.16 Mobile lime treatment mixing plant in the U.K. (after Boardman & Maclean, 1996)

2.5.1.2 Direct mixing methods

Direct mixing methods require excavation of the contaminated material, transportation to a designated area of the site, placement of the material in layers and subsequent mixing of reactive agents using mechanical plant. This method is particularly useful for treating waste in lagoons.

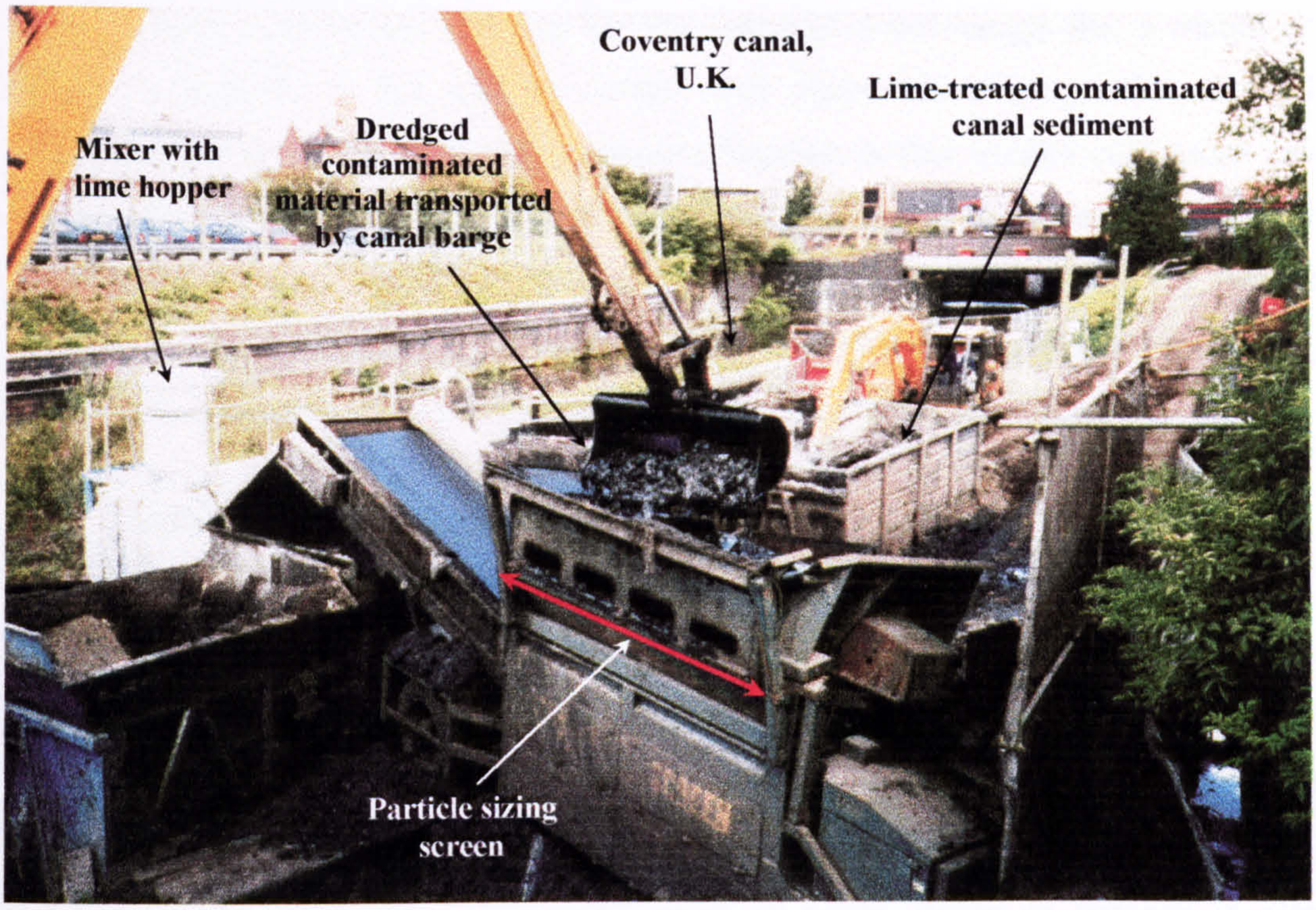

Figure 2.17 Mobile lime treatment of contaminated canal sediment in the U.K.

2.5.1.3 Drum processing methods

Drum processing methods involve the placement of the contaminated material in drums where it is mixed with the reactive agent and allowed to set. The material and the drum are subsequently co-disposed.

Relative to the other methods plant processing has considerable advantages because it ensures adequate mixing of contaminated material and reactive agent. There are three key steps utilised during plant processing:

- pre-treatment to homogenise, grade or dewater the material as well as perhaps a soil washing process to concentrate contaminants,
- mixing the wastes with reactive ingredients to create a pumpable slurry or a material compatible with standard earth moving machinery, and
- placement and curing.

Curing of pumpable material has the potential disadvantage that a mould or lagoon is required. It also ensures contact with water where compaction of solid material may not. When material is placed in lagoons in this fashion cold joints can occur which are areas of weakness where water can access with the potential for mobilisation of contaminants. Apart from traditional disposal routes for treated materials, there are reported cases such as, Emery (1980) and MacKay *et al* (1993), where treated material has been used successfully as a construction base.

2.5.2 In-situ methods of application

2.5.2.1 Surface clay-reagent mixing

The usual procedure for surface clay-lime mixing and other cementitious reagents involves spreading the reagent onto the surface and mixing to a depth of 200-400mm using a purpose-built rotavator or standard excavation equipment. This approach is often used to stabilise road foundations and is illustrated by Smith (1996). Application of stabilisation and solidification to waste stored in lagoons is also typically performed using conventional construction equipment, such as backhoe excavators and draglines. Effective mixing is very difficult to achieve. The primary purpose of these operations is usually to improve the physical characteristics of the material (U.S.EPA, 1990-A). Slurry spreading onto the surface of a material to be treated is less successful due to its propensity to flow, and thus achieves a non-uniform distribution. With respect to lime treatment it was traditional practice to allow the clay-lime mix to stand for a period of typically 24 h, either in a stockpile or for single layer treatment *in situ*, in order that complete lime distribution could occur. This process, known as mellowing, was considered vital for full modification of the clay minerals. Current thinking, however, suggests that immediate water content adjustment (where necessary) and compaction is more beneficial in achieving a long-term strength gain (Holt & Freer-Hewish, 1996). Glendinning *et al* (1998) also suggested that the compaction of the clay-lime mix is important to achieve the intimacy of contact of the modified clay particles necessary for the full benefits of the reaction to be achieved. In addition a minimum air void content should be aimed for since this will again aid the reaction process. For these reasons the water content should be slightly higher than the optimum water content determined for the clay-lime mix and an appropriate level of compaction should be applied to achieve a dry density close to the maximum achievable. Figure 2.18 highlights the water content – dry

density relationships for eight soils (Table 2.17) compacted according to the standard Proctor method.

Table 2.17 Key to soil properties for Figure 2.18

No.	Description	Sand	Silt	Clay	Liquid Limit	Plasticity Index
1	Well-graded loamy sand	88	10	2	16	---
2	Well-graded sandy loam	72	15	13	16	---
3	Med-graded sandy loam	73	9	18	22	4
4	Lean sandy silty clay	32	33	35	28	9
5	Lean silty clay	5	64	31	36	15
6	Loessial silt	5	85	10	26	2
7	Heavy clay	6	22	72	67	40
8	Poorly graded sand	94	---6---		---	---

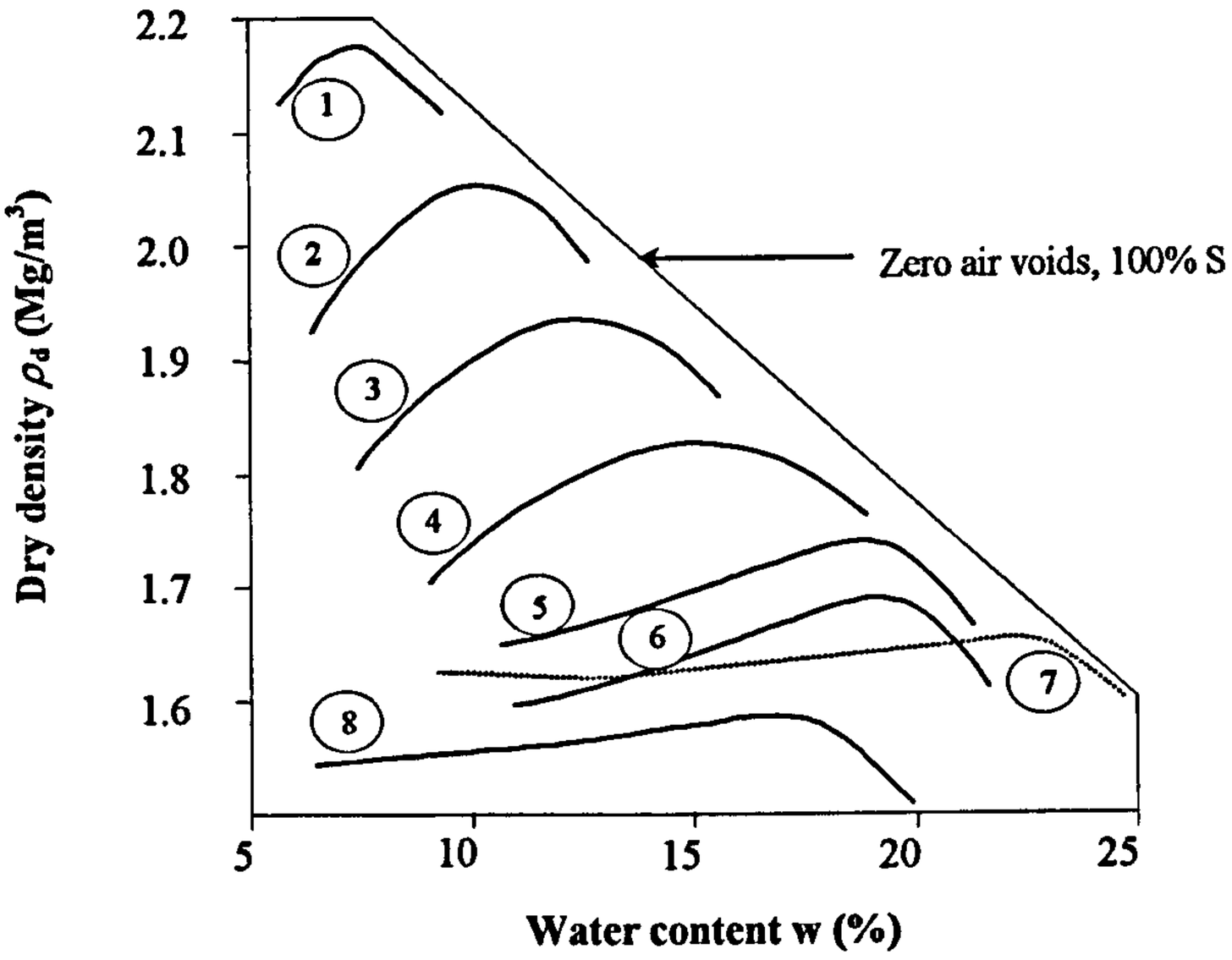

Figure 2.18 Water content-dry density relationships for eight soils compacted according to the standard Proctor method (after Johnson and Sallberg, 1960)

Glendinning *et al* (1998) state that immediate compaction would undoubtedly be beneficial for contaminated soil treatment, as long as thorough mixing is possible, since the pozzolanic reaction bonds that form at an early stage would assist with contaminant retention and minimise the flow of water through the stabilised material.

2.5.2.2 Deep clay-reagent mixing

An alternative treatment *in situ* for deep deposits is to form reagent columns, which are cylindrical columns of stabilising reagent mixed with clay typically 0.5-1.0m in diameter. The technique for lime columns was developed in Sweden (Broms & Boman, 1976) for stiffening and strengthening soft, wet clayey soils. A lime content of typically 10% is used, the lime being incorporated through the stem of an auger that is first driven into the ground to an appropriate depth. The rotation of the auger is reversed as the lime is fed into the soil, causing mixing and a degree of compaction. Such a technique could provide a suitable containment measure if continuous lime columns were constructed around the edge of a contaminated mass, such as a dredge tip. Care would be needed in design to ensure intimate mixing, as high a compacted density and thus as low a permeability as possible in the constructed columns. Indeed the technique could be used to create an underlying clay-reagent blanket *in situ* by constructing a series of continuous piles over the whole site, but only feeding reagent into perhaps the lowermost one metre of the internal columns. Construction of a surface clay-reagent layer would complete the barrier, although such a layer would need to be designed to cope with significant settlements. This technique was used extensively by the company Bachy Environmental on behalf of ICI Explosives in the winter and spring of 1994-1995. The technique is illustrated in Figure 2.19. The site was situated on a peninsula on the Southwest coast of Scotland 30 miles south west of Glasgow, England. The site was formally a landfill and was the repository for most of the waste from the chemical manufacturing operations on the site for 40 years. Records of the site combined with a site investigation confirmed that areas of the landfill contained waste of a low pH including, high ammonium and a host of heavy metals to a depth of 5 meters. The site was remediated due to the migration of contaminant in the groundwater towards environmentally sensitive areas. Much of the contamination from the manufacture of silicone was described as "friable to crystalline or slightly 'rubbery' grey/white silicone gel with dilute hydrochloric acid". Laboratory trials were performed using the 'Colmix process' which was a slurry mixture incorporating cement, PFA and lime. After small-scale field trials samples of treated waste were sampled by redrilling and by casting samples in the laboratory. These samples were subjected to permeability tests, acid neutralisation capacity tests, strength tests and leachability tests. The results highlighted the acceptably high pH nature of the final product which would reduce the solubility of

metals whilst also producing a material with a permeability less than 1×10^{-7} m/s and strength of greater than 100kPa and 200kPa after 7 and 28 days respectively. Based on this information the full-scale works were undertaken. In total using a specially designed auger to inject the slurry and compact the material 2,407 columns with a cross sectional area of $0.765m^2$ were produced to a depth of 5m. Assessment of the in-situ strength created by the works was performed by in-situ dynamic penetration tests and confirmation of the success of the treatment was to be assessed by resampling the site 12months after treatment. It is evident from Bachy (1995) that although the initial site investigation was very thorough the monitoring of the development of the treated site was not. One clear argument is that there are not any recommended tests specifically for stabilisation and solidification processes, so what should be measured is difficult to assess? Clearly the investigators did assess the main controlling factors of pH, permeability and strength, however, although adding to expense more frequent monitoring of these variables *in situ* would have been appropriate. It is difficult to criticise the process because the precise details of the site and all the works performed were not available at this time. However, it is clear that the development of sites such as this are essential to develop understanding and allow further implementation of the technology in other environments.

International Waste Technologies and Geo Con, Inc. have developed a similar in-ground mixing method in the U.S.. The process was evaluated under the U.S. EPA Superfund Innovative Technology Evaluation (SITE) Program in 1988 (U.S.EPA, 1990-B). Other in-situ stabilisation/solidification processes are under development and scheduled for demonstration under the SITE program (U.S.EPA,1992-A, U.S.EPA, 1992-B). An established ground improvement (solidification) technique incorporating jet grouting also has potential for application. Barry (1982) examined this concept in a report for the U.K. Department of the Environment where two significant disadvantages were identified:

- Even permeation of the treatment agent into the ground was difficult to ensure, and
- Due to the need for sufficient overburden pressure to withstand the injection pressures required, treatment depth was limited to in excess of 2m. However, it was highlighted that temporary surcharging may overcome this limitation.

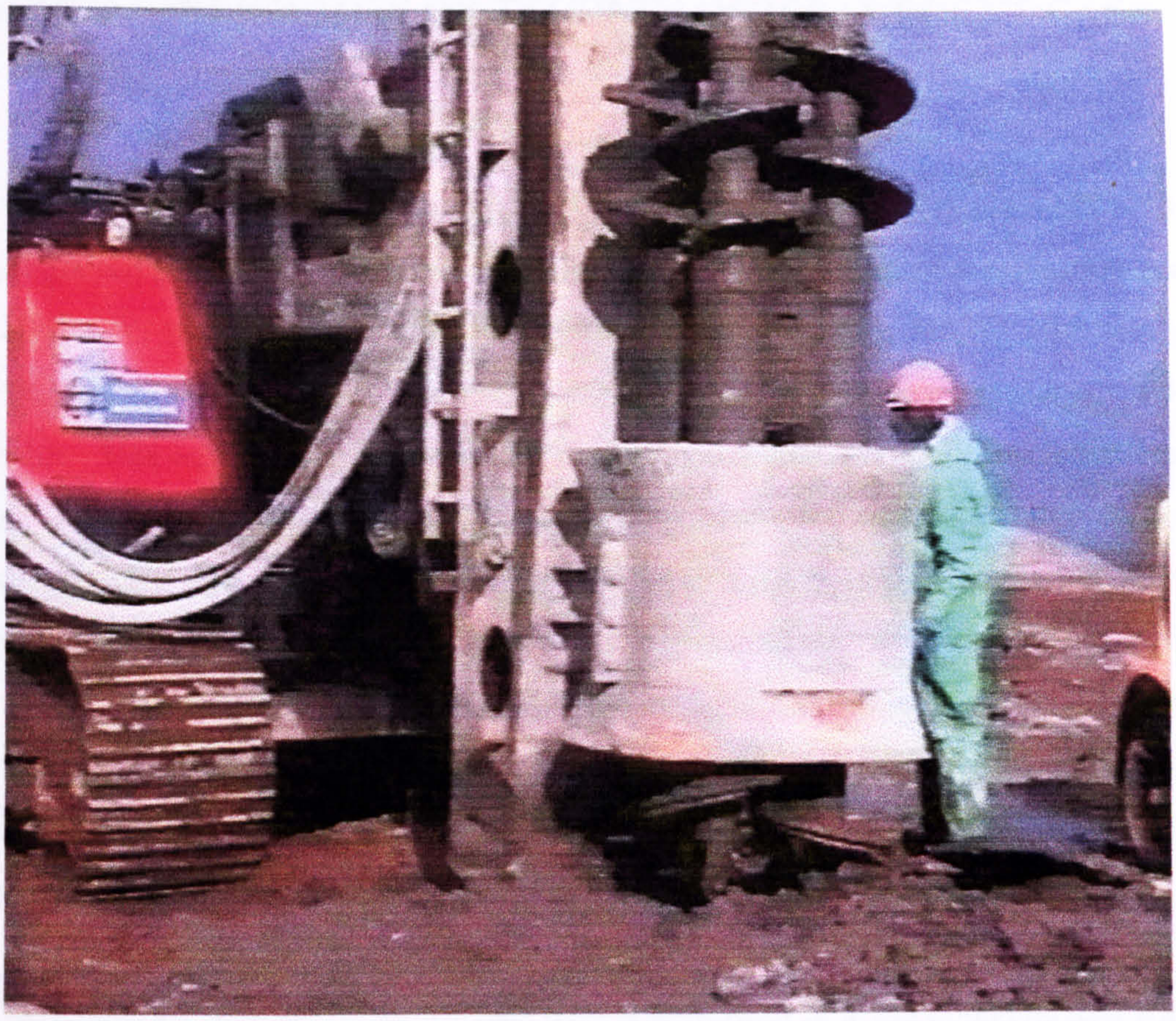

Figure 2.19 Deep clay-reagent mixing (From Bachy Environmental advertisement video of ICI Explosives site remediation project, 1995)

A variation of this technique Soilcrete® Jet Grouting is described by Smith (1998). During this process, soil is loosened by the high pressure action of water, often sheafed in a cone of air (jet-cutting). The loosened soil is partially removed to the surface via air-lift pressure as the remaining soil is simultaneously mixed with cementitious or cement/bentonite grout. Columns can be made to overlap, thus treating all of the soil. The columns have diameters of 0.5-1.8m, depending on soil type. Compressive strengths of up to 10MPa can be achieved in granular soils and 5MPa can be achieved in cohesive soils. It is suggested that some binding of inorganic contaminants can be expected and that permeabilities in the range of 1×10^{-6} to 1×10^{-9}m/s can be achieved. A variation of the jet-cutting process, in which the soil is displaced by clean material introduced at the base of the hole, has been applied to permit ex situ treatment of the displaced soil.

2.6 SITE APPLICATION OF TECHNOLOGIES / RECENT CASE STUDIES

Recent large scale case studies by NATO and reported by Hinsenveld (1993) highlight the difficulties in reviewing the limited number of applied stabilisation and solidification technologies in the field. Even on the scale of a NATO pilot study, results lacked the detailed information required to critically compare one method to another. This was not helped by the fact that many manufacturers of propriety mixes keep details of their additives out of the public domain for reasons of commercial confidentiality. The cases within the NATO/CCMS Pilot Study all applied cement, pozzolanic material or lime stabilisation and solidification agents. The sites available to the researchers were large with metal and organic contamination providing the ideal opportunity to test the viability of stabilisation and solidification technologies. Table 2.18 summarises the site-specific details for each of the three processes reviewed. The studies reviewed were :

- EIF Ecology, France. In-situ surface lime stabilisation of a site contaminated with a variety of hydrocarbons and heavy metals.
- TREDI, France, using the Prefix process (specific reagent unknown) to stabilise a former industrial disposal site contaminated mainly with chromium, sulphates and sulphides.
- Hazcon, presently IM-Tech, United States, applying *ex-situ* treatment with Portland cement to a site containing large amounts of organic components. It is a propriety process using a patented non-toxic chemical called Chloranan (U.S.EPA, 1989-B). Chloranan is claimed to neutralise the inhibiting effects that organic contaminants have on the hydration of cement-based materials.

Table 2.18 Site details of the NATO/CCMS case studies (adapted from Hinsenveld, 1993)

Process/technique *Manufacturer*	*Lime stabilisation* *EIF-Ecology*	*Petrifix* *TREDI*	*Portland cement* *Hazcon (presently IM-Tech)*
Country	**France**	**France**	**United States**
City	**Site A: Marais de Ponteau-Lavera (near Marseille)** **Site B: Bourron Marlotte**	**Site C: Nesle-Somme** **Site D: Bellay-Aln**	**Douglassville, PA**
Area(m^2)	**Site B: 4,200**	----	**Total of five areas in the site: 200,000**
Depth (m)	**Site B: 6-7**	**Site C: 5** **Site D: 2.5**	**Unknown**
Amount of soil to be treated	**Site A: 22,000m^3** **Site B: 22,680 tonnes**	**Site C: 6,804 tonnes** **Site D: 8,165 tonnes**	**200,000m^3**
Source	**Site A: Industrial residues of the Levere petrochemical plant (sludges and sediments)** **Site B: Industrial residues from an old refinery (mainly acid tars and filtration residues)**	**Site C: Industrial residues** **Site D: Sludges from tannery plant wastewater treatment**	**Oil recycling facility, with wastewater sludge, recycled oil and filtercake**
Type of soil	**Site A: Not known** **Site B: Top layer-light viscous material; middle layer-aqueous liquid; bottom layer-sticky material (composition unknown)**	**Site C: Black-coloured sludges and silty material** **Site D: Not known**	**Five different wastes: Site A: Oily sludge from wastewater treatment** **Site B: Oily filtercake** **Site C: Oil and oily water** **Site D: Sludge (landfarming area)** **Site E: Plant processing areas**
Type and concentrations of contaminants	**Site A: Not known** **Site B: Not known**	**Site C: Concentrations in leachate: COD up to 450 mg/l; iron up to 47mg/l; ammonia up to 80mg/l; traces of copper and zinc (concentrations in material itself unknown)** **Site D: Chromium 8,700mg/kg; sulphide 475mg/kg; sulphates 500mg/kg; nitrogen 350,000mg/kg (35%)**	**Lead 3,000-22,000mg/kg (0.3-2.2%); oil and grease 10,000-250000mg/kg (1-25%); VOCs 0-150mg/kg; semivolatile organics 12-530mg/kg; PCBs 1.2-54mg/kg; pH 2.6-7.0**
Main lesson learned	**Absence of data concerning the original waste characteristics and concentrations makes evaluation and technology transfer impossible.**		**Leachate characteristics of treated material alone are not sufficient for a good evaluation; leachate quality from both treated and untreated waste was identical. The raw material feed system and the blender may be critical in the process**

2.6.1 Evaluation of operations

Site A, Marias De Ponteau-Lavera 50km west of Marseille is an old salt marsh by the coast in which was dumped residues from the lava petro-chemical plant for 15 years between 1955 and 1974. The activities on this site were described by the Agence Nationale pour la Recuperation et l'Elimination des Dechets (ANRED), (1988). An initial assessment of the of the quantities and nature of the waste to be treated on the site led to trials of the following disposal possibilities:

- Incineration in an industrial waste incinerator,
- Recycling as feed stock in a cement factory,
- Incineration in a thermal power plant, and
- Recycling in an oil refinery.

These approaches were deemed unsuccessful due to the heterogeneity of the material. Consequently a stabilisation and solidification operation was carried out in 1978. A patented solidification process was adopted based mainly on the use of lime as the reactive agent. The method of agent addition was not specified, however, from the date of treatment it was likely that there would be no specialised mixing equipment. Treated samples were taken via the excavation of a number of trenches and samples removed from 3 horizons described as the surface treated zone, mid-treated zone and below treated zone. The report was not clear about the depth or year of excavation, however, a backhoe excavator was required and the report implies that excavation was immediately after treatment. No characterisation of the levels of contaminants prior to treatment was reported.

Site B, Bourron Marlotte was an ancient sandpit on the edge of the forest of Fountainebleau near Paris that had been used as a dumping site until 1971 by an old refinery. The site was remediated in 1985 using the EFI Ecologie stabilisation process. No information was provided about the method of addition of the stabilisation reagent or indeed the year when samples were recovered for testing. Treated samples were recovered in the same manner as site A. A significant observation during excavation was the sandy soil under the treated zone appeared to be still contaminated with untreated tar. Limited characterisation of the levels of contaminants prior to treatment is reported in Table 2.19. Although not mentioned in

the report (ANRED, 1988), the levels of sulphates and chemical oxygen demand (COD) shown in Table 2.19 could suggest that the site was undergoing natural attenuation via anaerobic digestion of the organic pollution by bacteria. The site may not have required stabilisation if the dispersion of contamination was at a similar rate to degradation.

Table 2.19 INSA test results of untreated material from Site B-Bourron Marlotte (ANRED, 1988)

Measurement	Upper layer	Middle layer	Bottom layer
pH	3.5	2.05	2.10
Resistivity (units unknown)	7,900	232	232
COD (mg/kg)	4,800	1,960	52,000
Sulphates (mg/kg)	260	1,829	41,220
Hydrocarbons (mg/kg)	15	20	< 0.1

Site C, Nesle-Somme near Paris was an industrial waste dump in silty material overlying a chalky aquifer which was subsequently contaminated with nitrogen compounds and metals. The site was discovered during the first national inventory of hazardous dumps carried out in 1978. The waste consisted mainly of black coloured sludges and silty material. Analysis of leachates indicated COD up to 450mg/l, iron up to 47mg/l, ammonia up to 80mg/l and traces of copper and zinc. In 1980 the site was stabilised by TREDI using the Petrifix prior to site development in 1985. Again details of the year of sampling were not given. For testing and evaluation purposes, two samples were removed from 0-1.5m (humus soil) and a third at about 4m where the treated material was black and crumbly with a strong smell of organics and ammonia.

Site D, Bellay-Ain near Lyon was a number of wastewater disposal lagoons for a tanning factory. Once these lagoons reached capacity in 1980 the local authority insisted the sludge was pre-treated prior to disposal since it contained 8,700mg/kg (8.7%) chromium, 475mg/kg sulphides, 500mg/kg sulphates and 0.35% nitrogen. Treatment took place in 1982 again by TREDI using the Petrifix process. The treated sludge was disposed at a low swampy area with lush vegetation. Excavation of the

swampy site revealed a humus soil layer 0.80m deep followed by approximately 1.20m of treated material under which some material appeared untreated to a depth of approximately 2.5m where original soil was found. Suprisingly two samples were taken from the upper layer with only one taken from the treated material with no other samples taken from the apparently untreated layer.

Treated material from the four sites was subjected to limited physical and chemical analysis. A single set of physical tests to determine permeability and unconfined compressive strength were carried out on the material at the mid depth of excavation. The results of these physical tests are summarised in Table 2.20

Table 2.20 Physical characteristics of treated material from the French sites (adapted from ANRED, 1988)

Sample (Middle layer of excavation)	**Permeability (m/s)**	**Unconfined compressive strength (kg/cm^2)**
Site A	7.9×10^{-6}	4.7
Site B	1.2×10^{-5}	3.8
Site C	3.4×10^{-8}	1.1
Site D	---	1.0

Chemical testing was based around two French leaching tests. One test called the INSA test was designed for testing waste material to assess the appropriateness for disposal of the waste in special industrial waste landfills. The main features of the INSA test are:

- extraction liquid – demineralised water saturated with CO_2 and air ($pH \approx 5$),
- tested material crushed into particle sizes < 4mm,
- 100g of material mixed with 1 litre of extraction fluid,
- waste material and extraction fluid agitated for 16 hours then analysed, and
- a second extraction on the same material was carried out.

The second leaching test called the oedometric pressure-leaching test was based on the use of a pressure permeater. This test developed by the French is

described by ANRED (1988) and apparently takes into account the specific characteristics of solidification techniques. Figure 2.20 shows a cross section of the apparatus.

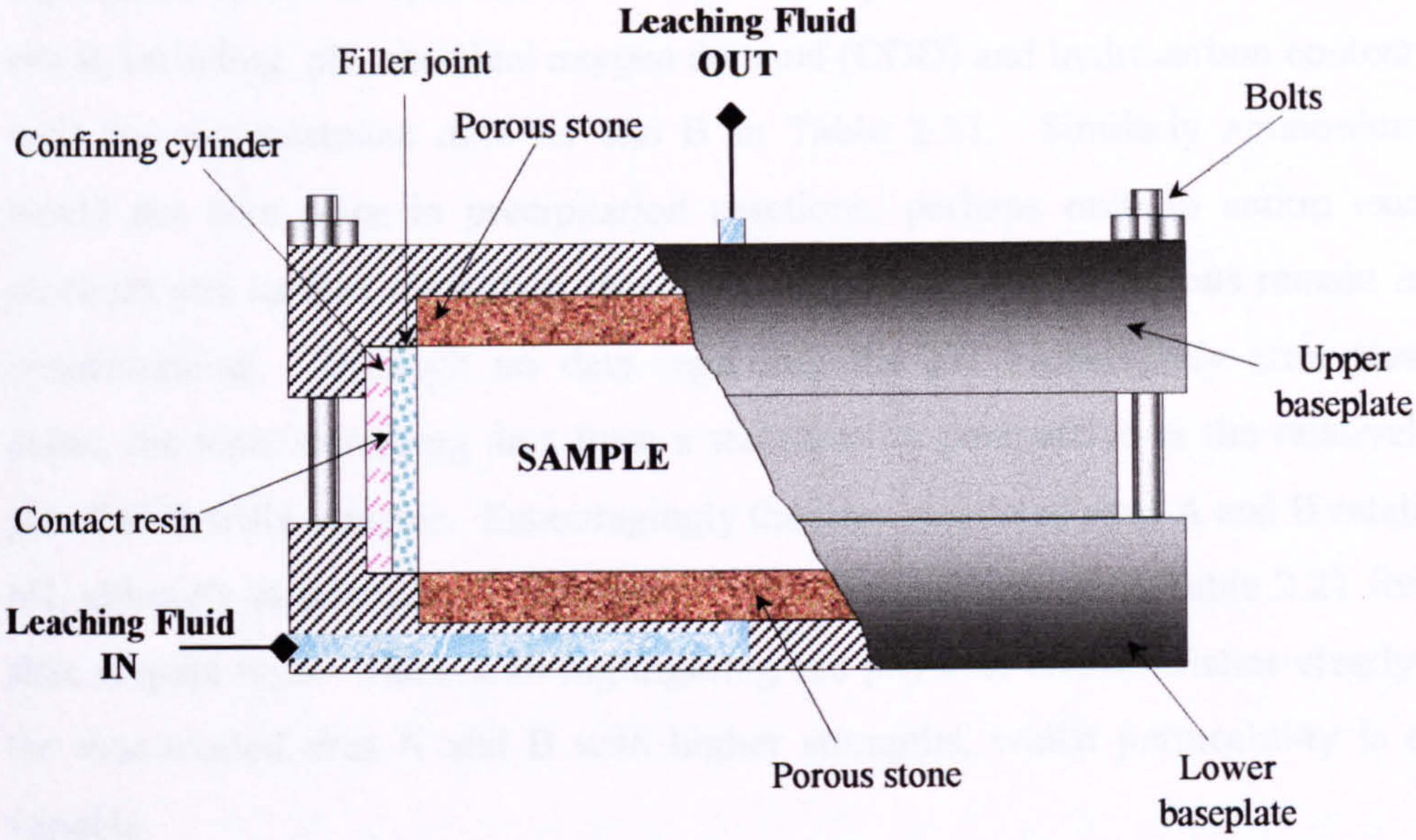

Figure 2.20 Oedometric pressure leaching apparatus (adapted from ANRED, 1988)

The test initially evaluates the permeability if the treated material and is then operated as a leaching cell. The pressure of the inputted leaching fluid is adjusted in order to achieve a discharge of 0.01 cm^3/s ($36cm^3$/hour). Successive extractions are made and it is possible to add separately the extracted quantities of every contaminant and to represent their variation as a function of the quantity of liquid discharged through the sample. According to ANRED (1988) this function is hyperbolic and its interpretation allows the evaluation of the total quantity of the considered contaminant that can be extracted if the volume of extraction liquid or the time of extraction was infinite. The resulting figure is considered as the maximum extractable quantity of the considered contaminant (mg/kg), hence a long-term scenario.

A significant evaluation of the efficiency of the stabilisation and solidification treatment at these old sites remains difficult, mainly due to the lack of knowledge of the initial physical and chemical characteristics of the untreated material as well as the quantities of reagent added to stabilise the material. The important factor that can be interpreted from the data in the tables is that the metal concentrations appear low. Although it is not possible to relate this data to the untreated material, low metal

concentrations would be expected at high pH. It is also clear that levels of sulphates and ammonium ions are high. This would also be expected since at moderate to high pH it would not be expected that negative sulphate ions would be stabilised. This is highlighted by the comparison of the one set of pre-treatment data in Table 2.19 for site B, including, pH, chemical oxygen demand (COD) and hydrocarbon content (HC) with the post-treatment data for site B in Table 2.21. Similarly ammonium ions would not take place in precipitation reactions, perhaps only in cation exchange reactions and surface adsorption reactions, suggesting why these ions remain in high concentrations. Although no data regarding the pH immediately after treatment exists, the most disturbing data from a stabilisation perspective is the relatively low pH of all Petrifix samples. Encouragingly the lime stabilised sites A and B retain high pH, although surprisingly the leachability of lead highlighted in Table 2.21 for these sites is quite high. Table 2.20 highlighting the physical characteristics clearly show the lime-treated sites A and B with higher strengths, whilst permeability is clearly variable.

Comparison of the INSA test leachable fractions of chemicals from Tables 2.21 and 2.22 with those of the Oedometric permeameter in Table 2.23 show surprisingly similar results. This is significant due to the clear difference in the testing method.

Perhaps the most important point to be taken from these pilot studies is the need for a thorough scientific approach to investigation and reporting data. Only by this approach will it be possible to improve knowledge in the large scale application of the stabilisation and solidification technology.

Table 2.21 INSA test data for lime-treated Site A-Marias De Ponteau-Lavera and Site B-Bourron Marlotte (adapted from ANRED, 1988)

Sample	Extraction	pH	Conductivity mS/s	TOC	COD	Cu	Pb	Cd	Co	Va	Ni	HC
A1	1	12.7	5.6	900	2800	6.2	25	0.4	< 0.5	< 0.5	1.0	12
(upper)	2	12.7	5.4	490	2000	3.7	21	0.2	< 0.5	< 0.5	0.8	8
	Total			1390	4800	9.9	46	0.6	< 0.5	< 0.5	1.8	20
A2	1	12.7	6.4	1170	3200	11.1	24	0.3	< 0.5	< 0.5	1.3	11
(middle)	2	12.7	5.6	419	1400	4.6	19	0.4	< 0.5	< 0.5	0.8	7
	Total			1589	4600	15.7	43	0.7	< 0.5	< 0.5	2.1	18
A3	1	12.1	5.9	3080	9100	3.6	< 2	0.4	< 0.5	< 0.5	1.2	5
(Lower)	2	9.3	1.6	845	2100	1.5	< 2	0.5	< 0.5	< 0.5	0.5	3
	Total			3926	11800	5.1	—	0.9	< 0.5	< 0.5	1.7	8

Sample	Extraction	pH	Conductivity mS/s	TOC	COD	Fe	Pb	Cd	S_2^-	SO_4	Ni	HC
B1	1	8.4	1.7	2100	5400	0.6	< 0.2	—	< 0.5	—	—	5.0
(upper)	2	7.8	1.6	1270	3050	0.4	< 0.2	0.3	0.6	6350	—	23
	Total			3370	8450	1	< 0.2	0.3	—	—	—	28
B2	1	12.5	5.3	1440	3500	0.5	4.0	0.4	1.8	10360	—	11
(middle)	2	11.1	1.8	2040	6100	0.6	—	0.3	< 0.5	10550	—	10
	Total			3480	9600	1.1	4.0	0.7	—	20360	—	21
B3	1	7.8	2.15	2920	7700	0.5	< 0.2	0.3	< 0.5	12130	—	4.0
(Lower)	2	7.7	1.95	898	3600	0.6	—	0.2	< 0.7	935	—	5.0
	Total			3818	10300	1.1	—	0.5	—	2205	—	9.0

Note : All values are in mg/kg except pH and conductivity.

Table 2.22 INSA test data for Petrifix treated Site C-Nesle-Somme and Site D-Bellay-Ain (adapted from ANRED, 1988)

Sample	Extraction	pH	Conductivity MS/s	TOC	COD	Cu	Fe	Zn	NH_4
C1	1	7.6	1.1	411	1000	< 0.5	0.8	< 0.2	549
(upper)	2	7.6	0.57	105	280	< 0.5	1.0	0.5	144
	Total			516	1280		1.8	0.5	693
C2	1	7.8	0.92	61	120	< 0.5	0.8	0.6	513
(middle)	2	7.9	0.49	16	60	< 0.5	0.9	0.5	108
	Total			77	180		1.7	1.1	621
C3	1	7.7	0.94	35	130	< 0.5	0.5	0.5	522
(Lower)	2	7.8	0.41	9	70	< 0.5	0.4	0.9	126
	Total			44	200		0.9	1.4	648

Sample	Extraction	pH	Conductivity mS/s	TOC	COD	Ca	Fe	Cr	NH_4
D1	1	7.7	1.1	230	800	1280	0.4	0.8	1280
(upper)	2	7.8	0.72	161	220	1150	0.5	< 0.5	1150
	Total			391	1020	2430	0.9	0.8	2430
D2	1	9.6	0.82	1260	3200	560	0.3	0.9	560
(middle)	2	8.2	0.48	260	750	410	0.6	1.1	410
	Total			1520	3950	970	0.9	2.1	970
D3	1	7.8	0.92	55	250	620	1.4	< 0.5	620
(Lower)	2	7.9	0.56	31	150	850	0.5	< 0.5	850
	Total			86	400	1470	1.9		1470

Note : All values are in mg/kg except pH and conductivity.

Table 2.23 Oedometric pressure leaching test data of treated mid-depth material from Sites A,B,C and D.

Sample	pH	Conductivity mS/s	TOC	COD	Cu	Pb	Cd	Co	Va	Ni	HC
A2	12.7	5.6	1166	3200	4.8	10.6	0.11	0.08	----	1.27	11.8
Sample	**pH**	**Conductivity mS/s**	**TOC**	**COD**	**Fe**	**Pb**	**Cd**	**S_2^-**	**SO_4**	**Ni**	**HC**
B2	12.6	5.8	1690	4760	0.26	3.26	0.12	0.5	5434	----	5.9
Sample	**pH**	**Conductivity MS/s**	**TOC**	**COD**	**Cu**	**Fe**	**Zn**	**NH_4**			
C2	8.5	0.4	60	160	0.06	5.1	0.03	271			
Sample	**pH**	**Conductivity mS/s**	**TOC**	**COD**	**Ca**	**Fe**	**Cr**	**NH_4**			
D2	9.2	0.44	1200	2680	315	0.6	< 0.05	132			

Note : All values are in mg/kg except pH and conductivity.

2.6.2 The HAZCON process

The major objective of the HAZCON solidification SITE programme demonstration test discussed by U.S.EPA (1989-B) was to develop reliable performance and cost information. The summary of projects in Table 2.18 indicates the area for the test was a former oil reprocessing plant in Douglassville, PA, containing a wide range of organic and heavy metal contaminants. Six sites were treated and are referred to as the Lagoon North (LAN), Lagoon South (LAS), Filter Cake Storage Area (FSA), Drum Storage Area (DSA), Plant Facility Area (PFA), and Landfarm Area (LFA). The contaminated soil was excavated and screened to remove aggregate and debris greater than 3 inches in diameter. The material was then fed to the Hazcon Mobile Field Blending Unit (MFU) along with cement and Chloranan. Cement was used on an approximately 1:1 ratio with soil, whilst the soil-Chloranan ratio was 10:1. The MFU utilised a mixing screw to blend the four feed components. Trial tests were performed where treated material was placed in 0.7645m^3 moulds and allowed to cure. Whilst curing took place the excavation holes were lined with impervious plastic liners and partially filled with clean soil. After 48-96 hours curing, the solidified blocks were placed in the lined excavations and covered with clean soil. The blocks were sampled at 28 days along with the surrounding clean soil. Samples were removed in three phases: before treatment, as a slurry exiting the MFU for analysis after 7 days of curing, and then the buried blocks after 28 days curing. Physical tests performed were:

- bulk density (results summarised in Table 2.24),
- moisture content,
- permeability (results summarised in Table 2.24),
- unconfined compressive strength of the solidified cores (results summarised in Table 2.24), and
- weathering tests – freeze/thaw and wet/dry.

Chemical tests as well as the following leaching tests were performed to identify metal and organic constituents:

- Toxicity Characteristic Leaching Procedure (TCLP) – Standard leaching procedure used for measuring leachability of contaminants (results in Table 2.25),
- ANS 16.1-simulates leaching from the intact solidified core in relatively stagnant groundwater regimes, and
- MCC-1P-simulates leaching from the intact solidified core in relatively stagnant groundwater regimes.

The latter two tests are used by the nuclear industry to model leaching behaviour. In an attempt to predict the long-term integrity of the stabilised and solidified mass X-ray diffraction was carried out to try to identify crystalline structure in the solid. Scanning electron microscopy was also used to attempt to characterise porosity and hydration products by viewing the presence of fractures and unreacted soil/waste material. Some of the important physical and chemical results are summarised in Tables 2.24 and 2.25.

Table 2.24 Physical properties of the HAZCON material during the SITE programme (U.S.EPA, 1989-B)

Location	Untreated Soil		28-Day Cores		
	Bulk Density (g/ml)	Permeability (cm/s)	Bulk Density (g/ml)	Permeability (cm/s)	Unconfined compressive strength (kPa)
DSA	1.23	0.57	1.95	1.8×10^{-9}	7674
LAN	1.40	1.8×10^{-3}	1.61	4.0×10^{-9}	3606
FSA	1.60	Impermeable	1.51	8.4×10^{-9}	1510
LFA	1.68	2.0×10^{-2}	1.84	4.5×10^{-9}	6515
PFA	1.73	7.7×10^{-2}	2.07	5.0×10^{-10}	10852
LAS	1.59	1.5×10^{-5}	1.70	2.2×10^{-9}	6129

Table 2.25 Chemical properties of the HAZCON material during the SITE programme (U.S.EPA, 1989-B).

Location	TCLP Leachate Concentrations (mg/l)					
	Untreated Soil			28-Day Cores		
	VOC*	BNA*	Pb	VOC	BNA	Pb
DSA	0.02	ND	1.5	0.38	ND	0.007
LAN	0.02	1.02	31.8	0.05	1.45	0.005
FSA	1.03	2.81	17.9	0.72	2.79	0.400
LFA	5.10	0.010	27.7	0.37	0.10	0.050
PFA	1.10	0.010	22.4	0.84	0.11	0.011
LAS	0.05	0.010	52.5	0.11	0.73	0.051

* VOC-Volatile Organic Carbon

BNA-Base Neutral Acid Extractable

A summary of the key results reported from HAZCON 'SITE' demonstration were as follows:

- The volume of the solidified soils compared to the untreated soils increased by approximately 120%.
- The unconfined compressive strength varied from 1430kPa-10200kPa and importantly found to be inversely proportional to the oil and grease concentration.
- The TCLP leach data suggest that the metals were immobilised despite the organic contamination present.
- The TCLP leach data performed on treated and untreated showed similar concentrations of volatile organics and BNAs in their respective leachates, suggesting no success at stabilising non-polar organic molecules as expected.
- The microstructural study of the solidified soil showed the following:
  - High porosity
  - Brownish aggregates passed through the process unaltered
  - Mixing was not efficient
  - Encapsulation is a major part of the solidification process
- The cost of the treatment was $205/ton utilising the Mobile Field Blending Unit in 1989.

2.6.3 Conclusions to the pilot studies

The results of the French and U.S. pilot studies highlight that the processes of stabilisation and solidification are very poorly understood and data is not reported to a suitable high degree to make significant analytical conclusions based upon the chemistry of the reactions taking place. Indeed it is often the case that comparisons of processes are reported by individuals with a potential bias for one process over another. This is often the case in arguments comparing cement treatment relative to CaO treatment, irrespective of the fact that cement is over 70% CaO. A case in fact is a document comparing the French technologies to the HAZCON process. The author describes the process of contaminant retention :

'In the EIF Ecology lime stabilisation process, the contaminants are essentially trapped due to the low solubility in the high pH environment of the mix. Release, therefore, strongly depends on the acid neutralisation capacity of the stabilised product. In general, lime as a sole binder is not very effective'

In many respects the high pH and acid neutralisation capacity are valid statements. However the author fails to describe the considered irreversible solidification reaction associated with the crystallisation of calcium silicates and calcium aluminates which creates a medium of low permeability and high stability. The author goes on to describe the HAZCON cement process:

'In the HAZCON process, heavy metals are retained in the stabilised product mostly by physical entrapment and precipitation. The buffering capacity of the stabilised material leads to a strong reduction in leachate concentrations.'

Due to the nature of both stabilisation methods, if they were both applied in an optimum individual design mix, the results are likely to be similar since both methods rely on precipitation at high pH and subsequent solidification due to re-crystallisation. One concession is made by the fact Chloranan may be a potential benefit in treating heavy metals in an organically contaminated environment. However, without comparison with pure cement stabilisation under similar contamination circumstance claims are hard to substantiate.

2.7 CHEMICAL ANALYSIS OF CONTAMINATED MATERIALS

2.7.1 Introduction

Much of the chemical analysis performed on contaminated material is to assess which elements and compounds are present and how mobile they are in an aqueous environment. Subsequently, the methods adopted to assess this chemical behaviour can be divided into two categories. Firstly, it is important to determine the total content of all elements and compounds within a material, which may become mobile due to passage of solutions and chemical transformations. Generally for inorganic materials and contaminating compounds this is achieved by aggressive reaction of the contaminated material with acids, termed acid digestion. In the context of a material such as clay much of the silicate and aluminate content are very stable and insoluble in concentrated nitric and hydrochloric acid. Therefore, if a total elemental analysis is to be carried out hydrofluoric acid must be used. Unfortunately, much specialised equipment is required since this acid is so dangerously aggressive that it dissolves virtually all materials.

The second category of analysis attempts to investigate the mobility of the elements from the contaminated material into the surrounding environment. This process is termed leaching behaviour. The ideal leaching test and model, which does not yet exist, would aim to predict how materials behave naturally in a specific fluid-soil or fluid-waste environment. With respect to heavy metal contaminated soils, this focuses on modelling the movement of metals in a variety of forms through a soil structure toward water resources and hence enable prediction of the long-term effects on the ecosystem.

To provide the best data relating to the actual leachability of metals at a specific site, in-situ measurements could be considered to provide the most complete representation. This would have to occur over large time-scales to account for changes in the environmental surroundings, including, temperature, rainfall, periodic rain acidity and the subsequent effects that these parameters have on biological activity. Based upon an analysis of this data, a treatment could be designed and applied to that particular site under those particular conditions and that particular time. However, those conditions could vary considerably in the longer-term and the initial assessment cannot occur indefinitely. For this reason, many testing approaches

attempt to emulate longer-term behaviour by exaggerating conditions in the short-term (aggressive tests). It is not necessarily possible or economically viable to control environmental parameters such as temperature, leach rates, or long-term freeze-thaw effects *in situ*, hence environmental conditions are emulated and manipulated in a laboratory environment. This in itself creates difficulties for the researcher because many environmental conditions cannot be adequately or cost effectively modelled in the laboratory. This includes factors such as:

- leaching fluid (leachant),
- material heterogeneity and physical behaviour of the macrostructure, and
- the presence and activity of biological species in conditions ranging from aerobic to anaerobic.

From these simplified considerations it is clear that no leach model or testing method can fully emulate the entire scope of environmental effects and therefore results from any such tests must be cautiously interpreted with an understanding of the materials physico-chemistry and compared solely on a relative basis. Research must aim to minimise variability, providing useable information, which may or may not be used to *estimate* long-term behaviour.

A substantial compilation and evaluation of leaching tests was composed by Löwenbach, 1978 on behalf of the U.S. EPA. Lewin *et al*, 1994 made significant use of this report when producing the U.K. National Rivers Authority Interim NRA guidance (R & D Note 301) for a U.K. leach test. Due to the existence of such thorough material for assessing leaching tests, this section only attempts to provide the basic fundamental concepts. For more detailed information about leach test approaches and methodology Löwenbach (1978) and Lewin *et al* (1994) should be consulted.

Many batch-leaching tests were initially developed for assessment of the short-term impact of wastes to landfill. Development was due to the complexity, time dependence and resultant cost of column leaching methods. The first batch testing methods were probably developed in the United States of America by the United States Environmental Protection Agency (EPA) and have undergone several refinements over the last two decades. Since the development of the batch extraction tests, several other tests very similar to the initial EPA tests have been developed

throughout the world to satisfy the individual requirements of a country's environmental governing body. It is very difficult to investigate batch tests and compare their results since for example in the USA, the nuclear industry has one testing method, the EPA has another test method outlined in the Code of Federal Regulations (CFR) and the American Standards of Testing and Materials (ASTM) has two different tests. It is also a fact that certain states in the USA have their own testing methods, for example the Minnesota Pollution Control Agency (MPCA) "Land Disposal Leach Test"; the Illinois Environmental Protection Agency test (IEPA); the IU Conversion Systems test (IUCS) which was an adaptation of the early Pennsylvanian Department of Environmental Resources test (DER), (Welsh *et al*, 1981). The Waste Research unit at the Harwell Laboratory in the U.K. has also developed a test as well as the UK National Rivers Authority.

The situation is clearly complicated with many organisations setting their own testing criteria and standards. Hence, a general review of the mechanisms will be provided.

The types of test recently categorised by Environment Canada, Wastewater Technology Centre (1990), are summarised in Figure 2.21, and will thereafter be briefly described.

Extraction tests are performed by placing a leachant in contact with a potentially contaminated material for a specific duration without replacement of the leachant at any time. A sample of leachate is removed throughout the test or more usually at the end of the test after solid separation and is chemically analysed to determine the soluble elemental fraction. Most extraction tests conform to one of the following categories: agitated extraction tests; non-agitated extraction tests; sequential extraction tests and concentration build-up tests.

2.7.2 Agitated batch leaching tests

Agitated extraction tests achieve equilibrium or steady state conditions as quickly as possible by mixing, stirring or shaking the contaminated material with the leachant. The tests measure the chemical properties of the system rather than rate-limiting mechanisms. The methods of mixing samples can be important since it determines the level of particle abrasion. Methods of mixing commonly adopted are illustrated in Figure 2.22.

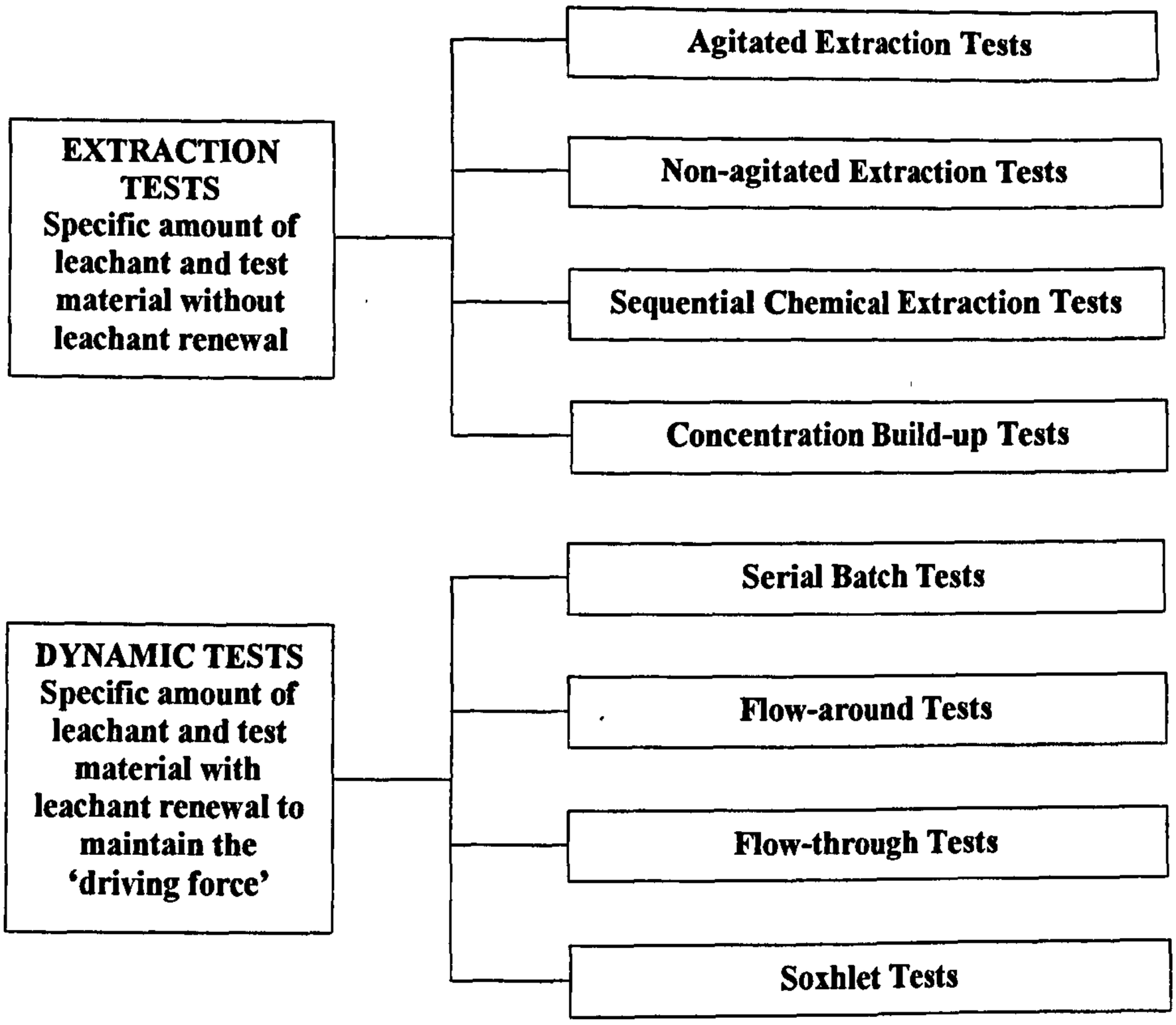

Figure 2.21 Leaching test categories (Adapted from Environment Canada, 1990 and reported by Lewin *et al*, 1994)

Sequential extraction tests involve separation of the waste from the previous leachant and adding this solid to a fresh leachant hence potentially allowing further leaching to occur. In theory the sequential extraction can be unlimited and may be analogous to column leaching. Some tests are performed with increasingly aggressive leachants. Lewin *et al* (1994) states that the resulting fractions of this type of test are not well defined in terms of chemical speciation and do not provide quantitative data, therefore they cannot be applied to field conditions.

Non-agitated tests involve placing a monolithic mass into a leachate bath and monitoring chemical changes within the batch solution. This is usually modelled by diffusion mechanisms and essentially provides data on rate limiting physical mechanisms in the leaching process from the monolithic samples rather than chemical characteristics of the material. These tests have been generally developed for application to radioactive waste.

Concentration build up tests involve repeatedly contacting aliquots of fresh contaminated material with the same leachate at very low cumulative liquid to solid ratios and monitoring the subsequent chemical changes.

To highlight the shear variability of agitated leachate tests currently being used throughout the world Löwenbach (1978) and Lewin *et al* (1994) provide a summary in Table 2.26.

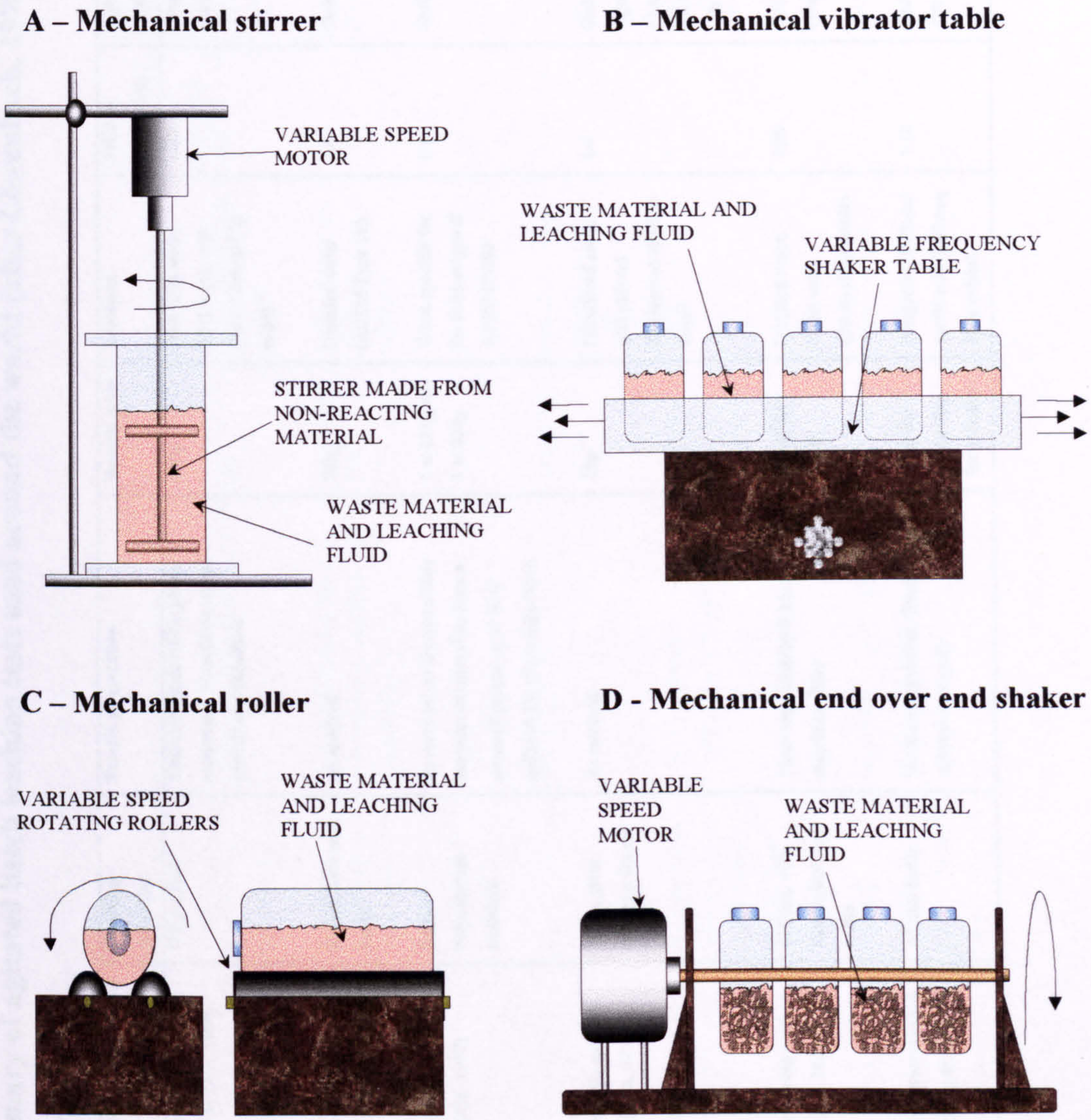

Figure 2.22 Mixing methods for extraction tests

Table 2.26 Summary of agitated batch leaching tests used around the world (after Löwenbach, 1978 and Lewin *et al*, 1994)

Test name	Development status	Leaching container	Sample preparation	Sample mass	Leachant	Solid to liquid ratio	Agitation method	Duration of test	Method of leachate separation
Extraction Procedure Toxicity Test (EP Tox, U.S. EPA 1310)	Regulatory method (U.S. EPA, 1980)	Unspecified	Non-monolithic waste: phase separation. Monolithic waste: particle size reduction.	100g	Deionised water 0.5N acetic acid (max 2.0meqH^+/g solid)	1:20	Unspecified, continuous	24 to 48h	0.45μm filtration
ASTM D3987 shake test (1979)	Research method (ASTM, 1979)	Round, wide neck bottle	As received	700g	Distilled water (ASTM Type IV)	1:4	Shaking	48h	0.45μm filtration
IUCS modified 48 hour shake leaching test	Research method (IUCS, 1977)	3 litre Polyethylene container	As received, or for monolithic samples: circular slice from a standard proctor or 3" × 6" cylinder. No phase separation	5 at 125g and 1 at 500g	Water specific for the field or type II ASTM D1193	1:4	Shaking	1,2,4,8,24 and 48h	0.45μm filtration
Minnesota Pollution Control Agency (MPCA) land disposal leach test	Research method (MPCA, 1977)	2 litre, glass separator funnel	As received	25g	1)Buffered acetic acid pH=4.5 2)deionised distilled water	1:4	Shaken vigorously for 60 seconds and left to stand for 24h	24h	Medium porosity ashless (<0.1 ash) filtration
Leachate Extraction Procedure (LEP), Ontario	Regulatory method (MOE, 1985)	1250ml, wide neck cylindrical bottle	Phase separation by 0.45μm membrane filter	50g of dry solids	Distilled water, acetic acid (2.0meqH^+/g solids)	1:20	End over end (10rpm)	24h	0.45μm filtration
Quebec R.s.Q., Q-2, R12.1	Regulatory method developed in (1987)	>1 litre bottle	No phase separation. Grinding. No structural integrity	100g dry solids. 50g for volatiles	Inorganics: buffered acetic acid (0.82meq H^+/g solids)	1:10	End over end (10 to 20 rpm)	24h	30 min decantation, 0.45μm filtration.

Table 2.26 Summary of agitated batch leaching tests used around the world.... Continued (after Löwenbach, 1978 and Lewin *et al*, 1994)

Test name	Development status	Leaching container	Sample preparation	Sample mass	Leachant	Solid to liquid ratio	Agitation method	Duration of test	Method of leachate separation
Waste Extraction Test (WET), California	Regulatory method (SOC, 1985)	Polyethylene or glass container	Milling 0.45µm filtration	50g	0.2M sodium citrate at pH5.0	1:10	Shaker table or rotary method	48h	Centrifugation, 0.45µm filtration
Toxicity Characteristics Leaching Procedure (TCLP, U.S. EPA 1311)	Standard method (U.S. EPA, 1986)	Any material compatible with sample, zero headspace extractor (ZHE) for volatiles	Cutting/crushing and grinding. Solid/liquid phase separation. No structural integrity	100g (25g for ZHE	Buffered acetic acid 1)pH=4.93 2)pH=2.88	1:20	End over end (30rpm)	18h	0.6 to 0.9µm borosilicate glass fibre filter combines liquid phase with extract
TCLP variant, U.S. EPA 1311	Modified TCLP (U.S. EPA, 1989-C)	As U.S. EPA 1311	As U.S. EPA 1311	As U.S. EPA 1311	Simulated acid rain (sulphuric/nitric acid)	As U.S. EPA 1311	As U.S. EPA 1311	As U.S. EPA 1311	As U.S. EPA 1311
Equilibrium Extraction (EE), Environment Canada.	Published research method (EC, 1990)	Inorganic: 250ml wide neck plastic sample bottle. Organic: 500ml glass	Inorganic: Grinding Organic: Pestle and mortar	Inorganics 40g Organics 80g	Distilled water	1:4	National Bureau of standards rotary extractor	7 days	0.45µm vacuum screen
Multiple Batch Leach Testing (MBLP), Environment Canada	Published research method (Constable and Côté, 1986)	1 to 2 litre Square polyethylene or glass bottle	Remove free liquid. Reduce particle size to <9.5mm	Variable to fill 90% of bottle	Distilled water. Acidic water buffer to pH4.5. Synthetic municipal waste	1:4 or 1:20	Slow rotary tumbling	24h	0.45µm filtration

Table 2.26 Summary of agitated batch leaching tests used around the world.... Continued (after Löwenbach, 1978 and Lewin *et al*, 1994)

Test name	Development status	Leaching container	Sample preparation	Sample mass	Leachant	Solid to liquid ratio	Agitation method	Duration of test	Method of leachate separation
French Leach Test AFNOR, X 31-210	Proposed standard for hazardous waste (AFNOR, 1988)	Straight wall 1.5litre bottle	Remove free liquid, reduce particle size to < 9.4mm	100g	Demineralised water	1:10	Roller or Shaker	16h	0.45μm filtration or centrifugation
Material Characterisation Centre MCC-3	Regulatory method (radioactive wastes)	Teflon container 20ml to 1 litre	Crush monolithic waste form into two fractions 74 to 149μm and 180 to 425μm	>1g	Choice of high purity water, silicate water, brine, repository water	1:10	Rolling and rocking	Variable: 28 days to several years	N/A
Italian CNR-IRSA	Regulatory method (1986). (Cernuschi *et al*, 1990)	Not known	Not known	Not known	1) Acetic acid 0.5N, pH=5 2) CO_2 saturated water	1:16	Continuous stirring	24h	Not known
German leachability by water. DIN 38414-S4	German standard method. (Din-Normen, 1984)	200ml wide necked flask	Sample reduction only if particles >10mm. No grinding	100g	Deionised water	1:10	Initial gentle swirl or flask inversion only	24h	Filtrational centrifugation
Proposed test in Draft EC Landfill Directive	Modified DIN 38414-S4. (CEC, 1991)	Wide necked glass bottle	Sampling reduction by crushing only if particles > 10mm	100g (dry solids)	Deionised water	1:10	Shake, rotating bottle by 180^0 once per minute	24h	Centifugation, 0.45μm filtration
UK National Rivers Authority Test	Guidance method (Lewin *et al*, 1994)	Not given	Particles< 5mm	100g	Deionised water acidified to pH 4.5 with acetic acid	1:5	Shaking	24h	0.45μm filtration

2.7.3 Dynamic leaching tests

Dynamic tests are tests, which involve continuous or intermittent renewal of the leachant to retain a high concentration difference between the solid and liquid phase. This is analogous to potential difference in electronics. Although these tests are potentially more complex, expensive and time consuming than batch tests, they do provide data relating to the kinetics of contaminant mobilisation and the likely complex mechanisms related to leaching.

Column flow through leaching tests are probably the most well known dynamic test. Leachant is continually passed through a laboratory or undisturbed field sample for as long as desired by the researcher, potentially years. Lewin *et al*, (1994) states that these methods are not considered to be suitable for regulatory purposes due to the poor reproducibility and lengthy duration of the tests. Figure 2.23 shows a simplified model of the apparatus required.

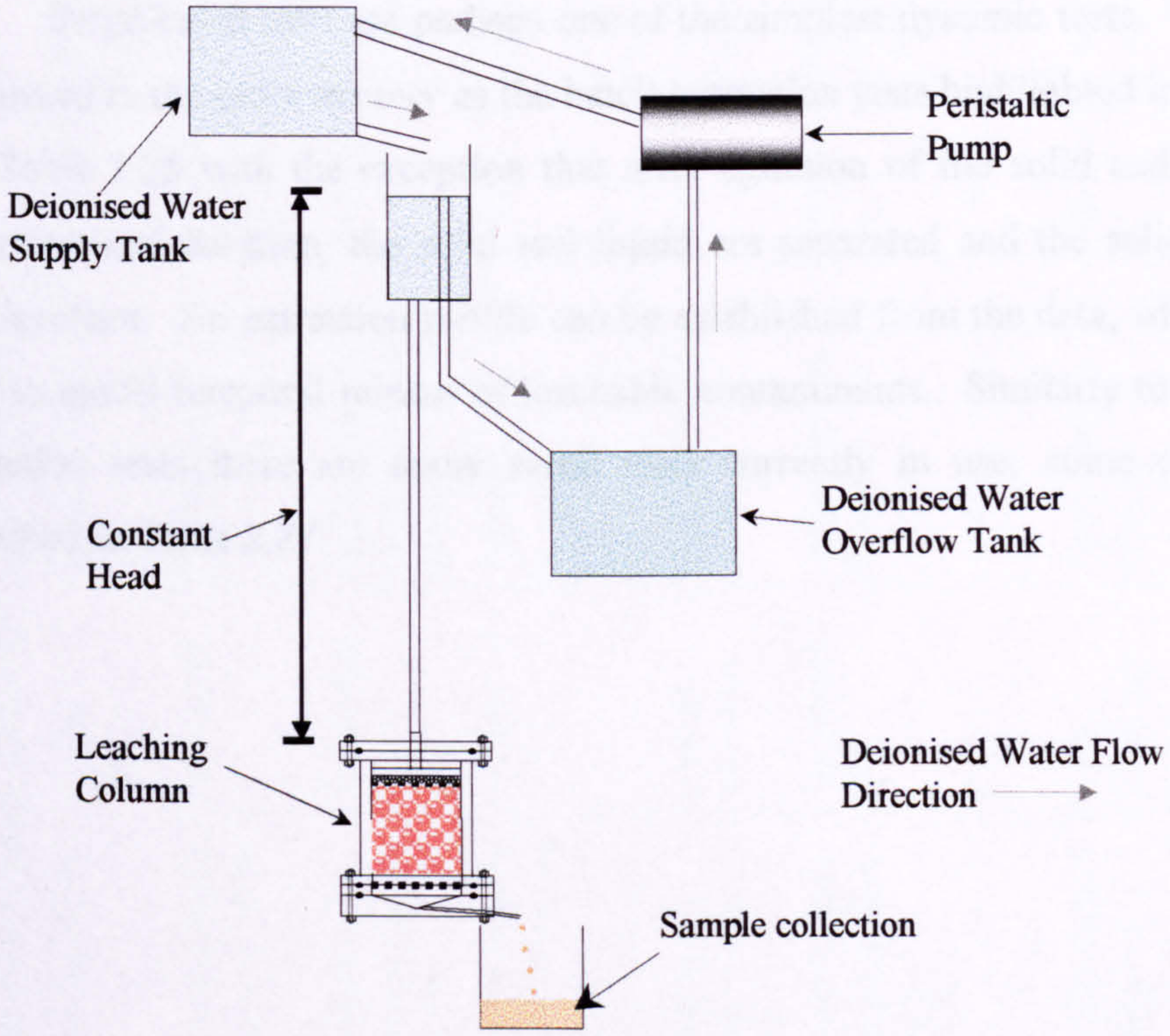

Figure 2.23 Simplified column leaching apparatus

Clearly one of the large limitations of this test is the velocity of flow of water through the sample. Forcing the leachant through the sample at higher pressures

could increase this, but how representative would this accelerated leaching be relative to the environment? Tests by Griffin *et al* (1976) overcame the low permeability and low flow through clay samples of landfill leachate by addition of sand to the clay samples. Although the permeability difficulty was overcome, there was clearly the potential for leachate reactions with the sand. A potential improvement on the technique in the 1990's would be to replace the sand with very small diameter Teflon beads.

Flow around tests generally used by the nuclear industry for radioactive waste repository studies can allow leachant to flow around monolithic samples, changing the leachant continuously or intermittently. Periodically either the monolithic mass and or the leachant is removed for chemical analysis. Soxhlet test apparatus applies a similar principle although leachant is boiled, condensed and repeatedly recirculated through or around the sample. The data produced is believed to provide information on the maximum amount of a contaminant that can be removed under extreme circumstances. These tests have also been used in radioactive studies.

Serial batch tests are perhaps one of the simplest dynamic tests. The tests are performed in the same manner as the batch extraction tests highlighted in Figure 2.22 and Table 2.26 with the exception that after agitation of the solid and liquid for a predetermined duration, the solid and liquid are separated and the solid added to a new leachant. An extraction profile can be established from the data, which could be used to model temporal release of leachable contaminants. Similarly to the standard extraction tests there are many serial tests currently in use, some of which are described in Table 2.27.

Table 2.27 Summary of serial agitated batch leaching tests used around the world (after Löwenbach, 1978 and Lewin *et al*, 1994)

Test name	Development status	Leaching container	Sample preparation	Sample mass	Leachant	Solid to liquid ratio	Agitation method	Duration of test	Method of leachate separation	Number of elutions
Multiple Extraction Procedure (MEP, U.S. EPA 1320)	Standard test method (U.S. EPA, 1986-B)	Same as EPTox	Same as EPTox	Same as EPTox	Acetic acid Synthetic acid Distilled water	1:20	Same as EPTox	Same as EPTox	Same as EPTox	10
Monofill Waste Extraction Procedure (MWE, U.S. EPA)	Technical resource document (Gaskill *et al*, 1986)	Wide neck bottle	Particle size reduction to <9.5mm or to structural integrity	Unspecified	Distilled water or site water	1:10	Rotary tumbler	18h	Settling and filtration	4
Graded serial batch test US Army	Research method for waste and soil (Long *et al*, 1987)	Unspecified	Unspecified	300g	Distilled water	1:2 or3or6or 12or24or48or96	Gentle periodic shaking 4 to 5 times a day	Until steady state conditions achieved	Vacuum filtration	>7
ASTM D4793-88 Sequential Batch Extraction	Standard method (1988) (ASTM, 1991)	2 litre wide necked bottle	Drying phase separation	100g	Reagent water (Type II D1193)	1:20	None	24h	0.45µm membrane filter	10
Waste Research Unit Leach Test (WRU) AERE Harwell (UK)	Standard method (Young & Wilson, 1982)	50ml wide neck flask	Crushing and vacuum filtration	100g	Distilled water Dilute acetic acid buffered (pH5)	One bed volume (first 5 elutions), 10 bed volumes (more than six elutions)	Mechanical flask shaker	2 to 80 hours Steady state	Vacuum filtration	5
Standard Leach (v) Test (SLT Cascade Test). The Netherlands, BEOP-31	Standard research method for combustion residues (Van Der Sloot *et al*, 1984)	1 litre polyethylene bottle	Crushing/sieving. Drying	40g	Demineralised water acidified to pH4 with nitric acid	1:20	Shake/roll	23h	Settling and 0.45µm filtration	5

Table 2.27 Summary of serial agitated batch leaching tests used around the world.... Continued (after Löwenbach, 1978 and Lewin *et al*, 1994)

Test name	Development status	Leaching container	Sample preparation	Sample mass	Leachant	Solid to liquid ratio	Agitation method	Duration of test	Method of leachate separation	Number of elutions
NVN 2508-Cascade Test	Dutch pre-standard (1988)	1 litre polyethylene bottle	Dry sample to constant mass, crushing, sieving to <3mm	40g	Demineralised water acidified to pH4 with nitric acid	1:20or40or60or80 or100	Shake/roll	23h	Settling and 0.45µm filtration	5
NVN 5432-Maximum Leachability Test	Dutch pre-standard (DPS, 1991)	Pyrex 1 litre glass beaker	Crush/grind to 565-125µm	8g	Demineralised water (pH 7 and pH4)	1:100	Magnetic stirrer	3h	Settling and 0.45µm filtration	2
Leachability by water (DIN 38414-S4	German standard method (Din-Normen, 1984)	200ml wide neck flask	Sampling reduction only if particles>10mm. No grinding	100g	Deionised water	1:10	Initial gentle swirl or flask inversion only	24h	Filtration/centri fugation	1-4
Standard Leach Test Procedure R, University of Wisconsin (SLT)	Past standard (1974) (Hamm, 1977)	Square flask	Remove liquid phase by 0.45µm pressure filtration	40g (wet mass)	Synthetic landfill leachate	1:10	Rotating shaker	24h	0.45µm filtration	3
EC draft waste acceptance test for proposed landfill directive	Draft CEN TC 292 (WG2) (CEN, 1993)	Not specified	Minimal (so similar to in situ material)	100g	As appropriate (pH4-7)	1:2 & 1:8	Any provided flask, contents not allowed to settle	6h, 18h	Filtration/cent rifugation (0.45µm)	2

2.7.4 Leach test parameters

Many leach test parameters significantly affect the elution of elements or compounds into solution. Some of the most important are:

- solid to liquid ratio (agitated tests only),
- composition of leaching solution,
- sample preparation method,
- leaching period,
- contact method,
- test environmental conditions,
- solid and leachate separation method, and
- sample storage and sample analysis method.

2.7.4.1 Solid to liquid ratio

Solid to liquid ratio clearly has an effect on the quantity of soluble elements found in the final leachate after a dynamic test. However, the effect of doubling the quantity of solid to liquid is not necessarily directly linearly proportional to the quantity of elements or compounds found in the resultant leachate. This depends on how much available soluble material is present and upon final equilibrium conditions. It is therefore conceivable that at very low solid to liquid ratios more mg of an element may be released into the final leachate per kg of solid waste present than for a high solid to liquid ratio. It is also possible that at low solid to liquid ratios some elements will become mobile that were not mobile at higher solid to liquid ratios. However, it is important to keep solid to liquid ratio high enough to avoid over dilution of important elements to the point where they are below the detection limits of analytical equipment. High ratios also have the potential to limit the effects of sampling errors.

Solid to liquid ratio could also partially govern the rate of particle breakdown since it influences particle contact time with solution. This factor can be significant when dealing with expansive materials such as sodium bentonites. Indeed if a material such as sodium bentonite can absorb many times its own mass in water (e.g. Wyoming Bentonite $\approx$ 500%) then it has a clear minimum solid to liquid ratio.

Solid to liquid ratio can be interpreted as dry solid to liquid ratio or indeed wet solid to liquid ratio. This is an important factor since some tests may require the water content of the solid to be taken into account when the leachate is added therefore creating an effective dry solid to liquid ratio. Alternatively, some tests may stipulate that the material is oven dried prior to testing. Although it is generally considered standard practice to dry material in an oven at 105 ± 0.5^{0}C, in circumstances where a contaminated material has been stabilised or solidified, drying may significantly change the chemistry of precipitates or other chemical species. This hypothesis is based on the fact that some reactions are exothermic (produce energy) or endothermic (require energy). Therefore by applying energy in the form of heat, exothermic reactions may be inhibited and endothermic reactions may be promoted. Cation exchange and surface adsorption are examples where such a theory would be relevant (see Appendix 2-Table A2.1). Furthermore the structure of clay minerals, more precisely c-axis spacing (see Table 2.10) can be significantly affected by temperature which could translate directly to chemical behaviour.

2.7.4.2 Leachant composition

Leachant composition is critical when determining contaminant release and has been subject to substantial investigation. In terms of practical application for prediction of in-situ behavioural characteristics, actual site water is likely to be preferable, although this may be subject to a very limited 'shelf' life and subsequently storage conditions are important. Many attempts particularly in the landfill industry have been made to produce synthetic chemical leachants to simulate actual site conditions. Although this could provide flexibility, clearly specific sites can vary significantly. A direct result of these considerations is that a standard solution is required, hence, deionised water is often stipulated. Lewin *et al*, 1994 states that many tests require leachant to simulate rain. Carbon dioxide saturated deionised water can be used for this purpose. This is relatively simple to produce by allowing the deionised water to equilibrate overnight with air, producing water with a pH of 5.6. According to Lewin *et al* (1994), the median pH of rainwater samples collected at Warren Springs Laboratory's national monitoring network in 1990 was pH5.5. The appropriateness of this mild acid leachant is further verified by the acidic conditions created in surface soil layers via organic degradation processes producing elevated

CO_2 levels discussed in Section 2.4.8 (the origin of hydrogen ions in soil which may damage stabilised soils) and illustrated in Figure 2.15.

Many dynamic leaching tests are designed as semi-predictive tests and utilise aggressive leachants which contain weak acids such as acetic acid, strong acids such as nitric acid/hydrochloric acid mixtures or complexing agents which have a high affinity for certain elements, essentially stripping contaminants from the waste or soil. Aggressive acids are usually added either as a fixed quantity at the beginning of a test or added gradually throughout the entire test to retain a specific constant pH. Aggressive acids will dissolve precipitates and the high hydrogen ion concentration could exchange with contaminants at any potential cation exchange site. The implication of adding such acids are especially detrimental to stabilised materials since the strong acid has the potential to neutralise the pH-dependent benefits of some stabilisation and solidification methods. The stabilisation and solidification methods directly affected include, lime stabilisation, cement stabilisation, adsorption stabilisation such as modified clays and any combination of these methods. For the purposes of contaminated land investigations, it is generally not appropriate to use strong acids or complexing agents.

2.7.4.3 Sample preparation methods

The importance of sample preparation including drying and crushing of the sample depends on the sample being tested. If the material to be tested consists of inherently large particles such as colliery spoil or landfill material is it appropriate to dry and crush the larger particles into smaller particle to increase surface contact with the leachant. In this particular example, this may be valid due to the relatively high porosity of the material. However, for solidified products resulting from lime or cement addition it could be argued that the solidified monolithic mass with the desired low permeability partly relies on its bound nature to retain some elemental species. In this example, complete crushing prior to testing may not provide representative behavioural characteristics. Although this hypothesis is valid this produces a circumstance where the material is not easily tested using a rapid agitated batch test, and suggests that the only representative approach would be a column-leaching test. A column test is probably preferable but not necessarily resource economic. Perhaps an appropriate compromise would be to develop a test involving partial breakdown of

a monolithic mass into smaller representative particle sizes that could be tested in a rapid agitated batch test.

2.7.4.4 Leaching period

The leaching period is of interest since it controls, although not solely, particle abrasion and subsequent breakdown. Furthermore, the leaching period will determine whether equilibrium conditions are reached. Maximum species concentrations in a batch test will occur upon attainment of equilibrium. Equilibrium is a unique thermodynamic state of a system depending only on temperature. Subsequently this state provides a framework within which comparisons to other systems may be made. True equilibrium, or steady state conditions are unlikely to be reached in natural systems. For such systems the extent of the reaction which is related to equilibrium may be a more useful concept (Löwenbach, 1978). Equilibrium conditions of rapid agitated batch tests can be considered to have been reached when the total dissolved solids (elements) have reached steady state conditions. This can be measured indirectly via monitoring conductivity. Another useful indicator is when pH reaches steady state, as this is a measure of H^+ ion concentration. Both these methods are particularly useful when considering lime or cement stabilised materials due to the high Ca^{2+} ion content and the very high pH induced by reagent addition.

The leaching period of column tests is also important since the contaminated material is continually subjected to fresh leachant over a time-period dependent on pore-volume and permeability. Therefore the driving force for desorption is constant resulting in time-dependent desorption curves.

2.7.4.5 Contact method

The contact method variable is directly associated with the leaching period in the sense that the two together affect particle breakdown. Figure 2.22 illustrates typical contact methods for rapid agitated batch tests that usually involve interaction within a sealed container. Clearly the level to which the container is filled is also relevant since this governs the amount of air and also $CO_{2(g)}$ present and the degree to which the solid and liquid can be agitated within the confined space.

The contact method is also of importance in column tests since the shape and orientation of the confined material as well as the pressure at which the leachant is passed though the sample governs the sample structural breakdown. Sample shape

(height to diameter ratio) can have a large influence on end effects that result in non-uniform flow through the ends of the sample. This can directly affect the quantities of contaminant removed from a sample. Pressurised leachant flow is often desirable for materials of very low permeability to reduce the time of a test that can take many months or even years if not pressurised.

2.7.4.6 Test environmental conditions

Probably the most dominant test environmental condition is temperature, which affects the results of both extraction and dynamic tests. Temperature affects both the solubility and importantly the rate of reactions. Thus, changes in the temperature of a system may change the reaction mechanism. For convenience most leaching tests are performed at room temperature without any temperature control although raised temperatures are sometimes applied to simulate the effects of self heating radioactive wastes or biological activity in landfill sites. It is clear, however, that large changes in temperature from summer to winter will affect attenuation and desorption reactions and subsequently the results of a series of tests.

2.7.4.7 Solid and leachate separation methods

This is generally not a significant factor for samples where solids settle within a few minutes and the solution can be decanted through filter papers. Lewin *et al* (1994) states glass fibres should be used when hydrophobic, low solubility organic molecules are expected in the leachate, since they could have a high affinity for filters composed of an organic polymer. 0.45μm membrane filters, such as cellulose acetate, should be used for metal species in place of glass. Filter papers do pose a particular problem for sequential rapid extraction batch tests since the material on the filter must be placed in a fresh container with fresh leachant. In some cases, the filter paper is also placed in the fresh container. It is therefore especially desirable to use a filter paper that does not contain elements that may be released into solution or alternatively attenuate elements from the waste.

Centrifugation is often used in tests. Where possible this should be avoided since batch tests are usually designed to mix waste and leachant in a specific manner for a specified time period and the action of centrifugation can cause particle abrasion and if not refrigerated, significant heat which may significantly affect the leachate.

Furthermore, each waste solution must be considered independently since the speed of revolution and time duration of centrifugation required to separate the solid from the liquid will vary from sample to sample. In circumstances involving thixotropic wastes, centrifugation may be the only method capable of separating the liquid from the solid. However, it must be remembered that in these circumstances the separation technique is particularly aggressive and perhaps produces a leachate that does not reflect the true quantitative properties of the original waste-solution mixture. It is also important that flocculating agents are not added to force solid liquid separation since this will clearly alter the chemistry of the mixture.

2.7.4.8 Sample storage and sample analysis method

There are many standards including ASTM standards that specify procedures for appropriate sample storage methods that largely depend on the types of contaminants present. In almost every case, particularly for metal contaminated solutions, it is specified that the sample should be acidified using very pure acids to pH 4 and stored at 4^0C to prevent biological activity. Clearly, if acids are added care should be taken since HCl would not be suitable if anion analysis for Cl is required. The choice of analytical method may depend on the facilities available, however, some methods are more sensitive than others for specific elements. Methods such as Inductively Coupled Argon Plasma Atomic Emission Spectroscopy (ICP), Atomic Absorption spectrometry (AA) or Graphite Furnace (GF) are often used.

2.7.4.9 Further significant factors affecting leachate generation

In Table 2.28, Löwenbach (1978) summarises the significance of pH, redox potential, buffer capacity, complexation capacity, ionic strength, dielectric constant and surface area and suggests how these variables may affect leachate generation.

Table 2.28 Definition and significance of factors affecting leachate generation (after Löwenbach, 1978 and reported by Lewin *et al*, 1994)

Factor	Definition	Significance	Remarks
pH	pH is defined as the negative log of hydrogen ion concentration. pH is an indirect measure of the electrochemical potential of protons.	The hydrogen ion concentration is an important factor affecting reaction rate and thus pollutant solubilities.	The pH of rainwater is controlled primarily by dissolved CO_2. With rare exceptions, proton exchange and associated processes occur so rapidly that such systems may be treated in terms of shifts of true equilibrium.
Redox potential	The redox potential of a system as defined by Nernst equation. In natural systems, redox potential is taken as the measured potential differences between an inert electrode and a reference electrode.	The redox potential is a measure of the oxidising capacity of a system and provides a framework within which redox and hydrolysis reactions may be compared.	Redox potential determines, in part, the aerobic conditions under which a material is leached. Low electron activity represents strongly oxidising conditions while high electron activity corresponds to strongly reducing conditions.
Buffer capacity	The buffer capacity of a system is defined as the response of that system, in terms of pH change, to the addition of an acid or a base.	Buffer capacity defines the resistance of a system to changes in pH upon the addition of acids or bases.	Naturally occurring leachate exists as a highly buffered system. Total acidity and alkalinity together with pH operationally define buffering capacity.
Complexation capacity	Complexation is defined as the formation of a complex from a metal ion with a natural or negative ion by means of one or more chemical bonds.	The effects of complexation vary from the solubility of specific metals to causing their precipitation, depending on the complexing agent and metal ion. Complexation affects the solubilities, reactions and modes of transport of leached materials.	The most effective complexing agents are generally organic compounds. Fulvic and humic acids are two naturally occurring complexing agents of possible significance in terms of heavy metal transport.

Table 2.28 Definition and significance of factors affecting leachate generation (after Löwenbach, 1978 and reported by Lewin *et al*, 1994).....continued.

Factor	Definition	Significance	Remarks
Ionic strength	The ionic strength of a solution, I, is defined as $I = \frac{1}{2}\sum C_i Z_i^2$, where C_i is the concentration of an ion in moles per litre, Z_i is its charge and the sum is taken over all ions in the solution.	Ionic strength has a significant effect on reaction rate and therefore influences the solubility of ionic species. In general, the solubility of an ionic salt is roughly proportional to $\sqrt{I}$ for dilute solvents.	The ionic strength is generally calculated rather than measured directly. The ionic strength together with the dielectric constant defines in part the polarity of a medium.
Dielectric constant	The dielectric constant is defined by ε in the equation $F = QQ^1 \sqrt[2]{\varepsilon r}$ where F is the force of attraction between two charges Q and Q^1 separated by the distance r in a uniform medium.	The dielectric constant is related to the solvating power of the eluant. It increases with addition of ionic species. Polar substances become more soluble with increasing dielectric constant, while non-polar substances become less soluble	The dielectric constant of a system is determined by both the molecular nature of the system (e.g. polarisability) and the composition of the system. The dielectric constant together with ionic strength defines in part the polarity of a system.
Surface area	The surface area is somewhat difficult to define operationally but practically involves the measurement of some property that qualitatively depends on the extent of surface development and can be related (by means of theory) to absolute surface area. Suitable methods of determination include particle or pore size measurement and permeability studies.	Heterogeneous reactions of solids and liquids are often governed by surface processes that occurs at a rate directly proportional to the surface area of a solid, in addition to the reagent concentration in the liquid phase. Finely divided particles have a greater solubility than large crystals. The surface energy of particles smaller than 1μ may become large enough to effect surface properties.	Different methods of surface area measurement will lead to different results. For the purpose of discussing leachate generation within a landfill, methods based on permeability studies or particle size measurement are most useful. Particle size of materials deposited in landfill usually decreases with time due to physical and chemical weathering processes.

2.8 LABORATORY LEACHING TEST RESEARCH

Much research has been performed in the field of the leachability of contaminating elements and compounds from wastes, although very little has been carried out on stabilised wastes and that which has been carried out is of limited quality for determining reaction processes. The majority of previous research has focussed on the effects of changing the operating parameters of rapid agitated batch leaching tests.

Paule (1981) performed a statistical analysis investigating three experimental variables:

1. the extractor (60 and 180 cycles per minute (cpm)) shaker tables illustrated in Figure 2.22B, and the National Bureau of Standards (NBS) mixer illustrated in Figure 2.22D,
2. the solid/liquid ratios 1/4, 1/10, and 1/20, and
3. the mixing time (24 and 48h).

These tests were carried out on the ASTM Special Fly Ash using only distilled water as the leaching agent. During the tests, fifteen elements were extracted by two independent laboratories and analysed by a third laboratory using Inductively Coupled Plasma spectroscopy (ICP). The elements investigated were aluminium, vanadium, magnesium, silicon, boron, barium, calcium, chromium, potassium, molybdenum, sodium, nickel, arsenic, iron, and selenium. By statistical comparison, the 60cpm shaker table at the 1/4 solid to liquid ratio and at 24 hour test interval showed the greatest variability. Analysis of pH, aluminium and vanadium show the 60cpm shaker table results were all low relative to the 180cpm shaker table and the NBS mixer results. However, magnesium and silicon showed the opposite effect. For all the extractors boron, barium, calcium, potassium, molybdenum, sodium and nickel were of a lower value for lower solid to liquid dilution ratios. Paule (1981) proposed the following potential models :

1. All extractable material is physically leached from the solid and the use of lower solid to liquid ratios simply dilutes the extracted material by an amount proportional to the liquid content as illustrated in Figure 2.24.

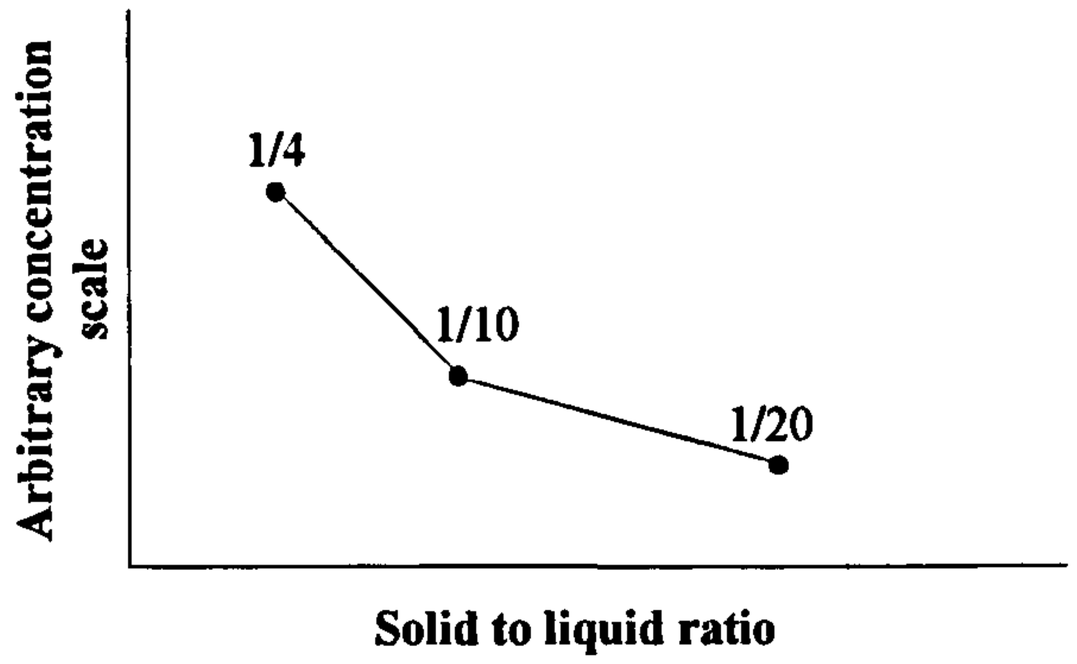

Figure 2.24 Diluted solution theory

This type of curve was obtained for, aluminium, boron, barium, calcium, chromium, iron, potassium, magnesium, molybdenum, sodium, nickel and selenium.

2. Alternatively, there is a large supply of extractable material in the solid to saturate the leaching liquid at all experimental dilutions. This would result in constant concentration at all experimental dilutions as illustrated in Figure 2.25. This was observed for vanadium and arsenic. However, for vanadium using the 60cpm extractor, the results were low. This could be due to the fact that the other two methods caused some degree of particle abrasion, thus potentially releasing more vanadium. However, it would be expected that this would also result in the release of greater concentrations of the other elements, which was not observed.

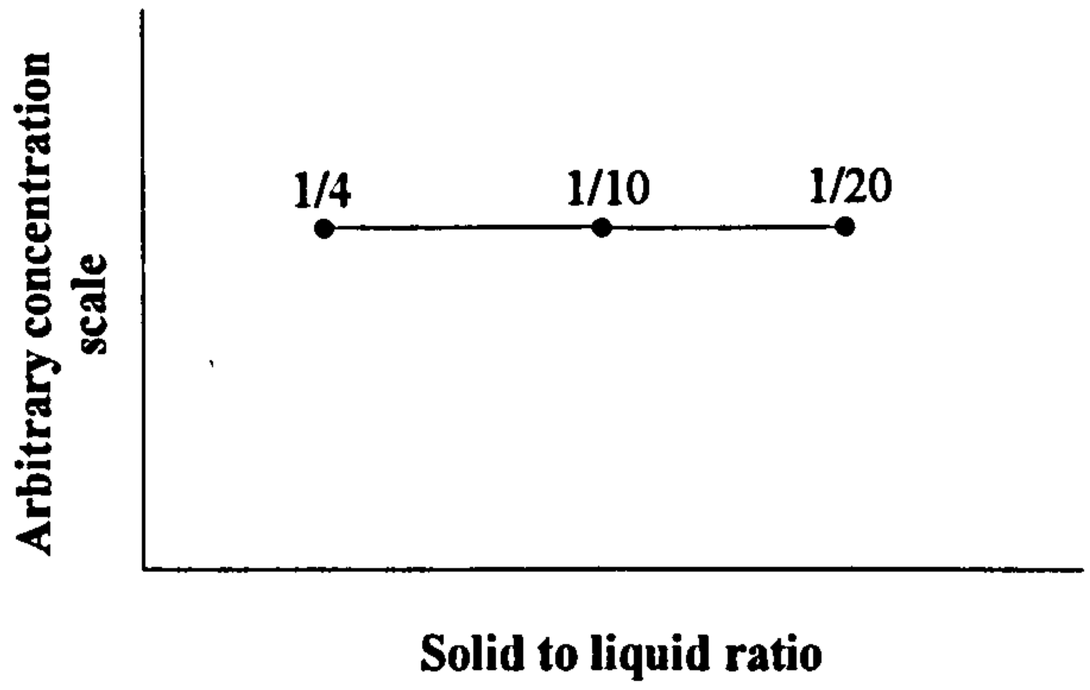

Figure 2.25 Saturated solution theory

3. As the aluminium, magnesium and silicon concentration changes are generally in opposite directions, there may be chemical equilibrium involved, such that a low aluminium concentration observed with the 60cpm shaker table can occur with high magnesium and silicon concentrations for this extractor. Similarly, the 1/4 to 1/20 dilution of aluminium for both the 180cpm shaker table and the NBS mixer could result in the observed increases in magnesium and silicon concentrations for these extracts. The flat dilution curves for arsenic and vanadium could be a result of similar equilibrium, except in this case the increase in concentration due to shifted chemical equilibrium is approximately balanced by the dilution in going from 1/4 to 1/20.

Larson *et al* (1981) carried out the EPA Extraction Procedure on wastes from electroplating factories, chlorine production and glass etching. Column leaching to simulate a landfill was achieved by mixing these wastes with municipal wastes and exposing them to a fixed quantity of deionised water each week. The EP Test is a prediction test to see whether a material can be categorised as hazardous, but, as currently designed, it did not always predict which constituents might represent the greatest pollution problems when co-disposed with municipal waste. Larson *et al* suggests that the EP Test will probably over estimate the release of cadmium, copper, lead and mercury. No arsenic or selenium was found in any EP Test extracts although it was found in large scale test cell leachates.

Welsh *et al* (1981) compared three acid extraction batch leaching protocols: the Minnesota Pollution Control Agency (MPCA) 'Land Disposal Leach Test' (1978), the proposed ASTM 'Leaching of Waste Materials, method B test (1978)' and the EPA proposed 'Extraction Procedure (1978). Boiler ash, an incinerator ash and an industrial wastewater treatment sludge were tested with respect to arsenic, chromium, lead and silver. All extractions utilised the stirrer extractor in Figure 2.22A. Each test on a particular waste with each method had a different final pH. It was found generally that greater amounts of metals were extracted at lower pH levels regardless of the test procedure used.

Jackson *et al* (1981) evaluated leaching of a standard fly ash by three batch extraction methods and compared these results with those obtained from column leach tests. Three types of mixer were utilised in the testing, see Figures 2.21B, 2.21C and 2.21D. Five solid to liquid ratios, 1/4, 1/10, 1/20, 1/40, and 1/80 were studied.

Leaching times ranging from 1 hour to 96 hours were used to assess the leachability of selenium, chromium and arsenic. Column test methods had leachant application rates of 1.8, 2.2, 2.4, and 3.5 mm/year/acre. With respect to the batch testing, the selenium results showed that after one hour leaching, time does not play an important role. As the solid to liquid ratio decreases, the amount of selenium leached per gramme of sample increases. Larger quantities were also leached using the reciprocating mixer in Figure 2.22D. The four lowest solid to liquid ratios tested with the roller mill mixer shown in Figure 2.22C produced the most consistent levels of pH, selenium and chromium, while the shaker table in Figure 2.22B gave the least consistent results. It was suggested that the shaker table at 70cpm does not give enough agitation to keep the sample mixed with the leaching fluid, where as the NBS mixer probably causes some particle abrasion. After six hours leach time, it was found that there was no significant agitation time relationship for chromium with any of the mixers. Examination of the arsenic results using the shaker table and NBS mixer indicates that after twelve hours leach time, the amount of arsenic leached does not exhibit a consistent pattern. The data for the roller mill mixer relating to arsenic were too scattered to be conclusive. As the solid to liquid ratio decreases, the concentration of the metals in the leachates also increases for any of the mixers. Whether a forty-eight hour leach test time is necessary is uncertain, i.e. although concentrations of metals did increased in some cases with increased test duration, there is no consistency in these increases. For these reasons, the NBS mixer utilising a 20/1 liquid to solid ratio and a leach time of twelve hours was chosen for comparison with the column leach test. The similarity in the quantities of element leached is apparent by observation of Table 2.29.

pH values of the final leachate for the column tests ranged from 8.1 to 9.2 while the batch tests range from 9.8 to 10.4. During column tests, selenium concentrations levelled out at 250µg/l after about twenty days testing, where as the chromium concentrations decreased throughout the entire sixty day period, at which the final value was 50µg/l. The amount of arsenic leached over the first five days declined very rapidly and then appeared to level out until day twenty, when the leachates from all four columns began to increase in arsenic concentration. Application rate data indicated that the leaching of arsenic was leach rate dependent, which agreed with the batch test data.

Table 2.29 Concentration of Selenium, Chromium, and Arsenic leached using the batch extraction and column test methods. (K. Jackson *et al* 1981)

Batch Test, 20/1 Liquid to solid Ratio. 12 hours Leach Time, NBS Mixer, µg/l	Contaminant	Column Leach Tests, at the end of 60 Days, µg/l
250	Selenium	270
62	Chromium	50
819	Arsenic	2362

Sack *et al* (1981) also evaluated fly ash leachability using batch extraction leaching procedures, specifically the EPA Extraction Procedure and the ASTM method. The acidified EPA procedure was found to extract more metals on a mg/kg of ash basis, although the ASTM method gave higher solution concentration. The EP method used a solid to liquid ratio of 1/20, a leachate buffered to pH 5.0 and a twenty-four hour leach time, where as the ASTM method used 350g of ash in 1400ml of water over forty-eight hours. For the contact times studied, i.e. two to forty-eight hours, no one elution time could be chosen which would allow equilibrium for all the parameters. Although certain elements evidenced sensitivity to the presence (aerobic conditions) or absence (anaerobic conditions) of oxygen, no pattern was found. During repeated extraction of the same fly ash with fresh leachate, release of metals was found to be highly pH-dependent. Most of the mobilisation tended to occur in the first two extractions for the acid test, while release occurred more gradually for five to seven extractions using de-ionised water.

Perhaps one of the most important studies in the UK was carried out by the National Rivers Authority (NRA). The main objective of the study reported by LeJeune *et al* (1996) was to validate the use of the NRA Interim Guidance Note on leaching tests for contaminated land. The strategy of the study was to assess the variability of results within laboratories and between laboratories when reference materials were leached under standard conditions. The two reference contaminated soils were typical of metalworks soils and gasworks soils. Initial analysis of the material highlighted an approximately 25% variability in the material of which 10% was apportioned to analytical error. Six samples of each material were sent to four laboratories and a single-step NRA batch leach test and a two-step sequential batch test were performed. Statistical analysis of the data highlighted significant differences between the data sets of the four laboratories for half the elements or compounds analysed. Furthermore, there was no evidence for systematic under-reporting or over-

reporting of individual elements or compounds by any particular laboratory. Intra-laboratory variability was particularly high for Pb and to a lesser extent Fe. The variability of the data was so high that it was expressed that acceptance limits would have to be set with very high tolerance bands. The researchers advised that variability could be reduced by using larger samples, conducting more tests, possibly taking more finely divided particles. In addition, there was no clear advantage in using the two-step sequential leach test so the additional cost and complexity was not justified.

Many more leach test comparisons have been performed by researchers on specific waste materials using a variety of tests monitoring the release of specific elements of interest. Examples include: leach testing of foundry process wastes, Boyle *et al* (1983); development of a Canadian data base on waste leachability, *Côté et al* (1983); the effect of storage on leaching properties of metal-finishing sludges, Saunders *et al* (1983); column leach testing of solid industrial wastes, Darcel *et al* (1983); chromium-bearing waste slag: evaluation of leachability when exposed to simulated acid precipitation, Kilau *et al* (1984); testing of hazardous wastes to assess their suitability for landfill disposal, Young & Wilson (1982); interpreting results from serial batch extraction tests of waste and soil, Houle & Long (1980); a comparative field and laboratory study of fly ash leaching characteristics, Dodd *et al* (1981); use of batchwise extraction procedure for coal ash disposal evaluation, Villaume *et al* (1981); modified leach test incorporating an elutriation step for the evaluation of metal sludges, Penland *et al* (1981); a comparison of groundwater quality at selected landfills to leaching test results, Rinaldo-Lee *et al* (1981), compilation and evaluation of leaching test methods, Löwenbach (1978).

Very few tests have been carried out specifically to investigate the behaviour of stabilised contaminated soil. Dermatas (1994) investigated the effectiveness of a lime based treatment in immobilising Cr^{3+} using a flow through leach test with acidic and water leachants. The tests were performed on mixtures of clay and sand that had been contaminated by 4040mg of solid chromium nitrate (Cr^{3+}) per kg of solid 'soil'. Quicklime (CaO) was added at 10% and sodium sulphate was added at 5%, both contents on a dry weight basis of the dry mixes. Samples were compacted using a standard compactive effort. Soil permeability was shown to increase because of lime treatment and the sulphate addition did not appear to affect permeability. Essentially, for the flow through tests, no chromium was leached from the treated montmorillonite-sand specimens whereas significant quantities were leached from the

untreated and treated kaolinite-sand specimens. Comparison of the leaching results to pH for the kaolinite samples emphasised that as pH dropped the Cr leachability dramatically increased.

Akhter *et al* (1990) carried out similar work using cement, lime and pozzolanic agents such as fly ash and slag to immobilise As, Cd, Cr and Pb at levels of 10,000ppm in Mississippi loess soils. Leachability was assessed using the U.S. EPA Toxicity Test. They concluded that in no case does fly ash improve the performance when mixed with other binding agents. Slag offers superior performance compared to fly ash in any combination and has potential for general utility in practice. They also conclude that Type I Portland cement is a very versatile and dependable reagent compared to the other agents such as lime, particularly in the cases of As and Cr. They also argue that in the case of lime addition the leaching results are marginally acceptable. Again, the difficulty in accepting the conclusions is because in the tests, cement was added at a much higher percentage than lime and the pozzolanic additives were not added in similar proportions. Some of this data is summarised in Table 2.30. Since the mix designs are so highly variable between the two added fixing agents and the type of lime used has not been stated, the results highlighted in Table 2.30 do not necessarily lead to the conclusions stated.

Cartledge *et al* (1990) carried out similar leach tests on cement treated Cd and Pb hydroxide sludges. They discovered very low leachate concentrations of Cd in the cement treated sample whilst Pb samples treated with cement leached a considerably higher proportion of Pb and would represent a serious threat to groundwater. They concluded that the Cd-cement system involved $Cd(OH)_2$ which provides nucleation sites for precipitation of calcium silicate hydrate 'gel' and calcium hydroxide with a very impervious coating. However, the Pb-cement system involves hydroxide, sulphate, and nitrate mixed salts (nitrate from added $Pb(NO_3)$), which retard cement hydration reactions by forming an impervious coating around cement clinker grains. It is also suggested that as pH in the cement pore waters undergoes fluctuations during the progress of hydration, the Pb salts undergo solubilisation and reprecipitation on leachable surfaces of the cement matrix.

Table 2.30 Leachability of elements in soil stabilised with added pozzolanic agents (after Akhter *et al* (1990)

Weight of additive per 100g of soil					Leachate EP, ppm
Cd (10,000ppm)					
Cement	Fly ash	Slag	Lime	Silica	
21	0.0	21	0.0	0.0	0.02
0.0	0.0	41	1.2	0.0	0.08

Weight of additive per 100g of soil					Leachate EP, ppm
Pb (10,900ppm)					
Cement	Fly ash	Slag	Lime	Silica	
22	0.0	22	0.0	0.0	0.18
0.0	0.0	44	1.3	0.0	0.55

Weight of additive per 100g of soil					Leachate EP, ppm
As (12,200ppm)					
Cement	Fly ash	Slag	Lime	Silica	
22	0.0	22	0.0	0.0	57.7
44	0.0	0.0	0.0	0.0	4.56
0.0	0.0	109	3.3	0.0	74.9

Weight of additive per 100g of soil					Leachate EP, ppm
Cr^{6+} (12,200ppm)					
Cement	Fly ash	Slag	Lime	Silica	
26	0.0	26	0.0	0.0	58.5
0.0	0.0	129	3.9	0.0	38.5

Young *et al* (1984) carried out an investigation to determine the ability of chemical treatment to reduce the leaching of metals from fly ash. Samples of fly ash were treated with Portland cement, chemically pure lime, and phosphoric acid and subjected to a column leaching process. Leachates were sampled and analysed using X-ray fluorescence and atomic absorption spectrometry. Results concluded that

Portland cement or lime reduced the quantity of leached arsenic by 40 to 80% relative to the control sample, whereas those treated with phosphoric acid yielded 50 times more arsenic. Portland cement reduced the total leached quantity of lead, selenium, copper, calcium, and total dissolved solids from 30 to 50% below the total leached quantities for untreated ash samples. Young *et al* (1984) concluded that generally samples treated with Portland cement showed the most uniform reduction in leachate concentrations and that compaction and curing of the chemically treated ash samples showed little improvement in the ability to control the amount and types of metals appearing in the leachates.

The difficulty with accepting aspects of this work relate to the fact that the type of chemically pure lime used was not stated i.e. either CaO, Ca(OH) or perhaps even $CaCO_3$. The maximum leached quantities of mercury and particularly lead in the fly ash were 0.0002μg/L and 0.011μg/L. These levels are so low that it is difficult to accept the absolute value even with a suggested error of 30% for the lead samples. Any differences brought about by addition of even a chemically pure fixing agent could have a significant contaminated fraction at these low detection levels and affect the leached quantity. Furthermore, the levels stated comparing control samples with cement treated samples and lime-treated samples show significantly different proportions of potential error with no apparent explanation in the text.

In conclusion, there is a clear lack of understanding regarding determination of appropriate chemical testing methods for assessment of lime-treated clay soils. Furthermore, it is evident that there is rarely an attempt to understand the mechanisms of contaminant interactions. There is a clear need to investigate the mechanisms of stabilisation and solidification reactions and to try to develop simple chemical batch tests to fulfil this requirement.

CHAPTER 3.0

3.0 RESEARCH PHILOSOPHY

Stabilisation and solidification agents, including lime and lime-based products, have been successfully used worldwide for the treatment of contaminated soils. However, the technique has not been used extensively in the UK. This is associated with the fact that the technique has been used unsuccessfully when applied inappropriately or without full understanding of the mechanisms. This has occurred, for example, at sites with large mixtures of organic and inorganic waste such as old gasworks (e.g. Portsmouth, 1998). There has been a move in the UK to begin to remediate contaminated land rather than dig it up and dispose of it in landfill. Stabilisation and solidification will prove important in this process due to its inherently low cost. However, to achieve this aim there needs to be a development of tests within the UK to measure the success or failure of stabilisation and solidification. When this has been achieved contractors will be able to tender for remediation projects knowing that it is possible to supply a client with guarantees as to the longer-term outcome of a stabilisation and solidification approach.

The literature has shown that there are several mechanisms controlling the success or failure of stabilisation and solidification of contaminated clay soils. These are:

- Clay natural attenuation of inorganic contamination.
- Modified clay natural attenuation of organics.
- Precipitation of metals at high pH.
    - Metal hydroxide solubility variations to be considered.
- Dissolution of clay structure and re-crystallisation of cementitious 'gels'.
    - Effects of contaminants on this solidification.

The mechanisms involving natural attenuation (cation exchange) are well understood and frequently investigated although they have seldom been considered specifically in the context of stabilisation and solidification. Solidification mechanisms are poorly understood and little research has been carried out to determine how clay dissolves and how this varies from one clay type to another.

Site-based research has usually been performed as a side issue to the main remediation project. This has resulted in incomplete pre-treatment and/or post-treatment physical and chemical investigations.

As a result of the current understanding and the incomplete and inconclusive research to date, the research reported in this thesis aimed to investigate the fundamental physico-chemical developments of lime-treated refined minerals containing high purity contaminants. Metal contaminants were chosen due to their presence at most contaminated sites and the fact that they are usually readily treatable with stabilisation and solidification. The contaminants Pb^{2+} and Fe^{3+} were chosen due to their frequent presence at contaminated sites and the fact that they have significantly different charge. English China Clay was chosen as one mineral for investigation because it was known that this mineral developed very small amounts of predominantly pH-dependent structural charge. Wyoming Bentonite was chosen as the second mineral because it represented the opposite extreme to English China Clay by having large quantities of predominantly permanent negative charge as well as pH-dependent charge sites. Since these minerals represented opposite extremes of structural charge development, it was felt that other clay minerals would exhibit physico-chemical behaviour between these extremes.

It was the aim to perform physical and chemical tests on sample mixes based on the two clays over three curing periods, after 7 days curing to allow for natural attenuation and metal precipitation (stabilisation) and after 175 days and 301 days curing to assess the developments of solidification. Two quicklime contents were chosen for each of the clays and, because it was important to assess the time-dependent developments for materials with no lime and/or no contamination, a full suite of control samples was required. This resulted in 9 mix designs for each clay.

The literature demonstrated that contaminated material was usually tested in rapid batch extraction tests often using an acidic leachant. Although the principle of a rapid cheap extraction test was a valuable concept, the use of an acidic leachant was considered inappropriate for assessing the mechanisms of a remediation technique that relies upon a high pH environment. Furthermore, natural attenuation mechanisms were also considered important to the understanding of stabilisation and solidification. These mechanisms would not be clear if the leachant contained high quantities of H^+ ions. Hence, an approach was formulated to use de-ionised water as a leachant in a batch extraction test. It was hoped that this would provide a more realistic extraction

environment in which to measure chemical changes brought about by cation exchange and mineral dissolution and re-crystallisation.

From the perspective of regulatory control, environmental scientists have been aware of the limitations of batch extraction tests to assess the leachability of contaminants from materials incorporated in a monolithic mass. Consequently this effect was examined by testing 10mm and 20mm monolithic masses. Due to the fact that the suggested batch extraction test no longer followed any standard protocols it was deemed necessary to investigate how the presence of monolithic masses was affected by adjusting the batch test parameters used to control the level of mixing. These included:

- Solid to liquid ratio,
- Mixer rotation speed,
- Test duration, and
- Initial size of monolithic mass.

To remove the effects of changing temperature conditions it was considered necessary to perform the tests in a regulated thermal environment of $11.5^0C \pm 0.5^0C$.

Chemical and physical analysis had to be performed using the resources available within the laboratory. Hence, chemical analysis of solutions was performed using Inductively Coupled Argon Plasma Atomic Emission Spectroscopy. Resources including the initial purchase cost and the final disposal through the University health and safety organisation stipulated that only small contaminated samples could be produced hence physical testing was limited to undrained shear strength measurements using the shear vane and also Atterberg Limit tests. This also limited the exposure of contaminated materials to a general geotechnical engineering laboratory where the health and safety of personnel were of paramount importance and subject to considerable regulation.

3.1 AIMS AND OBJECTIVES

The thesis aim is to determine whether the addition of lime to clay minerals can stabilise metal ionic contaminants by removing them from the aqueous phase.

Fulfilment of this aim will be achieved by meeting the following objectives:

- Develop a chemical batch leaching test which is suitable for assessing lime (specifically CaO) stabilised clays,

- Determine the leachability of contaminants (specifically $Pb(NO_3)_2$ and $Fe(NO_3)_3$) in the short term and longer term from lime treated contaminated clay,

- Investigate the soluble chemistry of the lime-clay reaction. Specifically, determine any substantial chemical behaviour changes from the short term to the longer term relative to control tests,

- Assess the effects of contaminants on the soluble chemistry of the lime-clay reactions and the effects of the lime-clay reactions on the contaminants,

- Determine physical changes by performing simple index tests, and finally,

- Compare the changes in the physical behaviour and water-soluble chemical behaviour to determine whether the lime-clay-contaminant reactions occur simultaneously or concurrently.

CHAPTER 4.0

4.0 EXPERIMENTAL METHODOLOGY

Prior to the commencement of this laboratory-based experimentation and final specification of the objectives, a clear outline of the experimental approach was prepared. This provided a well defined and logical progression to the experimentation, ensuring completion within the restricted time-scale and budget, and also allowed for the development of new ideas as the programme progressed. In outline, the experiments consisted of mixing lime with clays contaminated with heavy metals and monitoring the performance of the resulting mixes. Performance was measured in terms of the strength of the lime-clay mixes and leachability of the contaminants.

4.1 MATERIALS SPECIFICATION

4.1.1 Clay minerals

Two clay minerals were used in the investigations, English China Clay Grade 50 a white powder, was supplied by Watts, Blake, Bearne and Co. of Newton Abbott, Devon, UK. Wyoming Bentonite a light grey powder, was supplied by Steetley Minerals Ltd. of Middlesborough, UK (see Figure 4.1).

The dominant mineral composition of the English China Clay is well ordered kaolinite and muscovite, with minor constituents being quartz, feldspar and tourmaline. Some of the chemical and physical characteristics are described by the supplier in Table 4.1. For the purposes of this study the important characteristics described in the table are:

- the predominantly kaolinite nature ($Si_4Al_4O_{10}(OH)_8$),
- the high quantities of both silicon and aluminium oxides in similar proportions,
- the presence of mica (e.g. $KMg_3(AlSi_3O_{10})(OH)_2$ with K or Na exchangeable ions) and quartz (SiO_2) in low but potentially significant quantities,
- the 0% carbon content reducing the complexity of the chemical reactions,
- the slightly acidic pH, and
- the low surface area predicted for a kaolinite material in Table 4.1.

The Wyoming Bentonite clay is predominantly sodium montmorillonite with minor constituents of quartz and feldspars. The supplier's data in Table 4.2 summarise the mineral composition illustrating:

- the very high montmorillonite content, which along with the feldspars has a very high cation exchange capacity,
- the very high silicon oxide content relative to a high aluminium oxide content,
- the presence of significant proportions of iron, calcium, magnesium and sodium oxides,
- the high amount of 'structurally bound' water; and
- the very high, although significantly variable, liquid limit value.

Table 4.1 Mineralogical and chemical composition of English China Clay (adapted from Watts Blake Bearne & Co. PLC, 1998)

CHEMICAL	ULTIMATE ANALYSIS	MINERALOGICAL CONSTITUENT	CALCULATED COMPOSITION (RATIONAL ANALYSIS)
SiO_2	48.0 %		
TiO_2	0.1 %	Kaolinite	69 %
Al_2O_3	36.1 %		
Fe_2O_3	1.0 %	Potash Mica	24 %
CaO	0.1 %		
MgO	0.2 %	Soda Mica	1 %
K_2O	2.8 %		
Na_2O	0.1 %	Quartz	5 %
Loss on ignition	11.6 %		
Carbon	----	Carbonaceous matter	0 %
pH	5.0		
Surface area (by nitrogen adsorption)	12 m^2/g		

Table 4.2 Mineralogical and chemical composition of Wyoming Bentonite clay (adapted from Steetley Minerals Ltd, 1998)

CHEMICAL	CHEMICAL COMPOSITION (RANGE %)	MINERALOGICAL CONSTITUENT	CALCULATED COMPOSITION (X-RAY ANALYSIS)
SiO_2	62 - 66		
Al_2O_3	20 - 24	Montmorillonite	92 %
Fe_2O_3	3 - 4.5		
CaO	0.5 - 1.3		
MgO	1.7 - 2.3	Quartz	3%
K_2O	0.3 - 0.6		
Na_2O	2 - 4		
Bound Water	5.50	Feldspars	5%
Bulk Powder Density	800 - 950 kg/m^3		
Liquid Limit	600 - 750		

4.1.2 Lime used in laboratory investigations

The lime used throughout the experimental programme and referred to in this thesis is fine ground quicklime; calcium oxide ($CaO_{(s)}$) Grade SG60 supplied by Buxton Lime Industries (BLI). The physical untreated nature of the material is illustrated in Figure 4.1

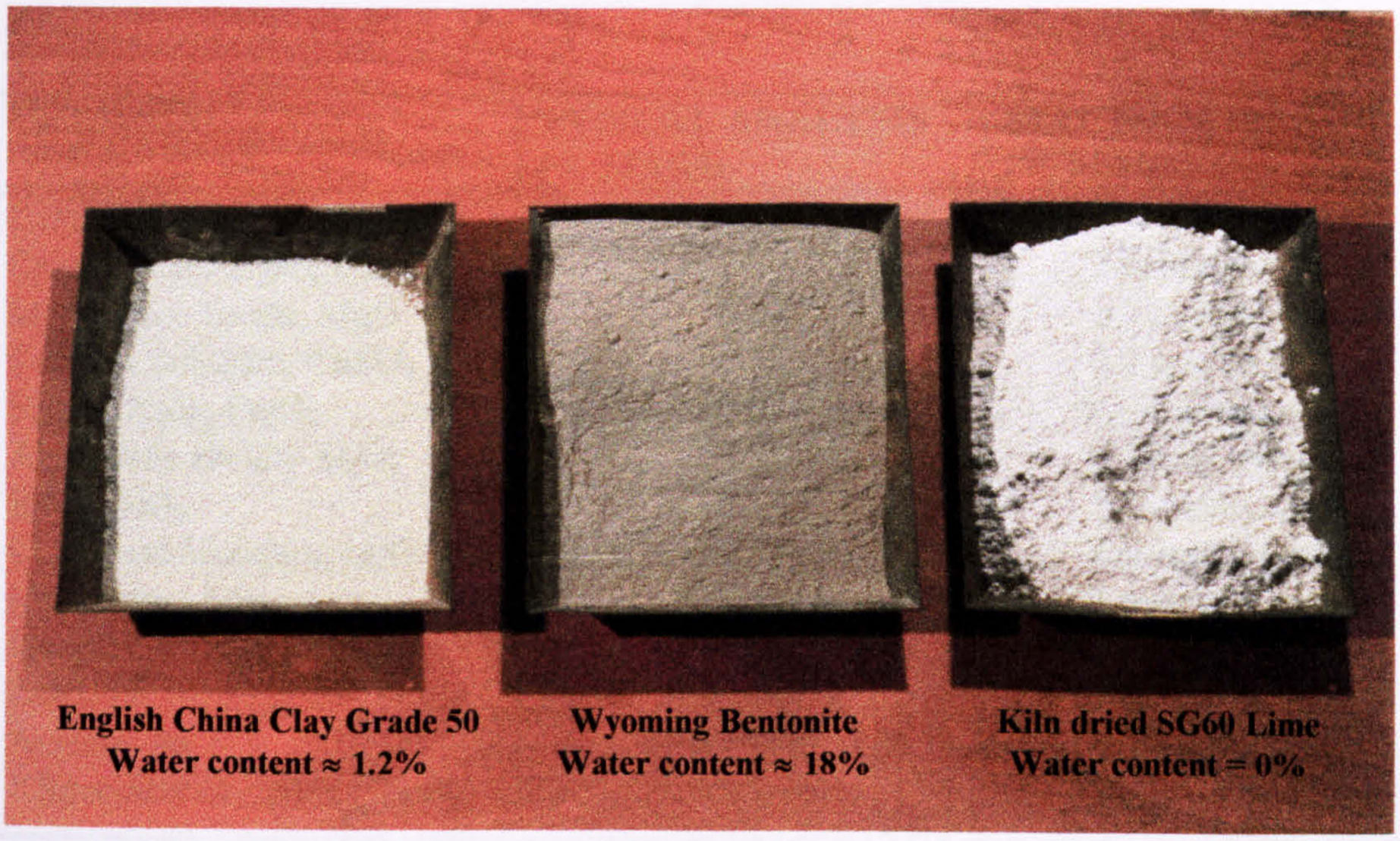

Figure 4.1 The untreated nature of the clay and the lime supplied

To ensure consistent chemical composition, all lime used during testing had been permanently stored in a kiln at or above 450°C for no longer than one month due to the gradual agglomeration of particles within that time in the kiln. Lime stored for longer than this period had been discarded. A minimum period of storage had been specified as 24 hours to ensure complete dehydration prior to use. Lime for use in all experimentation has been removed from the kiln and passed through a 420μm sieve whilst still hot and used immediately to reduce the potential for hydration and carbonation in the atmosphere. The particle size of SG60 highlighted in Table 4.4 ensured that obtaining the fraction < 420μm was a simple operation not requiring particle crushing hence reducing handling time in the atmosphere. Table 4.3 lists the principal components of the lime as being $CaO_{(s)}$ and $CaCO_{3(s)}$. The presence of forms of Mg, Fe, Al, Si, Mn, Pb in the lime is important, since these elements have been investigated in the main chemical batch testing programme discussed later. Analytical grade $CaO_{(s)}$ would have been used in preference to Grade SG60 to remove the interference of the trace elements in the chemical reactions and subsequent analysis. However, costs were inhibitive for the quantities required. It is also clear that in practice a form of lime similar to SG60 would be used *in situ*.

Table 4.3 Chemical composition of quicklime (CaO) SG60 (BLI, 1998)

CHEMICAL	TYPICAL ANALYSIS (% MASS)	SPECIFICATION * (% MASS)
Calcium Oxide, CaO	95.63	93.0 minimum
Calcium Carbonate, $CaCO_3$	2.23	7.0 maximum
Magnesium Oxide, MgO	0.47	1.0 maximum
Calcium Sulphate, $CaSO_4$	0.12	0.2 maximum
Ferric Oxide, Fe_2O_3	0.07	0.15 maximum
Aluminium Oxide, Al_2O_3	0.11	0.2 maximum
Silica, SiO_2	0.74	1.0 maximum
Combined Moisture, H_2O	0.63	1.0 maximum
Manganese, Mn	160 ppm	200 ppm maximum
Fluorine, F	70 ppm	100 ppm maximum
Lead, Pb	2 ppm	5 ppm maximum
Arsenic, As	0.4 ppm	1 ppm maximum

* Specification limits given at 95% confidence levels

Table 4.4 Physical composition of quicklime SG60 (BLI, 1998)

PHYSICAL	TYPICAL ANALYSIS (% MASS)	SPECIFICATION * (% MASS)
Grading : % passing 3.35mm	100	99.50 minimum
75 μm	54.7	30 minimum
Bulk density	1250kg/m^3	----
* Specification limits given at 95% confidence levels		

4.1.3 Contaminating metals added during the investigations

The reagents added to simulate inorganic metal contamination were lead (II) nitrate ($Pb(NO_3)_{2(s)}$) providing the lead (II) ion (Pb^{2+}) and, iron (III) nitrate ($Fe(NO_3)_3.9H_2O_{(s)}$) providing the iron (III) ion (Fe^{3+}). Both were of analytical reagent grade, supplied in solid form by Fisher Scientific of Loughborough. The two reagents were chosen due to their prevalence at many contaminated sites and their properties highlighted below:

- $Pb(NO_3)_{2(aq)}$ and $Fe(NO_3)_{3(aq)}$ are both acidic,
- $Pb(NO_3)_{2(aq)}$ and $Fe(NO_3)_{3(aq)}$ precipitate at high pH, and
- The charge to ion radius (ionic potential, see Figure 6.4) are significantly different which would create interesting differences in attenuation.

$Fe(NO_3)_3.9H_2O_{(s)}$ was chosen since it is relatively innocuous compared with lead. $Pb(NO_3)_{2(s)}$ was chosen since it was considered necessary to apply the technique to at least one environmentally toxic and problematic element that exhibits an amphoteric nature.

The nitrate form of these chemicals has been chosen for their high solubility (hence a potential for high cation mobility) and to limit the effects of the anion on the lime-induced pozzolanic stabilisation reactions. All nitrates are soluble and as such will not react with any elements released from the clays to form precipitates. Nitrates are also not currently reported to inhibit the stabilisation and solidification reactions. The high solubility allowed small volumes of reagents to be added in solution, allowing the relatively low water contents required to obtain optimum dry density to be achieved

easily. The high solubility also ensured a high degree of mixing of the reagents with the clay minerals resulting in more evenly distributed attenuation reactions.

Table 4.5 illustrates the respective chemical composition of these reagents. The trace elements were present in very small quantities. There were however slight differences in the quantities of trace elements present in the $Fe(NO_3)_3.9H_2O_{(s)}$ relative to the $Pb(NO_3)_{2(s)}$ that could have been significant. The chemical batch test analysis can detect levels of elements to fractions of a part per million, hence, it was important to mention their presence. The reported parts per million in Table 4.5 are on the basis of mass of ion to mass of compound added.

Table 4.5 Chemical composition of the $Fe(NO_3)_3.9H_2O$ and $Pb(NO_3)_2$ (Fisher, 1996)

$Fe(NO_3)_3.9H_2O_{(s)}$		$Pb(NO_3)_{2(s)}$	
LOT ANALYSIS	**QUANTITY**	**LOT ANALYSIS**	**QUANTITY**
Molecular Mass	404.00 g/mol	Molecular Mass	331.20g/mol
Acidity	0.06600 meq/g	pH (5%, aq. Soln.)	3.510
Assay	98.97 %	Assay	99.45 %
Calcium, Ca	**2.100 ppm**	**Calcium, Ca**	**< 0.500 ppm**
Total chloride, Cl^-	< 0.00050 %	Total chloride, Cl^-	< 0.00050 %
Copper, Cu	< 2.000 ppm	Copper, Cu	< 0.500 ppm
Potassium, K	< 2.000 ppm	Potassium, K	< 2.000 ppm
Magnesium, Mg	**2.600 ppm**	**Magnesium, Mg**	**< 0.200 ppm**
Sodium, Na	**< 2.000 ppm**	**Sodium, Na**	**< 10.000 ppm**
Total phosphorus, P	< 2.000 ppm	Total phosphorus, P	< 10.000 ppm
Lead, Pb	**5.600 ppm**	**Iron, Fe**	**< 1.000 ppm**
Total sulphur, S	< 4.000 ppm	Total sulphur, S	< 10.000 ppm
Total silicon, Si	**< 0.400 ppm**	**Total silicon, Si**	**< 0.500 ppm**
Zinc, Zn	13.000 ppm	Zinc, Zn	< 0.500 ppm

Bold characters are especially relevant to later chemical analysis.

Variable decimal places represent the degree of accuracy of the measurement equipment.

4.1.4 The water quality used at different stages of the investigations

Two grades of water were used throughout the study. The water used in all aspects of reagent and sample preparation and experimentation (unless otherwise stated) was prepared according to B.S. 3978 Grade 1 (BSI, 1987) and is hereafter referred to as ICP water. The lowest grade water hereafter referred to as RO water has been produced by purification of standard mains water using deioniser units

supplied by Purite Limited, Thame, Oxon, England. The mains water has been passed initially through a granular activated carbon filter, primarily to remove chlorine from the water. The water has then been passed through a Purite RO 100 reverse osmosis unit. This water provided typically 96% rejection of mineral ionisable impurities and 99.8% rejection of organics and bacteria. With medium hardness waters (up to 200ppm total dissolved solids) the quality achieved can be compared to that of single distilled water. The applications for this water were non-critical glassware rinsing and for the initial stages of cleaning laboratory soil mixers and spatulas. The RO water has been stored in 40 litre tanks and passed through a Purite STILLplus HP system to produce the B.S. 3978 Grade 1 ICP water on demand. This ICP water system comprised a N340 nuclear ion exchange cartridge, a C340 organic removal cartridge, a type BF02 (0.2μm) bacterial filter and a conductivity meter. The system is illustrated in Figure 4.2. The typical quality of this ICP water was critical for all chemical analysis and an analysis is detailed in Table 4.6.

Table 4.6 Typical ICP water quality (Purite, 1998)

IMPURITY			**TYPICAL QUALITY ACHIEVED**		
Conductivity at 25^0C			0.05 μS cm (18 megohm cm)		
Heavy Metals			0.0001 ppm		
Total Organic Carbon (T.O.C.)			< 30 ppb		
pH			Neutral		
Bacteria and Pyrogrens			99 % plus rejection		
Supplier suggested Applications	General Laboratory	Reagent Make Up	Glassware Rinsing	Atomic Absorption and ICP	Haematology

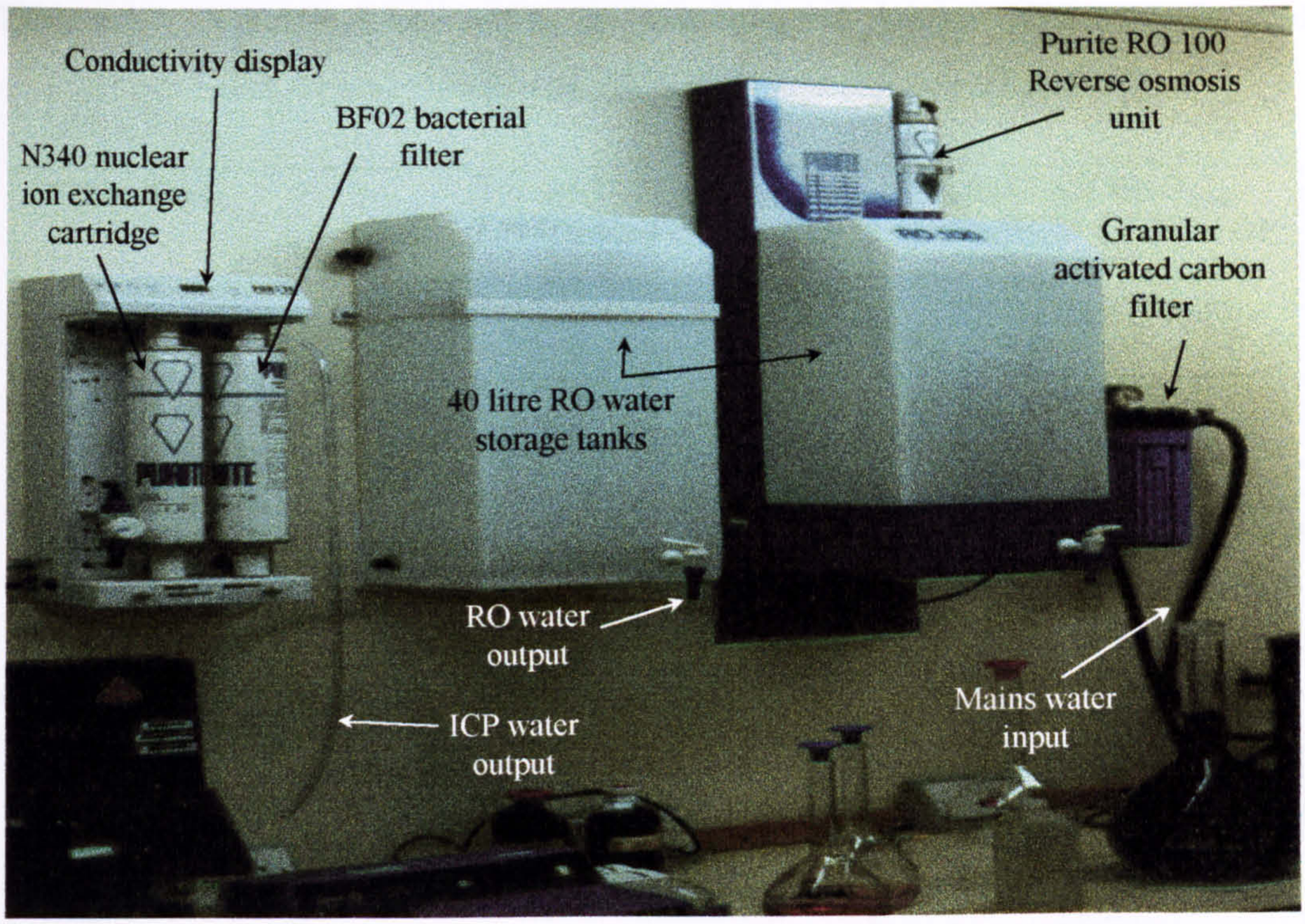

Figure 4.2 Water purification system for RO and ICP water production

4.1.5 Application and quality of acids used during the investigations

Where contaminated solids have been acid digested to determine acid digestible metal fractions or where chemical samples required stabilising prior to storage and subsequent chemical analysis, small quantities of high purity 'Aristar' nitric acid ($HNO_{3(aq)}$) and hydrochloric acid ($HCl_{(aq)}$) reagents supplied by B.D.H. Laboratory supplies, Poole were used. In all other situations such as acid washing batch leaching test containers or glassware to remove chemical residues a lower purity, less expensive GPR nitric acid has been used. Details of the high purity of these acids are shown in Table 4.7. It was clear that the addition of these acids to samples being preserved for sensitive chemical analysis would not significantly affect the results.

Table 4.7 Chemical impurities in concentrated Aristar Hydrochloric acid and Aristar Nitric acid (BDH Laboratory Supplies, 1998)

CHEMICAL	ARISTAR $HCl_{(aq)}$ MAXIMUM LIMITS OF IMPURITIES AFTER IGNITION (PPM)	ARISTAR $HNO_{3(aq)}$ MAXIMUM LIMITS OF IMPURITIES AFTER IGNITION (PPM)
Phosphate and silicate (as PO_4)	**0.1**	**0.1**
Sulphate (SO_4)	**0.2**	**0.5**
Aluminium (Al)	**0.005**	**0.02**
Arsenic (As)	0.005	0.005
Cadmium (Cd)	0.003	0.005
Calcium (Ca)	**0.005**	**0.05**
Chromium (Cr)	0.005	0.01
Cobalt (Co)	0.005	0.005
Copper (Cu)	0.002	0.005
Iron (Fe)	**0.1**	**0.2**
Lead (Pb)	**0.002**	**0.005**
Magnesium (Mg)	**0.005**	**0.01**
Manganese (Mn)	**0.005**	**0.005**
Mercury (Hg)	0.001	0.001
Nickel (Ni)	0.005	0.005
Potassium (K)	0.001	0.01
Sodium (Na)	**0.005**	**0.1**
Strontium (Sr)	0.005	0.01
Tin (Sn)	0.05	0.1
Vanadium (V)	0.01	0.01
Zinc (Zn)	0.005	0.01
Ammonium (NH_4)	0.5	----
Barium (Ba)	0.005	----
Molybdenum (Mo)	0.005	----
Free Chlorine (Cl)	0.5	----
Bromide and Iodide (Br)	50	----
(as sulphates)	**5**	----
Gold (Au)	----	0.01
Silver (Ag)	----	0.01
Chloride	----	0.1

Bold characters are especially relevant to later chemical analysis.

4.2 EQUIPMENT

4.2.1 Sample mixing and compaction equipment

All clay, contaminant and lime samples were mixed together using the z-blade mixer illustrated in Figure 4.3

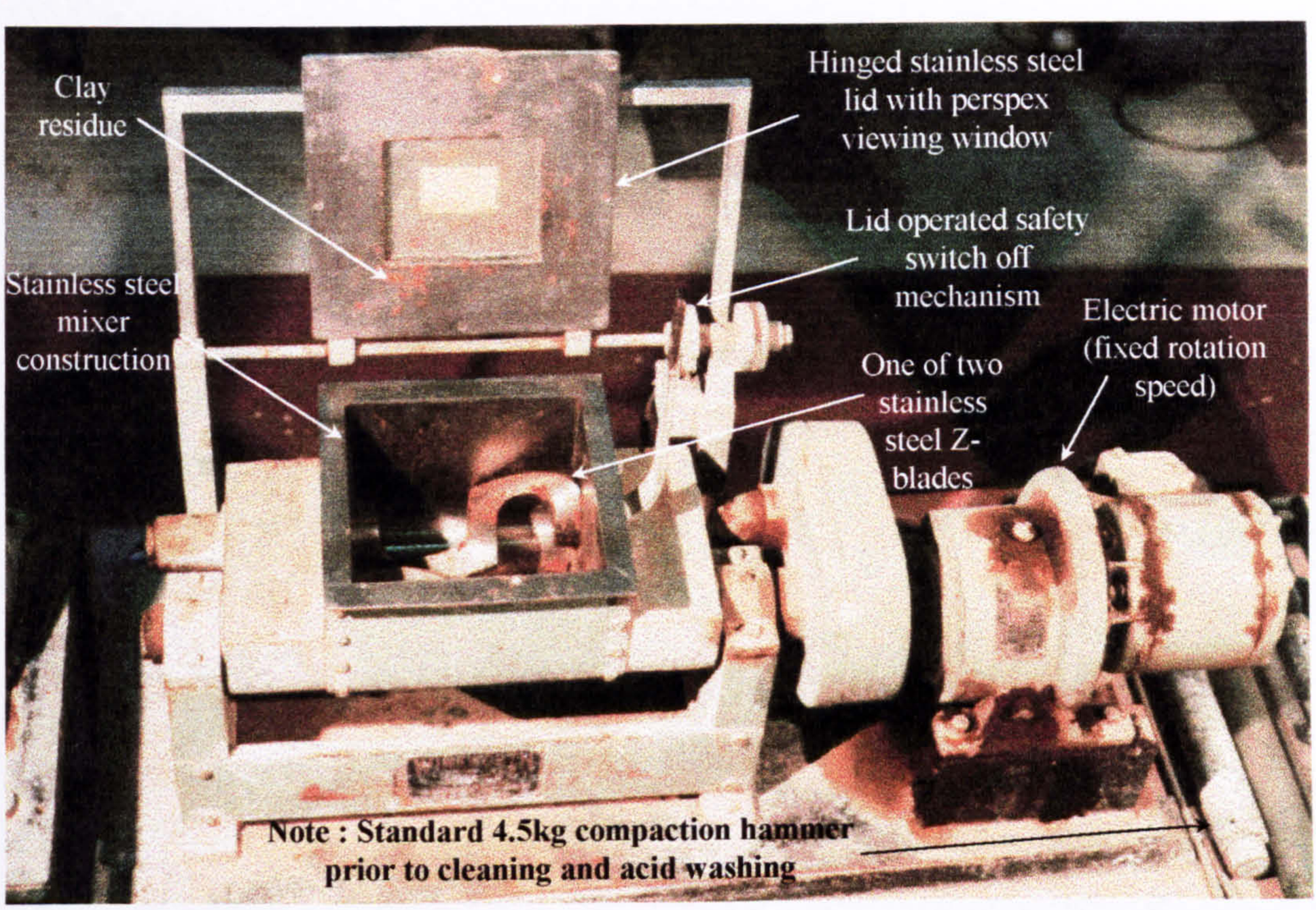

Figure 4.3 Z-blade mixing equipment prior to cleaning and acid washing

Prior to each mix all clay was cleaned from the mixer and the mixer washed with a 50% dilution of acetic (ethanoic) acid, a weak acid. $HNO_{3(aq)}$ would have been a more satisfactory cleaning agent, however, it was important not to damage the stainless steel construction of the mixer or potentially the mixer bearings. After acid washing, the mixer was rinsed with RO water twice and finally with ICP water.

Compaction was performed via two methods. Preliminary optimum water content compaction curve tests for the clay lime mixes were performed using a standard mechanical proctor compaction machine. The finalised mixes were compacted using a standard hand held 4.5kg hammer due to the dimensions of the compaction moulds (see note on Figure 4.3).

4.2.2 Chemical measurement

4.2.2.1 Batch test equipment

The batch testing equipment was based on the end over end mixer design of the ASTM Designation : D3987-85 Standard Test Method for Shake Extraction of Solid Waste with Water (ASTM, 1988). The mixer was designed to rotate 6×2l containers (a total mass of approximately 15kg) end over end about their centroid at speeds variable from zero to 300rpm within a cold room environment set at $11.5^0C \pm 0.5^0C$. The details of the constructed mixer are illustrated in Figure 4.4.

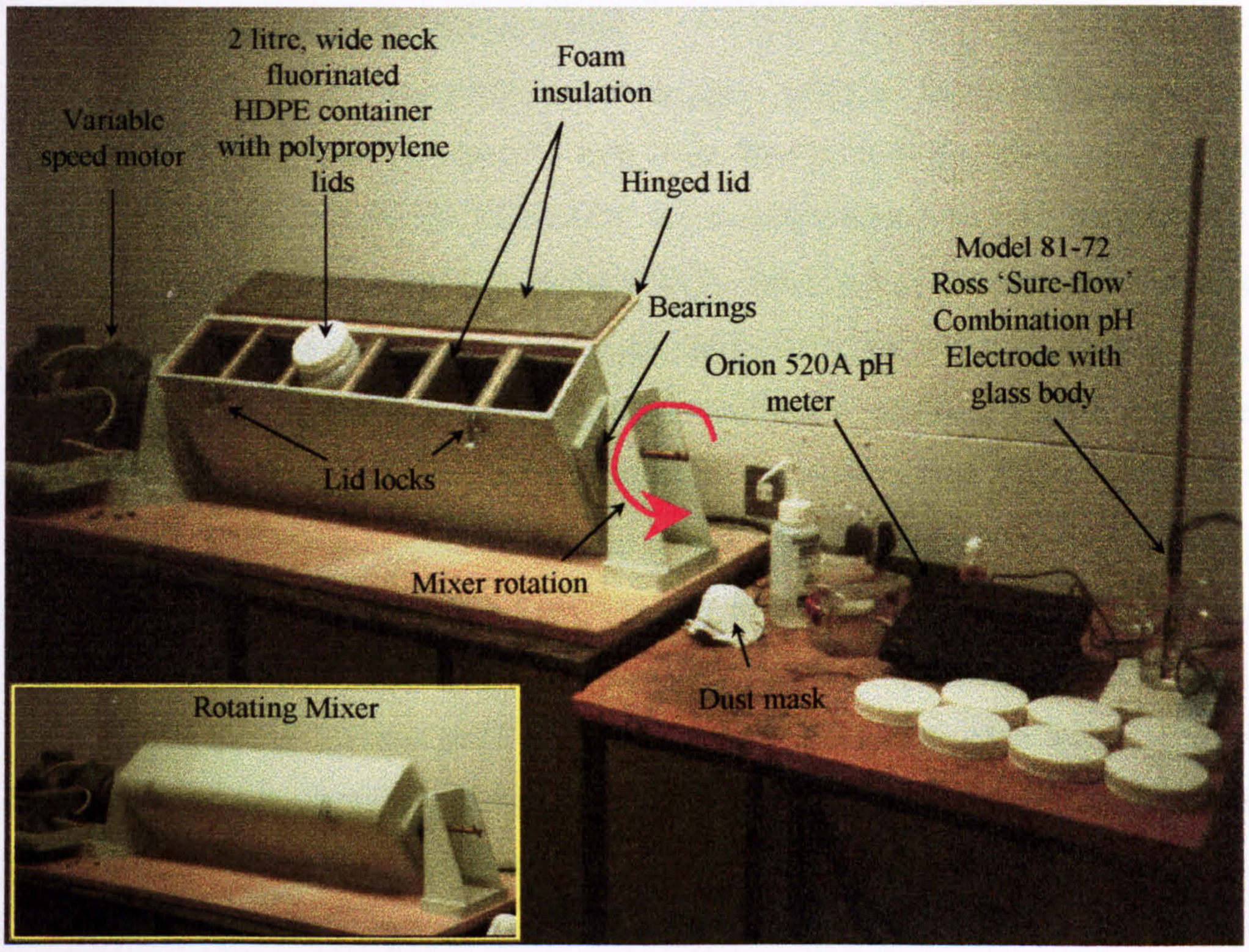

Figure 4.4 Constructed batch test mixer

The 2l containers used in conjunction with the mixer during the batch tests were Nalgene fluorinated high-density polyethylene (FHDPE) with wide necks and leak-proof polypropylene lids, specifically designed as short-term leaching containers. These were supplied by Fisher Scientific of Loughborough. Ideally Teflon containers would have been used for all testing, however cost was inhibitive since 18 containers were required to carry out the daily testing programme.

The batch mixer was located and run in a cold room especially constructed for the purpose of this testing programme. The dimensions of the room were 3m wide by 8m long by 3m high. The cold room plant consisted of an evaporator, a condensing unit, a thermostat to control the temperature and a clock to control the periodic defrosting of the condensing unit. This unit was designed to maintain a temperature range capability of 0^0C-16^0C when placed in a laboratory environmental air temperature of 16^0C-34^0C with lighting and mechanically induced heating loads. Design and installation was carried out by T.S. Refrigeration of Leicester.

4.2.2.2 pH and conductivity measurement

pH measurement was performed throughout using an Orion 520A pH meter supplied by QuadraChem Laboratories Ltd., East Sussex, in conjunction with a series of three Model 81-72 Ross 'SURE-FLOW' combination electrodes with glass bodies. The three electrodes were used in a rotation cycle dependent on the electrode cleaning requirements. All electrodes were cleaned according to the manufacturers instructions, however after use in Wyoming Bentonite based sludges, it was necessary to stand the electrode in 'Triton X' (a strong detergent) to remove residue and to keep the electrode within the required operating parameters. The probe was classified as being within operating parameters when the probe measured 0mV ± 35mV when placed in pH 7 buffer solution. Probes were calibrated prior to each measurement using three buffers pH 4.0, pH 7.0 and pH 9.2. Fresh buffers were used each day to ensure consistency of measurement. Before the pH buffers were used they were left in the cold room to achieve the correct temperature. These electrodes had a pH range of 0 - 14 over a temperature range of 0 - 100^0C. They were particularly recommended for use at pH>12 or <2 and had superior performance in 'dirty', difficult environments such as soil suspensions, sludges, colloids, viscous, and organics (Orion, 1998). For convenience, in conjunction with the pH electrodes, an Orion model 917005 epoxy construction automatic temperature compensation probe was used to correct pH readings to the equivalent pH at 25^0C.

The conductivity meter used in all testing was a Hanna Instruments HI 9033 Multi-range conductivity meter with automatic temperature compensation.

4.2.2.3 Solution separation techniques and ICP analysis

All solutions created by the batch tests and acid digestion tests requiring filtration were filtered through 150mm diameter Whatman No. 542 Hardened Ashless Filterpapers. All funnels and conical flasks used in this process were of plain borosilicate glass construction. Where filtration was not possible or not completely satisfactory, centrifuging was used. Where centrifuging was utilised, acid washed Nalgene Oakridge 50ml capacity Polysulfone centrifuge tubes were used. These were proved to be the most resistant to very high pH conditions. Although Teflon tubes have a higher resistance to the chemical attack, they must be used in a cooled centrifuge not available for this research. The centrifuge itself was a Hettich Universal 30F with an operating range of 0-11000 revolutions per minute (rpm).

All filtered solutions created for chemical analysis were stored in acid washed Nalgene 125ml capacity FHDPE wide necked bottles and stored in a cold room at $4 \pm 1^{o}C$. No sample was stored for longer than 48 hours before chemical analysis. All solution chemical analysis performed (unless stated otherwise) was to determine the soluble concentrations of Ca, Pb, Fe, Al, Si, Mg, Mn, and Na. This was achieved using an Atom Scan Inductively Coupled Argon Plasma Atomic Emission Spectrometer supplied by Thermo Jarrell Ash, and is illustrated in Figure 4.5

4.2.3 Physical analysis equipment

Liquid and plastic limits were carried out using the cone penetrometer equipment illustrated in Figure 4.6 and to an adapted British Standard methodology described in Section 4.6.

4.3 MATERIALS CHARACTERISATION

To establish a clear and successful programme of research it was essential to characterise the behaviour of the materials being used. Much of the chemical and mineralogical information has been obtained from the respective manufacturers and suppliers. The testing of other physical and chemical properties as well as general initial material preparation will be discussed in detail below.

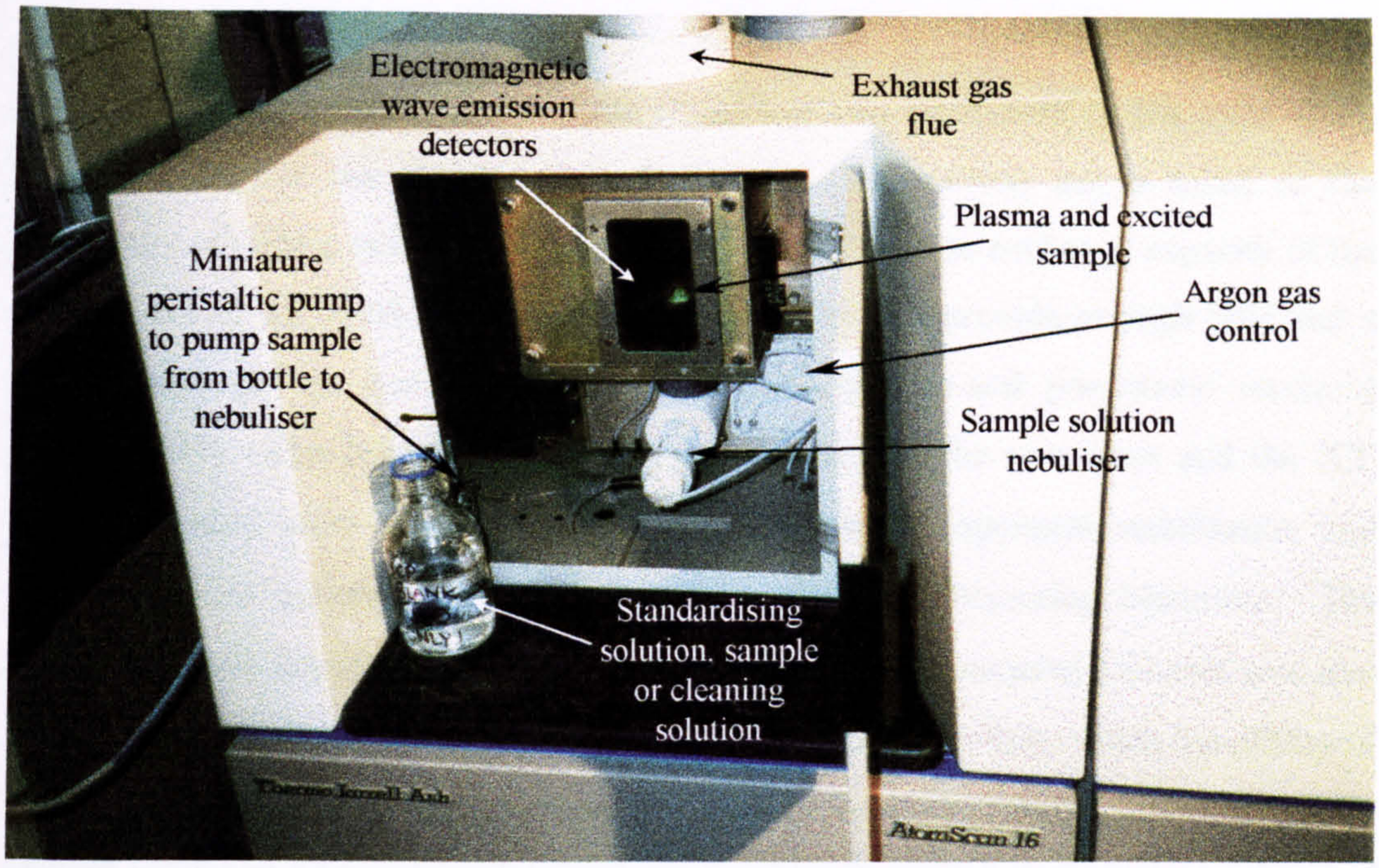

Figure 4.5 Computer controlled inductively coupled argon plasma atomic emission spectrometer

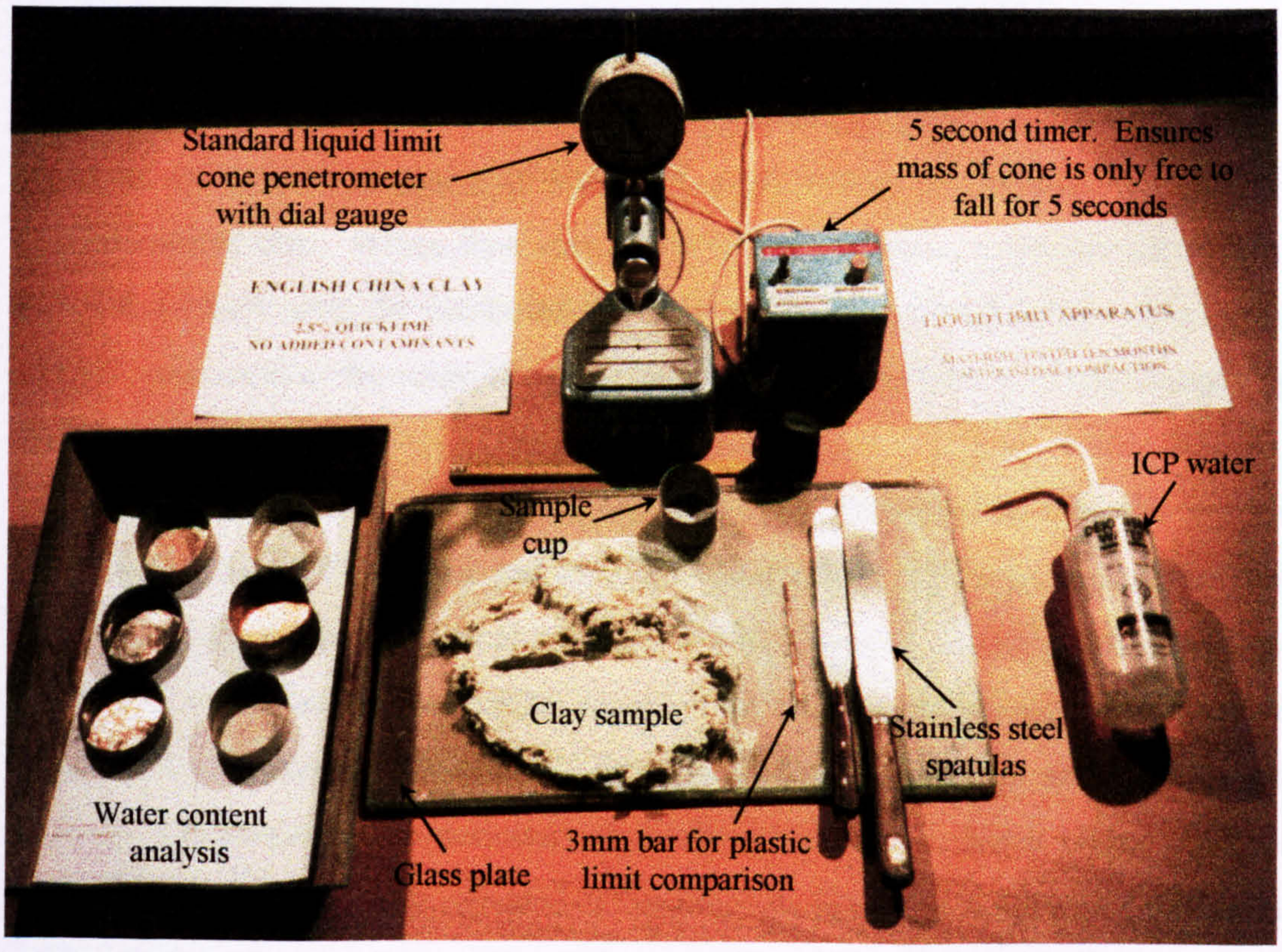

Figure 4.6 Liquid and plastic limit analysis equipment

4.3.1 Lime requirement

The initial consumption of lime (ICL) test was performed to BS 1924 (BSI, 1990A). The test was developed by Eades and Grim (1966) and is based on the philosophy of adding sufficient lime to a soil to satisfy cation exchange capacity of the soil and satisfy all initial or short-term reactions yet still provide enough lime and a high enough pH to sustain the strength-producing lime-soil pozzolanic reactions (Little, 1995). The ICL test was performed on each of the two clays and the ICL values obtained were the basis for all mix designs for optimum stabilisation and solidification of uncontaminated English China Clay and Wyoming Bentonite. The quantity of lime determined by the ICL test on the uncontaminated minerals was also added to the contaminated samples. This provided the datum from which the effects of addition of contaminants were assessed. Variations in physical and chemical behaviour depend on the concentration of calcium and hydroxide ions and since the addition of contaminating metal cations may reduce the quantity of hydroxide ions in solution through precipitation reactions, the differences observed were significant. The concentration of calcium ions affects the degree of cation exchange which can occur and since cation exchange is involved in the initial modification reactions this was also significant. Hence it was very important to add the same quantities of lime to both contaminated and uncontaminated samples to be able to compare results. Lime was added to an uncontaminated clay based on a percentage of the dry mass of the uncontaminated clay. Where lime was added to a contaminated clay this percentage was added based upon the combined dry mass of clay and contaminant. The error incurred was small as the mass of contaminant was only small (20g of contaminant in 4000g of clay).

The initial consumption of lime test (ICL) was performed in accordance with BS 1924 for English China Clay and an adapted method for Wyoming Bentonite. This was because the inherent physical swelling characteristics of Wyoming Bentonite on addition of water made it impossible to carry out the test by adding only 100ml of water to 20g of Wyoming Bentonite. In order to obtain a solution whereby the pH could be determined it was necessary to perform the tests at much higher solid to liquid ratios. The tests were repeated as described by BS 1924 but at a range of solid to liquid ratios, including 20g : 300ml, 20g : 520ml and 20g : 1000ml. Although it was evident at specific lime contents that lower solid to liquid ratios resulted in lower pH

values as predicted by the equation for pH (Equation 4.1), the maximum pH plateau at each of these solid to ratios occurred within half of one percent percentage lime addition.

$$pH = -Log_{10}[H^{+}\text{concentration (mole/dm}^3)] \qquad \textbf{Equation 4.1}$$

On this basis a close approximation of the optimum lime content was determined. Rogers *et al* (1997) investigated in detail the effects of solid to liquid ratio on the ICL value.

4.3.2 Compaction

Compaction control was considered to be an influential factor in this study because it affected the interpretation of virtually every aspect of the physical and chemical testing hereafter. The compaction of materials containing a variety of inorganic compounds created a situation with conflicting interests in respect to test data comparison. In the final application of this treatment method *in situ*, the aim of compaction is to maximise density and therefore minimise voids and permeability. Based on this hypothetical ideal, the first and most appropriate condition for a contaminated site would be to determine the optimum compaction conditions for each specific soil condition and contaminant condition. The addition of a single anion or cation in solution can have a large effect on the level of compaction of a clay. This behaviour is dependent on the chemical structure of the mineral. If the mineral has the capacity for cation exchange, which is the case for Wyoming Bentonite, flocculation of particles may occur. Investigations of the addition of lime to clays frequently refer to this phenomenon as modification. It is also reasonable to suggest that the development of the pozzolanic reactions over various curing times are affected by the initial compaction conditions, since this has direct influence on particle spacing and subsequently crystallisation reactions.

For a standard compactive effort at the optimum water content an optimum dry density of 1200kg/m^3 was achieved for Wyoming Bentonite alone whereas on the addition of 2.5% lime an optimum dry density of 1070kg/m^3 was achieved. The compactability issue was complicated further on the addition of lime with $Fe^{3+}_{(aq)}$ and $Pb^{2+}_{(aq)}$ cations due to the precipitation of the insoluble metal hydroxides and increased

flocculation. In the context of this research, a varying level of compaction for each clay, each lime content, each contaminant and all the associated mix combinations of these would have made comparison of physical and chemical data difficult.

In order that the time-dependent effects of the contaminants on the lime-stabilised clays could be determined the optimum water content for a specific compactive effort was determined for each of six clay and lime mixtures not accounting for the effects of the added contaminants. This resulted in six optimum water contents. When Pb^{2+} or Fe^{3+} ions were added to these six mixtures, the optimum water contents of the respective uncontaminated sample was used, thus allowing for direct comparison of the effects of contaminant addition.

Two compaction test methods were adopted to determine the compaction characteristics of the clay lime mixes. The first method was performed in accordance with BS 1377 (BSI, 1990B). This method was used solely for English China Clay with no added lime or contaminants. An automatic compaction machine set for a 1l 'Proctor' mould and a 50mm diameter circular faced 2.5kg hammer falling 300mm, 27 times on each of the three compaction layers in the 1l mould was employed for this purpose. This resulted in a compactive effort of 596 kJm^{-3} being applied.

As previously discussed the addition of lime causes a chemical reaction with a clay mineral changing its physical properties. The initial modification is almost instantaneous and further reactions are time-dependent. To obtain the compaction characteristics of this modified clay the time between mixing the lime with the hydrated clay and the moment the mix is compacted had to be accounted for. Additionally re-use of this modified clay after a single compaction was not appropriate since properties were changing within seconds to minutes of mixing. Hence to obtain a series of dry density and water content relationships the clay water content had to be adjusted prior to the addition of lime. For these reasons an adaptation of BS (1377) was performed on mixes of both English China Clay and Wyoming Bentonite where lime was added. This adapted method was also used for Wyoming Bentonite with no added lime or contaminants. It was found that water added to previously hydrated Wyoming Bentonite would not mix thoroughly due to the hydrated clay agglomerating into large pieces with the additional water acting only to lubricate the movement of this mass around the inside of the mixer. The following mixes were investigated with the adapted method.

- English China Clay with 0.5% lime,
- English China Clay with 1.5% lime,
- English China Clay with 2.5% lime,
- Wyoming Bentonite with no added lime,
- Wyoming Bentonite with 2.5% lime,
- Wyoming Bentonite with 7.0% lime, and
- Wyoming Bentonite with 10.0% lime.

In all cases the percentage lime addition was based on the dry mass of clay present. The initial consumption of lime (ICL) values for English China Clay and Wyoming Bentonite were 1.5% and 7% respectively. In both cases a lime content both higher and lower was chosen with 2.5% lime allowing direct comparison of water content-compaction characteristics of both clays.

The method for the above stated mixes was varied from BS1377 in the following ways :

1. Twenty four hours prior to compaction testing, the unhydrated clay to be used in testing was placed in a sealed polythene bag to prevent water loss or gain and a sample taken for water content analysis.

2. The equivalent of 4kg dry mass of clay (to the nearest 0.01g) was placed in the mixer with the required mass of water to achieve the desired water content for compaction.

3. The sample was sealed in the mixer to reduce loss of water from evaporation and thoroughly mixed for 20 minutes. If lime had not been added, the sample was then mixed for a further 20 minutes. If required, lime was evenly distributed over the mixing clay in the desired percentage, and allowed to mix for the further 20 minutes.

4. Water content was measured prior to performing a compaction test according to BS1377. Over a ten minute period, the clay was broken into 20mm pieces and the compaction test was performed. At the end of the test a further measurement of water content was made and compared with that immediately prior to mixing to evaluate losses due to evaporation throughout the test.

5. The mixer was cleaned and washed with single distilled water, dried and a new clay sample added.

6. Steps 1 to 5 were repeated continuously at incremental values of water contents until the relationship between water content and dry density was observed.

4.3.3 Levels of contamination

Literature illustrates that contamination can be present in hugely varying concentrations from hundreds of parts per million to tens of thousands of parts per million. A level of 5000ppm of contamination was chosen primarily because 5000ppm would react with significant quantities of hydroxide ions and because of the risk associated in using higher levels in the laboratory. The large effects due to flocculation on Atterberg Limits and shear strength due to small additions of ions such as Ca^{2+} ions are highlighted by Anson & Hawkins (1998). This highlighted that a concentration of 5000ppm of contamination would have a significant effect on measured properties. The quantity of contaminant was added based on a mass of Fe^{3+} ion and Pb^{2+} ion to dry mass of clay basis and not based of the equivalent number of moles of Fe^{3+} ion to Pb^{2+} ion for the following reasons :

1. Lead is very toxic via ingestion, inhalation and absorption through the skin, hence it was not desirable to use unnecessarily high quantities in the laboratory.

2. The resulting varying amount of positive charge from adding 5000 ppm $Pb^{2+}_{(aq)}$ and 5000 ppm $Fe^{3+}_{(aq)}$ would provide useful information regarding the varying effects of $OH^-_{(aq)}$ removal from the system hence the effects on the initial and longer-term time-dependent strength increases brought about by lime addition. Ultimately this

could indicate whether the initial increase in strength is truly due to cation exchange and that subsequent strength increase is due to the production and crystallisation of calcium-aluminium-silicates.

3. The cost of adding the mole equivalent of each ion was inhibitive.

4.4 LABORATORY 'FULL-SCALE' SAMPLE PREPARATION

4.4.1 Introduction

The high cost of the contaminants required that the quantity of clay in each mix was not significantly greater than that required to fulfil the test requirements for that particular mix. A proportion of each mix combination of lime, clay and contaminant was to be tested on twelve occasions; four batch tests with varying operating parameters repeated at three different curing periods. The ASTM D3987-85 Standard Test Method for Shake Extraction of Solid Waste with Water (ASTM, 1988) recommended batch test containers should be between 80% - 90% full by volume. Knowing the volume of the containers the solid to liquid ratio of each batch test and the relative densities of each of the compacted clay-water-contaminant and lime mixes it was possible to calculate precisely the required mass of sample for each batch test. This enabled detailed planning and calculation of costs. Sixteen kilograms of each mix design were required to fulfil the test requirements. Limitations in the number of batch tests physically possible in a single day required six batch tests on each of four consecutive days. This combined with the limited four kilogram mechanical mixer capacity led to four mixes of the same mix design compacted into four separate compaction tubes over a four day period. Although this could not have been avoided, the clear disadvantage was the potential for slight variations in mix quantities of clay, contaminant and lime.

4.4.2 Contaminant preparation

In order to achieve a consistent level of mixing of the clay and contaminant, the contaminant was added as a solution. To simplify addition of contaminant solutions to

the clays bulk quantities of the required solutions were prepared such that each 200ml of ICP water contained 20.0000g ± 0.0001g of either the Fe^{3+} or Pb^{2+} ion.

4.4.3 Clay-contaminant-lime mix preparation

The full-scale testing samples were prepared and compacted in a similar manner to that described in Section 4.3.2. This was performed as follows :

1. Approximately 4kg of untreated clay of known water content measured to ± 0.01g was placed in the mechanical mixer (see Figure 4.3).

2. The mass of water to be added to achieve the required water content for compaction was calculated. If a contaminant was not to be added to the mix, this mass of ICP water was added to the clay and mixed for 20 minutes. Where contaminant was added to the mix, the effective dry mass of clay in the mixer was calculated and the required mass of contaminant ion to be added to the effective dry mass of clay to achieve the required 5000ppm contaminant to dry clay ratio calculated. The volume of contaminant solution was then calculated along with the extra ICP water needed to achieve the required final clay water content for compaction. The volume of contaminant solution to be added was measured precisely using pipettes and burettes. The contaminant solution and the extra ICP water were mixed together and added to the clay in the mechanical mixer and mixed thoroughly for 20 minutes. After this period a sample of the mixture was taken to measure water content and the remainder removed from the mixer and sealed in polythene bags for 24 hours at $11.5^0C \pm 0.5^0C$ to allow for any cation exchange or adsorption to occur. Where a contaminant was not added, these samples were also stored for 24 hours at $11.50^0C \pm 0.5^0C$ to ensure consistency in the methodology.

3. After 24 hours storage and cleaning of the mixer, the mass of the bag and clay was measured and the contents of the bag placed in the mixer again. Measuring the mass of the emptied bag allowed the precise mass of the clay in the mixer to be calculated. Using the measured water content of the clay in the bag the effective dry mass of clay and contaminant in the mixer was calculated. Based on this

effective dry mass of clay and contaminant, the required mass of lime to be added was calculated. This mass of lime was evenly distributed over the mixing clay mixture and allowed to mix for 20 minutes. In the event that lime was not added, the sample was still mixed for 20 minutes. Where contaminants were added the lime added to the mixture was based on the combined dry mass of clay and contaminant because in the field the precise mass of contamination may not be easily assessed from one region to another.

4. The sample mixes were broken into pieces of 20mm or less and compacted into pre-weighed twin wall HDPE pipes 2% wet of the optimum water contents measured in the preliminary compaction tests under the compactive effort of 596 kJm^{-3}. The precise details for the compaction of the full-scale samples is illustrated in Table 4.8.

5. The compacted samples were trimmed and the material density determined. The samples were sealed to the atmosphere by pouring molten paraffin wax at 40 ± 5.0^{0}C on each end of the sample in the mould and allowing it to solidify on cooling. The samples were stored at 11.5^{0}C ± 0.5^{0}C until required for testing at each of the three time-dependent curing periods, 7days, 175days and 301days. The process was repeated for the three other mixes of the same clay, contaminant and lime proportions and then for all other mix specifications. One sample preparation was carried out on each of 72 days to allow for consistency of curing period when samples were batch tested on 72 consecutive days for each of the three curing periods. Hence mixing occurred over 72 consecutive days and batch testing over 216 days. Figure 4.7 illustrates one of the standard compacted samples waiting for shear strength determination and subsequent extraction for batch testing at 301 days after initial compaction.

Table 4.8 Compaction specifications of full-scale mixes in twin-walled plastic pipes

	CLAY / CONTAMINANT / LIME MIX DESIGN					
	ENGLISH CHINA CLAY			WYOMING BENTONITE		
SPECIFICATION	Clay only or Clay + 5000ppm Fe^{3+} or Clay + 5000ppm Pb^{2+} (NO ADDED LIME)	Clay only or Clay + 5000ppm Fe^{3+} or Clay + 5000ppm Pb^{2+} (1.5% LIME)	Clay only or Clay + 5000ppm Fe^{3+} or Clay + 5000ppm Pb^{2+} (2.5% LIME)	Clay only or Clay + 5000ppm Fe^{3+} or Clay + 5000ppm Pb^{2+} (NO ADDED LIME)	Clay only or Clay + 5000ppm Fe^{3+} or Clay + 5000ppm Pb^{2+} (2.5% LIME)	Clay only or Clay + 5000ppm Fe^{3+} or Clay + 5000ppm Pb^{2+} (7.0% LIME)
Required water content according to initial compaction tests (%).	29.30	34.45	35.65	46.00	58.30	60.60
Mould diameter (m).	0.150	0.150	0.150	0.150	0.150	0.150
Total compacted depth (m).	0.130	0.130	0.130	0.170	0.170	0.170
Compaction hammer mass (kg).	4.5	4.5	4.5	4.5	4.5	4.5
Compaction hammer fall height (m).	0.450	0.450	0.450	0.450	0.450	0.450
Number of compaction layers in mould.	3	3	3	3	3	3
Number of compaction hammer drops per layer.	23	23	23	30	30	30
Applied compactive effort.	596	596	596	596	596	596

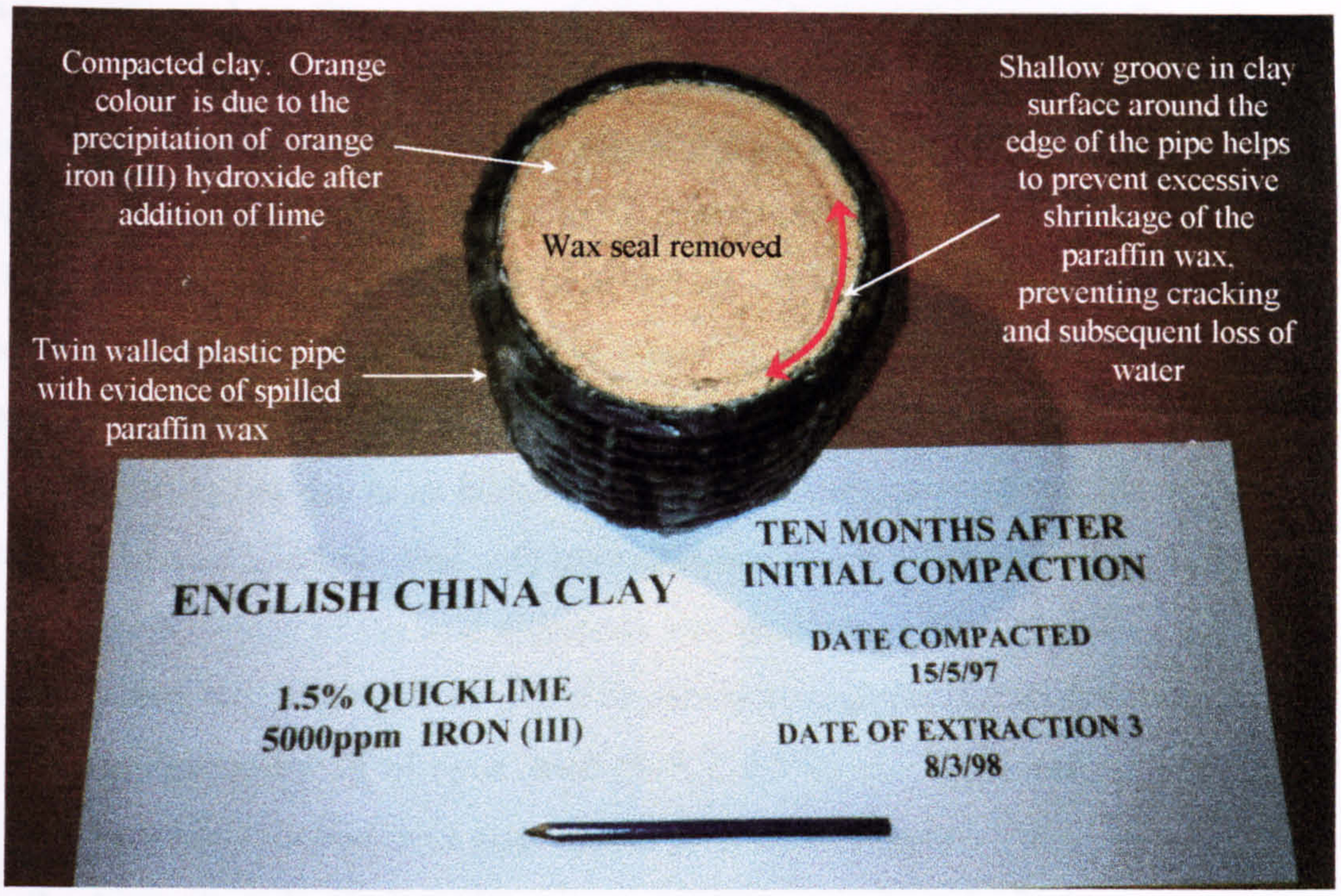

Figure 4.7 Compacted sample for full scale laboratory testing

4.5 BATCH TESTING

The aim of batch testing was to measure changes in the concentrations of the water soluble contaminants, lime and elements from the clay structure due to the time-dependent lime reactions. To assess the effect of the batch test parameters on the changes in concentration of soluble elements a series of batch tests with varying operating conditions were performed.

4.5.1 Pre-batch test clay analysis via acid digestion

Prior to initiation of the batch tests it was necessary to determine the most important chemical elements involved during the lime reactions and assess which elements were most likely to be released into solution during the whole batch-testing schedule for all mix designs. This was important due to the very high financial and time cost of ICP analysis. Clearly soluble Ca, Fe, and Pb had to be measured since their reactions within the clay environment were of immediate interest. To determine

the other significant elements for analysis a very aggressive series of acid digestions were performed on three samples of each uncontaminated untreated clay using a mixture of nitric and hydrochloric acids. One sample was acid digested once, another acid digested twice and the third acid digested three times. Comparison of data from these three samples determined the most appropriate number of acid digestions for future tests to determine the total acid soluble fractions. Complete digestion and analysis of the clay was not possible since this would have required the use of hydrofluoric acid to dissolve the silicates and aluminates. This compound was banned from the laboratory due to its health and safety implications as well as the fact that it can only be used in conjunction with laboratory equipment constructed from Teflon.

The methodology of the acid digestions was determined by a laboratory approved method, since resulting solutions would be passed through the ICP analysis equipment:

1. Approximately 1g of oven dried (105 $\pm$ 0.5^{0}C) clay measured to 0.1mg was placed into each of three acid washed glass conical flasks.
2. Approximately 40ml of ICP water was added to each of the flasks.
3. Via a pipette precisely 2.7ml of Aristar concentrated HCl and 1.3ml of Aristar concentrated HNO_3 were added to each of the three conical flasks.
4. Further ICP water was added until the total volume of each flask was approximately 50ml.
5. An acid washed stirrer magnet was added to each flask and the flasks placed on a heated magnetic stirrer in a fume cupboard where the samples were allowed to simmer gently, gradually evaporating the solution until only 5ml of solution remained in the flask.
6. Approximately 40ml of ICP water was added to each of the three flasks. One sample was gently warmed and filtered into a volumetric flask.
7. Stages 3,4,5 were repeated for the other two samples.
8. Approximately 40ml of ICP water was added to each of the flasks. Again one sample was gently warmed and filtered into a volumetric flask.
9. Stages 3,4,5 and 8 were repeated for the final flask.
10. The residues of each sample were all rinsed into the volumetric flasks with ICP water and the volume made up to precisely 100ml or 200ml.
11. Samples were shaken and stored at 4 $\pm$ 0.5^{0}C until ICP analysis.

12. Stages 1 to 11 were repeated for the other clay type.

The ICP analyser (Figure 4.5) was standardised (calibrated) using three 'multiquant' solutions to analyse the solutions produced from the above acid digestions, which enabled the system to rapidly test the concentration ± 20% of several elements. The elements included: Mg, Al, Ca, Cr, Mn, Fe, Co, Ni, Cu, Zn, As, Se, Sr, Ag, Cd, Ba, Hg, Pb, Bi, Li, Ti, Be, V, B, Sn, Na, Zr, P, K, Mo, and W. Based on an analysis of the acid soluble concentrations of these elements from the clay minerals, the following eight elements were considered significant and included in the ICP analysis of batch test solutions: Fe, Pb, Ca, Na, Si, Mg, Al and Mn.

4.5.2 Batch testing methods and undrained shear strength measurements

Each batch test was performed on a daily basis in the order in which the samples were created, thus allowing each sample to be tested at exactly the same time interval after initial mixing and compaction. The batch tests were performed on 4 samples of each design mix detailed in Table 4.8. Each of the four compacted samples from each of the 9 mix designs were allocated to one of the following set of batch testing parameters:

- 6 hour test duration, 30 rpm mixer rotation speed,
- 24 hour test duration, 30 rpm mixer rotation speed,
- 6 hour test duration, 60 rpm mixer rotation speed, and
- 24 hour test, 60 rpm mixer rotation speed.

Once allocated to one of the series of parameters, the sample was tested under these parameters for each of the three time periods i.e. 7 days, 175 days and 301 days. Due to the limited availability of time during one day, only one mixer could be operated on a daily basis, hence, one set of the above mentioned parameters were tested each day. The mixer illustrated in Figure 4.4 was therefore designed to hold six containers to test the following material parameters under each of the 4 batch test mixing parameters:

- 10mm solidified cubes, 1:10 solid to liquid ratio (0.170kg of dry solid),
- 20mm solidified cubes, 1:10 solid to liquid ratio (0.170kg of dry solid),

- 10mm solidified cubes, 1:20 solid to liquid ratio (0.090kg of dry solid),
- 20mm solidified cubes, 1:20 solid to liquid ratio (0.090kg of dry solid),
- 10mm solidified cubes, 1:40 solid to liquid ratio (0.045kg of dry solid), and
- 20mm solidified cubes, 1:40 solid to liquid ratio (0.045kg of dry solid).

After 301 days (approximately 10 months), only the samples previously tested in 6 hour 30rpm and 24 hour 30 rpm batch tests were tested for a third time. This was carried out to free time for other tests and reduce costs.

Twenty four hours prior to a batch test, the water content of the sample was assessed from the residues of a series of three shear vane measurements taken on the sample prior to extraction. The shear vane tests were performed in accordance with BS 1377 (BSI, 1990B) with the exception of the requirements for depth of vane penetration and the spacing of measurements. Unfortunately each plastic mould contained the samples to be tested at three time periods, subsequently limiting the available depth of penetration of the shear vane to 40mm. The spacing suggested by the standard for a circular mould was also not followed since this would have significantly disturbed a large proportion of the sample required to remain in tact for the batch tests. This made it impossible to follow the precise British Standard test method, although the approach remained consistent throughout. The method is illustrated in Figure 4.8.

After performing the strength test one third of a compacted sample was removed in one circular piece by cutting the tube and sample with a high tensile strength stainless steel wire. The removed sample was stored in a sealed plastic bag over night and the remaining compacted sample in the plastic tube was re-sealed with paraffin wax. Both the removed and re-sealed samples were stored in the cold room at $11.5^0C \pm 0.5^0C$.

On the morning of a batch test the solidified sample was cut using a stainless steel cheese wire and a scalpel into 10mm and 20mm cubes. The six 2l containers were filled with the required amount of wet material of the appropriate cube size to achieve the desired dry mass content to a precision of 0.01g. The mass of water in the solid material was calculated and further ICP water was added to achieve the desired dry solid to liquid ratio. To ensure that the material remained at 11 ± 0.5^0C desired for the test, the added ICP water was stored at 11 ± 0.5^0C over night prior to addition to

the 2l containers. The containers were then placed in the mixer in Figure 4.4 and the test initiated. During the 6 hour tests the mixer was stopped every hour for 10 minutes whilst pH and conductivity of the six samples was monitored. During 24 hours tests the mixer was stopped every 2 hours for the first 6 to 8 hours to monitor pH and conductivity. The 24 hour tests were then allowed to run over night and pH and conductivity measured at the end of the test. At the end of the test the samples were left undisturbed for 10 minutes and approximately 200ml of solution filtered through Whatman 542 hardened ashless filter papers. It was clear that all English China Clay solids separated easily from the solution making filtration the most favoured method of separation. However, Wyoming Bentonite exhibited a high degree of physical behavioural variation dependent on the contaminant and lime mix designs. It was clear that at high lime contents and iron (III) contents the solid material flocculated allowing significant separation of solid from liquid, hence, filtration was the most favoured method to ensure uniformity in methodology. This flocculation is evident in Figure 4.9.

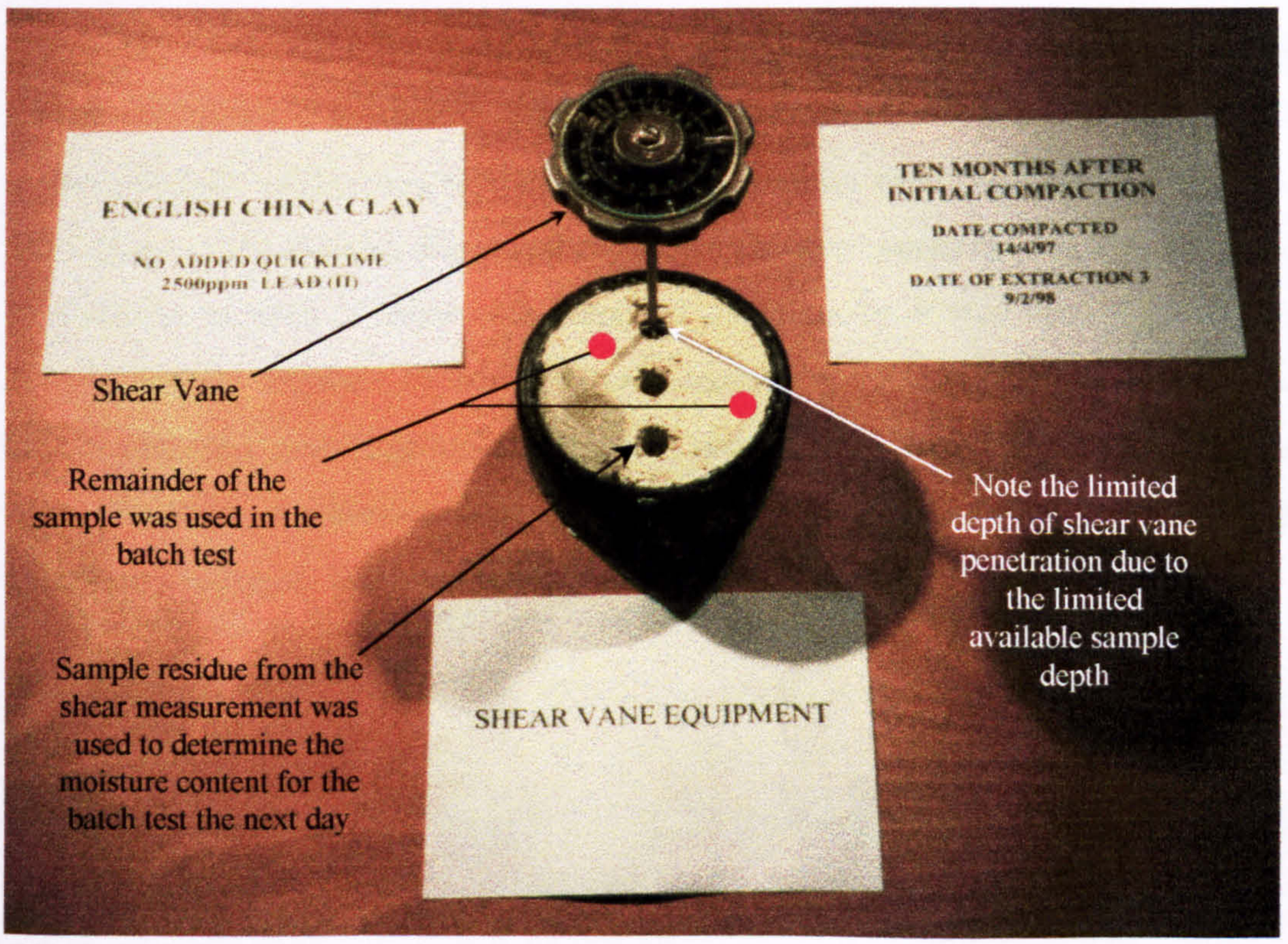

Figure 4.8 Shear strength measurement

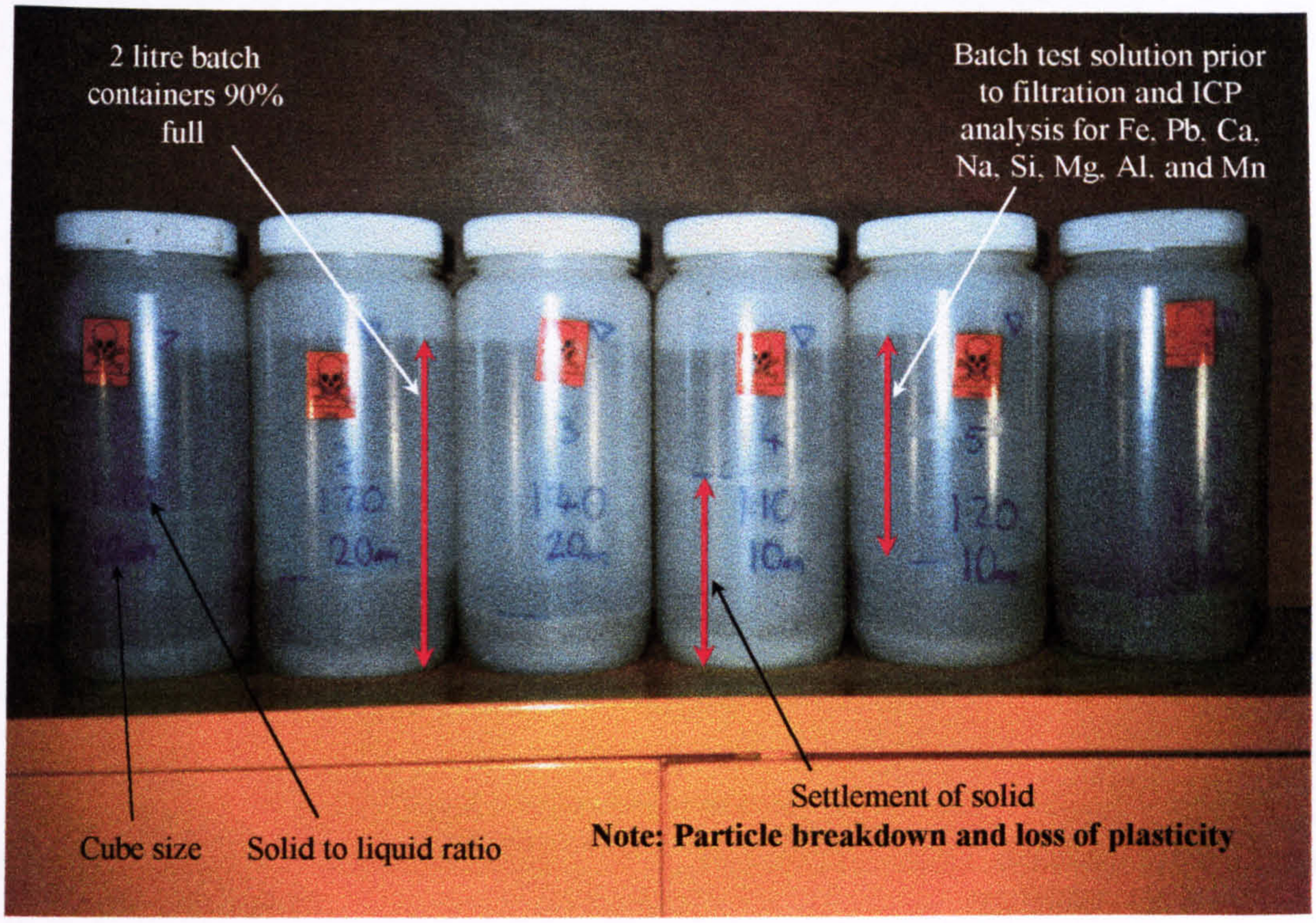

Figure 4.9 Wyoming Bentonite with 7.0% lime settling after a batch test

However, some Wyoming Bentonite mixtures required up to 6 hours filtering and others could not be filtered. Where filtration was possible over a long time period, a portion of the sample was filtered and another portion centrifuged at 11000rpm for 30 minutes. This allowed direct comparison of the two separation methods for these troublesome samples. Clearly where samples could not be filtered centrifugation was the only option. Figure 4.10 shows an uncontaminated, untreated Wyoming Bentonite sample requiring centrifugation after a batch test with the liquid fraction having been removed. There is a distinct difference in physical characteristics when compared with the treated Wyoming Bentonite sample illustrated in Figure 4.9.

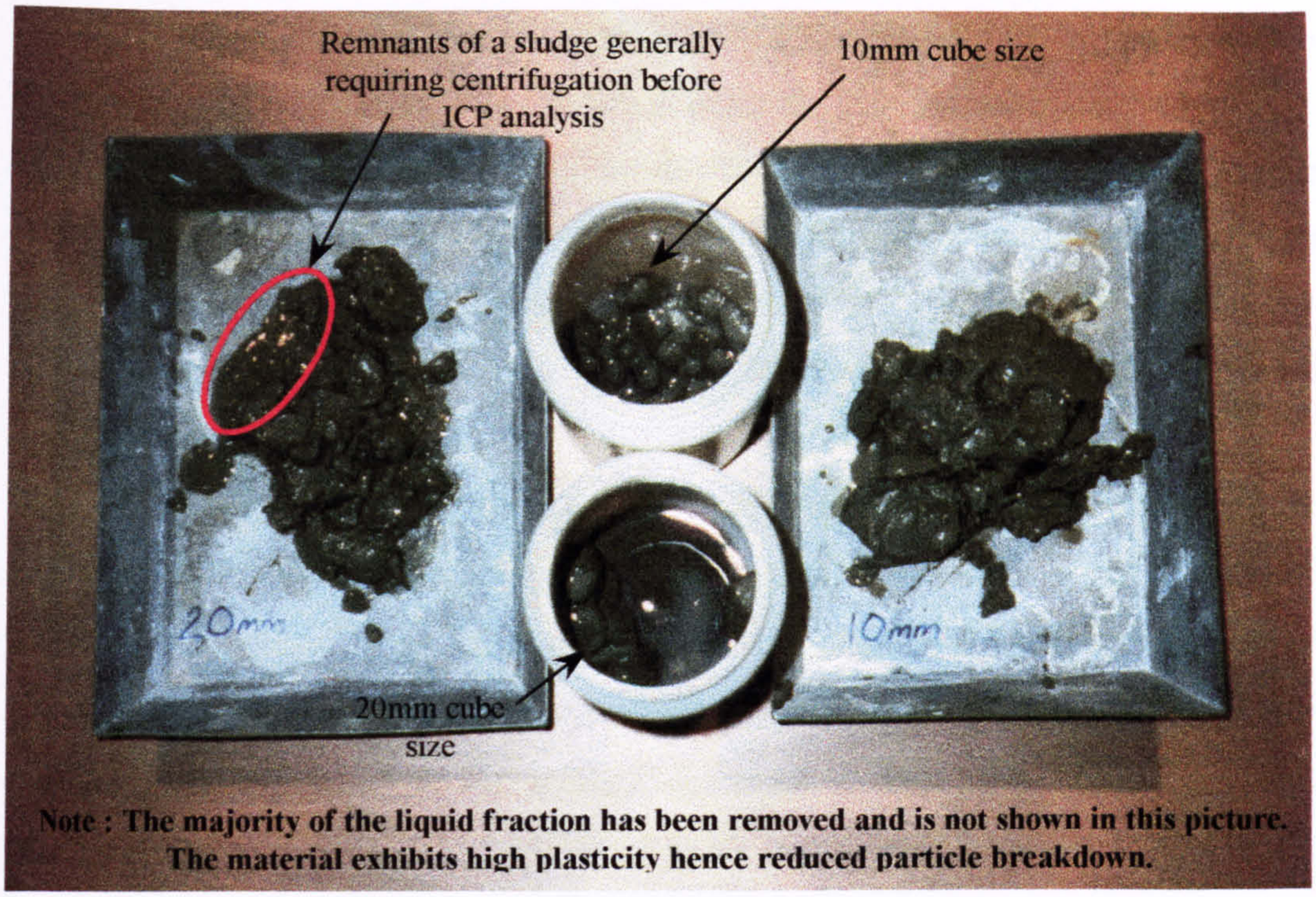

Figure 4.10. Uncontaminated, untreated Wyoming Bentonite after a batch test with solution removed.

It was apparent however that certain samples and indeed certain solid to liquid ratios centrifuged better than others did. It was often evident that a slightly green, but translucent solution was produced by centrifugation. The difficulties encountered with centrifugation included the fact that a faster speed and duration of centrifugation was required to achieve complete separation of solid and liquid. A faster centrifugation speed was not possible due to the lack of equipment that could operate at these higher rotational velocities. A longer duration was also not possible since the centrifuge was not cooled, hence, the spinning samples generated significant heat. This could have the effect of changing the chemistry and the separation properties of the solid and liquid fractions and also caused distortion and on several occasions disintegration of the centrifuge tubes. Furthermore, it was not desirable to add a flocculating agent since this would clearly alter the chemistry of the material rendering the resulting chemical analysis difficult to interpret. Subsequently all samples were centrifuged at the same speed and duration. Therefore the degree of solid and liquid separation of the centrifuged samples was directly dependent on their respective physico-chemistry and the results could be interpreted on a relative basis and be related to physical behaviour.

All sample solutions were stored in 200ml fluorinated HDPE bottles at 4 ± 0.5^{0}C for no longer than 24 hours at which point the samples were analysed by ICP. Precisely 1/2ml of concentrated Aristar nitric acid was added to every 100ml of sample to reduce the pH and preserve the sample. Acid was not added to centrifuged samples since the small quantities of mineral present reacted violently with acid and the low storage temperatures to produce a gelatinous material which could not be passed through the ICP analyser.

During the third batch testing period (301 days), where possible, due to the constraints of material properties linked to mix design, the residues of samples from 6 hour 30 rpm tests, 10m and 20mm cube size, and 1:10 solid to liquid ratios were wet sieved. The solid retained on a 63µm sieve was oven dried at 105 ± 0.5^{0}C and acid digested twice according to the method described in Section 4.5.1, and precisely analysed by ICP for the eight significant elements discussed in Section 4.5.3.

During a four day testing period where batch tests were being performed on samples of the same mix design the 2 litre batch containers were simply washed and rinsed several times with ICP water and allowed to air dry prior to use the next day. However, after four days testing when the mix design changed a new set of acid washed containers were used, whilst the other used containers were acid washed.

It should also be noted that all liquids, wet solids, or sludges resulting from the preparation of sample mixes or produced from the batch tests or other related tests were concentrated into a dry solid by evaporating the liquid in a fume cupboard. The resulting solid material was sealed and stored in heavy duty plastic bags prior to disposal in landfill by the University Health and Safety Organisation. Each week a volume of approximately 100 litres of contaminated sludge was disposed of in this manner.

4.5.3 Inductively coupled argon plasma atomic emission spectrometer analysis

Based upon the results of the initial ICP 'multiquant' analysis of the acid digested samples (detailed in Section 4.5.1) an estimation of the likely elemental release concentrations from the batch tests was made. Hence a program was written for the ICP spectrometer which was standardised to search for elements in solution at or below the following concentrations: Fe (10.00ppm), Pb (10.00ppm), Ca (10.00ppm

and 100ppm), Na (10.00ppm), Si (5.00ppm), Mg (10.00ppm), Al (2.00ppm), Mn (1.00ppm). Although not all solutions could be filtered or collected from each batch test sample, it was still possible to quantitatively analyse a small representative fraction of the solution. In determining the elemental concentration, the ICP spectrometer control system assumes that the sample analysed comes from a sample of 1 litre in volume, hence, it is a simple calculation to determine what the actual value is for the particular volume of liquid present in each batch test solid to liquid ratio.

Where an element concentration was significantly below the level for which the equipment was standardised, the level of element detected was usually slightly overestimated or alternatively described as below detection limits. For example, if a 10ppm Ca solution was tested with the above mentioned program, the 10ppm Ca standard would produce a result of 10ppm Ca whilst the 100ppm Ca standard would produce a result of approximately 12ppm. This behaviour varied slightly from one element to another due to variations in the wavelengths emitted and subsequently detected for each specific element under analysis. Where a sample solution contained more of an element than the spectrometer was standardised to detect the concentration was usually underestimated or described as saturated. To overcome this problem the ICP analyser was programmed and standardised to detect higher concentrations. However, for each specific element there is a specific maximum concentration that can be detected for a specific wavelength. Usually there were two or three wavelengths that could be used for each specific element, each with a higher or low detection concentration capability. The difficulty associated with changing the detected wavelength for a specific element was that some wavelengths interfered with each other potentially producing rogue results. Hence, it was important to check the manufacturers instructions for information regarding wavelength interference of one element relative to another and balance this factor with the required range of maximum and minimum detection limits. One solution to the problem of very high concentrations of a specific element was to precisely dilute the sample to a concentration that was easily within the detection range of a wavelength that did not interfere with a wavelength of another element. Hence, when samples varied significantly from one batch test to another it was often necessary to analyse a sample three or four times at several dilutions to obtain precise concentrations of all the elements required.

4.5.4 Sample mix acid digestions after 301 days curing

After 301 days 1 sample from each of the 18 mix designs along with 1 quicklime sample and each of the untreated unhydrated clays was dried at 105±0.5^{0}C for 24 hours, crushed with a pestle and mortar and acid digested twice according to the method described in Section 4.5.1. The samples were precisely analysed by ICP (not multiquant analysis approximation) for the eight selected elements. The purpose for this study was to check that all the contaminants were present in proportions of 5000ppm and that no cross contamination occurred during the preparation of the mix designs. It was also an intention to determine whether the presence of the contaminants and / or lime affected the acid soluble fractions of the selected elements in the mix designs after a substantial curing period. Results from these tests could suggest mechanisms that govern long-term stability behaviour.

4.6 ATTERBERG LIMITS

Liquid limit and plastic limit (i.e. Atterberg) tests were performed on one sample from each of the 18 mix designs at the same time periods as the batch tests i.e. 7 days, 175 days and 301 days. Samples were extracted from the same mould for each mix design for all three time periods to ensure direct comparability. The methods were performed using the equipment illustrated in Figure 4.6 according to BS 1377 (BSI, 1990B) with the exception of sample preparation. Due to the formation of precipitates in many of the mix designs it was not felt appropriate that the samples were dried in the oven. This would have affected the hydration of precipitates that were considered of potential importance with regard to crystallisation and physical behaviour. A particle size analysis performed on untreated clay using a sedimentation technique showed that 98% of English China Clay was below 15μm and 51% was below 2μm whilst 98% of Wyoming Bentonite was below 15μm and 84% was below 2μm. It was therefore clear that drying and crushing were certainly not required for samples that had not been solidified with lime. Where samples had solidified on addition of lime the samples were not dried, but were crushed at their extracted water content using a pestle and mortar. Once particles appeared to be approximately 1mm in diameter further water was added to the mixture and further particle crushing was performed

using a strong spatula. This process was continued, often for up to 6 hours, until a consistent smooth mixture was created. Clearly, similarly to the plastic limit test, this approach to the liquid limit test was subjective and dependent on the operator. The test was therefore performed by the same operator to try to limit any potential variability in the sample preparation.

4.7 THE POTENTIAL FOR VARIABILITY AND EXPERIMENTAL ERROR

4.7.1 Introduction

The ability to identify and reduce sources of experimental error and therefore maximise repeatability and confidence was as important as the fundamental concepts upon which the research was based. If the measured data were highly variable or were obtained with little or no control then it becomes invalid to base any arguments conclusively and therefore science has not been significantly developed by the research process. In one sense the concept of a sound research approach was one of the 'foundation stones' of this project because of the relatively poor execution and / or reporting of preceding research.

This section has been structured in an order that follows the progression of the research and highlights when and why some specific decisions were made without the benefits of hindsight. Within each section, an estimate of the potential error is provided.

4.7.2 Initial material characterisation

The initial particle size distribution performed using a sedimentation technique was important to highlight that Wyoming Bentonite had a higher proportion of very fine material than English China Clay. The analysis was performed by an external laboratory and a chemical dispersant was used to overcome the swelling properties of the Wyoming Bentonite. Due to the limited information provided by the laboratory it was difficult to assess potential error although the important factor was not the absolute values of particle size determined but the relative difference between samples, which could affect compaction.

Subsequent to the particle size distribution the ICL tests were performed. The most likely error associated with this test was due to the variation in test methodology adopted for the Wyoming Bentonite assessment. Due to variations in the test the ICL value determined for Wyoming Bentonite was a best estimate. In the context of the research this was not a significant difficulty because all Wyoming Bentonite samples were treated with same best estimated ICL lime content. A further consideration for any test where the measurement of pH is important is that one pH probe design will give different pH measurements to another. This is due to the fact that there are specific probes designed to measure extremes of pH from the highly acidic to the strongly alkaline. To limit the 'drift' in the pH scale associated with using an inappropriate pH probe, special probes to measure very alkaline sludges were purchased and prior to each pH measurement the probe was calibrated with three solutions of known pH, one acidic, one neutral and one alkaline. Section 4.2.2.2 describes in detail the precautions taken when measuring pH to limit the potential for error. The pH probes used throughout the study had a manufacturer's stated accuracy of ± 0.01 pH divisions. However previous experience has shown that in solutions of high pH containing mineral particles an accuracy of ± 0.10 pH divisions was more likely. The fact that the pH measurements were conducted in a thermally controlled environment also ensured that the readings did not vary due to temperature variations.

4.7.3 Determination of acid soluble mineral fractions and ICP analysis

Determination of the acid soluble fractions of the treated and untreated minerals had several potential sources of error that were minimised. The use of very precise balances (accurate to ± 0.0001g), pipettes (accurate to ± 0.01ml), volumetric flasks (accurate to ± 0.5ml) and very expensive pure concentrated acids and B.S. 3978 Grade 1 de-ionised water limited controllable error to insignificant proportions. If there had been an error of ± 0.0001g when measuring 1g of sample for an acid digestion test this would have resulted in an error of ± 0.01%. Hence for a clay sample containing 10000mg/kg Ca the accuracy of the measurement would be 10000mg/kg ± 1mg/kg. If there had been a final volumetric error of ± 1ml in a 100ml volumetric flask the error would only have been ± 1%. Hence for a clay sample containing 10000mg/kg Ca the accuracy of the measurement would be 10000mg/kg ± 100mg/kg.

Where error could have occurred was when samples were filtered through a filter paper that in itself contained chemical elements. However, discussion of this point with the manufacturers 'Whatman' suggested that the problem existed for all of their products that were within the resource capacity of the research. Furthermore, any likely error would be constant throughout the research so changes in chemistry would still be notable and not be due to changes in the composition of the filter material. The company 'Whatman' were unable to suggest what the likely error would be after passing solutions through their papers but reassuringly described it as negligible.

The focus on the potential variability of elements from this analysis was therefore on the actual ICP analytical technique. Here there were many influencing factors. Essentially the process worked by injecting a very fine spray of sample (almost a gas) at a known controlled rate into very pure argon gas that had been highly excited (plasma). Some of the energy from the plasma excited electrons in the atoms of elements present in the solution to higher energy orbitals within the atom. The electrons were not stable in these higher energy orbitals and as a result fell to lower energy orbitals and in doing so emitted electromagnetic radiation of specific wavelengths. This resulted in the atoms of a specific element releasing one or two wavelengths that were only released by the atoms of that element. These wavelengths were detected by electromagnetic sensors and converted into an electrical signal that the computer showed as intensity peaks where essentially the area below the peak related to the concentration of the element in the sample solution. Unfortunately when analysing mixtures of elements some wavelengths were within a very narrow wavelength range and the radiation from different elements interfered with each other producing larger intensity peaks and consequently higher measured concentrations than those actually present in the sample. This was overcome in this research by choosing to detect wavelengths that were sufficiently separated so as not to mutually interfere. One potential drawback was that some wavelengths were more sensitive than others and could detect lower levels of the desired element. Therefore the determination of some elemental concentrations were precise to parts per billion whilst others were precise to a tenth of a part per million. The magnitude of this variability is highlighted in Table 4.9.

Table 4.9 Wavelengths measured during precise ICP analysis including maximum and minimum detection limits

Element	Primary detection wavelength / line (nm)	Minimum detection limit (mg/l or mg/kg)	Maximum detection limit (mg/l or mg/kg)
Calcium (Ca)	393.366	0.0003	15.0000
Silicon (Si)	251.611	0.005	250.000
Aluminium (Al)	167.081	0.015	750.000
Sodium (Na)	588.995	0.10	5000.00
Lead (Pb)	220.353	0.14	7000.00
Iron (Fe)	259.940	0.015	750.000
Magnesium (Mg)	279.553	0.001	50.000
Manganese (Mn)	257.610	0.003	150.000

Once the wavelengths that did not interfere had been chosen the system had to be calibrated using solutions of known standard element concentration. It was therefore necessary to estimate the concentration of an element that was required to be measured, and prepare a standard to that concentration, which in itself could induce a small error. Standards were prepared from solutions containing 1000mg/l of the desired element. To create a standard of 10mg/l in a 1l volumetric flask 10ml of the 1000mg/kg standard was added to a 1l volumetric using a 10ml pipette accurate to ± 0.01ml and the volumetric flask filled with ICP water. Therefore if there was a volumetric error of ± 0.01ml in the pipette measurement this would have resulted in an accuracy of ± 0.1%. Hence the 10mg/l sample would have contained 10mg/l ± 0.01mg/l and all samples analysed after calibration using this one elemental standard would have an accuracy of ± 0.01mg/l.

The calibration process essentially told the system that the area under an intensity plot related to a specific concentration. If the actual concentration of the sample was say 10 to 30% above the standard concentration the error would have been large because the system could not have identified this size of intensity peak. However, if it were 10 to 30% below the standard it was likely to be insignificant. To complicate matters these effects varied slightly from one element to another. Hence

with the initial acid digestion tests (not those performed on samples after 301 days curing) a 'multiquant' analysis of 32 elements was performed. The standard for this 'multiquant' test was a mixture of a few elements and the system essentially estimates the concentration of the other elements. The results of this test were therefore ± 30 to 40%. However it did provide an estimate of what elemental concentrations to expect so that the batch test analysis could be carried out precisely.

On the basis of the results of the multiquant testing two standard solutions were created for future precise analysis. One standard was created containing eight element concentrations and the system was programmed to analyse the wavelengths of these elements which would not interfere and would be suitable to analyse the batch test solutions. The other standard was the B.S. 3978 Grade 1 de-ionised water that was essentially the blank control solution. Each batch test sample was analysed by this programme and any element that was measured to be significantly above the standard concentration was either re-analysed using another standard of higher concentration or if the system was close to the maximum concentration detection limits the sample was diluted. If the analysed elemental concentration was significantly below the standard concentration then there was no alternative but to analyse the sample after the system had been calibrated with a lower standard concentration. Furthermore, the system was programmed to analyse each element four times and average the result as well as calculate the variation between each of the four analyses. To further improve confidence in the data and to overcome the fact that as the system temperature increased the results were sometimes affected, immediately after standardisation, during and after a series of analysis the standard was analysed against itself. If there was variation in the results of analysis of the standard greater than 1% (for a standard of 10ppm this equates to 10ppm ± 0.1ppm) then the system was re-standardised and the previous samples were analysed again. This was clearly quite laborious but ensured that the main potential for error was limited to the standardisation of the ICP equipment. This potential for error cannot really be calculated since it varies with experience and from one operator to another and indeed one laboratory to another. This error was therefore limited or kept constant by ensuring that analysis was performed throughout by a single operator on the same equipment.

4.7.4 Preparation of compacted samples

After completion of the acid digestion tests and analysis the preliminary compaction tests were performed. Perhaps the most significant source of variability was between the Wyoming Bentonite samples without lime addition and those with lime addition. The samples without lime had such a high degree of cohesion that frequently material would adhere to the compaction equipment. This was limited as far as possible by continual cleaning of the apparatus. This difficulty did not arise for the lime-treated samples due to the flocculation processes. It was therefore evident that all Wyoming Bentonite samples with no added lime would behave in a consistent manner. This was highlighted by comparison of the full-scale compaction results and the preliminary data in Figure 5.4 and 5.5. To reduce error each full-scale result illustrated was the average obtained from the preparation of four samples. The preliminary and full-scale results are very similar and the variations are predominantly associated with the fact that the full-scale testing samples were compacted wet of optimum and in some cases contained added contaminants. However, the preparation of these contaminated samples could contain some error, specifically in respect to the addition of the contaminants. Although the mass of contaminant added to the prepared solutions was measured to ± 0.0001g and the volume of contaminated solution added to the clay in the mixer was measured to ± 0.2ml the acid digestion data of 1.0000g ± 0.0001g after 301 days suggest that only 4200ppm of Pb was present in the mineral. This is a potential error of 16%. It may be hypothesised that this error is linked to digestion of only 1g of material and that some contaminant is retained on the organic molecules of the filter paper media. The latter point is highly unlikely because of the highly acidic nature of the filtered solution. The former point is also unlikely because in the one case when an arithmetic error resulted in the addition of only 2500ppm Pb, the acid digestion data suggested that only 2100ppm Pb was present, half the quantity measured for all samples. This suggested three possibilities to explain the variation. The first was that the standard used to measure the soluble Pb concentration was not significantly close to the actual soluble Pb concentration present in solution thereby inducing error, which was later found not to be the case. The second hypothesis was that the acid digestion was not sufficient to remove attenuated Pb from exchange sites or that Pb was incorporated in the pozzolanic reaction products. This was also

unlikely because exactly the same behaviour was seen for the Wyoming Bentonite with high permanent charge and for English China Clay with pH-dependent charge. The third hypothesis was that during the sample mixing phase and addition of the contaminant to the mixer some contaminated solution was lost onto the surfaces of the mixer and not incorporated into the samples. If this was the case then it would be likely the same effect would be seen in the Fe^{3+} ion contaminated samples. This was indeed the case and can be seen in the data when the iron present naturally in the clay without contamination is accounted for along with the effect due to sample dilution on addition of lime. For English China Clay this process resulted in an added soluble Fe concentration of approximately 4100ppm. This was the same level of error assessed for the Pb^{2+} ion contaminated samples. For Wyoming Bentonite the amount of soluble Fe added appeared to be slightly higher although it is suggested that this was due to partial dissolution of Fe from the clay matrix during the high pH conditions of curing for 301 days prior to acid digestion.

The effect of the reduced contaminant content on the interpretation of data obtained from the experimentation was not important because it remained constant for all samples and the resulting data has been interpreted on a relative basis.

4.7.5 Batch testing

The potential for error in the chemical batch tests was very difficult to assess. All the tests were performed in precisely the same manner and all equipment was thoroughly washed with a nitric acid solution and rinsed with B.S. 3978 Grade 1 de-ionised water to eliminate cross-sample contamination. It was therefore important to assess the repeatability of the tests. Although no test was repeated exactly, it was found that tests involving changes in rotation speed and cube size were the same after chemical analysis of pH, conductivity and the eight selected elements. On this basis essentially each experiment was performed four times (two cube sizes at two rotation speeds). Each of these tests showed the same time-dependent chemical characteristic behaviour for the specific clay, contaminant and lime mix design. However, error could have occurred during the preparation of the tests where a mass of clay and a mass of water were measured. The mass of clay and mass of water added to each batch test container was measured to within $\pm$ 0.01g. For a batch test with a 1:20 solid

to liquid ratio the mass of effective dry solid added was 90.00g ± 0.01g (± 0.01%) and the mass of water added was 1800.00 ± 0.01g (± 0.0006%). This level of error would clearly have little influence on the results of the soluble element analysis. Hence the estimated error in the soluble elemental results for 1:20 solid to liquid ratio batch tests could be listed as follows:

Estimated error due to test preparation	± 0.0106%
Estimated error due to ICP calibration	± 0.1%
Estimated error due to diluting the elements in the sample solution by 100 times if required (i.e. 1ml in 100ml)	± 1%

The maximum estimated error in the concentrations of soluble elements from the batch tests would therefore be approximately ± 1.2%. Analysis of a batch test solution resulting in a soluble Ca concentration of 100mg/l would therefore realistically contain 100mg/l ± 1.2mg/l. This level of accuracy is clearly lower than the detection limits of the ICP equipment for any of the elements listed in Table 4.9 and was therefore likely to be the controlling factor in the chemical analysis of samples where the solid and liquid fractions were easily separated by filtration methods.

4.7.6 Shear strength measurements

This procedure was performed three times for each sample and because there were four samples of the same design mix, the final undrained shear strength value obtained was the average of 12 readings. Clearly by not performing the test precisely to British Standard recommendations the results were open to error. It was the relative differences between sample mixes at varying curing times that was significant and not necessarily the absolute value obtained. However, the maximum variation between any of the 12 readings at any one curing time and for any one sample mix was 10kPa. This result was for the Wyoming Bentonite sample contaminated with Pb^{2+} ions and with 7.0% lime added and cured for 7 days. The average undrained shear strength measurement for the sample was 140kPa, 5kPa below the maximum capacity of the shear vane, which could have accounted for the high variability observed in the

measurements. Generally the variation between the 12 undrained shear strength readings per mix design at any one curing time did not vary by more than ± 3kPa.

4.7.7 Atterberg limit measurements

Atterberg Limit tests are renowned for being highly subjective. All tests were performed precisely as described in the British Standards apart from the fact that prior to testing samples were not dried prior to crushing and performing the test. This was a very difficult decision to make and was an educated assessment on the likely effects of drying on the hydration properties of precipitated metal ions and potential changes in the behaviour of attenuated ions. To limit repeatability error a single person performed the tests. This would not only help to limit variations due to the subjective nature of the tests themselves but would also ensure that samples were crushed to the same degree by hand prior to commencing the test. Due to the fact that each test took on average 6 to 8 hours to perform (particularly for Wyoming Bentonite samples) and the fact that the tests were performed at specific curing times it was not possible to repeat an entire test. Purely from observation all the English China Clay liquid limit determinations were performed without any difficulty and there were essentially no deviations of the data from the linear regression line (water content against cone penetration). Hence the data could be interpreted with a high level of confidence. The same was also true of the Wyoming Bentonite samples with either added lime and/or contaminants. The addition of divalent and trivalent cations resulted in a material which was easier to mix with water and this improved the repeatability of cone penetrations at each water content. In contrast the untreated, uncontaminated Wyoming Bentonite produced highly variable results at each water content. Although this may have been attributed to variations in water content throughout the mixed sample every effort was made to ensure consistent mixing was performed. With the exception of the untreated, uncontaminated Wyoming Bentonite sample the estimated error in the liquid limit values of the other samples is ± 2%.

Several plastic limit determinations were made on each mix design. With the exception of the untreated, uncontaminated Wyoming Bentonite the procedure was readily producing plastic limit values within ± 1% water content. In contrast English China Clay plastic limits were only within ± 2% water content. This was attributed to

the fact that the English China Clay was quite 'silty' compared to the highly plastic Wyoming Bentonite.

Analysis of the above discussions highlights that in the majority of cases the likely variability is reduced to proportions that are difficult to measure. The tests were performed in precisely the same way, which was likely to induce the same degree of variability between samples. Since the results were interpreted on a relative basis small levels of variability were not likely to lead to misinterpretation of the large physico-chemical changes observed.

CHAPTER 5.0

5.0 RESULTS

The results in chapter 5 are divided into the following sections:

- The preliminary characterisation of the chemical (acid digestion and ICL) and compaction properties of the minerals studied,
- the effects of the chemical batch test operating parameters, including solid to liquid ratio, test duration, rotation speed, initial cube size and curing period on the pH, conductivity and leaching concentrations of elements from each of the clay-lime-contaminant mixes,
- detailed results from one set of batch test operating parameters highlighting the important curing time-dependent trends in pH, conductivity and element release for each of the clay-lime-contaminant mixes,
- the solubility of elements after acid digestions of the samples cured for 301 days, and
- the changes in physical behaviour with curing time in terms of undrained shear strength and Atterberg limits.

5.1 PRELIMINARY MATERIAL CHARACTERISATION

5.1.1 Particle size distribution

Untreated English China Clay and Wyoming Bentonite particle size distribution by sedimentation (illustrated in Figure 5.1) confirmed the prominence of clay particles (< 2μm) in the clay samples.

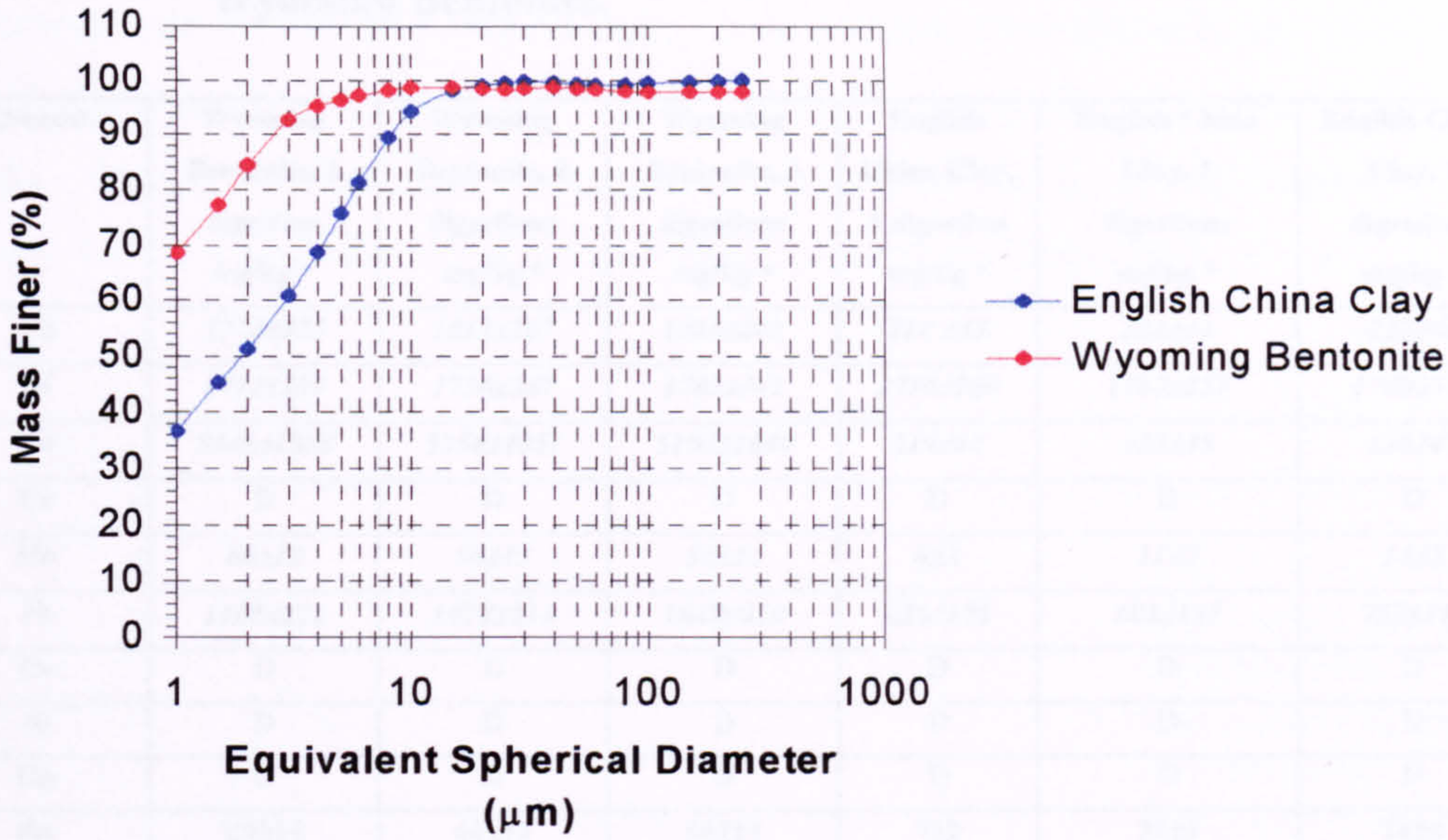

Figure 5.1 Particle size distribution of clay samples by sedimentation

5.1.2 Acid soluble clay fractions

The results displayed in Table 5.1 show the quantity of acid soluble elements present in the untreated clay minerals (± 20%) achieved by the series of acid digestions. The highlighted italic elements in Table 5.1 represent the most likely elements to yield information of value after stabilisation and solidification reactions relevant to this test programme. It is also apparent by inspection that the optimum number of acid digestions is 2.

Table 5.1 Aquarega soluble elements in English China Clay and Wyoming Bentonite.

Element	Wyoming Bentonite, 1 digestion mg/kg *	Wyoming Bentonite, 2 digestions mg/kg *	Wyoming Bentonite, 3 digestions mg/kg *	English China Clay, 1 digestion mg/kg *	English China Clay, 2 digestions mg/kg *	English China Clay, 3 digestions mg/kg *
Mg	***1374±275***	***1333±267***	***1306±261***	***214 ±43***	***221±44***	***228±46***
Al	***1793±359***	***1736±347***	***1703±341***	***1796±360***	***1787±357***	***1780±356***
Ca	***5341±1068***	***5256±1051***	***5153±1030***	***219±44***	***223±45***	***236±47***
Cr	D	D	D	D	D	D
Mn	***60±12***	***66±13***	***56±11***	***8±2***	***11±2***	***14±3***
Fe	***1105±221***	***1070±214***	***1049±210***	***626±125***	***683±137***	***757±151***
Co	D	D	D	D	D	D
Ni	D	D	D	D	D	D
Cu	D	D	D	D	D	D
Zn	69±14	64±13	64±13	7±2	28±6	18±4
As	D	D	D	D	D	D
Se	D	D	D	D	D	D
Sr	162±32	156±31	152±30	36±7	50±10	50±10
Ag	D	D	D	D	D	D
Cd	D	D	D	D	D	D
Ba	81±16	78±16	85±17	110±22	152±30	171±34
Hg	D	D	D	D	D	D
Pb	***D***	***D***	***D***	***D***	***D***	***D***
Bi	D	D	D	D	D	D
Li	D	D	D	D	D	D
Ti	D	D	D	D	D	D
Be	D	D	D	D	D	2±0.5
V	D	D	D	D	D	D
B	31±6	36±7	36±7	D	18±4	19±4
Sn	D	D	D	D	D	D
Na	***11380±2276***	***10680±2136***	***10389±2078***	***D***	***D***	***D***
Zr	69±14	68±14	62±12	728±146	707±141	668±134
Si	***2271±454***	***2210±442***	***2161±432***	***1547±309***	***1837±367***	***1855±371***
P	153±31	155±31	154±31	183±37	237±47	280±56
K	D	D	D	D	D	D
Mo	D	D	D	D	D	D
W	112±22	112±22	105±21	119±24	128±26	104±21

Notes: * mg of element per kg of clay.

D = below detection limits.

Bold italic characters represent chosen elements.

5.1.3 Initial consumption of lime tests

The results of the adapted initial consumption of lime test (ICL) on Wyoming Bentonite are depicted in Figure 5.2. It is evident that the ICL for Wyoming Bentonite lies between 5% and 8 % lime addition and probably the lower end of this range. Figure 5.3 illustrates the results of the standard ICL test on English China Clay. An ICL value of 1.5% was determined for English China Clay.

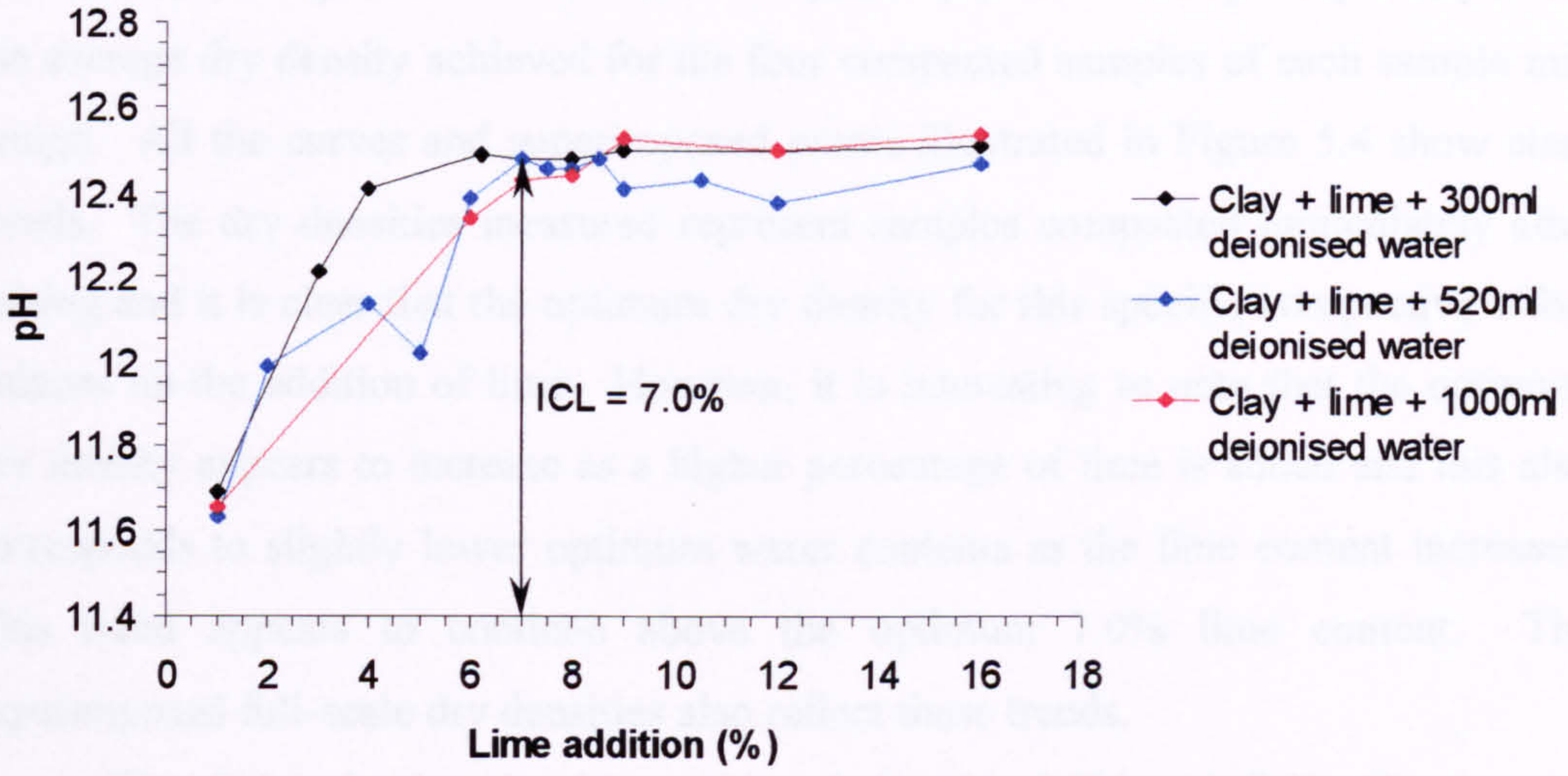

Figure 5.2 Results of the adapted initial consumption of lime test on Wyoming Bentonite

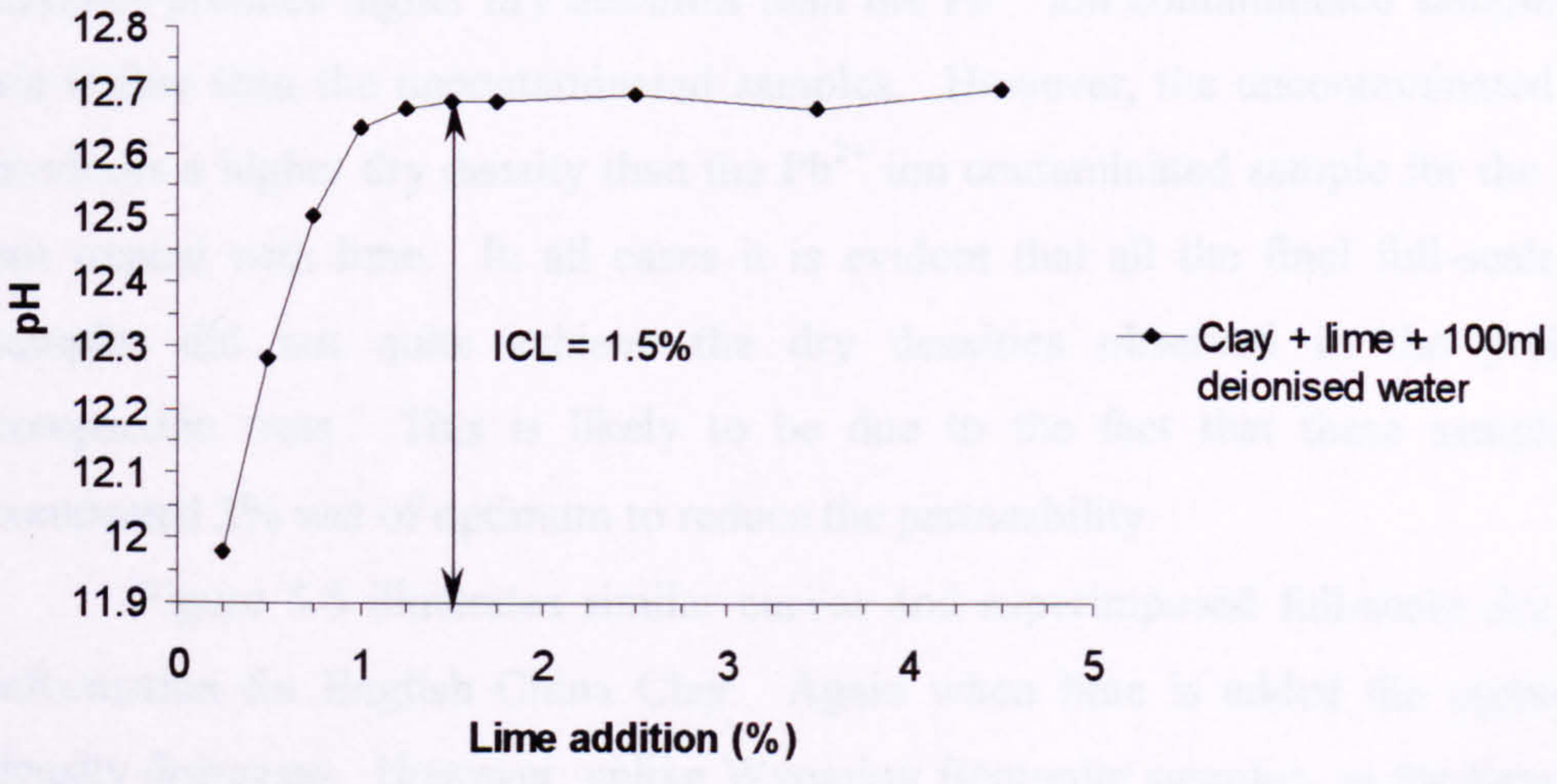

Figure 5.3 Results of the initial consumption of lime test on English China Clay

5.1.4 Preliminary dry density-water content investigations

The test data portrayed in Figures 5.4 and 5.5 were the basis upon which the main test programme clay samples were compacted, as described in Chapter 4.0. Figure 5.4 shows a series of dry density-water content curves for Wyoming Bentonite with varying additions of lime with no contaminants. The superimposed black, red and blue points represent the full-scale lime-treated contaminated and uncontaminated samples (i.e. not the preliminary compaction tests that were performed to characterise the materials) compacted in the twin-walled plastic pipes. Each superimposed point is the average dry density achieved for the four compacted samples of each sample mix design. All the curves and superimposed points illustrated in Figure 5.4 show clear trends. The dry densities measured represent samples compacted immediately after mixing and it is clear that the optimum dry density for this specific compactive effort reduces on the addition of lime. However, it is interesting to note that the optimum dry density appears to increase as a higher percentage of lime is added and this also corresponds to slightly lower optimum water contents as the lime content increases. This trend appears to continue above the optimum 7.0% lime content. The superimposed full-scale dry densities also reflect these trends.

The full-scale dry densities achieved for the 2.5% and 7.0% lime-treated samples coloured blue and red respectively in Figure 5.4 also highlight trends dependent on the contaminant present. In both these cases the Fe^{3+} ion contaminated samples produce higher dry densities than the Pb^{2+} ion contaminated samples which are higher than the uncontaminated samples. However, the uncontaminated sample produces a higher dry density than the Pb^{2+} ion contaminated sample for the samples not treated with lime. In all cases it is evident that all the final full-scale testing samples did not quite achieve the dry densities observed in the preliminary compaction tests. This is likely to be due to the fact that these samples were compacted 2% wet of optimum to reduce the permeability.

Figure 5.5 illustrates similar curves and superimposed full-scale dry density information for English China Clay. Again when lime is added the optimum dry density decreases. However, unlike Wyoming Bentonite samples, as the lime content increases the optimum dry density appears to decrease with a corresponding increase in the optimum water content. It is also clear that the sample treated with 2.5% lime produces similar values to the optimum 1.5% lime content. These trends are also evident in the full-scale samples. With the exception of the 2.5% lime-treated

samples, the full-scale dry density data suggest that the highest dry densities are achieved for uncontaminated samples with lower values obtained for Pb^{2+} ion contaminated samples and even lower values for Fe^{3+} ion contaminated samples. For the full-scale 2.5% lime-treated sample, the Fe^{3+} ion contaminated sample has a higher dry density than the Pb^{2+} ion contaminated sample. These trends relating dry density with lime content for the contaminated English China Clay and the Wyoming Bentonite are illustrated further in Figure 5.6.

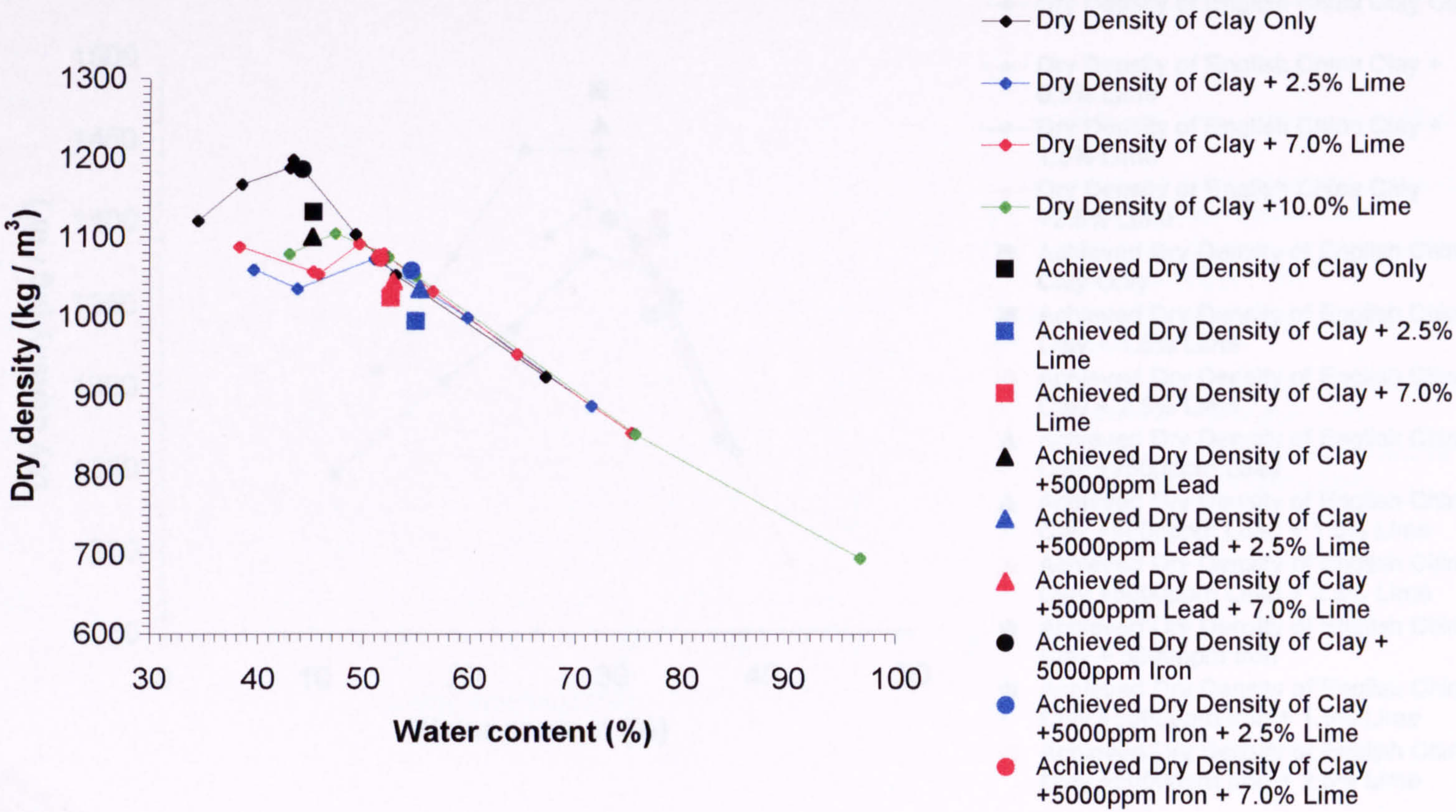

Figure 5.4 Variation of dry density with water content for Wyoming Bentonite samples.

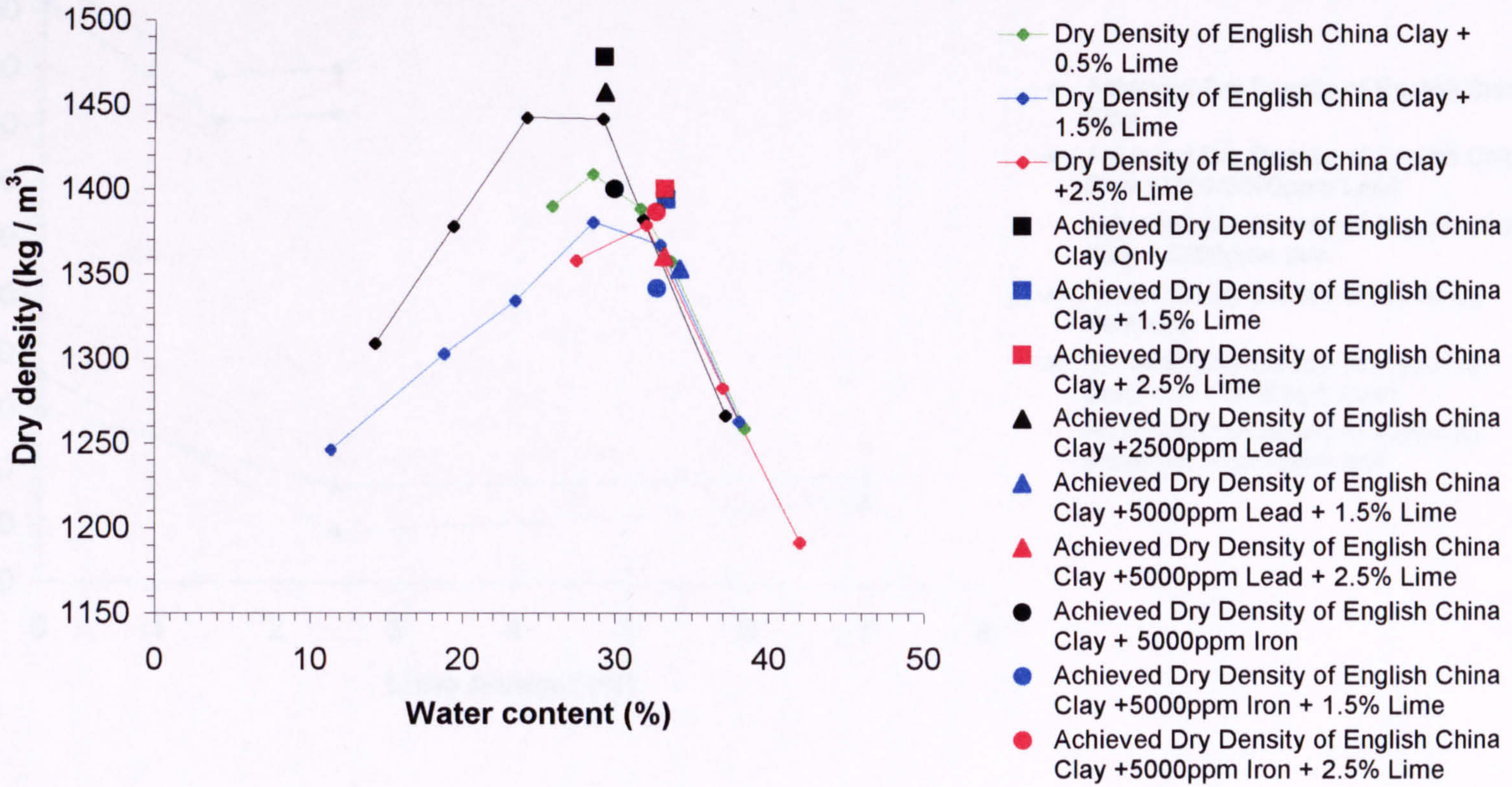

Figure 5.5 Variation of dry density with water content for English China Clay samples.

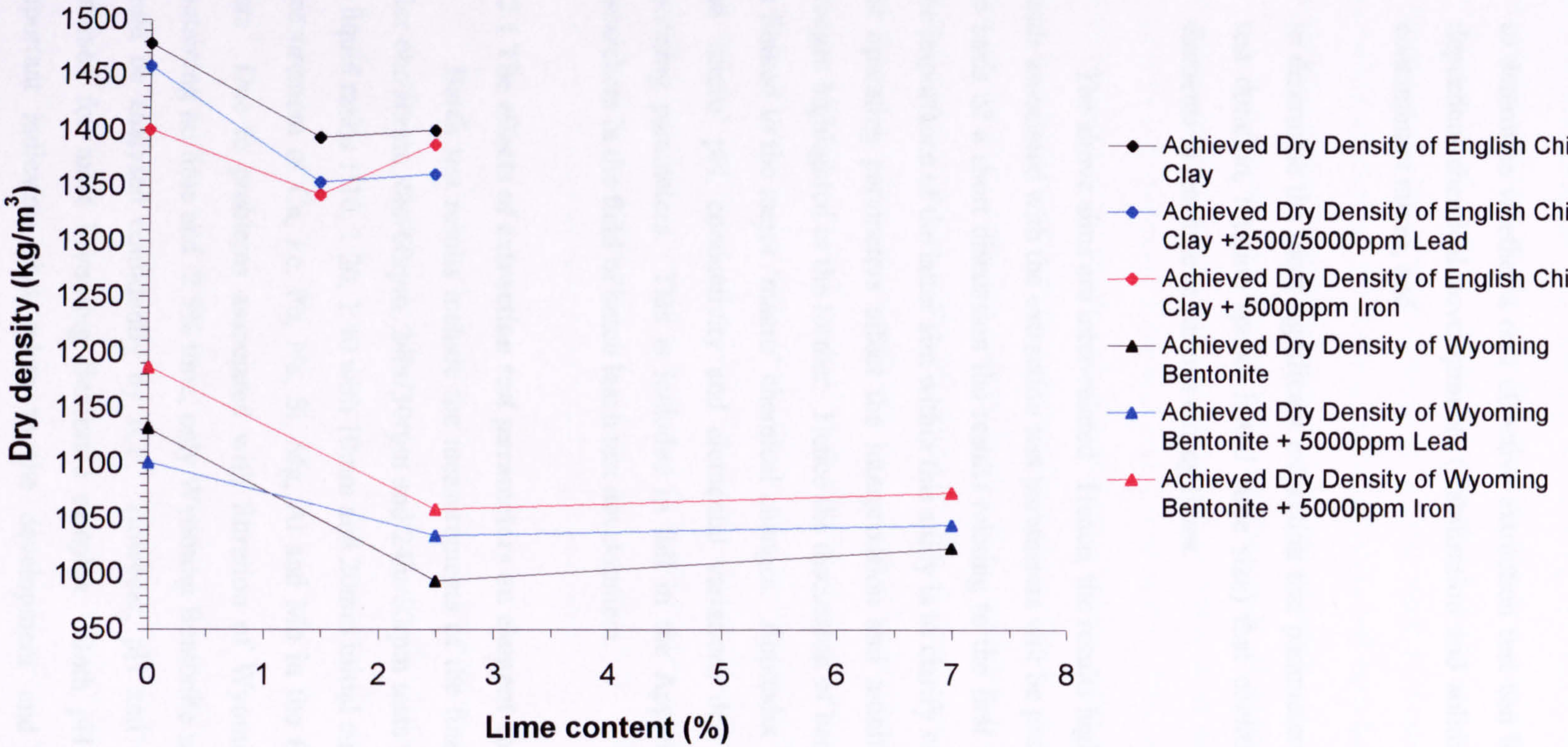

Figure 5.6 Variation of maximum dry density with percentage lime addition for English China Clay and Wyoming Bentonite on the addition of Fe^{3+} and Pb^{2+} cations (full-scale test samples)

5.2 BATCH EXTRACTION TESTS

The chemical batch tests were designed and with two primary aims:

- to determine whether a cost effective extraction test can be used to assess time-dependent chemical developments (stabilisation and solidification) of clay-lime-contaminant mixes, and
- to determine the most significant extraction test parameters (solid to liquid ratio, test duration, rotation speed, initial cube size) that control the concentration of elements in leachate at various curing times.

The above aims are inter-related. Hence, the results highlighting the important trends associated with the extraction test parameters will be presented initially, and on the basis of a short discussion the results relating to the first aim will be presented. The importance of the latter aim within this study is to clarify whether or not the batch test operating parameters affect the interpretation and monitoring of the chemical changes highlighted in the former. Hence the discussion of batch test parameters will be limited to the major 'macro' chemical changes. Appendix A presents all 'macro' and 'micro' pH, conductivity and elemental variations due to varying batch test operating parameters. This is included in full in the Appendix for the benefit of researchers in the field of batch leach test development.

5.2.1 The effects of extraction test parameters on element concentrations

Batch test results include the measurements of the final pH and conductivity after 6hr/30rpm, 6hr/60rpm, 24hr/30rpm and 24hr/60rpm tests on samples at the solid to liquid ratios 1:10, 1:20, 1:40 with 10mm and 20mm initial cube sizes as well as ICP measurement of Ca, Fe, Pb, Na, Si, Mg, Al and Mn in the final solutions of these tests. Due to problems associated with filtration of Wyoming Bentonite samples containing no lime and 2.5% lime, only Wyoming Bentonite samples with 7.0% lime could be analysed confidently by ICP. However, pH and conductivity data was obtained for most Wyoming Bentonite samples. Both pH and conductivity are important indicators that relate to the development and changes in chemical

stabilisation and solidification reactions. pH measurements provide data that help predict how pH sensitive charge sites are behaving and whether contaminants will be precipitated as well as the likelihood for continued solidification reactions. Conductivity, essentially measuring the quantity of dissolved solid, also provides information relating to the development of chemical reactions and highlights the development and success of stabilisation and solidification reactions. To make judgements on these measurements it is important to know how the batch test parameters affect these pH and conductivity results and how these results relate to the leachability of ions (including contaminants) into solution.

At a specific solid to liquid ratio the result of reducing initial cube size, increasing rotation speed and increasing test duration is to cause increased particle breakdown and increased solid and liquid interaction. This results in the solid and liquid phases moving closer to a chemical equilibrium. Increasing the proportion of water in the extraction test by reducing the solid to liquid ratio has a different effect. This results in a complete change in the final equilibrium condition by diluting element concentrations. Dilution of the soluble element concentrations, such as Ca released from a lime-treated material, can promote further dissolution of this element if more element is present to allow this change or permit the dissolution of another element which may not have been soluble at higher solid to liquid ratios. Dilution also has a disadvantage because it is possible that the dilution process will dilute an element concentration to below analytical detection limits. On this basis the effects of changing the extraction test parameters initial cube size, rotation speed, and test duration will be considered prior to solid to liquid ratio.

5.2.1.1 English China Clay sample variations due to changing initial cube size

The effect of varying cube size on the pH, conductivity and elemental release in batch tests varied between English China Clay and Wyoming Bentonite lime-contaminant mixes. Hence the results of each mineral type will be presented independently.

Generally for English China Clay samples with no added contaminants or lime increasing the initial cube size had no appreciable effect on the pH of the final batch test solutions at any solid to liquid ratio or curing period. However, at 7 days curing and the solid to liquid ratio 1:10 the 20mm cubes produced an increase in solution conductivity of between 1% to 4% depending on the other batch test parameters

(Table 5.2-reference A). English China Clay samples with Pb^{2+} ion contamination and no lime produced higher pH values at the lower 1:40 solid to liquid ratio for 10mm cubes at any curing period, although there was very little effect on the final solution conductivity (Table 5.2-reference B). English China Clay samples with Fe^{3+} ion contamination and no lime showed no appreciable variations in either pH or conductivity at any solid to liquid ratio or curing period (Table 5.2-reference C). Table 5.4 summarises the general trends in element concentrations associated with increasing the initial cube size and it is evident that for English China Clay samples with no added lime there were no apparent measurable changes between cube sizes, although small reductions in soluble Ca and Fe did occur for the Fe^{3+} ion contaminated samples.

With the exception of the Fe^{3+} ion contaminated samples, all English China Clay-lime-contaminant mixes showed no appreciable change in pH or conductivity when the initial cube size was changed at any curing period or solid to liquid ratio. For samples with only 1.5% lime the conductivity occasionally fluctuated and this appeared to be directly related to small fluctuations in the concentration of Ca in solution. This phenomenon appeared most predominant for the uncontaminated and Pb^{2+} ion contaminated samples (Table 5.2-reference D, E, G, H). The Fe^{3+} ion contaminated samples at both 1.5% and 2.5% lime content illustrated that the 10mm cube sizes frequently produced higher pH values although this trend was not consistent. Furthermore, these samples exhibited no appreciable variability in conductivity due to changing the initial cube size (Table 5.2-reference F, I).

Table 5.4 illustrates that frequently for English China Clay-contaminant-lime mixes the *larger* cube size produced higher Ca concentrations. However, only the Pb^{2+} ion and uncontaminated samples (not Fe^{3+}) with 2.5% lime produced small increases in Al concentrations, whilst all other elements analysed for showed no apparent change.

5.2.1.2 Wyoming Bentonite sample variations due to changing initial cube size

Wyoming Bentonite-contaminant mixes with no added lime illustrated the general trend where the smaller 10mm initial cube size produced a final leachate with lower pH and higher conductivity than the 20mm initial cube size at any curing period (Table 5.3-reference A-C). For the samples where filtration and ICP analysis was

possible the higher conductivity related to higher combined concentrations of Ca and Na in solution hence the higher conductivity.

Wyoming Bentonite with no contamination and 2.5% lime produced the result where the 10mm cube tests had generally higher solution pH and conductivity, particularly at 7 days and 175 days curing. This result was less pronounced during 24 hour tests probably due to increased particle breakdown (Table 5.3-reference D, E). Similar samples contaminated with either Pb^{2+} or Fe^{3+} ions with 2.5% lime exhibited little variation between cube sizes in pH or conductivity at any solid to liquid ratio or curing time (Table 5.3-reference F, G). For all clay-contaminant mixes with 7.0% lime there were also no clear trends between cube sizes relating to pH (Table 5.3-reference H-J). Furthermore, conductivity fluctuated depending on the combined concentrations of Ca and Na present in solution, a trend highlighted in Table 5.4.

Table 5.2 English China Clay end of batch test pH and conductivity trends associated with increasing initial cube size

Reference	Sample mix	Rotation speed		Test duration		Solid to liquid ratio			7 Days curing				175 Days Curing				301 Days curing			
									pH		Conductivity µS/cm		pH		Conductivity µS/cm		pH		Conductivity µS/cm	
		30 rpm	60 rpm	6 hour	24 hour	1:10	1:20	1:40	10 mm cubes	20 mm cubes	10 mm cubes	20 mm cubes	10 mm cubes	20 mm cubes	10 mm cubes	20 mm cubes	10 mm cubes	20 mm cubes	10 mm cubes	20 mm cubes
A	ECC-no contaminants-0% lime	X		X		X			6.12	6.03	9.7	11.4	5.89	5.90	18.3	18.3	5.76	5.74	17.5	17.5
B	ECC-Pb-0% lime	X			X			X	5.59	4.85	82.0	81.0	5.07	4.97	81.0	81.0	5.24	4.99	81.0	82.0
C	ECC-Fe-0% lime	X			X		X		2.67	2.65	2060	2030	2.66	2.65	2010	2010	2.69	2.70	2100	2100
D	ECC-no contaminants-1.5% lime	X			X		X		12.40	12.39	3180	3300	11.68	11.66	1109	1112	11.57	11.44	858	863
E	ECC-Pb-1.5% lime	X			X		X		12.40	12.34	3140	3170	11.78	11.82	1398	1414	12.10	12.11	1314	1325
F	ECC-Fe-1.5% lime	X			X		X		11.69	11.70	1902	1999	11.55	11.46	1903	1815	11.32	11.26	1840	1811
G	ECC-no contaminants-2.5% lime	X			X		X		12.66	12.66	5430	5450	12.07	12.07	1725	1715	11.85	11.82	1150	1147
H	ECC-Pb-2.5% lime	X			X		X		12.59	12.58	5150	5220	12.03	12.06	1864	1862	12.00	12.00	1434	1516
I	ECC-Fe-2.5% lime	X			X		X		11.99	12.09	2780	2810	11.87	11.78	2620	2620	11.83	11.82	2620	2650

Note : ECC = English China Clay (kaolinite)

Table 5.3 Wyoming Bentonite end of batch test pH and conductivity trends associated with increasing initial cube size

Reference	Sample mix	Rotation speed		Test duration		Solid to liquid ratio			7 Days curing				175 Days Curing				301 Days curing			
									pH		Conductivity µS/cm		pH		Conductivity µS/cm		pH		Conductivity µS/cm	
		30 rpm	60 rpm	6 hour	24 hour	1:10	1:20	1:40	10 mm cubes	20 mm cubes	10 mm cubes	20 mm cubes	10 mm cubes	20 mm cubes	10 mm cubes	20 mm cubes	10 mm cubes	20 mm cubes	10 mm cubes	20 mm cubes
A	WB-no contaminants-0% lime	X		X			X		10.12	10.24	946	675	10.19	10.21	823	583	10.11	10.14	830	620
B	WB-Pb-0% lime	X		X			X		9.83	9.92	866	573	9.74	9.80	805	525	9.79	9.79	854	603
C	WB-Fe-0% lime	X		X			X		8.48	8.57	1664	1464	8.80	8.90	1561	1371	8.91	9.05	1572	1145
D	WB-no contaminants-2.5% lime	X		X				X	11.66	11.55	1100	949	11.13	11.04	672	579	11.10	11.05	760	657
E	WB-no contaminants-2.5% lime	X			X			X	11.56	11.60	1243	1243	11.26	11.25	873	863	11.22	11.20	881	865
F	WB-Pb-2.5% lime	X		X			X		11.80	11.78	1915	1931	11.34	11.34	1264	1219	11.31	11.21	1276	1159
G	WB-Fe-2.5% lime	X		X			X		11.70	11.69	2680	2670	11.11	11.09	1916	1905	11.04	11.05	1882	1875
H	WB-no contaminants-7.0% lime	X		X			X		12.55	12.60	7290	7360	11.97	11.97	2070	2180	11.83	11.82	1920	2040
I	WB-Pb-7.0% lime	X		X			X		12.58	12.57	6830	7120	12.06	12.08	2130	2260	11.75	11.69	1724	1629
J	WB-Fe-7.0% lime	X		X			X		12.37	12.36	6340	6440	11.90	11.91	2850	2860	11.78	11.82	2530	2490

Note : WB = Wyoming Bentonite (Na-montmorillonite)

Table 5.4 **Summary of the general changes in end of batch test element concentration due to increasing batch test cube size from 10mm to 20mm for *filtered* samples only.**

Mineral and mix design	Elements determined in final batch test leachate							
	Ca	Fe	Pb	Na	Si	Mg	Al	Mn
English China Clay only	⇔	⇔	⇔	⇔	⇔	⇔	⇔	⇔
English China Clay only + 2500ppm Pb	⇔	⇔	⇔	⇔	⇔	⇔	⇔	⇔
English China Clay only + 5000ppm Fe	⇓(Small)	⇓	⇔	⇔	⇔	⇔	⇔	⇔
English China Clay + 1.5% lime	Fluctuates	⇔	⇔	⇔	⇔	⇔	⇔	⇔
English China Clay + 1.5% lime + 5000ppm Pb	⇑T	⇔	⇔	⇔	⇔	⇔	⇔	⇔
English China Clay + 1.5% lime + 5000ppm Fe	Fluctuates	⇔	⇔	⇔	⇔	⇔	⇔	⇔
English China Clay + 2.5% lime	⇑ (Large)	⇔	⇔	⇔	⇔	⇔	⇑	⇔
English China Clay + 2.5% lime + 5000ppm Pb	⇑ (Large)	⇔	⇑T	⇔	⇔	⇔	⇑	⇔
English China Clay + 2.5% lime + 5000ppm Fe	⇑ (Large)	⇔	⇔	⇔	⇔	⇔	⇔	⇔
Wyoming Bentonite + 5000ppm Fe *(7 days curing only)*	⇓ (Large)	⇑	⇔	⇓ (Large)	⇔	⇔	Fluctuates	⇔
Wyoming Bentonite + 2.5% lime + 5000ppm Pb *(7 days curing only)*	Fluctuates	⇔	⇔	Fluctuates	Fluctuates	⇔	⇔	⇔
Wyoming Bentonite + 2.5% lime + 5000ppm Fe	Fluctuates	⇔	⇔	Fluctuates	⇔	⇔	⇔	⇔
Wyoming Bentonite + 7.0% lime	Fluctuates	⇔	⇔	FluctuatesT	FluctuatesT	⇔	FluctuatesT	⇔
Wyoming Bentonite + 7.0% lime + 5000ppm Pb	Fluctuates	⇔	⇔	FluctuatesT	FluctuatesT	⇔	FluctuatesT	⇔
Wyoming Bentonite + 7.0% lime + 5000ppm Fe	Fluctuates	⇔	⇔	⇓	⇓	⇔	FluctuatesT	⇔

Notes: All changes are small unless stated otherwise

⇑ = Increase, ⇓ = Decrease, ⇔ = No significant change.

(Small) = Small increase in solution concentration of element.

(Large) = Large increase in solution concentration of element.

(Fluctuates) = Varies between samples.

T = Changes are also time-dependent and may differ from one curing time to another (concentrations generally higher at 7 days curing)

5.2.1.3 English China Clay sample variations due to changing rotation speed and test duration

Due to limited resources comparisons relating to changes in rotation speed were only possible on samples cured for 7 days and 175 days for both English China Clay and Wyoming Bentonite mixes. Furthermore, the behaviour of samples due to changes in rotation speed occasionally varied with test duration. Studying these two parameters highlighted the fact that rotation speed, test duration and initial cube size were inter-related and therefore associated with time-dependent physico-chemical changes due to stabilisation and solidification.

English China Clay with no contaminants or lime exhibited little variability in either pH or conductivity due to increasing rotation speed (Table 5.5-reference A). However, generally 24 hour tests produced small decreases in both pH and conductivity, particularly during 60rpm tests (Table 5.6-reference A). English China Clay-contaminant mixes with no lime exhibited little change in pH or conductivity due to increasing rotation speed (Table 5.5-reference B, C). However, increasing test duration resulted in small reductions in the pH for both contaminants whilst only the Fe^{3+} ion contaminated sample exhibited an associated small increase in conductivity (Table 5.6-reference B, C). Tables 5.9 and 5.10 highlight very small changes in leachate element concentrations due to increasing rotation speed and test duration for these mix compositions with no lime added. Increasing both parameters had similar effects on soluble element concentrations although clearly test duration has more influence on the soluble Si concentrations of the contaminated mixes. The effects on the soluble element species present are generally small and vary depending on the contaminant present. This is reflected in the limited changes in both conductivity and pH.

English China Clay with no contamination and 1.5% lime and the similar sample contaminated with Pb^{2+} ion contamination exhibited little change in pH due to increasing rotation speed although occasionally there was evidence of a slight increase in conductivity. The similar sample with Fe^{3+} ion contamination exhibited small increases in both pH and conductivity due to increasing rotation speed and this was particularly evident after 7 days curing (Table 5.5-reference D-F). The effect of increasing test duration on the clay-contaminant mixes with 1.5% lime was to increase both pH and conductivity and again the effect was most apparent after 7 days curing (Table 5.6-reference D-F).

English China Clay samples with no contaminants and 2.5% lime exhibited no clear trends for pH and conductivity relating to either increasing rotation speed or test duration (Tables 5.5 and 5.6-reference G). This was due to large inter-sample variations over the three curing periods. However the similar contaminated samples did exhibit some trends. The sample with Pb^{2+} ion contamination generally exhibited no significant change in pH when rotation speed was increased although conductivity did increase for 60 rpm tests over a 6 hour duration after 7 days curing (Table 5.5-reference H). The sample contaminated with Fe^{3+} ions generally exhibited little change in either pH or conductivity on increasing rotation speed although at 7 days curing the 24hr/60rpm test did produce lower pH levels (Tables 5.5 and 5.6-reference I). The effect of increasing test duration is clear for the contaminated samples with 2.5% lime. Both pH and conductivity increase and the effect is most predominant after 7 days curing and during 30rpm tests.

Generally Tables 5.3 and 5.4 illustrate clear tends for all samples with lime added. However, increasing rotation speed has no clear effect on Ca concentrations since they appear to fluctuate between samples and between curing periods. Other elemental concentrations appear to be relatively unaffected by increased test duration. However, increasing test duration increases Ca concentration for all mixes with added lime although these increases vary significantly with curing time. Furthermore, soluble Al concentration also varies in a fluctuating manner with the exception of the Fe^{3+} ion contaminated sample with 1.5% lime which exhibits increases with increasing duration. This suggests that the sample with Fe contamination has a significantly different physico-chemistry to the other mixes which requires further investigation. The high variability of the soluble Al concentrations for the lime-treated samples also suggests that Al is an important element in the chemistry of the lime-treated English China Clay samples.

5.2.1.4 Wyoming Bentonite sample variations due to changing rotation speed and test duration

The effects of varying rotation speed and test duration on Wyoming Bentonite samples with no contaminants or lime were highly variable with no apparent distinguishable trends (Tables 5.7 and 5.8-reference A). Increasing the rotation speed for the Wyoming Bentonite samples with contaminants and no lime resulted in no obvious change in pH or conductivity (Table 5.7-reference B, C). However,

increasing the test duration on these contaminated samples resulted in a lower final pH and higher conductivity particularly for the higher solid to liquid ratios (Table 5.8-reference B, C).

Wyoming Bentonite-contaminant-2.5% lime and Wyoming Bentonite-contaminant-7.0% lime mixes exhibit very similar behaviour although the increases are more evident at the higher lime content. Increasing rotation speed and duration had no apparent effects on pH although conductivity did appear to increase. This was particularly evident for samples after 7 days curing and during tests of 6 hours in duration. With the exception of the contaminated samples with 2.5% lime increasing test duration tended to increase the conductivity particularly at 7 days and 175 days curing for tests at the higher rotation speed. These trends are highlighted in Tables 5.7 and 5.8 reference D-I.

Table 5.9 and 5.10 illustrate that the changes in soluble element concentrations due to increasing rotation speed and test duration relate to Ca, Na, Si and Al. The changes in Al and Si are small and the elements that are most likely to affect conductivity measurements are the fluctuating levels of soluble Ca and Na that are involved in the cation exchange reactions.

In conclusion it is evident that increasing test duration and rotation speed will enable the closed system of the batch test to move closer to a chemical equilibrium condition. However, the measured variations in pH, conductivity and soluble elements between mix designs is complicated due to the variable effects of the interacting contaminants. This is particularly evident for samples treated with lime where the contaminants inhibit the solidification reactions.

Table 5.5 English China Clay end of batch test pH and conductivity trends associated with increasing rotation speed

Reference	Sample mix	Initial cube size		Test duration		Solid to liquid ratio			7 Days curing				175 Days Curing				301 Days curing			
									pH		Conductivity µS/cm		pH		Conductivity µS/cm		pH		Conductivity µS/cm	
		10 mm	20 mm	6 hour	24 hour	1:10	1:20	1:40	30 rpm	60 rpm	30 rpm	60 rpm	30 rpm	60 rpm	30 rpm	60 rpm	30 rpm	60 rpm	30 rpm	60 rpm
A	ECC-no contaminants-0% lime		X	X			X		6.08	6.17	13.9	13.7	5.94	5.96	11.6	12.2	---	---	---	---
B	ECC -Pb-0% lime		X	X			X		5.13	4.96	153	154	5.00	4.87	150	153	---	---	---	---
C	ECC -Fe-0% lime		X	X			X		2.68	2.72	1920	1950	2.66	2.71	1913	1921	---	---	---	---
D	ECC -no contaminants-1.5% lime		X	X			X		12.33	12.30	3300	3316	11.79	11.62	1049	1152	---	---	---	---
E	ECC -Pb-1.5% lime		X	X			X		12.42	12.42	3130	3140	11.77	11.77	1318	1364	---	---	---	---
F	ECC -Fe-1.5% lime		X	X			X		11.12	11.39	1592	1759	11.07	11.25	1540	1647	---	---	---	---
G	ECC -no contaminants-2.5% lime		X	X			X		12.55	12.42	5870	5350	12.22	12.00	2630	1656	---	---	---	---
H	ECC -Pb-2.5% lime		X	X			X		12.53	12.56	5170	5340	11.81	12.05	1699	2010	---	---	---	---
I	ECC -Fe-2.5% lime		X	X			X		11.90	11.91	2700	2710	11.87	11.92	2470	2560	---	---	---	---

Note : ECC = English China Clay (kaolinite)

No data available for 60 rpm tests at 301 days curing

Table 5.6 English China Clay end of batch test pH and conductivity trends associated with increasing test duration

Reference	Sample mix	Initial cube size		Rotation speed		Solid to liquid ratio			7 Days curing				175 Days Curing				301 Days curing			
									pH		Conductivity µS/cm		pH		Conductivity µS/cm		pH		Conductivity µS/cm	
		10 mm	20 mm	30 rpm	60 rpm	1:10	1:20	1:40	6 hour	24 hour	6 hour	24 hour	6 hour	24 hour	6 hour	24 hour	6 hour	24 hour	6 hour	24 hour
A	ECC-no contaminants-0% lime		X		X		X		6.17	5.87	13.7	12.3	5.96	5.83	12.2	11.6	---	---	---	---
B	ECC -Pb-0% lime		X	X			X		5.13	4.79	153	153	5.00	4.82	150	152	4.88	4.88	152	155
C	ECC -Fe-0% lime		X	X			X		2.68	2.65	1920	2030	2.66	2.65	1913	2010	2.69	2.70	1964	2100
D	ECC -no contaminants-1.5% lime		X	X			X		12.33	12.39	3300	3300	11.79	11.98	1049	1106	11.54	11.44	757	863
E	ECC -Pb-1.5% lime		X	X			X		12.42	12.34	3140	3170	11.77	11.82	1318	1414	11.65	12.11	1261	1325
F	ECC –Fe-1.5% lime		X	X			X		11.12	11.70	1592	1999	11.07	11.46	1540	1815	10.94	11.26	1546	1811
G	ECC -no contaminants-2.5% lime		X		X		X		12.42	12.41	5350	5780	12.00	12.25	1656	2630	---	---	---	---
H	ECC -Pb-2.5% lime		X		X		X		12.56	12.50	5340	5010	12.05	11.99	2010	1771	---	---	---	---
I	ECC -Fe-2.5% lime		X		X		X		11.91	11.81	2710	2740	11.92	11.85	2560	2530	---	---	---	---

Note : ECC = English China Clay (kaolinite)

No data available for 60 rpm tests at 301 days curing

Table 5.7 Wyoming Bentonite end of batch test pH and conductivity trends associated with increasing rotation speed

Reference	Sample mix	Initial cube size		Test duration		Solid to liquid ratio			7 Days curing				175 Days Curing				301 Days curing			
									pH		Conductivity µS/cm		pH		Conductivity µS/cm		pH		Conductivity µS/cm	
		10 mm	20 mm	6 hour	24 hour	1:10	1:20	1:40	30 rpm	60 rpm	30 rpm	60 rpm	30 rpm	60 rpm	30 rpm	60 rpm	30 rpm	60 rpm	30 rpm	60 rpm
A	WB-no contaminants-0% lime		x	x			x		10.24	10.09	675	663	10.21	10.21	583	613	---	---	---	---
B	WB-Pb-0% lime		x	x			x		9.92	9.81	573	643	9.80	9.83	525	636	---	---	---	---
C	WB-Fe-0% lime		x	x			x		8.57	8.83	1464	1241	8.90	8.86	1371	1210	---	---	---	---
D	WB-no contaminants-2.5% lime		x	x			x		11.69	11.44	1317	1263	11.20	11.15	785	817	---	---	---	---
E	WB-Pb-2.5% lime		x	x			x		11.78	11.92	1931	2450	11.34	11.38	1219	1328	---	---	---	---
F	WB-Fe-2.5% lime		x	x			x		11.69	11.63	2670	2650	11.09	11.00	1905	1950	---	---	---	---
G	WB-no contaminants-7.0% lime		x	x			x		12.60	12.49	7360	7420	11.97	11.98	2180	2450	---	---	---	---
H	WB-Pb-7.0% lime		x	x			x		12.57	12.57	7120	7040	12.08	12.05	2260	2320	---	---	---	---
I	WB-Fe-7.0% lime		x	x			x		12.36	12.46	6440	7210	11.91	11.90	2860	3060	---	---	---	---

Note : WB = Wyoming Bentonite (Na-montmorillonite)

No data available for 60 rpm tests at 301 days curing

Table 5.8 Wyoming Bentonite end of batch test pH and conductivity trends associated with increasing test duration

Reference	Sample mix	Initial cube size		Rotation speed		Solid to liquid ratio			7 Days curing				175 Days Curing				301 Days curing			
									pH		Conductivity µS/cm		pH		Conductivity µS/cm		pH		Conductivity µS/cm	
		10 mm	20 mm	30 rpm	60 rpm	1:10	1:20	1:40	6 hour	24 hour	6 hour	24 hour	6 hour	24 hour	6 hour	24 hour	6 hour	24 hour	6 hour	24 hour
A	WB-no contaminants-0% lime		X	X			X		10.24	10.18	675	935	10.21	10.20	583	896	10.14	9.93	620	907
B	WB-Pb-0% lime		X	X			X		9.92	9.71	573	1054	9.80	9.79	525	935	9.79	9.63	603	991
C	WB-Fe-0% lime		X	X			X		8.57	8.83	1464	1241	8.90	8.67	1371	1838	9.05	8.70	1145	1846
D	WB-no contaminants-2.5% lime		X		X		X		11.44	11.47	1263	1610	11.15	11.21	817	1168	---	---	---	---
E	WB-Pb-2.5% lime		X		X		X		11.92	11.88	2450	2170	11.38	11.33	1328	1382	---	---	---	---
F	WB-Fe-2.5% lime		X		X		X		11.63	11.68	2650	2630	11.00	11.00	1950	2040	---	---	---	---
G	WB-no contaminants-7.0% lime		X		X		X		12.49	12.56	7420	7570	11.98	12.01	2450	2730	---	---	---	---
H	WB-Pb-7.0% lime		X		X		X		12.57	12.38	7040	7180	12.05	11.97	2320	2810	---	---	---	---
I	WB-Fe-7.0% lime		X		X		X		12.46	12.41	7210	7410	11.90	11.97	3060	3400	---	---	---	---

Note : WB = Wyoming Bentonite (Na-montmorillonite)

No data available for 60 rpm tests at 301 days curing

Table 5.9 **General changes in element concentration due to increasing batch test rotation speed from 30rpm to 60rpm for *filtered* samples only.**

Mineral and mix design	Elements determined in final batch test leachate							
	Ca	Fe	Pb	Na	Si	Mg	Al	Mn
English China Clay only	⇔	⇔	⇔	⇔	⇔	⇔	⇔	⇔
English China Clay only + 2500ppm Pb	Fluctuates^{D}	⇔	⇑ (Small)	⇔	⇔	⇔	⇔	⇑ (Small)
English China Clay only + 5000ppm Fe	⇓ (Small)	⇓ (Small)	⇓ (Small)	⇔	⇔	⇔	⇔	⇔
English China Clay + 1.5% lime	Fluctuates^{T}	⇔	⇔	⇔	⇔	⇔	⇔	⇔
English China Clay + 1.5% lime + 5000ppm Pb	Fluctuates^{T}	⇔	⇑ (Large^{T})	⇔	⇔	⇔	⇔	⇔
English China Clay + 1.5% lime + 5000ppm Fe	Fluctuates^{T}	⇔	⇔	⇔	⇔	⇔	⇔	⇔
English China Clay + 2.5% lime	Fluctuates^{T}	⇔	⇔	⇔	⇔	⇔	Fluctuates	⇔
English China Clay + 2.5% lime + 5000ppm Pb	Fluctuates^{T}	⇔	⇓ (Small^{T})	⇔	⇔	⇔	⇔	⇔
English China Clay + 2.5% lime + 5000ppm Fe	⇑ (Large^{T})	⇔	⇔	⇔	⇔	⇔	⇔	⇔
Wyoming Bentonite + 7.0% lime	Fluctuates^{TD}	⇔	⇔	Fluctuates^{TD}	⇓ (Small^{T})	⇔	⇔	⇔
Wyoming Bentonite + 7.0% lime + 5000ppm Pb	Fluctuates^{TD}	⇔	⇔	Fluctuates^{TD}	⇔	⇔	⇔	⇔
Wyoming Bentonite + 7.0% lime + 5000ppm Fe	⇑^{TD}	⇔	⇔	Fluctuates^{TD}	⇔	⇔	⇑^{T}	⇔

Notes: ⇑ = Increase, ⇓ = Decrease, ⇔ = No Significant change.

(Small) = Small increase in solution concentration of element.

(Large) = Large increase in solution concentration of element.

(Fluctuates) = Increases or decreases when solid to liquid ratio increases from 1:20 to 1:40 but then decreases or increases respectively when solid to liquid ratio increases from 1:20 to 1:10.

T = Changes are also time-dependent and may differ from one curing time to another.

D = The stated behaviour clearly varies with test duration

Table 5.10 **General changes in element concentration due to increasing batch test duration from 6 hours to 24 hours for *filtered* samples only.**

Mineral and mix design	Elements determined in final batch test leachate							
	Ca	Fe	Pb	Na	Si	Mg	Al	Mn
English China Clay only	⇔	⇔	⇔	⇔	⇔	⇔	⇔	⇔
English China Clay only + 2500ppm Pb	⇔	⇔	⇑ (Large^{T})	⇔	⇑ (Small)	⇑ (Small)	⇔	⇑ (Large)
English China Clay only + 5000ppm Fe	⇓ (Small^{T})	⇓ (Small)	⇓ (Small)	⇔	⇑ (Small)	⇔	⇔	⇔
English China Clay + 1.5% lime	⇑ (Large^{T})	⇔	⇔	⇔	⇔	⇔	⇔	⇔
English China Clay + 1.5% lime + 5000ppm Pb	⇑ (Large^{T})	⇔	⇔	⇔	⇔	⇔	Fluctuates	⇔
English China Clay + 1.5% lime + 5000ppm Fe	⇑ (Large^{T})	⇔	⇔	⇔	⇔	⇔	⇑ (Large)	⇔
English China Clay + 2.5% lime	⇑ (Large^{T})	⇔	⇔	⇔	⇔	⇔	Fluctuates^{T}	⇔
English China Clay + 2.5% lime + 5000ppm Pb	⇑ (Large^{T})	⇔	⇔	⇔	⇔	⇔	Fluctuates^{T}	⇔
English China Clay + 2.5% lime + 5000ppm Fe	⇑ (Large^{T})	⇔	⇔	⇔	⇔	⇔	Fluctuates^{T}	⇔
Wyoming Bentonite + 7.0% lime	Fluctuates^{T}	⇔	⇔	Fluctuates^{T}	⇑ (Small)	⇔	⇓ (Small^{T})	⇔
Wyoming Bentonite + 7.0% lime + 5000ppm Pb	Fluctuates^{T}	⇔	⇔	Fluctuates^{T}	⇔	⇔	⇑ (Small^{T})	⇔
Wyoming Bentonite + 7.0% lime + 5000ppm Fe	Fluctuates^{T}	⇔	⇔	⇑ (Large^{T})	⇔	⇔	⇔	⇔

Notes: ⇑ = Increase, ⇓ = Decrease, ⇔ = No Significant change.

(Small) = Small increase in solution concentration of element.

(Large) = Large increase in solution concentration of element.

(Fluctuates) = Increases or decreases when solid to liquid ratio increases from 1:20 to 1:40 but then decreases or increases respectively when solid to liquid ratio increases from 1:20 to 1:10.

T = Changes are also time-dependent and may differ from one curing time to another.

5.2.1.5 English China Clay and Wyoming Bentonite sample variations due to changing solid to liquid ratio

It was evident from the above discussion of the effects of initial cube size, rotation speed and test duration on the observed changes in pH and conductivity were relatively small. Therefore, it is reasonable to assess the effects of solid to liquid ratio for one set of initial batch test parameters. The data discussed in this section was from 6 hour / 30 rpm tests with an initial cube size of 20mm.

Figure 5.7 illustrates the effects of increasing solid to liquid ratio on the end of batch test solution pH values of English China Clay samples. It was evident that increasing solid to liquid ratio resulted in a larger increase in pH as the lime content increased. These increases were of a greater magnitude when increasing the solid to liquid ratio from 1:40 to 1:20 than from 1:20 to 1:10 although the trends appeared very similar in nature. It was also clear that as the lime content increased the spread in the increase in pH results for the various contaminated mixes reduced implying that the lime content was predominantly controlling the change.

Consideration of the increase in solid to liquid ratio from 1:40 to 1:20 showed that all contaminated samples with no added lime displayed a decrease in pH whilst the uncontaminated sample displayed an increase in pH. This was not the case for the similar increase in solid to liquid ratio 1:20 to 1:10 where all samples with no added lime displayed a decrease in pH. The reduction in pH of the contaminated samples on increasing solid to liquid ratio was understandable because of the acidic nature of the contaminants. If there were higher solids content then there were more acidic contaminants present hence a reduction in pH. Furthermore, as the pH reduced there were fewer positive charge sites on the clay surface to adsorb metal ions. This was likely to have an effect on both pH and conductivity due to changes in equilibrium.

The increase in pH of the uncontaminated samples due to increasing solid to liquid ratio from 1:40 to 1:20 and the subsequent reduction due to increasing solid to liquid ratio from 1:20 to 1:10 was probably due to changes in ion equilibrium concentrations and not absolute variations in solid content. The latter point regarding absolute variations in solid content should be explained. For samples tested with a solid to liquid ratio 1:40, 1:20 and 1:10, 0.045kg, 0.090kg and 0.170kg of effective dry solid was added respectively to the batch test containers. It could be suggested that it was not simply doubling the solid to liquid ratio which was important to monitor changes in pH but also that it was important to precisely double the solid

content. This was not carried out during the tests because the volume of the batch test containers was not large enough to contain 0.180kg of dry solid at the solid to liquid ratio 1:10 and it was not considered that a reduction in dry solid to 0.170kg would be significant so long as the solid to liquid ratio was controlled. The effect was also clear for the Wyoming Bentonite samples illustrated in Figure 5.8. A further consideration may be that as the volume of ICP water present reduces so does the volume of dissolved oxygen that could impact on the redox conditions of the system and therefore pH.

Although curing period had an effect, the results were too scattered to determine a specific pattern of behaviour. An interesting point to note is that there was no change in the increase in pH of the Fe^{3+} ion contaminated English China Clay samples with 2.5% lime addition at all curing periods due to an increase in solid to liquid ratio from 1:20 to 1:10 whilst there was a significant increase due to a lime addition of 1.5%. It was also clear that for the Fe^{3+} ion contaminated English China Clay with 1.5% lime the increase in pH due to the change in solid to liquid ratio from 1:20 to 1:10 was related to curing time. In fact as curing time increased the increase in pH increased. This suggested a time-dependent change in the physico-chemical behaviour of the Fe^{3+} ion contaminated sample. The effect was also evident for 24hr/30rpm, 6hr/60rpm and 24hr/60rpm batch tests. The likely reason was that at 1.5% lime addition there was an equilibrium being established with time between dissociation of $Ca(OH)_2$ and the high concentration of Fe in solution. It is feasible that as curing period increased and solid to liquid ratio increased from 1:20 to 1:10 that there were increases in the quantity of soluble Fe adsorbed onto the surfaces of the English China Clay resulting in a change in solution equilibrium allowing further dissolution of $Ca(OH)_2$. The Fe^{3+} ion contaminated English China Clay sample with 2.5% lime added saturated both the 1:20 and 1:10 solid to liquid ratios with hydroxide (OH^-) ions hence there was no measurable change in pH.

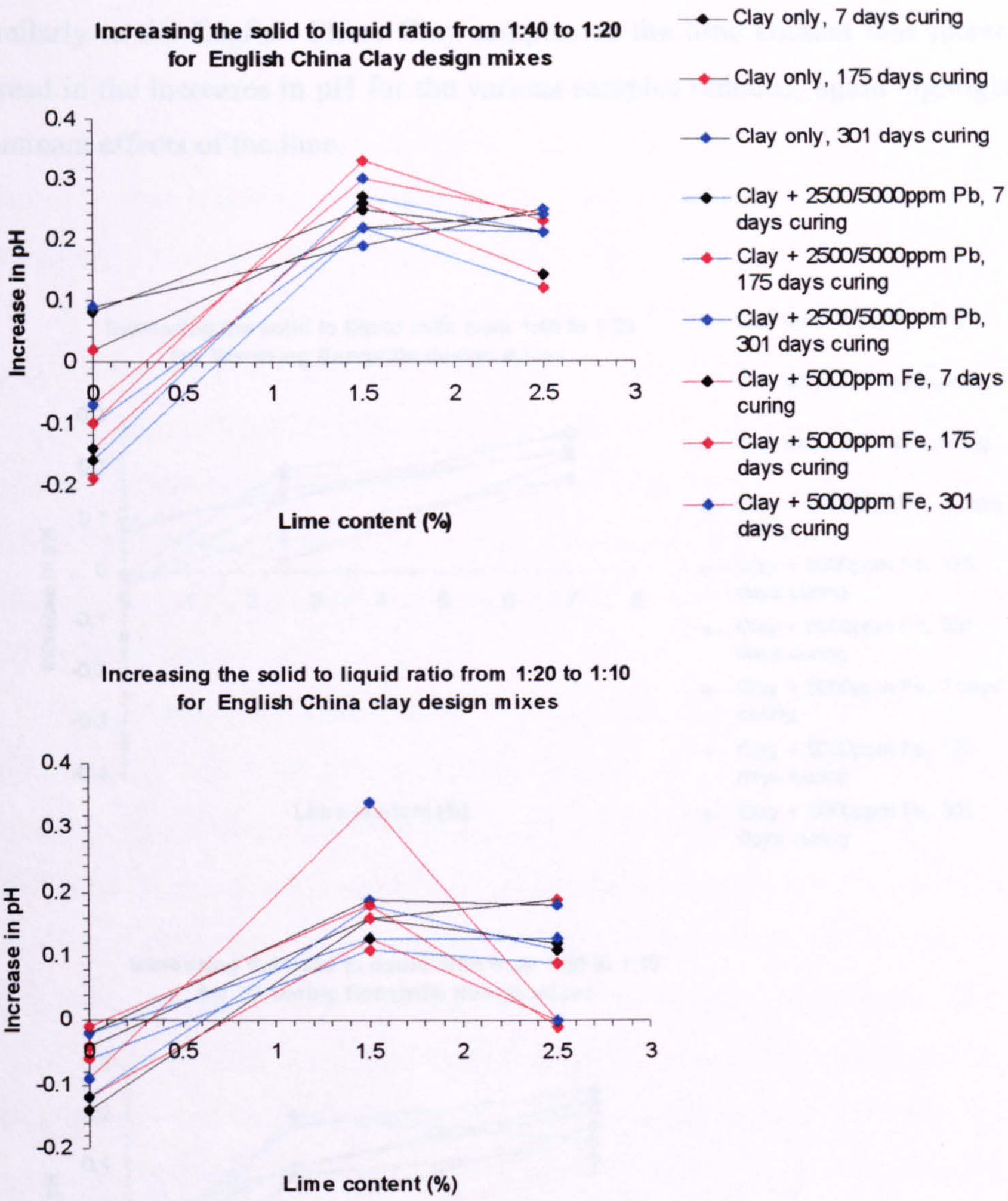

Figure 5.7 **The increases in end of batch test pH with percentage lime addition due to increasing the solid to liquid for English China Clay design mixes**

Figure 5.8 highlights similar pH behaviour for the Wyoming Bentonite design mixes. The most apparent differences include the fact that as the percentage lime increased from 0% to 2.5% to 7.0% the increase in pH continually increased. It was clear however that the largest increase in the increase of pH occurred due to the initial small input of lime similarly to the English China Clay samples. Furthermore, it was apparent that the Fe^{3+} ion contaminated sample increases in pH were the lowest, often negative suggesting dilution of OH^- ions whilst the uncontaminated and Pb^{2+} ion

contaminated sample pH increases were higher and very similar in magnitude. Similarly to the English China Clay samples as the lime content was increased the spread in the increases in pH for the various samples reduced, again highlighting the dominant effects of the lime.

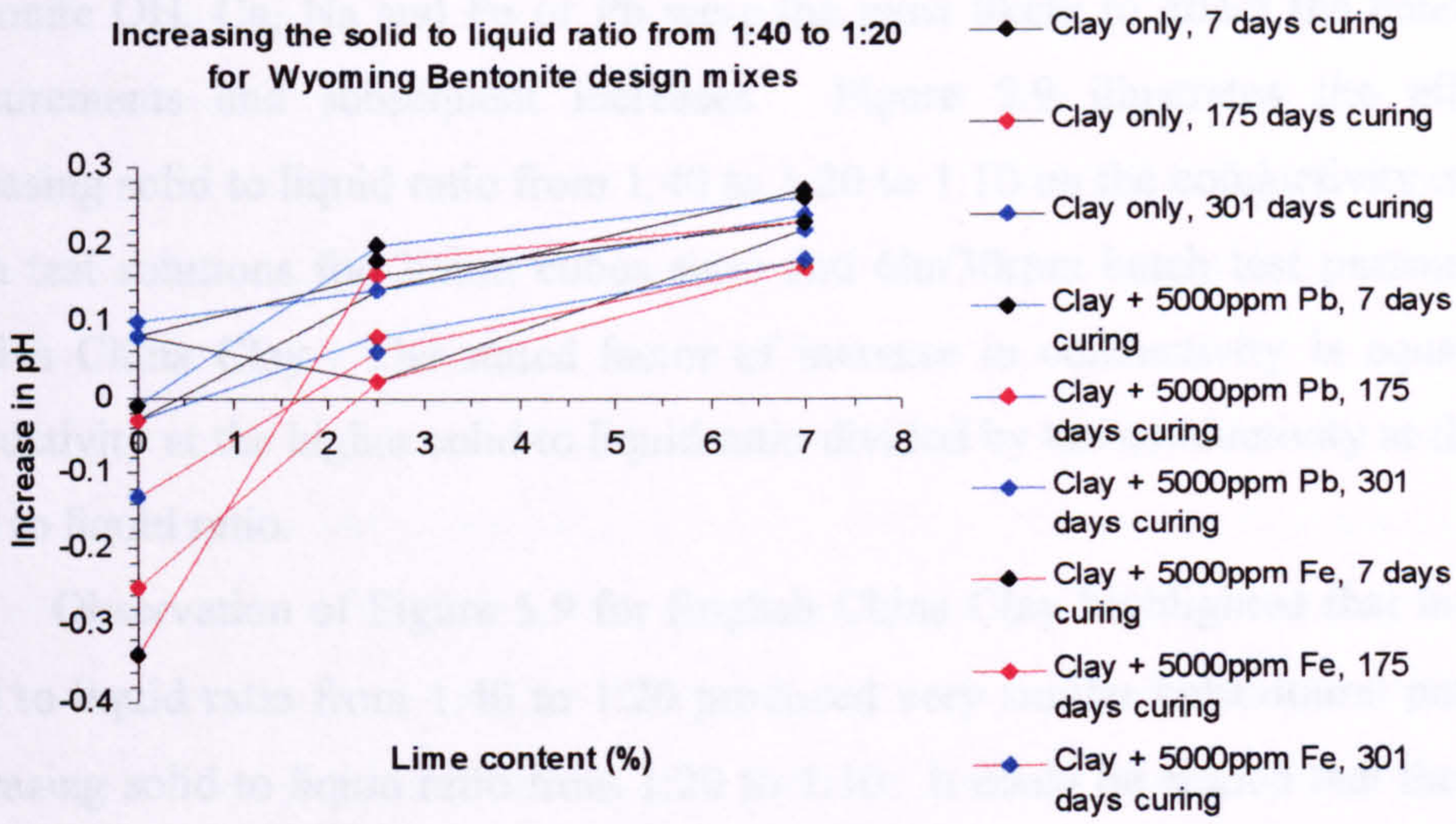

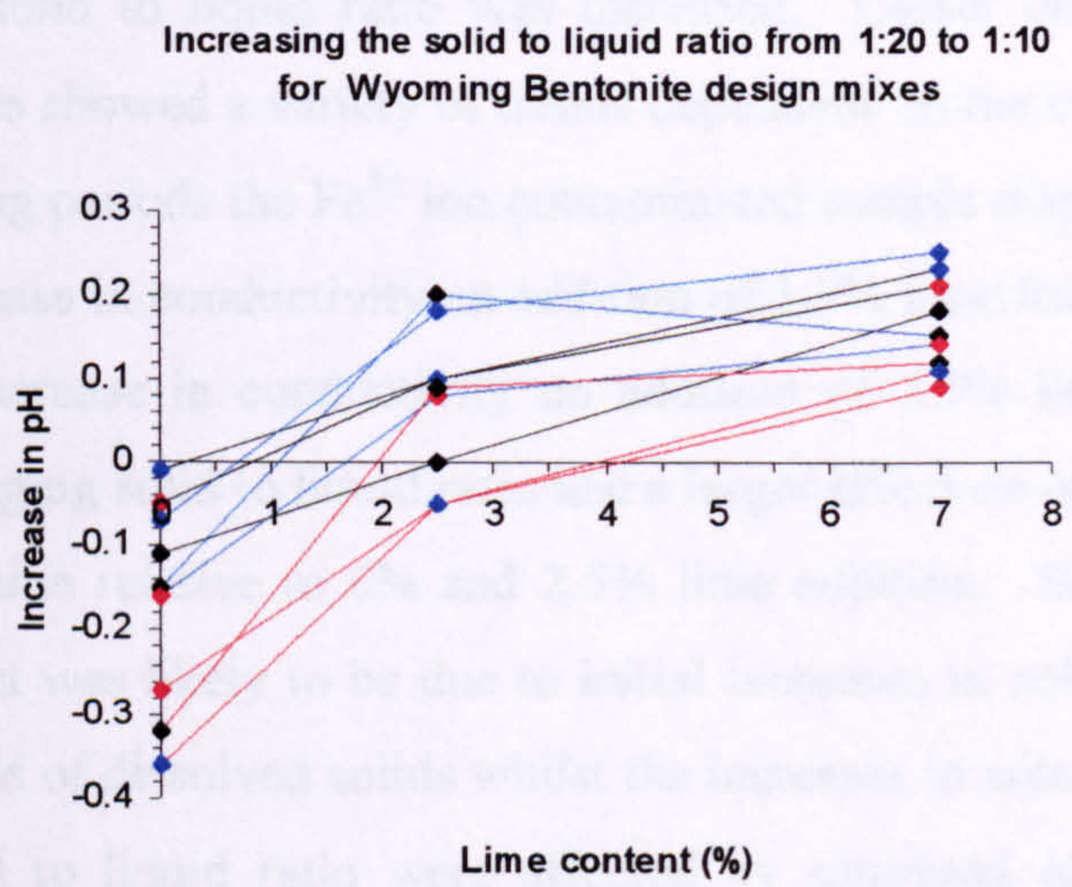

Figure 5.8 **The increases in end of batch test pH with percentage lime addition due to increasing the solid to liquid for Wyoming Bentonite design mixes**

The trends for hydrogen ion concentration (pH) appeared relatively clear. The changes in levels of dissolved solids (conductivity) due to changing the solid to liquid ratio, which includes all cations and anions, was also significant. Previous ICP analysis had shown that for English China Clay samples the most significant dissolved solids affecting conductivity, other than hydrogen ions and hydroxide ions, were soluble Ca and the respective soluble Fe or Pb. With respect to Wyoming Bentonite OH, Ca, Na and Fe or Pb were the most likely to affect the conductivity measurements and subsequent increases. Figure 5.9 illustrates the effects of increasing solid to liquid ratio from 1:40 to 1:20 to 1:10 on the conductivity of end of batch test solutions for 20mm cubes sizes and 6hr/30rpm batch test parameters for English China Clay. The stated factor of increase in conductivity is equal to the conductivity at the higher solid to liquid ratio divided by the conductivity at the lower solid to liquid ratio.

Observation of Figure 5.9 for English China Clay highlighted that increasing solid to liquid ratio from 1:40 to 1:20 produced very similar behavioural patterns to increasing solid to liquid ratio from 1:20 to 1:10. It could be argued that the general trend was a decrease in the increase in conductivity with increasing lime content when the solid to liquid ratio was increased. Closer observation of the specific design mixes showed a variety of trends dependent on the contaminant present. Firstly at all curing periods the Fe^{3+} ion contaminated sample displayed an increase in the factor of increase in conductivity on addition of 1.5% lime followed by a decrease in the factor of increase in conductivity on addition of 2.5% lime. This variation showed that changing solid to liquid ratio had a larger effect on conductivity readings at 1.5% lime addition relative to 0% and 2.5% lime addition. Similarly to the pH variations this effect was likely to be due to initial increases in solid to liquid ratio allowing higher levels of dissolved solids whilst the increases in conductivity after further increases in solid to liquid ratio were affected by saturated solutions. Although the absolute values were very similar for the change in solid to liquid ratio from 1:40 to 1:20 the 7 day cured sample increases were consistently slightly higher than the 175 day cured sample increases which were higher than the 301 day cured sample increases. This implies that as curing period increased, increasing the solid to liquid ratio had less effect on the increase in conductivity, hence indicating a degree of solidification.

Consideration of the Pb^{2+} ion contaminated sample showed that as the lime content increased the effect of increasing solid to liquid ratio reduced. It was also

clear that as curing time increased this effect reduced significantly implying a degree of solidification. At first observation the uncontaminated sample appeared to behave in a rather illogical fashion. However, the absolute conductivity values measured relative to the contaminated samples were very low hence only a slight variation in absolute magnitude related to significant factors of increase. Subsequently at 0% lime addition the increasing factor of increase in conductivity due to increasing curing time signified a release of elements with curing time. On addition of lime to the uncontaminated sample the effect of the Ca and OH was significant and there were more dissolved solids. As the curing time increased the solid to liquid ratio had less effect on conductivity due to the involvement of Ca in the crystallisation processes, a resultant effect of solidification and stabilisation.

The result of increasing the solid to liquid ratio of Wyoming Bentonite batch tests showed similar behaviour (Figure 5.10). As the lime content increases there was a general reduction in the factor of increase in conductivity due to changes in solid to liquid ratio. It was apparent that the change in solid to liquid ratio had the greatest effect on Fe^{3+} ion contaminated samples followed by Pb^{2+} ion contaminated samples and then uncontaminated samples which was a sign that the solutions were becoming saturated with dissolved solids.

An important feature illustrated by Figures 5.7 to 5.10 for both English China Clay samples and Wyoming Bentonite samples was that at the highest lime addition doubling the solid to liquid ratio increased pH from between approximately 0.1 and 0.2 pH divisions for both clays and all design mixes. Furthermore, the same change in solid to liquid ratio resulted in an increase in conductivity by a factor between 1.2 to 1.6.

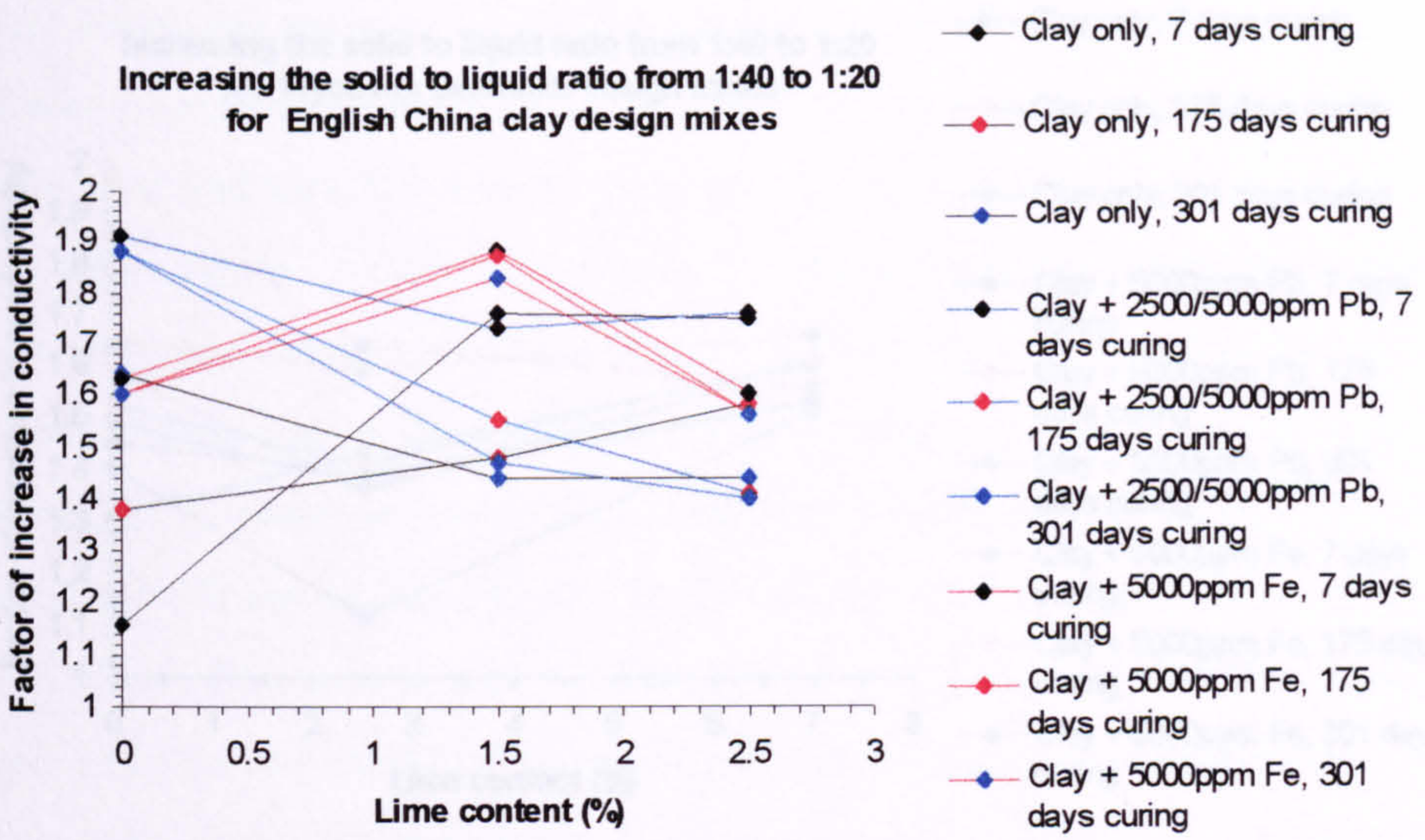

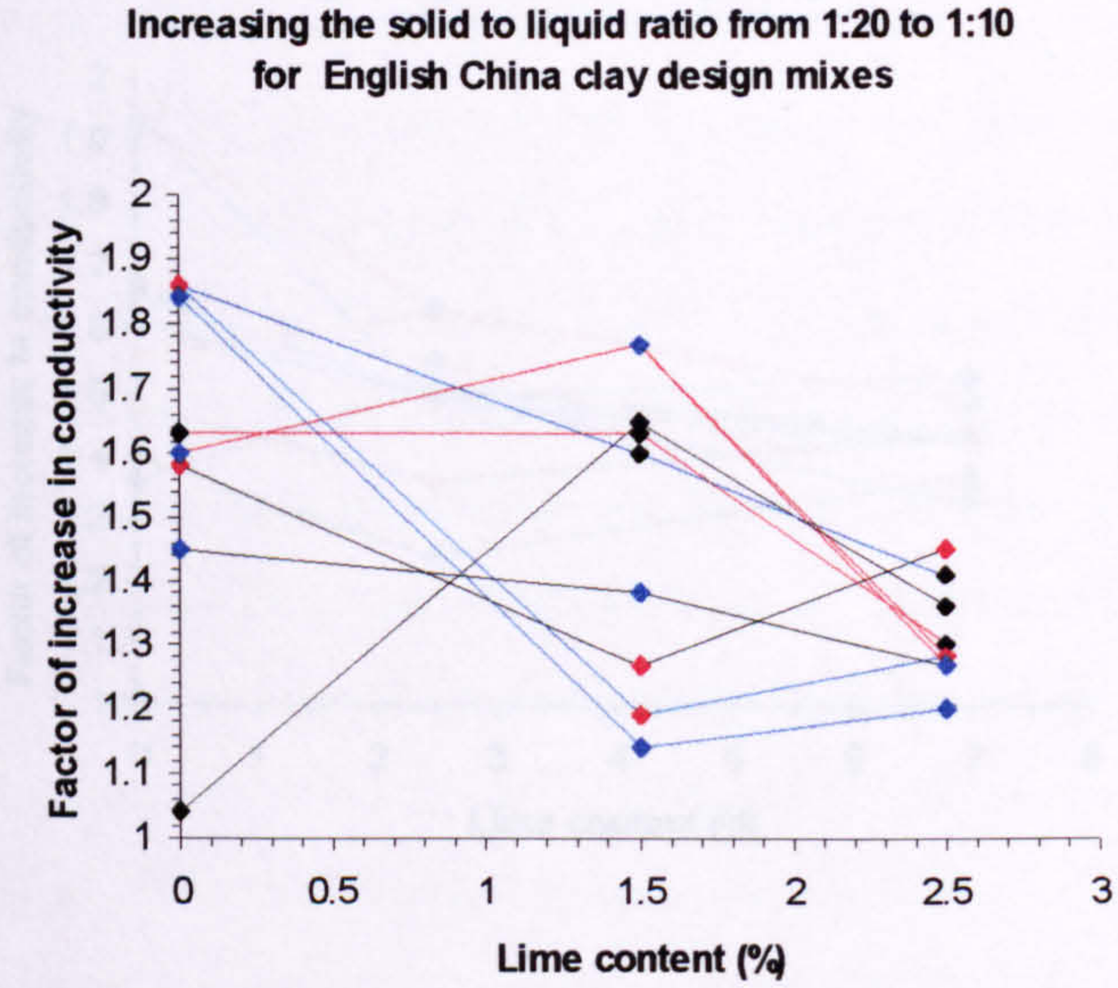

Figure 5.9 **The increases in end of batch test conductivity with percentage lime addition due to increasing the solid to liquid English China Clay design mixes.**

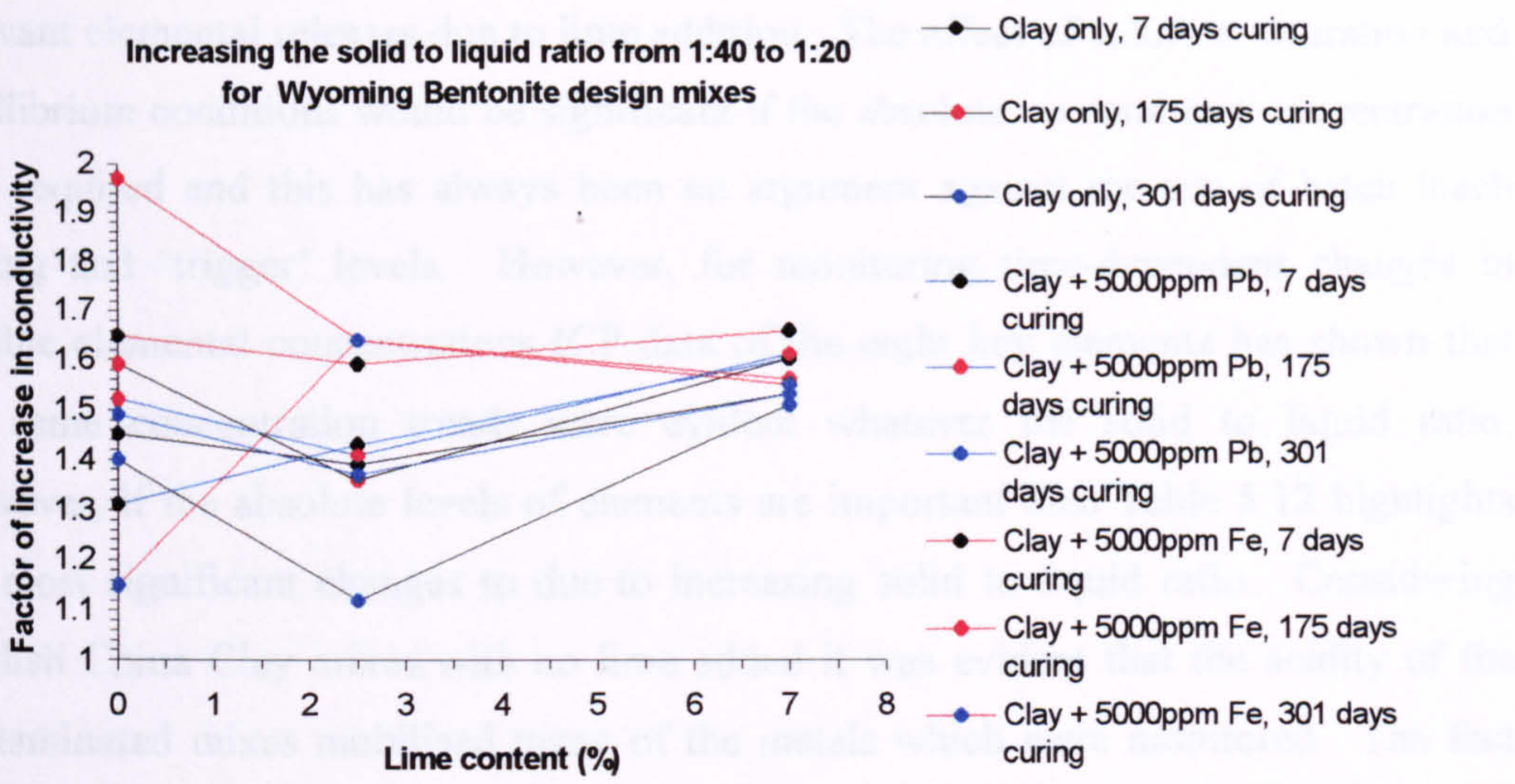

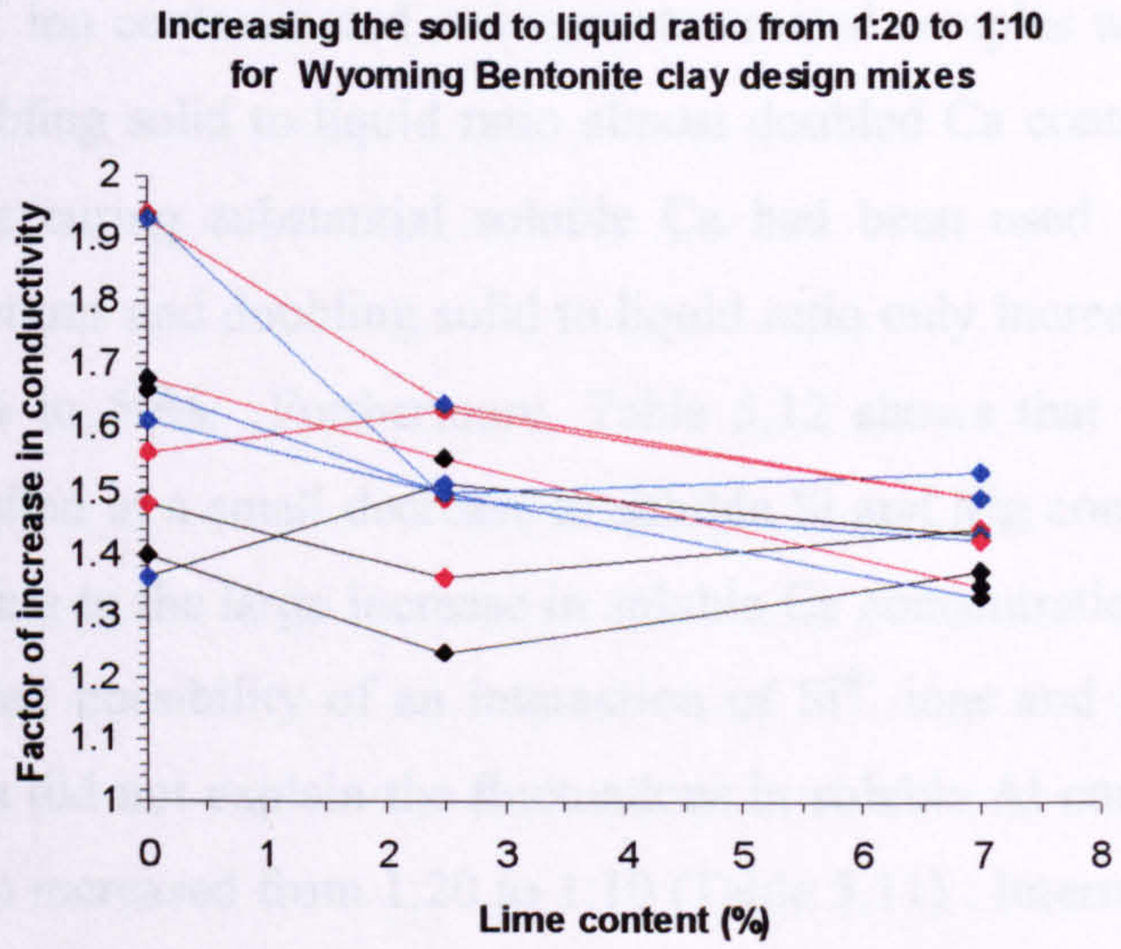

Figure 5.10 The increases in end of batch test conductivity with percentage lime addition due to increasing the solid to liquid for Wyoming Bentonite design mixes with 20mm cubes and 6hr/30rpm batch test parameters

With such distinct changes in pH and conductivity brought about by increasing solid to liquid ratio at high lime contents it was reasonable to suggest that

any solid to liquid ratio could be used to monitor time-dependent changes to the most relevant elemental releases due to lime addition. The effect of solution saturation and equilibrium conditions would be significant if the absolute contaminant concentration was required and this has always been an argument against the use of batch leach testing and 'trigger' levels. However, for monitoring time-dependent changes in soluble elemental concentrations ICP data of the eight key elements has shown that the same concentration trends were evident whatever the solid to liquid ratio. However, if the absolute levels of elements are important then Table 5.12 highlights the most significant changes to due to increasing solid to liquid ratio. Considering English China Clay mixes with no lime added it was evident that the acidity of the contaminated mixes mobilised many of the metals which were monitored. The fact that doubling solid to liquid ratio doubled element concentrations showed that the solutions were not saturated. The trends of the English China Clay mixes with either 1.5% or 2.5% lime were almost the same for each contaminant mix design. For the Pb^{2+} ion contaminated and uncontaminated samples with 1.5% lime at 7 days curing, doubling solid to liquid ratio almost doubled Ca content, however after 175 and 301 days curing substantial soluble Ca had been used in pozzolanic re-crystallisation reactions and doubling solid to liquid ratio only increased Ca concentrations by about 25% to 50%. Furthermore, Table 5.12 shows that increasing solid to liquid ratio resulted in a small decrease in soluble Si and Mg concentrations which was likely to be due to the large increase in soluble Ca concentration and possibly that there was a higher possibility of an interaction of Si^{4+} ions and Mg^{2+} ions with exchange sites. This did not explain the fluctuations in soluble Al concentration when solid to liquid ratio increased from 1:20 to 1:10 (Table 5.11). Interestingly at 7 days curing as solid to liquid ratio was doubled soluble Al concentration halved. At 175 days curing all soluble Al concentration values were similar in magnitude . At 301 days there was a further change where increasing solid to liquid ratio resulted in an increase in soluble Al concentration.

Table 5.11 Al concentration variations for uncontaminated English China Clay samples with 1.5% lime due to increasing solid to liquid ratio.

Curing time (Days)	Solid to liquid ratio		
	Al concentration for 1:10	Al concentration for 1:20	Al concentration for 1:40
7	1.76	3.10	4.87
175	13.39	14.78	11.53
301	15.37	12.59	9.89

The conclusion was therefore that there were potentially several reaction stages linked to stabilisation and solidification, which had varying equilibrium behaviour during closed batch tests. A likely mechanism was that at 7 days curing very little mineral dissolution had occurred. At 175 days sufficient dissolution had occurred to release significant quantities of Al into solution but limited re-crystallisation had occurred. Therefore, if soluble Ca concentrations were still high this may have partially controlled the quantity of Al in solution. At 301 days curing significant re-crystallisation had occurred with a large reduction in soluble Ca concentrations that resulted in an unsaturated solution where the soluble Al concentration was controlled by dilution processes. Direct evidence for this process lies in the data from the English China Clay mix with 5000ppm Fe^{3+} and 1.5% lime. Changes in soluble Ca concentrations due to changing solid to liquid ratio were the same as the other mixes at 7 days, but were not affected by increasing curing time. This suggested that no pozzolanic reactions were occurring and therefore the soluble Al concentrations were very low due to limited dissolution. A further argument could be that the constantly high Ca saturated solution equilibrium was such that Al was not dissolved into solution. However, the very fact that Ca concentrations remained high for Fe contaminated samples implies that no solidification was occurring. The trends for the mixes containing 2.5% lime were exactly the same although soluble Ca concentrations were slightly elevated.

The behaviour of the Wyoming Bentonite samples was similar with occasional exceptions. With the exception of one sample with added Fe^{3+} ions, the contaminated

samples with no lime could not be filtered and the ICP analysis of the centrifuged samples was not reliable. Understanding of these difficulties were not essential for discussion in this report therefore they were presented in Appendix A1. The samples with no lime or 2.5% lime that could be filtered behaved considerably differently to the Wyoming Bentonite samples with 7.0% lime (ICL value) which could be filtered.

Considering first the Fe^{3+} ion contaminated Wyoming Bentonite with no lime, the large increases in soluble Ca, Na, Mg and Mn when the solid to liquid ratio was doubled were likely to be due to increasing the available soluble solids content in an unsaturated solution and the fact that the mix was less alkaline than samples with added lime which could have influenced the release of Mn into solution. The effect on the release of Si and Al into solution were more difficult to understand especially if the solutions were not saturated. It was clear however that Ca, Na, Si, Mg, Al and Mn solution concentration variations with solid to liquid ratio changed with time suggesting that because little solidification was likely to occur at the reduced alkalinity that any soluble Si and Al could be due to cation exchange reactions. Both Si and Al have higher ionic potentials than Ca, Na, and Mg and if in an ionic form in solution they would be likely to be involve in exchange processes as previously stated. The reductions often seen for the soluble Si and Al on increasing solid to liquid ratio could therefore be linked to the fact that there was likely to be more disorder in the system and more opportunity to be involved in exchange reactions. A further more likely possibility was that because the Fe^{3+} ion contaminated Wyoming Bentonite still had significant plasticity there was a tendency for the material to agglomerate within the batch test vessel. Hence on increasing the solid to liquid ratio there was the potential for increased agglomeration and less particle-leachant interaction and therefore reduced soluble Si and Al concentration. It could be argued therefore that the same behaviour would be expected of the other elements such as Ca. This may not have been the case because the Ca may have been more readily available due to its exchange from the exchange sites by the added Fe^{3+} ions. It was likely therefore that the observed behaviour was a complex mix of all these interactions and equilibrium changes.

On addition of a small quantity of lime (2.5%), relative to the ICL value (7.0%), to the Pb^{2+} and Fe^{3+} ion contaminated Wyoming Bentonite the behaviour of doubling the solid to liquid ratio was complex. Many of the elemental releases fluctuated with curing time due to the cation exchange processes related to the initial

flocculation and then by a limited level of solidification. On a molecular level there were more Fe^{3+} contaminant ions present than Pb^{2+} ions and these Fe^{3+} ions satisfied more of the structural charge deficit on the Wyoming Bentonite. Therefore for the Fe^{3+} ion contaminated samples there was more Ca likely to be in solution to be affected by increasing solid to liquid ratio. The large time-dependent increases in soluble Na concentration were also a result of the exchange process. The behaviour of the other elements was likely to be related to the behaviour of the samples with no added lime and also the onset of limited solidification.

The samples with the ICL 7.0% lime content behaved more predictably which was expected because the system was probably saturated with Ca ions and had a consistently high pH thereby consistently promoting pozzolanic solidification reactions. The time-dependent fluctuating soluble Ca concentrations observed when increasing solid to liquid ratio were the result of slight differences in Na exchange and the availability of Ca to be involved in pozzolanic reactions. There was a slight variation in the binding properties of the cubes used in the batch tests due to contaminant affects and this would have an effect on particle breakdown and therefore the changes in ion exchange that could occur during the batch test. The Na concentration was linked to the exchange processes and the interaction of all potential exchanging ions in the system. It was therefore not unexpected with the high lime content that doubling solid to liquid ratio almost doubled soluble Na concentrations. The time-dependent variation in soluble Na release due to changing solid to liquid ratio was also linked to the pozzolanic solidification reactions because as the material solidified there was reduced breakdown of the monolithic cubes.

Comparing the changes in chemistry brought about by changing solid to liquid ratio did help develop understanding of some of the chemical processes occurring including equilibrium changes. It was also evident that solid to liquid ratio was the most important batch test variable out of all the variables tested (initial cube size, rotation speed, test duration, solid to liquid ratio). The second most important variable was test duration. The likely reasons for their importance were that solid to liquid ratio would change the final chemical equilibrium point whilst test duration would most likely to affect how close the chemical system got to reaching this equilibrium. Although changing the batch test parameters affected the resultant chemistry this could be considered insignificant if the changes of chemistry with time and lime content were still evident. This hypothesis is only valid so long as the test is

not being performed to compare the results to statutory 'trigger' levels. Since the basis of this study was to assess whether a batch test could indicate changes in the chemistry of clay-contaminant-lime mixes then it is apparent that any of the batch test parameters could be chosen to assess changes with time. It may be useful to mention at this stage that perhaps an understanding of the chemical developments with time of clay-contaminant-lime mixes is of more use in risk based regulatory control than comparing data with 'trigger' levels.

Table 5.12 General changes in element concentration due to doubling solid to liquid ratio for *filtered* samples only.

Mineral and mix design	Elements determined in final batch test leachate							
	Ca	Fe	Pb	Na	Si	Mg	Al	Mn
English China Clay only	⇑ (Small)	⇔	⇔	⇔	⇑ (Small)	⇔	⇔	⇔
English China Clay only + 2500ppm Pb	⇑ (Nearly doubles)	⇔	⇑ (nearly doubles)	⇑ (small)	⇑ (Nearly doubles)	⇑ (Nearly doubles)	⇔	⇑ (Nearly doubles)
English China Clay only + 5000ppm Fe	⇑ (Nearly doubles)	⇑ (Nearly doubles)	⇑ (small)	⇑ (small)	⇑ (Nearly doubles)	⇑ (Nearly doubles)	⇑ (Nearly doubles)	⇑ (Nearly doubles)
English China Clay + 1.5% lime	⇑ (Large^{T})	⇔	⇔	⇑ (Small)	⇓ (Small^{T})	⇓ (Small^{T})	Fluctuates^{T}	⇔
English China Clay + 1.5% lime + 5000ppm Pb	⇑ (Large^{T})	⇔	⇔	⇑ (Small)	⇓ (Small^{T})	⇓ (Small^{T})	Fluctuates^{T}	⇔
English China Clay + 1.5% lime + 5000ppm Fe	⇑ (Nearly doubles)	⇔	⇔	⇑ (Small)	⇓ (Small^{T})	Fluctuates^{T}	⇑	⇔
English China Clay + 2.5% lime	⇑ (Large^{T})	⇔	⇔	⇑ (Small)	⇓ (Small^{T})	⇓ (Small^{T})	Fluctuates^{T}	⇔
English China Clay + 2.5% lime + 5000ppm Pb	⇑ (Large^{T})	⇔	⇔	⇑ (Small)	⇓ (Small^{T})	⇓ (Small^{T})	Fluctuates^{T}	⇔
English China Clay + 2.5% lime + 5000ppm Fe	⇑ (Large)	⇔	⇔	⇑ (Small)	Fluctuates	Fluctuates	Fluctuates^{T}	⇔
Wyoming Bentonite only + 5000ppm Fe *(7 days curing only)*	⇑ (Nearly doubles^{T})	⇔	⇔	⇑ (Large^{T})	Fluctates^{T}	⇑ (Nearly doubles^{T})	⇓ (small^{T})	⇑ (Nearly doubles^{T})
Wyoming Bentonite + 2.5% lime + 5000ppm Pb *(7 days curing only)*	⇓ (Small^{T})	⇓ (Small^{T})	⇓ (Small^{T})	⇑ (Large^{T})	⇓ (Nearly halves)	⇓ (Small^{T})	⇔	⇔
Wyoming Bentonite + 2.5% lime + 5000ppm Fe	⇑ (Nearly doubles)	⇔	⇔	⇑ (Nearly doubles^{T})	Fluctates^{T}	Fluctates^{T}	⇔	⇔
Wyoming Bentonite + 7.0% lime	Fluctates^{T}	⇓ (Small^{T})	⇔	⇑ (Nearly doubles^{T})	⇓ (Small^{T})	⇓ (Small^{T})	⇑ (small^{T})	⇔
Wyoming Bentonite + 7.0% lime + 5000ppm Pb	Fluctates^{T}	⇓ (Small^{T})	⇔	⇑ (Nearly doubles^{T})	⇓ (Small^{T})	⇓ (Small^{T})	⇑ (small^{T})	⇔
Wyoming Bentonite + 7.0% lime + 5000ppm Fe	Fluctates^{T}	⇔	⇔	⇑ (Nearly doubles^{T})	⇓ (Small^{T})	⇓ (Small^{T})	Fluctuates	⇔

Notes: ⇑ = Increase, ⇓ = Decrease, ⇔ = No Significant change.

(Small) = Small increase in solution concentration of element due to doubling solid to liquid ratio.

(Large) = Large increase in solution concentration of element but not double the concentration.

(Nearly doubles) = Element solution concentration almost doubles due to doubling solid to liquid ratio.

(Nearly halved) = Element solution concentration almost halves due to doubling solid to liquid ratio.

(Fluctuates) = Increases or decreases when solid to liquid ratio increases from 1:20 to 1:40 but then decreases or increases respectively when solid to liquid ratio increases from 1:20 to 1:10.

T = Changes are also time-dependent and may differ from one curing time to another.

5.2.2 End of test pH and conductivity variations with curing time for English China Clay and Wyoming Bentonite samples

This section will present the results to examine whether a rapid cost effective extraction test can be used to assess time-dependent chemical developments (stabilisation and solidification) of clay-lime-contaminant mixes?

Not only will the chemical developments be illustrated in data from batch tests (6hr/30rpm, 1:20 solid to liquid ratio, 20mm initial cube size) but these data will be used to explain physical changes that have an effect on material durability. These changes in behaviour with time were the most significant observations during this study and as such will be discussed in detail.

At the end of a chemical batch test the final pH and conductivity of the solution and suspended solids provides substantial information about changes in the general quantity of dissolved solids and the very important H_30^+ ion concentration. If the tests are carried out at different curing times the changes in stabilisation and solidification reactions can be monitored via these simple pH and conductivity measurements. Although it is clear that some tests do not achieve equilibrium, the trends of all batch tests performed for a specific mix design are the same. The reasons for a sample not reaching equilibrium in the solution is due to the fact that the tests are essentially on small stabilised monolithic masses with continually changing strengths and plasticity properties. These strengths and plasticity properties change with the type of contaminant present and the quantity of lime added which in itself is a contaminant. Hence any batch test using any solid to liquid ratio, any cube size, any test duration and any test speed can be used to help explain the stabilisation and solidification reactions. The cautionary note must be that the choice of solid to liquid ratio may be important if very small soluble quantities of elements are involved which may be diluted below detection limits. The converse is also true if there are very high soluble concentrations of one element, equilibrium may reduce the concentration in solution of one ion due to the high concentration of another. In the case of lime treatment the soluble concentration of elements released during stabilisation and solidification have been shown to be high for the minerals studied. For these reasons the most time economic 6hr test duration, the most time economic 20mm cubes, the most energy economic 30rpm test speed, and the most time economic 1:20 solid to liquid ratio have been chosen for analysis. The 1:20 solid to liquid ratio was chosen since it shows high levels of important elements such as Si, Al, Na and Ca. In many

cases the 1:10 solid to liquid ratio required significant dilutions prior to ICP analysis which was very time consuming and required an initial analysis to determine the level of dilution required. This was not very time and material economic and could lead to increased experimental error. The 1:40 solid to liquid ratio diluted some elements to levels very close to the detection limits that could lead to a higher degree of experimental error. A consideration must also be made of the pH that results from the different solid to liquid ratios. If the pH was to reduce too significantly then some contaminants previously of low solubility could become significantly soluble which would not necessarily represent the behaviour of the monolithic mass.

Figure 5.11 illustrates the variation of end of batch test pH and conductivity for English China Clay and Wyoming Bentonite design mixes. Considering initially the pH data for both the English China Clay and Wyoming Bentonite mix designs there were a number of trends. As expected, generally for both clay design mixes the higher the percentage lime addition the higher the final pH values. For the English China Clay samples with 2.5% lime addition, the highest pH was generated for the uncontaminated sample followed by the Pb^{2+} ion contaminated sample and then the Fe^{3+} ion contaminated sample. At 1.5% lime addition the uncontaminated and Pb^{2+} ion contaminated samples produced very similar pH values whilst the Fe^{3+} ion contaminated sample pH values were significantly lower. Untreated English China Clay pH values were significantly lower and acidic. The variations due to contaminant addition were the same as those of the lime-treated samples although the magnitude of variation was far more exaggerated.

For the Wyoming Bentonite samples the variations due to lime addition were more distinct than those of the English China Clay samples due to the larger increases in lime addition. For the 7.0% lime addition, the highest pH was generated by the Pb^{2+} ion contaminated sample followed by the uncontaminated sample then the Fe^{3+} ion contaminated sample. The trends were the same for the 2.5% lime addition samples, whilst, similarly to the English China Clay mixes the samples with no lime addition, the highest pH was produced by the uncontaminated sample followed by the Pb^{2+} ion contaminated sample and the Fe^{3+} ion contaminated sample. It was evident that the pH of the uncontaminated Wyoming Bentonite samples were far higher than those of the uncontaminated English China Clay samples and this was due to the naturally high pH properties of the clay.

Perhaps the most significant observation was that uncontaminated and Pb^{2+} ion contaminated samples for both clays showed reductions in pH with increasing curing time. For lime-treated samples the largest decrease could be seen between 7 and 175 days curing with smaller reductions between 175 and 301 days. For samples not treated with lime there was also a reduction in pH although this appeared directly proportional to the curing period. Fe^{3+} ion contaminated samples did provide the exception. For English China Clay samples contaminated with Fe^{3+} ions and treated with both 1.5% and 2.5% lime there were only very small reductions in pH when curing period was increased. For Fe^{3+} ion contaminated samples not treated with lime there were slight increases in pH with curing period. The Wyoming Bentonite samples contaminated with Fe^{3+} ions and treated with 2.5% and 7.0% lime showed decreases in pH similar in magnitude to the other contaminated and uncontaminated samples. The Fe^{3+} ion contaminated Wyoming Bentonite sample with no lime addition showed higher increases in pH than the respective English China Clay sample.

Indirect consideration of the variation in dissolved solids content via solution conductivity measurements further illustrated the significance of the variation in pH readings with curing time. Generally for both clay samples the highest conductivities and hence quantities of dissolved solids were achieved by the samples with the highest percentage lime additions. However, this was not always true due to variations brought about by varying levels of crystallisation with increasing curing time. Consideration of the English China Clay samples with 1.5% lime illustrated that the Pb^{2+} ion contaminated sample had the highest conductivity values followed by the uncontaminated sample. Conversely at 2.5% lime addition the uncontaminated sample had the higher conductivity relative to the Pb^{2+} ion contaminated sample. Significantly for samples containing Fe^{3+} ion contamination the sample with 2.5% lime had the highest conductivity followed by the sample with no added lime followed by the sample with 1.5% lime. For English China Clay samples with no lime addition the highest conductivity was achieved by the Fe^{3+} ion contaminated samples followed by much lower conductivities for the Pb^{2+} ion contaminated samples and then the uncontaminated samples. The Pb^{2+} ion contaminated sample in this case was unduly low relative to the Fe^{3+} ion contaminated sample since only 2500ppm Pb^{2+} ions was added to this sample relative to the 5000ppm of Fe^{3+} ions to

the Fe^{3+} ion contaminated sample. This was an error during the initial stages of sample preparation.

Consideration of the conductivities of Wyoming Bentonite samples illustrated significantly different behaviour. For samples with 7.0% lime addition at 7 days curing the uncontaminated and Pb^{2+} ion contaminated samples had a higher conductivity than the Fe^{3+} ion contaminated samples. However, at 175 and 301 days curing both the uncontaminated and Pb^{2+} ion contaminated samples had lower conductivities and hence lower levels of dissolved solids relative to the Fe^{3+} ion contaminated sample. For samples with only 2.5% lime addition the trend was significantly different with the Fe^{3+} ion contaminated sample producing the highest conductivities at any curing period followed by the Pb^{2+} ion contaminated sample followed by the uncontaminated sample. For samples with no lime addition the Fe^{3+} ion contaminated sample had the highest conductivity followed by the Pb^{2+} ion and uncontaminated samples which had similar conductivity values. An important point to note was that the conductivities of the uncontaminated and Pb^{2+} ion contaminated Wyoming Bentonite samples with no lime were much higher than the respective English China Clay samples. However, the conductivities of the uncontaminated and Pb^{2+} ion contaminated Wyoming Bentonite samples with 2.5% lime were much lower than the respective English China Clay samples. This was likely to be linked to pH and the effects of cation exchange.

Perhaps the most significant difference between the English China Clay and Wyoming Bentonite conductivities was the change in conductivity with curing period. For English China Clay samples with lime added, as curing period increased there were very large decreases in conductivity for all samples with the exception of the Fe^{3+} ion contaminated samples. However, for Wyoming Bentonite with lime added the conductivity of all samples including the Fe^{3+} ion contaminated samples reduced significantly. The reductions in conductivity values were most significant for the higher lime contents. At 7 days curing the conductivity of the Fe^{3+} ion contaminated sample with 7.0% lime was lower than those of the other samples with 7.0% lime. However, at 175 and 301 days curing the converse was true. A further important factor to consider was that with the exception of the Fe^{3+} ion contaminated samples, the Wyoming Bentonite with 7.0% lime had only slightly higher conductivities than the English China Clay samples with only 2.5% lime.

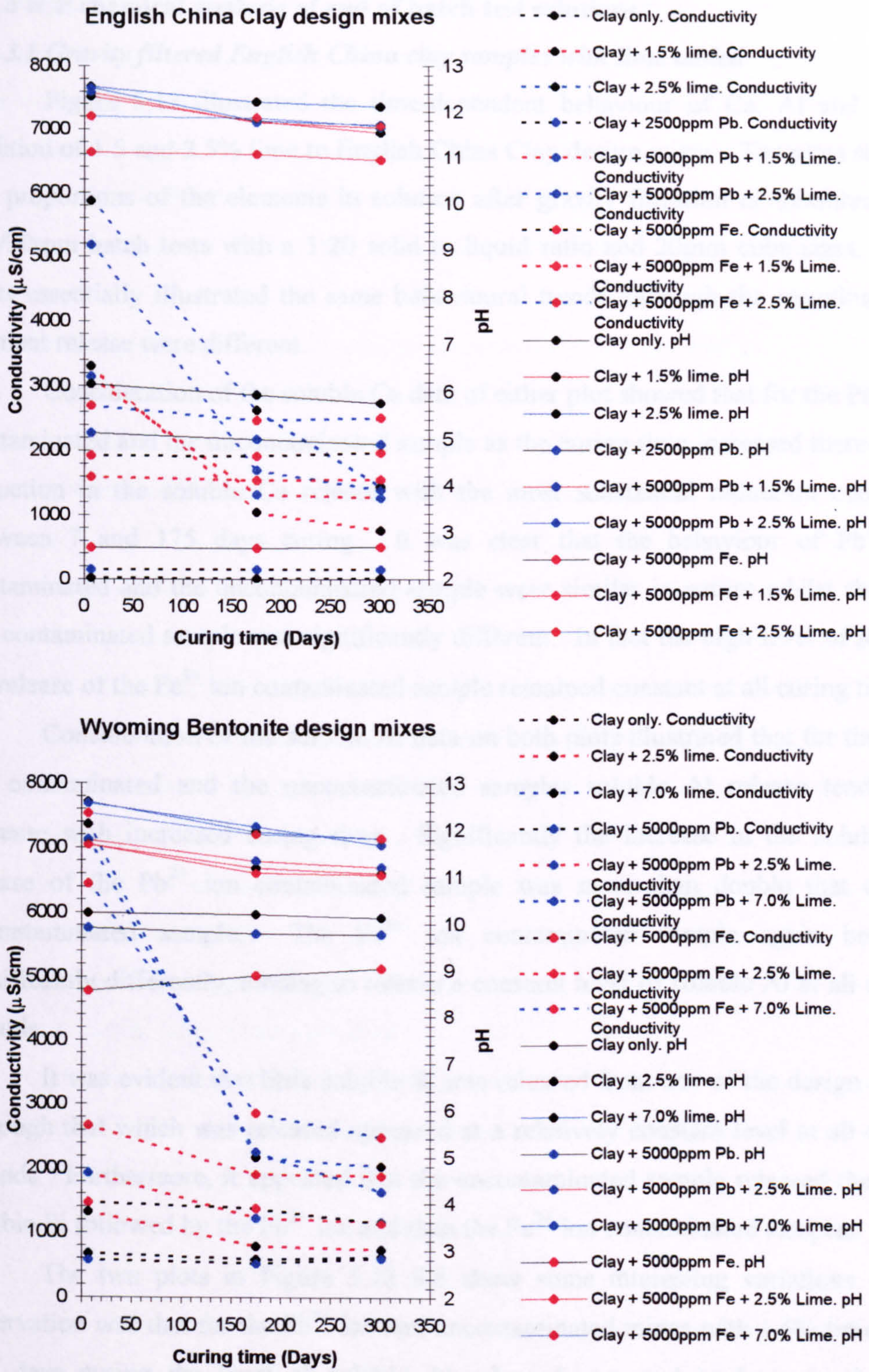

Figure 5.11 Variation of end of batch test pH and conductivity for English China Clay and Wyoming Bentonite design mixes. 1:20 solid to liquid ratio, 20mm cube size, 6hr/30rpm batch tests

5.2.3 ICP chemical analysis of end of batch test solutions

5.2.3.1 Gravity filtered English China clay samples with lime added

Figure 5.12 illustrated the time-dependent behaviour of Ca, Al and Si on addition of 1.5 and 2.5% lime to English China Clay design mixes. The plots showed the proportions of the elements in solution after gravity filtration of mixtures from 6hr/30rpm batch tests with a 1:20 solid to liquid ratio and 20mm cube sizes. Both plots essentially illustrated the same behavioural trends although the magnitudes of element release were different.

Consideration of the soluble Ca data of either plot showed that for the Pb^{2+} ion contaminated and the uncontaminated sample as the curing time increased there was a reduction in the soluble Ca release with the most substantial reduction occurring between 7 and 175 days curing. It was clear that the behaviour of Pb^{2+} ion contaminated and the uncontaminated sample were similar in nature whilst the Fe^{3+} ion contaminated sample was significantly different. In fact the high level of soluble Ca release of the Fe^{3+} ion contaminated sample remained constant at all curing times.

Consideration of the soluble Al data on both plots illustrated that for the Pb^{2+} ion contaminated and the uncontaminated samples soluble Al release tended to increase with increased curing time. Significantly the increase in the soluble Al release of the Pb^{2+} ion contaminated sample was more than double that of the uncontaminated sample. The Fe^{3+} ion contaminated sample again behaved significantly differently, tending to release a constant level of soluble Al at all curing periods.

It was evident that little soluble Si was released from any of the design mixes although that which was released appeared at a relatively constant level at all curing periods. Furthermore, it appeared that the uncontaminated sample released the most soluble Si followed by the Pb^{2+} ion and then the Fe^{3+} ion contaminated samples.

The two plots in Figure 5.12 did show some interesting variations. One observation was that for the Pb^{2+} ion and uncontaminated mixes with 1.5% lime after 175 days curing the level of soluble Al released appeared to have reached an optimum. A second observation involved the soluble Ca releases. It would be expected that the mixes including the higher percentage lime would release a higher level of soluble Ca and that was clearly the case for all samples. It was also not surprising that the Fe^{3+} ion contaminated sample with 1.5% lime released more soluble Ca than the Pb^{2+} ion contaminated or the uncontaminated samples with the

same lime content. However, on addition of 2.5% lime to these contaminated mixes and after 7 days curing the Fe^{3+} ion contaminated sample released less soluble Ca relative to the other samples. The potentially anomalous behaviour of the Fe^{3+} ion contaminated sample was also reflected in the soluble Al release after 7 days curing. The level of soluble Al released was significantly higher than the other two mixes, which was not the case for the Fe^{3+} ion contaminated sample with 1.5% lime.

5.2.3.2 Gravity filtered Wyoming Bentonite samples with lime added

Figure 5.13 illustrated the time-dependent behaviour of soluble Ca, Al, Si, Na and Mg on addition of 2.5 and 7.0% lime to Wyoming Bentonite design mixes. The plots showed the proportions of the elements in solution after gravity filtration of mixtures.

Observation of the soluble Ca plots of samples containing 7.0% lime revealed that as the curing time was increased the level of released soluble Ca significantly reduced in much the same way as the English China Clay samples, with the exception that the Fe^{3+} ion contaminated sample also showed a dramatic reduction in soluble Ca release with increased curing time. It was evident that again the Pb^{2+} ion and the uncontaminated samples released similar levels of soluble Ca after 7 days curing whilst the Fe^{3+} ion contaminated sample released more than double the quantity of soluble Ca. However, after 175 and 301 days curing time all design mixes released similar proportions of soluble Ca. Furthermore, the levels of soluble Ca released at these later curing times were almost zero.

Analysis of the soluble Na plots for samples with 7.0% lime content revealed that the soluble Na release was similar in nature to the soluble Ca plots with a few subtle differences. Firstly, the Pb^{2+} ion contaminated and the uncontaminated samples showed similar magnitudes of soluble Na release and similar levels of reduction with increased curing time. After 175 days curing the level of soluble Na release showed no significant further reduction and remained constant at a relatively high level of release. The Fe^{3+} ion contaminated sample behaved slightly differently, releasing more soluble Na than the other two samples and showing a reduced level of reduction with increased curing time but still essentially levelling off at a constant level after 175 days curing time.

Unlike the English China Clay plots the soluble Al release from the Wyoming Bentonite samples with 7.0% lime was quite low. Again the Pb^{2+} ion contaminated

and the uncontaminated samples released more soluble Al than the Fe^{3+} ion contaminated sample. However, for all samples as the curing period increased the soluble Al release increased in an almost linear manner. Again, unlike the English China Clay design mixes, it was the soluble Si release which was more prominent than the soluble Al release for the Wyoming Bentonite samples with 7.0% lime content. Although the soluble Si releases were clearly of a greater magnitude than the soluble Al releases the behavioural patterns with respect to the effects of the contaminants were the same.

An important point of note was that for other solid to liquid ratios and test durations the elemental release of soluble Si and Al for Wyoming Bentonite design mixes with 7.0% lime behaved slightly differently. The release of soluble Al tended to be significantly lower and the soluble Si release significantly higher.

Consideration of the soluble Mg plots in Figure 5.13 should be taken with caution due to the very low concentrations detected. With the exception of the Pb^{2+} ion contaminated sample reading at 301 days curing the level of soluble Mg released appeared relatively constant for all mixes at all curing periods. The results of the Wyoming Bentonite samples with 2.5% added lime should also be observed with caution unlike the samples containing 7.0% lime. This was due to the fact that the Fe^{3+} ion contaminated samples with 2.5% lime content reported in the plots were the only samples that could be gravity filtered. Although the batch test mixtures were sufficiently flocculated to enable filtration, the period of filtration was 12 hours compared to 10 minutes for the samples containing 7.0% lime. 12 hours could have been sufficient time for significant chemical changes. This may have been the reason that the Fe^{3+} ion contaminated samples with 2.5% lime content showed significantly elevated soluble Si, Al and Mg relative to the other samples that would not be expected.

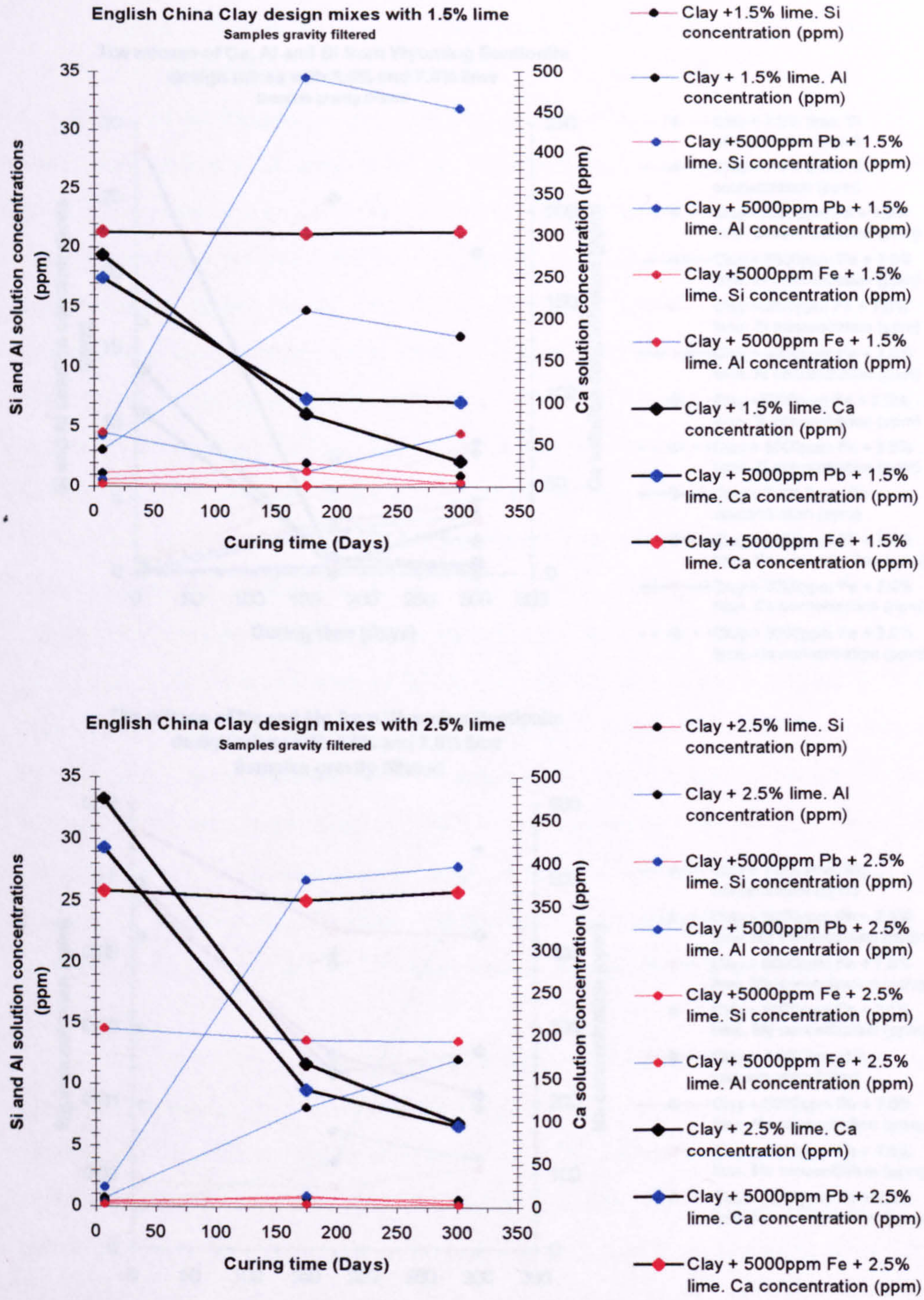

Figure 5.12 **Variation of end of test soluble Ca, Al and Si with curing time for English China Clay design mixes with 1.5 and 2.5% lime content. Solutions analysed were from gravity filtered 6hr/30rpm batch tests with a 1:20 solid to liquid ratio and 20mm cubes**

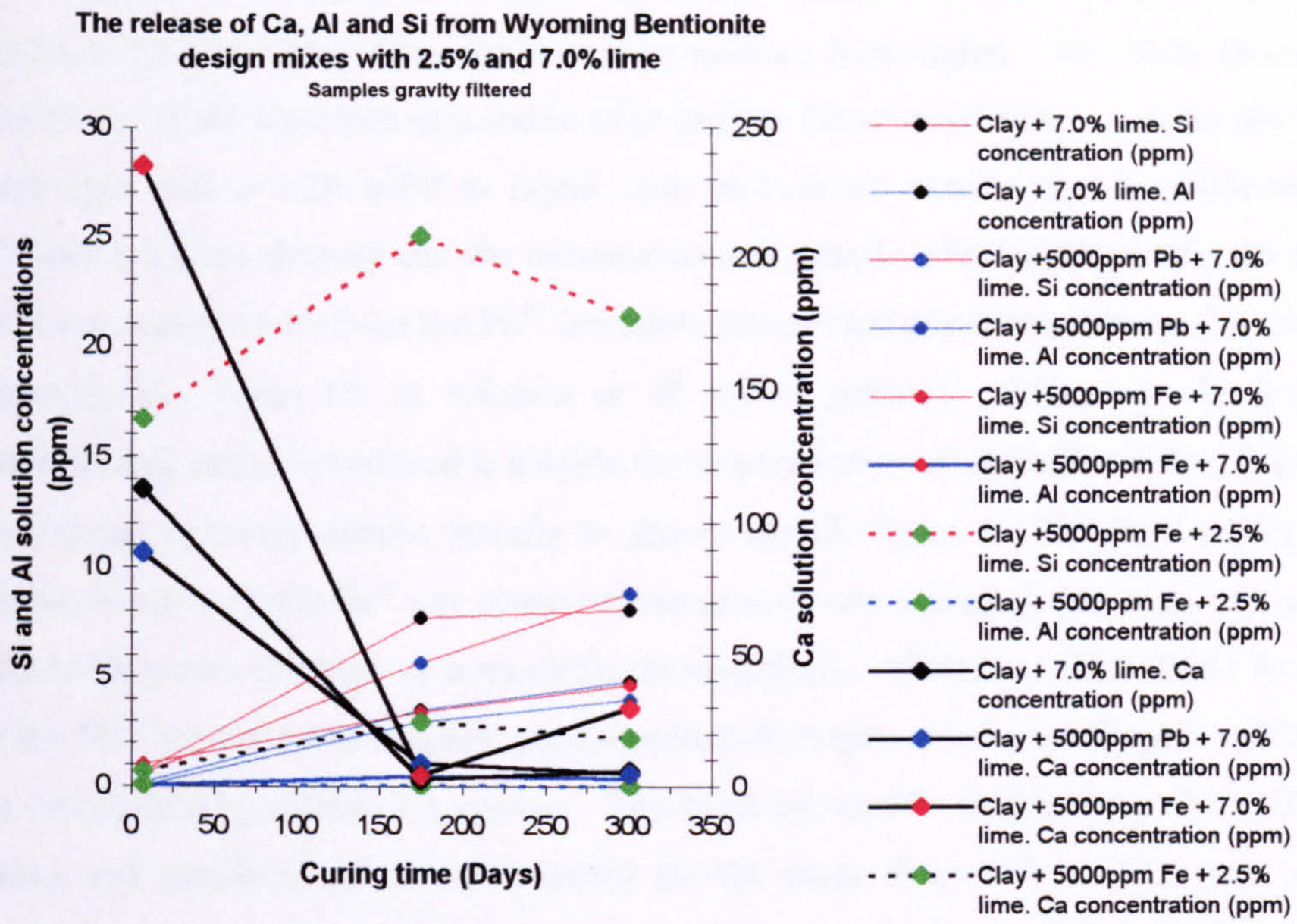

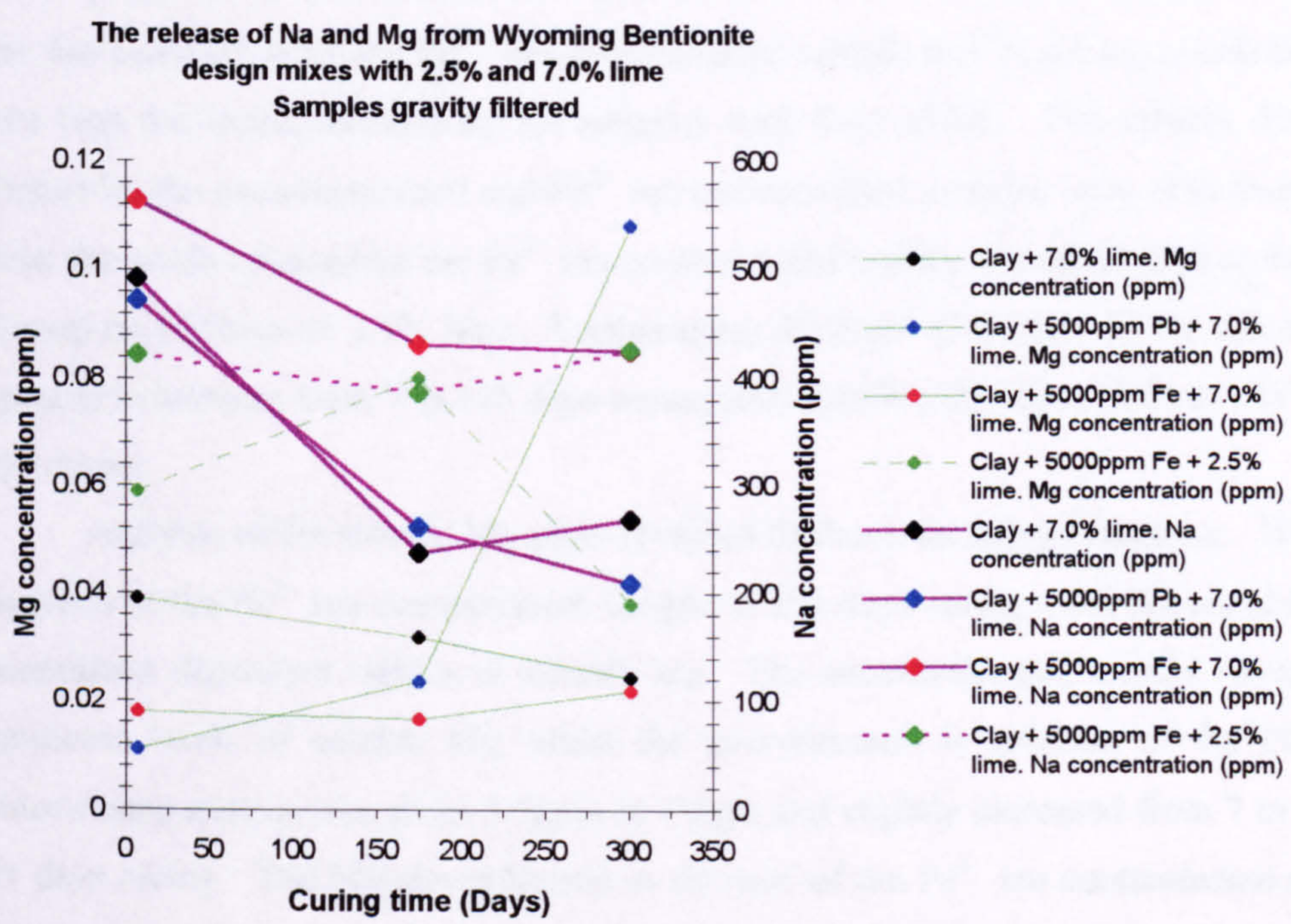

Figure 5.13 **Variation of end of test soluble Ca, Al, Si, Na and Mg with curing time for Wyoming Bentonite design mixes with 2.5 and 7.0% lime content. Solutions analysed were from gravity filtered 6hr/30rpm batch tests with a 1:20 solid to liquid ratio and 20mm cubes**

5.2.3.3 Gravity filtered English China clay samples with no lime added

Figure 5.14 illustrated the time-dependent behaviour of soluble Ca, Al, Si, Mg, Pb and Fe of English China Clay design mixes with no lime added. The plots showed the proportions of the elements in solution after gravity filtration of mixtures from 6hr/30rpm batch tests with a 1:20 solid to liquid ratio and 20mm cube sizes. Consideration of soluble Ca release showed that the uncontaminated sample released essentially no soluble Ca at any curing time whilst the Pb^{2+} ion contaminated sample released a constant level of approximately 6ppm Ca in solution at all curing periods. However, the Fe^{3+} ion contaminated sample produced a soluble Ca concentration of approximately 20ppm at 7 days curing reducing almost linearly to approximately 7ppm at 301 days curing. The soluble Si curve of the Fe^{3+} ion contaminated sample was precisely the same shape as the soluble Ca curve although of a much lower magnitude. However, the soluble Si curves for the Pb^{2+} ion contaminated and uncontaminated samples were significantly different to the corresponding soluble Ca curves. The level of soluble Si fell from 7 to 175 days curing and remained relatively constant at this level from 175 to 301 days curing. Furthermore, the level of soluble Si released by the uncontaminated sample was more than that released from the Pb^{2+} ion contaminated sample and in all cases substantially more than the levels released by the samples with lime added. The soluble Al levels released by the uncontaminated and Pb^{2+} ion contaminated samples were effectively zero whilst the levels released by the Fe^{3+} ion contaminated sample was again higher than that released on addition of 2.5% lime. Furthermore, the level of soluble Al for this sample appeared to increase from 7 to 175 days curing and significantly reduced from 175 to 301 days curing.

Analysis of the soluble Mg plots revealed further interesting behaviour. With the exception of the Fe^{3+} ion contaminated sample at 301 days curing there appeared to be a contaminant dependent release of soluble Mg. The uncontaminated sample released no significant levels of soluble Mg whilst the concentration in solution of the Pb^{2+} ion contaminated sample was about 3.5ppm at 7 days and slightly increased from 7 to 175 to 301 days curing. The Mg concentration in solution of the Fe^{3+} ion contaminated sample was about 7ppm and increased slightly from 7 to 175 days curing but then appeared to abruptly decrease from 175 to 301 days curing. Perhaps one of the most significant details of the plots was that the uncontaminated English China Clay mix design released no measurable soluble Pb or Fe, whilst the level of soluble Fe released from the Fe^{3+} ion contaminated sample showed a significant linear reduction with increasing curing time. Although unfortunately the Pb^{2+} ion contaminated sample contained only 2500ppm Pb^{2+}

ions rather than the desired 5000ppm Pb^{2+} ions the reduction of soluble Pb concentration with increasing curing time was visible in Figure 5.14.

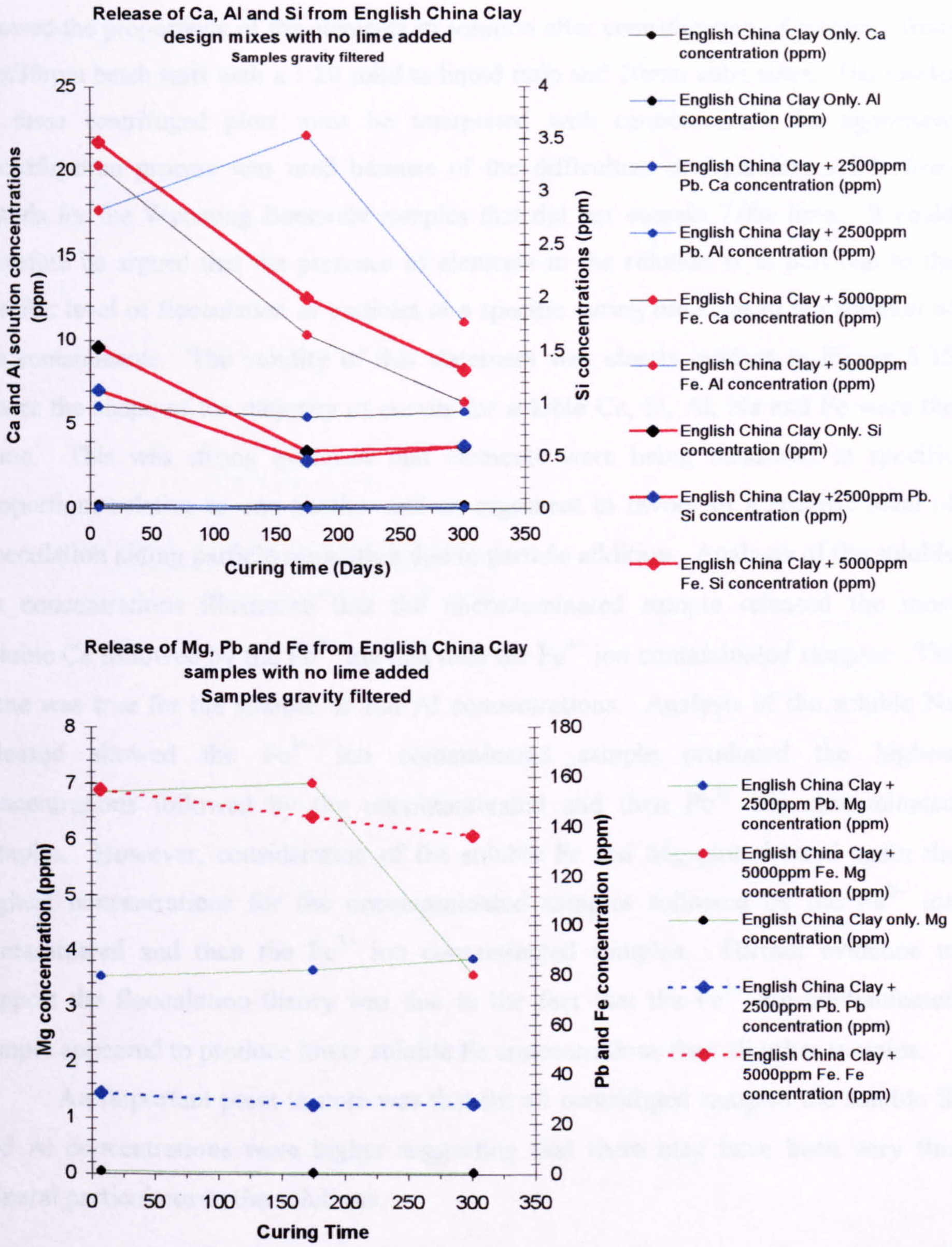

Figure 5.14 **Variation of end of test soluble Ca, Al, Si, Mg, Pb and Fe with curing time for English China clay design mixes with no lime added. Solutions analysed were from gravity filtered 6hr/30rpm batch tests with a 1:20 solid to liquid ratio and 20mm cubes**

5.2.3.4 Centrifuged Wyoming Bentonite design mixes with no lime added

Figure 5.15 illustrated the time-dependent behaviour of soluble Ca, Al, Si, Mg, Na, Pb and Fe of Wyoming Bentonite design mixes with no lime added. The plots showed the proportions of the elements in solution after centrifugation of mixtures from 6hr/30rpm batch tests with a 1:20 solid to liquid ratio and 20mm cube sizes. The results in these centrifuged plots must be interpreted with caution since the aggressive centrifugation process was used because of the difficulties in separating solids from liquids for the Wyoming Bentonite samples that did not contain 7.0% lime. It could therefore be argued that the presence of elements in the solution is in part due to the specific level of flocculation of particles at a specific curing time due to the addition of the contaminants. The validity of this statement was clearly evident in Figure 5.15 where the shape of the majority of curves for soluble Ca, Si, Al, Na and Fe were the same. This was strong evidence that elements were being measured in specific proportions relative to one another and an argument in favour of a specific level of flocculation aiding particle separation due to particle addition. Analysis of the soluble Ca concentrations illustrated that the uncontaminated sample released the most soluble Ca followed by the Pb^{2+} ion and then the Fe^{3+} ion contaminated samples. The same was true for the soluble Si and Al concentrations. Analysis of the soluble Na released showed the Fe^{3+} ion contaminated sample produced the highest concentrations followed by the uncontaminated and then Pb^{2+} ion contaminated samples. However, consideration of the soluble Fe and Mg plot showed again the highest concentrations for the uncontaminated samples followed by the Pb^{2+} ion contaminated and then the Fe^{3+} ion contaminated samples. Further evidence to support the flocculation theory was due to the fact that the Fe^{3+} ion contaminated sample appeared to produce lower soluble Fe concentrations than all other samples.

An important point to note was that for all centrifuged samples the soluble Si and Al concentrations were higher suggesting that there may have been very fine mineral particulates in the solutions.

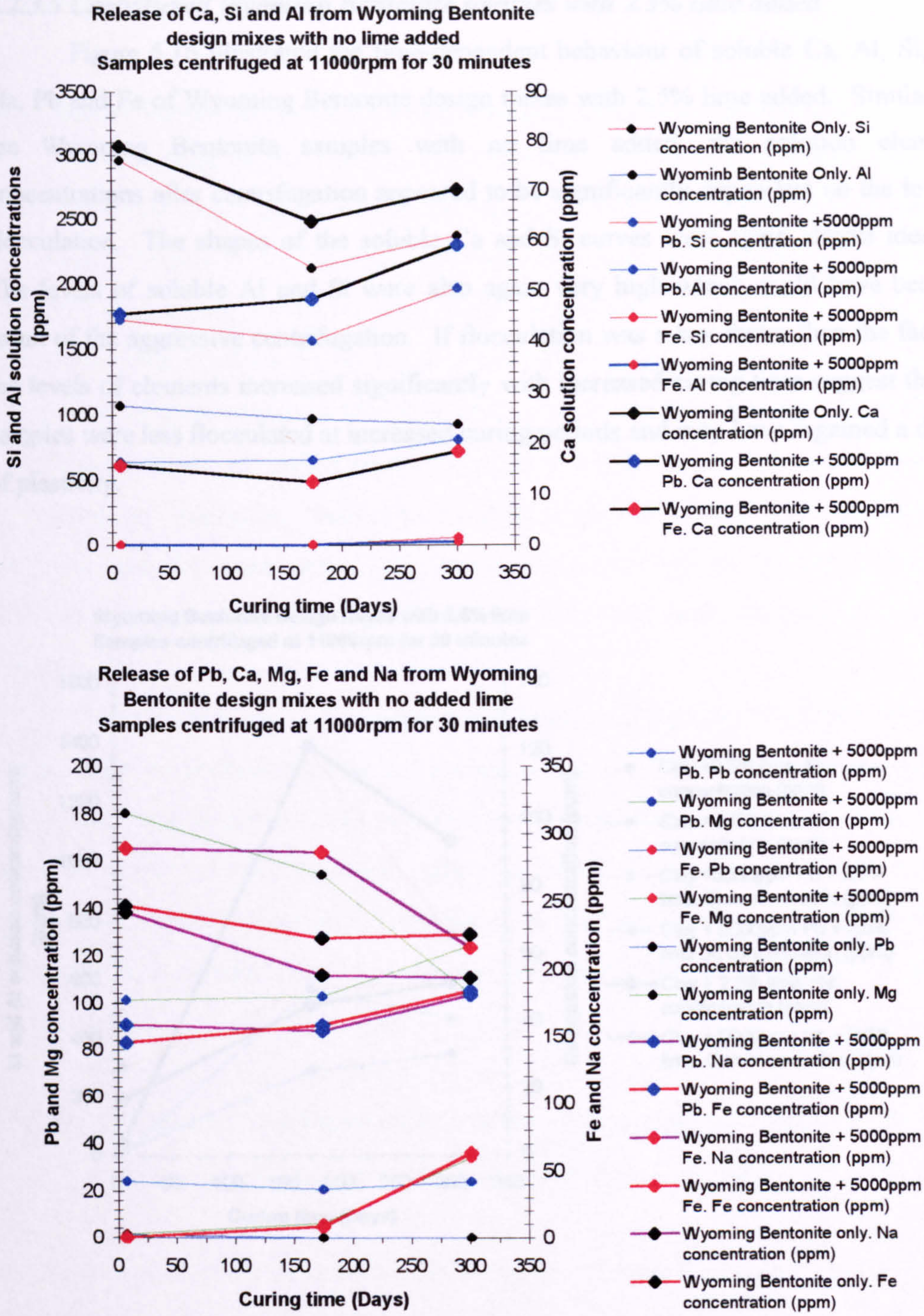

Figure 5.15 **Variation of end of test soluble Ca, Al, Si, Na, Mg, Pb and Fe with curing time for Wyoming Bentonite design mixes with no lime added. Solutions analysed were samples from 6hr/30rpm batch tests with a 1:20 solid to liquid ratio and 20mm cubes centrifuged at 11000rpm for 30 minutes**

5.2.3.5 Centrifuged Wyoming Bentonite samples with 2.5% lime added

Figure 5.16 illustrated the time-dependent behaviour of soluble Ca, Al, Si, Mg, Na, Pb and Fe of Wyoming Bentonite design mixes with 2.5% lime added. Similarly to the Wyoming Bentonite samples with no lime added, the solution elemental concentrations after centrifugation appeared to be significantly dependent on the level of flocculation. The shapes of the soluble Ca and Si curves were again almost identical. The levels of soluble Al and Si were also again very high which could have been the result of the aggressive centrifugation. If flocculation was a key factor then the fact that the levels of elements increased significantly with increased curing time suggest that the samples were less flocculated at increased curing periods and may have regained a degree of plasticity.

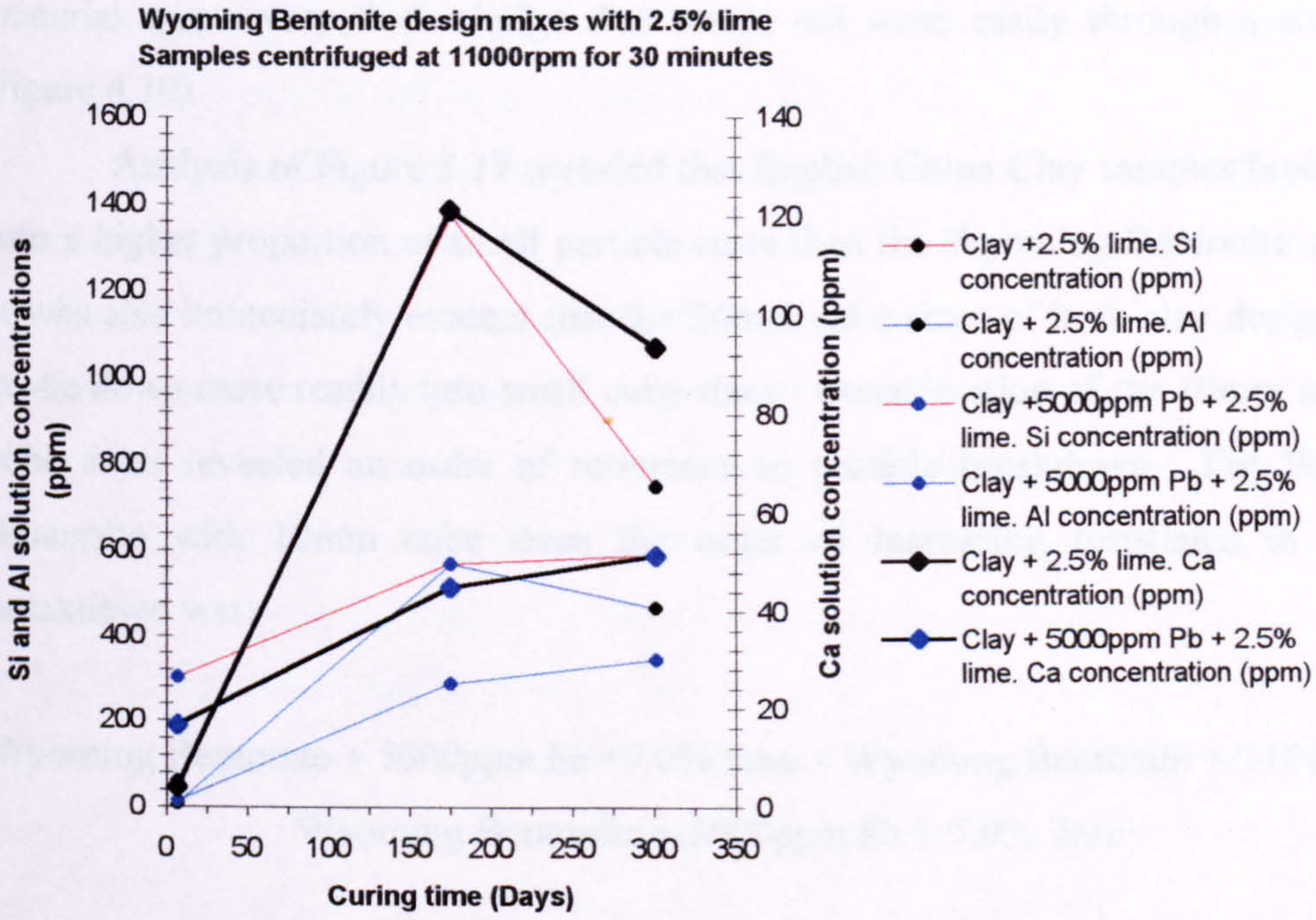

Figure 5.16 Variation of end of test soluble Ca, Al and Si with curing time for Wyoming Bentonite design mixes with 2.5% lime added. Solutions analysed were samples from 6hr/30rpm batch tests with a 1:20 solid to liquid ratio and 20mm cubes centrifuged at 11000rpm for 30 minutes

5.3 PHYSICAL BEHAVIOUR

5.3.1 End of batch test particle size distribution and chemical analysis

An analysis of the physical breakdown of the monolithic cubes during the batch tests provided a link between the chemical batch test results and the physical test results. Figure 5.17 illustrated the results of a series of wet sieving experiments after 301 days curing on the residues of 6hr/30rpm batch tests for 10mm and 20mm cube sizes with a 1:10 solid to liquid ratio. Tests were not performed on English China Clay samples with no added lime or English China Clay with 5000ppm Fe with 1.5% lime because all solids passed through a 63μm sieve. Tests were also not performed on Wyoming Bentonite samples with no added lime or Wyoming Bentonite samples with only 2.5% lime because the end of the batch test solid material was a very thick sludge that would not wash easily through a sieve (see Figure 4.10).

Analysis of Figure 5.17 revealed that English China Clay samples broke down into a higher proportion of small particle sizes than the Wyoming Bentonite samples. It was also immediately evident that the 20mm cube sizes of both clay design mixes broke down more readily into small cube sizes. Consideration of the 10mm or 20mm cube sizes revealed an order of resistance to particle breakdown. For Wyoming Bentonite with 10mm cube sizes the order of increasing resistance to particle breakdown was:

Wyoming Bentonite + 5000ppm Fe +7.0% lime < Wyoming Bentonite + 7.0% lime < Wyoming Bentonite + 5000ppm Pb + 7.0% lime.

A similar series in order of increasing resistance to particle breakdown could also be suggested for English China Clay samples with 10mm cubes:

English China Clay ≈ English China Clay + 5000ppm Fe ≈ English China Clay + 5000ppm Pb < English China Clay + 5000ppm Fe + 1.5% lime < English China Clay + 5000ppm Fe + 2.5% lime < English China Clay + 5000ppm Pb + 1.5% lime < English China Clay + 5000ppm Pb + 2.5% lime < English China Clay + 1.5% lime < English China Clay + 2.5% lime.

The order of increasing resistance to particle breakdown suggested above was based on the percentage of particles passing a 63μm sieve. However, it was apparent that for the English China Clay samples with no contaminants and added lime the chart showed a well graded material unlike the contaminated samples. Therefore if particle breakdown was considered on the basis of particles passing a 150μm sieve the order would have been significantly different.

5.3.2 Acid digestion

5.3.2.1 Acid digestion of particles from batch test mixtures retained on a 63μm sieve

In order to assess the chemistry of small particulates after the batch test samples from three of the design mixes retained on a 63μm sieve during the above mentioned particle size distribution were acid digested. For comparison a sample of the source design mixes stored in the plastic pipe curing containers was also acid digested, the results of which are displayed in Table 5.13.

Consideration of the English China Clay + 5000ppm Fe + 2.5% lime samples clearly showed that the orange coloured material retained on the sieve contained substantially more acid soluble Ca, Fe, Si, Mg, Al and Mn. This suggested that the particles retained on the sieve were hydrated lime particles with Fe^{3+} ion contamination on the surface. The Fe^{3+} ion contamination would be in either a precipitated form or be incorporated in re-crystallised cementitious compounds. This was confirmed by comparing these elemental releases with those of acid digested lime and dried untreated English China Clay shown in Table 5.14. Comparison of the Wyoming Bentonite + 5000ppm Fe + 7.0% lime illustrated similar behaviours. The material retained on the sieve contained more acid soluble Ca, Fe and Mn which again signified a high lime content. The levels of acid soluble Na, Mg and Al were significantly lower for the sieved retained material possibly suggesting a very low clay content. However, the low acid soluble Na content could have been due to the high cation removal of Na^{+} ions from the clay due to exchange reactions. Comparison of the Wyoming Bentonite samples + 5000ppm Pb + 7.0% lime showed similar behaviour in many respects, however the level of acid soluble Fe in the sieve retained sample was elevated and there was less acid soluble Pb on the sieved sample.

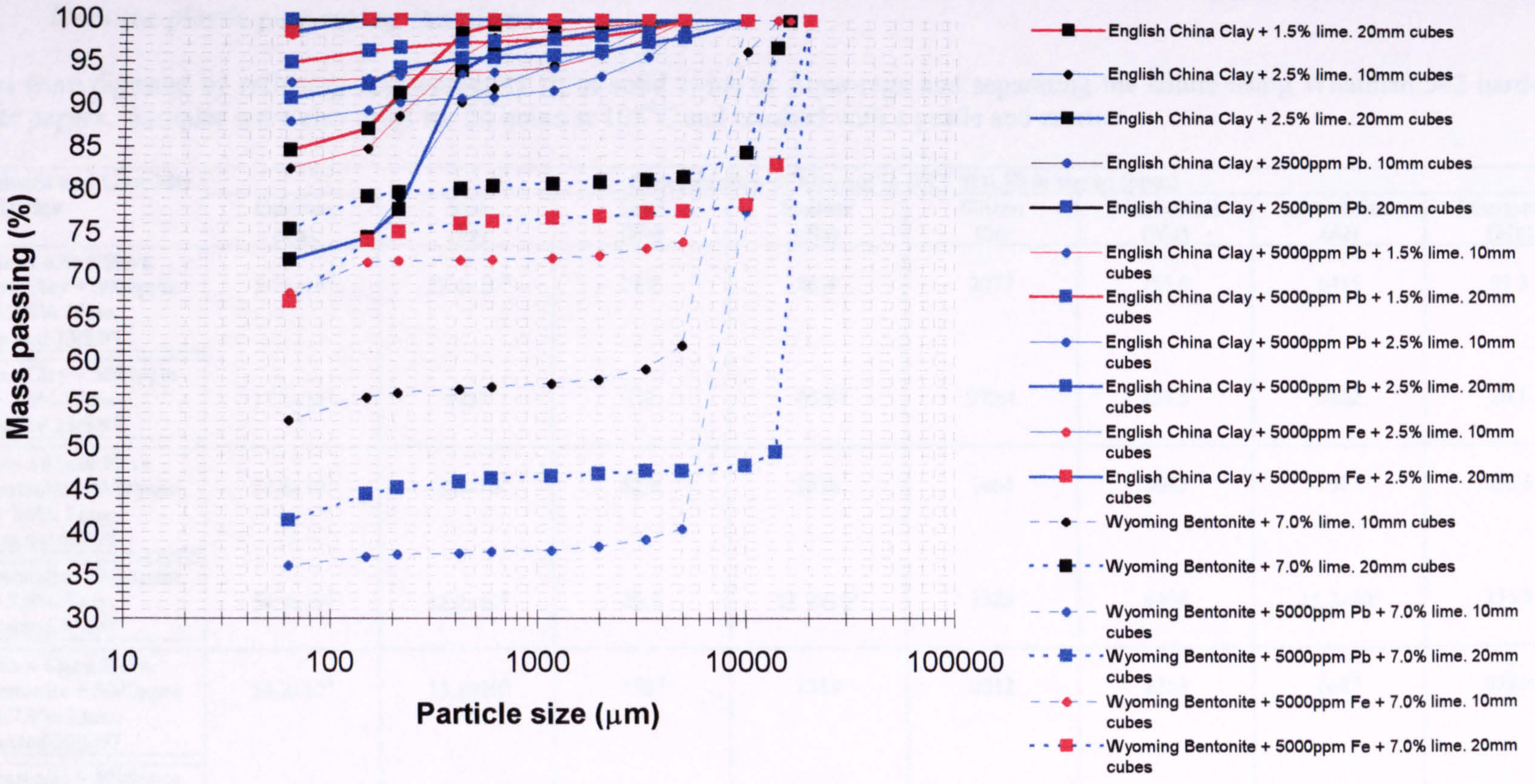

Figure 5.17 Grading of residue particles from 6hr/30rpm batch tests with a 1:10 solid to liquid ratio for English China Clay and Wyoming Bentonite design mixes after 301 days curing

Table 5.13 Comparison of acid digestion data of batch test material retained on 63µm sieve with the respective source material taken from the plastic pipe curing containers

All samples were digested by refluxing approximately 1g of solid twice in Aqua-rega and separating the solute using Whatman 542 hardened ashless filter papers. Samples were also dried for 24 hours at 105^{0}C and crushed with a pestle and mortar.

Clay, Contaminant and Lime Mix Design	Concentration of Element in DRY SOLID in mg/kg (ppm)							
	Calcium (Ca)	Iron (Fe)	Lead (Pb)	Sodium (Na)	Silicon (Si)	Magnesium (Mg)	Aluminium (Al)	Manganese (Mn)
Retained on a 63µm Sieve. English China Clay + 5000ppm Iron + 2.5% Lime. Compacted 23/5/97	56.3×10^3	23.6×10^3	21.8	86.4	2077	755.9	6415	91.3
English China Clay + 5000ppm Iron + 2.5% Lime. Compacted 23/5/97	17.1×10^3	4739	1.6	65.8	870.4	229.5	3862	20.1
Retained on a 63µm Sieve. Wyoming Bentonite + 5000ppm Iron + 7.0% Lime. Compacted 9/7/97	74.8×10^3	13.8×10^3	52.9	2558	1464	2642	7991	725.5
Wyoming Bentonite + 5000ppm Iron + 7.0% Lime. Compacted 9/7/97	54.9×10^3	12.2×10^3	26.1	11.7×10^3	1529	4404	15.3×10^3	235.8
Retained on a 63µm Sieve. Wyoming Bentonite + 5000ppm Lead + 7.0% Lime. Compacted 25/6/97	54.2×10^3	13.3×10^3	1527	2314	2512	2253	6687	838.9
Wyoming Bentonite + 5000ppm Lead + 7.0% Lime. Compacted 25/6/97	52.4×10^3	7764	4168	11.7×10^3	2055	4323	15.0×10^3	170.4

Note: Values stated are ± 0.1mg/kg

Table 5.14 Comparison of acid digestion data of English China Clay, Wyoming Bentonite and lime as supplied by the manufacturers

All samples were digested by refluxing approximately 1g of solid twice in Aqua-rega and separating the solute using Whatman 542 hardened ashless filter papers. Samples were also dried for 24 hours at 105^{0}C and crushed with a pestle and mortar.

Clay, Contaminant and Lime Mix Design	Concentration of Element in DRY SOLID in mg/kg (ppm)							
	Calcium (Ca)	Iron (Fe)	Lead (Pb)	Sodium (Na)	Silicon (Si)	Magnesium (Mg)	Aluminium (Al)	Manganese (Mn)
Untreated English China Clay (Material in form supplied by manufacturer)	248.7	627.7	2.7	85.7	563.7	185.3	4272	18.8
Untreated Wyoming Bentonite ((Material in form supplied by manufacturer)	7893	6365	33.3	11.7×10^3	3294	3090	8034	162.2
Untreated Lime (KILN DRIED DIRECT FROM MANUFACTURER)	633.7×10^3	264.2	0.1	89.0	739.2	2453	279.8	100.6

Note: Values stated are ± 0.1mg/kg

5.3.2.2 Acid digestion of compacted clay-lime-contaminant mixes

Due to the potential for errors arising from of cross contamination between samples during the mixing process, a sample of each design mix was also acid digested. The results of this process were illustrated in Tables 5.15 and 5.16. Analysis of the English China Clay data in Table 5.15 suggested no cross contamination from this source although the levels of metal ions present appear lower than those actually added. The levels of acid soluble Pb in the uncontaminated samples appeared slightly high especially when compared with the sample direct from the bag in Table 5.14. However, this was also the case for the levels of acid soluble Fe, Si and Mg which could suggest a chemical reaction occurring in the design mix sample which had a higher water content and had been stored for 301 days prior to testing.

It was important to note that the uncontaminated and Pb^{2+} ion contaminated mixes with added lime showed elevated levels of Si and Al relative to the uncontaminated sample with no lime added suggesting pozzolanic reactions. Furthermore, the Fe^{3+} ion contaminated sample with added lime also showed slightly elevated levels of acid soluble Si and Al but not to the same extent as the Pb^{2+} ion contaminated and uncontaminated samples with added lime. Only a small proportion of these increases could be due to the acid soluble Si and Al content found in the lime added (Table 5.14).

Analysis of the Wyoming Bentonite data in Table 5.16 showed similar trends to English China Clay. Although the uncontaminated samples with no lime showed elevated levels of acid soluble Pb and Fe this was consistent with the levels found in samples direct from the mineral supplier. In addition it was clear that the lime-treated samples showed significantly elevated levels of acid soluble Si, Al, Fe, Mg and Mn. The higher levels of acid soluble Si, Al and Fe could not be attributed simply to these elements being present in the added lime and were probably due to the effects of pozzolanic reactions. However, it was feasible to link a proportion of elevated Mg and Mn to that present in the lime. The possible exception to this was the level of Mn released from samples containing Fe^{3+} ion contamination, which were significantly elevated relative to all other samples. It was also evident that the Fe^{3+} ion contaminated samples with added lime released significantly less acid soluble Si although similar levels of Al relative to the other lime-treated samples. Hence the Fe^{3+} ions appeared to inhibit the release of acid soluble Si possibly as a result of

inhibiting the pozzolanic reactions. A further interesting observation was that all samples whether treated with lime or not released effectively the same levels of acid soluble Na. Furthermore, Pb^{2+} and Fe^{3+} ion contaminated samples with no added lime released more acid soluble Ca than the uncontaminated sample with no lime. Although initially this may have been attributed to increased cation exchange of Ca^{2+} ions naturally present on the exchange sites this was unlikely to be the case since it would have been expected that this Ca would be released anyway due to the acid digestion treatment.

Table 5.15 Acid digestion results of English China Clay design mixes after 301 days curing

Clay, Contaminant and Lime Mix Design	Concentration of Element in DRY SOLID in mg/kg (ppm)							
	Calcium (Ca)	Iron (Fe)	Lead (Pb)	Sodium (Na)	Silicon (Si)	Magnesium (Mg)	Aluminium (Al)	Manganese (Mn)
English China Clay only. Compacted 27/3/97	261.7	775.3	9.5	76.1	795.3	209.3	4125	9.4
English China Clay + 1.5% Lime. Compacted 4/4/97	9584	753.6	5.6	71.0	1174	240.4	6714	17.2
English China Clay + 2.5% Lime. Compacted 9/4/97	18.5×10^3	689.5	D 0.0000	60.7	1694	239.6	7099	13.8
English China Clay + 2500ppm Lead. Compacted 11/4/97	230.7	597.2	2100	78.00	980.9	174.9	3981	10.9
English China Clay + 5000ppm Lead + 1.5% Lime. Compacted 22/4/97	9361	649.8	4198	63.20	1572	218.0	5738	19.4
English China Clay + 5000ppm Lead + 2.5% Lime. Compacted 28/4/97	18.5×10^3	651.7	4226	66.8	1397	241.8	6476	20.4
English China Clay + 5000ppm Iron. Compacted 2/5/97	222.2	5013	7.712	65.8	432.8	187.2	3930	18.8
English China Clay + 5000ppm Iron + 1.5% Lime. Compacted 16/5/97	8617	4779	D 0.0000	70.4	844.1	205.9	3703	19.6
English China Clay + 5000ppm Iron + 2.5% Lime. Compacted 23/5/97	17.1×10^3	4739	1.6	65.8	870.4	229.5	3862	20.1

Note: Values stated are ± 0.1mg/kg

Table 5.16 Acid digestion results of Wyoming Bentonite design mixes after 301 days curing

Clay, Contaminant and Lime Mix Design	Concentration of Element in DRY SOLID in mg/kg (ppm)							
	Calcium (Ca)	Iron (Fe)	Lead (Pb)	Sodium (Na)	Silicon (Si)	Magnesium (Mg)	Aluminium (Al)	Manganese (Mn)
Wyoming Bentonite only. Compacted 28/5/97	7205	4867	35.4	12.2×10^3	2459	3341	10.5×10^3	54.7
Wyoming Bentonite + 2.5% Lime. Compacted 3/6/97	25.9×10^3	6944	33.7	12.0×10^3	3153	3570	10.4×10^3	152.7
Wyoming Bentonite + 7.0% Lime. Compacted 10/6/97	53.5×10^3	8554	53.09	11.0×10^3	7131	4543	18.0×10^3	158.6
Wyoming Bentonite + 5000ppm Lead. Compacted 13/6/97	7785	6347	4192	11.7×10^3	4392	3358	9876	141.3
Wyoming Bentonite + 5000ppm Lead + 2.5% Lime. Compacted 19/6/97	27.3×10^3	7175	4157	11.7×10^3	3254	3576	11.2×10^3	166.5
Wyoming Bentonite + 5000ppm Lead + 7.0% Lime. Compacted 25/6/97	52.4×10^3	7764	4168	11.7×10^3	2055	4323	15.0×10^3	170.4
Wyoming Bentonite + 5000ppm Iron. Compacted 4/7/97	10.0×10^3	11.6×10^3	29.5	11.4×10^3	2337	3335	9706	202.2
Wyoming Bentonite + 5000ppm Iron + 2.5% Lime. Compacted 14/7/97	27.8×10^3	11.2×10^3	27.0	11.4×10^3	1410	3613	10.7×10^3	196.1
Wyoming Bentonite + 5000ppm Iron + 7.0% Lime. Compacted 9/7/97	54.9×10^3	12.2×10^3	26.1	11.7×10^3	1529	4404	15.3×10^3	235.8

Note: Values stated are ± 0.1mg/kg

5.3.3 Shear strength measurements

There was a hypothesis that the breakdown of particles in the batch tests represented by the particle size distribution in Figure 5.17 was related to shear strength of the various clay-contaminant-lime mixes. The hypothesis was based on the fact that as shear strength increased the particle breakdown would reduce during the batch tests. The order of increasing shear strength at 301 days curing for English China Clay (ECC) was:

ECC + 5000ppm Fe < ECC + 5000ppm Fe + 1.5% lime < ECC only < ECC + 2500ppm Pb < ECC + 1.5% lime < ECC + 5000ppm Fe + 2.5% lime < ECC + 2.5% lime or ECC + 5000ppm Pb + 1.5% lime or ECC + 5000ppm Pb + 2.5% lime.

The final three mixes could not be placed in order because all measurements were above the capacity of the shear vane i.e. greater than 145kPa. The order suggested by the mass of particles below 63μm after the batch tests was:

ECC + 5000ppm Fe or ECC only or ECC + 5000ppm Pb < ECC + 5000ppm Fe + 1.5% lime < ECC + 5000ppm Fe + 2.5% lime < ECC + 5000ppm Pb + 1.5% lime < ECC + 5000ppm Pb + 2.5% lime < ECC + 1.5% lime < ECC + 2.5% lime.

The order of increasing shear strength at 301 days curing for Wyoming Bentonite (WB) was:

WB + 5000ppm Fe < WB only < WB + 2.5% lime < WB + 5000ppm Pb + 2.5% lime < WB + 5000 Fe + 2.5% lime < WB + 7.0% lime < WB + 5000ppm Fe + 7.0% lime or WB + 5000ppm Pb + 7.0% lime

The order suggested by the mass of particle below 63μm after the batch tests was:

WB + 5000ppm Fe +7.0% lime < WB + 7.0% lime < WB + 5000ppm Pb + 7.0% lime

It was clear that the particle breakdown during batch tests was not simply linked to the shear strength. However, this does not mean that the release of elements during the batch test cannot be linked to physical properties.

Analysis of the English China Clay shear strengths in Figure 5.18 does reveal several trends. Firstly at 7 days curing with no lime present the Pb^{2+} ion contaminated sample had a higher shear strength than the uncontaminated sample which was again higher than the Fe^{3+} ion contaminated sample. Again at 7 days curing, on addition of 1.5% lime, the strength of the Pb^{2+} ion contaminated sample increased the most significantly followed by only small increases for the uncontaminated and Fe^{3+} ion contaminated samples. An addition of 2.5% lime resulted in a linear increase in the shear strength of the Pb^{2+} ion contaminated sample followed by an increase in the shear strength of the Fe^{3+} ion contaminated sample with no significant change in the uncontaminated sample. Consideration of the effects of curing time on the mix designs revealed further trends. Increasing curing time resulted in slight increases in shear strength for the Fe^{3+} ion contaminated samples that were especially notable at the higher lime contents. In addition, it was apparent that even without the addition of lime the shear strength of the uncontaminated sample increased by about 10% over 301 days curing. This was not due to a change in the water content because this was monitored and seen to remain unchanged with curing time. Probably the most significant trend was that the Pb^{2+} ion contaminated sample with 1.5% lime achieved the highest shear strength at both 175 and 301 days curing. However, for samples with 2.5% lime added the shear strengths of both the Pb^{2+} ion and uncontaminated samples achieved the maximum measurable shear strength of the shear vane, significantly higher than the respective Fe^{3+} ion contaminated sample.

The shear strength results of Wyoming Bentonite illustrated in Figure 5.18 were not quite so distinct. However, it was clear that the uncontaminated sample and the Fe^{3+} and Pb^{2+} ion contaminated samples with no added lime increased in strength from 7 days curing to 301 days curing. For the samples with 2.5% added lime the Pb^{2+} ion contaminated samples and Fe^{3+} ion contaminated samples appeared to produce higher shear strengths than the uncontaminated samples at both 175 and 301 days curing. It was also clear from the rate of increase in shear strength of the contaminated samples that the addition of 2.5% lime had a more significant effect on these samples than the uncontaminated sample. Furthermore, it was apparent that for the samples with 2.5% added lime curing time had very little effect on the shear

strength of Fe^{3+} ion contaminated samples and the uncontaminated samples whereas there was a large increase in the shear strength of the Pb^{2+} ion contaminated samples when curing time increased from 7 to 175 days. When 7.0% lime was added to the mixes the Fe^{3+} and Pb^{2+} ion contaminated samples produced similar shear strengths at 7 days curing whilst all samples recorded shear strengths beyond the range of the shear vane at both 175 and 301 days curing.

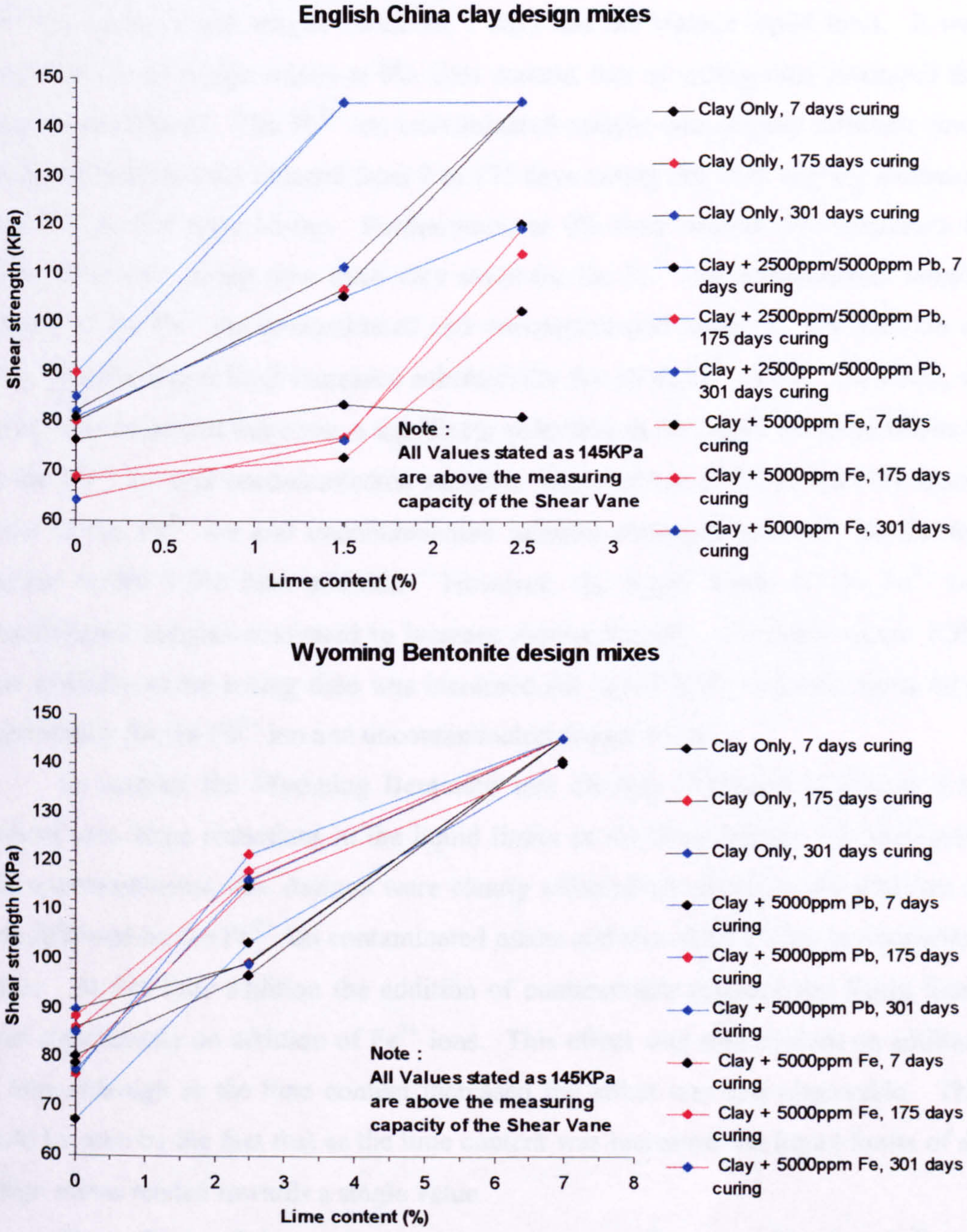

Figure 5.18 Shear strength variation with lime addition at various curing times for English China Clay and Wyoming Bentonite design mixes.

5.3.4 Atterberg limit test results

5.3.4.1 Liquid limits

Figure 5.19 illustrated the variation in the liquid limit characteristics of English China Clay and Wyoming Bentonite design mixes with lime at varying curing periods. It was immediately evident that the two clay minerals behaved differently. Observation of the English China Clay plots revealed that as the lime content increased for all design mixes the liquid limit also increased. At 0% lime content the Pb^{2+} ion contaminated sample cured for 7 days had the highest liquid limit. It was clear that for all design mixes at 0% lime content that as curing time increased the liquid limit reduced. The Pb^{2+} ion contaminated sample was slightly different since the liquid limit initially reduced from 7 to 175 days curing and then slightly increased from 175 to 301 days curing. Furthermore, at 0% lime content the reductions in liquid limit with curing time were very small for the Fe^{3+} ion contaminated sample relative to the Pb^{2+} ion contaminated and uncontaminated samples. On addition of 1.5% lime the liquid limit increased substantially for all design mixes. However, as curing time increased there was a significant reduction in the liquid limits particularly for the Pb^{2+} ion and uncontaminated samples. On addition of 2.5% lime the liquid limits of the Pb^{2+} ion and uncontaminated samples remained generally unaffected relative to the 1.5% lime addition. However, the liquid limits of the Fe^{3+} ion contaminated samples continued to increase almost linearly. Similarly to the 1.5% lime addition, as the curing time was increased the liquid limits reduced, again most significantly for the Pb^{2+} ion and uncontaminated design mixes.

In contrast the Wyoming Bentonite mix designs illustrated in Figure 5.19 showed very large reductions in the liquid limits as the lime content was increased. The uncontaminated mix designs were clearly affected the most by the addition of lime followed by the Pb^{2+} ion contaminated mixes and then the Fe^{3+} ion contaminated mixes. At 0% lime addition the addition of contaminants reduced the liquid limit, most significantly on addition of Fe^{3+} ions. This effect was also evident on addition of lime although as the lime content increased the effect was less observable. This could be seen by the fact that as the lime content was increased the liquid limits of all design mixes tended towards a single value.

The effects of increasing curing time were diverse. For the Fe^{3+} ion contaminated sample there was little effect on the liquid limit. For the Pb^{2+} ion contaminated sample at all lime contents increasing curing time reduced the liquid

limit. Furthermore, the effect was most noticeable between 7 and 175 days curing. For the uncontaminated Wyoming Bentonite sample at 0% lime the liquid limit appeared to increase significantly between 7 and 175 days curing and then reduce significantly between 175 and 301 days curing. On addition of lime to the sample the tendency was for a reduction in the liquid limit with increased curing time.

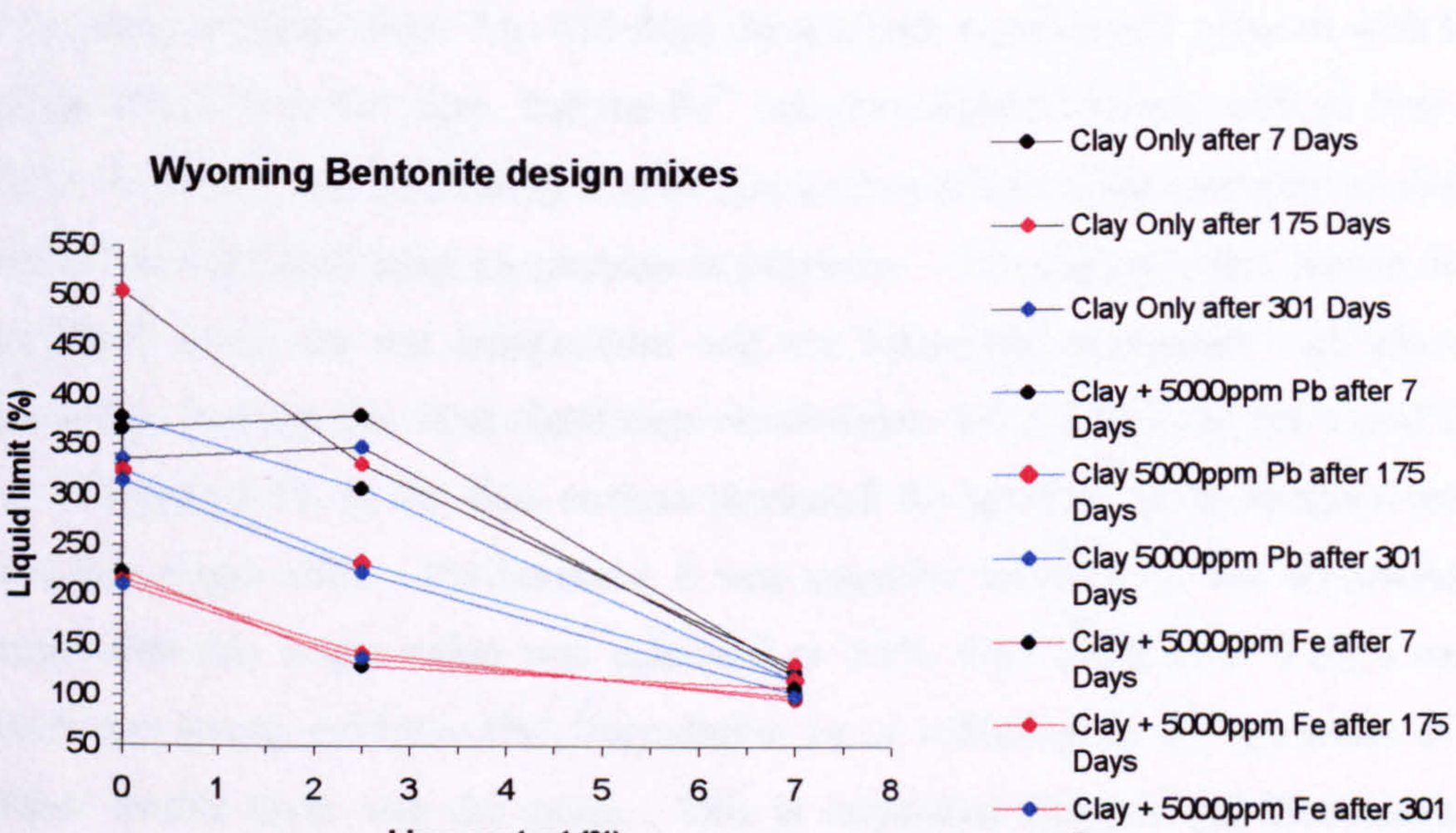

Figure 5.19 Liquid limit variation of English China Clay and Wyoming Bentonite design mixes with lime content at varying curing periods

Figure 5.20 illustrated how the gradients of the liquid limits plots of water content against cone penetration for English China Clay and Wyoming Bentonite design mixes varied with lime content and curing period. The English China Clay plot showed a high level of variability that was difficult to decipher. Essentially the plot showed that there was no significant change in the gradient as the lime content increased. However, as the lime content increased there was a slight divergence of the results increasing the range from the maximum to minimum gradient value which did not appear to be directly dependent on contaminant or curing time.

The Wyoming Bentonite plot showed many trends since the effect of adding contaminants and lime resulted in very large changes in the gradient. Indeed comparison of Figure 5.20 with the liquid limit plot in Figure 5.19 showed that the two were almost identical. It was apparent therefore that the effects on the liquid limits due to adding contaminants and lime were due, in part, to the changing gradient of the line. Figure 5.20 identified that as the lime content increased for all design mixes the gradient significantly reduced. The Pb^{2+} ion contaminated and uncontaminated samples also behaved similarly. Generally at all lime contents as the curing time increased from 7 to 175 days the gradient significantly reduced with little change from 175 to 301 days. For the Fe^{3+} ion contaminated sample with no lime and with 2.5% lime it was interesting to note that as the curing period increased so did the gradient perhaps indicating an increase in plasticity. This suggests that plastic limits and liquid limits are not independent and are inherently associated with physico-chemistry. Perhaps the most significant observation, and similarly to the liquid limit plot in Figure 5.19, as the lime content increased the gradient of all samples tended towards a single value. Furthermore, it was apparent for the Fe^{3+} ion contaminated sample that this single value was achieved at 2.5% lime addition at 7 days curing which was strong evidence that flocculation i.e. a reduction in the thickness of the diffuse double layer was the cause. This is important because this phenomena is suggested as a way of measuring appropriate quantities of lime addition for treating clay soils.

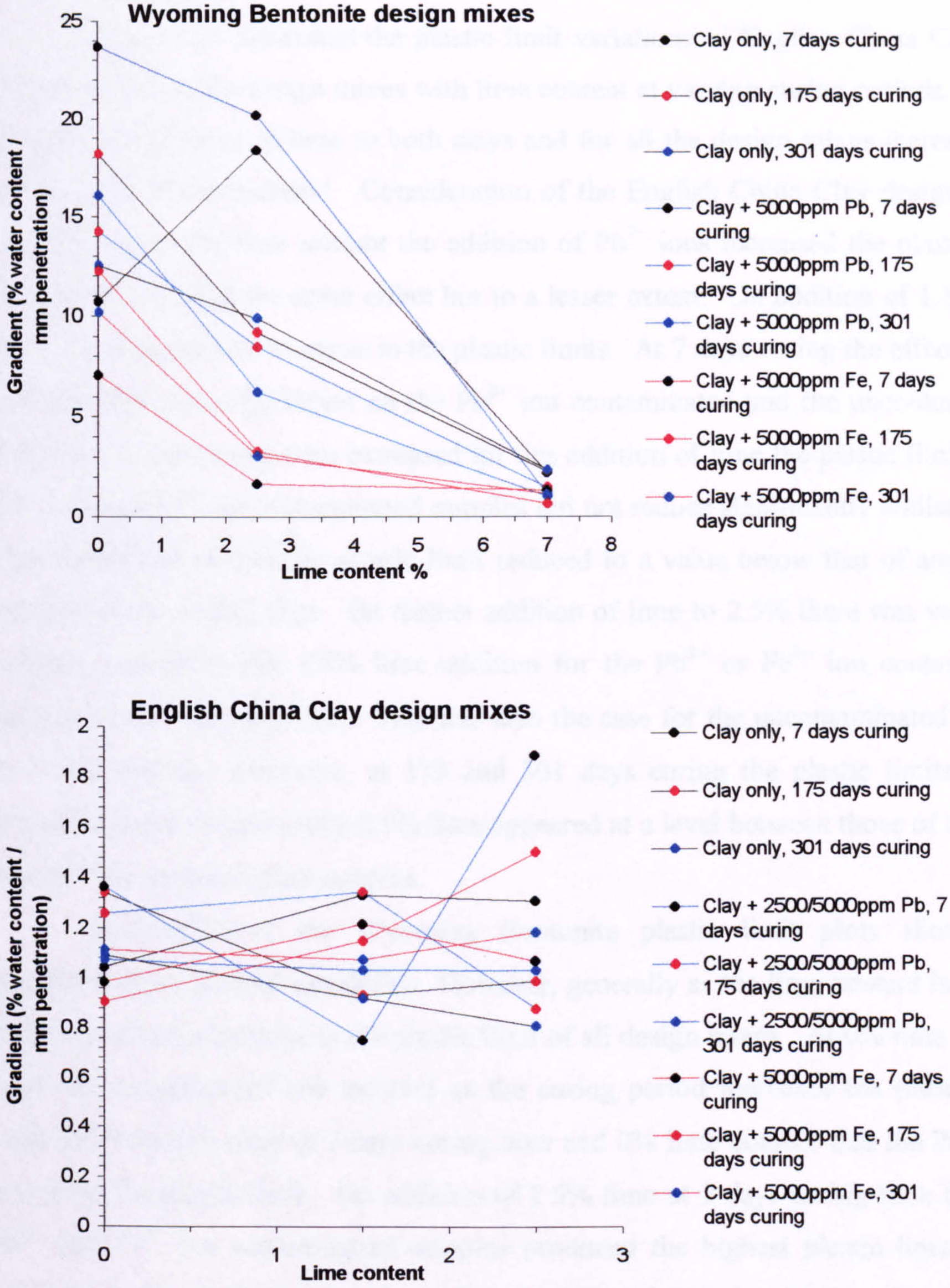

Figure 5.20 **Influence of lime content and curing period on the water content : cone penetration relationship for English China Clay and Wyoming Bentonite**

5.3.4.2 Plastic limits

Figure 5.21 illustrated the plastic limit variations of English China Clay and Wyoming Bentonite design mixes with lime content at varying curing periods. It was evident that addition of lime to both clays and for all the design mixes increases the plastic limit of the material. Consideration of the English China Clay design mixes showed that at 0% lime content the addition of Pb^{2+} ions increased the plastic limit whilst Fe^{3+} ions had the same effect but to a lesser extent. On addition of 1.5% lime there was a significant increase in the plastic limits. At 7 days curing the effect of this addition was most significant on the Pb^{2+} ion contaminated and the uncontaminated samples. As the curing time increased for this addition of lime the plastic limit of the Pb^{2+} ion and Fe^{3+} ion contaminated samples did not reduce significantly whilst for the uncontaminated sample the plastic limit reduced to a value below that of any of the samples at any curing time. On further addition of lime to 2.5% there was very little increase relative to the 1.5% lime addition for the Pb^{2+} or Fe^{3+} ion contaminated samples at any curing period. This was also the case for the uncontaminated sample at 7 days curing. However, at 175 and 301 days curing the plastic limits of the uncontaminated samples with 2.5% lime appeared at a level between those of the Pb^{2+} and Fe^{3+} ion contaminated samples.

Observation of the Wyoming Bentonite plastic limit plots showed an apparently high level of variability. However, generally as the lime content increased there was a linear increase in the plastic limit of all design mixes. At 0% lime content (with the exception of one sample) as the curing period increases the plastic limit reduced. It is also clear at 7 days curing time and 0% lime content that the Pb^{2+} ions increased the plastic limit. On addition of 2.5% lime at 7 days curing time both the Pb^{2+} and Fe^{3+} ion contaminated samples produced the highest plastic limit values followed by the uncontaminated sample. At 175 and 301 days curing time the Fe^{3+} ion contaminated sample had the highest plastic limit followed by the Pb^{2+} ion contaminated sample and then the uncontaminated sample. On addition of 7.0% lime at 7 days curing time the uncontaminated sample produced the highest plastic limit value followed by the Pb^{2+} ion and then the Fe^{3+} ion contaminated samples. At 175 and 301 days curing time Fe^{3+} ion contaminated sample produced the highest plastic limit value followed by the Pb^{2+} ion contaminated sample and then the uncontaminated sample. It was generally evident that for samples with added lime as

the curing period increases the plastic limit reduced and the effect was not obviously affected by the presence of a particular contaminant.

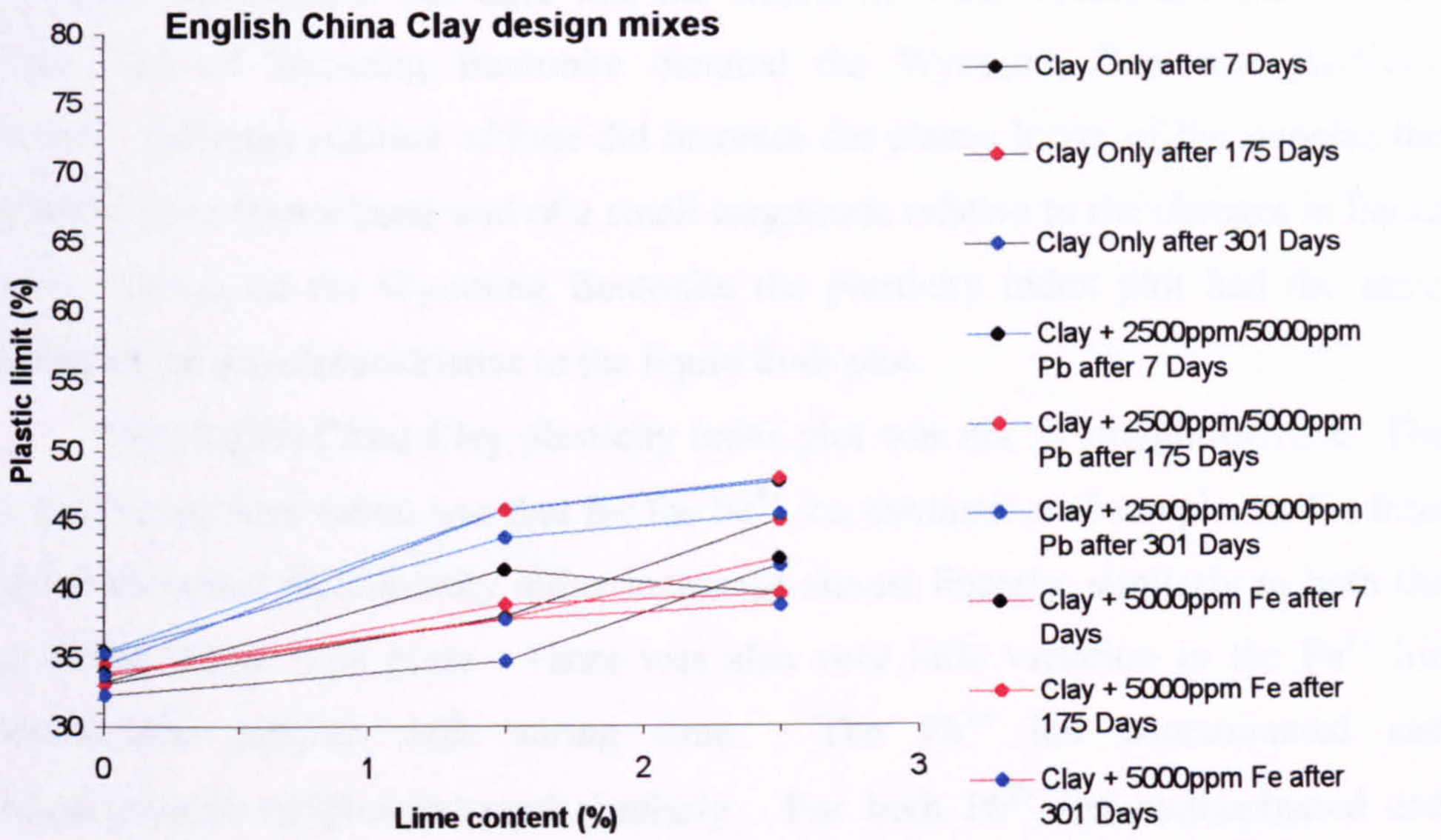

Figure 5.21 Plastic limit variation of English China Clay and Wyoming Bentonite design mixes with lime content at varying curing periods

5.3.4.3 Plasticity index

Figure 5.22 illustrated the plasticity index variation of English China Clay and Wyoming Bentonite design mixes with lime content at varying curing periods. From an initial observation it was clear that the effects of contaminants and lime on the liquid limit of Wyoming Bentonite dictated the Wyoming Bentonite plasticity indexes. Although addition of lime did increase the plastic limits of the samples the increases were almost linear and of a small magnitude relative to the changes in liquid limits. Hence for the Wyoming Bentonite the plasticity index plot had the same general shape and characteristics to the liquid limit plot.

The English China Clay plasticity index plot was not so straightforward. The most apparent observation was that for the Fe^{3+} ion contaminated samples as the lime content increased the plasticity index increased almost linearly, similarly to both the liquid and plastic limit plots. There was also very little variation in the Fe^{3+} ion contaminated samples with curing time. The Pb^{2+} ion contaminated and uncontaminated samples behaved similarly. For both Pb^{2+} ion contaminated and uncontaminated mixes at all lime contents the plasticity index reduced between 7 and 175 days curing and then increased slightly from 175 to 301 days curing. Consideration of the uncontaminated samples showed that as the lime content increased from 0% to 2.5% at all curing periods the plasticity index increased slightly. On further addition of lime at 7 days curing the plasticity index continued to increase whilst at 175 and 301 days curing this increase in lime content resulted in a slight reduction in the plasticity index. Consideration of the Pb^{2+} ion contaminated sample showed that as the lime content increased from 0% to 2.5% at 7 days the plasticity index increased only to decrease significantly on addition of more lime. However, the plasticity index of the Pb^{2+} ion contaminated samples at 175 and 301 days curing tended to decrease almost linearly as lime content increased.

Evidently there are associations between physical and chemical properties of lime-treated contaminated clays. These associations will be discussed in detail in Chapter 6. In addition explanations of the physico-chemical behaviour will be postulated.

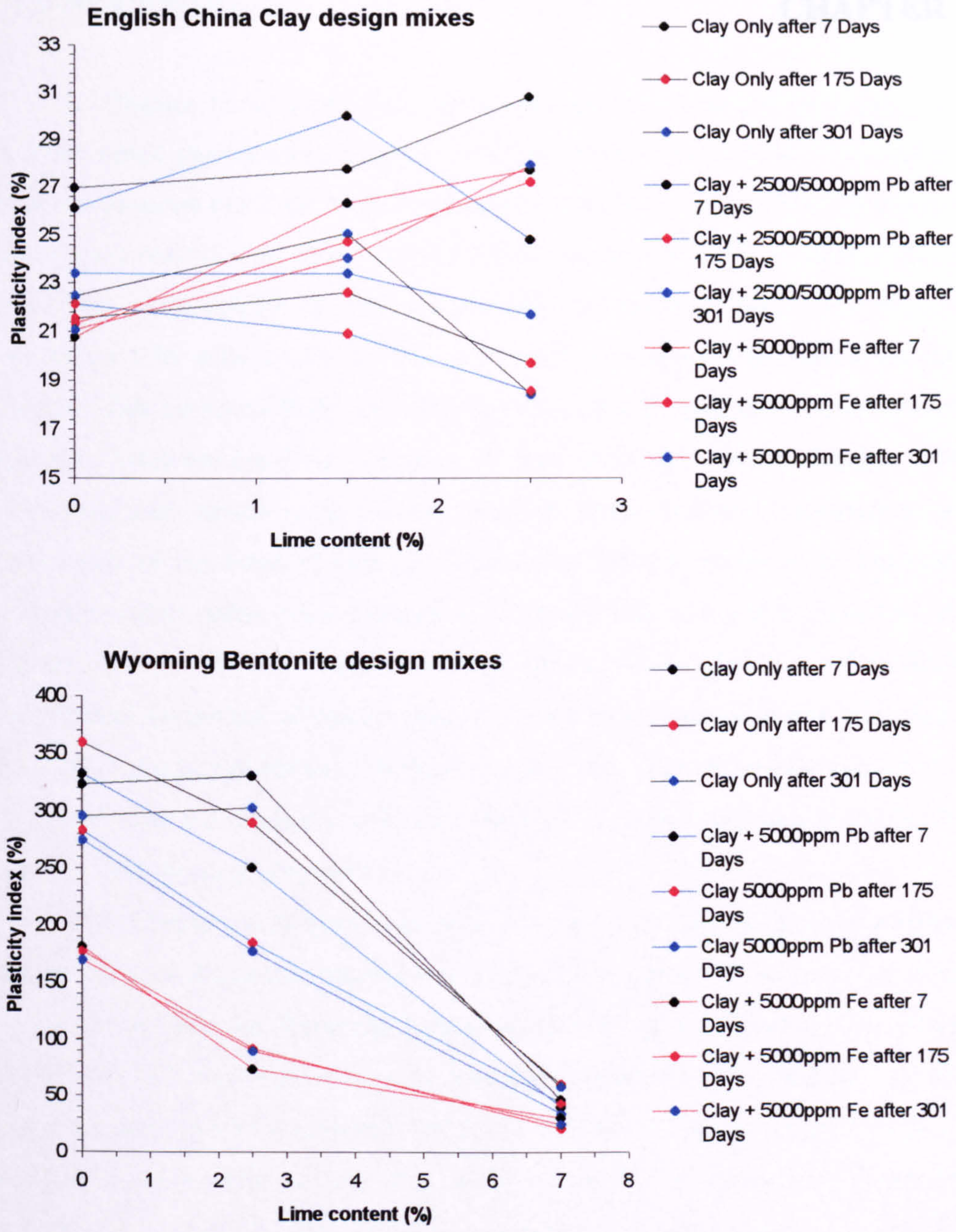

Figure 5.22 Plasticity index variation of English China Clay and Wyoming Bentonite design mixes with lime content at varying curing periods

CHAPTER 6.0

6.0 DISCUSSION

In Chapter 5 the results from the laboratory investigations were presented in an order which characterised the materials and allowed the effects of changing the batch test parameters for each of the mix designs to be assessed. Having established that the parameters of the batch test, with the exception of solid to liquid ratio, have little effect on the release of ions into solution, one series of batch tests (6hr/30rpm tests with a 1:20 solid to liquid ratio and 20mm cube sizes) was chosen for further analysis. This section will discuss the pH and conductivity of the solutions resulting from these batch tests, and the effects on pH and conductivity due to changing solid to liquid ratio and variations in solution element concentration. Subsequent to the presentation of the basic chemistry of the batch tests, a transition to the physical behaviour will be made via a discussion of the particle size grading analysis of the residues of a specific set of batch tests and aggressive acid digestion of all samples. The physical properties of shear strength, liquid limits, plastic limits and plasticity index of all the design mixes will then be discussed. The discussions of the results will hypothesise the mechanisms linking the time-dependent changes in the batch test chemistry and physical properties.

This Chapter could have been structured in a way that illustrated the effects of lime on the time-dependent physico-chemical developments of the two clay minerals English China Clay and Wyoming Bentonite. Following this discussion the effects of the Pb^{2+} and Fe^{3+} contaminant ions on these time-dependent lime reactions could have been discussed. Indeed Boardman *et al* (1999-A) discuss the time-dependent physico-chemical developments of lime-clay mixes from this perspective. Furthermore, Boardman *et al* (1999-B) discuss the time-dependent physico-chemical developments of lime-clay-contaminant mixes and Boardman *et al* (1999-C) discuss appropriate short-term and long-term testing procedures for contaminated soils treated with pH-dependent stabilisation and solidification agents.

However, this chapter was not structured in this way because it was important to consider the changes in physico-chemical developments in terms of ionic interactions prior to, and after the onset of, pozzolanic reactions to understand the mechanisms involved in contaminant retention. This was important because the ionic interactions were different at high and low pH, and both immediately after mixing and after a long curing time. As $Pb(NO)_2$ and $Fe(NO)_3$ can be considered to be acidic

ionic contaminants with specific physico-chemical interactions, hydrated CaO ($Ca(OH)_2$) can be considered to be an alkaline ionic contaminant with specific physico-chemical interactions. The minerals studied have opposite extremes of permanent negative charge and develop varying pH-dependent charge attracting both cations and anions. Hence understanding the mechanisms governing the interaction of these ions with the minerals provides a model from which other ionic interactions can be postulated and considered in the context of other remediation approaches, such as modified mineral attenuation, phyto-remediation, electro-osmosis, and slurry wall or landfill liner retention barrier systems. Furthermore, although other contaminating ions will behave differently when exposed to varying soil pH conditions, the retention processes and the soil physical characteristics will be more easily predicted.

Interpretation of the contents of this chapter can made from the alternative perspective as follows:

- To find information on the clay-lime mix interactions refer to Sections: 6.1.2, 6.1.3.1, 6.2.1, 6.2.2.1, 6.2.3.1, 6.2.3.3, 6.2.4.1, 6.2.4.3, 6.3.3.1, 6.4.1.2 and 6.4.2.2.
- To find information on the clay-lime-contaminant interactions refer to Sections: 6.1.3.2, 6.2.2.2, 6.2.3.2, 6.2.4.2, 6.2.4.4, 6.3.3.2, 6.4.1.2 and 6.4.2.2.

6.1 PRELIMINARY MATERIAL CHARACTERISATION

6.1.1 Initial particle size and chemical characterisation

The initial particle size distribution of the untreated clay minerals (Figure 5.1) confirmed that Wyoming Bentonite contained a much higher proportion of particles $< 2\mu m$ (84%) relative to the English China Clay (51%). This was relevant because it was directly linked to the available mineral surface area for chemical interactions. The acid soluble fractions of these minerals were also substantially different. These initial classification results provided useful information for test and analysis design. The Wyoming Bentonite samples had significantly higher acid soluble levels of Ca, Mg, Mn, Fe and Na whilst the levels of acid soluble Al and Si were very similar. The majority of the Ca and Na were likely to come from the cation exchange sites of the Wyoming Bentonite. Although the English China Clay sample was predominantly kaolinite (Table 4.1 reported 69%) with essentially no permanent charge the mineral

was not pure and contained a small proportion of Quartz and Micas which explained the presence of some of the elements. Although a proportion of the other elements, including Mg, Mn, Fe, Al and Si, may also have been from cation exchange sites, especially in the Wyoming Bentonite, it was likely that some originated from the clay mineral structure itself. This was significant since for both clay minerals the levels of Al and Si which were acid soluble were similar in magnitude and could be directly compared in the batch tests to show the differing stabilisation and solidification behaviour of the two minerals. It could be expected that once stabilisation and solidification reactions were in progress, similar levels of Si and Al from the two minerals would be soluble. This was not the case and will be discussed in detail later and compared with the precise acid digestion data collected after 301 days.

6.1.2 Mechanisms controlling the initial consumption of lime test (ICL)

The results of the initial consumption of lime (ICL) tests on the minerals were clear for the English China Clay. However, interpretation of the results from the adapted Wyoming Bentonite test required a degree of speculation. It was evident from Figure 5.2 that the requirement to add additional water to perform the test affected the ICL value. It could be expected that the addition of excess water to the Wyoming Bentonite tests would reduce the expected pH of the solutions, particularly at the lower lime additions, by definition of the pH measurement.

$$pH = -\log_{10}(\text{Hydrogen ion concentration, mol/dm}^3) \qquad \textbf{Equation 6.1}$$

By a similar argument it was evident that the asymptote upon which the ICL was based could be shifted to a higher percentage lime addition. Analysis of Figure 5.2 did however show that these variations were relatively small and that the ICL value of 7.0% for Wyoming Bentonite was likely to be reasonably accurate.

Arguments about the mechanisms governing the determination of the ICL value of different clay minerals have been complex and diverse, but highly important with respect to predicting the lime required to develop stabilisation and solidification within a soil. An explanation of the mechanisms governing the determination of the ICL value will be suggested below because it is also relevant to later discussions. Although ultimately there are many inter-dependent factors occurring simultaneously, the chemical processes involved in determination of the ICL value have been associated with the mineral characteristics illustrated in Figure 6.1.

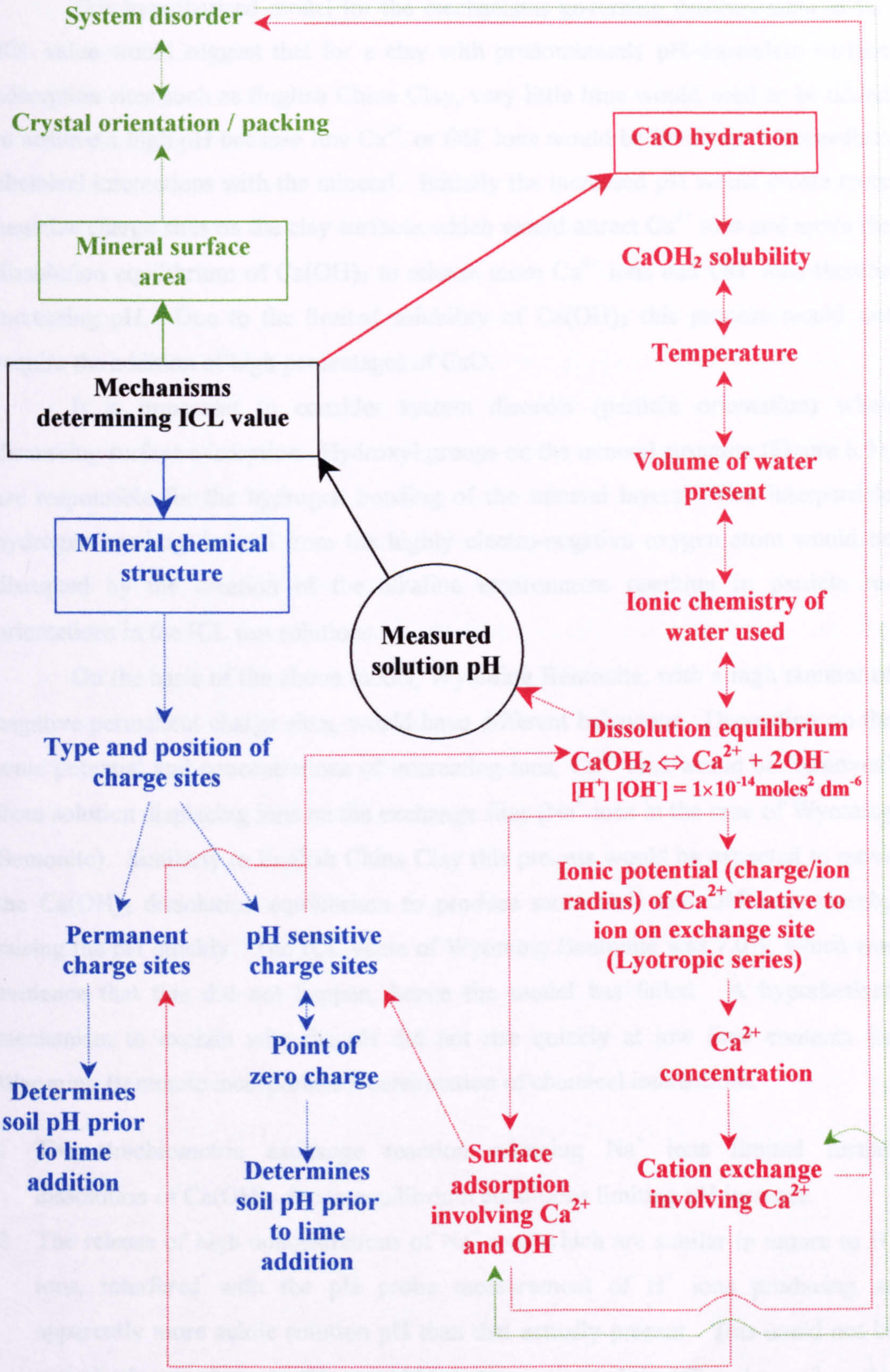

Figure 6.1 Hypothesised principles governing ICL test

This hypothesised model for the mechanisms governing determination of the ICL value would suggest that for a clay with predominantly pH-dependent surface adsorption sites such as English China Clay, very little lime would need to be added to achieve a high pH because few Ca^{2+} or OH^- ions would be involved in immediate chemical interactions with the mineral. Initially the increased pH would create more negative charge sites on the clay surfaces which would attract Ca^{2+} ions and move the dissolution equilibrium of $Ca(OH)_2$ to release more Ca^{2+} ions and OH^- ions thereby increasing pH. Due to the limited solubility of $Ca(OH)_2$ this process would not require the addition of high percentages of CaO.

It is important to consider system disorder (particle orientation) when discussing surface adsorption. Hydroxyl groups on the mineral structure (Figure 6.3), are responsible for the hydrogen bonding of the mineral layers. This interparticle hydrogen bonding derived from the highly electro-negative oxygen atom would be disrupted by the creation of the alkaline environment resulting in particle re-orientations in the ICL test solutions.

On the basis of the above model, Wyoming Bentonite, with a high number of negative permanent charge sites, would have different behaviour. Depending on the ionic potential and concentrations of interacting ions, Ca^{2+} ions would be 'removed' from solution displacing ions on the exchange sites (Na^+ ions in the case of Wyoming Bentonite). Similarly to English China Clay this process would be expected to move the $Ca(OH)_2$ dissolution equilibrium to produce more Ca^{2+} and OH^- ions thereby raising the pH quickly. The ICL value of Wyoming Bentonite was 7.0%, which was evidence that this did not happen, hence the model has failed. A hypothesised mechanism to explain why the pH did not rise quickly at low lime contents for Wyoming Bentonite incorporates a combination of chemical interactions:

1. The stoichiometric exchange reaction releasing Na^+ ions limited further dissolution of $Ca(OH)_2$ due to equilibrium conditions limiting pH increase.
2. The release of high concentrations of Na^+ ions which are similar in nature to H^+ ions, interfered with the pH probe measurement of H^+ ions producing an apparently more acidic solution pH than that actually present. This could not be entirely the case because this would have over-estimated the ICL value and on this basis significant stabilisation at lower lime contents would have been expected, which was not the case.

3. The Wyoming Bentonite had a higher number of surface adsorption (hydroxyl) sites than English China Clay. Montmorillonite does have surface hydroxyl sites which would be involved in chemical interactions (Figure 6.3) and the increased surface area due to particle orientations and disorder would suggest that these sites would be more available for chemical interactions. However, Wyoming Bentonite had a significantly higher ICL value than English China. It was previously suggested that the release of Na^+ ions into solution due to cation exchange with Ca^{2+} ions would reduce the dissolution of lime. Alternatively as a higher quantity of solid lime was added more Na^+ ions were displaced which had a higher solubility than the Ca^{2+} ions thereby allowing more dissolution of $Ca(OH)_2$. As the Ca^{2+} ions were interacting with exchange sites OH^- ions were attracted to the Ca^{2+} at the edges of these sites resulting in the unexpected low pH. This would also explain some of the pozzolanic dissolution phenomena to be discussed later where the location of mineral dissolution varied for different minerals. Furthermore, the gradual addition of lime would cause the water between interacting layers to be excluded resulting in particle flocs surrounded by water. These changes in particle orientation and disorder in solution would also have an effect on future chemical interactions. A simplified image of this process and the effects of system disorder are illustrated in Figure 6.2.

On the basis of the ideas relating to the mechanisms controlling the ICL determination it would be possible to hypothesise the outcomes of testing contaminated soils, varying the ICL solid to liquid ratio, and varying the soil mineralogy. These ideas are open to considerable conjecture by various investigators. Investigations by Ho and Handy (1963A and 1963B) would tend to support the hypothesis via measurements of zeta potential (a quantity related to the net negative or positive charge by the clay particles in dilute suspension) of lime-treated Bentonite aged either for several days ('fresh') or a year ('aged'). Their results showed that Ca^{2+} ion saturated Bentonite had a zeta potential of about –20 millivolts. Small additions of lime caused a slight increase in this value and larger additions generated a modest decrease for both fresh and aged samples. Na saturated Bentonite had a zeta potential of about –40 millivolts; additions of lime up to about 6 percent caused strong proportional reductions to –26 millivolts for fresh samples and –22 millivolts for the aged samples, whereas higher additions of lime caused no further change. However,

Diamond and Kinter (1965) disputed the ideas of ionic interactions with Bentonite because ionic interactions were often above the cation exchange capacity of the mineral and suggested that physical adsorption of the CaO molecule was more likely. These latter ideas were disputed by Ho and Handy (published in Diamond and Kinter, 1965) and pH-dependent surface ionic adsorption was the suggested mechanism.

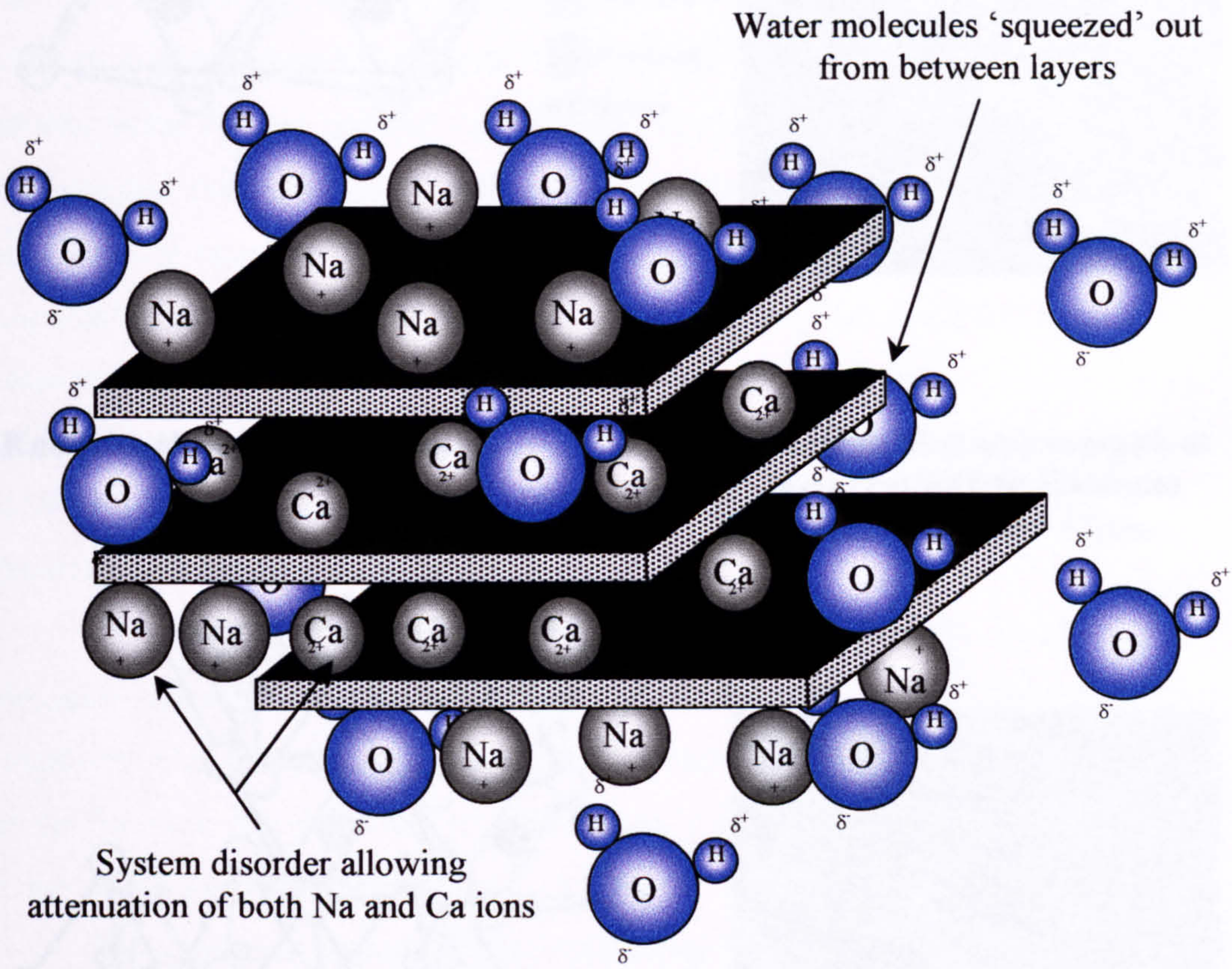

Figure 6.2 Monovalent and divalent cations between multiple clay surfaces

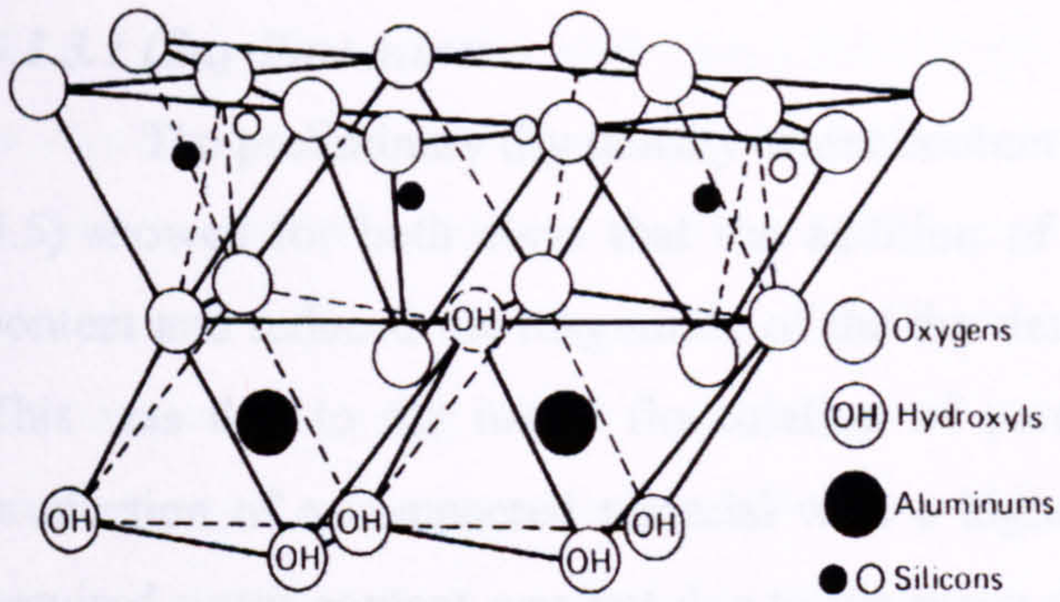

Kaolinite chemical structure.

Electron photomicrograph of well-crystallized Kaolinite. Picture width = 17μm.

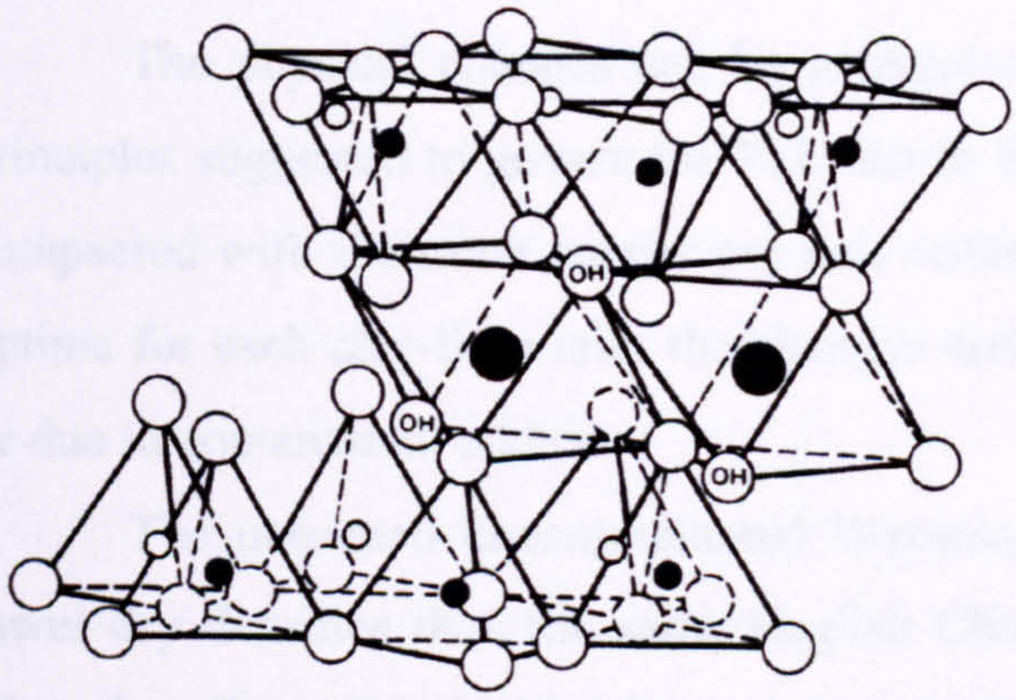

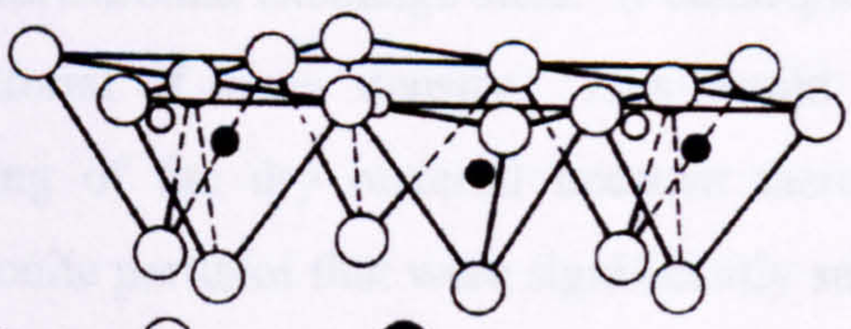

Montmorillonite chemical structure.

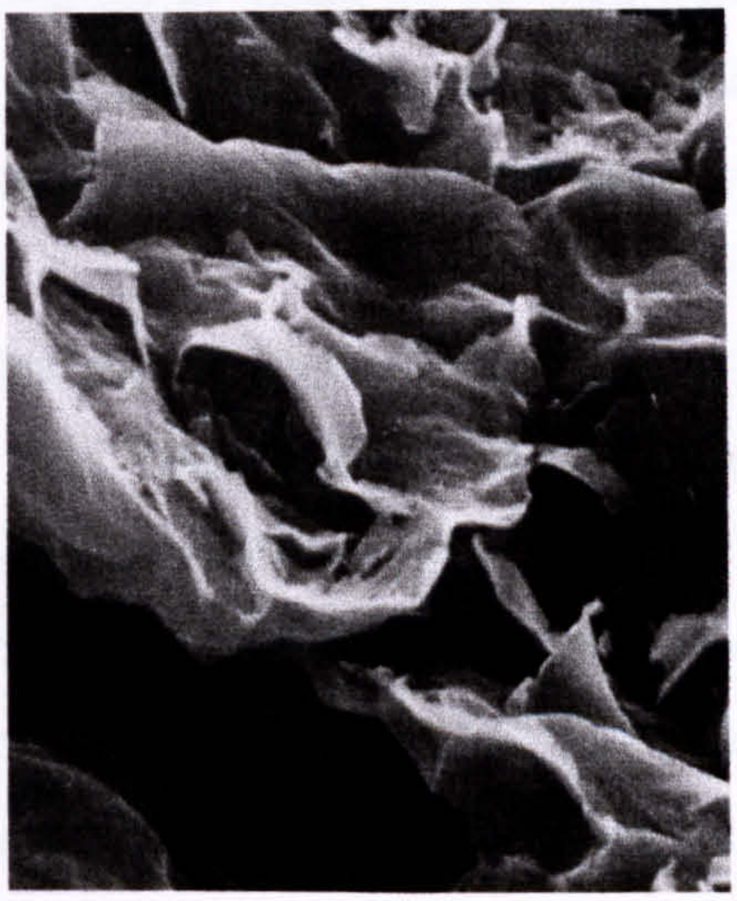

Electron photomicrograph of montmorillonite (Bentonite). Picture width = 7.5μm.

Figure 6.3 Natural chemical structures of Kaolinite and Montmorillonite relative to visual particle orientations (SEM; after Mitchell, 1976)

6.1.3 Dry density water-content relationships

6.1.3.1 Clay-lime mixes

The preliminary dry density-water content compaction curves (Figures 5.4 and 5.5) showed for both clays that the addition of lime increased the optimum water content and reduced the magnitude of the dry density at this optimum water content. This was due to the initial flocculation of particles on addition of lime and the production of a compacted material with a higher proportion of voids. The higher required water content was not due to the water required to hydrate the lime because the measured water content was carried out at 105 ± 0.5^{0}C, not sufficient to reverse the hydration reaction. Hence this extra required water was also a result of the flocculation reactions. More water was needed to reduce the resistance to shearing to a minimum so that density was maximised i.e. to remove suctions. The dry densities achieved for the final design mixes (Figure 5.6) also illustrated this behaviour. Furthermore, it was clear that the contaminant present affected the dry density due to cation exchange, where applicable.

The physical changes can be associated with many of the ionic interaction principles suggested to govern the ICL test in Section 6.1.2. Since all samples were compacted with the same energy per unit volume and 2% wet of the predetermined optima for each clay-lime mix, the changes seen with contaminants present can only be due to contaminant addition.

The untreated uncontaminated Wyoming Bentonite samples achieved much lower dry densities than the same English China Clay samples due to the fact that Wyoming Bentonite hydrated, retaining significant quantities of water within its structure around exchange sites. It consequently expanded significantly and produced a material of lower density. This would not have been expected from the initial grading of the dry material because there was a higher proportion of Wyoming Bentonite particles that were significantly smaller than those of English China Clay.

6.1.3.2 Clay-lime-contaminant mixes

The contaminated English China Clay samples with no lime added exhibited reduced dry density because the particle flocculation increased due to the addition of an ionic contaminant. On addition of lime the dry density achieved reduced further although the lime-treated contaminated samples still had lower dry densities. Several

mechanisms could be postulated. The first was that the OH^- ions liberated by the addition of lime reacted with the contaminant ions, hence moving the $Ca(OH)_2$ equilibrium to release more Ca^{2+} and OH^- ions and thereby increasing flocculation caused by the Ca^{2+}. However, the reduced quantity of Fe^{3+} ions would also reduce flocculation. Hence it would be feasible to suggest that a variety of ions in equilibrium of varying charge and radius can achieve a higher degree of flocculation than any one ion due to system disorder. The second hypothesis was that the contaminant precipitate produced on the addition of lime might partially bind particles together physically and hence impede compaction with a compaction hammer. A combination of these factors is feasible.

Wyoming Bentonite behaved differently to the English China Clay samples (Figure 5.6). Initially the Fe^{3+} ion contaminated sample had a higher dry density than either the uncontaminated or Pb^{2+} ion contaminated samples. This did not happen for the equiverlant English China Clay samples. Due to its structural differences Wyoming Bentonite was more likely to react to the processes of cation exchange and flocculation than the English China Clay. An explanation as to the different behaviour of the two clays was only evident by observation of the samples during compaction. It was clearly visible that wet untreated Wyoming Bentonite had very significant plasticity that made it very difficult to compact with a hammer due to adhesion to the base of the hammer. On addition Fe^{3+} ions the difficulties due to the plasticity reduced. However, on addition of lime the level of flocculation was so significant that dry density decreased. The flocculation was so rapid, within seconds of the addition of lime, that the material gained a level of increased strength and reduced plasticity which made it difficult to compact. This could help to explain why the dry densities increased marginally when the lime addition was increased from 2.5% to 7.0%. Some of these behavioural characteristics will become more apparent later during the discussion of the Atterberg Limits and the shear strength results. Plasticity was not a problem for compaction of the English China Clay simply due to its inherent low plasticity and very low cation exchange capacity.

It is important to note that the final design mix samples were deliberately mixed on the wet side of optimum to achieve the minimum permeability. Therefore the dry densities achieved were expected to be slightly lower than the optimums determined by the initial characterisation.

6.2 CORRELATION BETWEEN CHEMICAL MEASUREMENTS AND SHEAR STRENGTH

6.2.1 Introduction

Once the soluble element contents and specifically the soluble Ca, Al, Si and Na contents of the filtered end of batch solutions were known in conjunction with the end of batch test pH and conductivity, it was possible to use the end of batch test pH and conductivity alone (as illustrated in Figure 5.11) to explain many of the time-dependent chemical and physical properties of both clay-lime and clay-lime-contaminant interactions. Specifically pH and conductivity variations with curing time can be used to infer whether the stabilisation and solidification reactions were taking place without the need for complex chemical analysis. With care, the shear strength improvements have been associated with these changes.

Prior to discussion of the detailed 'micro' element chemical releases during batch tests the 'macro' processes governing release should be highlighted. There were four processes that governed the release of the Pb, Fe, Ca, Si, Al and Na into solution during batch tests.

1. Firstly there were the cation exchange reactions, which were predominantly associated with Pb^{2+}, Fe^{3+}, Ca^{2+} and Na^{+} ion releases from the Wyoming Bentonite samples only.

2. Secondly there were the stabilisation and solidification reactions, which in the longer-term created a strong material of low permeability which would limit the release of all elements and incorporate some of these elements in the crystallisation products. This mechanism was relevant to both clay minerals, although the mechanisms were different.

3. Thirdly the development of the solidification reactions with curing time affected how the cubes in the batch test broke down, and therefore the surface area in contact with the leachant and subsequently the element release with curing time. The process governing this mechanism were the

effects of the high pH creating more soluble Si and Al from dissolution reactions at the clay mineral surface.

4. Fourthly there was the method of separation of the solid and liquid phases at the end of the batch test. This latter mechanism was relevant for those Wyoming Bentonite mixes with lime additions below 7.0% where separation was via centrifugation. The success or otherwise of centrifugation appeared to be associated with the degree of flocculation of the mineral particles and resulted in the release into solution of very high levels of Ca, Fe, Si and Al, which disguised the changes in these element concentrations due to solidification reactions. The high levels of the elements found to be present were due to fine clay particulates held in suspension in solution, a situation noted by the cloudy nature of the supernatant. Therefore the changes being observed for the samples which were easily filtered were more likely to relate to cation exchange where appropriate, stabilisation and solidification reaction chemistry and particle breakdown (i.e. strength of the solidified mass). The difficulty therefore arose in distinguishing between the effects associated with changing solidification reactions and those of particle breakdown.

6.2.2 Measured chemical changes due to particle breakdown and time-dependent chemical reactions

6.2.2.1 Clay-lime mixes

On addition of lime to a sample a reduction in the particle breakdown would be generally expected due to increased strength properties associated with initial stabilisation reactions and subsequent time-dependent solidification reactions. If on addition of lime there were increases in elemental release with time this could not be associated with reduced particle breakdown but only with the chemistry related to stabilisation and solidification reactions. However, the problem arose when there was a reduction in elemental release and pH and conductivity since it was unclear whether these reductions were due to changes in chemistry or changes in particle breakdown. Both these mechanisms would be of benefit at limiting element migration *in situ*.

A hypothesis can be constructed for English China Clay to suggest that much of the release of elements was primarily due to chemical processes although it was not

possible to ascertain the precise proportion. The basis for the argument explained below is that if one of the lime-treated clays, either English China Clay or Wyoming Bentonite can be found, which breaks down into small particles, any reductions in conductivity or soluble Ca concentration are due to chemical changes and not due to partial breakdown of the monolithic masses.

Analysis of the particle breakdown curve for samples batch tested after 301 days curing in Figure 5.17 showed that for English China Clay mix designs with 1.5% lime content, at least 83% of particles by mass for both 20mm and 10mm initial cube sizes broke down into particles smaller the 63μm. Due to the time dependence of solidification it could be argued that particle breakdown of the English China Clay samples with 1.5% lime would be greater at 175 days curing and greater still at 7 days curing. This hypothesis was supported by the shear strength data in Figure 5.18 that illustrated that at 7 days curing the shear strength was much less than that at 301 days curing. Due to the high particle breakdown at the end of these batch tests after 301 days curing it was likely that the observed changes with curing time of pH (hydrogen ion concentration) and conductivity (dissolved solids) for the end of batch test solutions of English China Clay samples with 1.5% lime content in Figure 5.11 were predominantly due to chemical changes. The changes in conductivity and pH of the English China clay samples with 2.5% lime illustrated in Figure 5.11 were a similar shape even though there was less particle breakdown (70% < 63μm). This was evidence to suggest that the observed change in element release into solution (Si, Al and Ca) depicted in Figure 5.12 was predominantly due to chemical changes.

Distinguishing between chemical changes associated with the particle breakdown and time-dependent chemistry of Wyoming Bentonite samples was not as easy due to the high undrained shear strengths of the clay-lime mixes. This was compounded by the fact that it was not possible to sieve samples with only 2.5% lime addition due to the fact that the material obtained from the batch test was a thick sludge similar to that illustrated in Figure 4.10. However, increases in the soluble concentrations of Si discussed later and illustrated in Figure 5.13 confirmed that chemical changes were detectable irrespective of particle breakdown. To make further judgements about Wyoming Bentonite the contaminated samples had to be considered. These are discussed in Section 6.2.2.2.

6.2.2.2 Clay-lime-contaminant mixes

Figure 5.17 illustrated that contaminants significantly affected the breakdown of the cubes in the batch tests. The influence of contaminants on this process was more evident for Wyoming Bentonite mixes than English China Clay mixes. For any of the contaminant mixes with lime added the lowest mass passing a 63μm sieve after a batch test with 20mm cube sizes was 92% for English China Clay + Pb^{2+} ions + 2.5% lime whilst only 41% for Wyoming Bentonite + Pb^{2+} ions + 7.0% lime. For the uncontaminated Wyoming Bentonite sample with 7.0% lime the mass passing a 63 μm sieve was 41% clearly indicating the increased resistance of the Pb contaminated sample to particle breakdown. pH and conductivity data in Figure 5.11 illustrated that all these samples exhibited the similar reductions in pH and conductivity signifying that chemical processes were occurring.

6.2.3 Relationships between shear strength and soluble chemistry for English China Clay

6.2.3.1 Clay-lime mixes

Figure 5.18 highlighted the large increases in shear vane strength of English China Clay with increasing lime content and curing time. ICP chemical data in Figure 5.12 for uncontaminated English China Clay with 1.5% and 2.5% lime all showed increases in soluble Al concentrations, reductions in Ca concentrations and very low, relatively constant Si concentrations with increasing curing time. For English China Clay with a 2.5% lime content, the soluble Ca concentrations illustrated in Figure 5.12 reduced by a higher proportion with curing time than the sample with 1.5% lime whilst the Al concentrations again increased. The large reduction in Ca and increase in Al leached into solution at 175 and 301 days curing was not evident at 7 days, which suggested that at 7 days curing there was limited pozzolanic reaction activity and that activity increased with increasing curing time. Although not supported with data due to the limitations of the shear vane equipment, it was evident that the English China Clay samples with 2.5% lime resulted in higher undrained shear strengths. This suggested that substantial benefit was gained by adding lime above the ICL.

ICP data in Figure 5.12 illustrated that on addition of lime to English China Clay samples, only Al appeared to become more soluble with curing time with no

measurable Si activity. Although it would be expected that soluble Al would decrease due to re-crystallisation of calcium aluminate hydrates at the continued high pH, further dissolution would be expected hence retaining the high concentrations of soluble Al at longer curing times. However, the level of soluble Al would also be expected to reduce after a very long curing time due to a reduction in the pH and the re-crystallisation of cementitious reaction products on the surfaces of the mineral particles, the source of alumina. Perhaps this was not seen here due to testing at limited curing periods.

6.2.3.2 Clay-lime-contaminant mixes

The behaviour of the contaminated samples was different. Batch tests on English China Clay with Pb^{2+} or Fe^{3+} ion contamination and no lime exhibited an initial liberation of soluble Si at 7 days curing, with large reductions in Si concentration from 7 days to 175 days and subsequently 301 days (Figure 5.14). However, on addition of lime to this Pb^{2+} ion contaminated English China Clay sample, there were large reductions in soluble Ca concentrations and large increases in soluble Al concentrations with no soluble Si activity. For lime-treated English China Clay with 5000ppm Fe^{3+} ions there were very small reductions in soluble Ca concentrations and no increases in soluble Al. Instead of reductions in soluble Ca and increases in soluble Al there were essentially constant high levels of both elements at all curing periods. However, increasing the lime content for this sample from 1.5% to 2.5% lime resulted in higher constant concentrations of both Al and Ca in batch test solutions (Figure 5.12). It was also clear from Figure 5.12 that the higher lime content resulted in larger reductions with time in soluble Ca concentrations for the Pb^{2+} ion contaminated and uncontaminated samples. English China Clay had essentially no cation exchange capacity thus it was reasonable to suggest that changes in soluble Ca and Al concentrations were due to the formation of calcium-aluminate-hydrate gels as the pozzolanic reactions progressed. Significantly Pb^{2+} ion contaminated samples treated with 2.5% lime liberated nearly 2.5 times more soluble Al than all other lime-treated samples at 175 and 301 days curing (Figure 5.12). This could help explain why these samples showed larger shear strength increases than uncontaminated mixes with the same lime content (Figure 5.18). Interestingly English China Clay + 5000ppm Fe with 2.5% lime liberated more soluble Al at 7 days curing compared to all other mixes with the same lime content. This may explain its

apparent higher strength relative to the other samples with no lime and the uncontaminated English China Clay sample with 2.5% lime at 7 days curing. This trend of increased strength as leached Al concentration increased was reflected by all other lime-treated English China Clay samples.

The undrained shear strength of the lime-treated Fe^{3+} ion contaminated samples were low relative to the lime-treated uncontaminated samples and the Pb^{2+} ion contaminated samples (Figure 5.18). One suggested hypothesis incorporated two mechanisms. Firstly the quantities of $OH^-_{(aq)}$ required to react with the two different contaminants was substantially different. For every mole of the $OH^-_{(aq)}$ anion required to react with the added $Pb^{2+}_{(aq)}$ cation, 5.56 moles of $OH^-_{(aq)}$ was required to react with the added $Fe^{3+}_{(aq)}$ cation. Also for every mole of $Pb(OH)_{2(s)}$ precipitated there were 3.7 moles of $Fe(OH)_{3(s)}$ precipitated, hence more precipitate was present to interfere in the crystallisation of any pozzolanic reaction products. If crystallisation could not occur it was reasonable to suggest that Ca could remain at a constant level in some soluble form and be detectable using ICP and conductivity. These ideas were reflected in Figure 5.11. Where lime was present, with the exception of the Fe^{3+} ion contaminated sample, there were significant reductions with time in pH and conductivity with curing. Clearly as $pH = -Log_{10}[H_30^+]_{(aq)}$ where $[H_30^+]_{(aq)}$ represents hydrogen ion concentration in moles/dm^3, a small change in pH reflects a relatively large change in $[H_30^+]_{(aq)}$. The reduction in pH reflected an increase in $(H_30)^+_{(aq)}$, i.e. a reduction in $OH^-_{(aq)}$. The reductions in conductivity reflect the reduction in concentrations of all anions and cations, although perhaps the most significant being the ICP measured reductions in soluble Ca concentration and the reduction in hydroxide ions due to precipitation reactions. These reductions in pH were clearly evident for contaminated English China Clay samples with lime relative to the uncontaminated English China Clay samples with lime.

The second suggested mechanism for the reduced physical and chemical development of the Fe^{3+} ion contaminated samples with lime relate to the very slow creation of iron-aluminate-hydrates relative to calcium-aluminate hydrates. In a system of mixed Fe^{3+} and Ca^{2+} ions it would be likely that Fe^{3+} ions would be involved preferentially to Ca^{2+} ions, although this behaviour would have to be in equilibrium with the precipitation reaction involving the Fe^{3+} and OH^- ions.

The Pb^{2+} ion contaminated samples exhibit increased chemical activity and improved strength development particularly in the early stages of solidification. Pb^{2+}

ions have a similar charge and size to Ca^{2+} ions (Figure 6.4) and as such behave similarly during pozzolanic reactions. However, this cannot explain why more soluble Al was produced during the early stages of solidification reactions. This would suggest that the presence of Pb^{2+} ions aided the dissolution of the aluminates from English China Clay.

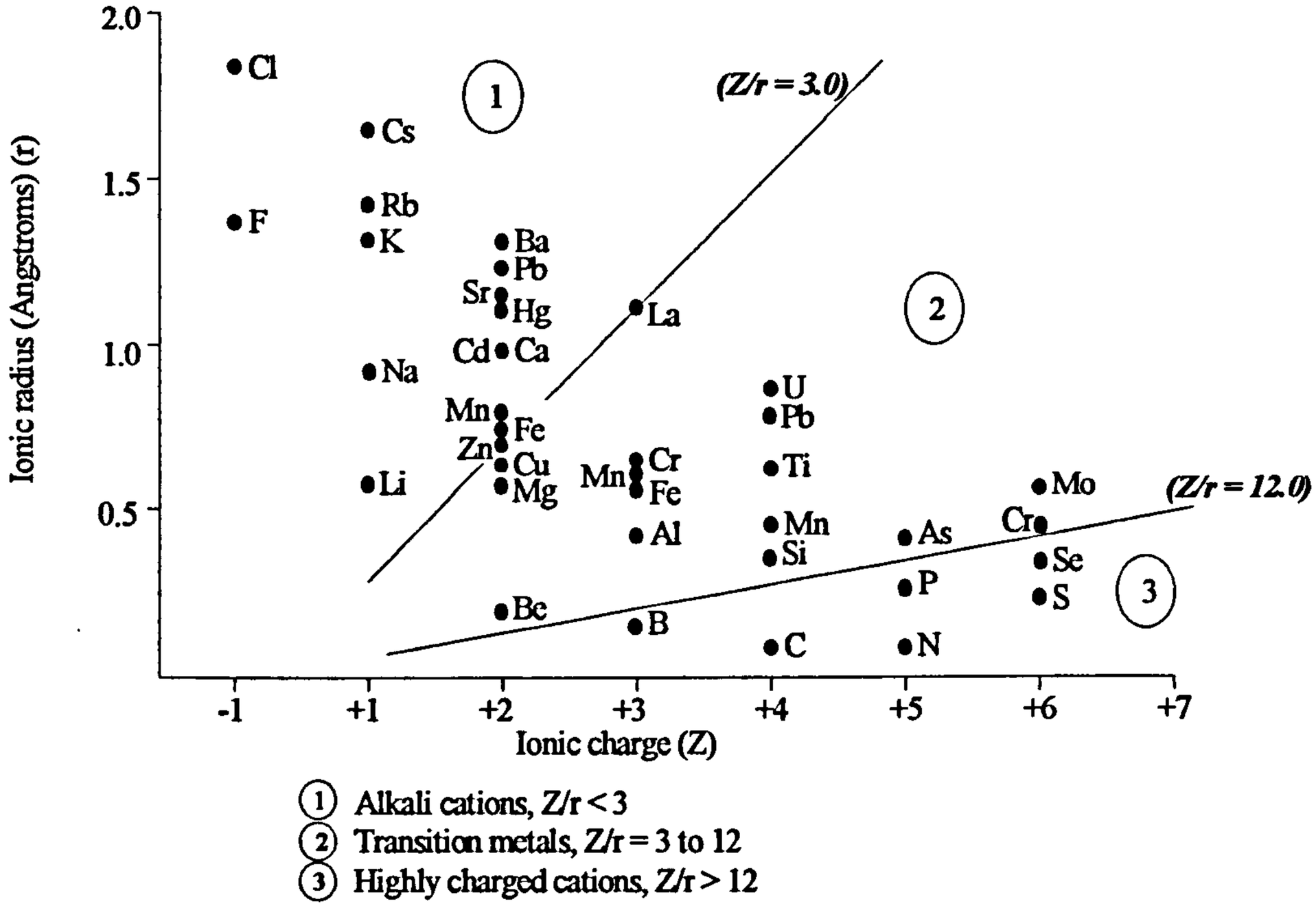

Figure 6.4 Ionic potentials (Z/r) of important ions found in soil (Loughnan, 1969)

Aside to the considerations due to the addition of contaminants, an important issue is the selective dissolution of Al relative to Si during pozzolanic reactions. This issue will be addressed in the next section.

6.2.3.3 Suggested mechanisms governing selective dissolution of the English China Clay structure due to pozzolanic reactions

Initial inspection of acid digestion data in Table 5.14 would suggest that the higher soluble Al than Si concentrations observed in batch test solutions due to pozzolanic reactions were due to lower levels of Si present in the mineral structure

(564mg/kg acid soluble Si relative to 4272mg/kg acid soluble Al). Caution should be used in interpreting such acid soluble data because the solubility of a mineral is significantly different in acid and alkaline environments. Figure 2.12 illustrates that in alkaline environments above pH 10.5 both silicon oxides and aluminium oxides are similarly susceptible to dissolution whilst below pH 3 (the condition during acid digestion) aluminium oxides are significantly more susceptible to dissolution than silicon oxides. On this basis the acid digestion did not necessarily reveal the relative quantities of soluble Al and Si. To obtain these data acid digestion using hydrofluoric acid would have been required, a chemical not permitted for use during this study due to health and safety restrictions. However, analysis of Figure 6.2 suggested a mechanism that would govern the release of Al preferentially to Si during solidification reactions. The hydroxyl group attached to the mineral surface responsible for interparticle hydrogen bonding was pH sensitive and at high pH the OH^- ions were attracted to the sites interacting with the hydrogen atom. This in turn created negative charges at these sites thus attracting Ca^{2+} ions. The attraction of the OH^- ions to these sites initiated mineral dissolution directly next to a source of Al atoms in the mineral structure. The fact that Ca^{2+} ions were also attracted to these sites resulted in a ready supply of Ca^{2+} to create the calcium-aluminate-hydrate gels prior to re-crystallisation.

However, it was found that that when no lime was added to the contaminated English China Clay samples Si became the most susceptible to dissolution. These samples were acidic when in solution (between pH 3 and pH 5; Figure 5.11). An initial suggestion could be that the Si^{4+} was displaced from surface adsorption sites by the sites becoming positively charged. This was unlikely because this Si release would be evident for the lime-treated samples after dissolution of these sites. One potential explanation was that because the hydroxyl sites become positively charged in acidic conditions excess H^+ ions were repelled from these sites and were attracted to the electronegative oxygen associated with the silicon atoms (Figure 6.3). It was at these sites where dissolution occurred. Hence dissolution according to acid environments illustrated in Figure 2.12 would occur.

6.2.4 Relationships between shear strength and soluble chemistry for Wyoming Bentonite

6.2.4.1 Clay-lime mixes

Figures 5.11 and 5.18 suggested that the chemical and strength behaviours of filtered Wyoming Bentonite samples were similar to those of English China Clay. In many ways this appeared to be the case but with the added effects due to the Wyoming Bentonite chemical structure and subsequent cation exchange capability releasing Na^+ and Ca^{2+} ions. This was evident by consideration of uncontaminated Wyoming Bentonite with 7.0% lime. The concentrations of soluble Ca illustrated in Figure 5.13 clearly decreased significantly with increasing curing time. Although still high the soluble Na concentrations also reduced with increasing curing time whilst the soluble Si concentrations increased significantly. Significantly virtually no soluble Al was liberated relative to soluble Si, unlike the English China Clay samples.

6.2.4.2 Clay-lime-contaminant mixes

The soluble Na and Ca concentrations for Wyoming Bentonite + 5000ppm Pb with 7.0% lime were similar to the uncontaminated Wyoming Bentonite sample with 7.0% lime. If the presence of Pb^{2+} ions was responsible for liberation of extra soluble Al in English China Clay with subsequent larger increases in vane strength of these samples, it is possible that the reduced amount of available soluble Si in the Wyoming Bentonite samples explains why the Wyoming Bentonite with Pb^{2+} ion contamination strength behaviour does not reflect the behaviour characteristics of English China Clay. It was consequently hypothesised that exchange of Pb^{2+} for Na^+ ions in the Wyoming Bentonite structure had reduced the effect of increased liberation of soluble Si on addition of Pb^{2+} ions, as was the case for increased soluble Al liberation on addition of Pb^{2+} ions to the English China Clay sample.

One of the most significant results for Wyoming Bentonite was for the Fe^{3+} ion contaminated sample with 7.0% lime. The presence of the Fe^{3+} ions did not significantly inhibit the pozzolanic reactions and the undrained shear strength increases were similar to the Pb^{2+} ion contaminated and uncontaminated samples treated with lime. The occurrence of pozzolanic chemistry for the Fe^{3+} ion contaminated Wyoming Bentonite sample was apparent by the reduction in pH and conductivity of the samples in Figure 5.79, unlike the equivalent English China Clay sample. To explain why Fe^{3+} ion contamination inhibited the pozzolanic reactions of

English China Clay and not Wyoming Bentonite a hypothesis involving three mechanisms was developed. Firstly, it could be argued that this effect was due to the higher (7.0%) lime content of the Wyoming Bentonite sample relative to the (2.5%) lime content of the English China Clay sample, resulting in a higher $OH^-_{(aq)}$ availability and increased pozzolanic activity. However, this was not necessarily the case because similar reductions in pH and conductivity occurred for the Wyoming Bentonite samples to which 5000ppm Fe^{3+} ion contamination and 2.5% lime were added (an addition well below the ICL for Wyoming Bentonite) and the English China Clay samples to which 5000ppm Fe^{3+} ion contamination and 2.5% lime were added (an addition above the ICL value). The second suggested mechanism was due to the inter-layer cation exchange sites attenuating significant quantities of Fe^{3+} ions from solution, resulting in reduced levels of precipitate interfering with pozzolanic solidification reactions. Thirdly iron-silicate-hydrate may have hydrated faster and crystallised to produce a stronger material than crystallised iron-aluminate-hydrate. Although this discussion is speculative, the difference between the predominant Al dissolution from English China Clay and Si dissolution from Wyoming Bentonite would be a significant factor. Due to the large conductivity and soluble Ca reductions with time, illustrated in Figures 5.11 and 5.13 respectively, it could be speculated that Fe^{3+} ions did not interact at all with the dissolved mineral and did not produce iron-silicate-hydrates but produced calcium-silicate-hydrates. This is a suggested area requiring further study.

6.2.4.3 Suggested mechanisms governing selective dissolution of the Wyoming Bentonite structure due to pozzolanic reactions

Inspection of Figure 6.3 suggested that the majority of edge sites of montmorillonite minerals were associated with the tetrahedral silicate structure. It was also hypothesised that if OH^- ions were attracted to Ca^{2+} ions on exchange sites as suggested in Section 6.2.1, then mineral dissolution could also be initiated at these sites, adjacent to tetrahedral silicates. The fact that small quantities of soluble Al were also produced via dissolution processes suggests that proportions of all Wyoming Bentonite mineral surfaces were involved in dissolution processes and that dissolution occurred into the mineral structure.

6.2.4.4 The influence of contaminants on pozzolanic reactions

It was evident that the cation exchange sites were very important and could affect which contaminant precipitated at high pH. Furthermore, cation exchange sites could control the quantity of contaminant precipitated and therefore reduce positive or negative effects of contaminants on pozzolanic reactions. Due to the fact that the pozzolanic reactions of the Fe^{3+} ion contaminated Wyoming Bentonite samples with 7.0% lime were relatively unaffected compared with the similar English China Clay samples it was important to try to gain more information from the data about these processes. It was considered important to distinguish what proportion of Pb^{2+} ions were removed by cation exchange and what proportion were removed by precipitation to aid analysis. It was apparent that a higher proportion of the 5000ppm Pb^{2+} ions were precipitated relative to the 5000ppm Fe^{3+} ions by observing the soluble Na concentrations of the samples with 7.0% lime content (Figure 5.13). It was clear that the uncontaminated and Pb^{2+} ion contaminated samples had similar soluble Na concentrations. Since Pb^{2+} ions have a slightly smaller ionic potential than Ca^{2+} ions (Figure 6.4), it was reasonable to suggest that Ca^{2+} ions could have occupied more exchange sites than the Pb^{2+} ions. Further evidence for this existed in Figure 5.13, where at 7 days curing i.e. during the natural attenuation period prior to solidification reactions, there were fewer Ca^{2+} ions released from the Pb^{2+} ion contaminated sample than the uncontaminated sample. However, Fe^{3+} ions have a higher ionic potential than Ca^{2+} ions hence they were likely to be attenuated preferentially to the Ca^{2+} ions. Again this was illustrated in Figure 5.13 at 7 days curing this by the significantly higher quantity of soluble Ca released than either the Pb^{2+} ion contaminated or the uncontaminated samples.

It was previously discussed that there was a higher number of Fe^{3+} ions present than Pb^{2+} ions, hence the higher concentrations of soluble Na in Figure 5.13 for the Fe^{3+} ion contaminated samples relative to the other samples could be explained. Based on these facts (including the ionic potentials of Ca^{2+}, Pb^{2+} and Fe^{3+} ions) and the fact that for the lime-treated samples no soluble Pb or Fe was detectable by ICP, clearly a higher proportion of Pb^{2+} ions was precipitated relative to Fe^{3+} ions. Therefore, it may have been expected that the Pb^{2+} ion contaminated Wyoming Bentonite sample would behave similarly to the uncontaminated English China Clay sample by having improved strength properties. There was one flaw in the hypothesis that more Pb^{2+} ions were precipitated than Fe^{3+} ions. If this were the case the pH of

these samples could be expected to reduce significantly. An explanation as to why this did not happen comes from Figure 5.11 and an analysis of the pH changes of contaminated English China Clay samples. Since removal of contaminant from solution was essentially only possible via precipitation reactions, and all lime-treated samples showed no evidence of contamination of either soluble Pb or Fe, then one would expect reductions in pH as a result. For both English China Clay samples with 1.5% and 2.5% lime these reductions were only apparent for the Fe^{3+} ion contaminated sample and not the Pb^{2+} ion contaminated sample (Figure 5.11). Therefore, for the Wyoming Bentonite sample that had a naturally higher pH than English China Clay it would also not have been expected to see reductions in pH due to the precipitation of Pb^{2+} ions. Subsequently for Wyoming Bentonite it was feasible that Pb^{2+} ions were precipitated and not necessarily attenuated.

6.2.4.5 Wyoming Bentonite at lime additions below the ICL value

The relationship between strength and chemistry was not as easy to determine for the 2.5% lime addition as for the 7.0% lime addition due to the inability to filter the material from these batch tests. Figure 5.18 showed that on addition of 2.5% lime, both Fe^{3+} and Pb^{2+} ion contaminated samples were stronger than the respective uncontaminated samples at any curing time. It was also evident for the 2.5% lime addition that the strength of the Fe^{3+} ion contaminated samples did not increase significantly with time where as that of the Pb^{2+} ion contaminated samples did. At this low level of lime addition reliable ICP data were not available. Therefore it was necessary to utilise the variation in pH and conductivity in Figure 5.11 to infer the chemical behaviour of the Wyoming Bentonite samples with 2.5% lime addition. Observation of the pH variation of all the samples with 2.5% and 7.0% lime showed a clear small reduction with curing time of all contaminated and uncontaminated samples, which was not the case for all the English China Clay samples with 2.5% lime. This suggests that more lime must be added to raise the pH to increase the pozzolanic reaction activity.

The processes controlling the increased strength of the contaminated samples was revealed by the conductivity data in Figure 5.11. The ions that were most likely to cause changes in conductivity were Ca^{2+}, Na^{+}, Fe^{3+}, Pb^{2+} and NO_3^{-}. For the Wyoming Bentonite samples with 7.0% lime the ICP data confirmed that the changes in conductivity with curing time were essentially due to reductions in soluble Ca and

Na concentrations (Figure 5.12). The higher conductivity of the Fe^{3+} ion contaminated samples with 7.0% lime at 175 and 301 days curing related partly to the higher soluble Na concentration, illustrated in Figure 5.12 and explained earlier by the preferential exchange of the Fe^{3+} ions than the Ca^{2+} ions or Pb^{2+} ions. The conductivity data clearly indicated that the increased strength of the Wyoming Bentonite samples with 2.5% lime was associated with the large differences in the conductivity between the mixes. Firstly the reduction in conductivity with time was likely to be due to the changes in Ca^{2+} and Na^{+} ions. These were significantly less at 2.5% lime content than for the samples with 7.0% lime content due to the reduced pH limiting the dissolution of silicates and hence re-crystallisation of calcium silicates. Therefore the removal of soluble Ca by this process was significantly less. Secondly the conductivity of the Fe^{3+} ion contaminated samples with 2.5% lime addition was consistantly higher than the Pb^{2+} ion contaminated samples with 2.5% lime addition which was consistantly higher than the uncontaminated samples with 2.5% lime addition. This was for the following reasons:

- The higher proportion of Fe^{3+} than the Pb^{2+} ions exchanging for Na^{+} ions resulted in higher concentrations of soluble Na, which were not necessarily involved in the re-crystallisation process after limited dissolution. However, the argument of a high proportion of Fe^{3+} ion rather than Pb^{2+} ion attenuation may not have been as valid here as it was for the samples with 7.0% lime content, because the reduced concentration of Ca^{2+} ions present on addition of only 2.5% lime reduced the competition for exchange sites and therefore potentially more Pb^{2+} ions would be exchanged for Na^{+} ions.
- Due to the charge on the Fe^{3+} ion contamination and the fact that more Fe^{3+} than Pb^{2+} ions were added, there would also be significantly more NO_3^- present in the Fe^{3+} ion contaminated samples than the Pb^{2+} ion contaminated samples. The Pb^{2+} ion contaminated samples also had significantly more ions in solution than the uncontaminated samples with 2.5% lime addition. However, this argument would also have been valid at any lime content because it was dependent on the contaminant added.

It is therefore likely to be the case that the attenuation of the contaminants resulted in the clear strength trends, a mechanism indicated by increasing Na availability in solution and measurable via conductivity.

6.2.4.6 Wyoming Bentonite behaviour for samples containing 0% lime

Wyoming Bentonite samples with no added lime behaved quite differently to the English China Clay samples. Figure 5.11 illustrated this, with the Wyoming Bentonite samples exhibiting significantly higher pH values than the English China Clay samples whilst the Pb^{2+} ion contaminated and uncontaminated samples produced significantly higher conductivity values. ICP analysis of centrifuged sludges produced in batch tests was illustrated in Figure 5.15, but appeared to show no obvious trends that could be related to the pH, conductivity or shear strength results. As previously explained the ICP data represented the degree of separation of the clay and leachant, which was directly linked to particle flocculation. This was apparent by observation of the behaviour of Si, Al and Ca. The clear pattern was that the Fe^{3+} ion contaminated samples apparently released the smaller quantities of each of the three elements, followed by the Pb^{2+} ion contaminated sample and then the uncontaminated sample. Since Fe^{3+} ions have a higher ionic potential than Pb^{2+} ions and that there were more Fe^{3+} ions present than Pb^{2+} ions, this order of element release was a flocculation effect. This hypothesis was supported by the fact that the Fe^{3+} ion contaminated sample released the most soluble Na and the least soluble Fe, a process indicating cation exchange. Since there was such a high degree of flocculation due to the addition of contaminants the particle separation via centrifugation for the Fe^{3+} ion contaminated samples the results perhaps showed similar detail as the filtered English China Clay samples. However, the chemistry of the other samples was obscured by the poor solid and liquid separation. It was clear however that the observed flocculation effects reflected in the ICP data of these centrifuged samples could reflect changes in Atterberg Limits which were also associated with flocculation.

Due to the poor solid and liquid separation an alternative extraction technique was required to identify the changes in the properties of the Wyoming Bentonite samples with no added lime compared with other samples. Acid digestion after 301 days curing was potentially more useful for these samples because the acid digested mixture was highly flocculated by the addition of high concentrations of H^+ ions hence easily filtered. This will be investigated in the next section.

6.3 ACID DIGESTION OF CLAY-CONTAMINANT-LIME MIXES

6.3.1 Introduction

The technique of acid digesting samples after a significant curing period revealed a great deal about the changes brought about by the addition of both lime and contaminants to the minerals. Significantly it revealed information regarding the pozzolanic reactions on addition of lime. This was achieved by analysing for increases in acid soluble Al, Si, Mg, Ca and Mn. One disadvantage of the aggressive acid analysis was that for minerals with significant cation exchange capacity, the majority of ions on exchange sites would be replaced predominantly with H^+ ions thereby eliminating, albeit partially, analysis incorporating cation exchange effects. The results of such an analysis on English China Clay and Wyoming Bentonite were illustrated in Tables 5.13 and 5.14 respectively.

Unlike the water-based batch tests, only 1g of material was acid digested. This would result in higher levels of variability between samples due to sampling error. Therefore, to help to illustrate the relevance of changes between samples, the absolute values obtained from acid digestions were represented in Figures 6.5 and 6.6 and not increases in acid soluble fractions relative to the untreated, uncontaminated minerals. In addition, because CaO additions were completely soluble in the acid mixture and the element concentrations were represented in mg per kg of clay, the element concentrations were corrected for the dilution effect due to the addition of lime.

6.3.2 Acid digestion of clay mixes with no added lime

6.3.2.1 Uncontaminated clay mixes

Figure 5.18 illustrated that from 7 days curing to 301 days curing there was an increase in the shear strength of Wyoming Bentonite with no lime or contaminants added. Acid digestion of the uncontaminated sample after 301 days curing (Table 5.16) and the untreated suppliers sample (Table 5.14) revealed material chemical changes due to curing of the compacted sample containing only de-ionised water. The cured sample exhibited reductions in acid soluble Ca, Fe, Si and Mn whilst levels of Al increased. It was possible that the hydration and expansion of the mineral

structure was such that changes in the cation exchange equilibrium occurred slowly with curing time, resulting in the strength increases.

Similarly to the Wyoming Bentonite samples the English China Clay samples with de-ionised water and no added lime (Table 5.15) which were compacted and cured for 301 days had slightly different behaviour on acid digestion than the material provided by the supplier (Table 5.14). It was clear that the sample with no contaminants had similar concentrations of acid soluble Ca, higher concentrations of acid soluble Fe, Si and Mg, and less Al. There were clearly chemical changes taking place for English China Clay samples suggesting that cation exchange suggested for Wyoming Bentonite was not likely. The process which was likely to be responsible is called the 'Gley' process and is discussed in detail in the next section.

6.3.2.2 Contaminated clay mixes

Similar strength increases to those of the uncontaminated samples occurred for the Fe^{3+} and Pb^{2+} ion contaminated Wyoming Bentonite samples with no lime, although the absolute shear strength values of the Fe^{3+} ion contaminated samples were higher than the similar Pb^{2+} ion contaminated samples. The difference in the absolute shear strength values were likely to be due to the flocculated material achieved immediately after mixing compacting to a different degree, as illustrated by Figure 5.4. However, the changes in shear strength with curing time for these samples were likely to be due to chemical changes. It could be argued that these chemical changes would also be affected by the initial compaction and subsequent particle spacing. However, the effects of changes in cation exchange behaviour would be observed after acid digestion because the high concentration of H^+ ions added during acid digestion would displace ions from these sites. The process that could account for the measured changes after acid digestion would be the isomorphous substitution of Ca, Fe, Si and Mn for Al in the Wyoming Bentonite structure.

Relative to the uncontaminated Wyoming Bentonite sample, the Pb^{2+} ion contaminated Wyoming Bentonite sample with no lime released similar levels of acid soluble Ca, Fe, and Mn and more Si, Mg. Furthermore, the Fe^{3+} ion contaminated sample released more acid soluble Ca, Al, and Mn and less Si.

The Pb^{2+} ion contaminated English China Clay sample had similar concentrations of acid soluble Ca and Mg, higher concentrations of Si and lower concentrations of Fe and Al than the uncontaminated English China Clay sample. The

Fe^{3+} ion contaminated sample had similar concentrations of acid soluble Ca and Mg, and lower concentrations of Si, and Al.

It was clear that the different contaminants in the samples induced release of different elements from the mineral structure. A recent paper by Lessovaia (1998) suggested a process called the 'Gley' process to explain this. The process is connected with the change of redox potential of soil via moistening. A material being reduced gains electrons whilst a material being oxidised loses electrons. As a result, the soil physical properties degrade and elements including Fe and Mn are reduced and become mobile, ultimately being removed from the soil. Although neither the acid digestion data nor the batch test data showed increases in Mn content, there were clear increases in mobility of the other elements. The further addition of the positive ions Pb^{2+} and Fe^{3+} and negative NO_3^- into the pore water solution would interact with this process by providing a source of electron acceptors and electron donors respectively. Figure 5.18 illustrated that, similarly to the Wyoming Bentonite, the 'Gley' process was likely to be responsible for strength increases with curing time of the untreated uncontaminated English China Clay samples.

6.3.3 Acid digestion of clay mixes with added lime

6.3.3.1 Uncontaminated clay mixes

The effect of adding lime to the clay mixes was complex. Analysis of the samples in Figures 6.5 and 6.6 revealed that as the percentage lime addition increased linearly, so did the acid soluble Ca fraction and this increase was essentially the same for all contaminated mixes. Back calculation indicated that the Ca concentrations measured related directly to the percentage lime added. This had the important implication that during the aggressive acid digestion process the re-crystallised calcium-aluminate-hydrates and calcium-silicate-hydrates were soluble. On the basis of this argument changes in acid soluble Si and Al release due to addition of lime should have been apparent.

At this stage it is important to remember that the water based batch tests suggested that for English China Clay samples Al was predominantly involved with solidification reactions whilst for Wyoming Bentonite Si was predominantly involved with solidification reactions. Figures 6.5 and 6.6 suggested different behaviour. For all clay-lime mixes the acid soluble Al concentrations were significantly higher than the acid soluble Si fractions. However, as the lime content was increased the acid

digestable concentrations of both Al and Si increased for both minerals which signified that pozzolanic reactions were occuring. This highlighted a very important fact relating to acid digestion data and pH variation in general. Figure 2.12 illustrated that above approximately pH 10 both aluminium oxides and silicon oxides were liable to dissolution whilst below pH 3 aluminium oxides were liable to dissolution and silicon oxides were almost insoluble. It was therefore foreseeable that whilst samples were in conditions of high pH such as those found after lime addition both calcium-aluminate-hydrates and calcium-silicate-hydrates were formed which were more soluble in acid than the original mineral aluminates or silicates.

6.3.3.2 Contaminated clay mixes

It is important to note that for all Wyoming Bentonite-contaminant-lime mixes the acid soluble levels of Na released were essentially constant. This, combined with the fact that soluble Ca levels related well to the percentage lime added, suggested that all ions on cation exchange sites were replaced by H^+ ions during acid digestion.

On addition of 2.5% lime to the Wyoming Bentonite-contaminant mixes, there were small increases in the acid soluble Al levels suggesting that some pozzolanic reactions had taken place. For the uncontaminated sample there was a similar increase in the soluble Si. Significantly for the contaminated samples there were reductions in the levels of acid soluble Si (Figure 6.5). This was contrary to the water based batch chemistry and suggested that a silicon compound was being formed which was less soluble in acid than water. Increasing the lime content of the samples to 7.0% further enhanced the acid soluble Al and Si trends. Furthermore, at this higher lime content less acid soluble Al was produced by the contaminated samples than the uncontaminated sample suggesting that the contaminants did tend to inhibit pozzolanic reactions.

Further to the solidification reactions involving Si and Al it would appear from Figure 6.5 that Mg, Fe and to a lesser extent Mn were also involved in solidification reactions. Interestingly the increases in acid soluble Fe with lime content increased in a similar way as the increases in Mn for the Fe^{3+} ion contaminated sample. The same was also true for the Pb^{2+} ion and uncontaminated samples.

The Wyoming Bentonite-contaminant mixes with 2.5% lime clearly showed a level of pozzolanic activity. However, Figure 5.18 showed that the strength increases at 301 days curing for the Fe^{3+} and Pb^{2+} ion contaminated samples due to the addition

of 2.5% lime were higher than those of the uncontaminated sample. For the Fe^{3+} ion contaminated sample most of the increase happened at 7 days, suggesting that the increase was related to flocculation effects. However, for the Pb^{2+} ion contaminated sample much of the strength increase happened after 7 days, suggesting a solidification reaction.

The acid soluble element trends of the English China Clay-contaminant-lime mixes were similar in nature to those of the Wyoming Bentonite, with the following exceptions:

- There were no high levels of acid soluble Na from the cation exchange sites.
- Although there were quantities of acid soluble Fe present, the levels did not increase with increasing lime content suggesting that Fe sites within the English China Clay were not significantly affected by the high alkaline conditions on addition of lime. Similarly there was no appreciable change in acid soluble concentrations of Mn or Mg.

Furthermore, the acid soluble levels of Si and particularly Al for all samples with or without lime were significantly less than those of the Wyoming Bentonite. Since the same quantity of material was acid digested for both English China Clay and Wyoming Bentonite, it could be argued that this was due to a lower surface area susceptible to dissolution. On this basis similar behaviour would have been expected at high pH resulting in reduced solidification reactions for English China Clay. Clearly this did not occur because there were significant strength increases similar to those of Wyoming Bentonite attributable to pozzolanic reactions. Therefore the quantity of acid soluble Si or Al from untreated clays prior to lime addition cannot be used as a guide to predict successful solidification. However, time-dependent changes in acid soluble elements can be used as an assessment tool for lime-treated clays.

Similarly to the water-soluble chemistry of the batch tests, the acid digestion tests highlight that there were no increases in the acid soluble levels of Al in the Fe^{3+} ion contaminated samples with lime after 301 days curing time. This suggested that there were no solidification reactions taking place.

A further disadvantage of the acid soluble data was that it did not indicate why the Pb^{2+} ion contaminated sample with lime had higher strength gains than the uncontaminated sample with lime. Figure 5.18 indicated that the Pb^{2+} ion contaminated sample with 1.5% lime at 301 days had significantly higher strength than the uncontaminated sample, whilst the acid digestion data suggested that uncontaminated sample produced more calcium-aluminate-hydrates than the Pb^{2+} ion contaminated sample.

It was clear therefore that acid digestion could provide information about the development of the chemistry of samples due to the addition of lime. However due to the different solubility of Si and Al compounds in the highly acid environment, it was difficult to see the changing trends between the clay types. It was also the case that the ability to observe the chemistry relating to precipitation, cation exchange, and the interaction of Ca in the formation of calcium-aluminate-hydrate and calcium-silicate-hydrate was lost by acid digestion. Furthermore, it was difficult to relate the changes in chemistry to observed changes in physical characteristics.

6.3.3.3 Acid soluble constituents of material retained on 63μm sieves after batch tests at 301 days

Time constraints during the testing programme dictated that only the solid residues of batch tests performed at 301 days could be graded. This grading was performed on material not filtered after a batch test. Acid digestion tests were very useful to determine the absolute quantities of elements (particularly metals) present in a graded material. Again due to time constraints it was only possible to determine the constituents of materials retained on 63μm sieves after some of these batch tests at 301 days curing (Table 5.13). Comparison of the English China Clay + 5000ppm Fe + 2.5% lime material retained on a 63μm sieve after the batch test and the material stored in the twin-walled pipe revealed that the material on the 63μm sieve contained approximately three times the quantity of Ca. Therefore, large proportions of the material on the sieve were particles of lime. It was therefore not surprising that levels of the contaminant were also high. This suggested that Fe^{3+} ions precipitated around the lime particle in lime-treated English China Clay mixes. It was also evident that there were significantly elevated levels of acid soluble Si, Mg, Al and Mn around or

incorporated in the particles, which would be consistent with high levels of pozzolanic reactions immediately adjacent to the lime particles.

The particles retained on a 63 μm sieve after tests on Wyoming Bentonite + 5000ppm Fe + 7.0% lime were significantly different. Although the level of Ca in the samples was higher than the general Wyoming Bentonite + 5000ppm Fe + 7.0% lime samples, it was not high enough to be predominantly composed of lime particles. The fact that the acid soluble Na levels in the material were low did not necessarily suggest that the material was not mineral based, since most of the acid soluble Na would have been exchanged by Ca and washed away in the solution on sieving. The particles contained more acid soluble Mn, less Mg and Al, and similar quantities of Fe and Si.

The particles retained on a 63 μm sieve after tests on Wyoming Bentonite + 5000ppm Pb + 7.0% lime were also unusual. Relative to the acid digestion data for the Wyoming Bentonite + 5000ppm Pb + 7.0% lime sample stored in the twin-walled pipes, the material retained on the 63μm sieve contained similar levels of acid soluble Ca, higher levels of Fe, Si, significantly higher levels of Mn, and lower levels of Pb, Na, Mg and Al. It was difficult to suggest what the material was although for both mixes the particles retained on the 63μm sieve were black in colour and granular in nature whilst smaller particulates were grey in colour. Since initial mineral classification determined that all Wyoming Bentonite particles were smaller than 63μm it was likely that the digested particles were agglomerations of a specific particle fraction within the clay containing significant quantities of Mn and Fe.

The significance of these data was in the different materials from the two minerals retained on the same sized sieve and the fact that for English China Clay the contaminant appeared to precipitate around the CaO particles, which in itself was likely to inhibit the development of pozzolanic reactions. Unfortunately data were not available for all samples. Consequently it was difficult to suggest reaction mechanisms. Evidently both acid-based and water-based chemical tests are beneficial so long as the results are interpreted with an appreciation of the differences between the tests.

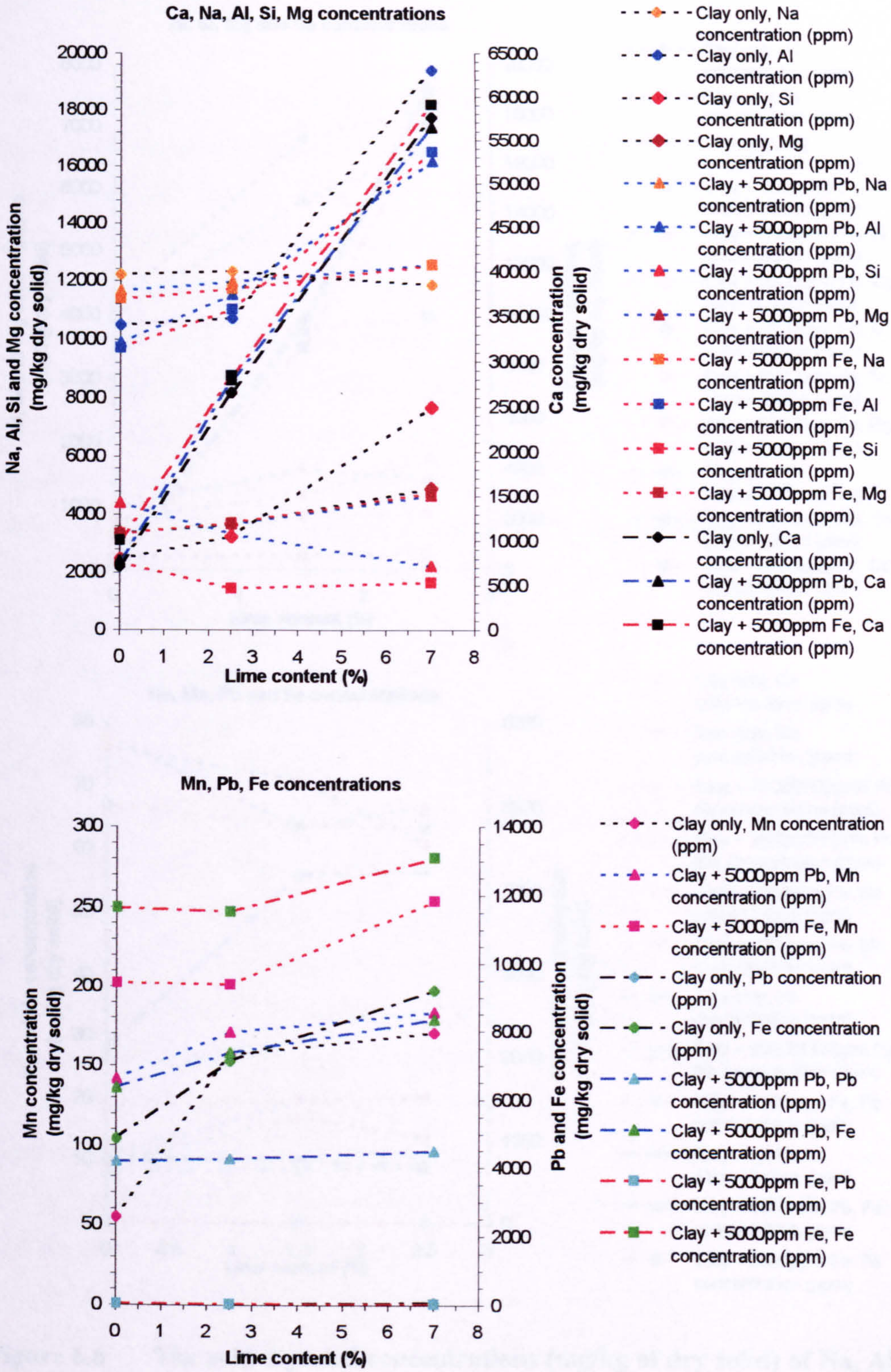

Figure 6.5 **The acid digested concentrations (mg/kg of dry solid) of Na, Al, Fe, Si, Mg, Ca, Pb and Mn in Wyoming Bentonite samples cured for 301 days**

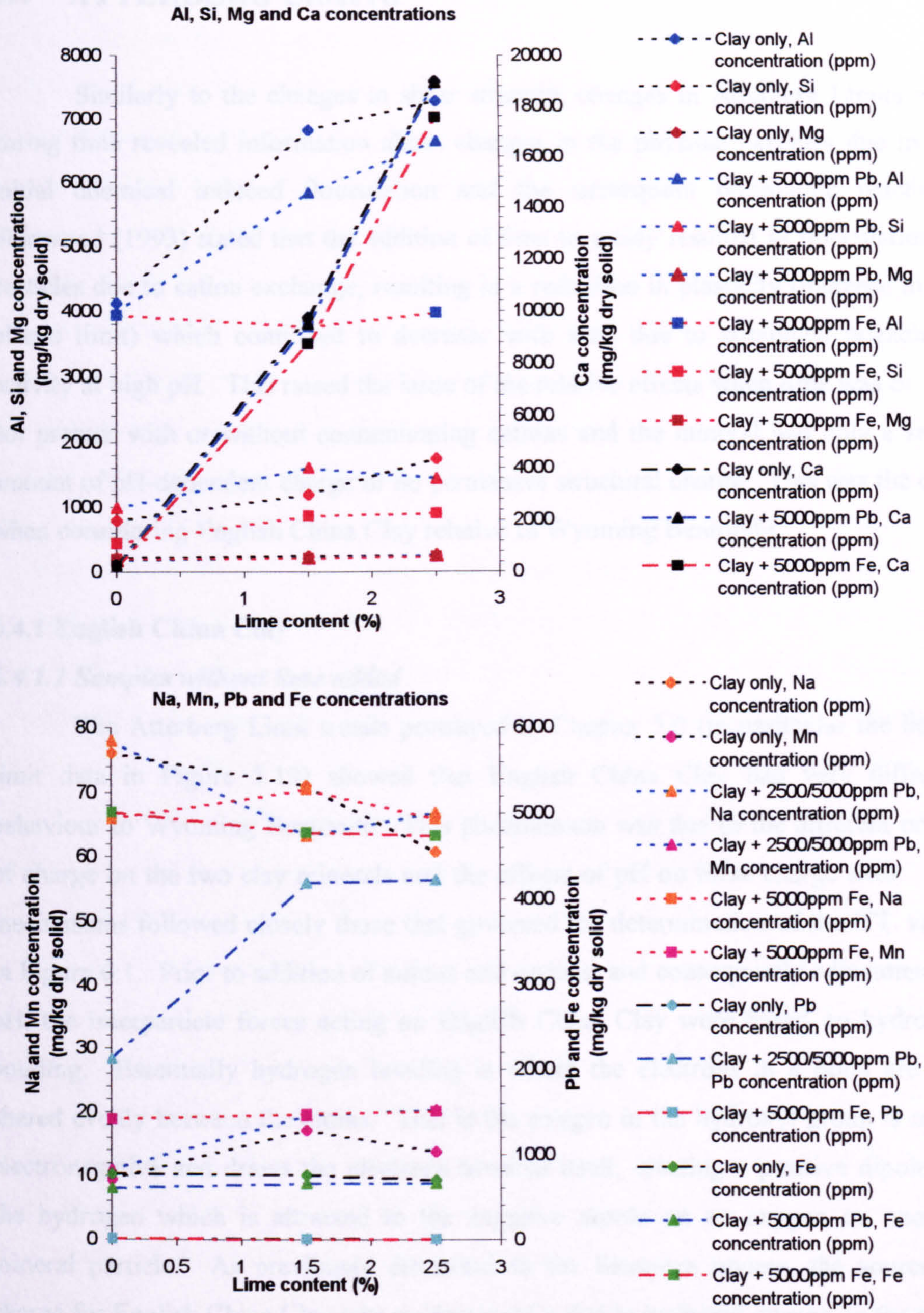

Figure 6.6 **The acid digested concentrations (mg/kg of dry solid) of Na, Al, Fe, Si, Mg, Ca, Pb and Mn in English China clay samples cured for 301 days**

NOTE: Pb CONTAMINATED ENGLISH CHINA CLAY SAMPLES WITH NO ADDED LIME ONLY CONTAINS 2500PPM Pb WHILST ALL OTHER SAMPLES CONTAIN 5000PPM Pb.

6.4 ATTERBERG LIMITS

Similarly to the changes in shear strength, changes in Atterberg Limits with curing time revealed information about changes in the physical particles due to the initial chemical induced flocculation and the subsequent pozzolanic reactions. Sherwood (1993) stated that the addition of lime to a clay resulted in flocculation of particles due to cation exchange, resulting in a reduction in plasticity (increase in the plastic limit) which continued to decrease with time due to continued pozzolanic activity at high pH. This raised the issue of the relative effects when lime was or was not present with or without contaminating cations and the mineral had only a small amount of pH-dependent charge or no permanent structural charge. This was the case when considering English China Clay relative to Wyoming Bentonite.

6.4.1 English China Clay

6.4.1.1 Samples without lime added

The Atterberg Limit trends portrayed in Chapter 5.0 (in particular the liquid limit data in Figure 5.19) showed that English China Clay had very different behaviour to Wyoming Bentonite. This phenomenon was due to the different origin of charge on the two clay minerals and the effects of pH on these charge sites. The mechanisms followed closely those that governed the determination of the ICL value in Figure 6.1. Prior to addition of anions and cations, and consequently adjustment of pH, the interparticle forces acting on English China Clay were based on hydrogen bonding. Essentially hydrogen bonding is where the electrons in a bond are not shared evenly between the atoms. That is the oxygen in the hydroxyl group is more electronegative and draws the electrons towards itself, creating a positive dipole on the hydrogen which is attracted to the negative dipole on an oxygen on another mineral particle. As previously discussed in the literature review, the source of charge for English China Clay was predominantly due to hydroxyl groups on the edge sites that were a source of pH-dependent charge. If the pore water was highly alkaline, the charge on the mineral was negative attracting cations such as H_30^+, Pb^{2+}, Ca^{2+} and Fe^{3+}. If the pore water was highly acidic, the charge on the mineral was positive attracting anions such as NO_3^- and OH^-. Since the pH at which English China Clay has no charge (either positive or negative) was not known, it was difficult to

state categorically the mechanisms occurring on addition of lead nitrate or iron (III) nitrate. End of batch test pH data in Figure 5.11 illustrated that the Fe^{3+} ion contaminated sample remained at a constantly low acidic pH, whilst that of the Pb^{2+} ion contaminated sample and the uncontaminated samples were at a much higher pH and that pH reduced with time. Care must be taken when considering these pH values since in the small pore water volume relative to the batch test volume the pH would be considerably lower and the change in pH more significant. However, the pH of the Fe^{3+} ion contaminated samples was so low that it would have been expected that the charge on the hydroxyl groups of the mineral was positive. If flocculation of the Fe^{3+} ion contaminated sample was occurring the mechanism could be that the positively charged hydroxyl groups were attracted together by sharing of an anion in solution. If this was the mechanism it is necessary to try to determine why the Pb^{2+} ion contaminated sample had a higher plastic limit than the Fe^{3+} ion contaminated sample. An explanation could lie in the fact that the Pb^{2+} ion contaminated sample had a much higher pH than the Fe^{3+} ion contaminated sample. If this pH was above the point of zero charge for the mineral the attraction of the Pb^{2+} ion would have been greater than the attraction of the NO_3^- ion for the Fe^{3+} ion contaminated sample, therefore producing a more highly flocculated material of lower plasticity and consequently higher plastic limit, as illustrated in Figure 5.21. This argument is valid because the Pb^{2+} ion is smaller than the NO_3^- ion and has a higher charge density. However, it was evident that the range of variation in the plastic limits illustrated in Figure 5.21 was only 3 % and, although the contaminated materials had clearly the higher plastic limits, caution must be observed in the interpretation of these results.

Analysis of the liquid limits illustrated in Figure 5.19 showed that the Fe^{3+} ion contaminated sample had the lowest liquid limit and this did not vary with curing time. However, the uncontaminated and Pb^{2+} ion contaminated samples with no lime at 7 days curing had much higher and similar liquid limits to the Fe^{3+} ion contaminated sample respectively. In addition, as the curing period increased the liquid limit of these two mixes reduced towards the liquid limit of the Fe^{3+} ion contaminated sample. Curiously, Figure 5.11 also noted a reduction in the pH of these two samples with time. Figure 5.18 showed that at 7 days curing the Pb^{2+} ion and uncontaminated samples had higher strengths. As previously stated this was in part due to the different levels of achieved compaction illustrated in Figure 5.6. This reduced compactability suggested that the Fe^{3+} ion contaminated sample was

flocculated to a higher degree than the other mixes, contrary to previous charge related arguments. Figure 5.18 also showed that the strength of the uncontaminated sample, and more so the Pb^{2+} ion contaminated sample, increased with curing time, which was not the case for the Fe^{3+} ion contaminated sample. Consideration of all these facts suggested that the liquid limit of samples with no lime present was not simply due to flocculation brought about by the pH-dependent charge. Since the Fe^{3+} ion contaminated sample was so acidic, Figure 2.12 suggests that silicon oxides and more so aluminium oxides will be dissolved. This would not necessarily occur to the same extent at the higher pH of the Pb^{2+} ion and uncontaminated samples. This idea was verified by the soluble Si and Al releases of the samples in Figure 5.14. If this was the case then perhaps even after only 7 days curing the effect was noticeable and the changes in liquid limit, plastic limit and subsequently plasticity index were not solely related to flocculation. With regard to the reductions in liquid limit with time for the Pb^{2+} ion and the uncontaminated sample, perhaps the explanation was related to the pH reduction and the gley effect mentioned previously.

6.4.1.2 Samples with lime added

The behaviour of English China Clay samples with lime was more difficult to understand. The most important point to aid understanding was that the pore water pH was highly alkaline. Furthermore, alkalinity often reduced significantly on addition of a contaminant due to precipitation reactions as well as reducing with time due to mineral dissolution and crystallisation. The importance of the changing pH was due to the position of the pH-dependent point of zero charge and the fact that at high pH the hydroxyl groups on the clay have a negative charge attracting cations. Therefore the mechanisms governing changes in Atterberg limits were:

- pH-variable charge on the mineral edge sites which, when alkaline, attracted cations, which in turn were attracted to the slight negative dipole on the oxygen of other mineral particles as well as the nitrate anions and hydroxide ions.
- Precipitation of the metal hydroxide which could bind particles together and limit the lime interaction with the mineral by coating particles.
- Contaminants could inhibit or improve the development of time-dependent pozzolanic reactions.

Since the pH of all English China Clay samples with lime was very high, between approximately pH 11.0 to pH 12.6 (from batch tests Figure 5.11), it was clear that charge sites on the hydroxyl groups would have been positive, although the mixes at the lower pH would have a slightly lower quantity of positively charged sites.

Figure 5.21 and 5.19 illustrated that in the case of English China Clay mixes there were increases in both plastic limit and liquid limit due to the addition of lime. The changes in plastic limit with time were small in magnitude and unclear. Clearly the addition of lime caused flocculation in all cases, and yet the Pb^{2+} ion contaminated samples had higher plastic limits than the Fe^{3+} ion contaminated samples. This was attributed firstly to the fact that, since English China Clay had such a low cation exchange capacity, there were more Fe^{3+} compounds precipitated than Pb^{2+} compounds, and consequently the Fe^{3+} ion contaminated samples were likely to be bound together better by hydrated precipitates. If this was the only mechanism responsible, the Fe^{3+} and Pb^{2+} ion contaminated samples would have been expected to have lower plastic limits than the uncontaminated sample and the Fe^{3+} ion contaminated sample to have had the highest liquid limit. Consequently there must also be a link with chemical reactions involving the clay mineral. It had been previously suggested that the Fe^{3+} ion contamination inhibited the dissolution of the English China Clay mineral, whilst the Pb^{2+} ion contamination appeared to aid dissolution and re-crystallisation and resulted in more rapid strength increases on addition of lime than the uncontaminated sample. This rate increase in the pozzolanic reactions due to the addition of Pb^{2+} ions was likely therefore to explain the very low plastic limit and high liquid limit of the Pb^{2+} ion contaminated samples.

The liquid limits of the Pb^{2+} ion and uncontaminated English China Clay with lime samples reduced with curing time whilst the liquid limit of the Fe^{3+} ion contaminated sample with lime did not. This was attributed to the fact that for the lime-treated samples containing Fe^{3+} ion contamination there were essentially no pozzolanic reactions since little mineral dissolution in the form of Al and/or Si, or reductions in pH or conductivity, was detected in the leachates of the batch tests. Figure 5.19 also illustrated that as the lime content of the Fe^{3+} ion contaminated mixes increased the liquid limit increased linearly with very little change with curing time relative to the other mixes. Since pozzolanic reactions were not responsible for the increases with increased lime content, the increase must have been related to

increased flocculation. Further evidence for this behaviour lay in the fact that the pH of Fe^{3+} ion contaminated sample was lower than the other samples due to higher levels of precipitation. Therefore increasing the pH would increase the number of negatively charged hydroxyl sites and therefore, when Ca^{2+} ions interacted with these sites more flocculation would occur. However, the Pb^{2+} ion contaminated and uncontaminated mixes in Figure 5.19 did not show the same linear increase in liquid limit with increasing lime content. The reductions in liquid limit with time must therefore be associated with the pozzolanic reactions. Indeed the reduced pH and soluble Ca content due to crystallisation processes found in the batch test data for these samples would also result in the reduced level of flocculation observed in Figure 5.19.

The effects of lime and contaminants on the liquid limits and plastic limits of English China Clay were therefore summarised in Figure 5.22. For Fe^{3+} ion contaminated English China Clay samples, as the lime content was increased there was a linear increase in the plasticity index. For the Pb^{2+} ion and uncontaminated mixes the behaviour was different. At 7 days curing as lime content was increased the plasticity index tended to increase. However, as curing time was increased, increasing the lime content resulted in a decrease in the plasticity index, particularly for the Pb^{2+} ion contaminated sample.

6.4.2 Wyoming Bentonite

The Atterberg Limits behaviour of Wyoming Bentonite samples were easier to explain than the English China Clay samples due to the fact that the majority of cation exchange capacity was due to permanent mineral structural charge, and not pH-dependent charge, and this permanent charge dominated physico-chemical developments.

6.4.2.1 Samples without lime added

Similarly to the English China Clay samples with no lime the differences in plastic limit due to the addition of contaminants was only small, up to 5% water content (Figure 5.21). However, Figure 5.19 illustrated that the variation in liquid limit due to contaminant addition was large, up to a water content of 300%. Clearly ionic contaminants had a very large effect on the liquid limit of Wyoming Bentonite and therefore inherently mineral structure orientation. The effects on the mineral

structure appeared to be related to flocculation, with the higher valency ions having the larger effect on the diffuse double layer. This was consistent with the Lyotropic series and the fact that there were also more Fe^{3+} ions present. Figure 5.19 did however suggest large fluctuations in the liquid limit of uncontaminated Wyoming Bentonite with no lime added. Although there were likely to be some chemical changes with time purely due to the addition of water it was not expected that these changes could cause such large fluctuations. Indeed the Wyoming Bentonite supplier's data stated a liquid limit in the range 400% to 600% due to the difficulties in measuring the liquid limit of untreated Na Wyoming Bentonite. Discussion with the supplier confirmed that the data in Figure 5.19 were not unexpected. However on addition of ions with a higher ionic potential the liquid limit test was far easier to perform and the results were repeatable.

Figure 5.19 showed that for the Pb^{2+} ion contaminated sample the liquid limit reduced as curing time was increased. This time-dependent change indicated a chemical reaction with time. There were two mechanisms that could have been partially responsible for the change.

- Although ICP data were not available to confirm the theory it was felt that because the ionic potential of Pb^{2+} ions was only slightly higher than that of Na^{+} ions, initially a relatively high degree of cation exchange occurred which resulted in some flocculation. As curing time progressed, further cation exchange occurred due to disorder and entropy considerations. This would not be expected for the Fe^{3+} ion contaminated sample, since Fe^{3+} ions have an ionic potential far higher than that of Na^{+} ions and Fe^{3+} ions were present in higher concentrations. This could have also explained why the phenomena occurred for the Pb^{2+} ion contaminated sample with a lime content (2.5%) well below the ICL of Wyoming Bentonite.
- The acid soluble data in Figure 6.1 showed that for samples with no lime present there were higher concentrations of soluble Si present in the Pb^{2+} ion contaminated sample with no lime relative to the other similar Fe^{3+} ion contaminated and uncontaminated samples. This suggests that Pb^{2+} ions were interacting with the mineral particularly at the sites of the clay adjacent to silicates possibly in turn suggesting that lead-silicate

compounds were being produced with time and thus increasing bonding between particles.

6.4.2.2 Samples with lime added

On addition of lime to Wyoming Bentonite the material became far more workable and the Atterberg Limit tests became easier to perform. The liquid limit continued to reduce and converge on a constant value for all mixes, whether uncontaminated or contaminated with Pb^{2+} or Fe^{3+} ions (Figure 5.19). It was clear however that the Fe^{3+} ion contaminated sample converged on this value on addition of only 2.5% lime. This effect was directly linked to cation exchange and flocculation due to ionic interactions with the charge sites on Wyoming Bentonite. This suggested that essentially the ions present with an ionic potential greater than that of Na^{+} ions would cause flocculation to occur until all Na^{+} ions were exchanged, resulting in the liquid limit converging. However, the plastic limit plot in Figure 5.21 showed that on addition of lime the plasticity of all samples continued to increase almost linearly with lime content with no apparent convergence. Combining the effect of both liquid limit and plastic limit in the plasticity index illustrated in Figure 5.22 revealed that the addition of lime produced a reduction in plasticity index which was almost linearly proportional to increasing lime content. It was also evident that the presence of ions with a higher ionic potential reduced the gradient of the plot. This did of course neglect the concentration factor regarding the increased quantity of Fe^{3+} ion contamination present relative to Pb^{2+} ion contamination.

6.4.3 Interpretation of Atterberg Limits

The above discussions raised the issue of the practical use of the Atterberg Limit tests in their current form for assessing a material under varying chemical conditions. As with all testing protocols, interpretation of the results must be considered with an understanding of the fundamental concepts upon which the tests are founded. This will be discussed below.

The liquid limit test relates to the water content required for a cone to penetrate a material by a pre-determined amount due to the input of a constant amount of energy. For the cone to penetrate it must overcome the material interparticle frictional forces causing both lateral and vertical particle movements, a process associated with the shearing action of the particles. Similarly the plastic limit relates

to the lowest water content that is able to retain sufficient suction to avoid cracking once a material has been rolled to specified dimensions. For both the tests the clear common factors are achieving shearing at unknown water contents due to predetermined methods of inducing shear, factors more usually associated with the rheology of a material and frequently assessed in sprayed concrete applications for the purposes of determining material workability. This is an interesting concept because it is not dissimilar to lime-treated clay minerals and the requirement to achieve a level of durability. On this basis the tests indicate changes in the physico-chemistry of a material associated with the interaction of water.

Particularly for the liquid limit test, the issue was related to the practical value in determining the water content to achieve a specific penetration when it was the change in water interaction over a range of water contents with the material which was of interest. It was more appropriate to interpret the variation in penetration ('shearing') over a range of moisture contents to understand the physico-chemical changes. Figure 5.20 achieved this by plotting the gradient of the linear portion of the standard liquid limit plot (% water content / mm penetration) against changing chemical conditions (lime content).

Figure 5.20 illustrated for Wyoming Bentonite that the trends associated with the '% water content / mm penetration' and lime content were consistent with the trends of liquid limit and lime content. This implied that the addition of highly charged ions primarily affected the way in which water interacted with the mineral charge sites. This was observed by the fact that less water was required to achieve the same physical penetration characteristics as lime was added. However, for English China Clay the trends associated with the '% water content / mm penetration' and lime content were not consistent with the trends of liquid limit and lime content. Limited change was observed in the '% water content / mm penetration' against lime plot whilst increases were seen in the liquid limit on addition of lime. Due to the very small pH-dependent charge it would not have been expected that the addition of ions would significantly affect how water interacted with the mineral. However, it was noted that the liquid limit increased on addition of lime to the English China Clay without an appreciable change in the '% water content / mm penetration' relationship, and reduced on addition of lime to Wyoming Bentonite and with a change in '% water content / mm penetration' (Figures 6.7 and 6.8). The reason for this was considered to be associated with the different type and location of charge sites and how these

affect particle orientation, and consequently how water can be physically present within these particle orientations.

On addition of lime to Wyoming Bentonite, the permanent charge sites had a more prominent effect than the surface pH-dependent charge sites (Figure 6.3). However, it should still be recognised that the pH-sensitive charge sites did still generate a small negative charge thereby attracting positively charged species. The c-axis spacing limited the amount of water that could physically fit into the space between attracted particles. This resulted in a 'soup' of flocculated particles of reduced plasticity in water with a net reduction in the interaction of water with the mineral structure. It was clear that the plasticity of the material would affect the liquid limit due to the way in which the liquid limit was measured, hence the two properties were not mutually exclusive.

On addition of lime to English China Clay only surface pH-dependent charge sites could immediately interact with the chemicals. Prior to lime addition these sites were utilised in hydrogen bonds, bonding the particles together (Figure 6.3). On addition of lime the OH^- ion was attracted to the $X\text{-}OH^{\delta+}$ (where X is the mineral structure; see Equation 2.3). This resulted in a breakdown of the mineral to mineral hydrogen bonds and produced a net negative charge on the hydroxyl groups. This in turn attracted dissociated Ca^{2+} ions along with its associated water. Therefore the net result of lime addition in the short-term was to reduce interparticle hydrogen bonding and attract Ca^{2+} ions and water into spaces between particles. Hence the English China Clay mineral structure could accommodate more water with its structure. In a similar way to the hydrogen bonding the presence of Ca^{2+} ions on the hydroxyl group could attract the electronegative oxygen on another mineral molecule. The resultant effect was a material of reduced plasticity but with the ability to retain more water within its structure.

It was clear from Figure 6.7 that lime interaction with clays of limited structural charge resulted in an increase in liquid limit, but the ratio of the water content to penetration did not change appreciably. However, it was clear from Figure 6.8 that lime interaction with clays of high structural charge resulted in an increase in liquid limit in the same way as a clay with low structural charge but also that the ratio of the water content to penetration reduced appreciably.

The ideas relating to Atterberg Limits above are hypothetical, but could help formulate a research project to develop a simple index test which could be used to measure associations between physical and chemical behavioural characteristics.

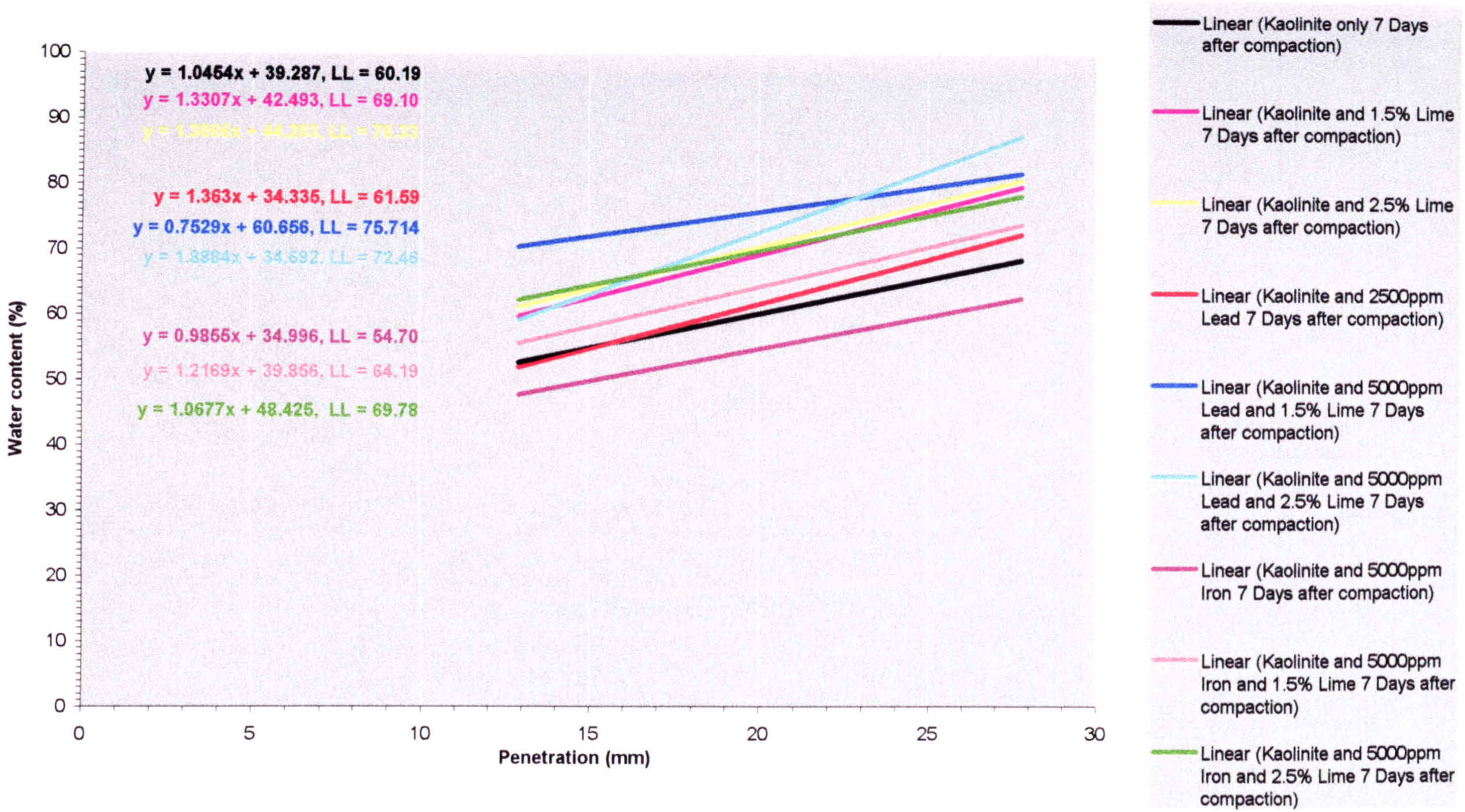

Figure 6.7 Variation of liquid limits of English China Clay on addition of cations 1 week after mixing

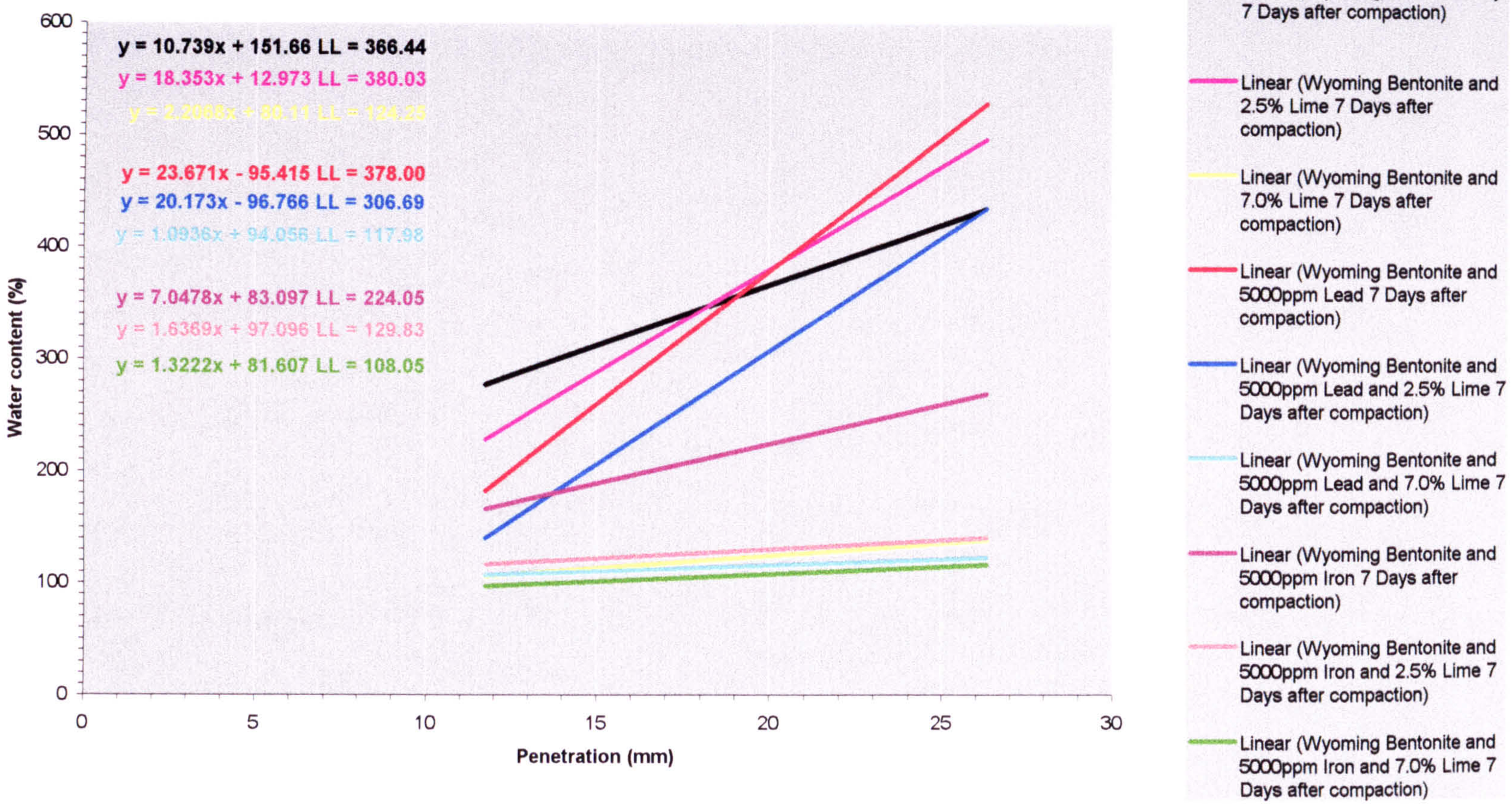

Figure 6.8 Variation of liquid limits of Wyoming Bentonite on addition of cations 1 week after mixing

CHAPTER 7.0

7.0 CONCLUSIONS

In Chapter 6 the results from the laboratory investigations were discussed. This discussion highlighted the physico-chemical relationships of clay-contaminant-lime mixes. This chapter will present the main significant conclusions of that discussion and on the basis of those conclusions proposals for further research will be recommended.

7.1 BATCH TEST DEVELOPMENT

The development of the chemical batch extraction test with de-ionised water as the leachant proved to be very successful for monitoring the clay-contaminant-lime interactions with time. However, to have confidence in the meaning of the results it was important to assess the effects on the chemistry due to adjustment of the operating parameters of the tests. The following batch test parameters had no appreciable effect on the leached concentrations of elements from the tested clay-contaminant-lime mixes:

- changing the initial cube size from 10mm to 20mm, and
- increasing test rotation speed from 30rpm to 60rpm.

Although test duration and solid to liquid ratio had an effect on the measured element concentrations in solution, so long as the tests operating with the same parameters were compared, the chemical trends remained the same. This was significant because from the perspective of regulatory control the absolute concentration value was important, whilst from the perspective of determining controlling mechanisms, relative changes were important. The effect of increasing the test duration from 6 hours to 24 hours was to move the closed chemical system closer towards a specific equilibrium condition. In the chemical extraction test, apart from pH, the solid to liquid ratio had the largest effect on the concentrations because it changed the final equilibrium condition. The changes highlighted were:

- for solutions not saturated with any particular element, doubling the solid to liquid ratio doubled element concentrations, and

- for solutions close to saturation with a particular element such as Ca, doubling the solid to liquid ratio significantly increased the concentration of that element (Ca) as well as often increasing the concentration of other elements. However, in some cases the solubility of other species reduced.

These trends were particularly relevant to lime-treated materials. Immediately after mixing clay and lime the soluble Ca concentrations saturated solutions, whilst after a significant curing period the soluble Ca had reduced via re-crystallisation processes to a level where solutions were not necessarily saturated. Therefore, it was important to consider curing time and solid to liquid ratio together. To prevent the generation of a saturated solution during batch tests, reducing the solid to liquid ratio was an option. However, the consequence of this was to reduce the soluble concentration of some elements including Si and Al to below analysis detection limits. In addition, too much dilution could have reduced the solution pH to the point where more contaminants were soluble, which would not have been representative of the compacted samples. Since all the batch tests performed revealed the same chemical changes and the fundamental mechanisms of clay-contaminant-lime interactions were important, the most economical test was recommended as the 6 hour / 30rpm test with a 1:20 solid to liquid ratio and a 20mm initial cube size.

7.2 LIME CLAY REACTION MECHANISMS

The two clays with significantly different quantities of structural charge, English China Clay (predominantly kaolinite) and Wyoming Bentonite (predominantly sodium-montmorillonite), behaved completely differently in both the modification and subsequent solidification phases after the addition of lime. During the initial modification reactions the interaction mechanisms of the lime with the minerals were as follows:

- **English China Clay**
  - After 7 days curing the solid CaO hydrated, releasing both Ca^{2+} cations and OH^- anions into the pore water of the compacted clay mixture. This was evident in the batch tests at 7 days due to the high solution pH and soluble Ca concentrations, which resulted in high solution conductivity. The very low soluble concentrations of either Si or Al in the batch test solutions indicated that no mineral dissolution had occurred, hence pozzolanic reactions had not yet begun.
  - The high pore water pH generated by the OH^- ions interacted with the hydroxyl groups on the clay structure generating pH dependent negative charge on the mineral at these sites. These negative sites, which were previously involved in hydrogen bonding with other mineral sheets, consequently attracted Ca^{2+} ions in the pore water solution. The result of this chemical interaction was particle flocculation and consequently increases in the undrained shear strength, plastic limit and the liquid limit of the material.
  - Addition of lime above the ICL value was of little benefit as it resulted in no improvement in the shear strength or plastic limit, and only with a marginal increase in the liquid limit.

- **Wyoming Bentonite**
  - After 7 days curing it was evident from the low soluble Ca concentration and high soluble Na concentration in the batch test solution that the Ca^{2+} cations from the lime had exchanged for Na^+ ions on the Wyoming Bentonite permanent negative charge sites. Similarly to English China Clay, the very low soluble concentrations of either Si or Al in the batch test solutions indicated that no mineral dissolution had occurred.
  - The resultant effect of the cation exchange reaction was flocculation of the mineral particles, and consequently a reduction in the plastic limit of the material and an increase in undrained shear strength.
  - In contrast to English China Clay, the result of flocculation was a reduction in the liquid limit. This was due to the higher ionic potential of the Ca^{2+} ions relative to the Na^+ ions reducing the c-axis spacing, thereby reducing the

potential for the material to retain, and consequently swell on the addition of water.

- The addition of lime below the ICL was found to be beneficial as it resulted in an increase in the undrained shear strength and a reduction in plasticity. These changes were marginal compared to the samples with the ICL value of lime addition.

The longer-term solidification developments of the two clays due to the addition of lime were identified as being due to the following mechanisms:

- **English China Clay**
  - After 175 days and 301 days curing the batch test solutions exhibited small reductions in pH and large reductions in conductivity relative to the samples cured for 7 days. The reduction in conductivity was attributable to reductions in soluble Ca concentrations in the clay pore water.
  - The reduction in Ca concentration was accompanied by a large increase in the soluble Al concentration although there was no Si present in solution. This indicated that the high pore water pH had initiated dissolution of Al from the mineral but not Si. The reduction in the soluble Ca concentration was a result of re-crystallisation of calcium-aluminate-hydrates.
  - The Al was dissolved from the mineral and not Si because of the location of the pH-dependent charge sites. These sites are located adjacent to sources of Al. Hence since the Ca^{2+} ions were attracted to the pH-dependent negative charge generated by the OH^- ions and the hydroxyl groups, all the components for pozzolanic reactions were present.
  - Associated with the above chemical interactions were large increases in the undrained shear strength of the material, reductions in the liquid limit and marginal reductions in the plastic limit.
  - Acid digestion data at 301 days curing illustrated that samples containing lime released significantly more Al than samples with no lime confirming that pozzolanic reactions were occurring.

- **Wyoming Bentonite**
  - Similarly to English China clay, after 175 days and 301 days curing, the batch test solutions exhibited reductions in both pH and conductivity. In contrast to English China Clay there were large reductions in the concentrations of both Ca and Na in the batch test solutions.
  - The reduction in Ca concentration was accompanied by a large increase in the soluble Si concentration and a moderate increase in the Al concentration in solution. This indicated that the high pore water pH had initiated dissolution of predominantly Si from the mineral. The reduction in the soluble Ca concentration was a result of re-crystallisation of calcium-silicate-hydrates. The predominance of calcium-silicate-hydrates was due to the mineral containing more Si and the fact that dissolution would have occurred near the cation exchange sites, the same location as the Ca^{2+} ions and the source of Si.
  - The above pozzolanic reactions were accompanied by increases in strength for the 2.5% and 7.0% lime content although, no change was observed in liquid or plastic limits.

7.3 STABILISATION/SOLIDIFICATION OF CONTAMINANTS

7.3.1 Stabilisation/solidification of contaminants

Stabilisation in the short-term of the Pb^{2+} and Fe^{3+} ion contaminated samples due to the addition of lime was controlled by the following processes:

- **English China Clay**
  - On addition of lime to the contaminated clay samples the high pH environment resulted in the contaminants being removed from the aqueous phase by precipitation of the ions as solid hydroxides. Due to the development of only small quantities of pH-dependent negative charge only a small proportion of each contaminant would be present on these sites.
  - At 7 days curing the batch test chemistry for the Pb^{2+} and Fe^{3+} ion contaminated samples was the same as the uncontaminated mix, showing no indication of pozzolanic reactions. There was also no contamination present in the aqueous phase.

- At 1.5% lime addition and 7 days curing the uncontaminated sample was stronger than the Fe^{3+} ion contaminated sample, which illustrated that the Fe^{3+} ions had a negative influence on the chemical improvements of the mineral. In contrast the Pb^{2+} ion contaminated sample with 1.5% lime was stronger than the respective uncontaminated sample, which illustrated that Pb^{2+} ions had a positive influence on the chemical improvements of the mineral.
- Increasing the lime content above the ICL requirement for the uncontaminated sample significantly improved the strength properties of both the contaminated samples.

- **Wyoming Bentonite**
  - Stabilisation of contaminants on Wyoming Bentonite was the product of cation exchange of the Pb^{2+} and Fe^{3+} ion contaminants for Na^{+} ions and the precipitation of the contaminant hydroxides at high pH due to the addition of lime. The cation exchange was evident by the high soluble Na concentrations in the batch test solutions from all the mixes.
  - Similarly to the English China Clay samples, the batch test data confirmed that there was no pozzolanic activity at 7 days curing.
  - Associated with the above attenuation reactions there were increases in shear strength which were attributed to flocculation of mineral particles. At 2.5% lime addition both the Pb^{2+} and Fe^{3+} ion contaminated samples had a higher shear strength than the uncontaminated samples, clearly a result of increased flocculation. However, at 7% lime addition all samples had similar strengths due to the saturation of the pore water solution with Ca^{2+} ions.
  - The plasticity of all samples reduced similarly. However as the concentration of ions in solution increased, the liquid limit reduced tending towards one specific value. This was associated with the increased flocculation due to the presence of contaminants reducing the c-axis spacing, and hence the ability of Wyoming Bentonite to swell on addition of water.

In the longer term the contaminants had significantly different effects on the solidification reactions:

- **English China Clay**
  - As the curing time increased from 7 days to 175 days to 301 days the batch test solution conductivity of the Pb^{2+} ion contaminated samples with either 1.5% or 2.5% lime reduced in a similar manner as the uncontaminated samples, with an associated reduction in the soluble Ca concentration. However, there was almost twice the concentration of soluble Al released from the Pb^{2+} ion contaminated sample suggesting that Pb^{2+} ions were aiding mineral Al dissolution.
  - Associated with the above chemical reactions were significant increases in undrained shear strength and reductions in the liquid limit, in a similar way to the uncontaminated sample. However, at 1.5% lime addition the Pb^{2+} ion contaminated sample had a significantly higher undrained shear strength than the uncontaminated sample with the same lime addition.
  - At 175 days and 301 days curing, the Fe^{3+} ion contaminated sample exhibited no reduction in soluble Ca concentrations. At the ICL value (1.5%) no appreciable Si or Al was water soluble and there were no changes with time. Associated with these chemical changes were small increases in undrained shear strength. However, above the ICL value high quantities of water soluble Si was produced at 7 days but there was no observed change with time. However, strength increased moderately. This suggested that Fe^{3+} ions were inhibiting the solidification process at two stages. The first stage was during the mineral dissolution and the second stage was due to Fe^{3+} ions, and not Ca^{2+} ions, reacting to form cementitious gels and thereby creating a material with lower undrained shear strength.

- **Wyoming Bentonite**
  - At 175 days and 301 days curing for all mixes at the ICL lime content the soluble Ca concentrations reduced to almost zero concentration and soluble Na concentrations reduced significantly, whilst soluble Si concentrations increased together with smaller increases in soluble Al concentrations. This resulted in a significant reduction in solution conductivity and a small reduction in pH. Associated with these processes

there were large increases in undrained shear strength for all clay-contaminant mixes at the ICL lime content. This suggested that the contaminant present neither impeded nor improved the dissolution or re-crystallisation processes.

- At lime contents below the ICL lime content (2.5%), and particularly at 175 and 301 days curing, the contaminated samples exhibited higher undrained shear strengths than the uncontaminated samples. Although elemental analyses were not available, there were very small reductions in solution pH and conductivity suggesting that there was a small amount of solidification occurring. However, the significant strength increases of these samples suggested that flocculation processes over a longer curing period were predominantly responsible.

7.4 FUTURE WORK

7.4.1 Author's comments

The development of pozzolanic reactions appeared to relate directly to reductions in hydroxide ions, which could be monitored by a pH probe, and large reductions in Ca^{2+} ions that correlated clearly to large reductions in batch test solution conductivity measured by a conductivity probe. Therefore, an ideal, but cheap and simple, test to monitor stabilisation and solidification reactions *in situ* is via long-term pH and conductivity measurements of the material in de-ionised water. Furthermore, it was apparent that physical developments could be associated with the fundamental chemistry of the stabilisation and solidification reactions. Essentially the behaviour of the mineral charge sites governed changes in physical properties in the short-term. In the longer-term it was hypothesised that the location of these charge sites and their behaviour relative to the OH^- ion governed where dissolution of the mineral was initiated.

The batch test data indicated that contaminants were successfully removed from solution so long as the pH remained high. In a carefully engineered environment the pH would remain high and metals which precipitate at this high pH would remain in the solid phase. The success of the process would necessarily be soil specific since different contaminants reacted in different ways with the clay-lime mixes. Nevertheless, the technique could prove to be of considerable practical

benefit. One limitation of the batch test is that it does not provide much information about how contaminants interact with pozzolanic reaction products or the re-crystallisation process. To understand this aspect of the lime reaction more clearly a future study of cementitious solidification products is required using x-ray diffraction techniques.

7.4.2 Proposals for future research

Many important conclusions about the selective dissolution of minerals on the addition of lime were made on the basis of the results from the water soluble batch tests. Furthermore, the suggested mechanisms relating to the effects of contaminants on these processes were also based on data from the batch tests. Therefore, it is important to assess the applicability of this batch test to 'real' soils having mixed mineralogy and particularly the effects that humic substances have on the reactions due to lime addition, and hence the results of the batch test. Based upon these foundations a database on the effects of various contaminants on the lime reaction of 'real' soils should be developed with the philosophy of not simply measuring leachability, but understanding their interactions with the fabric of the soil and therefore allowing a degree of predictability. It would then be possible to develop the batch test further into a simple test for use *in situ* whereby only simple pH and conductivity measurements would be required to assess the development of the stabilisation and solidification reactions. This has clear implications as to the appropriateness of current regulatory leach testing strategies world-wide and highlights the fact that an engineering approach needs to be developed. On the basis that acid based leaching tests 'destroy' the mechanisms which make stabilisation and solidification viable for contaminated sites, these tests are not appropriate for risk assessment purposes on the basis of achieving a specific regulatory value. They are useful in studying the development of stabilisation and solidification reactions when interpreted with an understanding of the reaction mechanisms.

Clearly the adsorption of problem contaminants onto exchange sites is an important factor which will increase the applicability of the process to problem remediation sites. This is particularly relevant to mixed organic and inorganic contaminated sites where organic contaminants can severely inhibit the potential benefits of lime addition. It is therefore imperative to assess and develop low cost adsorbents for both organic and inorganic contaminants. The difficulty lies in the

sheer number of organic contaminants and assessing the most prolific species on contaminated sites. On this basis it would be beneficial to construct a database of contaminants present on contaminated sites within the UK and Europe as well as identification of the chemical nature of the soil within which the contaminants lie. This is occurring slowly within the research community, although research approaches to date have not been sufficiently thorough to be of benefit to the general research community. There is also a clear need to have specific sites available to the research community with the support of the Environment Agency where developing remediation techniques can be assessed in a natural environment without excessive overheads.

7.5 SUMMARY

Development of the batch leaching test demonstrated that changing the operational parameters had no effects on the observed chemical *trends* associated with the time-dependent stabilisation and solidification reactions brought about by the addition of lime to clay minerals. It was also shown that successful solidification could be monitored using simple conductivity measurements without the need for expensive, complex elemental analysis.

The batch test highlighted that Pb^{2+} ion and Fe^{3+} ion contamination specifically, could be stabilised in the short-term and the longer term. This stabilisation and solidification process was attributed to a combination of natural attenuation and precipitation in the short-term and additionally incorporation into recrystalised silicate and aluminate hydrates in the longer-term.

The chemical reaction processes due to the addition of lime were found to be different for the two clay minerals. Furthermore there was a clear difference between the short-term reactions and the longer-term reactions. English China Clay and Wyoming Bentonite pozzolanic reactions were based on Al and Si dissolution from the respective mineral. This dissolution was only detectable in the longer-term suggesting that the short-term undrained shear strength increases and changes in Atterberg Limits were associated with ion exchange effects alone. Large increases in undrained shear strength were associated with increases in soluble Si and Al and reductions in soluble Ca, the result of solidification.

The difference between the dissolution of Si and Al from the two clay minerals had a significant impact on re-crystallisation. Pb^{2+} ions were found to enhance solidification by enhancing dissolution of Al from English China Clay, whilst Fe^{3+} ions were found to have inhibitive effects preventing interaction of Ca^{2+} ions in the formation of calcium aluminate hydrates. On re-crystallisation, the Pb^{2+} ion contaminated English China Clay samples had higher undrained shear strengths than the uncontaminated samples whilst the Fe^{3+} ion contaminated English China Clay samples had lower undrained shear strengths than the uncontaminated samples. Contaminants were found to have no appreciable influence on Wyoming Bentonite re-crystallisation.

Natural attenuation can reduce the leachability of ionic contaminants. However, the attenuation process is reversible in both the short term and the long term. Incorporation of precipitated contaminants into a stabilised matrix and incorporation of contaminant-silicate hydrates and contaminant-aluminate hydrates into this matrix reduces the longer-term contaminant mobility. Lime stabilisation is an effective remediation technique for ionic contamination when applied in an engineered environment. Furthermore, the simple batch test that was developed proved to be of considerable benefit in monitoring the success or failure of the process.

REFERENCES

ADAMS, F. 1984. Soil acidity and liming. Second Edition. Madison, WI, American Society of Agronomy.

ADRIANO, D. C. 1986. Trace elements in the terrestrial environment. Springer-Verlag, New York, USA.

AFNOR-Agence Francais de Normalisation, 1988. Dechets: Essai de Lixivitation X31-210, Paris, France.

ALTHER, G., EVANS, J. C., FANG, H-Y, & WITMER, K. 1985. Influence of inorganic permeants upon the permeability of Bentonite. *In*: JOHNSON, A. I., FROBEL, R. K., CAVALLI, N. J., & PETERSON, C. B. (eds*). Hydraulic Barriers in Soil and Rock.* ASTM STP 874. Philadelphia: American Society for Testing and Materials.

ANDERSON, W. C. (ed), 1994. Stabilization/solidification, American Academy of Environmental Engineers, Annapolis, MD,USA.

ANSON, R. W. W., & HAWKINS, A. B. 1998. The effect of calcium ions in pore water on the residual shear strength of kaolinite and sodium montmorillonite. *Géotechnique*, **48**, No.6, pp.787 - 800.

AGENCE NATIONALE POUR LA RECUPERATION ET L'ELIMINATION DES DECHETS (ANRED), 1988. Evaluation of solidification/stabilization processes. Département Industrie, France, RG/BP/MF8/0TAN/1.

ARNOLD, P. W. 1978, Surface-electrolyte interactions. In Greenland, D. J. and Hayes, M. H. B. (eds), The Chemistry of Soil Constituents, John Wiley, Chichester, UK,pp. 355-404.

ARMAN A., & MUNFAKH, G. A. 1970. Stabilization of organic soils with lime. Louisiana State University, Baton Rouge, USA, Engineering Research Bulletin 103.

ASTM, 1979. Proposed method for leaching for waste materials. 1979 Annual Book of ASTM Standards, Part 31 D3987 (water). American Society for Testing and Materials.

ASTM, 1988. Standard test method for shake extraction of solid waste with water. American society of testing and materials, D3987-85.

ASTM, 1991. Standard method for sequential batch extraction of waste with water, ASTM D4793-88. American society of testing and materials.

AKHTER, H., BUTLER, L. G., BRANZ, S., CARTLEDGE, F. K., & TITTLEBAUM, M. E. 1990. Immobilization of As, Cd, Cr, and Pb-containing soils by using cement or pozzolanic fixing agents. Journal of Hazardous Materials, **24**, pp. 145-155.

BACHY. 1995. Company promotional video, Bachy, UK.

BARNETT, S. 1998. Environmental requirements and consequences related to the closing of United States military bases in Europe. *In*: *Proceedings of the Fourth International Symposium and Exhibition on Environmental Contamination in Central and Eastern Europe.* CD-ROM. Warsaw, September, 1998.

BARRY, D. L. 1982. Treatment options for contaminated land (Report to the Department of the Environment), W.S. Atkins Research and Development, Epson, UK.

BDH LABORATORY SUPPLIES. 1998. Personal communication with BDH laboratory supplies, Poole, UK.

BELL, F. G. 1988. Stabilisation and treatment of clayey soils with lime. Ground Engineering, **21**, No.1, pp.10-15.

BERGGREN, B., & ODEN, S. 1972. Analysresultat Rorande Fungmetaller Och Kloerade Kolvaten I Rotslam Fran Svenska Reningsverk 1968-1971. Institutione fur Markvetenskap Lantbrukshogskolan, Uppsala, Sweden.

BERROW, M. L., & WEBBER, J. 1972. Trace elements in sewage sludges. J. Sci. Food Agric. **23**[1], pp.93-100.

BETTEKER, J. M., SHERRARD, J. H., & LUDWIG, D. D. 1986. Solidification/stabilisation of contaminated dredged material. Mid Atlantic Industrial Waste 18th Conference, Virginia, USA, pp.253-273.

BISHOP, P. L. 1990. Stabilization/solidification of contaminated soils: an overview. *In*: ARENDT, F., HINSENVELD, M., & VAN DEN BRINK, W. J. (eds). *Proceedings of the Third International KfK/TNO Conference on Contaminated Soil 90*. Kluwer Academic Publishers (Dordrecht), pp.1265-1274.

BLI. 1998. Personal communication with Buxton Lime Industries, Buxton, UK.

BOARDMAN, D. I., GLENDINNING, S., & ROGERS, C. D. F. 1999-A. Stabilisation and solidification: time-dependent physico-chemical developments of lime-clay mixes. Draft print submitted to Geotechnique.

BOARDMAN, D. I., GLENDINNING, S., & ROGERS, C. D. F. 1999-B. Stabilisation and solidification: time-dependent physico-chemical developments of lime-clay-contaminant mixes. Draft print to be submitted to Geotechnique.

BOARDMAN, D. I., GLENDINNING, S., & ROGERS, C. D. F. 1999-C. Appropriate short-term and long-term testing procedures for contaminated soils treated with pH dependent stabilisation and solidification agents. Draft print.

BOARDMAN, D. I., & MACLEAN, J. A. 1996. Lime treatment of metal contaminated sludges. *In*: ROGERS, C. D. F., GLENDINNING, S. & DIXON, N. (eds) *Lime stabilisation*. Thomas Telford, London, UK, pp.115-126.

BOARDMAN, D. I., GLENDINNING, S., & ROGERS, C. D. F. 1998. Lime Treatment for Clean Up of Metal Contaminated Soils. *In*: *Proceedings of the Fourth International Symposium and Exhibition on Environmental Contamination in Central and Eastern Europe*. CD-ROM. Warsaw, September, 1998.

BOHN, H., McNEAL, B., & O' CONNOR, G. 1985. Soil Chemistry, 2nd edition, Wiley-Interscience, Chichester, UK.

BOLT, G. H., & BRUGGENWERT, M. G. M. 1976. Soil Chemistry : A. Basic Elements, Elsevier Scientific Publishing Company, Oxford, UK.

BOYLE, W. C., HAM, R. K., PASTENE, J., & STANFORTH, R. 1983. Leach testing of foundry process wastes. *Hazardous and Industrial Solid Waste Testing: Second Symposium, ASTM STP 805*, CONWAY, R. A., & GULLEDGE, W. P., Eds., American Society for Testing and Materials, pp.67-88.

BRANDL, H. 1981. Alteration of soil parameters with lime. 10th International Conference on soil mechanics and foundation engineering, Stockholm, Sweden, **3**, pp.587-594.

BROHOLM, M. M., JONES, I., TORSTENSSON, D., & ARVIN, E. 1998. Groundwater contamination from coal carbonation plant. *In*: LERNER, D.N. & WALTON, N. R. G. (eds) 1998. *Contaminated Land and Groundwater: Future Directions.* Geological Society, London, UK. Engineering Geology Special Publications, **14**, pp.159-165.

BROMS, B. B., & BOMAN, P. 1976. Stabilisation of deep cuts with lime columns. *6th European Conference on Soil Mechanics and Foundation Engineering*, Vienna, Austria, pp.207-210.

BSI (1987). Water for laboratory use. *British Standard 3696*, British Standards Institution, London, UK.

BSI (1990A). Stabilized materials for civil engineering purposes. Methods of test for cement-stabilized and lime-stabilized materials. *British Standard 1924 : Part 2*, British Standards Institution, London, UK.

BSI (1990B). Methods of test for soils for civil engineering purposes. *British Standard 1377*, British Standards Institution, London, UK.

BURMISTROV, D., TARANENKO, V., & LINKOV, I. 1998. Dynamic modelling of radionuclides fate and transport in the Techa river and application for dose reconstruction. *In: Proceedings of the Fourth International Symposium and Exhibition on Environmental Contamination in Central and Eastern Europe.* CD-ROM. Warsaw, September, 1998.

CARTLEDGE, F. K., BUTLER, L. G., CHALASANI, D., EATON, H. C., FREY, F. P., HERRERA, E., TITTLEBAUM, M. E., & YANG, S. 1990. Immobilization mechanisms in solidification/stabilization of Cd and Pb salts using portland cement fixing agents. Environmental Science and Technology, **24**, pp.867-873.

CEC, 1991. Proposal for a council directive on landfill of waste. Official Journal of the European Communities. C190/1, 22 July 1991.

CEN, 1993. European leaching test for granular waste materials. Third Draft. CEN/TC292/WG2 Doc 25.

CERNUSCHI, S., GIUGLIANO, M., & PAOLI, I. D. E. 1990. Italian CNR-IRSA. Waste Management and Research **8**, pp.419-427.

CETO, N., PALAZZO, A., FELITTI, B., MARCY, K.,STARKOVA, I., & OSLAMENKO, V. 1998. Nizhnii Tagil mine tailings reclamation project. *In: Proceedings of the Fourth International Symposium and Exhibition on Environmental Contamination in Central and Eastern Europe.* CD-ROM. Warsaw, September, 1998.

CHRISTOFI, N., IVSHINA, I. B., KUYUKINA, M. S., & PHILP, J. C. 1998. Biological treatment of crude oil contaminated soil in Russia. *In*: LERNER, D.N. & WALTON, N. R. G. (eds) 1998. *Contaminated Land and Groundwater: Future Directions.* Geological Society, London, Engineering Geology Special Publications, **14**, pp.45-51.

COBBE, M. I., 1988. Lime-modification of kaolinite-illite clays. Civil Engineering Technology. February.

CONSTABLE, T. W., & CÔTÉ, P. L. 1986. Development and application of a multiple batch leaching procedure. Environment Canada Report EPS 3/AT/1.

CÔTÉ, P. L., & CONSTABLE, T. W. 1983. Development of a Canadian data base on waste leachability. *Hazardous and Industrial Solid Waste Testing: Second Symposium, ASTM STP 805*, CONWAY, R. A., & GULLEDGE, W. P., Eds., American Society for Testing and Materials, pp.53-66.

CSIZER, Z., & RICHARDSON, M. 1998. Effective environmental management for the pharmaceutical chemical industry: part 1 guidelines for governments, NGOs and other officials. *In*: *Proceedings of the Fourth International Symposium and Exhibition on Environmental Contamination in Central and Eastern Europe.* CD-ROM. Warsaw, September, 1998.

DANIELS, W. L., STUCZYNSKI, T. PANTUCK, K., CHANEY, R., & PISTELOK, F., 1998. Low cost stabilization of toxic, metalliferous smelter wastes in Poland. *In*: *Proceedings of the Fourth International Symposium and Exhibition on Environmental Contamination in Central and Eastern Europe.* CD-ROM. Warsaw, September, 1998.

DARCEL, F. C., 1983. Column leach testing of solid industrial wastes. *Hazardous and Industrial Solid Waste Testing: Second Symposium, ASTM STP 805*, CONWAY, R. A., & GULLEDGE, W. P., Eds., American Society for Testing and Materials, pp.127-140.

DAVIS, G. 1998. BTEX plumes and vapour phase emissions: can natural attenuation cope? *In*: *Proceedings of the Fourth International Symposium and Exhibition on Environmental Contamination in Central and Eastern Europe.* CD-ROM. Warsaw, September, 1998.

DEEGEN, J. 1987A. Looking back at Love Canal. Environmental Science and Technology, **21**, No.4, pp.328-331.

DEEGEN, J. 1987B. Looking back at Love Canal. Environmental Science and Technology, **21**, No.5, pp.421-426.

DELANEY, B. T., UHLMAN, K., & PENDEXTER, W. S. 1998. Characterisation of the complex flow geometry of DNAPLs in the vadose zone. *In*: *Proceedings of the Fourth International Symposium and Exhibition on Environmental Contamination in Central and Eastern Europe.* CD-ROM. Warsaw, September, 1998.

DERMATAS, D. 1994. Leachability study of chromium contaminated soils to assess the long-term effectiveness of a remediation technology. Geoenvironment 2000, pp.449-462.

DIAMOND, S., & KINTER, B. 1965. Mechanisms of soil lime stabilisation. Highway Research Record, No.92, Highway Research Board, National Research Council, Washington DC, USA, pp.83-102.

DIN-NORMEN. DIN 38414-S4, 1984. Determination of leachability by water (S4). German standard methods for the examination of water, waste water and sludge. Sludge and sediments (group S).

DODD, D. J. R., GOLOMB, A., CHAN, H. T., & CHARTIER, D. 1981. *Hazardous Solid Waste Testing: First Conference, ASTM STP 760*, R. A. Conway and B. C. Malloy, Eds., American Society for Testing and Materials, pp.164-185.

DPS, 1991. Dutch Pre-Standard NVN5432. Waste materials, construction materials and stabilised waste products. Part 1-determination of maximum leachability.

DRAGUN, J. 1988. The soil chemistry of hazardous materials. Hazardous materials control research institute, Silver spring, Maryland.

DRAWBAUGH, R. B. 1998. Environmental management systems in the military sector. *In*: *Proceedings of the Fourth International Symposium and Exhibition on Environmental Contamination in Central and Eastern Europe.* CD-ROM. Warsaw, September, 1998.

DUMBLETON, M. J. 1962. Investigations to assess the potentialities of lime for soil stabilisation in the United Kingdom. Road Research Technical Paper No. 64, Transportation Research Laboratory, Crowthorne, Berks., UK.

DURFER, C.N., & BECKER, E. 1964. Public water supplies of the 100 largest cities in the United States. U. S. Geol. Surv., Water-Supply Pap. **1812**.

EADES, J. L., & GRIM, R. E. 1960. Reaction of hydrated lime with pure clay minerals in soil stabilization. Highway Research Board. Bulletin 262, pp.51-63.

EADES, J. L., & GRIM, R. E. 1966. A quick test to determine lime requirements of lime stabilisation. Highway Research Record, No.139, Highway Research Board, National Research Council, Washington D.C., USA, pp.61-72.

EBENS, R. J., & SHACKLETTE, H. T. 1982. Geochemistry of some rocks, mine spoils, stream sediments, soils, plants, and waters in the western energy region of the conterminous United States. U. S. Geol. Surv. Prof. Pap. **1237**.

EC. 1990. Compendium of waste leaching tests. Report EPS 3/HA/7. Environment Canada, Waste Water Technology Centre.

EISENMAN, G. 1961. On the elementary origin of equilibrium ionic specificity. In A. Kleinzeller and A. Kotyk (eds.), Symposium on Membrane Transport and Metabolism. New York Academic Press, pp.163-179.

ELEJALDE, C., RUIZ, F. R., & GOMEZ, G. 1992. Speciation of metals in soils and mobilization by acid-base treatment. Toxicological and Environmental Chemistry, **37**, pp.49-60.

EL-RAWI, N. M., & AWAD, A.A. 1981. Permeability of lime stabilized soils. Transportation Engineering Journal, January, pp.25-35.

EMERY, J. J. 1980. Stabilization of industrial sludge for fill applications. Proceedings Seventh International Congress on the Chemistry of Cement (Paris), **4**.

ENVIRONMENT CANADA. 1990. Compendium of waste leaching tests. Report EPS 3/HA/7. Environment Canada, Waste Water Technology Centre.

EVANS, J. C., BRYCE, R. W., BATES, D. J., & KEMNER, M. L. 1990. Hanford site ground-water surveillance for1989, PNL-7396. Pacific Northwest Laboratory, Richland, WA.

FEIGE-MUNZIG, 1998. Risk assessment for occupational health and safety protection in the remediation of contaminated sites. *In*: *Proceedings of the Fourth International Symposium and Exhibition on Environmental Contamination in Central and Eastern Europe.* CD-ROM. Warsaw, September, 1998.

FERGUSON, C., DARMENDRAIL, D., FREIER, K., JENSEN, B. K., JENSEN, J., KASAMAS, H., URZELAI, A., & VEGTER, J. (eds). 1998. Risk assessment for contaminated sites in Europe. Volume 1. Scientific basis. LQM Press, Nottingham, UK.

FIRSOVA, E. V., GUERMAN, K. E., PERETROUKHIN, V.F., & KHIJNYAK, T. V. 1998. Bioaccumulation of long-lived radionuclides in freshwater silt. *In*: *Proceedings of the Fourth International Symposium and Exhibition on Environmental Contamination in Central and Eastern Europe.* CD-ROM. Warsaw, September, 1998.

FISHER. 1996. Personal communication with Fisher Scientific, Loughborough, Leicestershire, UK.

FOSSBERG, E. 1965. Some fundamental engineering properties of stabilized clay. Proceedings, 6th International Conference of Soil Mechanics and Foundation Engineering, Montreal, Canada.

FRETWELL, B. A., BURGESS, W. G., JEFFRIES, N. L., & DOTTRIDGE, J. 1998. Distribution of volatile organic compounds in porewater of the seasonally unsaturated Chalk aquifer. *In*: LERNER, D.N. & WALTON, N. R. G. (eds) 1998. *Contaminated Land and Groundwater: Future Directions.* Geological Society, London, Engineering Geology Special Publications, **14**, pp.219-226.

FRINK, C. R., & VOIGT, G. K. 1977. Potential effects of acid precipitation on soils in the humid temperate zone. Water, Air, and Soil Pollution **7**, pp.371-388.

FURMAN, C., & COCHRAN, S. R. 1985. Case study investigations of remedial response programs at uncontrolled hazardous waste sites. *In*: *Land Disposal of Hazardous Waste. Proceedings of the Eleventh Annual Research Symposium*, Cincinnati, OH, EPA-600/9-85-013. Cincinnati, OH, U.S. Environmental Protection Agency.

FURR, K. A., LAWRENCE, A.W., TONG, S. S. C., GRANDOLFO, M. G., HOFSTADER, R. A., BACHE, C.A., GUTEMANN, W. H., & LISK, D. J. 1976. Multielement and chlorinated hydrocarbon analysis of municipal sewage sludge of American cities. Environ. Sci. Technol. **10**, pp.683-687.

GASKILL, A. Jr., ALLEN, C. C., & TINESDALE, R. S. 1986. A procedure for estimating monofilled solid waste leachate composition, 2nd edition, USEPA-SW924.

GILBERT, M., & R. VAN BLADEL. 1970. Thermodynamics and thermochemistry of the exchange reaction between NH_4^+ and Mn^{2+} in a montmorillonite clay. J. Soil Sci. **21**, pp.38-49.

GLENDINNING, S. 1995. Deep stabilization of slopes using lime piles. PhD. Thesis, Loughborough University, Leicestershire, UK.

GLENDINNING, S., & BOARDMAN, D. I. 1996. Lime treatment of metal contaminated clay soils. *In: Proceedings of the 32nd Annual Conference of the Engineering Group of the Geological Society and the Hydrogeological Group.* Eds. Lerner, D. N., & Walton, N., University of Portsmouth, UK., pp.249-258.

GLENDINNING, S., ROGERS, C. D. F., & BOARDMAN, D. I. 1998. Lime stabilisation of inorganic contaminants in clays. *In:* LERNER, D. N. & WALTON, N. R. G. (eds). *Contaminated Land and Groundwater: Future Directions.* Engineering Geology Special Publications, Geological Society, London, England, **14**, pp.19-28.

GRABAR, S., & KUCAR, S. 1998. Management of inorganic-galvanic sludges using industrial facilities in the Republic of Croatia. *In: Proceedings of the Fourth International Symposium and Exhibition on Environmental Contamination in Central and Eastern Europe.* CD-ROM. Warsaw, September, 1998.

GRIFFIN, R. A., & SHIMP, N. F. 1975. Attenuation of pollutants in municipal landfill leachate by clay minerals, Final Report for EPA Contract 68-03-0211, Cincinnati, Ohio, USA.

GRIFFIN, R. A., & SHIMP, N. F. 1976. Effect of pH on exchange-adsorption or precipitation of lead from landfill leachates by clay minerals. Environmental Science and Technology, **10** (13), pp.1256-1261.

GRIFFIN, R. A., SHIMP, N. F., STEELE, J. D., RUCH, R. R., WHITE, W. A., & HUGHES. 1976. Attenuation of pollutants in municipal landfill leachate by passage through clay. Environmental Science and Technology, **10** (13), pp.1262-1267.

GUTSCHICK, K. A. 1978. Lime stabilization under hydraulic conditions. Presented at the 4th International Lime Congress, Hershey, PA. Available from the National Lime Association, Washington, DC, USA.

HADJIHRISTOVA, M. 1998. Use of constructed wetlands for the treatment of copper refinery effluent feasibility study. *In*: *Proceedings of the Fourth International Symposium and Exhibition on Environmental Contamination in Central and Eastern Europe.* CD-ROM. Warsaw, September, 1998.

HAMM, R. K. 1977. Development of a standard leaching test – second progress report. University of Wisconsin, USA.

HARRIS, M. R., HERBERT, S. M., & SMITH, M. A. 1995. Remedial treatment for contaminated land, volume IX: Ex-situ treatment of contaminated soils, sediments and sludges, Construction Industry Research and Information Association, London, UK. Special publication 108.

HARTY, J. R., & THOMPSON, M. R. 1973. Lime reactivity of tropical and sub-tropical soils. Highway Research Board, No.442, National Research Council, Washington D.C., USA, pp.102-112.

HAYES, M. H. B., & SWIFT, R. S. 1978. The Chemistry of Soil Constituents, John Wiley, Chichester, UK.

HELLING, C. S., CHESTERS, G., & COREY, R. B. 1964. Contribution of organic matter and clay to soil cation exchange capacity as affected by the pH of the saturating solutions. Soil Science Society of America Proceedings, **28**, pp.517-520.

HERCULES AEROSPACE COMPANY.1991. A petition for the reclassification of TNT process red water to a secondary material. Radford Army Ammunition Plant, Radford, Virginia, USA.

HERRIN, M., & MITCHELL, H. 1961. Lime-soil mixtures. Highway Research Board. Bulletin 304, pp.99-138.

HILL, G., & HOLMAN, J. 1989. Chemistry in Context, Third Edition, Thomas Nelson and Sons Ltd., UK.

HILT, G. H., & DAVIDSON, D. T. 1960. Lime fixation of clayey soils. Highway Research Board Bulletin, No.262, Highway research Board, National Research Council, Washington D.C., USA, pp.20-32.

HINSENVELD, M. 1993. Stabilization/solidification technologies. *In* : *NATO/CCMS Final Report Volume 1 – Demonstration of Remedial Action Technologies for Contaminated Land and Groundwater.* Environmental Protection agency, EPA/600/R-93/012a.

HO, C., & HANDY, R. L. 1963A. Characteristics of lime retention by montmorillonitic clays. Highway Research Record No.29, pp.55-69.

HO, C., & HANDY, R. L. 1963B. Electrokinetic properties of lime-treated Bentonites. Paper presented at 12th National Conference on clays and clay minerals, Atlanta, Ga., Oct.

HOLT, C. C., & FREER-HEWISH, R. J. 1996. Lime treatment of capping layers in accordance with the current specification for highway works. *In*: ROGERS, C. D. F., GLENDINNING, S. & DIXON, N. (eds) *Lime stabilisation.* Thomas Telford, London, pp.51-61.

HOULE, M. J., & LONG, D. E. 1980. Interpreting results from serial batch extraction tests of wastes and soils. Proceedings of the 6th Annual Research Symposium. EPA 600/9-80-010. United States Environmental Protection Agency.

HUTCHINSON, T. C., & HAVAS, M. (eds). 1980. Effects of Acid Precipitation on Terrestrial Ecosystems. New York: Plenum Press.

IUCS. 1977. Shake test for evaluation of the leaching potential for land disposal of waste materials. I.U. Conversion Systems Incorporated. Philadelphia, Pennsylvania, USA.

JACKSON, K., BENEDIK, & JACKSON, L. 1981. Comparison of three solid waste batch leach testing methods and a column leach test method. *Hazardous Solid Waste Testing: First Conference, ASTM STP 760*, R. A. CONWAY & B. C. MALLOY, Eds., American Society for Testing and Materials, pp.83-98.

JAN, M. A., & WALKER, R. D. 1963. Effect of lime, moisture, and compaction on a clay soil. Highway Research Record 29, pp.1-12.

JAUZEIN, M. 1998. Personal communication and lecture notes. European Union Advanced Study Course 'Soil Remediation', Vienna, Austria, 12 July 1998.

JOHNSON, A. W., & SALLBERG, J. R. 1960. Factors that influence field compaction of soils. Bulletin 272, Highway Research Board.

KHAN, A. Q., & THOMAS, G.A. 1980. Pseudo love canal of the united kingdom: in-situ decontamination and rehabilitation of a hazardous chemical dump problems of uncontrolled disposal sites. *In*: *Proceedings of U.S. EPA National Conference on Management of Uncontrolled Hazardous Waste Sites*, Washington, D.C., October 15-17, 1980. Silver Spring, MD: Hazardous Materials Control Research Institute.

KILAU, H. W., & SHAH, I. D. 1984. Chromium-bearing waste slag: evaluation of leachability when exposed to simulated acid precipitation. *Hazardous and Industrial Waste Management and Testing: Third Symposium, ASTM STP 851*, JACKSON, L. P., ROHLIK, A. R., & CONWAY, R. A., Eds., American Society for Testing and Materials, pp.61-80.

KISSELEVA, E., KOSITSKAYA, L., KUZMENOK, O., & POTAPNEV, M. 1998. Long-lasting alterations in the immune system of Chernobyl accident victims. *In*: *Proceedings of the Fourth International Symposium and Exhibition on Environmental Contamination in Central and Eastern Europe.* CD-ROM. Warsaw, September, 1998.

KOPP, J. F., & KRONER, R. C. 1991. Trace metals in waters of the United States, U. S. Environmental Protection Agency, Washington, D.C., USA.

KUCAR, S., METES, A., SUBASIC, D., & KOPRIVANAC, N. 1998. Waste reduction in the printing ink industry: from theory to practice. *In*: *Proceedings of the Fourth International Symposium and Exhibition on Environmental Contamination in Central and Eastern Europe.* CD-ROM. Warsaw, September, 1998.

LANDRETH, R. E. 1982. Physical properties and leach testing of solidified/stabilised industrial wastes. Report Number EPA-600/2-82-099, US Environmental Protection Agency, Cincinnati, Ohio 45268, USA.

LARSON, R. J., MALONE, P. G., MYERS, T. E., & SHAFER, R. A. 1981. Evaluation of the extraction procedure testing of hazardous industrial wastes. *Hazardous Solid Waste Testing: First Conference, ASTM STP 760,* R. A. CONWAY & B. C. MALLOY, Eds., American Society for Testing and Materials, pp.139-150.

LEES, G. ABDELKADER, M. O., & HAMDANI, S. K. 1982. Effect of the clay fraction and mechanical properties of lime-soil mixtures. Highways and Transportation, **30**, Part 12, pp.8-16.

LEJEUNE, G., ROSENVEAR, A., & FOX, A. 1996. Pollution potential of contaminated sites-validation of leaching test. Research and Development Technical Report P10. Environment Agency, UK.

LESSOVAIA, S. 1998. Influence of the gley process on the mineral composition of soils. *In*: *Proceedings of the Fourth International Symposium and Exhibition on Environmental Contamination in Central and Eastern Europe.* CD-ROM. Warsaw, September, 1998.

LEWIN, K., BRADSHAW, K., BLAKEY, N. C., TURRELL, J., HENNINGS, S. M., & FLAVIN, R. J. 1994. Leaching tests for assessment of contaminated land – Interim NRA guidance. R & D Note 301. National Rivers Authority, Rivers House, Waterside Drive, Almondsbury, Bristol, UK.

LINDSAY, P., BELL, F. G., & HYTIRIS, N. 1998. Contamination of sediments in the Forth Estuary, Scotland. *In*: LERNER, D.N. & WALTON, N. R. G. (eds) 1998. *Contaminated Land and Groundwater: Future Directions.* Geological Society, London, Engineering Geology Special Publications, **14**, pp.179-187.

LITTLE, D. N. 1994. Handbook for stabilization of pavement subgrades and base courses with lime. National Lime Association. Kendall/Hunt, Dubuque, Iowa, USA.

LIVENS, F. R. 1991. Chemical reactions of metals with humic material. Environmental Pollution, **70**, pp.183-208.

LONG, D. E., HOWLE. M. J., WEATHERHEAD, D. C., & RICHAS, G. K. 1987. Migration of hazardous substances through soil, part IV. Development of a serial batch extraction method and application to the accelerated testing of seven industrial wastes. United States Army, Dugway Proving Ground, Report No: DRG-FR-87-015.

LOUGHNAN, F. C. 1969. Chemical weathering of silicate minerals. American Elsevier Publishing Co. Inc., New York.

LÖWENBACH, W. 1978. Compilation and evaluation of leaching test methods. United States Environmental Protection Agency. Report EPA-600/2-78-095. May 1978.

LUND, O. L., & RAMSEY, W. J. 1959. Experimental lime stabilization in Nebraska. Highway Research Board, Bulletin 231, pp.24-59.

LUTZ, E. J., & MINEHAN, L. J. 1986. Laboratory study to determine longterm stability of pozzolanically stabilised waste. Proceedings of HAZPRO ' 86, Baltimore, April 1986. Puduan, USA, pp.295-303.

MACKAY, M., & EMERY, J. J. 1993. Practical stabilization of contaminated soils, Land Contamination and Reclamation, **1**, Number 3, pp.149-155.

MACKAY, D. M. 1998. Is cleanup of VOC-contaminated groundwater feasible? *In*: LERNER, D. N. & WALTON, N. R. G. (eds) 1998. *Contaminated Land and Groundwater: Future Directions.* Geological Society, London, Engineering Geology Special Publications, **14**, pp.13-11.

MALONE, P. G., & LARSON, R. 1983. Scientific basis of hazardous waste immobilization. *Hazardous and Industrial Solid Waste Testing: Second Symposium, ASTM STP 805*, CONWAY, R. A. & GULLEDGE, W. P. Eds., American Society for Testing and Materials, pp.168-177.

MANAHAN, S. E. 1991. Environmental Chemistry. 5th. ed. Lewis Publishers, Chelsea, MI.

MARSHALL, C. E, (1975), The physical chemistry and mineralogy of soils. Vol. I: Soil Materials, Robert E. Krieger Publishing Co., New York.

MATEOS, M. 1964. Soil lime research at Iowa State University. Proc. A.S.C.E. Journal of Soil Mechanics and Foundation Division, **90**, S.M.2, pp.127-153.

McBRIDE, M. B. 1994. Environmental Chemistry of Soils. Oxford University Press, New York.

McCALLISTER, L. D., & PETRY, T. M. 1992. Leach tests on lime-treated clays. Geotechnical Testing Journal, **15**, Number 2, pp.106-114.

MITCHELL, J. K. 1976. Fundamentals of Soil Behaviour. John Wiley & Sons, New York.

MOE. 1985. Ministry of the Environment regulation 309/leachate extraction procedure. Government of Ontario.

MOORE, J. C., & JONES, R. L. 1971. Effect of soil surface area and extractable silica, alumina and iron on lime stabilisation characteristics of Illinois soils. Highway Research Record No.315, Highway Research Board, National Research Council, Washington D.C. USA, pp.87-92.

MORTLAND, M. M. 1970. Clay-organic complexes and interactions. Adv. Agron. **22**, pp.75-117.

MORTLAND, M. M., SHAOBAI, S., & BOYD, S. A. 1986. Clay-organic complexes as adsorbents for phenol and chlorophenols. Clays Clay Miner. **34**, pp.581-585.

MOSSOM, J. 1998. Personal communication at the EU advanced study course 'Soil remediation – an overall approach to a complex subject', Vienna, Austria, July 13-18, 1998. ICCET centre for environmental technology, Imperial Collage, London, UK.

MPCA. 1977. Minnesota Pollution Control Agency. Division of solid wastes land disposal leach test.

MUVRIN, B., KAVEDZIJA, Z., ABRAHAM, Z., & KRULIJAC, I. 1998. Measures for eliminating soil pollution by spilled hydrocarbons. *In*: *Proceedings of the Fourth International Symposium and Exhibition on Environmental Contamination in Central and Eastern Europe.* CD-ROM. Warsaw, September, 1998.

MYASOEDOV, B. F. 1998. Radioactive environment contamination and abilities of the modern radiochemistry in the field of nuclear waste disposal and monitoring. *In*: *Proceedings of the Fourth International Symposium and Exhibition on Environmental Contamination in Central and Eastern Europe.* CD-ROM. Warsaw, September, 1998.

NEWMAN, A. C. D. (ED). 1987. Chemistry and Clay Minerals. Mineralogical Society, Longman Group Ltd.

OLIVER, B. G., & COSGROVE, E. G. 1975. Metal concentrations in the sewage, effluents, and sludges of some southern Ontario wastewater treatment plants. Environ. Lett. 9, pp.75-90.

PAULE, R. C. 1981. Analysis and modelling of the leaching process. *Hazardous Solid Waste Testing: First Conference, ASTM STP 760*, R. A. CONWAY & B. C. MALLOY, Eds., American Society for Testing and Materials, pp.112-135.

PENLAND, J. L., STEWARD, F. A., & LANCY, L. E. 1981. Modified leach test incorporating an elutriation step for the evaluation of metal sludges. *Hazardous Solid Waste Testing: First Conference, ASTM STP 760*, R. A. CONWAY & B. C. MALLOY, Eds., American Society for Testing and Materials, pp.186-200.

POBORSKI, P. S. 1998. Solving contaminated land problems: risk based decision-making for potential clean-up projects. *In: Proceedings of the Fourth International Symposium and Exhibition on Environmental Contamination in Central and Eastern Europe.* CD-ROM. Warsaw, September, 1998..

PORTSMOUTH, 1998. Personal communication on a site visit to an old gasworks in the town of Portsmouth, UK.

PRITCHARD, P. H., & COSTA, C. F. 1991. EPA's Alaska oil spill bioremediation project. *Environmental Science and Technology*, **25**, pp.372-379.

PURITE. 1998. Personal communication with Purite Ltd., Thame, Oxon, UK.

QUIGLEY, R. M., & DINARO, L. R. 1978. Clay mineral weathering controls on lime and cement stabilisation of Southwestern Ontario clay borrow. Highway Research Record No.690, Highway Research Board, National Research Council, Washington D.C. USA, pp.5-8.

RANGANATHAM, B. V. 1961. Soil structure and consolidation characteristics of black cotton clay. Geotechnique, **11**, p.331.

RILEY, R. G., ZACHARA, J. M., & WOBBER, F. J. 1992. Chemical contaminants on DOE lands and selection of contaminant mixtures for subsurface science research. DOE/ER-0547T.U.S.Dept. of Energy, Office of Energy Research, Subsurface Science Program, Washington, DC.

RINALDO-LEE, M. B., KUNES, T. P., & NICHOLS, D. G. 1981. A comparison of groundwater quality at selected landfills to leaching test results. *Hazardous Solid Waste Testing: First Conference, ASTM STP 760*, R. A. CONWAY & B. C. MALLOY, Eds., American Society for Testing and Materials, pp.201-214.

RITCHIE, G. S. P., & POSNER, A. M. 1982. The effect of pH and metal binding on the transport properties of humic acids. Journal of Soil Sciences, **33**, pp.233-247.

RIVETT, M. O., FEENSTRA, S., & CHERRY, J. A. 1998. The relevance of a DNAPL-tracer test conducted at Base Borden, Canada, to solvent groundwater contamination in the UK. *In*: LERNER, D.N. & WALTON, N. R. G. (eds) 1998. *Contaminated Land and Groundwater: Future Directions.* Geological Society, London, Engineering Geology Special Publications, **14**, pp.235-241.

ROGERS, C. D. F., GLENDINNING, S., & ROFF, T. E. J. (1997). Modification of clay soils for construction expediency. *Proceedings of the Institution of Civil Engineers Geotechnical Engineering*, **125**, pp.1 – 8.

ROGERS, J. C., DANIELS, K. L., GOODPASTURE, S. T., & KIMBROUGH, C. W. 1989. Oak Ridge Reservation environmental report for 1988, ES/ESH-8/Vol. 1. Martin Marietta Energy Systems, Inc., Oak Ridge, TN, USA.

ROSS, S. 1989. Soil processes. Routledge, London.

RURY, P. M., & LITTLE, A. D. 1998. A risk-based decision protocol for reuse of Belarussian military installations. *In*: *Proceedings of the Fourth International Symposium and Exhibition on Environmental Contamination in Central and Eastern Europe.* CD-ROM. Warsaw, September, 1998.

SACK, W. A., BOOMER, B. A., TARANTINO, J. T., KEEFER, G. B., SEALS, R. K., & MILLER, M. 1981. Evaluation of fly ash leachability using batch leaching procedures. *Hazardous Solid Waste Testing: First Conference, ASTM STP 760* R. A. CONWAY & B. C. MALLOY, Eds., American Society for Testing and Materials, pp.61-82.

SAUNDERS, F. M., WILLIAMS, F. M., & KUTZ, R. G. 1983. Effect of storage on leaching properties of metal-finishing sludges. *Hazardous and Industrial Solid Waste Testing: Second Symposium, ASTM STP 805*, CONWAY, R. A., & GULLEDGE, W. P., Eds., American Society for Testing and Materials, pp.89-107.

SCHACHTSCHABEL, P. (1940), Untersuchungen über die sorption der Tonmineralien und organishen Boden-kolloide. Kolloid Beihefte, **51**, pp.199-243.

SCHNITZER, M., & DESJARDINS, J. G. 1969. Chemical characteristics of a natural soil leachate from humic podzol. Canadian Journal of Soil Science, **49**, pp.151-158.

SCHNITZER, M., & HANSON, E. H. 1970. Organo-metallic interactions in soils: 8 An evaluation of methods for determination of stability constants of metal-fulvic acid complexes. Soil Science, **109**, pp.333-340.

SCHNITZER, M. 1977. The chemistry of humic substances. In: Environmental Geochemistry, **1**, Chapter 7, Ed. Nriagu, J. O.. Ann Arbor Science, Michigan.

SCHOFIELD, R. K. 1949. Effect of pH on electric charges carried by clay particles. Journal of soil science **1**, pp.1-8.

SHERWOOD, P. T. 1993. 'The effect of lime on soils', Soil stabilisation with cement and lime. Transportation Research Laboratory, State-of-the-Art Review, HMSO, London, England.

SMITH, D. G., & LORIMAR, J. W. 1964. An examination of the humic acids of *Sphagnum* peat. Canadian Journal of Soil Science, **44**, pp.76-87.

SMITH, J. H. 1996. Construction of lime or lime plus cement stabilised cohesive soils. *In*: ROGERS, C. D. F., GLENDINNING, S. & DIXON, N. (eds) *Lime stabilisation*. Thomas Telford, London, pp.13-26.

SMITH, M. A. 1998. Stabilization/solidification processes. In: NATO/CCMS Pilot Study-Evaluation of Demonstrated and Emerging Technologies for Treatment and Clean-Up of Contaminated Land and Groundwater. EPA542-R-98-001a.

SOC. 1985. Criteria for identification of hazardous and extremely hazardous wastes. State of California code title 22 Article 11 1800.M5 – 1800.28.

SOUNDARAJAN, R., BARTH, E. F., & GIBBONS, J. J. 1990. Using an organophilic clay to chemically stabilize waste containing organic compounds. Hazard. Mater. Control **3** [1], pp.42-45.

SOUNDARAJAN, R.1998. A comprehensive approach for the management of radioactive wastes. *In*: *Proceedings of the Fourth International Symposium and Exhibition on Environmental Contamination in Central and Eastern Europe.* CD-ROM. Warsaw, September, 1998.

SOWINSKI, M. 1998. Risk assessment and risk management for optimizing environmental management decisions in Central and Eastern Europe. *In*: *Proceedings of the Fourth International Symposium and Exhibition on Environmental Contamination in Central and Eastern Europe.* CD-ROM. Warsaw, September, 1998.

SPARKS, D. L. 1995. Environmental soil chemistry. Academic Press, London.

STANCZYK, T. F., SENEFELDER, B. C., & CLARKE, J. H. 1982. Solidification / stabilisation processes appropriate to hazardous chemicals and waste spills. Hazardous Material Spills, Milwaukee, WI, USA, pp.79-84.

STEETLEY MINERALS LTD. 1998. Personal communication with Steetley Minerals Ltd, Middlesborough, UK.

STENNER, R. D., CRAMER, K.H., HIGLEY, K. A., JETTE, S.J., LAMAR, D. A., McLAUGHLIN, T. J., SHERWOOD, D. R., & HOUTEN, N. C. V. 1988. Hazard ranking system evaluation of CERCLA inactive waste sites at Hanford : evaluation methods and results, PNL-6456, Vol.1. Pacific Northwest Laboratory, Richland, WA.

STEVENSON, F. J., 1977. Binding of metal ions by Humic Acids. The chemistry of humic substances. In: Environmental Biochemistry, Volume 2, Chapter 33, Ed. Nriagu, J. O. Ann Arbor Science, Michigan.

STRZELECKI, R., WOLKOWICZ, S., WOLKOWICZ, W., MOAMONT-CIEOELA, K., MOSE, D. G., SZABO, Z., IVAHNENKO, T., & MUSHRUSH, G. W. 1998. Evaluation of geological Radon potential in two regions in Southwestern and Southern Poland. *In: Proceedings of the Fourth International Symposium and Exhibition on Environmental Contamination in Central and Eastern Europe.* CD-ROM. Warsaw, September, 1998.

TALIBUDEEN, O. 1981. Cation exchange in soils. In: Greenland, D. J. and Hayes, M. H. B. (eds), The Chemistry of Soil Processes, John Wiley & Sons Ltd, Chichester, pp.115-177.

TAYLOR, W. H., Jr., & ARMAN, A. 1960. Lime stabilization using pre-conditioned soils. Highway Research Board, Bulletin 262, pp.1-19.

THOMPSON, M. R. 1965. Influence of soil properties on lime-soil reactions. Public works, 96, No. 8, August.

THOMPSON, M. R. 1966. Shear strength and elastic properties of lime-soil mixtures. Highway Research Record 139, pp.1-14.

TORSTENSSON, D., THORNTON, S. F., BROHOLM, M. M., & LERNER, D. N. 1998. Hydrochemistry of pollutant attenuation in groundwater contaminated by coal tar wastes. *In*: LERNER, D. N. & WALTON, N. R. G. (eds) 1998. *Contaminated Land and Groundwater: Future Directions.* Geological Society, London, Engineering Geology Special Publications, **14**, pp.149-157.

TOUCHETTE, T., CADOW, R. E., & CONLEY, T. 1998. Environmental security in contingency operations: an environmental handbook and video for soldiers. *In*: *Proceedings of the Fourth International Symposium and Exhibition on Environmental Contamination in Central and Eastern Europe.* CD-ROM. Warsaw, September, 1998.

TOURTELOT, H. A. 1971. Chemical compositions of rock types as factors in our environment. *In*: CANNON, H. L. & HOPPS, H. C. (eds) 1971. *Environmental Geochemistry in Health and Disease.* Geol. Soc. Am., Boulder, CO, **123**, pp.13-29.

TOWNSEND, D. C., & KYLM, T. W. 1966. Durability of lime-stabilized soils. Highway Research Record No. 139. Highway Research Board, National Research Council, Washington, DC, pp.25-41.

ULFIG, K., TIEN, A., PLAZA, G., WORSZTYNOWICZ, A., & HAZEN, T. (1998). Microbial changes in petroleum-contaminated soil during bioremediation at a polish petroleum refinery. *In*: *Proceedings of the Fourth International Symposium and Exhibition on Environmental Contamination in Central and Eastern Europe.* CD-ROM. Warsaw, September, 1998.

U.S.EPA. 1980. Test method for the evaluation of solid waste, physical chemical methods. Office of solid wastes. United States Protection Agency. USEPA Report number: SW-846.

U.S.EPA, 1986. Hazardous waste management system; identification and listing of hazardous waste; notification requirements; reportable quantity adjustments; proposed rule. Federal Register 51(114):21648-21693.

U.S.EPA, 1986-B. Multiple extraction procedure method 1310. Test method and structural test methods for evaluation of solid wastes. USEPA Report number: SW-846. United States Environmental Protection Agency.

U.S. EPA. 1987. Federal Register, 52(155): 29999, August 12, 1987.

U.S.EPA. 1989. Corrective action: technologies and applications, Seminar Publication, EPA/625/4-89/020. United States Environmental Protection Agency.

U.S.EPA. 1989-B. Hazcon solidification process. PA-Applications Analysis Report, EPA/540/A5-89/001. United States Environmental Protection Agency.

U.S.EPA, 1989-C. Performance testing of method 1312-QA support for RCRA testing. EPA/600/4-89/022. United States Environmental Protection Agency.

U.S.EPA. 1990-A. Handbook on the *in situ* treatment of hazardous waste-contaminated soil. EPA/540/2-90/002. United States Environmental Protection Agency.

U.S.EPA. 1990-B. International waste technologies / Geo-con *in situ* stabilization/solidification. Applications Analysis Report, EPA/540/A5-89/004. United States Environmental Protection Agency.

U.S.EPA. 1991. Innovative treatment technologies overview and guide to information sources, Office of Solid Waste and Emergency Response, EPA/540/9-91/002. United States Environmental Protection Agency.

U.S.EPA. 1992-A. Hazardous waste control: Nomix® technology, *In*: *The Superfund Innovative Technology Evaluation Program: Technology Profiles*, Fifth Edition, EPA/540/R-92/077, United States Environmental Protection Agency, pp.100-101.

U.S.EPA. 1992-B. S. M. W. Seiko Inc: *In situ* solidification and stabilization. *In*: *The Superfund Innovative Technology Evaluation Program: Technology Profiles*, Fifth Edition, EPA/540/R-92/077, United States Environmental Protection Agency, pp.156-157.

U.S. EPA. 1993. Handbook : Approaches for the remediation of federal facility sites contaminated with explosive or radioactive wastes. Report Number EPA/625/R-93/013, United States Environmental Protection Agency., Cincinnati, Ohio 45268.

U.S. PUBLIC HEALTH SERVICE. 1962. Public health service drinking water standards, U. S. Gov. Printing Office, Washington, DC.

VAN DER SLOOT, H. A., PIEPERS, O., & KOK, A. 1984. A standard leaching test for combustion residues. Bureau Energie Onderzoek, Netherlands Projecten BEOP-31.

VAN OLPHEN, H. 1977. An introduction to clay colloid chemistry for clay technologists, geologists and soil scientists, 2nd edn. John Wiley and Sons, Chichester.

VILLAUME, J. F., MIDDLESWORTH, B. C., & UNITES, D. F. 1981. Use of batch-wise extraction procedure for coal ash disposal evaluation. *Hazardous Solid Waste Testing: First Conference, ASTM STP 760*, R. A. CONWAY & B. C. MALLOY, Eds., American Society for Testing and Materials, pp.99-111.

WALLACE, S., BURGESS, W., DOTTRIDGE, J., KIM, A., ZAMFIRESCU, D., & ZAMFIRESCU, F. 1998. Characterization of extensive hydrocarbon contamination of an alluvial aquifer, Poiesti, Romania. *In*: LERNER, D.N. & WALTON, N. R. G. (eds) 1998. *Contaminated Land and Groundwater: Future Directions.* Geological Society, London, Engineering Geology Special Publications, **14**, pp.189-193.

WALTON, N. R. G., & HIGGINS, A. 1998. The legacy of contaminated land in Portsmouth: its identification and remediation within a socio-political context. *In*: LERNER, D.N. & WALTON, N. R. G. (eds) 1998. *Contaminated Land and Groundwater: Future Directions.* Geological Society, London, Engineering Geology Special Publications, **14,** pp.29-36.

WANG, J. W. H., MATOES, M., & DAVIDSON, D. T. 1963. Comparative effects of hydraulic, calcitic, and dolomitic limes and cement in soil stabilization. Highway Research Record 29, pp.42-54.

WATTS BLAKE BEARNE & CO. PLC. 1998. Personal communication with Watts Blake Bearne & Co. Newton Abbot, Devon, UK.

WELSH, S. K., GAGNON, J. E., & ELANABARAWY, M. T. 1981. Comparison of three acid extraction-leaching test protocols. *Hazardous Solid Waste Testing: First Conference, ASTM STP 760,* R. A. CONWAY & B. C. MALLOY, Eds., American Society for Testing and Materials, pp.28-39.

WCISLO, E. 1998, Risk assessment as a tool for guiding phytoremediation activities: a case study- the Bytom site, Poland. *In*: *Proceedings of the Fourth International Symposium and Exhibition on Environmental Contamination in Central and Eastern Europe.* CD-ROM. Warsaw, September, 1998.

WELLS, N., & WHITTON, J.S. 1977. Element composition of tomatoes grown on four soils mixed with sewage sludge. N. Z. J. Exp. Agric. **5,** pp.363-369.

WENG, C. H., & HUANG, C. P. 1994. Treatment of metal industrial wastewater by flyash and cement fixation. Journal of Environmental Engineering, **120**(6), pp.1470-1487.

WHITE, R. E. 1979. Introduction to the principles and practice of Soil Science. Blackwell Scientific, Oxford.

WHITTAKER, H., COPPER, D. A., WITAKERE, R., MALERS, J., MILLERS, J., & KOKARS, V. 1998. Remediation studies of a spill of SAMIN missile fuel at a former Soviet base in Latvia. *In*: *Proceedings of the Fourth International Symposium and Exhibition on Environmental Contamination in Central and Eastern Europe.* CD-ROM. Warsaw, September, 1998.

WILK, C. M., 1997. Stabilisation of heavy metals with Portland Cement: research synopsis. Waste Management Information, Public Works Department, Portland Cement Association, 5420 Old Orchard Road, Skokie, Illinois 60077.

WILDING, L. P., & RUTLEDGE, E. M. 1966. Cation exchange capacity as a function of organic matter, total clay and various clay fractions in a soil toposequence. Soil Society of America Proceedings, **30**, pp.782-785.

WINNICKI, T. 1998. Brackish water management on Polish copper mining area. *In*: *Proceedings of the Fourth International Symposium and Exhibition on Environmental Contamination in Central and Eastern Europe.* CD-ROM. Warsaw, September, 1998.

WRIGHT, W. R., & FOSS, J. E. 1972. Contribution of clay and organic matter to the cation exchange capacity of Maryland soils. Soil Science Society of America Proceedings, **36**, pp.115-118.

YOUNG, P. J., & WILSON, D. C. 1982. Testing of hazardous wastes to assess their suitability for landfill disposal. AERE Harwell, Environmental and Medical Sciences Division. AERE-R 10737.

ZHANG, P. C., & SPARKS, D. L. 1993. Kinetics of phenol and aniline adsorption and desorption on an organo-clay. Soil Sci. Soc. Am. J. **57**, pp.340-345.

ZHANG, Z. Z., SPARKS, D. L., & SCRIVNER, N. C. 1993. Sorption and desorption of quaternary amine cations on clays. Environmental science and technology **27**, pp.1625-1631.

ZOLKOV, E. 1962. Influence of chlorides and hydroxides of calcium and sodium on consistency limits of a fat clay. Highway Research Board, Bulletin 309, pp.109-115.

APPENDIX 1

DETAILED PRESENTATION OF THE BATCH TEST RESULTS AND THE EFFECT OF THE INITIAL OPERATING PARAMETERS ON THE SOLUTION CHEMISTRY

A1.2 BATCH EXTRACTION TESTS

Batch test results include the development of pH and conductivity during 6hr/30rmp, 6hr/60rpm, 24hr/30rpm and 24hr/60rpm tests on samples at three solid to liquid ratios and two different cube sizes as well as ICP measurement of Ca, Fe, Pb, Na, Si, Mg, Al and Mn in the final solutions of these tests. As a result of the complexity and volume of data as well as the requirement to highlight variations induced by changing operating parameters each specific clay design mix will be presented independently.

A1.2.1 English China Clay with no contaminants or lime

A1.2.1.1 Solid : liquid ratio

Inspection of Figures A1.7- A1.10 clearly illustrates that solid to liquid ratio has the most influential effect on conductivity out of the parameters tested. Increases in solid to liquid ratio in distinct increments results in discrete increases in conductivity within the range 5μS/cm to 20μS/cm. In all cases as the test duration increases so does the conductivity. pH values at specific solid to liquid ratios are very similar and are in the range 5.7-6.2. Figure A1.9 (24hr/30rpm); Figure A1.10 (24hr/60rpm) and Figure A1.7 (6hr/30rpm) do however indicate that as solid to liquid ratio increases, pH tends to decrease.

Tables A1.2 to A1.11 also highlight that as solid to liquid ratio and conductivity increases, in many cases soluble Ca and Si in solution increases although some variability is evident at the low levels measured. All other elements, Fe, Pb, Na, Mg, Al and Mn show very low levels below or near detection limits.

A1.2.1.2 Cube Size

Figures A1.7 to A1.10 illustrate that all pH and conductivity values for specific solid to liquid ratios do not change with varying cube size. Chemical data in Tables A1.2 to A1.9 do however highlight that generally at the smaller cube sizes more Ca, Na are released with no observable significant differences for the other elements

A1.2.1.3 Rotation speed and test duration

Comparison of Figure A1.7 (6hr/30rpm) and Figure A1.8 (6hr/60rpm) at 7 and 175 days curing time shows little change in final pH values and conductivity with increased rotation speed. These plots are very similar to the 24 hours tests although the higher rotation speeds generate slightly higher pH values. Increased test duration appears to release less Ca and more Si and Mg. It is also evident that the longer test duration creates slightly higher pH values. Inspection of Tables A1.2 to A1.9 suggests that at higher rotation speeds more Ca, Si and Mg are released whilst the other element are below detection limits. Furthermore, increasing test duration tends to produce higher concentrations of Si, Mg and lower concentrations of Ca

A1.2.1.4 Curing Time

In all cases the tests carried out at 7 days show the most variability in conductivity and pH between initial cube sizes at the same solid to liquid ratios. It is also evident that the scatter of pH values is most pronounced for the 24hr tests. Tables A1.2 to A1.11 indicate that as curing time increases the already low levels of soluble Si, Na, Mn and Mg decrease further whilst Al levels increase and all other elements remain relatively constant.

Figure A1.7 Conductivity and pH characteristics for English China Clay with no contaminants or lime during 6hr/30rpm Batch Tests

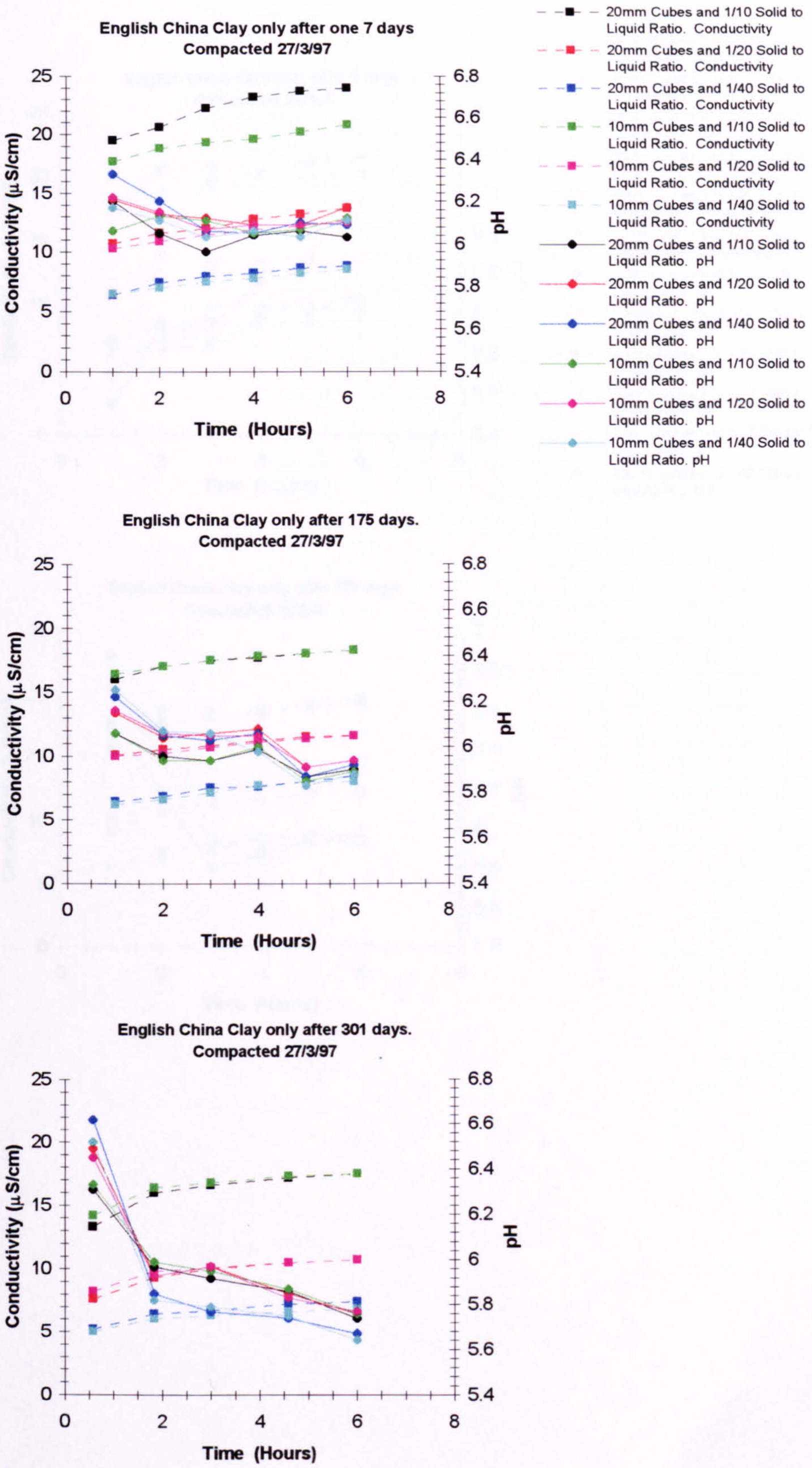

Figure A1.8 Conductivity and pH characteristics for English China Clay with no contaminants or lime during 6hr/60rpm Batch Tests

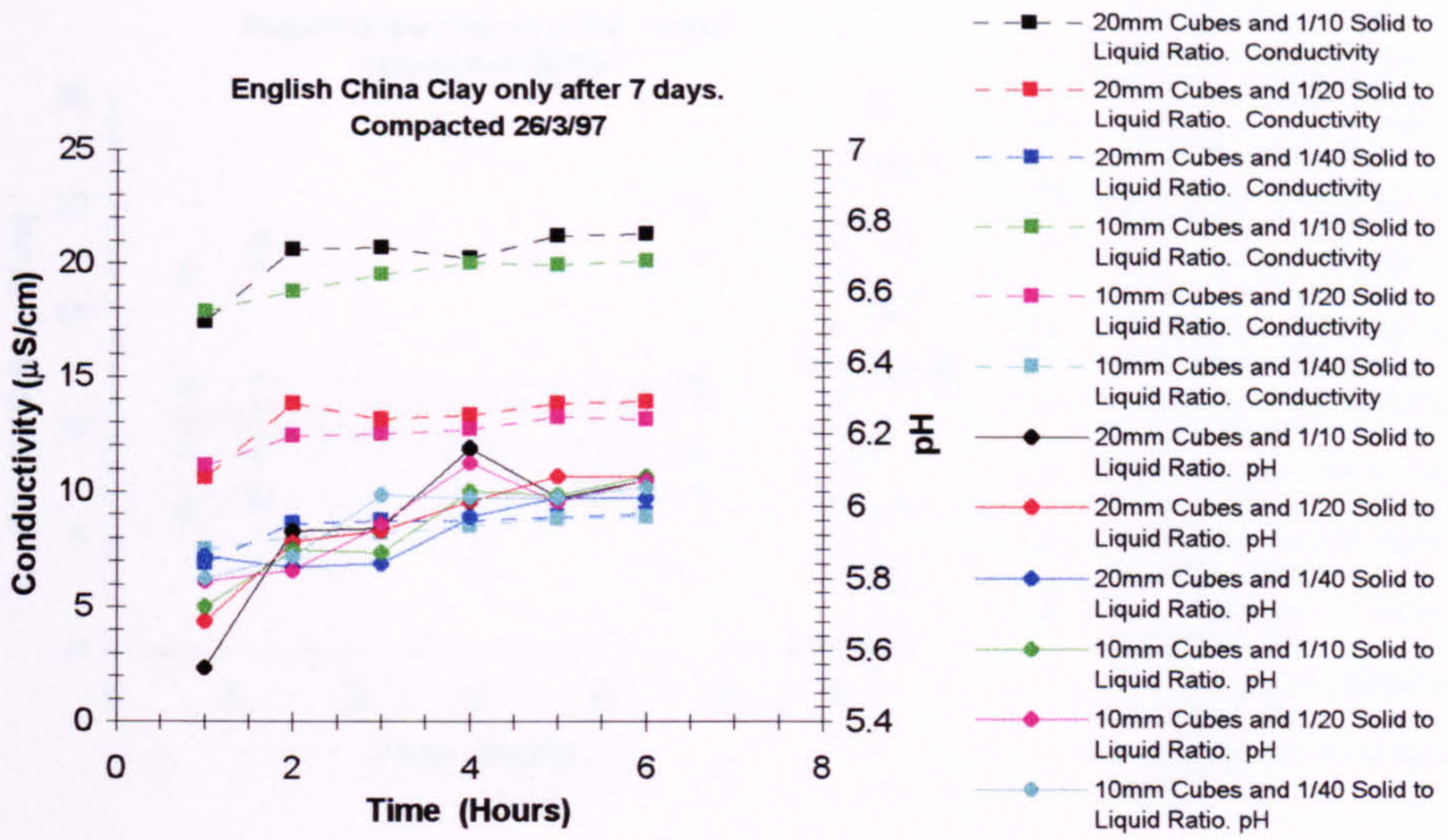

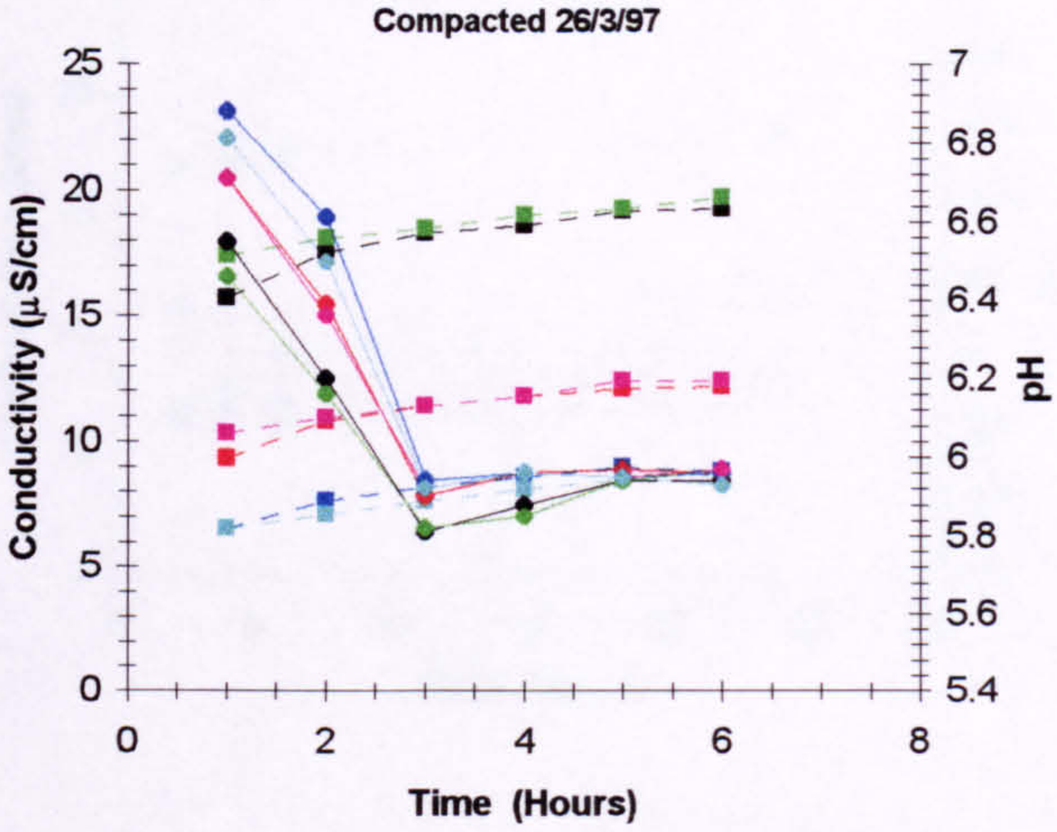

Figure A1.9 Conductivity and pH characteristics for English China Clay with no contaminants or lime during 24hr/30rpm Batch Tests

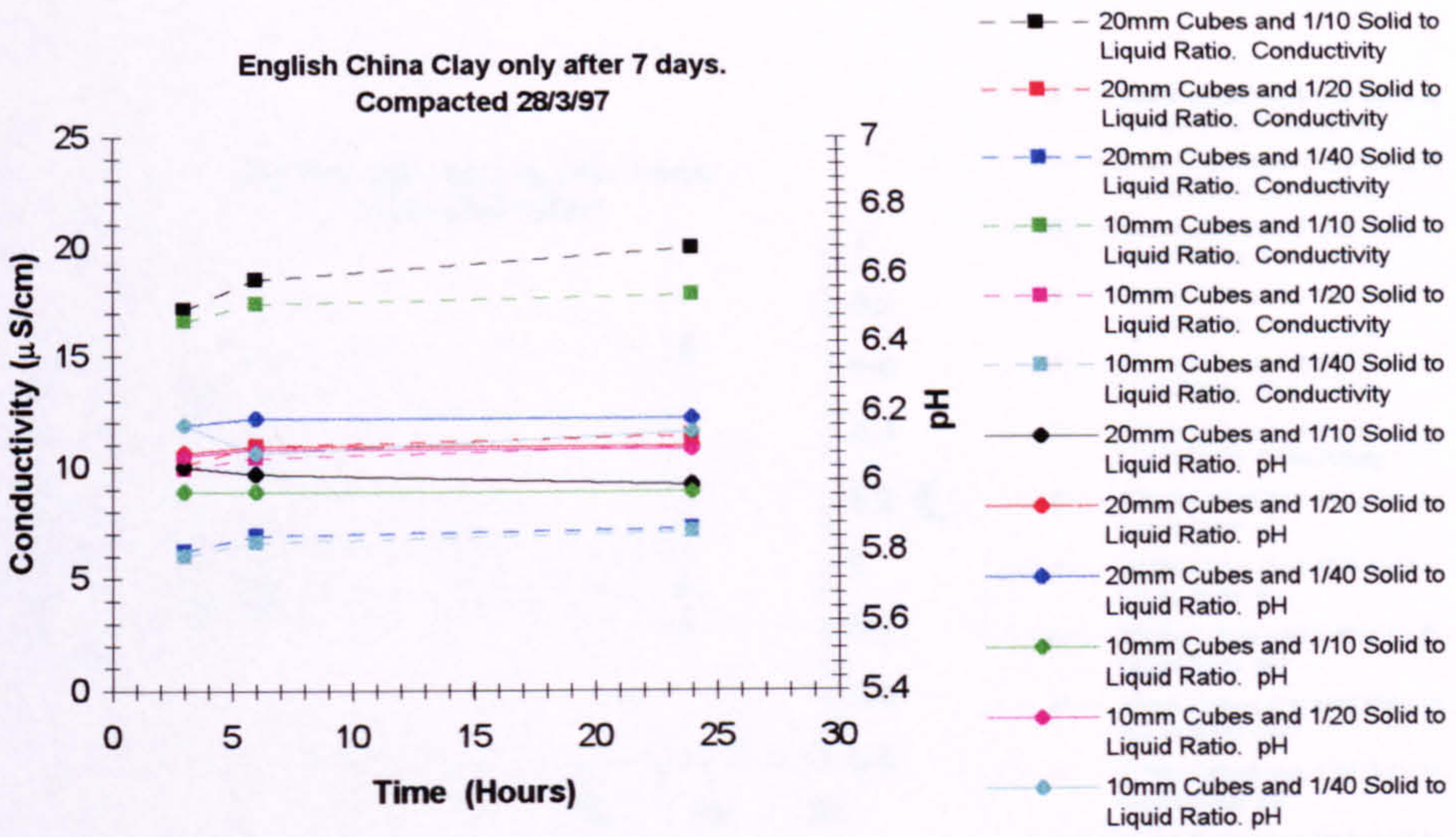

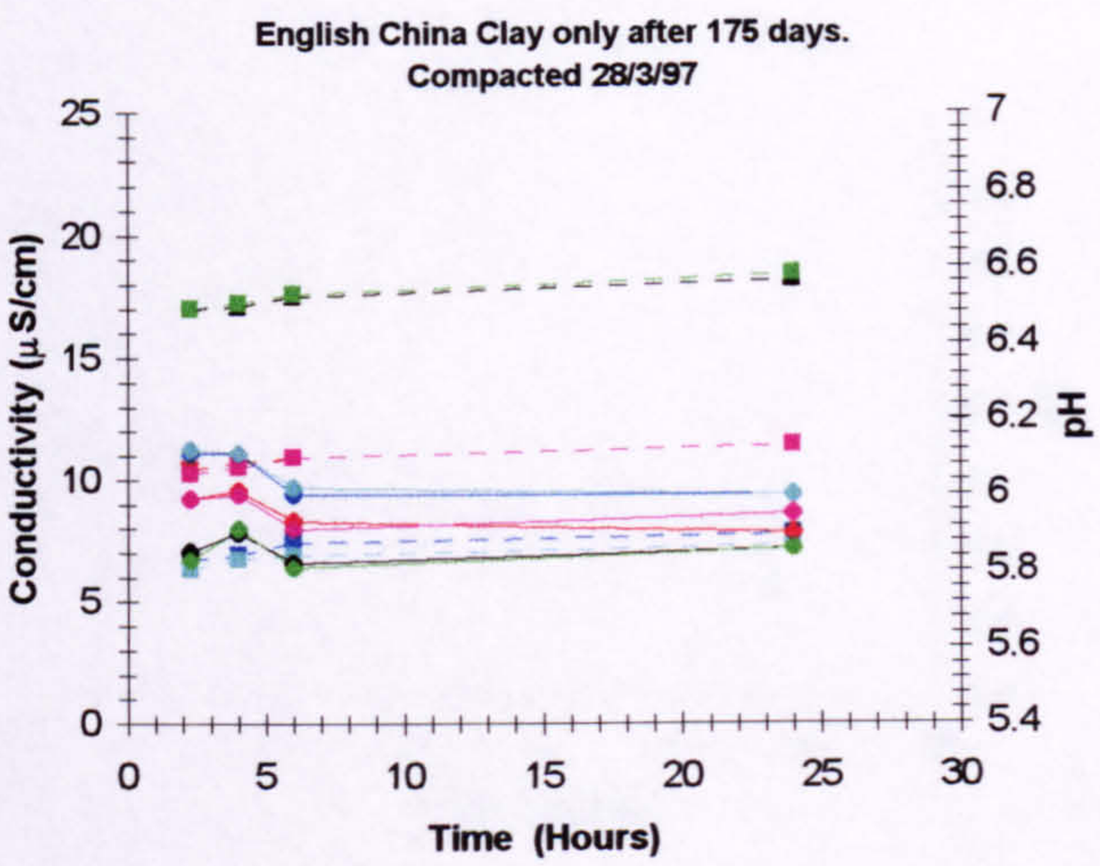

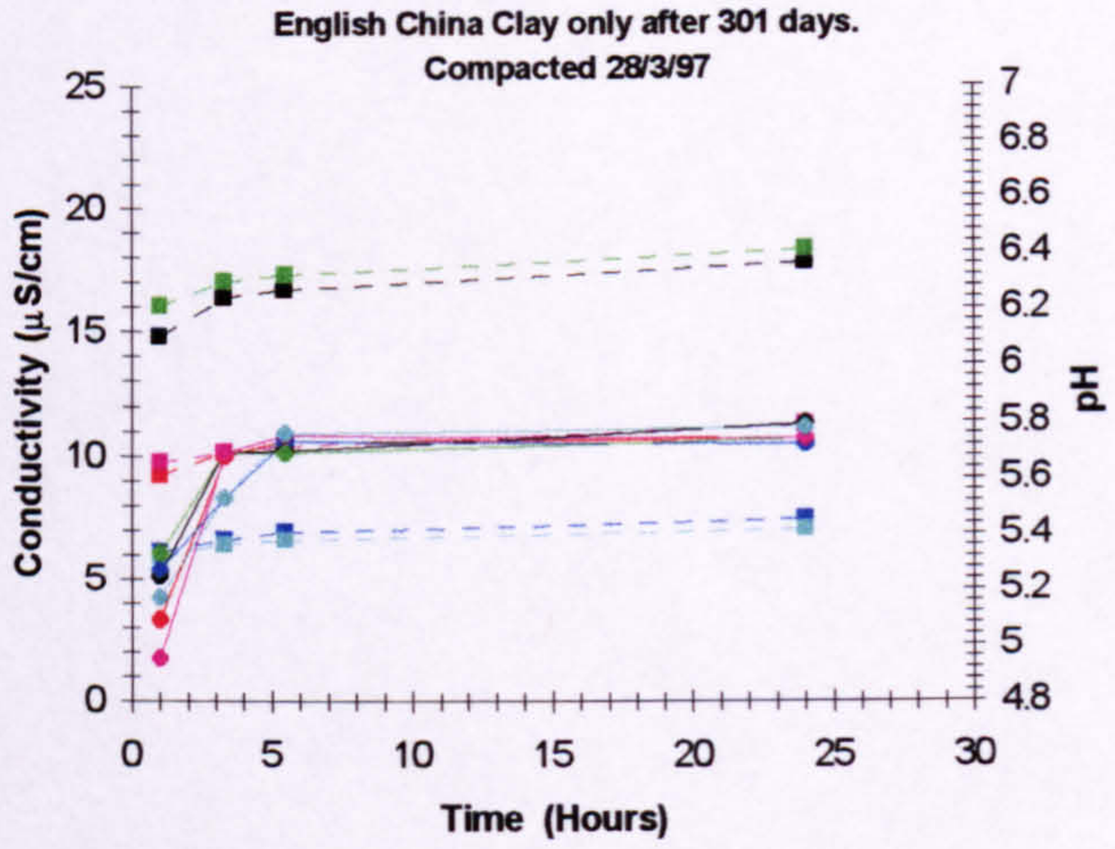

Figure A1.10 Conductivity and pH characteristics for English China Clay with no contaminants or lime during 24hr/60rpm Batch Tests

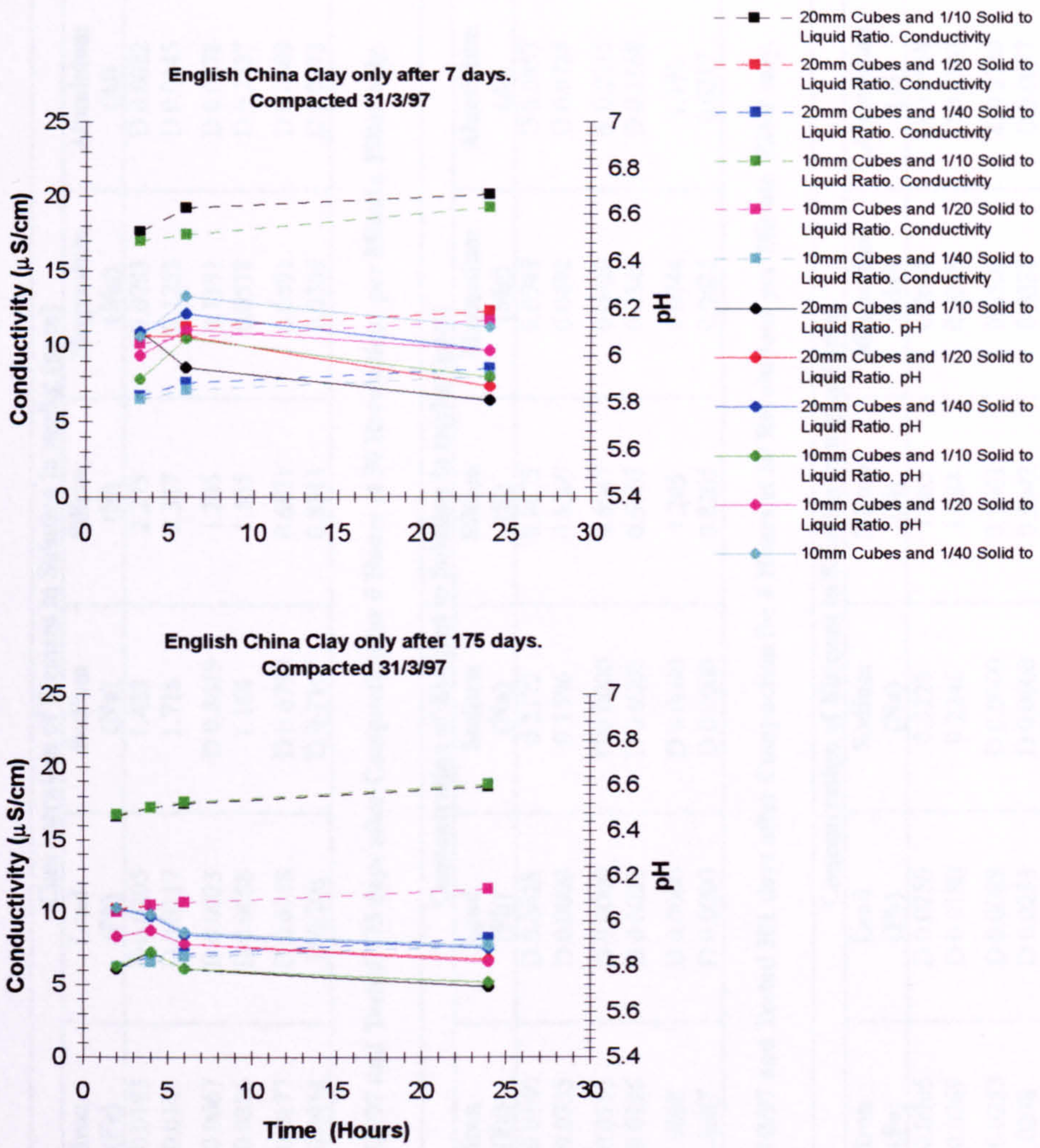

Table A1.2 ICP Data for Kaolinite only, Compacted on the 27/3/97 and Tested 7 days after Compaction for 6 Hours at 30 Revolutions per Minute. Filter only.

Solid to Liquid Ratio	Initial Cube Size (mm)	Concentration of Element in Solution in mg/kg (ppm)							
		Calcium (Ca)	Iron (Fe)	Lead (Pb)	Sodium (Na)	Silicon (Si)	Magnesium (Mg)	Aluminium (Al)	Manganese (Mn)
1/10	10	0.2224	D 0.0183	D 0.0205	1.423	2.275	0.0783	D 0.0022	D 0.0021
	20	0.3122	D 0.0143	D 0.0117	1.718	2.317	0.1253	D 0.0145	D 0.0032
1/20	10	0.2585	D 0.0067	D 0.0023	D 0.8619	1.245	0.1191	D 0.0378	D 0.0032
	20	0.1725	D 0.0386	D 0.0088	1.164	1.535	0.0518	D 0.2537	D 0.0021
1/40	10	0.2282	D 0.0177	D 0.0158	D 0.6790	0.6831	0.0591	D 0.0589	D 0.0021
	20	0.1539	D 0.0454	D 0.101	D 0.7167	0.8311	0.0359	D 0.0975	D 0.0023

Table A1.3 ICP Data for Kaolinite only, Compacted on the 27/3/97 and Tested 175 days after Compaction for 6 Hours at 30 Revolutions per Minute. Filter only.

Solid to Liquid Ratio	Initial Cube Size (mm)	Concentration of Element in Solution in mg/kg (ppm)							
		Calcium (Ca)	Iron (Fe)	Lead (Pb)	Sodium (Na)	Silicon (Si)	Magnesium (Mg)	Aluminium (Al)	Manganese (Mn)
1/10	10	0.5544	D 0.0140	D 0.0028	0.2172	0.8675	0.0748	D 0.0857	D 0.0014
	20	0.2551	D 0.0735	D 0.0000	0.1596	0.8507	0.0492	D 0.0728	D 0.0018
1/20	10	0.1963	D 0.0152	D 0.0000	D 0.0000	0.6047	0.0420	d. 0.2015	D 0.0013
	20	0.2281	D 0.0126	D 0.0025	D 0.0000	0.5503	0.0343	D 0.1168	D 0.0013
1/40	10	0.2631	0.0808	D 0.0000	D 0.0000	1.245	0.0744	1.195	D 0.0021
	20	0.2322	0.0687	D 0.0000	D 0.0000	0.8265	0.0628	0.6317	0.0053

Table A1.4 ICP Data for Kaolinite only, Compacted on the 27/3/97 and Tested 301 days after Compaction for 6 Hours at 30 Revolutions per Minute. Filter only.

Solid to Liquid Ratio	Initial Cube Size (mm)	Concentration of Element in Solution in mg/kg (ppm)							
		Calcium (Ca)	Iron (Fe)	Lead (Pb)	Sodium (Na)	Silicon (Si)	Magnesium (Mg)	Aluminium (Al)	Manganese (Mn)
1/10	10	0.6033	D 0.0905	D 0.0250	0.3229	1.065	0.0648	D 0.0868	D 0.0016
	20	0.2664	D 0.0269	D 0.0180	0.2246	1.024	0.0289	D 0.0563	D 0.0002
1/20	10	0.3981	d. 0.0253	D 0.0088	D 0.0000	0.7461	0.0508	d. 0.2330	D 0.0006
	20	0.2565	0.0298	D 0.0253	D 0.0000	0.5942	0.0323	D 0.0637	D 0.0005
1/40	10	0.2711	0.0489	D 0.0000	D 0.0000	0.7407	0.0301	0.4602	D 0.0007
	20	0.3741	0.1665	D 0.0000	0.2064	3.013	0.1204	2.924	D 0.0021

Note: 'D' indicates the stated value is below detection limits and the value stated is a system estimate.
'd' indicates the stated value is close to detection limits.

Table A1.5 ICP Data for Kaolinite only, Compacted on the 26/3/97 and Tested 7 days after Compaction for 6 Hours at 60 Revolutions per Minute. Filter only.

Solid to Liquid Ratio	Initial Cube Size (mm)	Concentration of Element in Solution in mg/kg (ppm)							
		Calcium (Ca)	Iron (Fe)	Lead (Pb)	Sodium (Na)	Silicon (Si)	Magnesium (Mg)	Aluminium (Al)	Manganese (Mn)
1/10	10	0.3369	D 0.0159	D 0.0060	1.491	2.353	0.1853	D 0.0457	D 0.0046
	20	0.2359	D 0.0120	D 0.0067	1.631	2.786	0.1416	D 0.1942	D 0.0039
1/20	10	0.2001	D 0.0162	D 0.0108	D 0.9943	1.588	0.1065	D 0.0248	D 0.0032
	20	0.2175	D 0.0057	D 0.0133	1.238	1.494	0.1074	D 0.0518	D 0.0034
1/40	10	0.1165	D 0.0081	D 0.0000	D 0.8647	0.9493	0.0309	D 0.0506	D 0.0012
	20	0.1618	D 0.0306	D 0.0000	D 0.6548	0.8570	0.0523	D 0.0400	D 0.0018

Table A1.6 ICP Data for Kaolinite only, Compacted on the 26/3/97 and Tested 175 days after Compaction for 6 Hours at 60 Revolutions per Minute. Filter only.

Solid to Liquid Ratio	Initial Cube Size (mm)	Concentration of Element in Solution in mg/kg (ppm)							
		Calcium (Ca)	Iron (Fe)	Lead (Pb)	Sodium (Na)	Silicon (Si)	Magnesium (Mg)	Aluminium (Al)	Manganese (Mn)
1/10	10	0.5695	D 0.0357	D 0.0000	0.4120	0.9779	0.1375	D 0.1191	D 0.0036
	20	0.3740	d. 0.0245	D 0.0059	0.3780	0.9279	0.0885	D 0.1016	D 0.0030
1/20	10	0.3147	d. 0.0166	D 0.0000	D 0.0000	0.5857	0.0684	D 0.1151	D 0.0029
	20	0.4108	0.0591	D 0.0000	D 0.0000	0.6146	0.0881	D 0.1450	d. 0.0047
1/40	10	0.3616	0.0428	D 0.0014	D 0.0000	0.7608	0.0644	0.5008	D 0.0027
	20	2.347	0.0519	D 0.0000	D 0.0000	0.7471	0.0554	0.4661	d. 0.0049

Note: 'D' indicates the stated value is below detection limits and the value stated is a system estimate.
'd' indicates the stated value is close to detection limits.

Table A1.7 ICP Data for Kaolinite only, Compacted on the 28/3/97 and Tested 7 days after Compaction for 24 Hours at 30 Revolutions per Minute. Filter only.

Solid to Liquid Ratio	Initial Cube Size (mm)	Concentration of Element in Solution in mg/kg (ppm)							
		Calcium (Ca)	Iron (Fe)	Lead (Pb)	Sodium (Na)	Silicon (Si)	Magnesium (Mg)	Aluminium (Al)	Manganese (Mn)
1/10	10	0.1201	D 0.0051	D 0.0038	1.392	2.909	0.0688	D 0.0217	D 0.0023
	20	0.1909	D 0.0172	D 0.0000	1.675	2.850	0.1104	D 0.0426	d. 0.0053
1/20	10	0.0817	D 0.0117	D 0.0017	D 0.8353	1.849	0.0518	D 0.1663	D 0.0031
	20	0.1152	D 0.0143	D 0.0000	D 1.042	1.684	0.0551	D 0.0687	D 0.0025
1/40	10	0.1177	D 0.0085	D 0.0038	D 0.7251	0.9910	0.1004	D 0.0801	D 0.0024
	20	0.1084	D 0.0096	D 0.0212	D 0.8624	1.004	0.0558	D 0.0534	D 0.0030

Table A1.8 ICP Data for Kaolinite only, Compacted on the 28/3/97 and Tested 175 days after Compaction for 24 Hours at 30 Revolutions per Minute. Filter only.

Solid to Liquid Ratio	Initial Cube Size (mm)	Concentration of Element in Solution in mg/kg (ppm)							
		Calcium (Ca)	Iron (Fe)	Lead (Pb)	Sodium (Na)	Silicon (Si)	Magnesium (Mg)	Aluminium (Al)	Manganese (Mn)
1/10	10	0.2737	D 0.0114	D 0.0000	0.2825	1.126	0.0502	D 0.1150	D 0.0034
	20	0.2202	D 0.0277	D 0.0000	0.1678	1.105	0.0441	D 0.0926	D 0.0030
1/20	10	0.1707	D 0.0118	D 0.0000	D 0.0000	0.7072	0.0320	D 0.1460	D 0.0013
	20	0.2285	D 0.0150	D 0.0000	D 0.0000	0.7417	0.0473	D 0.1933	D 0.0022
1/40	10	0.4166	0.1142	D 0.0000	D 0.0000	2.566	0.0919	2.795	D 0.0027
	20	0.2257	D 0.0277	D 0.0000	D 0.0000	0.6194	0.0442	d. 0.3338	D 0.0017

Table A1.9 ICP Data for Kaolinite only, Compacted on the 28/3/97 and Tested 301 days after Compaction for 24 Hours at 30 Revolutions per Minute. Filter only.

Solid to Liquid Ratio	Initial Cube Size (mm)	Concentration of Element in Solution in mg/kg (ppm)							
		Calcium (Ca)	Iron (Fe)	Lead (Pb)	Sodium (Na)	Silicon (Si)	Magnesium (Mg)	Aluminium (Al)	Manganese (Mn)
1/10	10	0.0663	d. 0.0398	D 0.0064	0.9598	1.577	0.0271	0.3031	D 0.0007
	20	0.1220	0.0103	D 0.0184	0.8440	1.409	0.0339	0.1958	D 0.0014
1/20	10	0.1385	d. 0.0120	D 0.0186	0.6095	0.8514	0.0276	d. 0.1578	D 0.0003
	20	0.0673	0.0310	D 0.0000	0.5189	1.034	0.0235	0.3141	D 0.0003
1/40	10	0.1117	d. 0.0184	D 0.0102	d. 0.3111	0.6196	0.0219	0.2231	D 0.0003
	20	1.489	0.0361	D 0.0003	0.5655	1.562	0.0683	1.008	D 0.0011

Note : 'D' indicates the stated value is below detection limits and the value stated is a system estimate.
'd' indicates the stated value is close to detection limits.

Table A1.10 ICP Data for Kaolinite only, Compacted on the 31/3/97 and Tested 7 days after Compaction for 24 Hours 60 Revolutions per Minute. Filter only.

Solid to Liquid Ratio	Initial Cube Size (mm)	Concentration of Element in Solution in mg/kg (ppm)							
		Calcium (Ca)	Iron (Fe)	Lead (Pb)	Sodium (Na)	Silicon (Si)	Magnesium (Mg)	Aluminium (Al)	Manganese (Mn)
1/10	10	0.3963	D 0.0049	D 0.0168	1.329	3.153	0.2897	D 0.0738	0.0090
	20	0.2698	D 0.0109	D 0.0000	1.349	3.175	0.0911	D 0.0693	d. 0.0057
1/20	10	0.1964	D 0.0068	D 0.0284	D 0.7236	1.889	0.0603	D 0.1596	D 0.0037
	20	0.1759	D 0.0043	D 0.0075	D 0.7240	1.650	0.1250	D 0.0174	D 0.0053
1/40	10	0.1266	D 0.0069	D 0.0000	D 0.4478	0.9586	0.0408	D 0.0604	D 0.0052
	20	0.1646	D 0.0172	D 0.0000	D 0.5005	1.520	0.0621	D 0.3894	D 0.0028

Table A1.11 ICP Data for Kaolinite only, Compacted on the 31/3/97 and Tested 175 days after Compaction for 24 Hours at 60 Revolutions per Minute. Filter only.

Solid to Liquid Ratio	Initial Cube Size (mm)	Concentration of Element in Solution in mg/kg (ppm)							
		Calcium (Ca)	Iron (Fe)	Lead (Pb)	Sodium (Na)	Silicon (Si)	Magnesium (Mg)	Aluminium (Al)	Manganese (Mn)
1/10	10	0.3095	d. 0.0149	D 0.0000	0.1102	1.221	0.0495	D 0.1387	D 0.0030
	20	0.3258	D 0.0242	D 0.0000	0.1287	1.125	0.0405	D 0.1025	D 0.0035
1/20	10	0.2783	D 0.0308	D 0.0000	D 0.0000	0.7651	0.0435	D 0.1616	D 0.0016
	20	0.2261	D 0.0185	D 0.0057	D 0.0000	0.8879	0.0341	D 0.3128	0.0085
1/40	10	1.529	0.0675	D 0.0000	D 0.0000	1.534	0.0431	1.418	D 0.0019
	20	0.3190	0.1186	D 0.0000	D 0.0000	2.560	0.0844	2.734	D 0.0021

Note: 'D' indicates the stated value is below detection limits and the value stated is a system estimate.
'd' indicates the stated value is close to detection limits.

A1.2.2 English China Clay with 2500ppm Pb and no lime

A1.2.2.1 Solid : liquid ratio

Inspection of Figures A1.11 to A1.14 highlights solid to liquid ratio has the largest effect on conductivity and pH. Unlike the uncontaminated sample with no lime, as solid to liquid ratio increases in discrete increments conductivity increases in discrete increments and pH decreases. Doubling the solid to liquid ratio doubles conductivity. The conductivity of the solid to liquid ratios 1:10, 1:20 and 1:40 are all generally approximately 290µS/cm, 150µS/cm and 80µS/cm respectively.

pH values range from 4.6-5.8 depending on the solid to liquid ratio. The lower solid to liquid ratios tend to produce more variable pH values between cube sizes for specific solid to liquid ratios although conductivity measurements remain similar.

Tables A1.12 to A1.21 illustrate doubling the solid to liquid ratio doubles the concentrations of Ca, Pb, Mg and Mn in solution, whilst Si concentrations nearly double and Na concentrations increase. At the 1:10 solid to liquid ratio the concentration of Ca≈10ppm, Pb≈80ppm, Na≈2ppm, Si≈3ppm, Mg≈8ppm and Mn≈0.6ppm, whilst Fe and Al are below detection limits.

A1.2.2.2 Cube Size

Figures A1.11 to A1.14 illustrate that generally the 10mm cube sizes produce slightly higher solution pH values, especially at the lower solid to liquid ratios. Considering conductivity the 10mm cubes achieve the plateaux value the quickest with both sizes ultimately producing the same final value. During the 30rpm tests the 10mm cubes generally release slightly more Ca whilst Pb, Na, Si, Mg and Mn appear in similar quantities for all cube sizes.

A1.2.2.3 Rotation speed and test duration

Comparison of Figures A1.11 to A1.13 illustrates that generally the 6hr/30rpm tests produce slightly higher pH values than 24hr/30rpm tests, although, conductivity is similar in all cases. With the exception of high variability at low solid to liquid ratios the 6hr/60rpm and 24hr/60rpm tests illustrated in Figures A1.12 and A1.14 do not show significant variation in pH and conductivity due to the extended test duration. Changing the rotation speed from 30rpm to 60rpm does not appear to

produce higher pH values for the 20mm cubes relative to the 10mm cubes for the lower solid to liquid ratios. In all cases the 6hr/60rpm tests (Figure A1.12) clearly produce the least variability between cube sizes at any solid to liquid ratio. However, although pH values do not vary significantly during 6hr tests, values tend to rise during 24hr tests at all curing time periods.

Comparison of Tables A1.12, A1.13, A1.14 and A1.17, A1.18, A1.19 illustrates that 24hr/30rpm tests release more Pb, Si, Mg, Mn and less Ca than 6hr/30rpm tests. This trend is also similar when comparing 24hr/60rpm and 6hr/60rpm tests. The other elements not mentioned due not appear to change significantly. The lower test rotation speeds release more Ca and less Pb, Na, Si, Mg and Mn for both 6hr and 24 hr tests.

A1.2.2.4 Curing Time

With the exception of the 1:40 solid to liquid ratio, increasing curing time results in the 10mm and 20mm cube sizes producing similar pH values. As curing time increases the final batch pHs reduce by approximately 0.1 depending on the initial solid to liquid ratio whilst conductivity values do not appear to change.

Analysis of Tables A1.12 to A1.21 illustrates that as curing time increases Pb and Si concentrations decrease whilst Na levels increase with Mg, Ca and Mn remaining relatively constant for specific solid to liquid ratios and test parameters.

Figure A1.11 Conductivity and pH characteristics for English China Clay with 2500ppm Pb and no lime during 6hr/30rpm Batch Tests

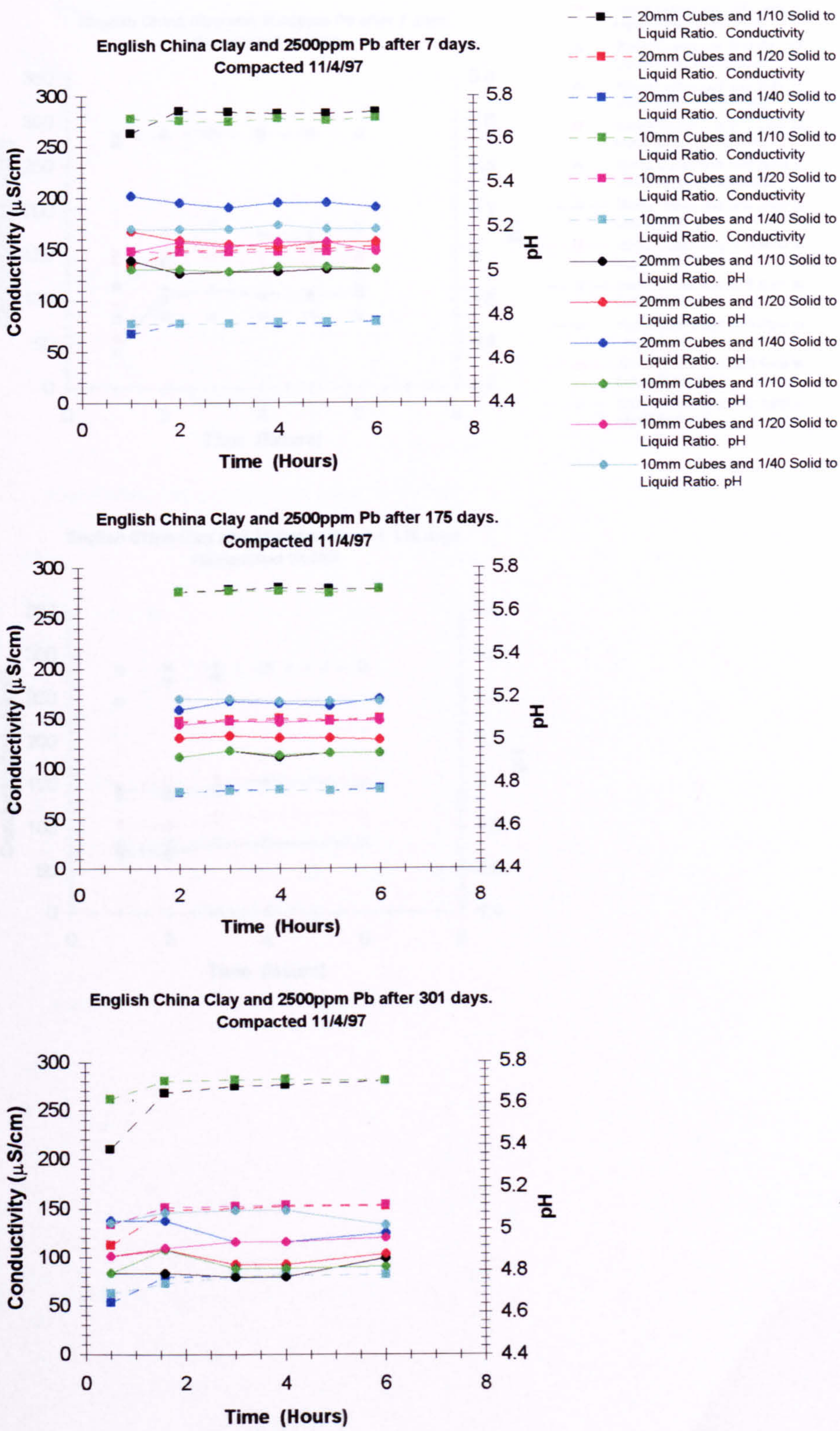

Figure A1.12 Conductivity and pH characteristics for English China Clay with 2500ppm Pb and no lime during 6hr/60rpm Batch Tests

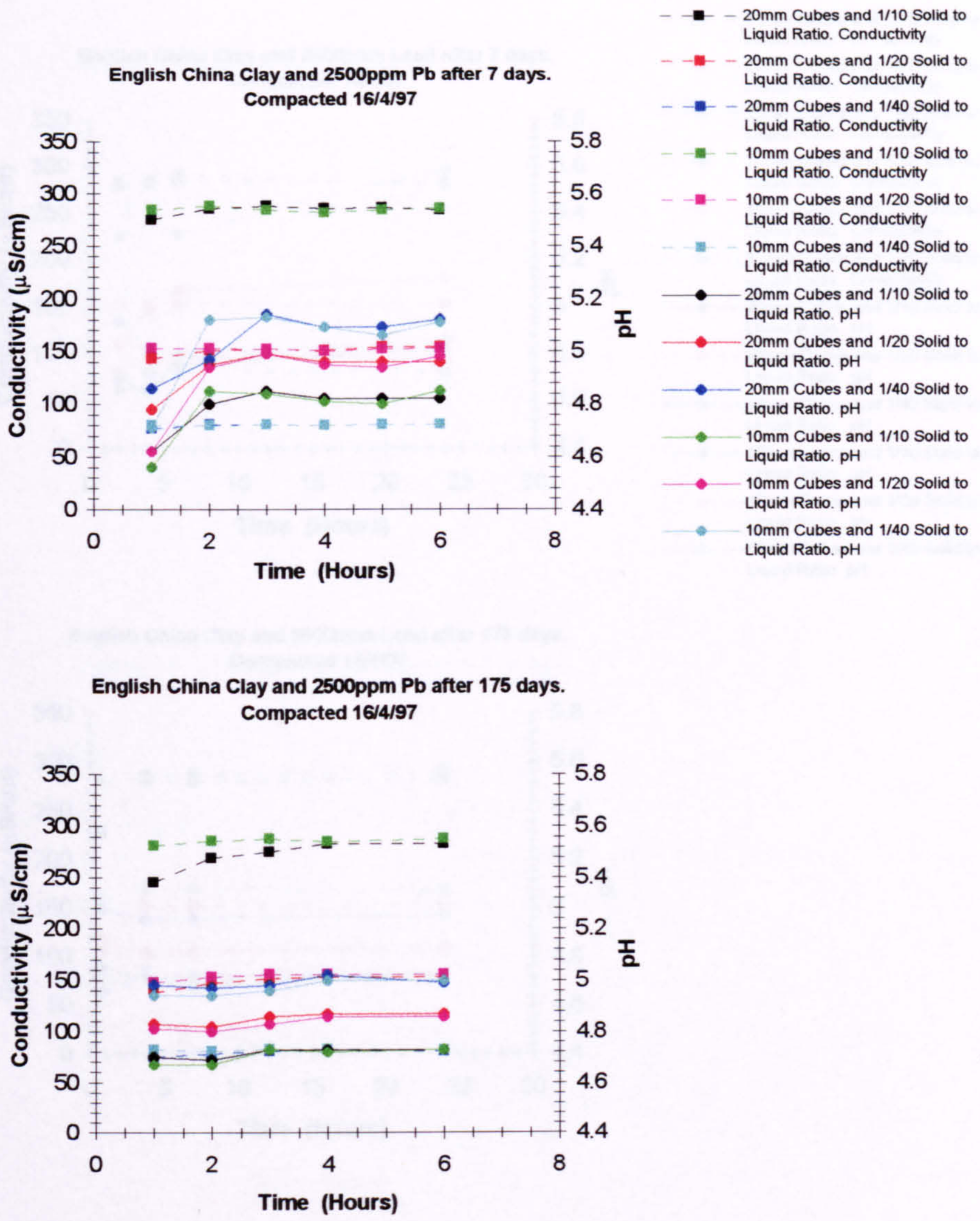

Figure A1.13 Conductivity and pH characteristics for English China Clay with 2500ppm Pb and no lime during 24hr/30rpm Batch Tests

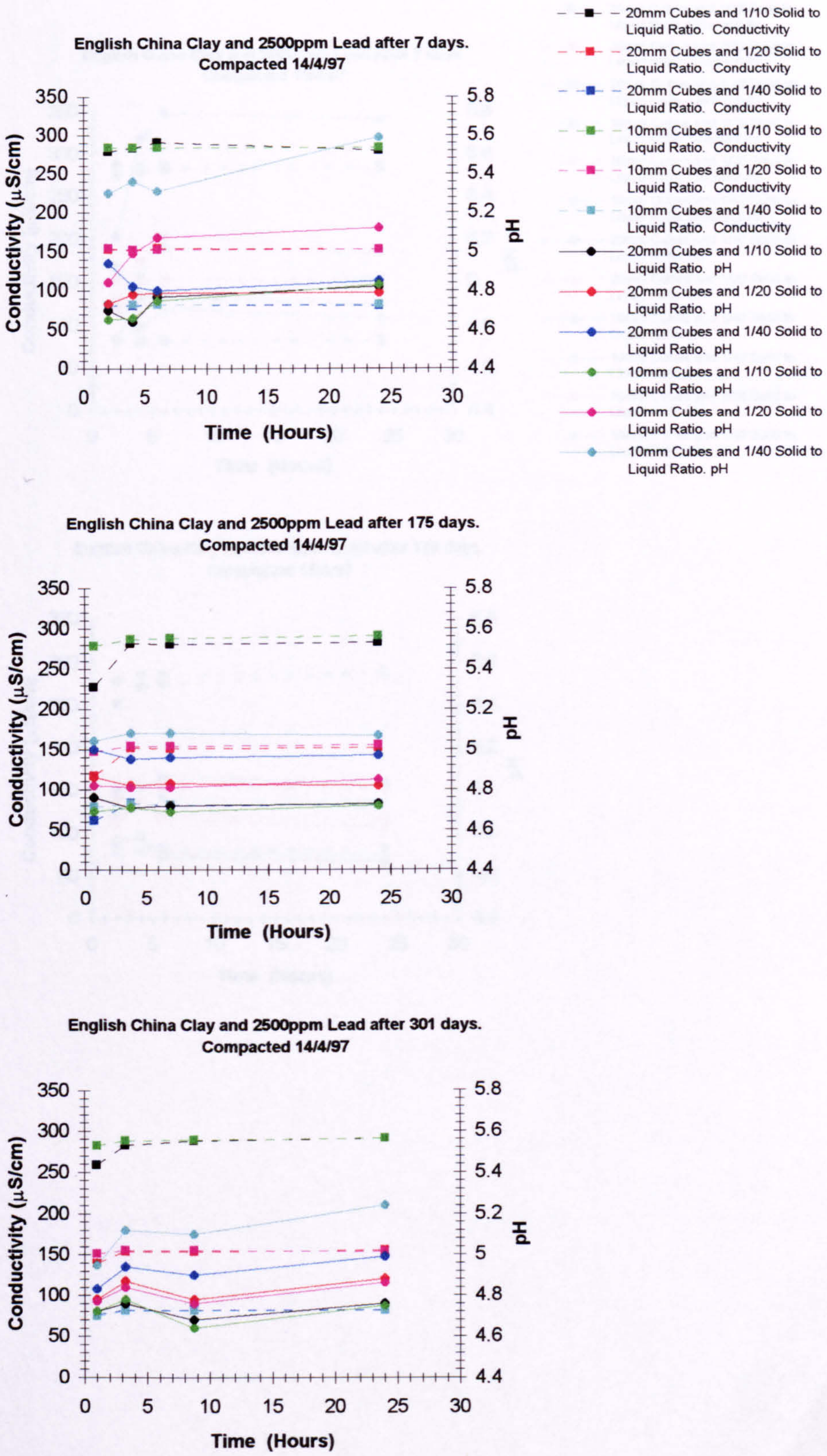

Figure A1.14 Conductivity and pH characteristics for English China Clay with 2500ppm Pb and no lime during 24hr/60rpm Batch Tests

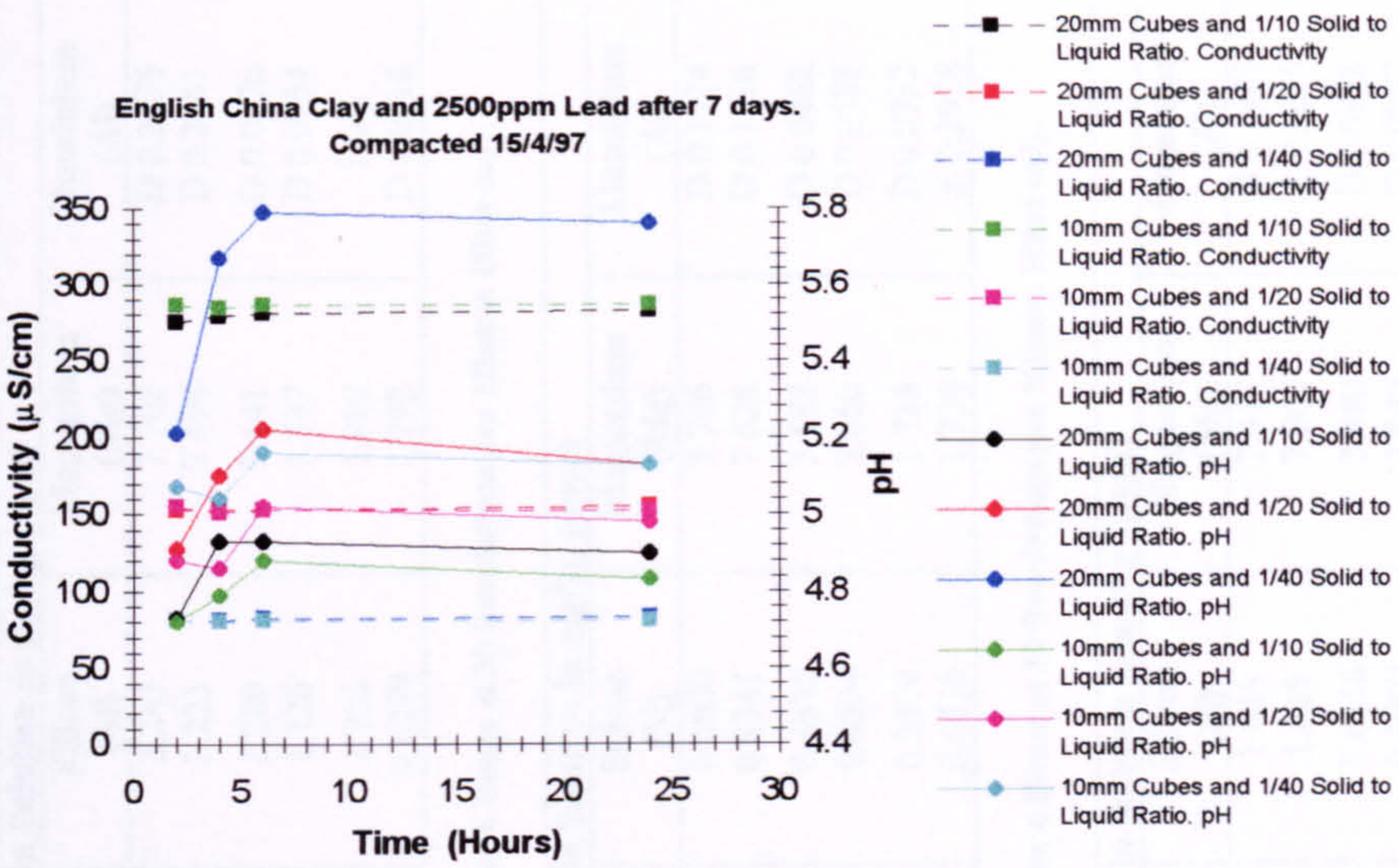

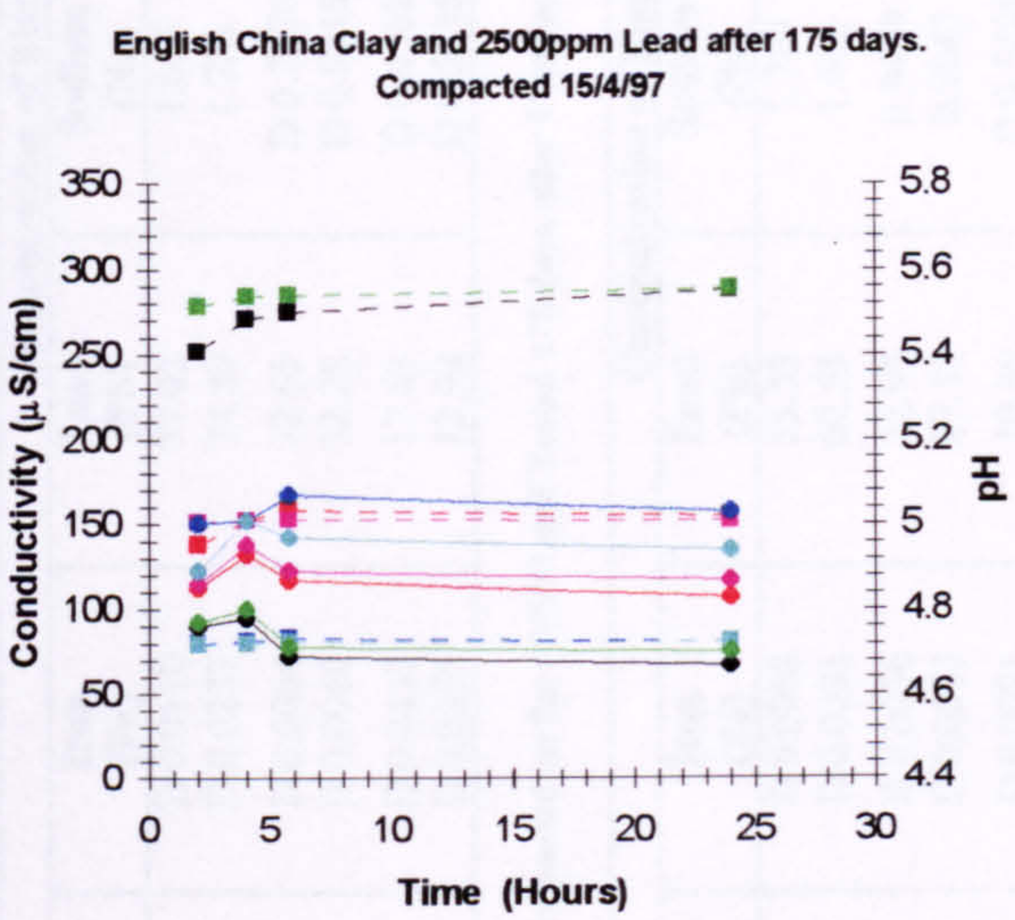

Table A1.12 ICP Data for Kaolinite and 2500ppm Lead, Compacted on the 11/4/97 and Tested 7 days after Compaction for 6 Hours at 30 Revolutions per Minute. Filter only.

Solid to Liquid Ratio	Initial Cube Size (mm)	Concentration of Element in Solution in mg/kg (ppm)							
		Calcium (Ca)	Iron (Fe)	Lead (Pb)	Sodium (Na)	Silicon (Si)	Magnesium (Mg)	Aluminium (Al)	Manganese (Mn)
1/10	10	12.83	D 0.0110	77.02	1.627	2.243	7.702	D 0.2675	0.3967
	20	12.37	D 0.0237	74.30	1.786	2.225	7.494	D 0.2661	0.3887
1/20	10	6.405	D 0.0064	32.65	D 0.7676	1.200	3.641	D 0.0876	0.1915
	20	6.077	D 0.0060	32.28	D 0.9919	1.126	3.537	D 0.0754	0.1820
1/40	10	2.719	D 0.0432	17.69	D 0.4562	2.786	1.980	1.661	0.1031
	20	3.848	D 0.0055	12.98	D 0.5735	0.6278	1.792	D 0.0518	0.0918

Table A1.13 ICP Data for Kaolinite and 2500ppm Lead, Compacted on the 11/4/97 and Tested 175 days after Compaction for 6 Hours at 30 Revolutions per Minute. Filter only.

Solid to Liquid Ratio	Initial Cube Size (mm)	Concentration of Element in Solution in mg/kg (ppm)							
		Calcium (Ca)	Iron (Fe)	Lead (Pb)	Sodium (Na)	Silicon (Si)	Magnesium (Mg)	Aluminium (Al)	Manganese (Mn)
1/10	10	14.06	D 0.0068	55.53	1.710	0.8600	7.706	D 0.1134	0.4403
	20	13.71	D 0.0091	60.53	1.658	0.8341	7.626	D 0.1316	0.4414
1/20	10	6.106	D 0.0036	22.97	0.9459	0.4678	3.583	D 0.0462	0.2046
	20	5.467	D 0.0045	27.57	0.9043	0.4594	3.650	D 0.0588	0.2125
1/40	10	2.907	D 0.0021	10.96	D 0.5400	0.2594	1.738	D 0.0382	0.0987
	20	3.144	D 0.0096	10.68	D 0.5950	0.4510	1.739	d. 0.2958	0.1000

Table A1.14 ICP Data for Kaolinite and 2500ppm Lead, Compacted on the 11/4/97 and Tested 301 days after Compaction for 6 Hours at 30 Revolutions per Minute. Filter only.

Solid to Liquid Ratio	Initial Cube Size (mm)	Concentration of Element in Solution in mg/kg (ppm)							
		Calcium (Ca)	Iron (Fe)	Lead (Pb)	Sodium (Na)	Silicon (Si)	Magnesium (Mg)	Aluminium (Al)	Manganese (Mn)
1/10	10	13.73	d. 0.0176	64.54	1.806	1.043	7.911	D 0.1915	0.4516
	20	13.43	d. 0.0359	66.98	1.831	1.025	7.864	d. 0.2013	0.4525
1/20	10	5.672	D 0.0145	30.12	1.093	0.6156	3.880	D 0.0818	0.2221
	20	5.770	D 0.0110	27.92	1.222	0.5967	3.849	D 0.0847	0.2205
1/40	10	2.854	D 0.0092	12.32	0.6961	0.3630	1.801	D 0.0468	0.1034
	20	2.967	d. 0.0033	12.34	0.7809	0.3551	1.838	D 0.0756	0.1044

Note: 'D' indicates the stated value is below detection limits and the value stated is a system estimate.
'd' indicates the stated value is close to detection limits.

Table A1.15 ICP Data for Kaolinite and 2500ppm Lead, Compacted on the 16/4/97 and Tested 7 days after Compaction for 6 Hours at 60 Revolutions per Minute. Filter only.

Solid to Liquid Ratio	Initial Cube Size (mm)	Concentration of Element in Solution in mg/kg (ppm)							
		Calcium (Ca)	Iron (Fe)	Lead (Pb)	Sodium (Na)	Silicon (Si)	Magnesium (Mg)	Aluminium (Al)	Manganese (Mn)
1/10	10	10.30	D 0.0128	72.11	1.814	2.520	7.964	D 0.4949	0.6344
	20	10.73	D 0.0110	80.40	1.847	2.424	8.053	D 0.3661	0.6395
1/20	10	5.194	D 0.0093	40.45	D 0.8611	1.183	3.917	D 0.1238	0.3170
	20	4.988	D 0.0105	37.38	d. 0.9775	1.261	3.863	D 0.1883	0.3068
1/40	10	2.675	D 0.0063	17.00	D 0.6030	0.6455	1.951	D 0.0628	0.1506
	20	2.522	D 0.0113	16.81	D 0.5858	0.8431	1.884	D 0.2207	0.1480

Table A1.16 ICP Data for Kaolinite and 2500ppm Lead, Compacted on the 16/4/97 and Tested 175 days after Compaction for 6 Hours at 60 Revolutions per Minute. Filter only.

Solid to Liquid Ratio	Initial Cube Size (mm)	Concentration of Element in Solution in mg/kg (ppm)							
		Calcium (Ca)	Iron (Fe)	Lead (Pb)	Sodium (Na)	Silicon (Si)	Magnesium (Mg)	Aluminium (Al)	Manganese (Mn)
1/10	10	9.199	D 0.0053	70.05	1.575	0.8048	7.985	D 0.1845	0.6777
	20	9.297	D 0.0065	69.42	1.743	0.8160	8.008	D 0.1891	0.6790
1/20	10	5.049	D 0.0016	33.03	0.8902	0.4522	4.114	D 0.0684	0.3503
	20	5.327	D 0.0032	32.33	1.298	0.4410	3.904	D 0.0548	0.3370
1/40	10	2.527	D 0.0125	14.53	D 0.6211	0.3633	1.938	D 0.1446	0.1673
	20	2.739	D 0.0000	12.23	0.7376	0.2313	1.819	D 0.0306	0.1559

Note: 'D' indicates the stated value is below detection limits and the value stated is a system estimate.
'd' indicates the stated value is close to detection limits.

Table A1.17 ICP Data for Kaolinite and 2500ppm Lead, Compacted on the 14/4/97 and Tested 7 days after Compaction for 24 Hours at 30 Revolutions per Minute. Filter only.

Solid to Liquid Ratio	Initial Cube Size (mm)	Concentration of Element in Solution in mg/kg (ppm)							
		Calcium (Ca)	Iron (Fe)	Lead (Pb)	Sodium (Na)	Silicon (Si)	Magnesium (Mg)	Aluminium (Al)	Manganese (Mn)
1/10	10	13.64	D 0.0070	80.69	1.670	3.028	7.930	D 0.2769	0.6078
	20	10.37	D 0.0097	81.01	1.840	3.188	8.163	D 0.3404	0.6328
1/20	10	6.949	D 0.0163	34.97	D 0.8716	1.967	3.690	D 0.3587	0.2905
	20	5.173	D 0.0134	35.93	D 0.9261	2.112	3.874	D 0.4078	0.2980
1/40	10	5.079	D 0.0026	12.17	D 0.4394	0.9041	1.732	D 0.0485	0.1350
	20	2.649	D 0.0062	16.63	D 0.4981	1.007	1.938	D 0.1261	0.1488

Table A1.18 ICP Data for Kaolinite and 2500ppm Lead, Compacted on the 14/4/97 and Tested 175 days after Compaction for 24 Hours at 30 Revolutions per Minute. Filter only.

Solid to Liquid Ratio	Initial Cube Size (mm)	Concentration of Element in Solution in mg/kg (ppm)							
		Calcium (Ca)	Iron (Fe)	Lead (Pb)	Sodium (Na)	Silicon (Si)	Magnesium (Mg)	Aluminium (Al)	Manganese (Mn)
1/10	10	9.561	D 0.0035	69.64	1.675	1.048	8.306	D 0.1745	0.6772
	20	9.730	D 0.0043	69.14	1.690	1.109	8.232	D 0.2043	0.6768
1/20	10	5.439	D 0.0027	33.62	0.9149	0.5624	4.059	D 0.0579	0.3406
	20	5.071	D 0.0031	33.61	1.024	0.5834	4.024	D 0.0791	0.3378
1/40	10	3.014	D 0.0016	13.44	D 0.6725	0.3340	1.927	D 0.0448	0.1593
	20	2.729	D 0.0031	13.75	0.7775	0.3129	1.898	D 0.0287	0.1569

Table A1.19 ICP Data for Kaolinite and 2500ppm Lead, Compacted on the 14/4/97 and Tested 301 days after Compaction for 24 Hours at 30 Revolutions per Minute. Filter only.

Solid to Liquid Ratio	Initial Cube Size (mm)	Concentration of Element in Solution in mg/kg (ppm)							
		Calcium (Ca)	Iron (Fe)	Lead (Pb)	Sodium (Na)	Silicon (Si)	Magnesium (Mg)	Aluminium (Al)	Manganese (Mn)
1/10	10	10.36	D 0.0169	71.75	1.875	1.291	7.735	d. 0.1742	0.6639
	20	10.43	D 0.0059	72.82	1.787	1.294	7.780	D 0.1988	0.6657
1/20	10	5.264	d. 0.0099	32.23	1.111	0.7151	3.770	D 0.0722	0.3260
	20	5.398	D 0.0133	33.35	1.065	0.9131	3.702	0.3080	0.3215
1/40	10	3.529	d. 0.0067	11.15	0.7256	0.4347	1.756	D 0.0636	0.1468
	20	2.914	0.0196	13.53	0.8071	0.7231	1.873	0.4507	0.1550

Note : 'D' indicates the stated value is below detection limits and the value stated is a system estimate.
'd' indicates the stated value is close to detection limits.

Table A1.20 ICP Data for Kaolinite and 2500ppm Lead, Compacted on the 15/4/97 and Tested 7 days after Compaction for 24 Hours at 60 Revolutions per Minute. Filter only.

Solid to Liquid Ratio	Initial Cube Size (mm)	Concentration of Element in Solution in mg/kg (ppm)							
		Calcium (Ca)	Iron (Fe)	Lead (Pb)	Sodium (Na)	Silicon (Si)	Magnesium (Mg)	Aluminium (Al)	Manganese (Mn)
1/10	10	10.21	D 0.0051	83.44	1.778	3.277	8.209	D 0.2969	0.6562
	20	10.75	D 0.0068	66.23	1.616	2.850	6.952	D 0.2292	0.5445
1/20	10	5.185	D 0.0067	38.33	D 0.9237	1.733	3.957	D 0.1363	0.3137
	20	6.775	D 0.0095	34.33	d. 1.052	2.168	3.747	D 0.5170	0.2989
1/40	10	2.619	D 0.0140	18.49	D 0.6115	1.077	1.954	D 0.1661	0.1543
	20	5.150	D 0.0047	11.18	D 0.5540	0.9642	1.725	D 0.0547	0.1340

Table A1.21 ICP Data for Kaolinite and 2500ppm Lead, Compacted on the 15/4/97 and Tested 175 days after Compaction for 24 Hours at 60 Revolutions per Minute. Filter only.

Solid to Liquid Ratio	Initial Cube Size (mm)	Concentration of Element in Solution in mg/kg (ppm)							
		Calcium (Ca)	Iron (Fe)	Lead (Pb)	Sodium (Na)	Silicon (Si)	Magnesium (Mg)	Aluminium (Al)	Manganese (Mn)
1/10	10	10.11	D 0.0041	67.45	1.821	1.088	8.305	D 0.1835	0.6798
	20	9.919	D 0.0049	67.82	1.934	1.081	8.296	D 0.1772	0.6807
1/20	10	5.863	D 0.0026	30.14	1.094	0.5605	3.990	D 0.0698	0.3354
	20	6.663	D 0.0018	29.37	1.017	0.5781	4.027	D 0.0345	0.3377
1/40	10	3.511	D 0.0024	13.47	0.7531	0.2933	1.943	D 0.0257	0.1592
	20	3.263	D 0.0008	12.76	D 0.6655	0.3135	1.841	D 0.0230	0.1546

Note : 'D' indicates the stated value is below detection limits and the value stated is a system estimate.
'd' indicates the stated value is close to detection limits.

A1.2.3 English China Clay with 5000ppm Fe and no lime

A1.2.3.1 Solid : liquid ratio

Inspection of Figures A1.15 to A1.18 shows that as solid to liquid ratio increases conductivity increases and pH decreases. Doubling the solid to liquid ratio increases conductivity by 1.5 in every case. The conductivity of the solid to liquid ratios 1:10, 1:20 and 1:40 are all generally approximately 1300µS/cm, 2000µS/cm and 3200 µS/cm respectively whilst pH values are approximately 2.55, 2.65 and 2.80 respectively.

Tables A1.22 to A1.31 show that as solid to liquid ratio doubles, the concentration of leachable Fe increases by 2.2 whilst Ca, Mg, Si, Al and Mn concentrations double and Na increases by a small amount. At 1:10 solid to liquid ratio after 7 days concentrations of Ca≈20ppm, Fe≈325ppm, Na≈2ppm, Si≈7ppm, Mg≈13ppm, Al≈37ppm and Mn ≈1.2ppm whilst Pb is below detection limits.

A1.2.3.2 Cube Size

In all cases at all solid to liquid ratios the 10mm cubes produce slightly higher pH values than 20mm cubes and often slightly higher conductivity. In most cases the 10mm cubes release slightly more Ca and Fe whilst Na, Si, Mg, Al, and Mn appear unaffected.

A1.2.3.3 Rotation speed and test duration

Comparison of Figures A1.15 and A1.17 illustrates that the 6hr/30rpm test again produces slightly higher pH values and slightly lower conductivity than 24hr/30rpm tests. These trends are mirrored in 60rpm tests illustrated in Figures A1.16 and A1.18. At the lowest solid to liquid ratio the pH and conductivity values are higher for 60rpm tests than 30rpm tests. This is most apparent for conductivity values. All tests appear to produce similar pH and conductivity variations throughout the tests although pH values clearly fall consistently over 24hr tests which is not so apparent during 6hr tests.

Inspections of the data in Tables A1.22 to A1.31 highlight that changing slightly reduces the concentrations of Ca, Fe, Pb and Na. It is clear however that increasing rotation speed does not affect Si, Mg, or Mn leachability whilst Al increases during 6hr tests at 7 days curing only. Increasing test duration increases Si

and Mn at 7days curing with no change in Mg. There is however an increase in Al content during 30rpm tests at 7 days curing although not during 60rpm tests. Levels of Ca, Na, Fe and Pb do generally tend to decrease with increasing test duration.

A1.2.3.4 Curing Time

In many tests at the lower solid to liquid ratios it is evident that after 175 days curing pH and conductivity have slightly reduced relative to 7 days. However after 301 days these values have returned to values similar in magnitude to those at 7 days. Analysis of the data Tables A1.22 to A1.31 indicates that between 7 days and 175 days levels of Fe and Si significantly reduce whilst levels of Mg, Al and Mn increase. No significant trends are observable for Na and Ca.

Figure A1.15 Conductivity and pH characteristics for English China Clay with 5000ppm Fe and no lime during 6hr/30rpm Batch Tests

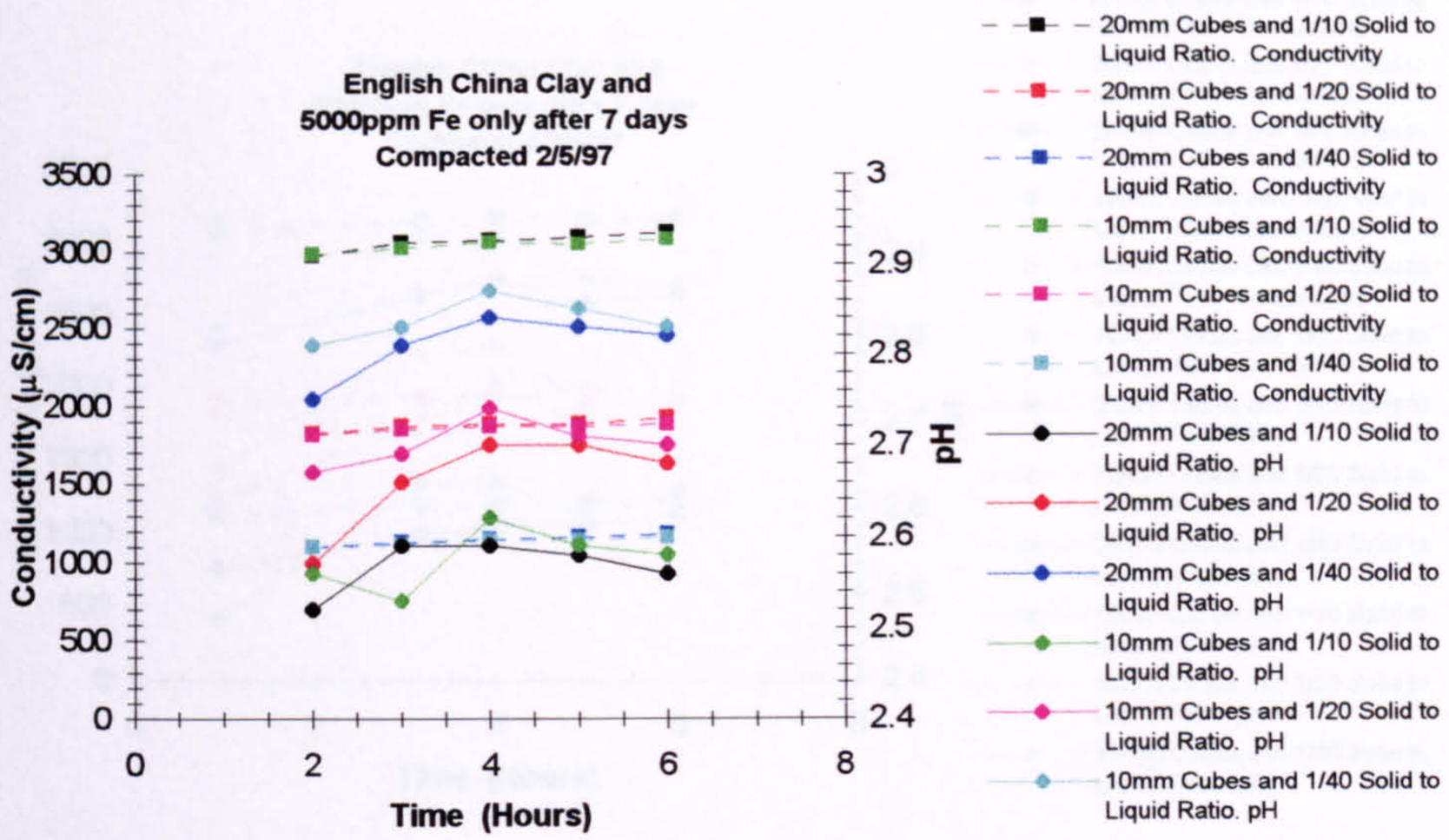

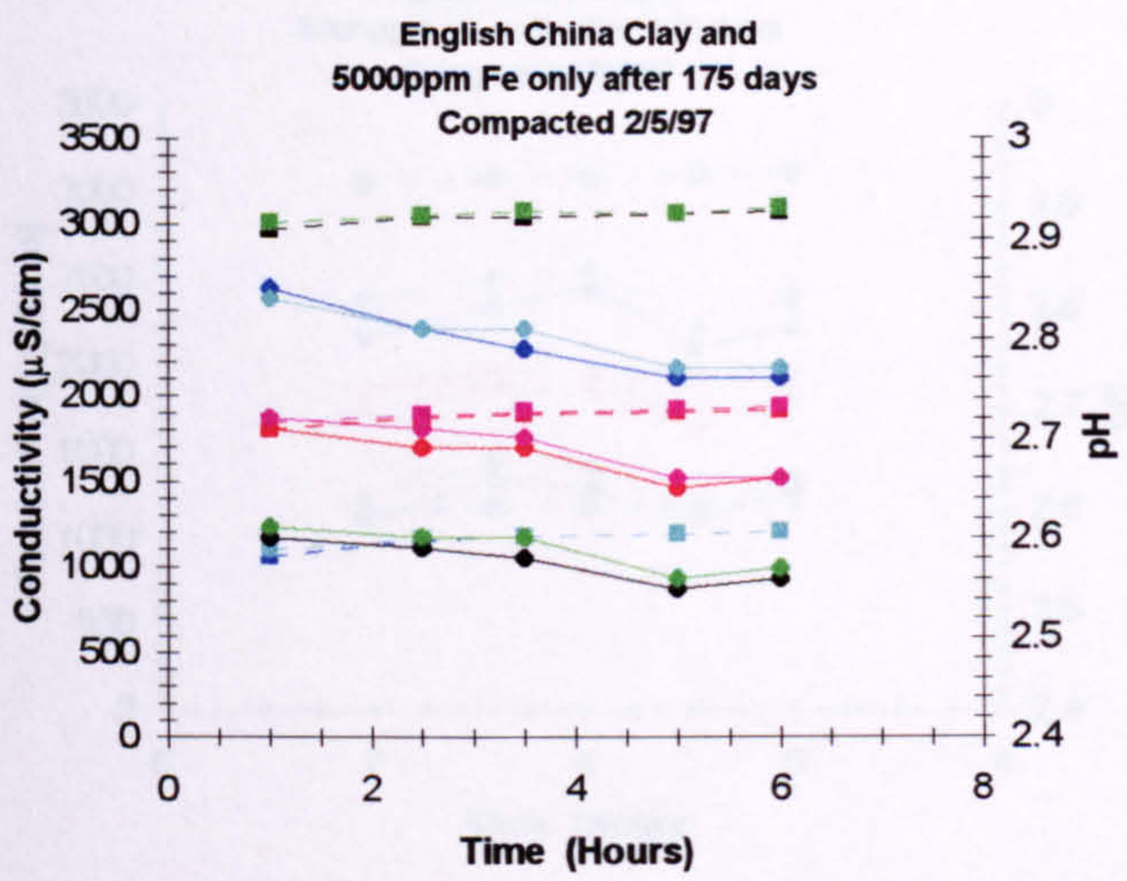

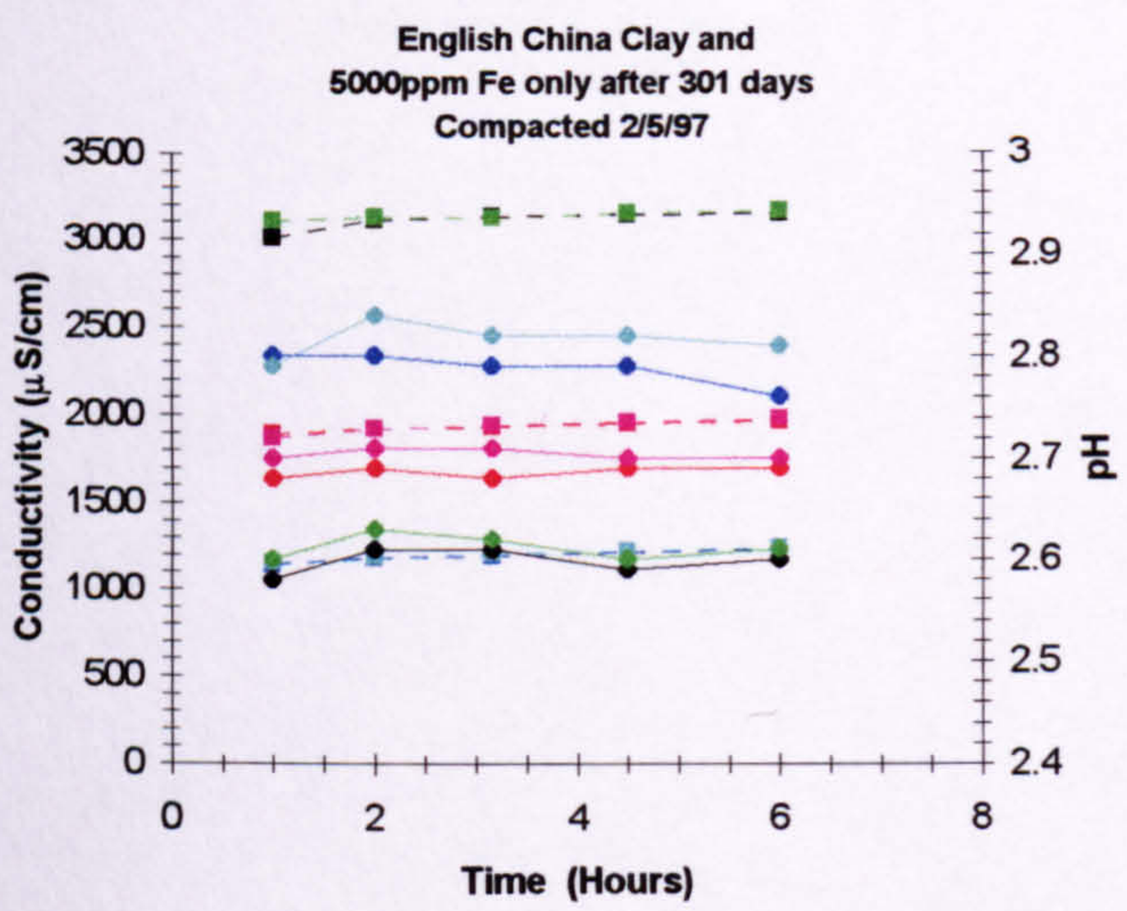

Figure A1.16 Conductivity and pH characteristics for English China Clay with 5000ppm Fe and no lime during 6hr/60rpm Batch Tests

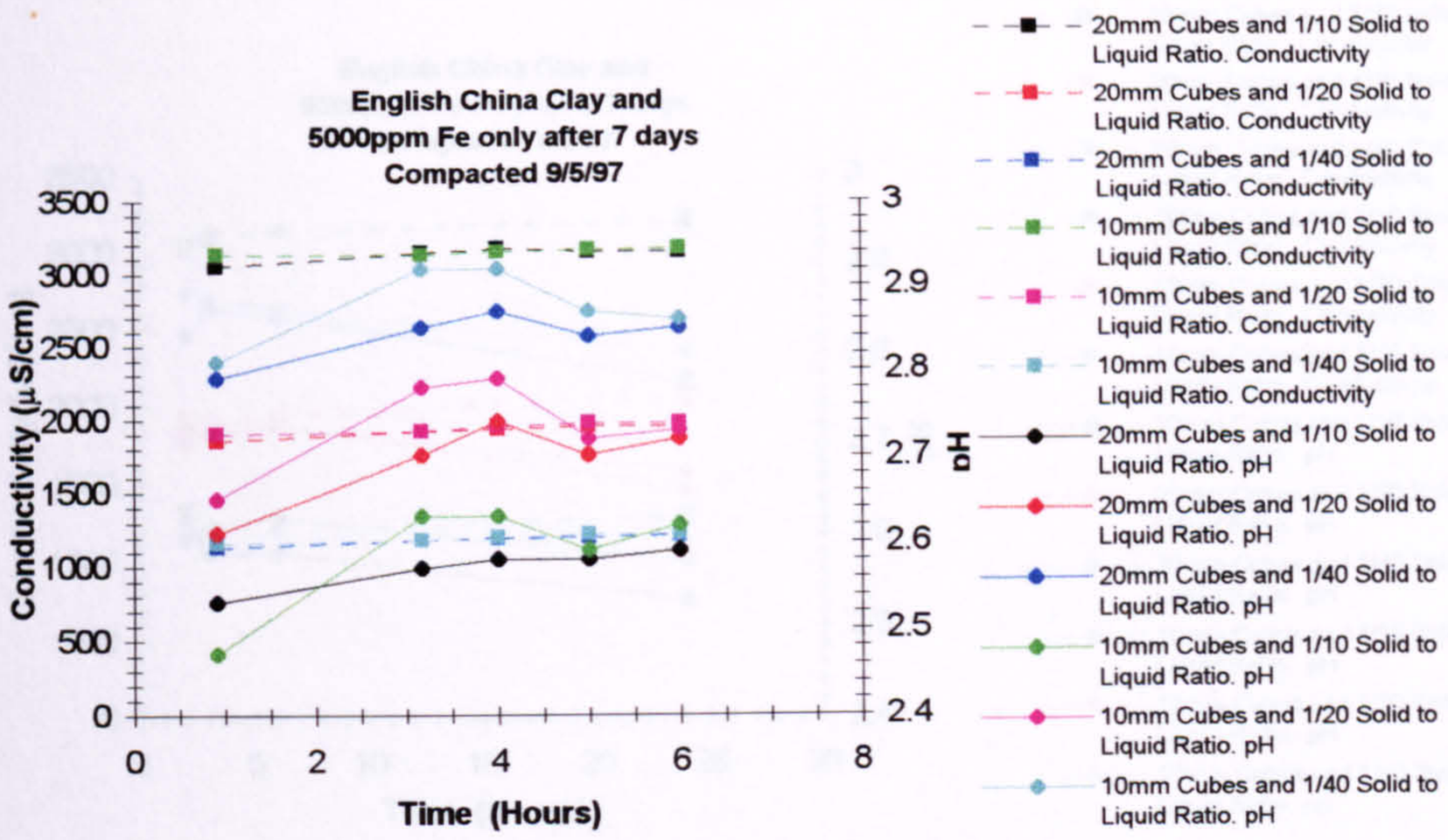

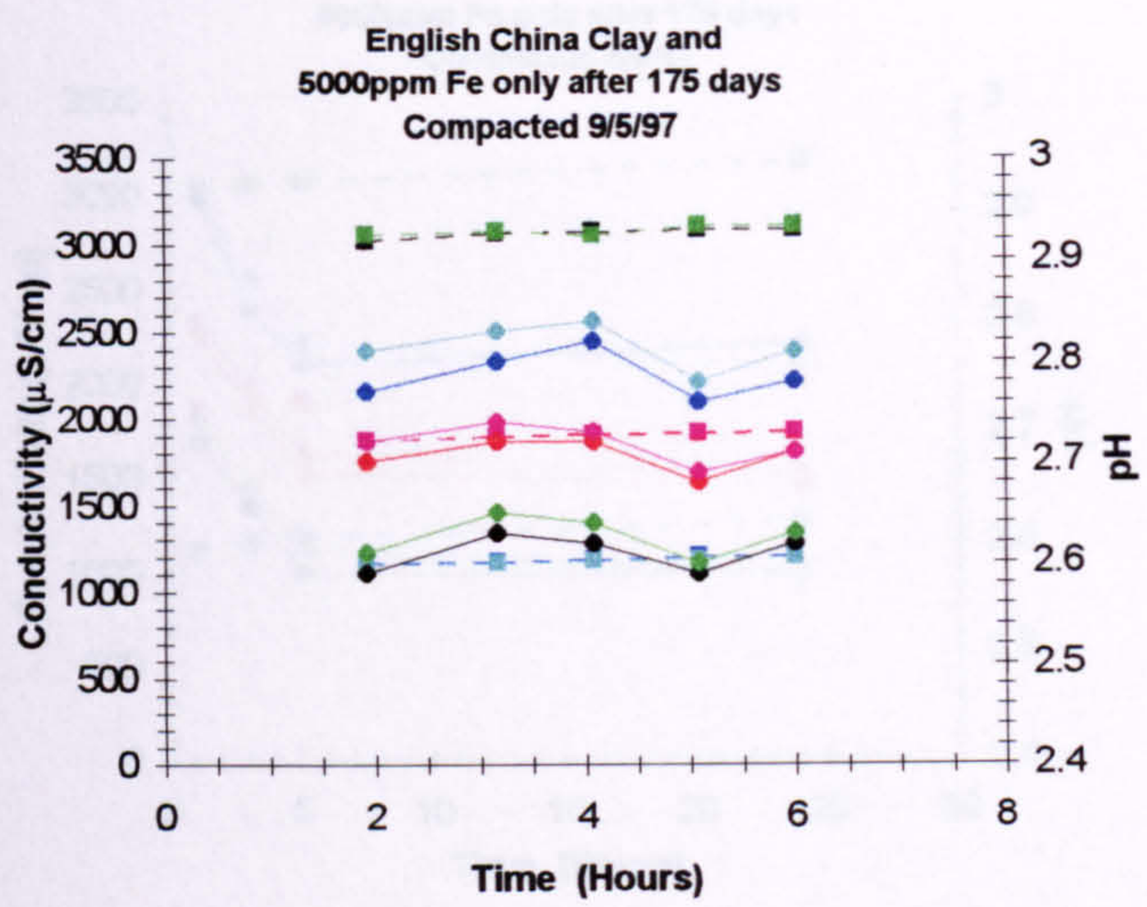

Figure A1.17 Conductivity and pH characteristics for English China Clay with 5000ppm Fe and no lime during 24hr/30rpm Batch Tests

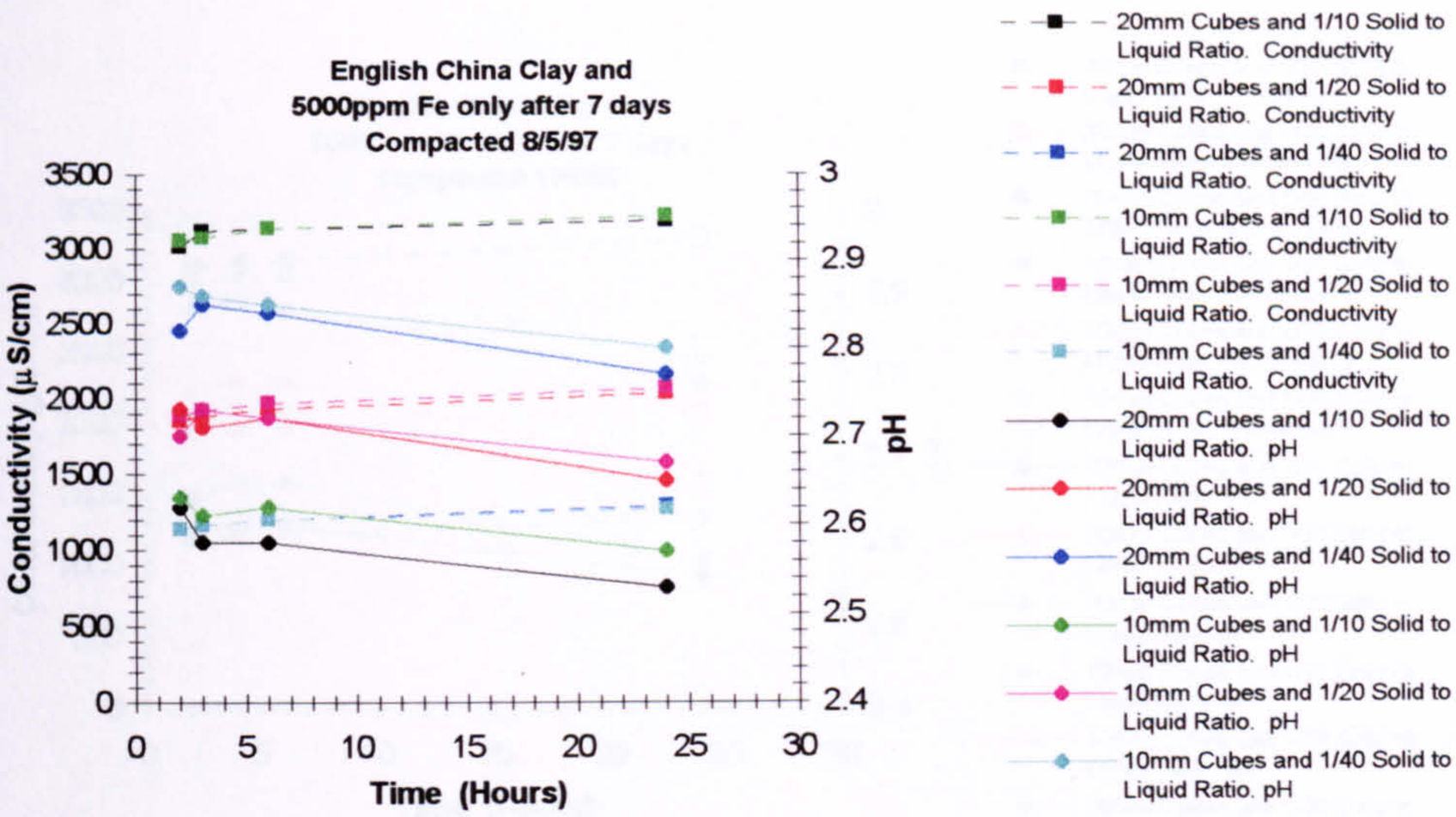

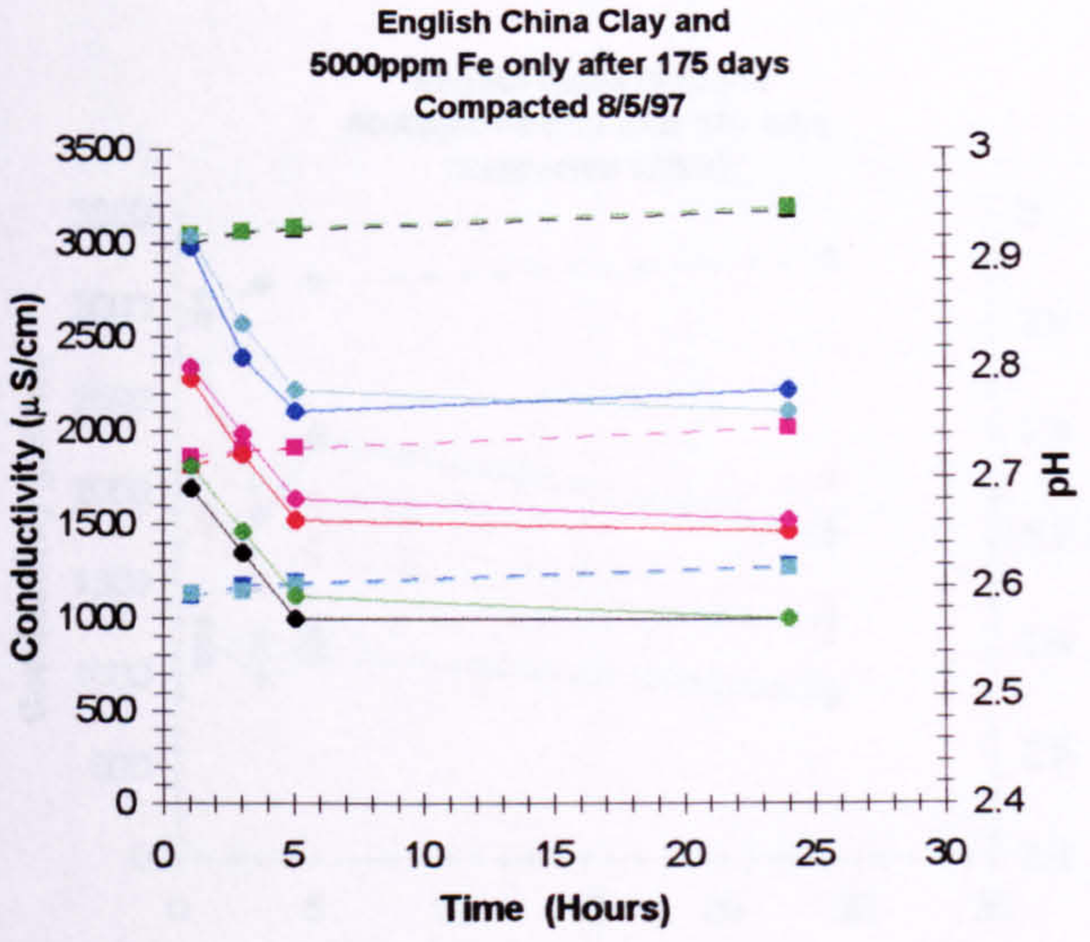

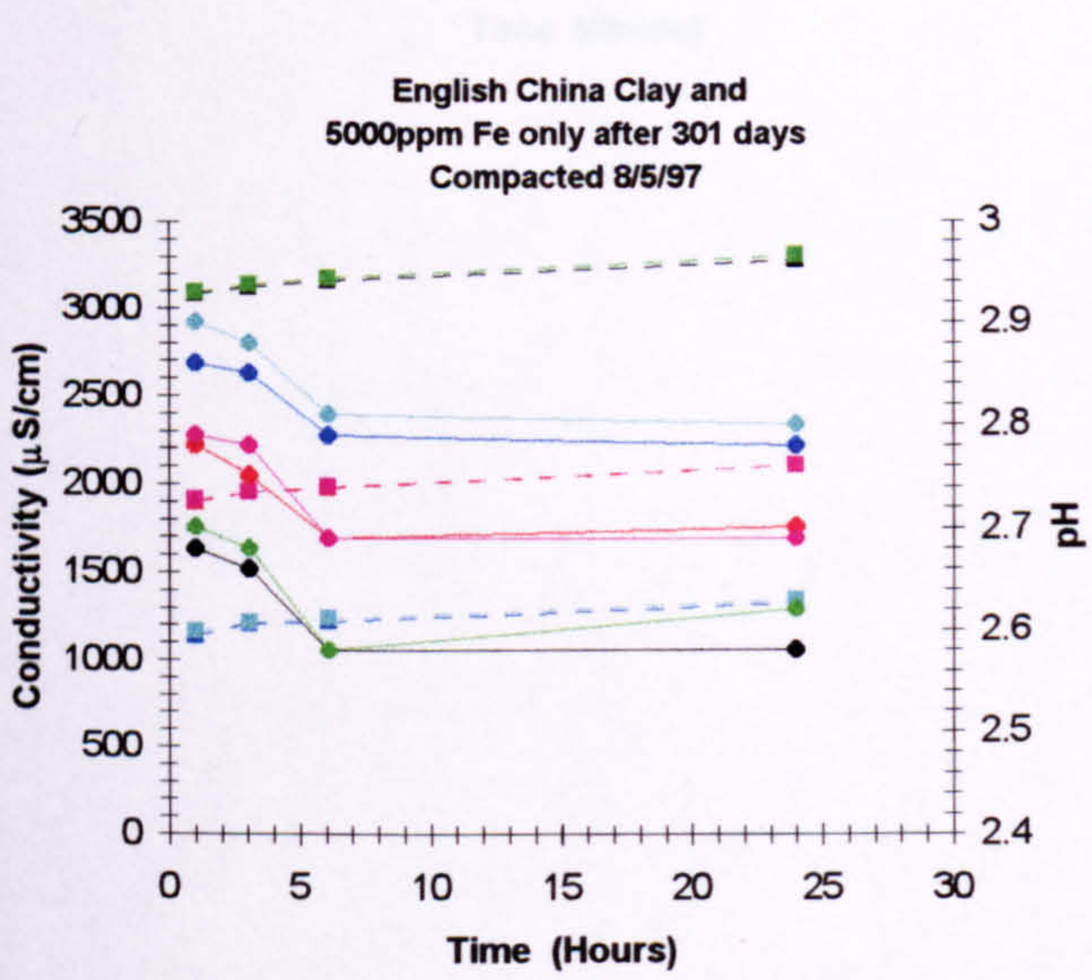

Figure A1.18 Conductivity and pH characteristics for English China Clay with 5000ppm Fe and no lime during 24hr/60rpm Batch Tests

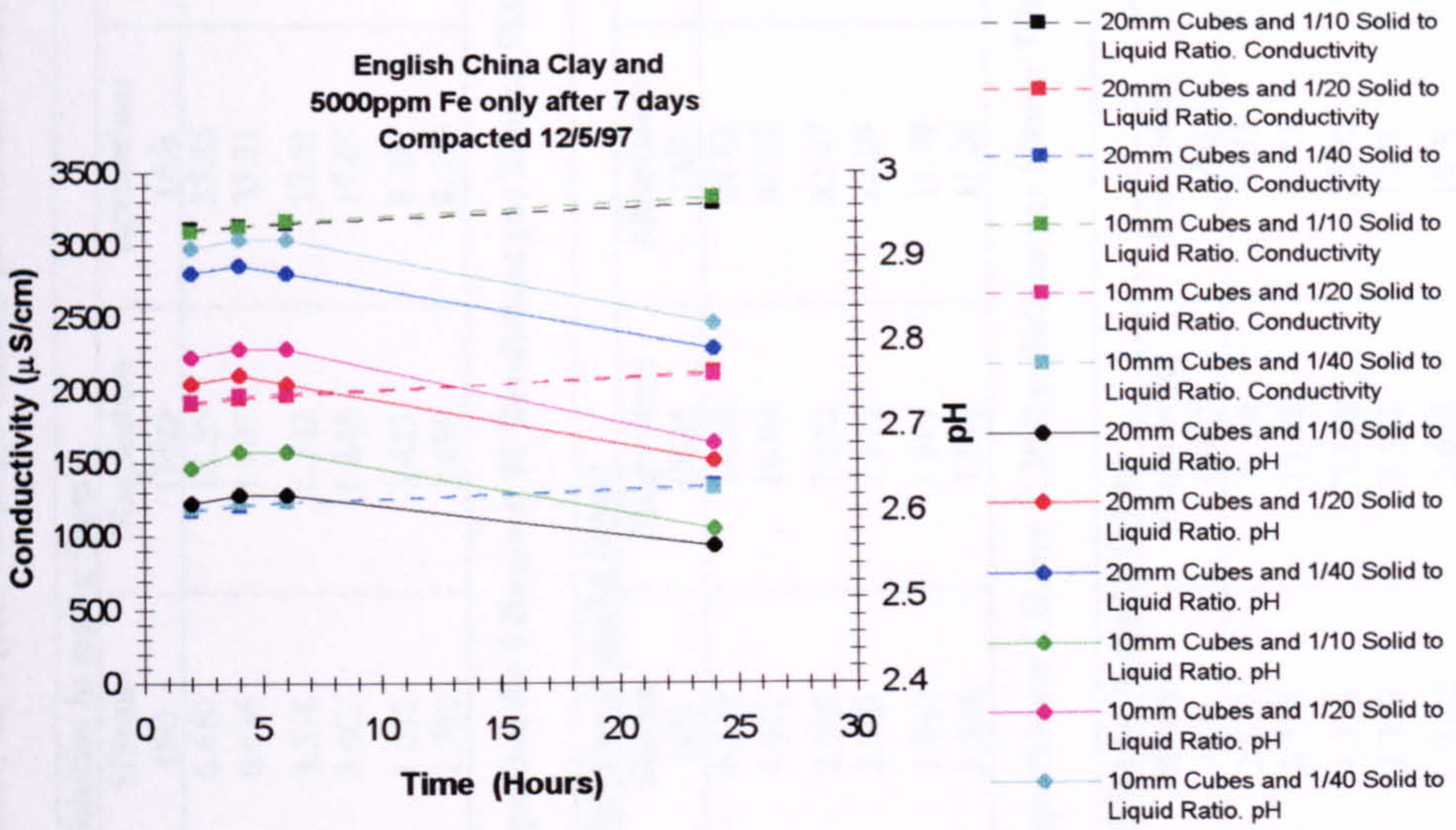

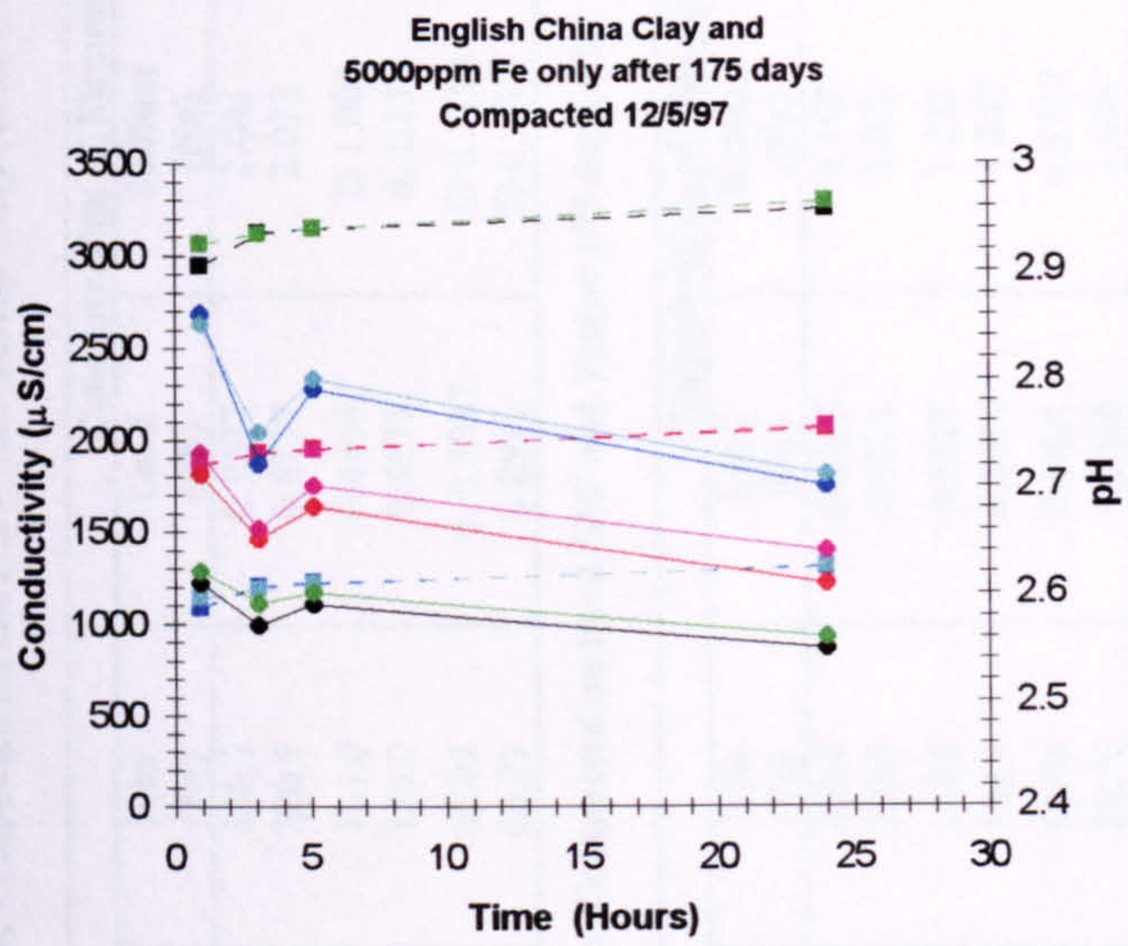

Table A1.22 ICP Data for Kaolinite and 5000ppm Iron, Compacted on the 2/5/97 and Tested 7 days after Compaction for 6 Hours at 30 Revolutions per Minute. Filter only.

Solid to Liquid Ratio	Initial Cube Size (mm)	Concentration of Element in Solution in mg/kg (ppm)							
		Calcium (Ca)	Iron (Fe)	Lead (Pb)	Sodium (Na)	Silicon (Si)	Magnesium (Mg)	Aluminium (Al)	Manganese (Mn)
1/10	10	40.33	336.7	0.9127	2.041	6.650	13.35	35.85	1.215
	20	35.59	326.9	0.8737	2.023	6.636	13.07	35.31	1.224
1/20	10	29.03	154.0	0.4466	D 1.002	3.318	6.742	17.61	0.6434
	20	20.28	155.0	0.4671	d. 1.119	3.467	6.849	17.67	0.6675
1/40	10	8.957	66.03	d. 0.3947	D 0.5794	1.612	3.422	8.481	0.3286
	20	17.18	64.99	0.8911	D 0.5745	1.790	3.499	8.750	0.3285

Table A1.23 ICP Data for Kaolinite and 5000ppm Iron, Compacted on the 2/5/97 and Tested 175 days after Compaction for 6 Hours at 30 Revolutions per Minute. Filter only.

Solid to Liquid Ratio	Initial Cube Size (mm)	Concentration of Element in Solution in mg/kg (ppm)							
		Calcium (Ca)	Iron (Fe)	Lead (Pb)	Sodium (Na)	Silicon (Si)	Magnesium (Mg)	Aluminium (Al)	Manganese (Mn)
1/10	10	21.88	309.4	0.6466	2.102	4.033	14.00	44.62	1.405
	20	21.94	309.6	0.8571	2.072	4.051	14.09	44.37	1.402
1/20	10	11.40	143.6	0.6257	1.223	2.035	7.152	22.47	0.7158
	20	10.38	144.4	0.1915	1.247	2.003	7.018	22.09	0.7025
1/40	10	5.517	59.96	0.1801	0.6737	1.680	3.699	11.49	0.3621
	20	5.520	59.96	0.1656	1.051	1.328	3.649	11.20	0.3562

Table A1.24 ICP Data for Kaolinite and 5000ppm Iron, Compacted on the 2/5/97 and Tested 301 days after Compaction for 6 Hours at 30 Revolutions per Minute. Filter only.

Solid to Liquid Ratio	Initial Cube Size (mm)	Concentration of Element in Solution in mg/kg (ppm)							
		Calcium (Ca)	Iron (Fe)	Lead (Pb)	Sodium (Na)	Silicon (Si)	Magnesium (Mg)	Aluminium (Al)	Manganese (Mn)
1/10	10	24.69	302.0	0.3059	1.920	2.533	14.00	41.33	1.459
	20	23.70	303.9	0.2666	1.925	2.538	13.91	41.41	1.460
1/20	10	11.30	139.4	0.2753	1.018	1.335	7.118	22.02	0.7414
	20	6.335	136.5	0.2785	0.6044	1.319	3.561	11.10	0.3670
1/40	10	6.143	52.62	0.3264	0.5812	0.9148	3.618	10.80	0.3620
	20	10.11	52.42	0.2225	1.080	1.282	6.789	21.57	0.7138

Note : 'D' indicates the stated value is below detection limits and the value stated is a system estimate.
'd' indicates the stated value is close to detection limits.

Table A1.25 ICP Data for Kaolinite and 5000ppm Iron, Compacted on the 9/5/97 and Tested 7 days after Compaction for 6 Hours at 60 Revolutions per Minute. Filter only.

Solid to Liquid Ratio	Initial Cube Size (mm)	Concentration of Element in Solution in mg/kg (ppm)							
		Calcium (Ca)	Iron (Fe)	Lead (Pb)	Sodium (Na)	Silicon (Si)	Magnesium (Mg)	Aluminium (Al)	Manganese (Mn)
1/10	10	24.09	327.9	0.5565	1.985	6.550	13.27	37.56	1.266
	20	22.78	318.5	0.4638	2.084	6.513	13.21	37.29	1.266
1/20	10	10.88	153.7	d. 0.3047	D 1.118	3.367	6.927	18.78	0.6784
	20	9.823	151.4	D 0.1930	1.215	3.304	6.824	18.51	0.6725
1/40	10	7.189	66.17	D 0.2300	D 0.9208	2.035	3.490	9.481	0.3363
	20	7.073	66.02	D 0.2349	D 0.6195	1.846	3.405	9.189	0.3365

Table A1.26 ICP Data for Kaolinite and 5000ppm Iron, Compacted on the 9/5/97 and Tested 175 days after Compaction for 6 Hours at 60 Revolutions per Minute. Filter only.

Solid to Liquid Ratio	Initial Cube Size (mm)	Concentration of Element in Solution in mg/kg (ppm)							
		Calcium (Ca)	Iron (Fe)	Lead (Pb)	Sodium (Na)	Silicon (Si)	Magnesium (Mg)	Aluminium (Al)	Manganese (Mn)
1/10	10	21.20	307.9	d. 0.1569	1.835	3.585	13.96	45.33	1.345
	20	20.64	305.3	d. 0.1483	1.890	3.560	13.66	45.47	1.353
1/20	10	9.561	138.8	D 0.0790	0.9811	1.765	6.970	22.90	0.6761
	20	10.89	141.8	D 0.0808	1.014	1.787	7.016	23.05	0.6770
1/40	10	5.316	55.98	D 0.0320	0.7726	0.9434	3.613	11.34	0.3402
	20	5.351	57.59	D 0.0442	0.7850	0.9388	3.613	11.39	0.3446

Note : 'D' indicates the stated value is below detection limits and the value stated is a system estimate.
'd' indicates the stated value is close to detection limits.

Table A1.27 ICP Data for Kaolinite and 5000ppm Iron, Compacted on the 8/5/97 and Tested 7 days after Compaction for 24 Hours at 30 Revolutions per Minute. Filter only.

Solid to Liquid Ratio	Initial Cube Size (mm)	Concentration of Element in Solution in mg/kg (ppm)							
		Calcium (Ca)	Iron (Fe)	Lead (Pb)	Sodium (Na)	Silicon (Si)	Magnesium (Mg)	Aluminium (Al)	Manganese (Mn)
1/10	10	19.96	319.2	D 0.0439	1.842	7.149	13.21	37.61	1.314
	20	21.53	321.7	D 0.1351	1.995	7.253	13.14	37.55	1.325
1/20	10	12.67	147.3	D 0.1424	D 1.043	3.774	6.888	19.19	0.7221
	20	13.53	143.8	D 0.3650	D 1.020	3.606	6.815	18.63	0.7060
1/40	10	5.706	61.94	D 0.1027	D 0.6022	1.961	3.421	9.368	0.3529
	20	6.516	60.60	D 0.1498	D 0.6513	1.931	3.393	9.046	0.3518

Table A1.28 ICP Data for Kaolinite and 5000ppm Iron, Compacted on the 8/5/97 and Tested 175 days after Compaction for 24 Hours at 30 Revolutions per Minute. Filter only.

Solid to Liquid Ratio	Initial Cube Size (mm)	Concentration of Element in Solution in mg/kg (ppm)							
		Calcium (Ca)	Iron (Fe)	Lead (Pb)	Sodium (Na)	Silicon (Si)	Magnesium (Mg)	Aluminium (Al)	Manganese (Mn)
1/10	10	25.04	298.4	0.5194	1.956	4.111	13.73	44.89	1.411
	20	34.93	302.2	D 0.0943	1.915	4.012	13.88	45.12	1.431
1/20	10	13.19	137.2	D 0.0406	1.126	2.034	7.068	22.67	0.7165
	20	14.29	131.2	0.2756	1.145	2.098	6.944	22.63	0.7075
1/40	10	11.74	51.21	0.4567	0.7978	1.782	3.572	11.81	0.3550
	20	6.707	52.70	0.6930	0.7588	1.190	3.547	11.15	0.3549

Table A1.29 ICP Data for Kaolinite and 5000ppm Iron, Compacted on the 8/5/97 and Tested 301 days after Compaction for 24 Hours at 30 Revolutions per Minute. Filter only.

Solid to Liquid Ratio	Initial Cube Size (mm)	Concentration of Element in Solution in mg/kg (ppm)							
		Calcium (Ca)	Iron (Fe)	Lead (Pb)	Sodium (Na)	Silicon (Si)	Magnesium (Mg)	Aluminium (Al)	Manganese (Mn)
1/10	10	23.12	305.0	0.2372	2.027	2.681	13.67	41.68	1.452
	20	22.54	300.5	0.1972	1.868	2.682	13.62	41.84	1.462
1/20	10	12.41	115.6	0.1390	1.107	1.932	7.107	23.47	0.7564
	20	12.94	129.9	0.2083	1.117	1.412	7.140	22.92	0.7517
1/40	10	6.242	39.41	0.2422	0.7414	0.9669	3.694	11.44	0.3819
	20	6.106	45.75	0.2282	0.7957	0.8645	3.617	11.07	0.3767

Note: 'D' indicates the stated value is below detection limits and the value stated is a system estimate.
'd' indicates the stated value is close to detection limits.

Table A1.30 ICP Data for Kaolinite and 5000ppm Iron, Compacted on the 12/5/97 and Tested 7 days after Compaction for 24 Hours at 60 Revolutions per Minute. Filter only.

Solid to Liquid Ratio	Initial Cube Size (mm)	Concentration of Element in Solution in mg/kg (ppm)							
		Calcium (Ca)	Iron (Fe)	Lead (Pb)	Sodium (Na)	Silicon (Si)	Magnesium (Mg)	Aluminium (Al)	Manganese (Mn)
1/10	10	19.77	323.4	D 0.0000	1.987	7.418	13.23	36.32	1.285
	20	19.43	320.5	D 0.0410	2.238	7.552	13.18	36.24	1.290
1/20	10	9.110	142.8	D 0.0127	1.183	3.771	6.863	18.23	0.6926
	20	9.813	143.5	D 0.0725	1.331	3.739	6.745	18.30	0.6875
1/40	10	4.888	61.58	D 0.0407	D 0.7593	1.971	3.536	9.229	0.3556
	20	4.798	58.08	D 0.0252	D 0.8046	1.936	3.357	8.997	0.3432

Table A1.31 ICP Data for Kaolinite and 5000ppm Iron, Compacted on the 12/5/97 and Tested 175 days after Compaction for 24 Hours at 60 Revolutions per Minute. Filter only.

Solid to Liquid Ratio	Initial Cube Size (mm)	Concentration of Element in Solution in mg/kg (ppm)							
		Calcium (Ca)	Iron (Fe)	Lead (Pb)	Sodium (Na)	Silicon (Si)	Magnesium (Mg)	Aluminium (Al)	Manganese (Mn)
1/10	10	20.90	300.2	D 0.0109	1.806	4.018	14.01	44.54	1.398
	20	20.78	300.6	D 0.0000	1.797	4.095	14.04	45.10	1.403
1/20	10	9.364	133.0	D 0.0131	1.018	2.171	7.039	22.70	0.6964
	20	9.086	133.7	D 0.0000	1.019	2.036	7.117	22.71	0.7040
1/40	10	5.230	51.41	D 0.0507	0.6547	1.056	3.623	11.29	0.3543
	20	5.083	52.37	D 0.0392	0.6763	2.917	3.598	12.75	0.3618

Note : 'D' indicates the stated value is below detection limits and the value stated is a system estimate.
'd' indicates the stated value is close to detection limits.

A1.2.4 English China Clay with no contaminants and 1.5% lime

A1.2.4.1 Solid : liquid ratio

Inspection of Figures A1.19 to A1.22 shows that as the solid to liquid ratio increases both conductivity and pH increases. At 7 days curing the conductivity of 6hr/30rpm tests with 20mm cube sizes (Figure A1.19) at the solid to liquid ratios 1:10, 1:20 and 1:40 are 5430μS/cm, 3300 μS/cm and 1870μS/cm respectively whilst pH values are 12.49, 12.33 and 12.08 respectively. At 175 days curing the conductivity values are 1337μS/cm, 1049μS/cm, 707μS/cm and pH values are 11.95, 11.79 and 11.57 respectively whilst at 301 days curing conductivity values are 1045μS/cm, 757μS/cm, 527μS/cm and pH values are 11.73, 11.54 and 11.35. Increasing the solid to liquid ratio at 7 days curing from 1:40 to 1:20 therefore increases conductivity by a factor of approximately 1.76 and pH by approximately 0.25 pH divisions. Increasing solid to liquid ratio further from 1:20 to 1:10 increases conductivity by a factor of approximately 1.65 and pH by approximately 0.16 pH divisions. At 175 days curing, conductivity increases by a factor of 1.48 and pH by 0.22 pH divisions for a change in solid to liquid ratio of 1:40 to 1:20. Increasing solid to liquid ratio from 1:20 to 1:10 at 175 days curing increases conductivity by a factor of 1.27 and pH by 0.16 pH divisions. These changes brought about by varying solid to liquid ratio and curing period are clearly evident visually by the spacing between pH and conductivity lines in Figure A1.19 (Also Figures A1.21 and A1.22).

Analysis of data Tables A1.32 to A1.41 illustrates that as solid to liquid ratio decreases and curing period increase, Ca concentrations significantly decrease by factors similar to those for conductivity changes. By observation of Table A1.32 for 20mm cubes and 6hr/30rpm tests at 7 days it is clear that increasing solid to liquid ratio from 1:40 to 1:20 results in an increase in concentration of Ca from 115ppm-276ppm. A reduction in Si from 1.88ppm-1.13ppm, Mg from 0.019-0.157 and Al from 4.87-3.10 also occurs. The similar increase in solid to liquid ratio from 1:20 to 1:10 results in an increase in Ca concentration from 276ppm-390ppm, Si from 1.12ppm-1.63ppm, Mg from 0.015ppm-0.018ppm and a reduction in Al from 3.10ppm-1.76ppm. For both these increases in solid to liquid ratio at 7 days during 24hr/30rpm tests and 24hr/60rpm tests, Tables A1.37 to A1.39 and A1.40 to A1.41 all show significant increases in Ca, whilst other elements show variable trends.

However at 175 days and 301 days curing all tests produce increases in Ca, Na and Al with increasing solid to liquid ratio.

A1.2.4.2 Cube Size

At solid to liquid ratios 1:20 and 1:40 the pH values related to 10mm cubes tends to be slightly higher than 20mm cubes. Where the resulting conductivity is higher, which can be for either 10mm or 20mm cubes, this appears to relate closely to the concentration of Ca in solution.

Inspection of Tables A1.32 to A1.41 illustrates that generally the larger initial cube size results in slightly higher concentrations of Na and Si whilst Al and Mg concentrations generally remain similar. These results are more consistent at 175 and 301 days curing.

A1.2.4.3 Rotation speed and test duration

No obvious trends in pH appear evident for increasing rotation speed at any curing time, although conductivity levels are slightly higher in some cases. It is clear that as the tests progress particularly for 24hr tests, pH generally continues to increase relative to 6hr tests.

Considering 6hr tests at 175 days curing (Table A1.33 and A1.36) increasing rotation speed results in a reduction in Ca, Na and Si concentrations whilst Al increases in concentration and other elements remain relatively unaffected.

Increasing test duration for 30rpm tests generally results in increases in Ca, Si concentrations whilst Na, Mg and Al concentrations remain unaffected. However increasing test duration for 60rpm tests at 175 days curing has similar effects although Na, Mg concentrations increases and Al concentrations reduce.

A1.2.4.4 Curing Time

Increasing curing time has a large effect on pH and conductivity as previously mentioned. These changes are most apparent between 7 days curing and 175 days curing although significantly changes are still occurring between 175 days and 301 days.

Analysis of the data Tables A1.32 to A1.41 illustrates that as curing period increases Ca concentrations significantly decrease, Mg, Al and Na concentrations

increase (Al very significantly) whilst all other elements remain relatively unaffected or are below detection limits.

Figure A1.19 Conductivity and pH characteristics for English China Clay with no contaminants and 1.5% lime during 6hr/30rpm Batch Tests

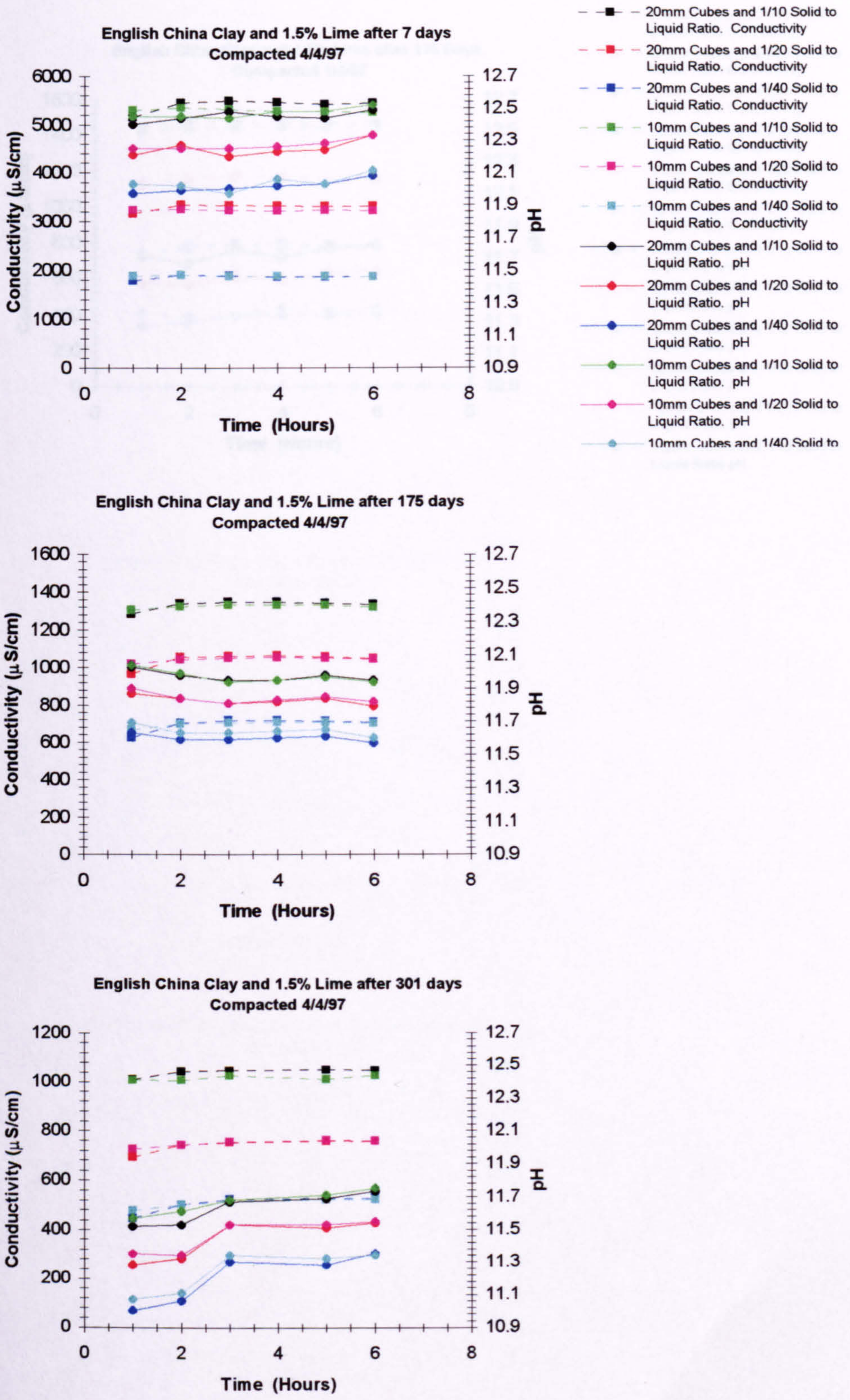

Figure A1.20 Conductivity and pH characteristics for English China Clay with no contaminants and 1.5% lime during 6hr/60rpm Batch Tests

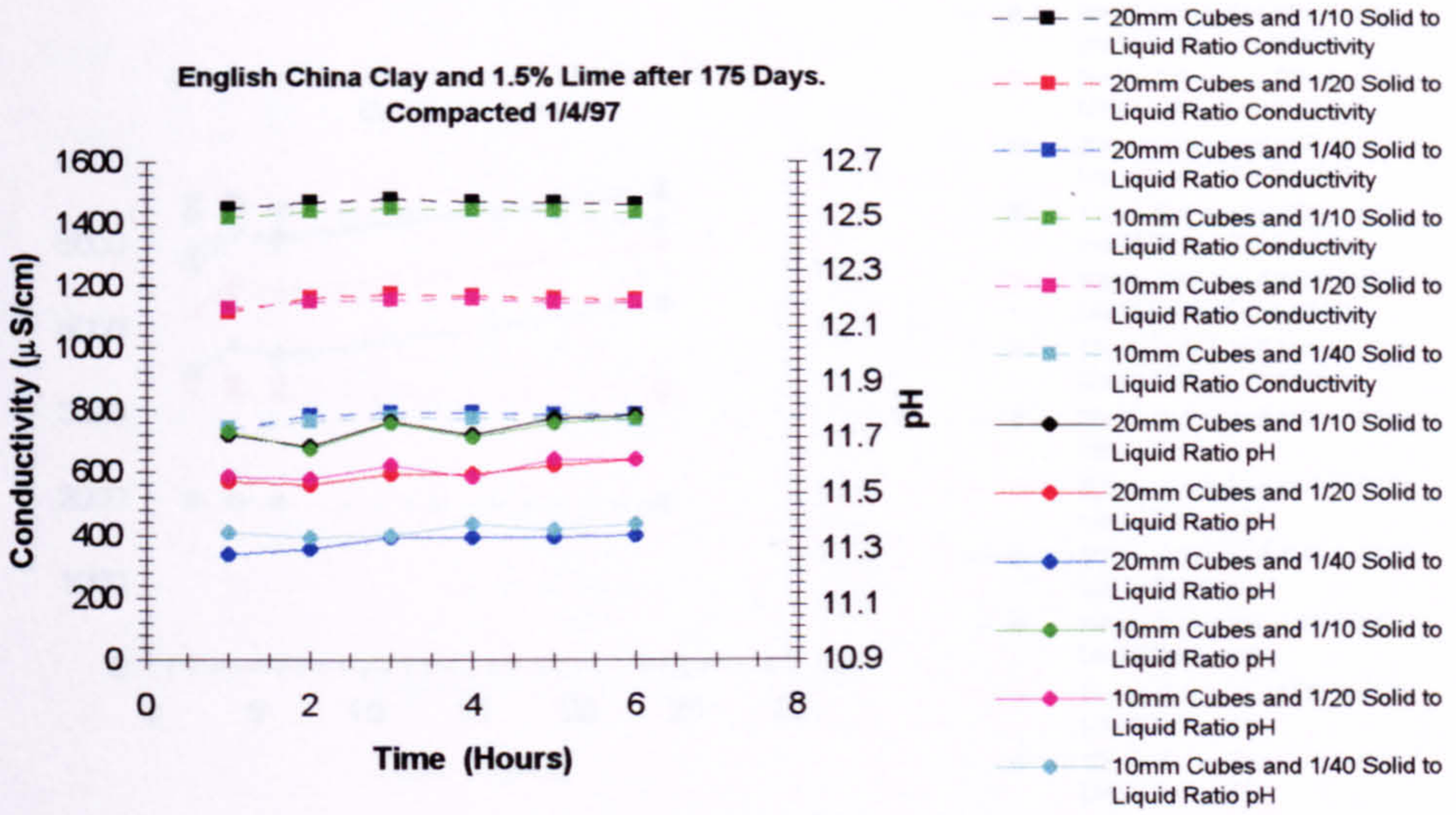

Figure A1.21 Conductivity and pH characteristics for English China Clay with no contaminants and 1.5% lime during 24hr/30rpm Batch Tests

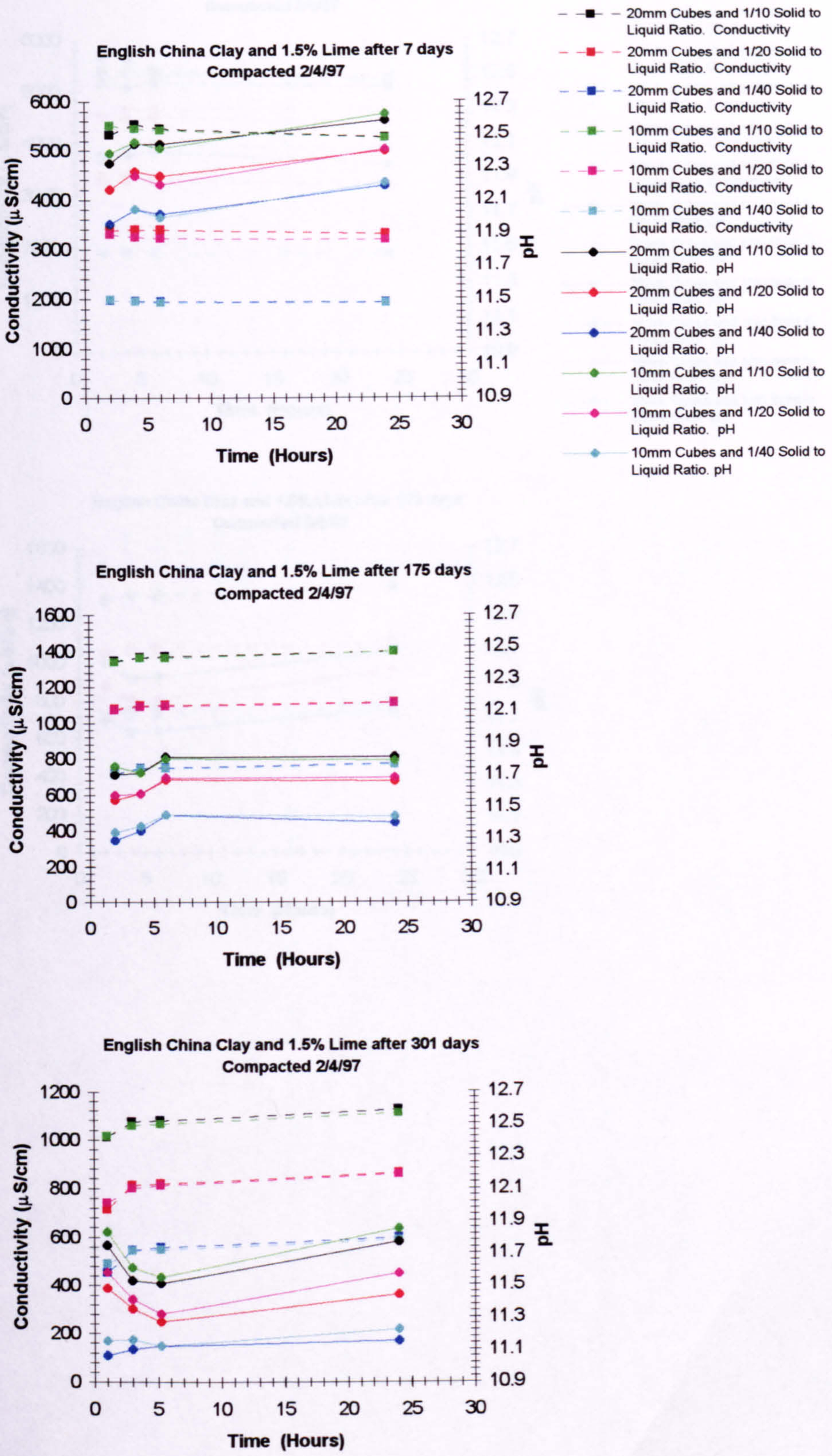

Figure A1.22 Conductivity and pH characteristics for English China Clay with no contaminants and 1.5% lime during 24hr/60rpm Batch Tests

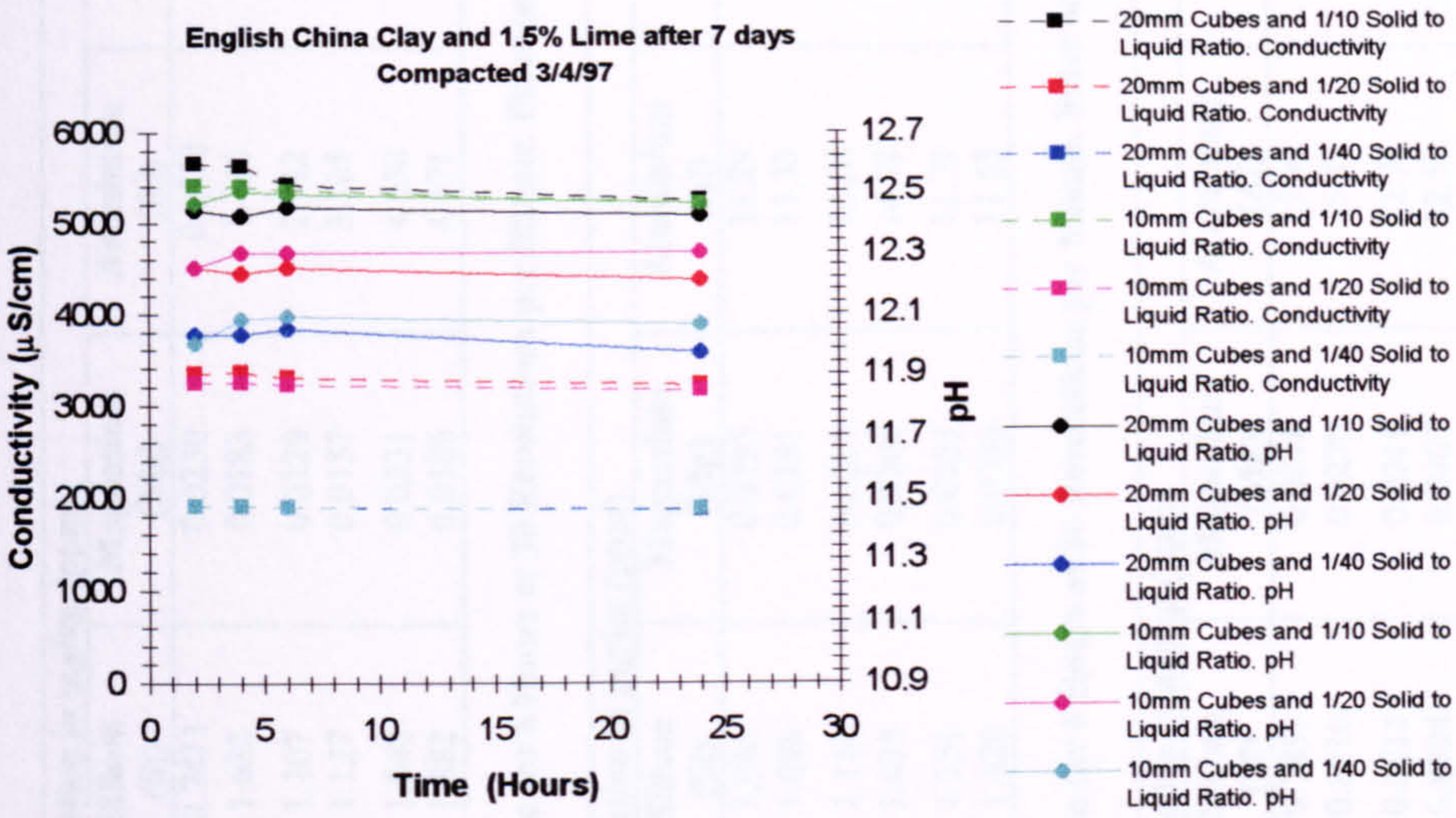

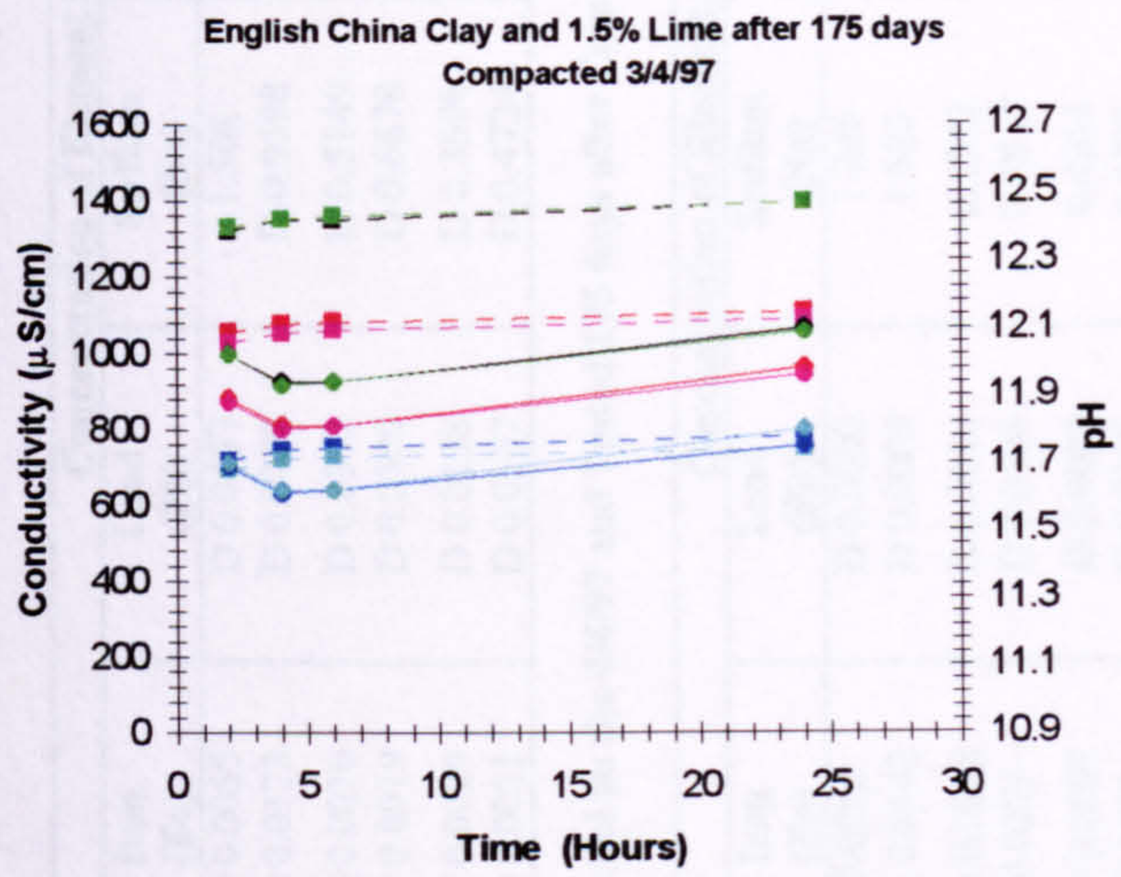

Table A1.32 ICP Data for Kaolinite and 1.5% Lime, Compacted on the 4/4/97 and Tested 7 days after Compaction for 6 Hours at 30 Revolutions per Minute. Filter only.

Solid to Liquid Ratio	Initial Cube Size (mm)	Concentration of Element in Solution in mg/kg (ppm)							
		Calcium (Ca)	Iron (Fe)	Lead (Pb)	Sodium (Na)	Silicon (Si)	Magnesium (Mg)	Aluminium (Al)	Manganese (Mn)
1/10	10	255.2	D 0.0055	D 0.0457	1.508	0.7411	0.0230	0.8593	D 0.0003
	20	390.0	D 0.0172	D 0.0000	D 0.9398	1.632	0.0183	1.766	D 0.0005
1/20	10	233.9	D 0.0010	D 0.0392	D 0.5149	1.107	0.0129	2.912	D 0.0001
	20	276.5	D 0.0019	D 0.0309	D 0.6878	1.127	0.0157	3.105	D 0.0007
1/40	10	124.6	D 0.0029	D 0.0138	D 0.3698	1.840	0.0231	4.530	D 0.0000
	20	115.8	D 0.0051	D 0.0107	D 0.4724	1.882	0.0186	4.871	D 0.0002

Table A1.33 ICP Data for Kaolinite and 1.5% Lime, Compacted on the 4/4/97 and Tested 175 days after Compaction for 6 Hours at 30 Revolutions per Minute. Filter only.

Solid to Liquid Ratio	Initial Cube Size (mm)	Concentration of Element in Solution in mg/kg (ppm)							
		Calcium (Ca)	Iron (Fe)	Lead (Pb)	Sodium (Na)	Silicon (Si)	Magnesium (Mg)	Aluminium (Al)	Manganese (Mn)
1/10	10	102.9	0.0220	D 0.0000	1.045	1.061	0.0295	13.29	d. 0.0003
	20	106.4	d. 0.0142	D 0.0000	1.623	1.098	0.0331	13.39	D 0.0001
1/20	10	89.41	D 0.0088	D 0.0000	0.7372	1.114	0.0279	14.04	D 0.0000
	20	87.47	0.0299	D 0.0000	0.6817	2.014	0.0305	14.78	d. 0.0001
1/40	10	64.84	D 0.0097	D 0.0000	0.4311	1.331	0.0253	11.71	D 0.0000
	20	62.61	0.0311	D 0.0000	0.8081	1.429	0.0386	11.53	d. 0.0005

Table A1.34 ICP Data for Kaolinite and 1.5% Lime, Compacted on the 4/4/97 and Tested 301 days after Compaction for 6 Hours at 30 Revolutions per Minute. Filter only.

Solid to Liquid Ratio	Initial Cube Size (mm)	Concentration of Element in Solution in mg/kg (ppm)							
		Calcium (Ca)	Iron (Fe)	Lead (Pb)	Sodium (Na)	Silicon (Si)	Magnesium (Mg)	Aluminium (Al)	Manganese (Mn)
1/10	10	63.51	d. 0.0050	D 0.0000	0.9943	0.7833	0.0278	15.40	D 0.0000
	20	78.84	D 0.0058	D 0.0000	1.042	0.8010	0.0270	15.37	D 0.0001
1/20	10	45.46	D 0.0083	D 0.0000	0.6654	0.8613	0.0219	12.74	D 0.0000
	20	30.12	D 0.0071	D 0.0000	0.6265	0.8794	0.0407	12.59	D 0.0000
1/40	10	24.06	d. 0.0082	D 0.0000	0.5108	0.8920	0.0297	10.01	D 0.0002
	20	25.05	d. 0.0030	D 0.0000	0.4108	0.8926	0.0282	9.895	D 0.0000

Note: 'D' indicates the stated value is below detection limits and the value stated is a system estimate.
'd' indicates the stated value is close to detection limits.

Table A1.35 ICP Data for Kaolinite and 1.5% Lime, Compacted on the 1/4/97 and Tested 7 days after Compaction for 6 Hours at 60 Revolutions per Minute.

Solid to Liquid Ratio	Initial Cube Size (mm)	Concentration of Element in Solution in mg/kg (ppm)							
		Calcium (Ca)	Iron (Fe)	Lead (Pb)	Sodium (Na)	Silicon (Si)	Magnesium (Mg)	Aluminium (Al)	Manganese (Mn)
1/10	10				Mechanical Failure of Reciprocating Mixer				
	20								
1/20	10								
	20								
1/40	10								
	20								

Table A1.36 ICP Data for Kaolinite and 1.5% Lime, Compacted on the 1/4/97 and Tested 175 days after Compaction for 6 Hours at 60 Revolutions per Minute. Filter only.

Solid to Liquid Ratio	Initial Cube Size (mm)	Concentration of Element in Solution in mg/kg (ppm)							
		Calcium (Ca)	Iron (Fe)	Lead (Pb)	Sodium (Na)	Silicon (Si)	Magnesium (Mg)	Aluminium (Al)	Manganese (Mn)
1/10	10	74.43	D 0.0081	D 0.0000	1.708	0.9145	0.0265	15.06	D 0.0001
	20	76.92	D 0.0141	D 0.0000	0.8817	0.8957	0.0233	15.16	d. 0.0001
1/20	10	74.97	D 0.0280	D 0.0000	0.6475	1.056	0.0277	16.18	D 0.0003
	20	41.20	D 0.0091	D 0.0000	0.5987	1.018	0.0308	16.11	D 0.0009
1/40	10	41.18	d. 0.0661	D 0.0000	0.4593	1.173	0.0312	13.02	D 0.0002
	20	58.06	D 0.0065	D 0.0000	0.4540	1.255	0.0255	13.25	D 0.0000

Note: 'D' indicates the stated value is below detection limits and the value stated is a system estimate.
'd' indicates the stated value is close to detection limits.

Table A1.37 ICP Data for Kaolinite and 1.5% Lime, Compacted on the 2/4/97 and Tested 7 days after Compaction for 24 Hours at 30 Revolutions per Minute. Filter only.

Solid to Liquid Ratio	Initial Cube Size (mm)	Concentration of Element in Solution in mg/kg (ppm)							
		Calcium (Ca)	Iron (Fe)	Lead (Pb)	Sodium (Na)	Silicon (Si)	Magnesium (Mg)	Aluminium (Al)	Manganese (Mn)
1/10	10	432.3	D 0.0015	D 0.0126	D 0.9225	0.6328	0.0116	1.375	D 0.0001
	20	437.9	D 0.0091	D 0.0297	D 1.031	1.306	0.0126	1.798	D 0.0000
1/20	10	231.7	D 0.0000	D 0.0081	D 0.5979	1.128	0.0106	3.265	D 0.0000
	20	272.7	D 0.0075	D 0.0081	D 0.7219	1.703	0.0178	4.154	D 0.0000
1/40	10	137.5	D 0.0007	D 0.0273	D 0.4600	1.656	0.0242	2.847	D 0.0021
	20	141.3	D 0.0000	D 0.0179	D 0.4791	0.3788	0.0185	D 0.3388	D 0.0000

Table A1.38 ICP Data for Kaolinite and 1.5% Lime, Compacted on the 2/4/97 and Tested 175 days after Compaction for 24 Hours at 30 Revolutions per Minute. Filter only.

Solid to Liquid Ratio	Initial Cube Size (mm)	Concentration of Element in Solution in mg/kg (ppm)							
		Calcium (Ca)	Iron (Fe)	Lead (Pb)	Sodium (Na)	Silicon (Si)	Magnesium (Mg)	Aluminium (Al)	Manganese (Mn)
1/10	10	109.0	d. 0.0132	D 0.0000	1.038	1.222	0.0193	12.14	d.0.0003
	20	110.2	d. 0.0209	D 0.0000	1.188	1.214	0.0259	12.49	d. 0.0009
1/20	10	89.03	0.0213	D 0.0000	0.6004	2.081	0.0434	14.07	0.0015
	20	89.65	d. 0.0128	D 0.0000	0.6221	1.478	0.0257	13.96	D 0.0002
1/40	10	70.67	D 0.0057	D 0.0000	0.4170	1.578	0.0269	12.15	D 0.0002
	20	69.18	D 0.0142	D 0.0000	0.5341	1.841	0.0253	12.36	D 0.0006

Table A1.39 ICP Data for Kaolinite and 1.5% Lime, Compacted on the 2/4/97 and Tested 301 days after Compaction for 24 Hours at 30 Revolutions per Minute. Filter only.

Solid to Liquid Ratio	Initial Cube Size (mm)	Concentration of Element in Solution in mg/kg (ppm)							
		Calcium (Ca)	Iron (Fe)	Lead (Pb)	Sodium (Na)	Silicon (Si)	Magnesium (Mg)	Aluminium (Al)	Manganese (Mn)
1/10	10	73.75	D 0.0011	D 0.0000	1.021	0.8374	0.0235	14.23	D 0.0000
	20	57.95	D 0.0006	D 0.0000	1.055	0.7705	0.0294	13.68	D 0.0000
1/20	10	49.58	D 0.0036	D 0.0000	0.5945	0.9228	0.0291	13.06	D 0.0001
	20	55.94	d. 0.0016	D 0.0000	0.6920	0.9577	0.0402	12.93	D 0.0002
1/40	10	31.31	D 0.0450	D 0.0000	0.5077	1.071	0.0294	10.38	D 0.0000
	20	31.66	D 0.0039	D 0.0000	0.5939	1.082	0.0521	10.35	D 0.0001

Note : 'D' indicates the stated value is below detection limits and the value stated is a system estimate.
'd' indicates the stated value is close to detection limits.

Table A1.40 ICP Data for Kaolinite and 1.5% Lime, Compacted on the 3/4/97 and Tested 7 days after Compaction for 24 Hours at 60 Revolutions per Minute. Filter only.

Solid to Liquid Ratio	Initial Cube Size (mm)	Concentration of Element in Solution in mg/kg (ppm)							
		Calcium (Ca)	Iron (Fe)	Lead (Pb)	Sodium (Na)	Silicon (Si)	Magnesium (Mg)	Aluminium (Al)	Manganese (Mn)
1/10	10	409.0	D 0.0000	D 0.0150	D 0.8321	0.4930	0.0104	1.076	D 0.0000
	20	476.2	D 0.0183	D 0.0016	1.741	0.7150	0.0328	1.175	D 0.0000
1/20	10	262.2	D 0.0011	D 0.0023	D 0.5314	1.144	0.0149	3.359	D 0.0000
	20	277.2	D 0.0026	D 0.0129	D 0.7293	1.259	0.0280	3.614	D 0.0015
1/40	10	139.8	D 0.0022	D 0.0015	D 0.4407	1.806	0.0272	4.390	D 0.0009
	20	143.7	D 0.0027	D 0.0102	D 0.4482	2.075	0.0243	5.489	D 0.0004

Table A1.41 ICP Data for Kaolinite and 1.5% Lime, Compacted on the 3/4/97 and Tested 175 days after Compaction for 24 Hours at 60 Revolutions per Minute. Filter only.

Solid to Liquid Ratio	Initial Cube Size (mm)	Concentration of Element in Solution in mg/kg (ppm)							
		Calcium (Ca)	Iron (Fe)	Lead (Pb)	Sodium (Na)	Silicon (Si)	Magnesium (Mg)	Aluminium (Al)	Manganese (Mn)
1/10	10	111.9	D 0.0082	D 0.0000	1.083	1.205	0.0236	12.91	d. 0.0004
	20	110.4	0.0237	D 0.0000	1.091	1.258	0.0364	13.23	d. 0.0008
1/20	10	88.33	0.0308	D 0.0000	0.7173	2.304	0.0405	14.66	d. 0.0006
	20	89.84	0.0228	D 0.0000	0.6787	1.367	0.0402	13.78	D 0.0010
1/40	10	69.44	D 0.0166	D 0.0000	0.6533	1.715	0.0481	12.41	d. 0.0002
	20	72.42	0.0711	D 0.0000	0.7802	1.670	0.0658	12.53	0.0031

Note : 'D' indicates the stated value is below detection limits and the value stated is a system estimate.
'd' indicates the stated value is close to detection limits.

A1.2.5 English China Clay with 5000ppm Pb and 1.5% lime

A very significant result is that even at the very high pH values illustrated in Figures A1.23 to A1.26, the levels of leachable Pb reported in Tables A1.42 to A1.51 are below detection levels despite the amphoteric nature of the element and after 301 days curing its soluble fraction is effectively zero.

A1.2.5.1 Solid : liquid ratio

Inspection of Figures A1.23 to A1.26 illustrates similar behavioural patterns to uncontaminated English China Clay with 1.5% lime. However the changes in pH and conductivity as solid to liquid ratio increases are slightly different.

Increasing solid to liquid ratio from 1:40 to 1:20 at 7 days for 20mm cubes during 6hr/30rpm tests (Figure A1.23) increased the end of test conductivity from 1820μS/cm to 3140μS/cm a factor of 1.73 whilst pH increased by 0.27 from 12.15 to 12.42. Similarly increasing solid to liquid ratio from 1:20 to 1:10 increased the end of test conductivity from 3140μS/cm to 5030μS/cm a factor of 1.60 whilst pH increased by 0.18 from 12.42 to 12.60. Increasing solid to liquid ratio from 1:40 to 1:20 at 175 days for 20mm cubes during 6hr/30rpm tests (Figure A1.23) increased the end of test conductivity from 852μS/cm to 1318μS/cm a factor of 1.50 whilst pH increased by 0.22 from 11.55 to 11.77. Similarly increasing solid to liquid ratio from 1:20 to 1:10 increased the end of test conductivity from 1318μS/cm to 1574μS/cm a factor of 1.19 whilst pH increased by 0.11 from 11.77 to 11.88.

As conductivity increased by specific factors due to changes in curing time and solid to liquid ratio these factors are similar to those changing Ca concentrations in solution. These trends are evident in Figures A1.23 to A1.26 and Tables A1.42 to A1.51.

Using the 6hr/30rpm tests with 20mm cube sizes as an example, increasing solid to liquid ratio from 1:40 to 1:20 to 1:10 at 7 days also reduces concentrations of Si from 1.12ppm to 0.603ppm to 0.429ppm respectively, Mg from 0.0212 to 0.0156 to 0.0095 respectively and Al from 5.12ppm to 4.28ppm to 1.28ppm respectively. However at 175 and 301 days, the 1:20 solid to liquid ratio releases the most Al, approximately 32ppm.

A1.2.5.2 Cube Size

At the lowest solid to liquid ratio 1:40, the 10mm cube size tends to produce the highest final pH at any curing time. However on the basis of conductivity the highest variation between cube sizes tends to occur at the highest solid to liquid ratios.

During 7 day curing tests, with the exception of 6hr/30rpm tests (Tables A1.42 to A1.44), the 10mm cube size released the most Ca. During 175 day and 301 day curing tests 20mm cubes appeared to release more Ca. Generally however it was the 10mm cubes at specific solid to liquid ratios that released more Na, Si, and Mg with Al remaining unaffected (Table A1.42 to A1.51).

A1.2.5.3 Rotation speed and test duration

The higher rotation speed during 6hr tests had no apparent effect on pH or conductivity at any test duration or curing period (Figures A1.23 to A1.26). At 7 days the higher rotation speed for both test durations released significantly more Ca, more Pb and less Na whilst generally all other elements remained unaffected. However at 175 days the higher 60rpm rotation speed released significantly less Ca than the 30rpm rotation speed at the solid to liquid ratios 1:20 and 1:40 for 24 hr tests and for all solid to liquid ratios for 6hr tests.

Increasing test duration at 7 days curing appears to have no appreciable effect on pH or conductivity. However comparison of at 175 days curing and 301 days curing suggests that increasing the test duration results in higher final pH and conductivity values. Ca leachability highlighted in Tables A1.42 to A1.51 is also higher at these higher pH and conductivity values. Comparison of 60rpm tests in Tables A1.45, A1.46, and A1.50, A1.51 at 7 and 175 days clearly illustrates that as test duration increased more Ca, Na, Si and Al are released. These trends are not as clear for 30rpm tests.

A1.2.5.3 Curing Time

It was previously mentioned that increasing curing time has significant effects on pH and conductivity. This is reflected as expected in massive reductions in Ca, increases in Na, increases and then reductions in Al and reductions in Si. Although present at levels near or at detection limits there are also reductions in Pb leachability.

Figure A1.23 Conductivity and pH characteristics for English China Clay with 5000ppm Pb and 1.5% lime during 6hr/30rpm Batch Tests

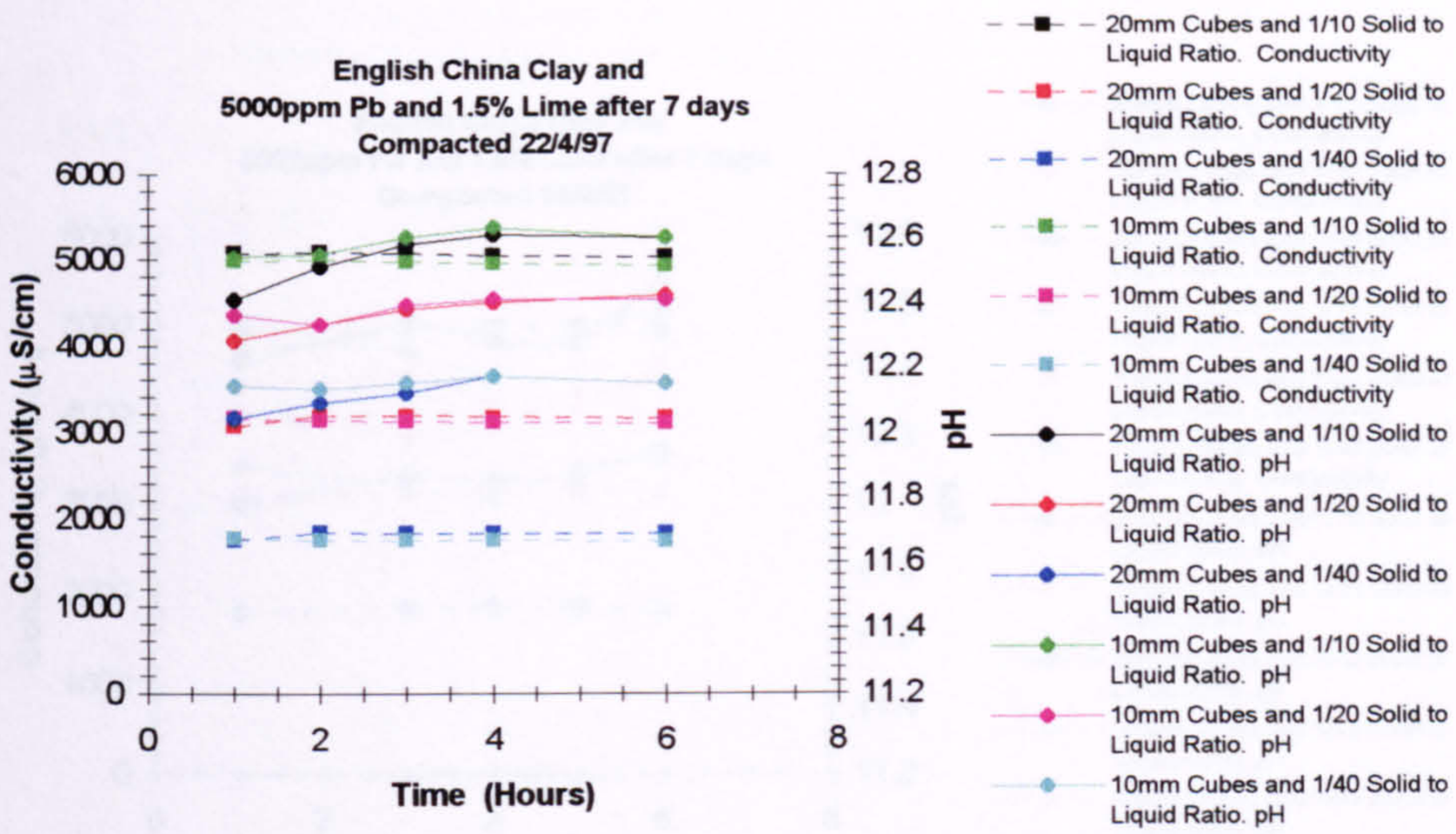

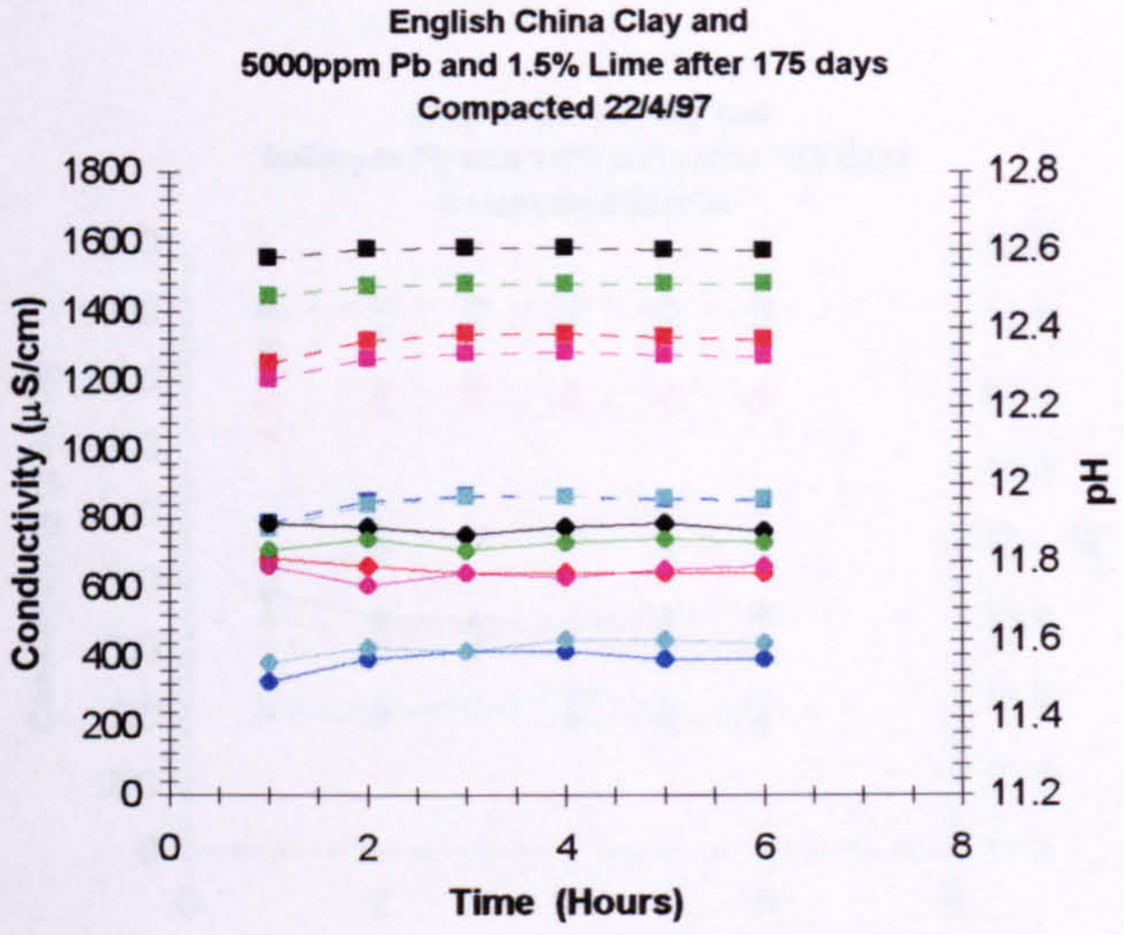

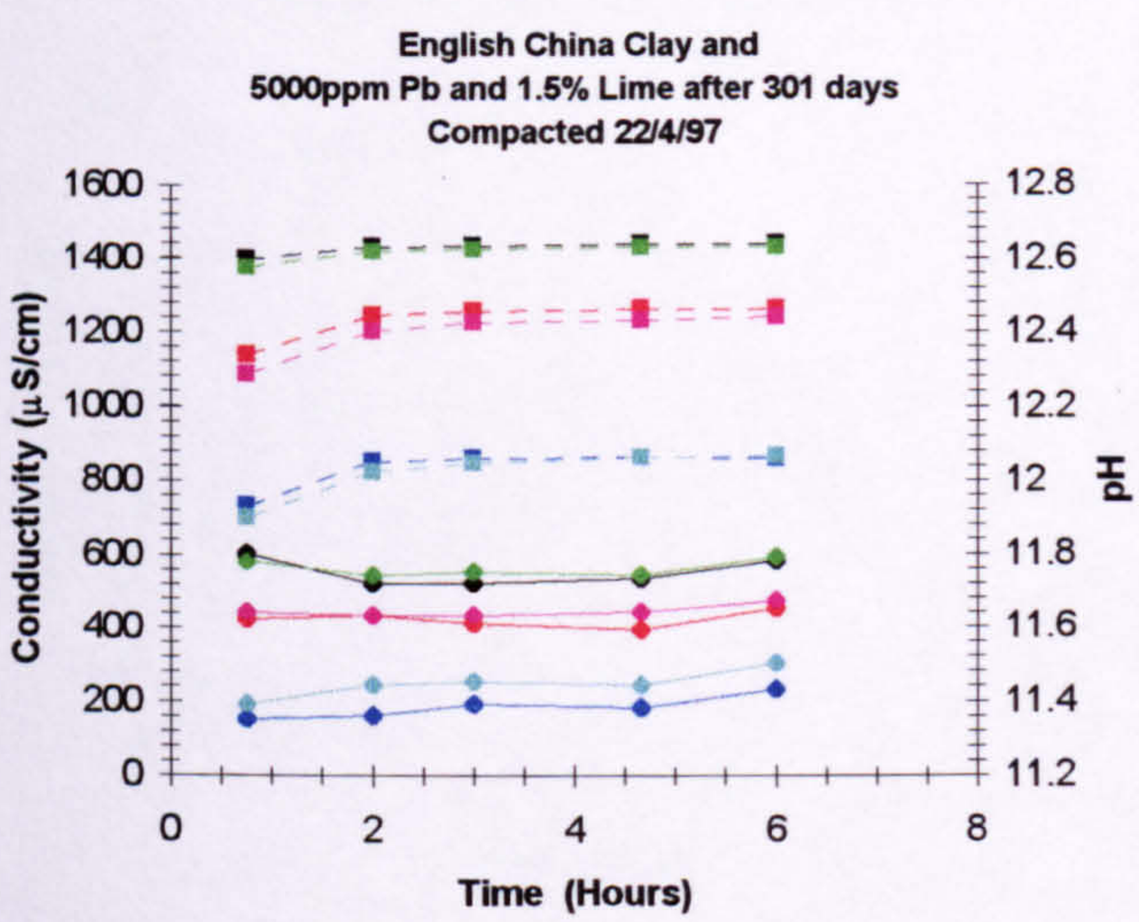

Figure A1.24 Conductivity and pH characteristics for English China Clay with 5000ppm Pb and 1.5% lime during 6hr/60rpm Batch Tests

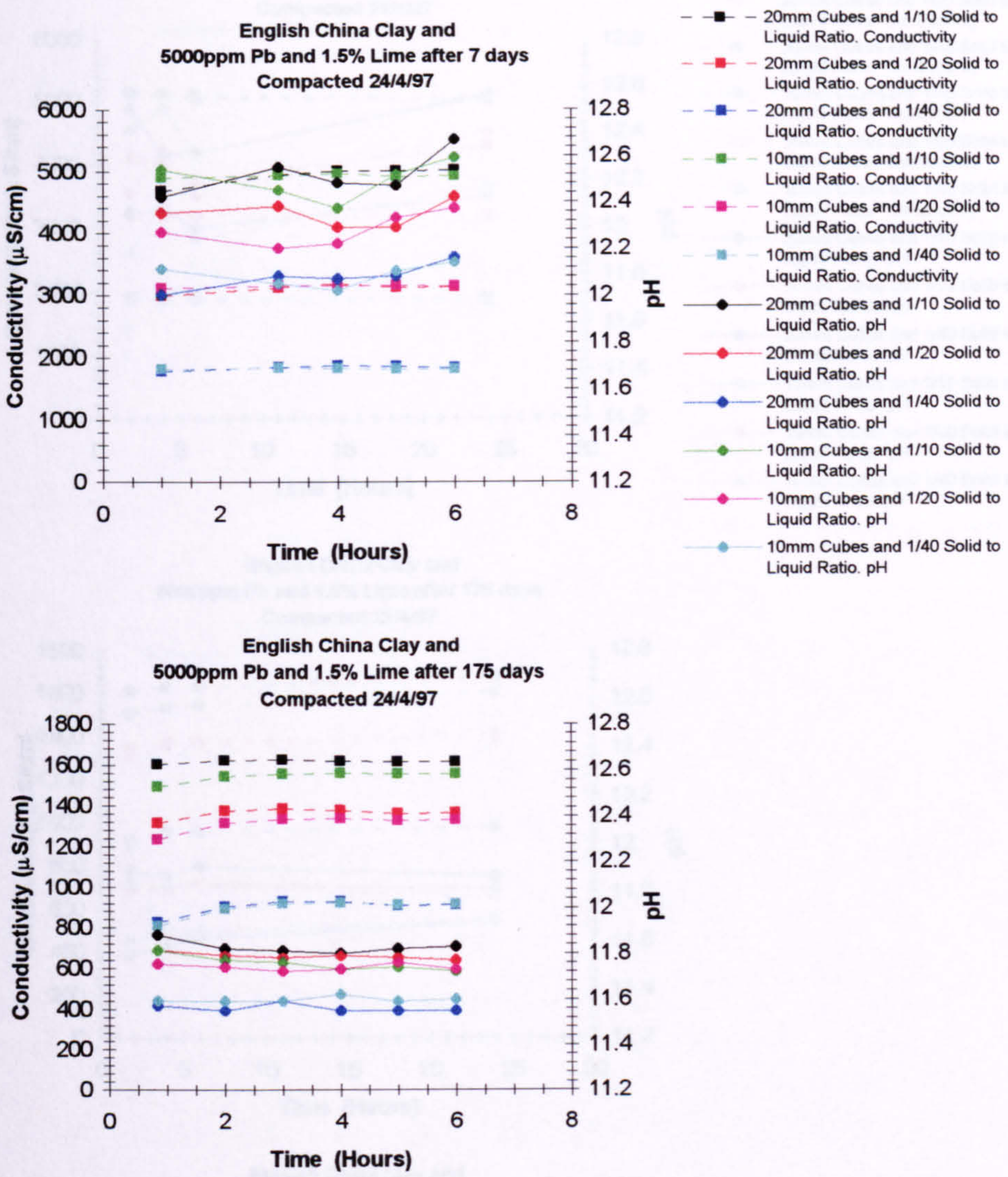

Figure A1.25 Conductivity and pH characteristics for English China Clay with 5000ppm Pb and 1.5% lime during 24hr/30rpm Batch Tests

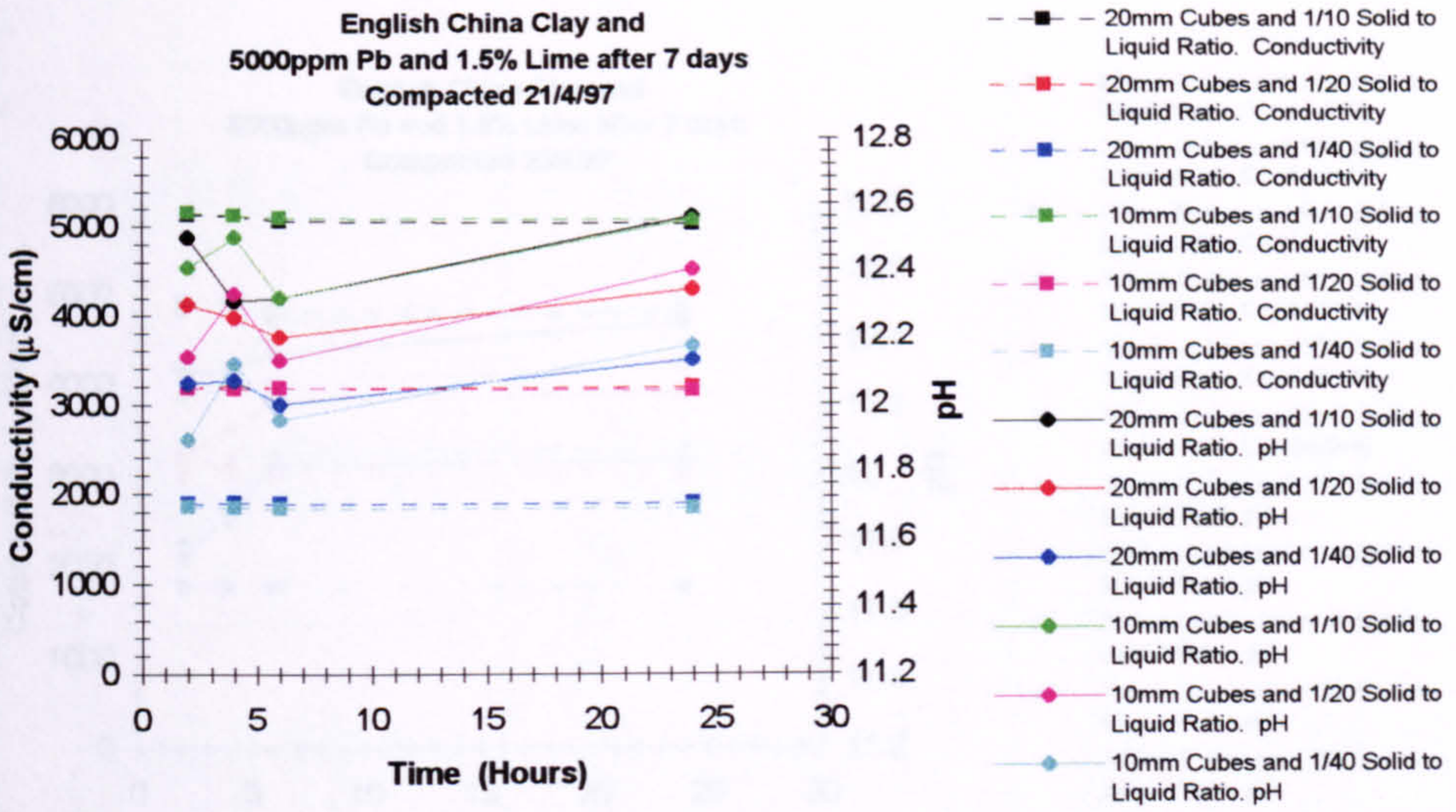

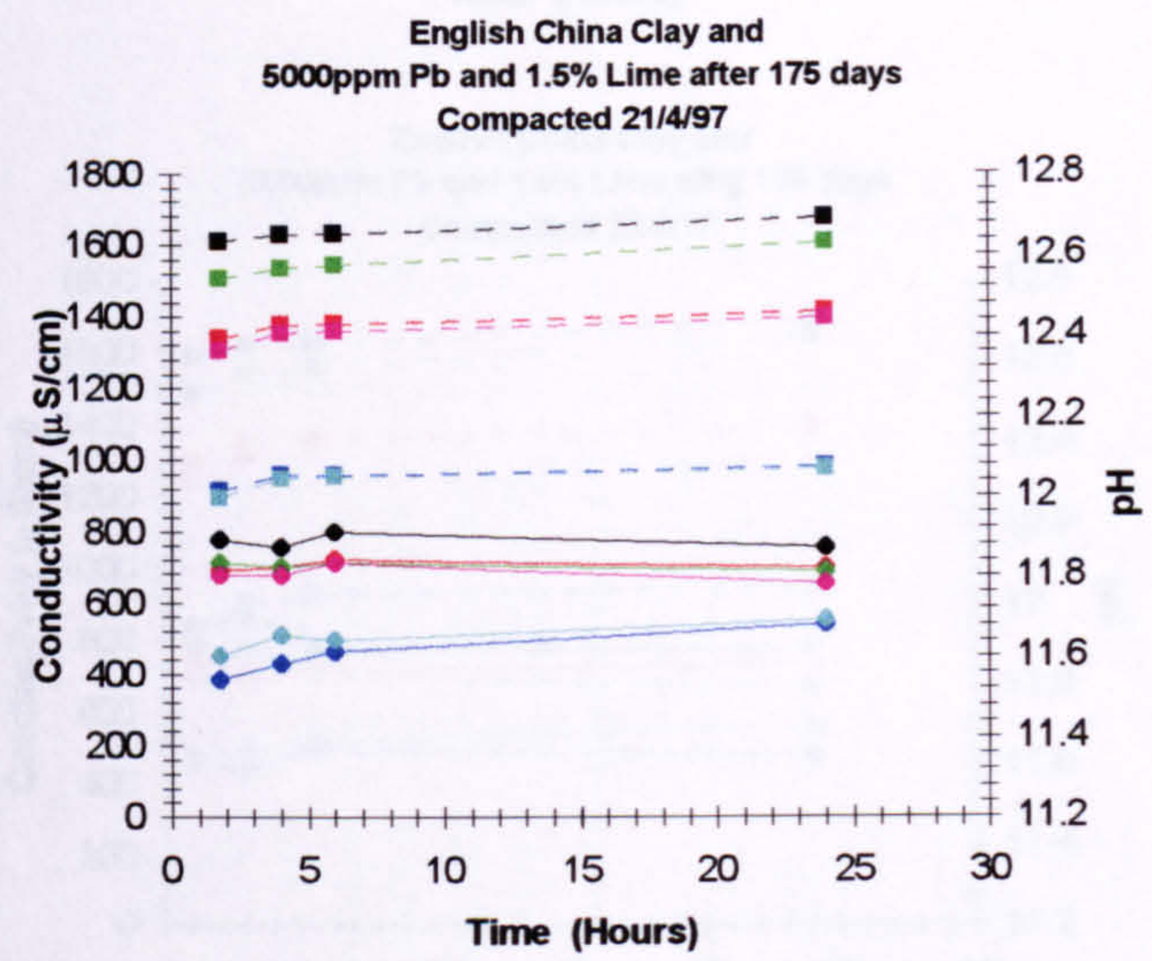

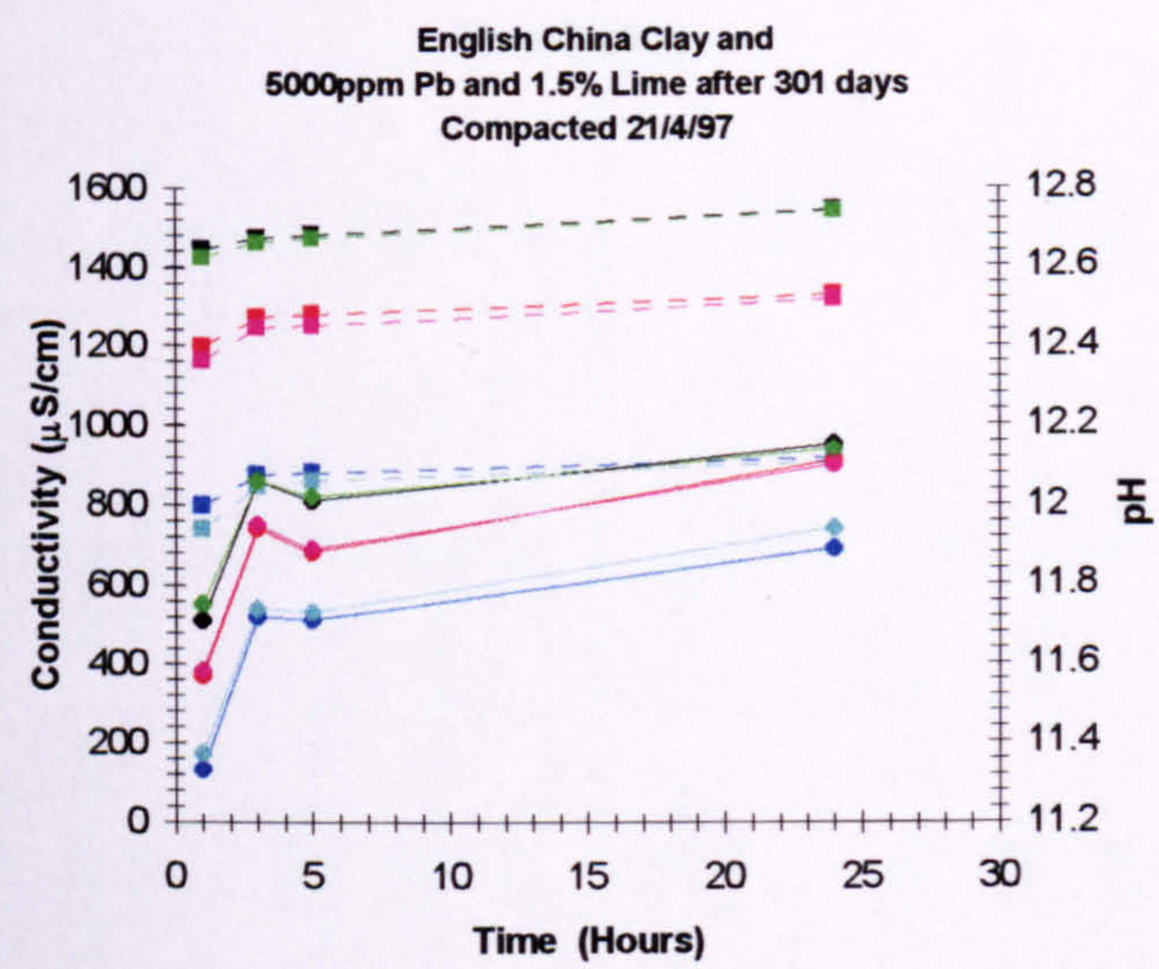

Figure A1.26 Conductivity and pH characteristics for English China Clay with 5000ppm Pb and 1.5% lime during 24hr/60rpm Batch Tests

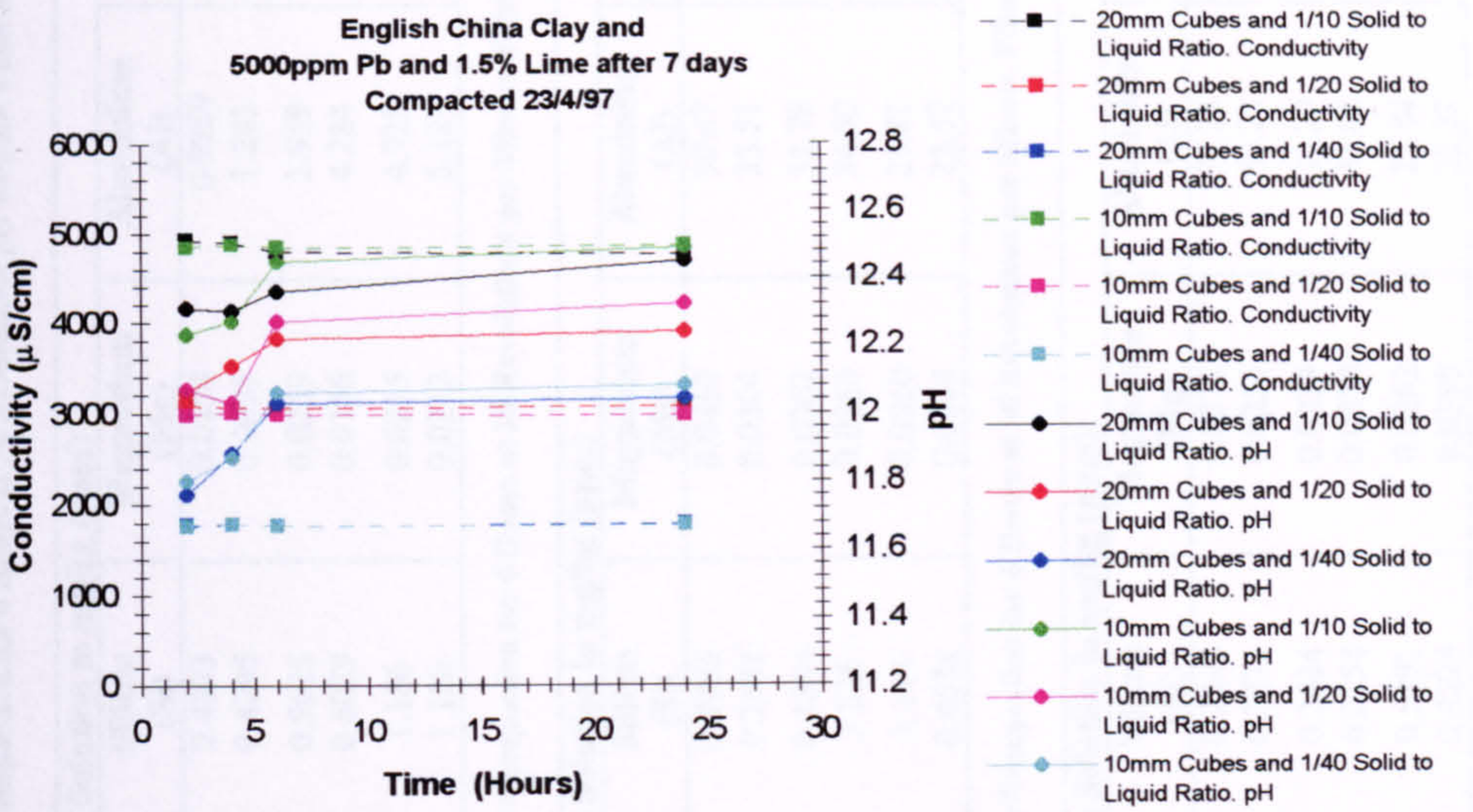

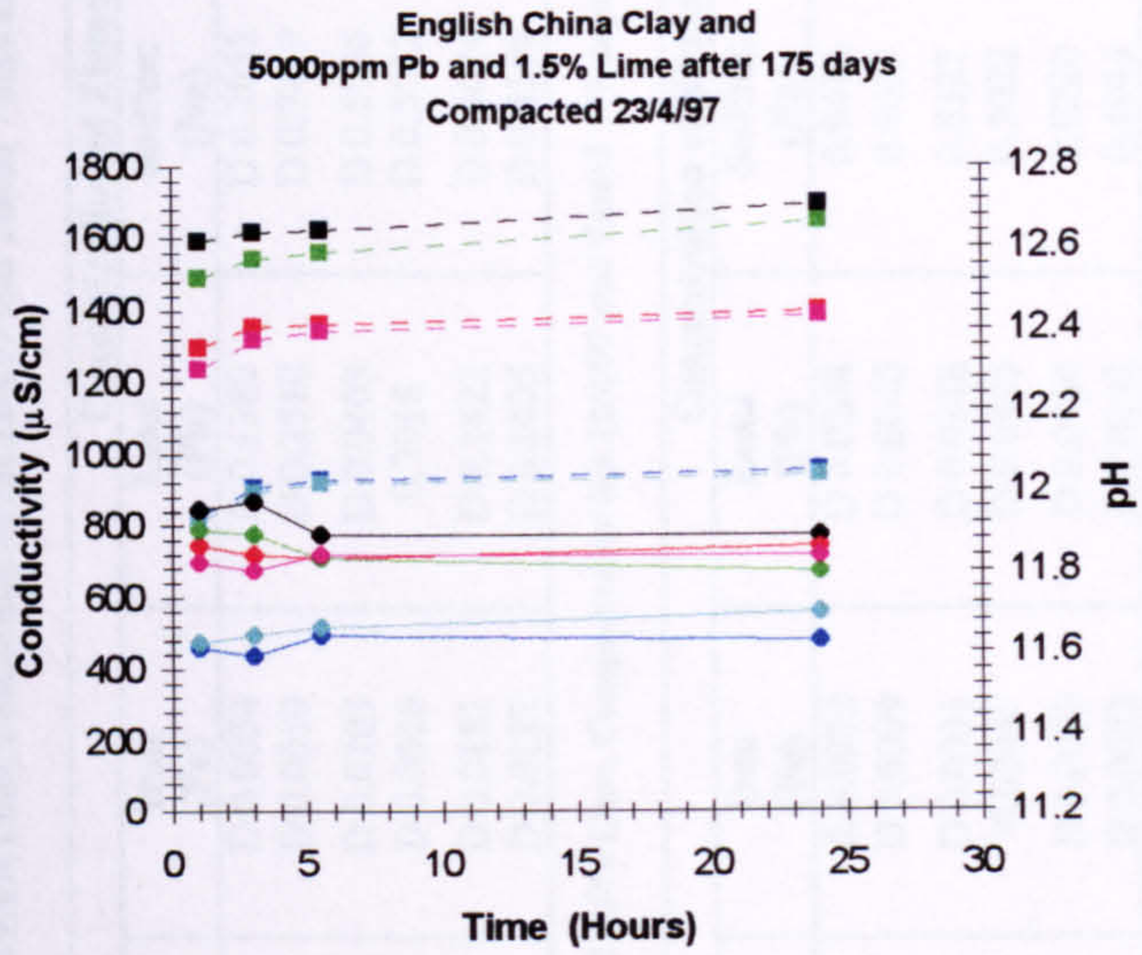

Table A1.42 ICP Data for Kaolinite and 5000ppm Lead and 1.5% Lime, Compacted on the 22/4/97 and Tested 7 days after Compaction for 6 Hours at 30 Revolutions per Minute. Filter only.

Solid to Liquid Ratio	Initial Cube Size (mm)	Concentration of Element in Solution in mg/kg (ppm)							
		Calcium (Ca)	Iron (Fe)	Lead (Pb)	Sodium (Na)	Silicon (Si)	Magnesium (Mg)	Aluminium (Al)	Manganese (Mn)
1/10	10	461.0	D 0.0034	D 0.1380	D 0.7855	0.4833	0.0154	0.9859	D 0.0000
	20	472.7	D 0.0010	D 0.2510	D 0.7419	0.4295	0.0095	1.283	D 0.0000
1/20	10	280.3	D 0.0103	D 0.0403	D 0.5936	0.9625	0.0259	3.959	D 0.0014
	20	248.9	D 0.0616	0.7918	D 0.5042	0.6039	0.0156	4.284	D 0.0028
1/40	10	131.7	D 0.0153	D 0.1422	D 0.5024	1.186	0.0255	4.729	D 0.0014
	20	156.5	D 0.0127	D 0.2405	D 0.3394	1.120	0.0212	5.127	D 0.0004

Table A1.43 ICP Data for Kaolinite and 5000ppm Lead and 1.5% Lime, Compacted on the 22/4/97 and Tested 175 days after Compaction for 6 Hours at 30 Revolutions per Minute. Filter only.

Solid to Liquid Ratio	Initial Cube Size (mm)	Concentration of Element in Solution in mg/kg (ppm)							
		Calcium (Ca)	Iron (Fe)	Lead (Pb)	Sodium (Na)	Silicon (Si)	Magnesium (Mg)	Aluminium (Al)	Manganese (Mn)
1/10	10	140.9	d. 0.0212	D 0.0244	0.9414	0.9786	0.0460	30.67	D 0.0000
	20	152.9	D 0.0009	D 0.0040	0.9023	0.2682	0.0304	33.51	D 0.0000
1/20	10	92.40	D 0.0051	D 0.0318	0.5527	0.4864	0.0362	32.78	D 0.0000
	20	105.3	0.0344	D 0.0825	0.5022	1.326	0.0363	34.50	D 0.0000
1/40	10	75.60	D 0.0099	D 0.0454	0.9220	1.143	0.0960	23.81	D 0.0001
	20	77.72	D 0.0021	D 0.0141	0.4044	0.4634	0.0344	23.57	D 0.0000

Table A1.44 ICP Data for Kaolinite and 5000ppm Lead and 1.5% Lime, Compacted on the 22/4/97 and Tested 301 days after Compaction for 6 Hours at 30 Revolutions per Minute. Filter only.

Solid to Liquid Ratio	Initial Cube Size (mm)	Concentration of Element in Solution in mg/kg (ppm)							
		Calcium (Ca)	Iron (Fe)	Lead (Pb)	Sodium (Na)	Silicon (Si)	Magnesium (Mg)	Aluminium (Al)	Manganese (Mn)
1/10	10	99.87	D 0.0064	D 0.0000	0.8639	0.2492	0.0271	30.28	D 0.0000
	20	100.2	D 0.0120	D 0.0000	0.8851	0.2275	0.0255	30.23	D 0.0000
1/20	10	95.45	D 0.0033	D 0.0000	0.6922	0.2424	0.0234	31.20	D 0.0000
	20	100.9	D 0.0000	D 0.0043	0.5742	0.2258	0.0358	31.82	D 0.0000
1/40	10	69.64	d. 0.0070	D 0.0000	d. 0.3131	0.5191	0.0262	22.84	D 0.0000
	20	72.57	D 0.0105	D 0.0000	0.5523	0.3223	0.0399	22.32	D 0.0000

Note: 'D' indicates the stated value is below detection limits and the value stated is a system estimate.
'd' indicates the stated value is close to detection limits.

Table A1.45 ICP Data for Kaolinite and 5000ppm Lead and 1.5% Lime, Compacted on the 24/4/97 and Tested 7 days after Compaction for 6 Hours at 60 Revolutions per Minute. Filter only.

Solid to Liquid Ratio	Initial Cube Size (mm)	Concentration of Element in Solution in mg/kg (ppm)							
		Calcium (Ca)	Iron (Fe)	Lead (Pb)	Sodium (Na)	Silicon (Si)	Magnesium (Mg)	Aluminium (Al)	Manganese (Mn)
1/10	10	514.3	D 0.0000	1.864	d. 0.9892	0.4366	0.0098	1.009	D 0.0000
	20	465.2	D 0.0027	0.5216	1.235	0.4769	0.0120	1.413	D 0.0000
1/20	10	306.4	D 0.0012	0.9175	D 0.6391	0.8239	0.0212	3.177	D 0.0000
	20	304.7	D 0.0066	0.7785	D 0.7532	0.6581	0.0200	4.217	D 0.0000
1/40	10	170.6	D 0.0062	D 0.2877	D 0.4500	1.109	0.0192	4.659	D 0.0000
	20	173.3	D 0.0046	D 0.2777	D 0.5611	1.145	0.0267	5.120	D 0.0002

Table A1.46 ICP Data for Kaolinite and 5000ppm Lead and 1.5% Lime, Compacted on the 24/4/97 and Tested 175 days after Compaction for 6 Hours at 60 Revolutions per Minute. Filter only.

Solid to Liquid Ratio	Initial Cube Size (mm)	Concentration of Element in Solution in mg/kg (ppm)							
		Calcium (Ca)	Iron (Fe)	Lead (Pb)	Sodium (Na)	Silicon (Si)	Magnesium (Mg)	Aluminium (Al)	Manganese (Mn)
1/10	10	83.95	D 0.0000	D 0.0083	0.8160	D 0.000	0.0293	5.327	D 0.0000
	20	98.51	D 0.0036	D 0.0000	0.7895	d.0.0842	0.0279	28.42	D 0.0000
1/20	10	73.00	D 0.0008	D 0.0000	0.5844	d. 0.0758	0.0382	26.48	D 0.0000
	20	69.55	D 0.0013	D 0.0000	0.5375	d. 0.0094	0.0365	19.75	D 0.0000
1/40	10	42.81	D 0.0011	D 0.0107	0.3460	D 0.0276	0.0327	13.86	D 0.0000
	20	42.44	D 0.0067	D 0.0134	0.4127	0.0432	0.0396	13.72	D 0.0001

Note: 'D' indicates the stated value is below detection limits and the value stated is a system estimate.
'd' indicates the stated value is close to detection limits.

Table A1.47 ICP Data for Kaolinite and 5000ppm Lead and 1.5% Lime, Compacted on the 21/4/97 and Tested 7 days after Compaction for 24 Hours at 30 Revolutions per Minute. Filter only.

Solid to Liquid Ratio	Initial Cube Size (mm)	Concentration of Element in Solution in mg/kg (ppm)							
		Calcium (Ca)	Iron (Fe)	Lead (Pb)	Sodium (Na)	Silicon (Si)	Magnesium (Mg)	Aluminium (Al)	Manganese (Mn)
1/10	10	489.9	D 0.0059	D 0.4553	D 0.8313	0.6951	0.0065	1.415	D 0.0000
	20	406.4	D 0.0128	D 0.2720	D 1.049	0.5214	0.0239	1.441	D 0.0006
1/20	10	290.7	D 0.0702	0.5715	D 0.4865	0.6388	0.0138	3.735	D 0.0006
	20	317.9	d. 0.0641	0.8861	D 0.7140	0.7464	0.0313	4.266	D 0.0020
1/40	10	192.0	0.0782	0.4834	D 0.3654	1.105	0.0264	4.700	D 0.0021
	20	186.8	D 0.0104	d. 0.3708	D 0.4444	1.100	0.0285	5.017	D 0.0007

Table A1.48 ICP Data for Kaolinite and 5000ppm Lead and 1.5% Lime, Compacted on the 21/4/97 and Tested 175 days after Compaction for 24 Hours at 30 Revolutions per Minute. Filter only.

Solid to Liquid Ratio	Initial Cube Size (mm)	Concentration of Element in Solution in mg/kg (ppm)							
		Calcium (Ca)	Iron (Fe)	Lead (Pb)	Sodium (Na)	Silicon (Si)	Magnesium (Mg)	Aluminium (Al)	Manganese (Mn)
1/10	10	178.3	D 0.0025	D 0.0096	1.097	0.3913	0.0130	27.71	D 0.0001
	20	184.5	D 0.0014	D 0.0133	0.8693	0.3237	0.0217	30.45	D 0.0000
1/20	10	144.8	D 0.0090	D 0.0236	0.6490	0.3850	0.0312	31.26	D 0.0002
	20	135.1	D 0.0113	D 0.0048	0.7137	0.4835	0.0299	30.71	D 0.0000
1/40	10	95.82	0.0255	0.2020	1.588	0.5341	0.0507	23.13	D 0.0003
	20	95.86	D 0.0012	D 0.0291	0.5029	0.5706	0.0365	23.56	D 0.0001

Table A1.49 ICP Data for Kaolinite and 5000ppm Lead and 1.5% Lime, Compacted on the 21/4/97 and Tested 301 days after Compaction for 24 Hours at 30 Revolutions per Minute. Filter only.

Solid to Liquid Ratio	Initial Cube Size (mm)	Concentration of Element in Solution in mg/kg (ppm)							
		Calcium (Ca)	Iron (Fe)	Lead (Pb)	Sodium (Na)	Silicon (Si)	Magnesium (Mg)	Aluminium (Al)	Manganese (Mn)
1/10	10	147.2	d. 0.0019	D 0.0000	1.082	0.2430	0.0317	26.56	D 0.0000
	20	170.1	d. 0.0001	D 0.0000	0.9718	0.2457	0.0271	26.62	D 0.0000
1/20	10	152.1	D 0.0032	D 0.0000	0.6706	0.2961	0.0240	29.20	D 0.0000
	20	135.7	D 0.0120	D 0.0000	0.7059	0.2673	0.0295	28.65	D 0.0000
1/40	10	78.04	D 0.0009	D 0.0000	0.5237	0.4463	0.0276	21.71	D 0.0000
	20	85.68	D 0.0095	D 0.0000	0.5090	0.4210	0.0265	21.68	D 0.0000

Note: 'D' indicates the stated value is below detection limits and the value stated is a system estimate.
'd' indicates the stated value is close to detection limits.

Table A1.50 ICP Data for Kaolinite and 5000ppm Lead and 1.5% Lime, Compacted on the 23/4/97 and Tested 7 days after Compaction for 24 Hours at 60 Revolutions per Minute. Filter only.

Solid to Liquid Ratio	Initial Cube Size (mm)	Concentration of Element in Solution in mg/kg (ppm)							
		Calcium (Ca)	Iron (Fe)	Lead (Pb)	Sodium (Na)	Silicon (Si)	Magnesium (Mg)	Aluminium (Al)	Manganese (Mn)
1/10	10	513.6	D 0.0074	0.6487	D 0.8849	0.5966	0.0326	1.775	D 0.0005
	20	495.5	D 0.0004	0.4852	D 0.8721	0.5058	0.0098	1.708	D 0.0003
1/20	10	309.7	D 0.0013	D 0.1607	D 0.4201	0.8493	0.0147	3.965	D 0.0004
	20	333.7	D 0.0114	1.130	D 0.4940	0.9366	0.0229	4.542	D 0.0003
1/40	10	187.0	D 0.0093	D 0.2674	D 0.3037	1.299	0.0249	5.238	D 0.0007
	20	162.8	D 0.0084	D 0.2193	D 0.3685	1.103	0.0268	5.049	D 0.0002

Table A1.51 ICP Data for Kaolinite and 5000ppm Lead and 1.5% Lime, Compacted on the 23/4/97 and Tested 175 days after Compaction for 24 Hours at 60 Revolutions per Minute. Filter only.

Solid to Liquid Ratio	Initial Cube Size (mm)	Concentration of Element in Solution in mg/kg (ppm)							
		Calcium (Ca)	Iron (Fe)	Lead (Pb)	Sodium (Na)	Silicon (Si)	Magnesium (Mg)	Aluminium (Al)	Manganese (Mn)
1/10	10	178.0	D 0.0003	D 0.0230	0.9132	0.3336	0.0255	28.31	D 0.0000
	20	183.6	D 0.0005	D 0.0090	0.8366	0.2930	0.0274	30.25	D 0.0000
1/20	10	100.4	D 0.0087	D 0.0000	0.6014	0.8598	0.0420	32.02	d.0.0001
	20	98.70	D 0.0090	D 0.0345	0.5627	0.5868	0.0365	31.56	D 0.0000
1/40	10	62.45	D 0.0005	D 0.0000	0.5271	0.5877	0.0481	22.94	D 0.0000
	20	75.51	D 0.0042	D 0.0056	0.4021	0.6507	0.0366	22.83	D 0.0000

Note: 'D' indicates the stated value is below detection limits and the value stated is a system estimate.
'd' indicates the stated value is close to detection limits.

A1.2.6 English China Clay with 5000ppm Fe and 1.5% lime

Similarly to the lime treated Pb contaminated samples, leachable Fe concentrations are found below detection limits in all batch tests performed.

A1.2.6.1 Solid : liquid ratio

Considering 6hr/30rpm tests (Figure A1.27) with 20mm cube sizes at 7 days curing, the conductivities at the solid to liquid ratios 1:40, 1:20 and 1:10 are 891μS/cm, 1592μS/cm and 2840μS/cm respectively whilst pH values are 10.98, 11.12 and 11.29 respectively. At 175 days curing end of test conductivity values are 823μS/cm, 1540μS/cm and 2730μS/cm respectively whilst pH values are 10.74, 11.07 and 11.25 respectively. There are no significant changes at 301 days curing.

Increasing solid to liquid ratio from 1:40 to 1:20 at 7 days curing increases conductivity from 891μS/cm to 1592μS/cm, a factor of 1.79 whilst pH increased by 0.14 pH divisions from 10.98 to 11.12. Increasing solid to liquid ratio from 1:20 to 1:10 increases conductivity from 1592μS/cm to 2840μS/cm a factor of 1.78 whilst pH increased by 0.17 pH divisions from 11.12 to 11.29.

Increasing solid to liquid ratio from 1:40 to 1:20 at 175 days curing increases conductivity from 823μS/cm to 1540μS/cm, a factor of 1.87 whilst pH increased by 0.33 pH divisions from 10.74 to 11.07. Increasing solid to liquid ratio from 1:20 to 1:10 increases conductivity from 1540μS/cm to 2730μS/cm a factor of 1.77 whilst pH increased by 0.18 pH divisions from 11.07 to 11.25. These trends are repeated in the other batch test results. Direct observation of Tables A1.52, A1.53 and A1.54 identifies that the factors of increase in conductivity with increasing solid to liquid ratio are directly related to Ca concentrations.

Inspection of Figures A1.27 to A1.30 highlights that the solid to liquid ratio 1:40 creates the most variability in pH between cube sizes. At all solid to liquid ratios and curing times conductivity apparently remains unaffected regardless of cube size. It is also apparent from analysis of Tables A1.52 to A1.61 that Ca concentrations decrease with decreasing solid to liquid ratio, Na and Al also decrease and Si concentrations increase whilst other elements remain relatively unaffected or below detection limits.

A1.2.6.2 Cube Size

Analysis of Figures A1.27 to A1.30 highlights that 10mm cubes tend to result in the highest solution pH and conductivity. However inspection of Tables A1.52 to A1.61 highlights no obvious trends in Al, Si or Ca content with cube size variation. This is also true for Na and Mg at 7 days curing. However after 7 days curing 10mm cube sizes generally release more Na, Mg and Al into solution.

A1.2.6.3 Rotation speed and test duration

Figures A1.27 and A1.28 illustrate that increasing rotation speed for 6hr tests substantially increased pH and conductivity particularly at higher solid to liquid ratios. Comparison of Figures A1.29 and A1.30 suggests that increasing rotation speed for 24 hr tests slightly reduce pH and conductivity values. Tables A1.52, A1.53 and A1.55, A1.56 show that increasing rotation speed for 6hr tests significantly increased Ca concentrations at 7 days curing with no significant subsequent change at 175days curing. Al levels significantly increase at all curing times whilst other elements remained unaffected. Consideration of 24hr tests in Tables A1.57, A1.58 and A1.60, A1.61, illustrates increasing rotation speed at 7 days curing reduces Ca concentration for specific solid to liquid ratios whilst at 175 days curing there is no significant difference. Na also tends to increase, although there is no significant variation in Al concentrations.

Increasing test duration for 30rpm tests illustrated in Figures A1.27 and A1.29 shows large increases in pH and conductivity at all curing times and solid to liquid ratios. Analysis of Tables A1.52 to A1.59 shows that as test duration increases Ca and Al increase significantly whilst Si and Mg exhibit moderate increases and Na concentration reduces. These trends are also similar for 60rpm tests.

A1.2.6.4 Curing Time

Increasing curing time from 7 days to 175 days results in a small reduction in conductivity and pH and only very small changes continue to occur between 175 days and 301 days. These trends are also reflected in the chemical data. Ca and Na concentrations reduce, Si concentrations moderately increase whilst Mg concentrations remain unaffected. For 6hr tests Al concentrations appear to significantly reduce from 7 days curing to 175 days curing then increase from 175 days curing to 301 days curing. However for 24 hr tests Al levels are high at 7 days curing and then increase slightly at 175 days and remain stable at this level at 301 days.

Figure A1.27 Conductivity and pH characteristics for English China Clay with 5000ppm Fe and 1.5% lime during 6hr/30rpm Batch Tests

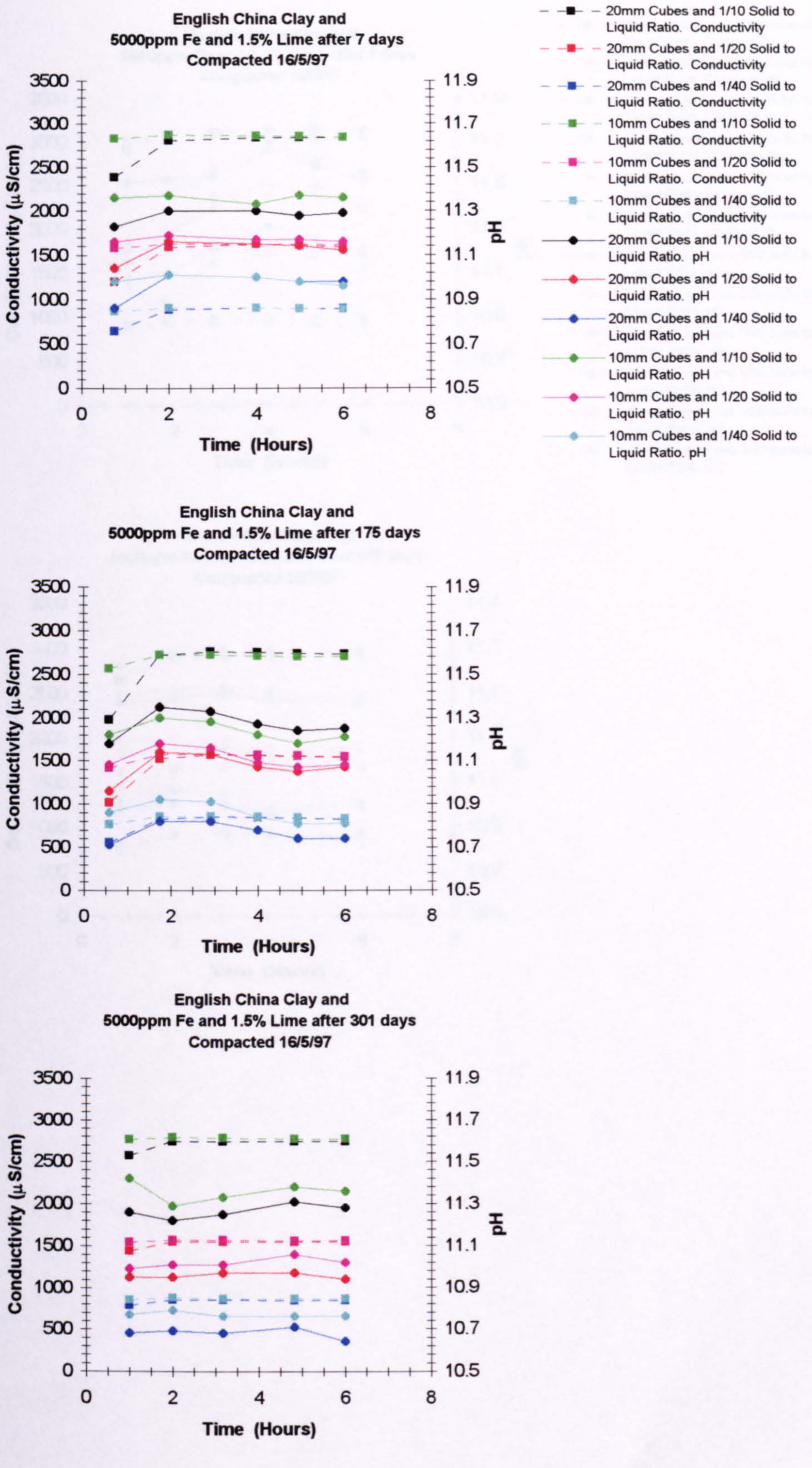

Figure A1.28 Conductivity and pH characteristics for English China Clay with 5000ppm Fe and 1.5% lime during 6hr/60rpm Batch Tests

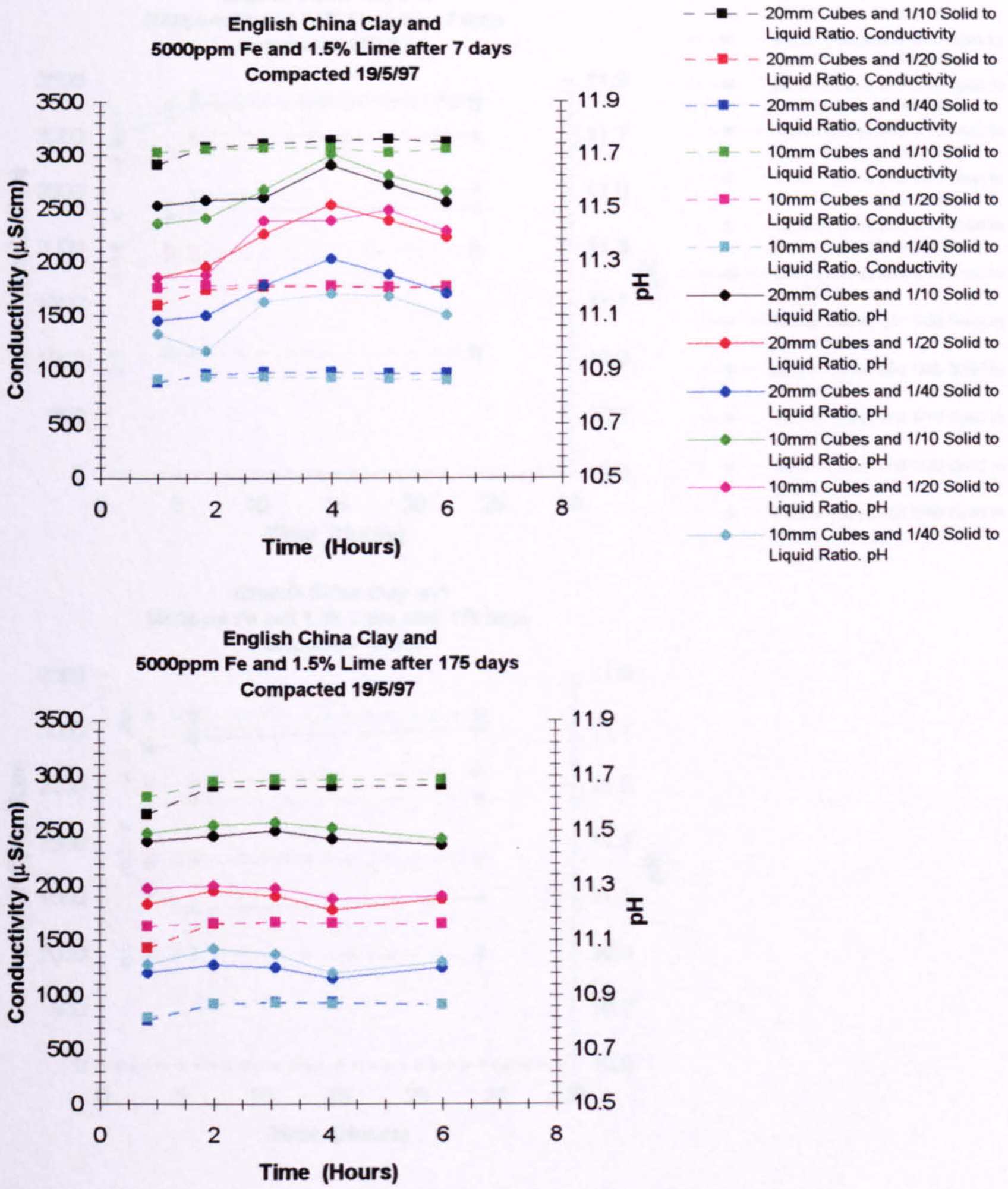

Figure A1.29 Conductivity and pH characteristics for English China Clay with 5000ppm Fe and 1.5% lime during 24hr/30rpm Batch Tests

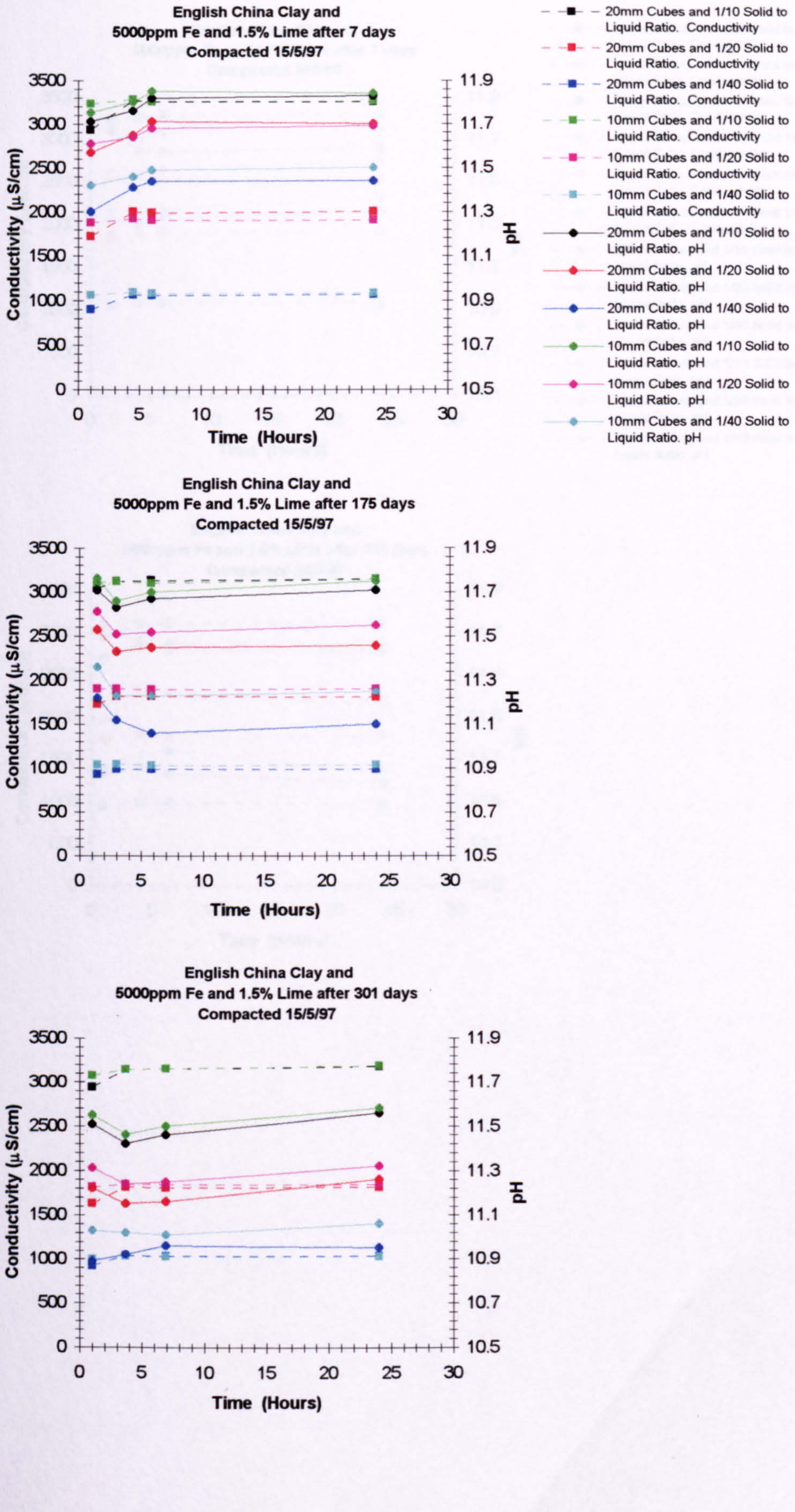

Figure A1.30 Conductivity and pH characteristics for English China Clay with 5000ppm Fe and 1.5% lime during 24hr/60rpm Batch Tests

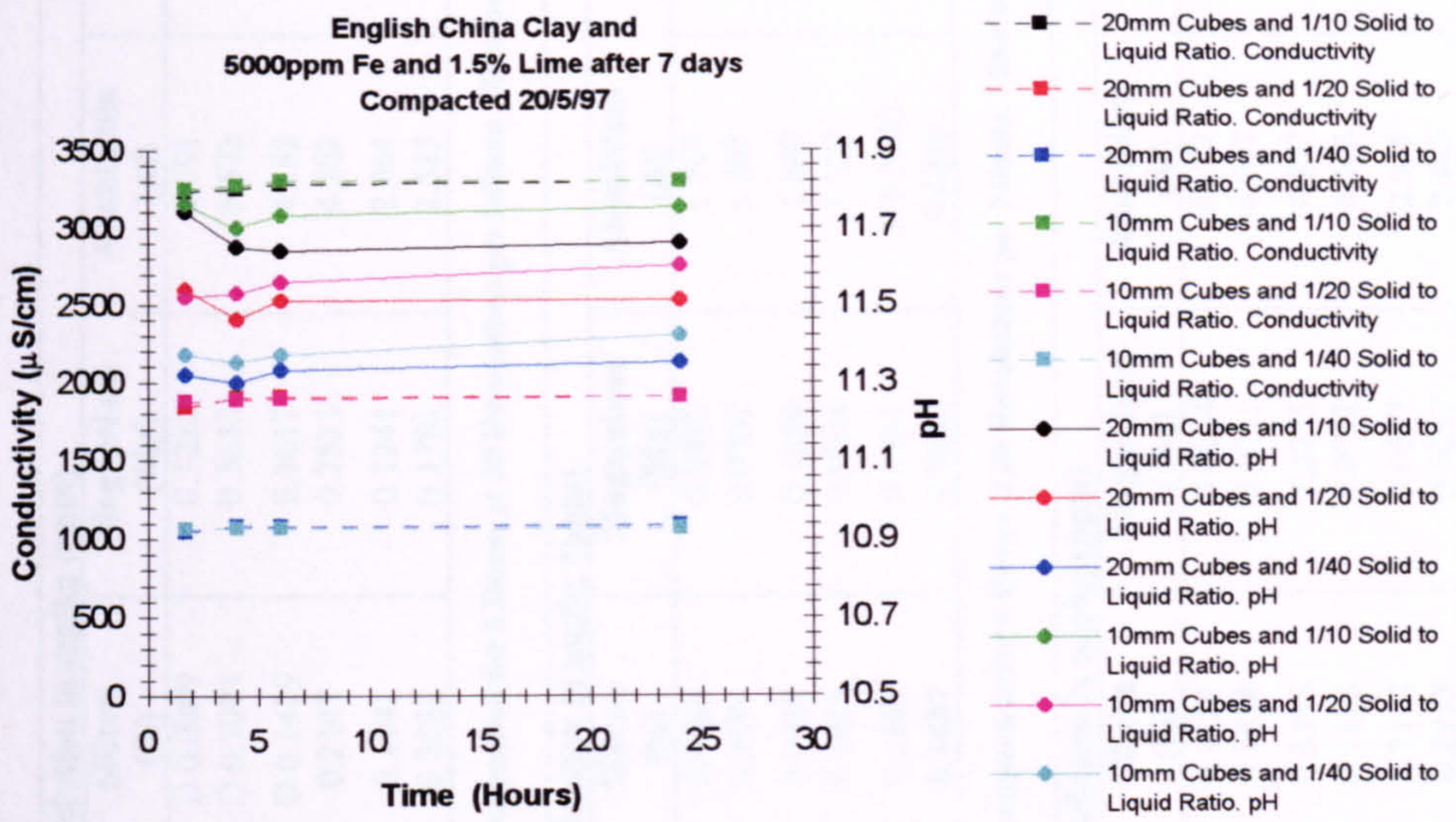

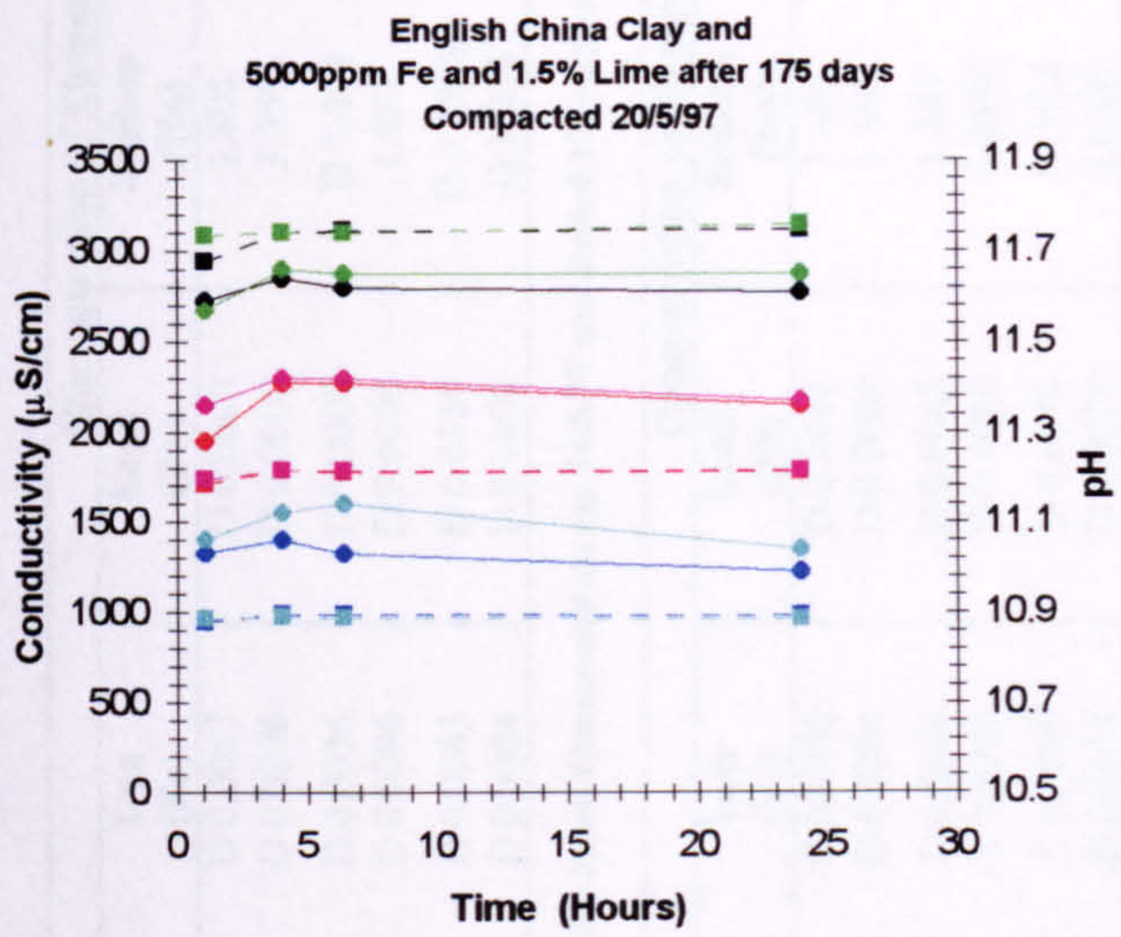

Table A1.52 ICP Data for Kaolinite and 5000ppm Iron and 1.5% Lime, Compacted on the 16/5/97 and Tested 7 days after Compaction for 6 Hours at 30 Revolutions per Minute. Filter only.

Solid to Liquid Ratio	Initial Cube Size (mm)	Concentration of Element in Solution in mg/kg (ppm)							
		Calcium (Ca)	Iron (Fe)	Lead (Pb)	Sodium (Na)	Silicon (Si)	Magnesium (Mg)	Aluminium (Al)	Manganese (Mn)
1/10	10	565.3	D 0.0057	D 0.0000	1.808	D 0.0809	0.1282	4.791	D 0.0001
	20	579.1	D 0.0206	D 0.0000	3.359	D 0.1094	0.3633	5.572	D 0.0008
1/20	10	311.1	D 0.0036	D 0.0000	D 1.004	D 0.1429	0.1017	4.182	D 0.0003
	20	304.6	D 0.0096	D 0.0000	1.951	0.2147	0.2523	4.562	D 0.0006
1/40	10	163.0	D 0.0085	D 0.0110	D 0.7288	0.1741	0.1241	2.361	D 0.0001
	20	166.6	D 0.0084	D 0.0000	D 1.024	0.3181	0.1781	2.513	D 0.0007

Table A1.53 ICP Data for Kaolinite and 5000ppm Iron and 1.5% Lime, Compacted on the 16/5/97 and Tested 175 days after Compaction for 6 Hours at 30 Revolutions per Minute. Filter only.

Solid to Liquid Ratio	Initial Cube Size (mm)	Concentration of Element in Solution in mg/kg (ppm)							
		Calcium (Ca)	Iron (Fe)	Lead (Pb)	Sodium (Na)	Silicon (Si)	Magnesium (Mg)	Aluminium (Al)	Manganese (Mn)
1/10	10	562.2	D 0.0000	D 0.0018	1.466	0.0986	0.0997	1.703	D 0.0012
	20	568.5	D 0.0004	D 0.0000	1.366	0.0694	0.0701	1.503	D 0.0006
1/20	10	301.5	D 0.0008	D 0.0045	1.047	0.0910	0.1050	1.840	d. 0.0003
	20	302.7	D 0.0006	D 0.0000	0.8686	0.1011	0.0704	1.327	D 0.0006
1/40	10	151.8	D 0.0000	D 0.0000	0.7612	0.1169	0.0991	d. 0.3580	d. 0.0005
	20	152.0	D 0.0017	D 0.0039	0.6289	0.1487	0.0997	0.6390	d. 0.0010

Table A1.54 ICP Data for Kaolinite and 5000ppm Iron and 1.5% Lime, Compacted on the 16/5/97 and Tested 301 days after Compaction for 6 Hours at 30 Revolutions per Minute. Filter only.

Solid to Liquid Ratio	Initial Cube Size (mm)	Concentration of Element in Solution in mg/kg (ppm)							
		Calcium (Ca)	Iron (Fe)	Lead (Pb)	Sodium (Na)	Silicon (Si)	Magnesium (Mg)	Aluminium (Al)	Manganese (Mn)
1/10	10	560.5	D 0.0043	D 0.0000	1.505	0.1124	0.0624	6.072	D 0.0007
	20	561.3	0.0151	D 0.0000	1.676	0.1438	0.0711	4.947	D 0.0004
1/20	10	300.0	0.0234	D 0.0000	0.8700	0.3375	0.0775	4.277	D 0.0003
	20	304.5	0.0195	D 0.0000	0.9412	0.3128	0.0792	4.458	D 0.0007
1/40	10	157.0	0.0185	D 0.0000	0.5019	0.3174	0.0597	2.918	D 0.0004
	20	156.5	0.0783	D 0.0000	0.6148	0.2955	0.0667	2.485	D 0.0003

Note: 'D' indicates the stated value is below *detection limits* and the value stated is a system estimate.
'd' indicates the stated value is close to detection limits.

Table A1.55 ICP Data for Kaolinite and 5000ppm Iron and 1.5% Lime, Compacted on the 19/5/97 and Tested 7 days after Compaction for 6 Hours at 60 Revolutions per Minute. Filter only.

Solid to Liquid Ratio	Initial Cube Size (mm)	Concentration of Element in Solution in mg/kg (ppm)							
		Calcium (Ca)	Iron (Fe)	Lead (Pb)	Sodium (Na)	Silicon (Si)	Magnesium (Mg)	Aluminium (Al)	Manganese (Mn)
1/10	10	590.9	D 0.0072	D 0.0343	2.115	D 0.1304	0.3136	6.391	D 0.0007
	20	603.6	D 0.0438	D 0.0592	2.491	0.1904	0.3933	6.169	D 0.0038
1/20	10	320.5	D 0.0052	D 0.0360	D 0.9125	d. 0.1507	0.1162	4.706	D 0.0000
	20	327.5	D 0.0065	D 0.0177	1.113	0.1536	0.1757	5.476	D 0.0000
1/40	10	165.8	D 0.0247	D 0.0203	D 0.7280	0.4867	0.1502	3.473	D 0.0006
	20	169.8	D 0.0052	D 0.0560	D 0.7154	0.2627	0.1825	3.603	D 0.0000

Table A1.56 ICP Data for Kaolinite and 5000ppm Iron and 1.5% Lime, Compacted on the 19/5/97 and Tested 175 days after Compaction for 6 Hours at 60 Revolutions per Minute. Filter only.

Solid to Liquid Ratio	Initial Cube Size (mm)	Concentration of Element in Solution in mg/kg (ppm)							
		Calcium (Ca)	Iron (Fe)	Lead (Pb)	Sodium (Na)	Silicon (Si)	Magnesium (Mg)	Aluminium (Al)	Manganese (Mn)
1/10	10	557.8	D 0.0000	D 0.0000	1.441	d. 0.0723	0.0669	2.204	D 0.0006
	20	554.6	D 0.0000	D 0.0000	1.524	D 0.0369	0.0643	2.094	D 0.0003
1/20	10	301.0	D 0.0000	D 0.0000	1.004	0.1157	0.0701	1.939	d. 0.0014
	20	292.1	D 0.0000	D 0.0194	0.8867	d. 0.0448	0.0624	1.587	D 0.0003
1/40	10	162.9	D 0.0094	D 0.0000	0.6694	0.1418	0.0667	1.777	D 0.0005
	20	159.3	D 0.0001	D 0.0000	0.7244	0.1136	0.0745	1.376	D 0.0009

Note: 'D' indicates the stated value is below detection limits and the value stated is a system estimate.
'd' indicates the stated value is close to *detection* limits.

Table A1.57 ICP Data for Kaolinite and 5000ppm Iron and 1.5% *Lime*, Compacted on the 15/5/97 and Tested 7 days after Compaction for 24 Hours at 30 Revolutions per Minute. Filter only.

Solid to Liquid Ratio	Initial Cube Size (mm)	Concentration of Element in Solution in mg/kg (ppm)							
		Calcium (Ca)	Iron (Fe)	Lead (Pb)	Sodium (Na)	Silicon (Si)	Magnesium (Mg)	Aluminium (Al)	Manganese (Mn)
1/10	10	640.4	D 0.0340	D 0.0000	1.473	0.2417	0.0542	11.02	D 0.0001
	20	624.4	0.0900	D 0.0000	1.406	0.2929	0.0596	10.92	D 0.0002
1/20	10	340.4	D 0.0138	D 0.0000	D 0.7770	0.4007	0.0573	8.348	D 0.0007
	20	357.0	d. 0.0573	D 0.0052	D 0.8939	0.5275	0.0766	9.388	D 0.0006
1/40	10	178.5	D 0.0171	D 0.0012	D 0.5470	0.4267	0.0745	5.142	D 0.0000
	20	184.2	D 0.0317	D 0.0171	D 0.6808	0.5205	0.0987	4.893	D 0.0003

Table A1.58 ICP Data for Kaolinite and 5000ppm Iron and 1.5% Lime, Compacted on the 15/5/97 and Tested 175 days after Compaction for 24 Hours at 30 Revolutions per Minute. Filter only.

Solid to Liquid Ratio	Initial Cube Size (mm)	Concentration of Element in Solution in mg/kg (ppm)							
		Calcium (Ca)	Iron (Fe)	Lead (Pb)	Sodium (Na)	Silicon (Si)	Magnesium (Mg)	Aluminium (Al)	Manganese (Mn)
1/10	10	580.8	D 0.0069	D 0.0000	1.347	0.3554	0.0353	13.22	D 0.0000
	20	585.7	D 0.0210	D 0.0000	1.357	0.6159	0.0353	13.71	D 0.0000
1/20	10	314.3	D 0.0036	D 0.0000	0.9307	0.2883	0.0446	9.842	D 0.0003
	20	315.9	D 0.0309	D 0.0000	0.8139	0.4959	0.0380	9.353	D 0.0001
1/40	10	151.2	D 0.0164	D 0.0000	0.7218	0.5204	0.0615	4.028	D 0.0001
	20	149.9	D 0.0029	D 0.0000	0.5819	0.2914	0.0475	5.063	D 0.0000

Table A1.59 ICP Data for Kaolinite and 5000ppm Iron and 1.5% Lime, Compacted on the 15/5/97 and Tested 301 days after Compaction for 24 Hours at 30 Revolutions per Minute. Filter only.

Solid to Liquid Ratio	Initial Cube Size (mm)	Concentration of Element in Solution in mg/kg (ppm)							
		Calcium (Ca)	Iron (Fe)	Lead (Pb)	Sodium (Na)	Silicon (Si)	Magnesium (Mg)	Aluminium (Al)	Manganese (Mn)
1/10	10	609.3	0.0136	D 0.0000	1.503	0.2115	0.0587	13.52	D 0.0000
	20	586.3	d. 0.0157	D 0.0000	1.422	0.2049	0.0456	12.81	D 0.0000
1/20	10	327.6	0.0410	D 0.0000	0.8307	0.5695	0.0585	9.412	D 0.0005
	20	310.4	d. 0.0228	D 0.0000	0.8855	0.4196	0.0562	8.268	D 0.0000
1/40	10	167.7	0.0449	D 0.0000	0.8296	0.2919	0.0772	5.714	D 0.0001
	20	162.8	d. 0.0111	D 0.0000	0.6393	0.2989	0.0594	5.506	D 0.0000

Note: 'D' indicates the stated value is below detection limits and the value stated is a system estimate.
'd' indicates the stated value is close to detection limits.

Table A1.60 ICP Data for Kaolinite and 5000ppm Iron and 1.5% Lime, Compacted on the 20/5/97 and Tested 7 days after Compaction for 24 Hours at 60 Revolutions per Minute. Filter only.

Solid to Liquid Ratio	Initial Cube Size (mm)	Concentration of Element in Solution in mg/kg (ppm)							
		Calcium (Ca)	Iron (Fe)	Lead (Pb)	Sodium (Na)	Silicon (Si)	Magnesium (Mg)	Aluminium (Al)	Manganese (Mn)
1/10	10	609.0	D 0.0167	D 0.0176	1.621	0.2630	0.0818	11.55	D 0.0002
	20	604.0	D 0.0062	D 0.0044	1.866	0.2594	0.0646	11.83	D 0.0003
1/20	10	329.0	D 0.0137	D 0.0420	D 1.036	0.3795	0.0715	8.822	D 0.0004
	20	318.8	D 0.0289	D 0.0339	D 0.9111	0.3784	0.0565	8.495	D 0.0003
1/40	10	165.0	D 0.0081	D 0.0207	D 0.6026	0.3728	0.0720	5.853	D 0.0003
	20	162.1	d. 0.0123	D 0.0379	d. 1.116	0.3801	0.0730	6.224	D 0.0009

Table A1.61 ICP Data for Kaolinite and 5000ppm Iron and 1.5% Lime, Compacted on the 20/5/97 and Tested 175 days after Compaction for 24 Hours at 60 Revolutions per Minute. Filter only.

Solid to Liquid Ratio	Initial Cube Size (mm)	Concentration of Element in Solution in mg/kg (ppm)							
		Calcium (Ca)	Iron (Fe)	Lead (Pb)	Sodium (Na)	Silicon (Si)	Magnesium (Mg)	Aluminium (Al)	Manganese (Mn)
1/10	10	579.5	D 0.0006	D 0.0000	1.355	0.2165	0.0501	13.39	D 0.0001
	20	582.4	D 0.0033	D 0.0000	1.313	0.2195	0.0379	12.77	D 0.0001
1/20	10	299.3	D 0.0000	D 0.0000	0.8545	0.2357	0.0710	8.482	D 0.0000
	20	302.9	D 0.0145	D 0.0000	0.7932	0.5275	0.0672	8.410	D 0.0003
1/40	10	151.7	D 0.0020	D 0.0000	0.5867	0.0416	0.0923	2.571	D 0.0006
	20	156.3	D 0.0034	D 0.0000	0.6258	0.3030	0.0827	4.827	d. 0.0007

Note : 'D' indicates the stated value is below detection limits and the value stated is a system estimate.
'd' indicates the stated value is close to detection limits.

A1.2.7 English China Clay with no contaminants and 2.5% lime

A1.2.7.1 Solid : liquid ratio

Inspection of Figures A1.31 to A1.34 shows that as the solid to liquid ratio increased both conductivity and pH increased. At 7 days curing the conductivity of 6hr/30rpm tests with 20mm cube sizes (Figure A1.31) at the solid to liquid ratios 1:10, 1:20 and 1:40 were 7970μS/cm, 5870μS/cm and 3350 μS/cm respectively whilst pH values were 12.67, 12.55 and 12.34 respectively. At 175 days curing the conductivity values were 3810μS/cm, 2630μS/cm and 1661μS/cm respectively whilst pH values were 12.41, 12.22 and 11.98. Increasing the solid to liquid ratio from 1:40 to 1:20 at 7 days curing from increased conductivity by a factor of 1.75 and pH by 0.21 pH divisions. Increasing solid to liquid ratio further from 1:20 to 1:10 increased conductivity by a factor of 1.35 and pH by 0.12 pH divisions. At 175 days curing conductivity increased by a factor of 1.58 and pH by 0.24pH divisions for a change in solid to liquid ratio of 1:40 to 1:20. Increasing solid to liquid ratio from 1:20 to 1:10 at 175 days curing increased conductivity by a factor of 1.45 and pH by 0.19 pH divisions.

Analysis of chemical data Tables A1.62 to A1.71 illustrate that as solid to liquid ratio decreased and curing period increased Ca concentration significantly decreased by factor similar to those for conductivity changes. Observation of Table A1.62 for 6hr/30rpm tests at 7 days and 20mm cube sizes shows clearly that increasing solid to liquid ratio from 1:40 to 1:20 resulted in an increase in concentration of Ca from 261ppm to 475ppm, a reduction in Si from 1.04ppm to 0.466ppm, Mg from 0.0143ppm to 0.0109ppm and Al from 0.692ppm to 0.0637ppm. At 175 days curing and 301 days curing all tests produced increases in Ca and Na whilst Al reduced with increasing solid to liquid ratio.

It is evident from Figures A1.31 to A1.34 that the solid to liquid ratio 1:40 results in the highest level of variability in pH values between the two cube sizes.

A1.2.7.2 Cube Size

By observation of Figure A1.31 to A1.34, 10mm cubes generally produced slightly higher pH values. Again where the resulting conductivity was found to be higher for either 10mm or 20mm cubes, Ca levels in the leachates were found to be

correspondingly higher. The larger cube size also tended to release higher concentrations of Na, Si, Mg and Al.

A1.2.7.3 Rotation speed and test duration

Comparison of 6hr tests at 7 and 175 days curing (Figures A1.31 and A1.34) illustrates that at all solid to liquid ratios the 60rpm tests tended to produce slightly lower pH and conductivity values. These trends were more defined at 175 days curing. During similar comparisons of 24hr tests at 7 days curing (Figures A1.33 and A1.34) it is clear that the 60rpm tests produced lower pH values but higher conductivity values at specific solid to liquid ratios. At 175 curing for 24hr tests, the 60rpm pH and conductivity values were both much higher than for the 30rpm tests. These differences in conductivity and pH are again in proportion to leachable Ca levels. Tables A1.62, A1.63 and A1.65, Mb illustrate that increased rotation speed during 6 hr tests did increase leached Si and Al. 24hr test data in Tables A1.67 to A1.68 and Tables A1.70 to A1.71 illustrate that the higher rotation speed generally produced more Ca, Si and less Al. Generally however higher concentrations of Ca and Mg were found at higher rotation speeds.

Increasing test duration has a variety of effects. 30rpm tests depicted in Figures A1.31 and A1.33 illustrate high variability in pH and conductivity. At 7 days curing the 24hr tests clearly produced higher pH values and lower conductivity values at specific solid to liquid ratios. At 175 days curing, 24hr tests resulted in lower pH and conductivity values. At 301 days curing pH values were higher whilst again conductivity was significantly lower at the higher test duration. Once again it appears that changes in conductivity were directly linked to changes in Ca concentration and is illustrated by the data in the tables. During the longer curing periods the 24hr tests released more Na, Si and Mg whilst Al showed no obvious trends. Comparison of 60rpm tests (Figures A1.32 and A1.34) illustrates that at 7 days curing, 24hr tests produced similar pH values but higher conductivities. However, at 175 days curing, 24 hr tests produced significantly higher pH and conductivities. Interestingly for 60rpm tests (Tables A1.65, A1.66 and A1.70, A1.71) 24hr tests produced less Na, Si, Mg and Al, the opposite of 30rpm tests.

A1.2.7.4 Curing Time

For all test parameters, increasing curing period for specific solid to liquid ratios dramatically reduced pH and conductivity. The change was most obvious between 7 and 175 days curing although still very significant between 175 and 301 days curing. The changes in conductivity with curing time were clearly reflected in changes in Ca concentrations, an example of which is shown in Tables A1.62 to A1.64. It is also clear at all solid to liquid ratios that increasing curing time tends to increase Na, Si, Mg and Al although in the case of Na, Si and Mg the optimum concentrations were achieved at 175 days curing and remained at a similar level after 301 days curing.

Figure A1.31 Conductivity and pH characteristics for English China Clay with no contaminants and 2.5% lime during 6hr/30rpm Batch Tests

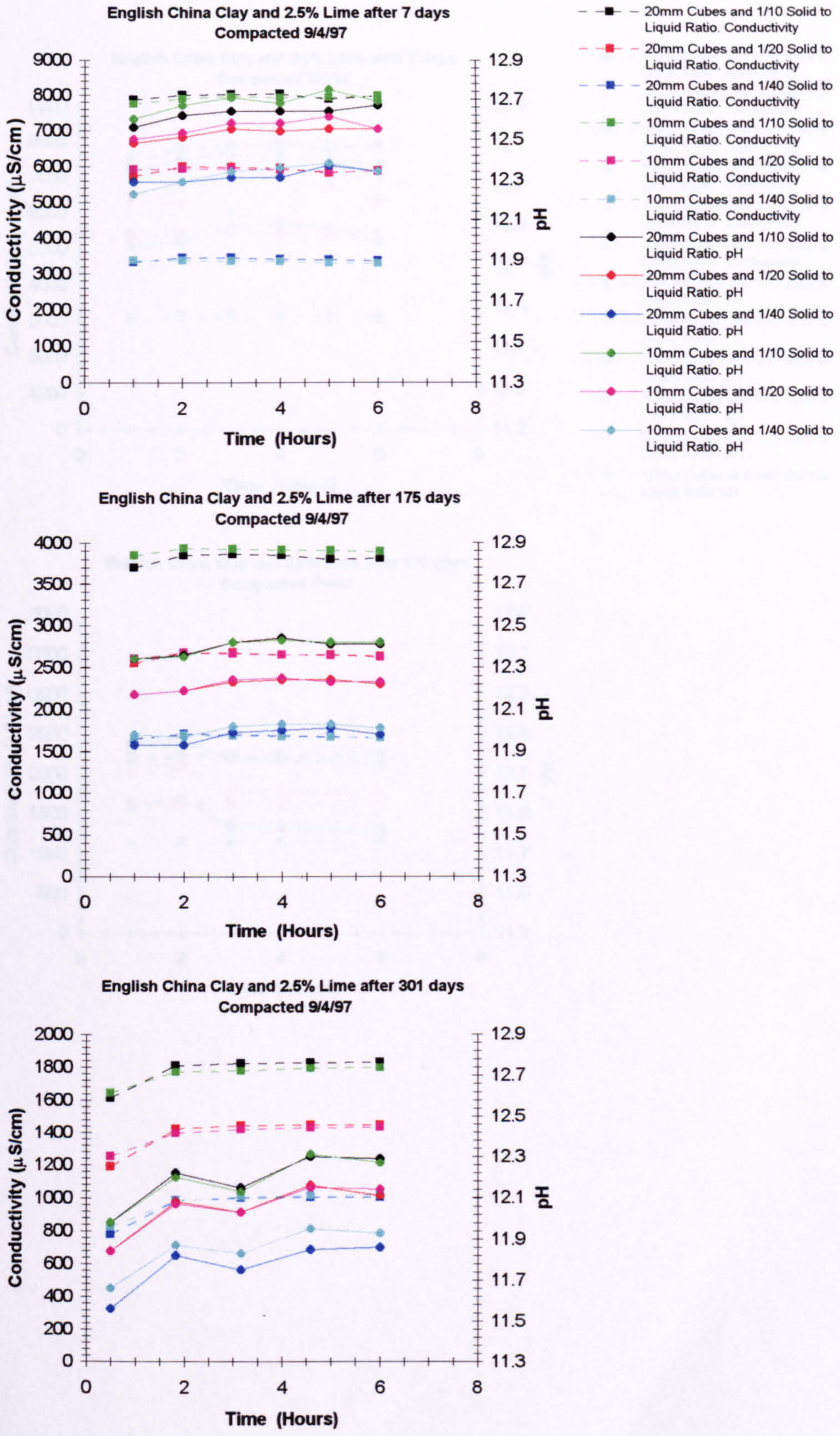

Figure A1.32 Conductivity and pH characteristics for English China Clay with no contaminants and 2.5% lime during 6hr/60rpm Batch Tests

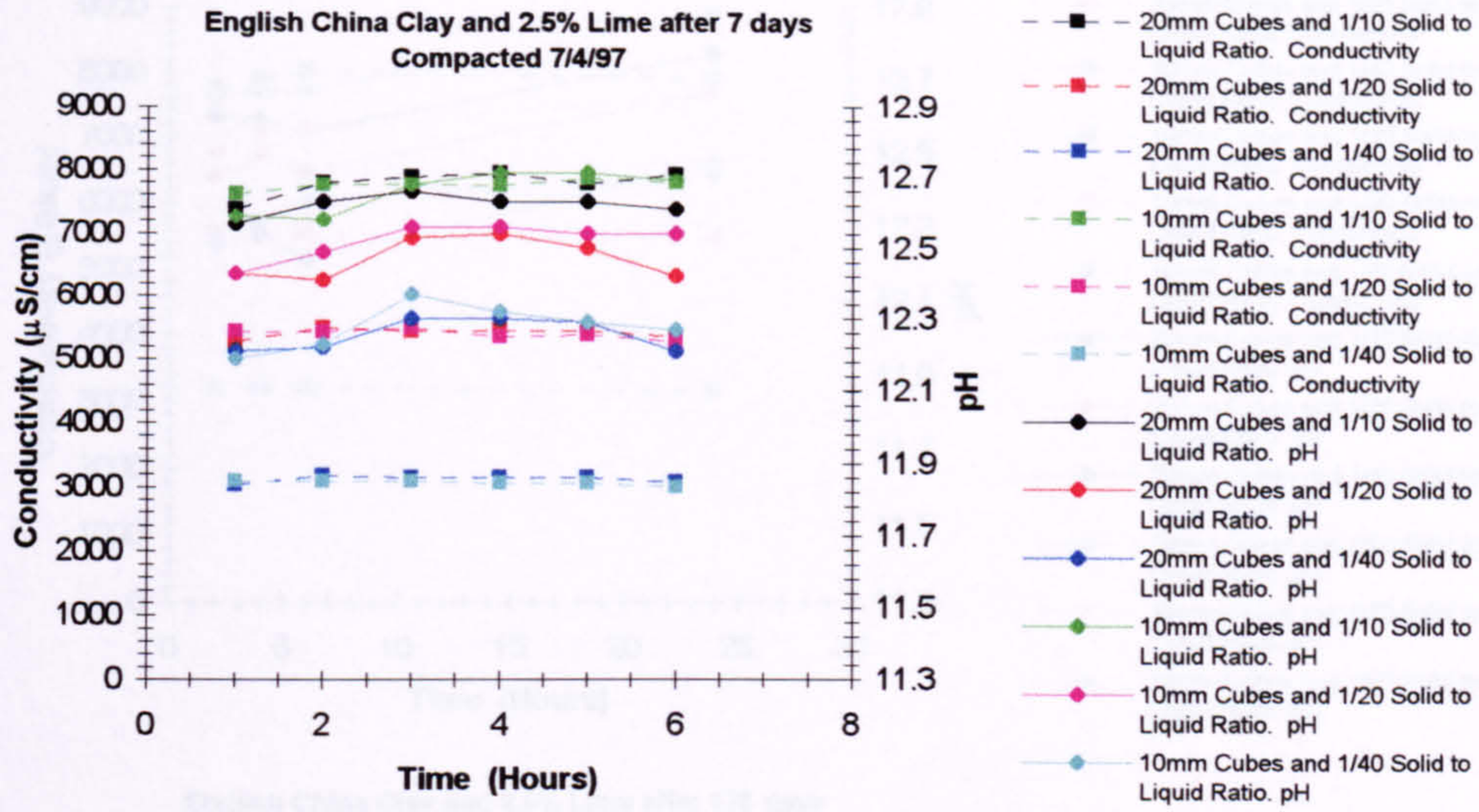

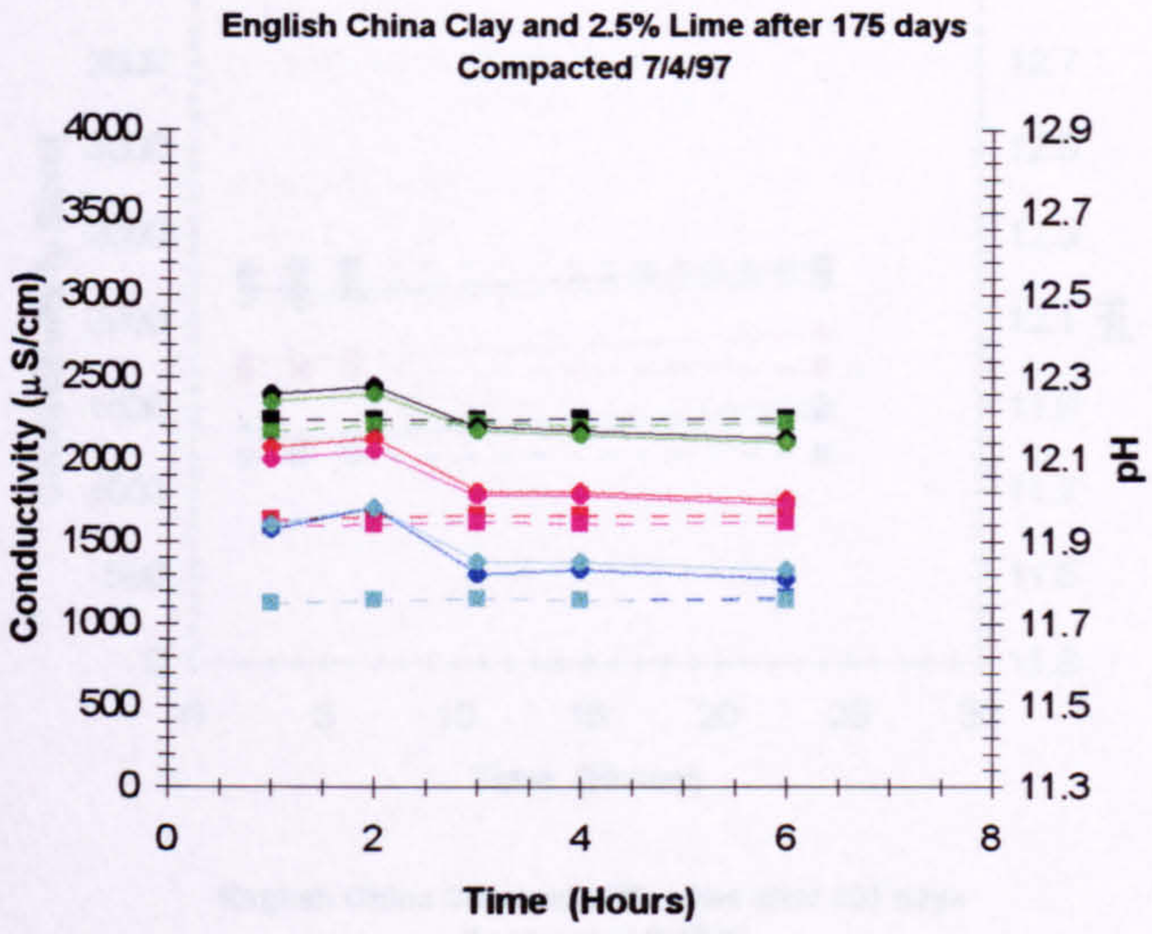

Figure A1.33 Conductivity and pH characteristics for English China Clay with no contaminants and 2.5% lime during 24hr/30rpm Batch Tests

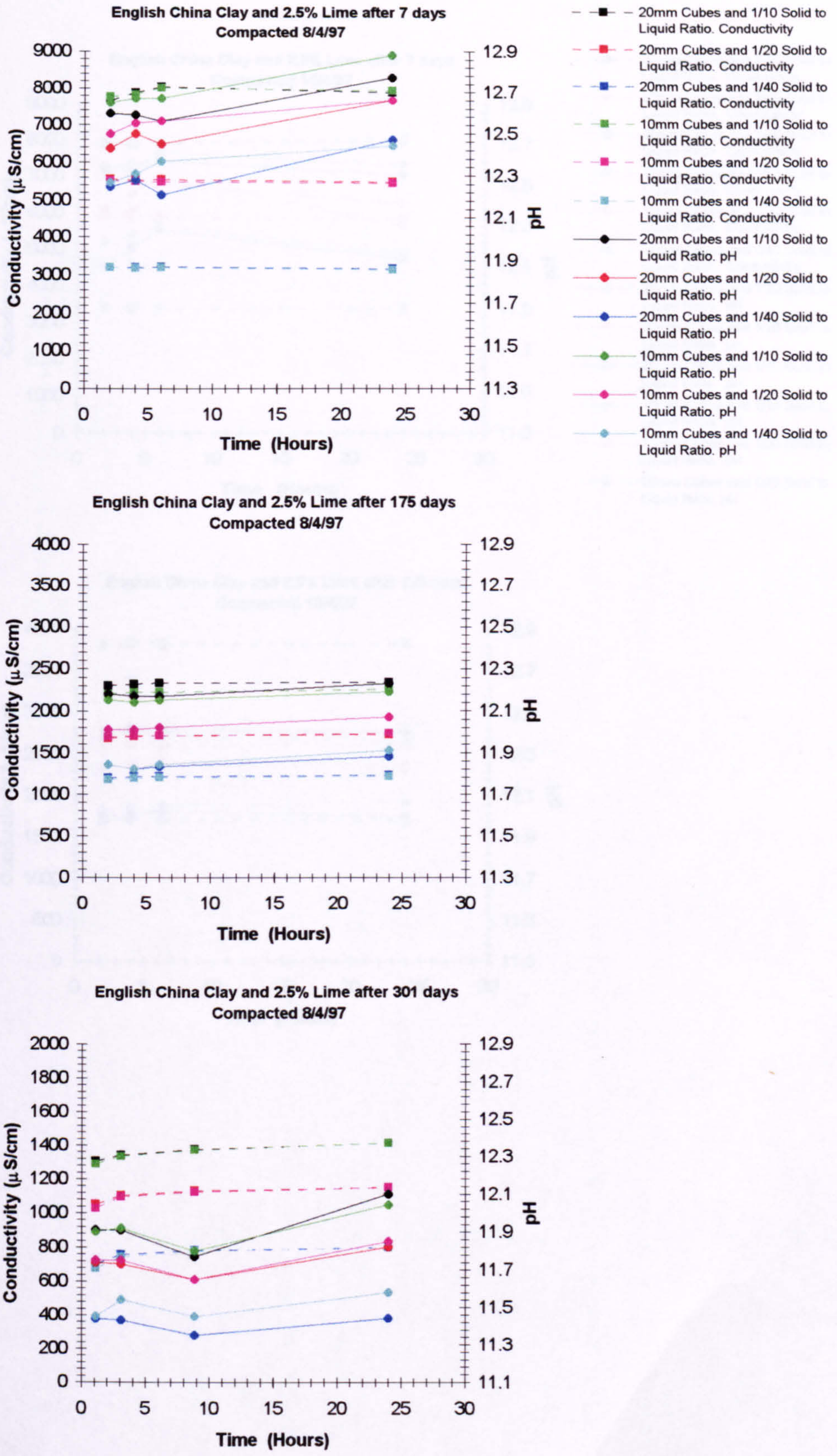

Figure A1.34 Conductivity and pH characteristics for English China Clay with no contaminants and 2.5% lime during 24hr/60rpm Batch Tests

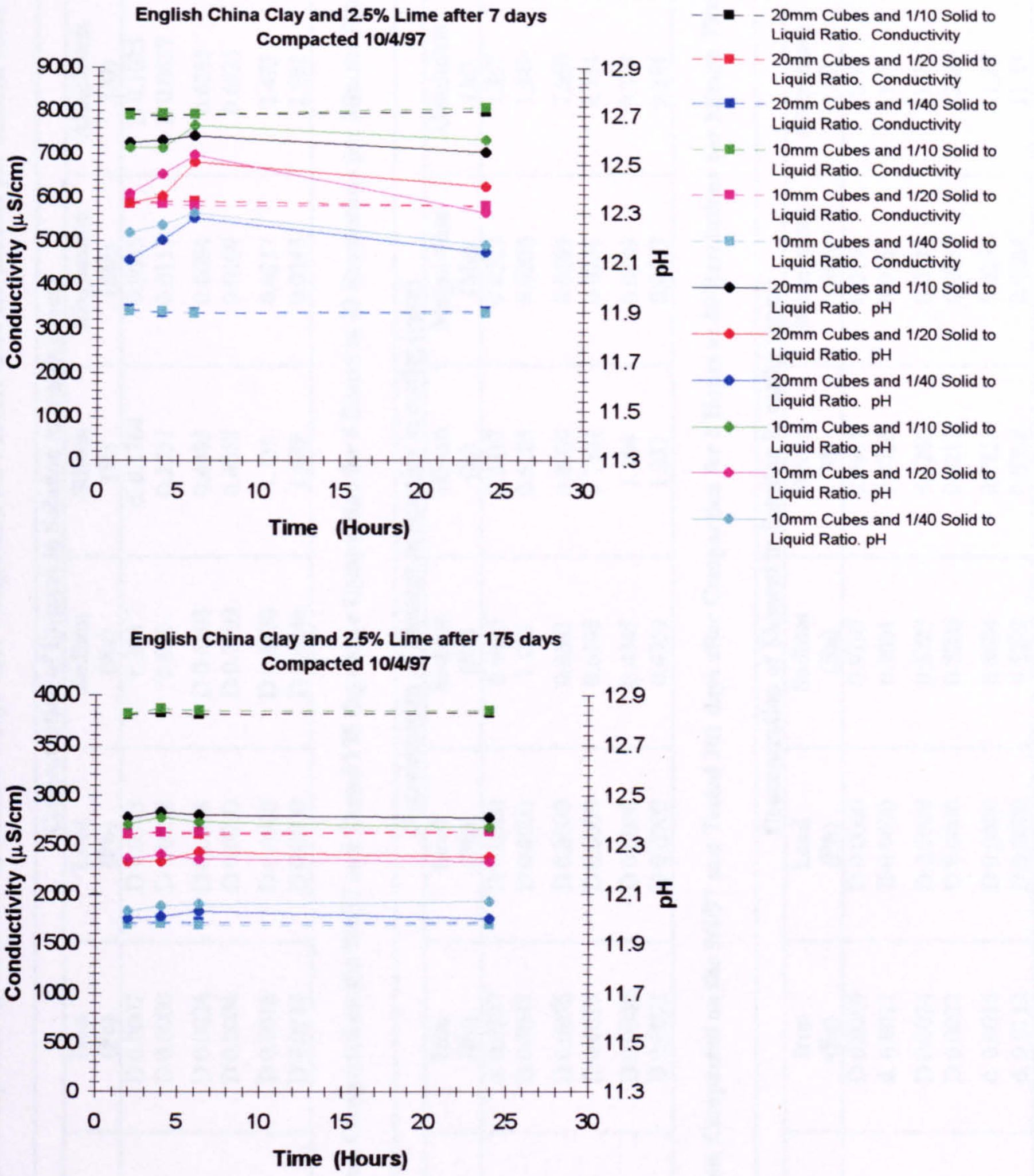

Table A1.62 ICP Data for Kaolinite and 2.5% Lime, Compacted on the 9/4/97 and Tested 7 days after Compaction for 6 Hours at 30 Revolutions per Minute. Filter only.

Solid to Liquid Ratio	Initial Cube Size (mm)	Concentration of Element in Solution in mg/kg (ppm)							
		Calcium (Ca)	Iron (Fe)	Lead (Pb)	Sodium (Na)	Silicon (Si)	Magnesium (Mg)	Aluminium (Al)	Manganese (Mn)
1/10	10	617.5	D 0.0007	D 0.0343	1.306	d. 0.1764	0.0085	D 0.1025	D 0.0000
	20	631.2	D 0.0000	D 0.0232	1.651	0.2351	0.0113	D 0.0637	D 0.0000
1/20	10	434.9	D 0.0024	D 0.0338	D 0.4403	0.4483	0.0084	0.6265	D 0.0002
	20	475.2	D 0.0004	D 0.0080	D 0.7503	0.4658	0.0109	0.6925	D 0.0001
1/40	10	143.8	D 0.0016	D 0.0000	D 0.8830	1.139	0.0217	2.473	D 0.0001
	20	261.8	D 0.0024	D 0.0000	D 0.4246	1.039	0.0143	2.681	D 0.0000

Table A1.63 ICP Data for Kaolinite and 2.5% Lime, Compacted on the 9/4/97 and Tested 175 days after Compaction for 6 Hours at 30 Revolutions per Minute. Filter only.

Solid to Liquid Ratio	Initial Cube Size (mm)	Concentration of Element in Solution in mg/kg (ppm)							
		Calcium (Ca)	Iron (Fe)	Lead (Pb)	Sodium (Na)	Silicon (Si)	Magnesium (Mg)	Aluminium (Al)	Manganese (Mn)
1/10	10	239.6	d. 0.0007	D 0.0000	0.9435	0.5817	0.0273	3.357	D 0.0001
	20	282.2	D 0.0047	D 0.0000	1.120	0.6283	0.0206	1.549	D 0.0005
1/20	10	196.0	D 0.0076	D 0.0000	0.6641	0.8020	0.0169	7.660	D 0.0007
	20	166.6	D 0.0073	D 0.0000	0.6195	0.7531	0.0231	8.154	D 0.0002
1/40	10	77.53	D 0.0040	D 0.0000	0.4345	1.164	0.0189	9.373	D 0.0000
	20	100.7	D 0.0075	D 0.0000	0.4759	1.237	0.0183	9.294	D 0.0002

Table A1.64 ICP Data for Kaolinite and 2.5% Lime, Compacted on the 9/4/97 and Tested 301 days after Compaction for 6 Hours at 30 Revolutions per Minute. Filter only.

Solid to Liquid Ratio	Initial Cube Size (mm)	Concentration of Element in Solution in mg/kg (ppm)							
		Calcium (Ca)	Iron (Fe)	Lead (Pb)	Sodium (Na)	Silicon (Si)	Magnesium (Mg)	Aluminium (Al)	Manganese (Mn)
1/10	10	124.6	D 0.0009	D 0.0000	0.9197	0.4975	0.0194	10.79	D 0.0000
	20	116.8	d. 0.0011	D 0.0000	0.9061	0.4763	0.0181	11.35	D 0.0000
1/20	10	67.53	D 0.0024	D 0.0000	0.5727	0.6260	0.0224	11.79	D 0.0002
	20	98.70	D 0.0022	D 0.0000	0.7206	0.6212	0.0238	12.07	D 0.0000
1/40	10	57.68	d. 0.0015	D 0.0000	0.3674	0.7853	0.0255	11.25	D 0.0000
	20	58.18	d. 0.0112	D 0.0000	0.5222	0.8068	0.0264	11.33	D 0.0001

Note: 'D' indicates the stated value is below detection limits and the value stated is a system estimate.
'd' indicates the stated value is close to detection limits.

Table A1.65 ICP Data for Kaolinite and 2.5% Lime, Compacted on the 7/4/97 and Tested 7 days after Compaction for 6 Hours at 60 Revolutions per Minute. Filter only.

Solid to Liquid Ratio	Initial Cube Size (mm)	Concentration of Element in Solution in mg/kg (ppm)							
		Calcium (Ca)	Iron (Fe)	Lead (Pb)	Sodium (Na)	Silicon (Si)	Magnesium (Mg)	Aluminium (Al)	Manganese (Mn)
1/10	10	671.4	D 0.0032	D 0.0174	D 0.9032	0.3829	0.0047	D 0.2515	D 0.0003
	20	728.7	D 0.0023	D 0.0000	D 1.040	0.3114	0.0132	D 0.0977	D 0.0000
1/20	10	417.9	D 0.0324	D 0.0034	D 0.6449	0.4553	0.0098	0.7695	D 0.0001
	20	446.7	D 0.0009	D 0.0000	D 0.7640	0.5427	0.0097	0.8295	D 0.0000
1/40	10	224.6	D 0.0020	D 0.0000	D 0.4988	1.155	0.0128	2.551	D 0.0000
	20	253.2	D 0.0000	D 0.0024	D 0.5011	1.262	0.0158	2.718	D 0.0000

Table A1.66 ICP Data for Kaolinite and 2.5% Lime, Compacted on the 7/4/97 and Tested 175 days after Compaction for 6 Hours at 60 Revolutions per Minute. Filter only.

Solid to Liquid Ratio	Initial Cube Size (mm)	Concentration of Element in Solution in mg/kg (ppm)							
		Calcium (Ca)	Iron (Fe)	Lead (Pb)	Sodium (Na)	Silicon (Si)	Magnesium (Mg)	Aluminium (Al)	Manganese (Mn)
1/10	10	191.6	D 0.0133	D 0.0000	1.059	0.7877	0.0331	9.605	d. 0.0005
	20	200.4	D 0.1322	D 0.0000	1.023	0.7630	0.0295	10.12	D 0.0000
1/20	10	145.4	D 0.0172	D 0.0000	0.6855	1.012	0.0216	10.93	d. 0.0000
	20	153.6	D 0.0110	D 0.0000	0.7746	0.9990	0.0218	11.31	D 0.0004
1/40	10	93.21	D 0.0123	D 0.0000	0.6550	1.171	0.0254	11.16	D 0.0004
	20	92.63	0.1728	D 0.0000	0.7604	1.942	0.0417	12.13	0.0015

Note : 'D' indicates the stated value is below detection limits and the value stated is a system estimate.
'd' indicates the stated value is close to detection limits.

Table A1.67 ICP Data for Kaolinite and 2.5% Lime, Compacted on the 8/4/97 and Tested 7 days after Compaction for 24 Hours at 30 Revolutions per Minute. Filter only.

Solid to Liquid Ratio	Initial Cube Size (mm)	Concentration of Element in Solution in mg/kg (ppm)							
		Calcium (Ca)	Iron (Fe)	Lead (Pb)	Sodium (Na)	Silicon (Si)	Magnesium (Mg)	Aluminium (Al)	Manganese (Mn)
1/10	10	715.3	D 0.0018	D 0.0221	D 1.072	0.2175	0.0109	D 0.0598	D 0.0000
	20	660.0	D 0.0002	D 0.0121	1.768	0.2628	0.0178	D 0.1124	D 0.0000
1/20	10	489.2	D 0.0012	D 0.0050	D 0.7849	0.4148	0.0110	0.9921	D 0.0000
	20	465.8	D 0.0011	D 0.0090	D 0.6853	0.4586	0.0103	0.9793	D 0.0000
1/40	10	264.0	D 0.0004	D 0.0202	D 0.4280	1.005	0.0157	3.039	D 0.0000
	20	236.5	D 0.0000	D 0.0125	D 0.5730	0.9651	0.0173	3.082	D 0.0000

Table A1.68 ICP Data for Kaolinite and 2.5% Lime, Compacted on the 8/4/97 and Tested 175 days after Compaction for 24 Hours at 30 Revolutions per Minute. Filter only.

Solid to Liquid Ratio	Initial Cube Size (mm)	Concentration of Element in Solution in mg/kg (ppm)							
		Calcium (Ca)	Iron (Fe)	Lead (Pb)	Sodium (Na)	Silicon (Si)	Magnesium (Mg)	Aluminium (Al)	Manganese (Mn)
1/10	10	184.4	D 0.0057	D 0.0000	1.105	0.7084	0.0157	9.510	D 0.0001
	20	208.8	D 0.0066	D 0.0000	1.023	0.6624	0.0159	9.580	D 0.0004
1/20	10	155.9	0.0507	D 0.0000	0.6627	2.834	0.0414	12.38	D 0.0008
	20	153.6	D 0.0061	D 0.0000	0.6820	1.017	0.0203	11.08	D 0.0001
1/40	10	96.51	D 0.0061	D 0.0000	0.5055	1.352	0.0243	11.54	D 0.0001
	20	96.66	D 0.0284	D 0.0000	0.5950	1.469	0.0273	11.84	D 0.0002

Table A1.69 ICP Data for Kaolinite and 2.5% Lime, Compacted on the 8/4/97 and Tested 301 days after Compaction for 24 Hours at 30 Revolutions per Minute. Filter only.

Solid to Liquid Ratio	Initial Cube Size (mm)	Concentration of Element in Solution in mg/kg (ppm)							
		Calcium (Ca)	Iron (Fe)	Lead (Pb)	Sodium (Na)	Silicon (Si)	Magnesium (Mg)	Aluminium (Al)	Manganese (Mn)
1/10	10	96.51	D 0.0062	D 0.0000	1.041	0.8375	0.0244	9.437	D 0.0000
	20	92.49	d. 0.0067	D 0.0000	1.105	0.8259	0.0324	9.350	D 0.0003
1/20	10	62.17	d. 0.0097	D 0.0000	0.6413	0.9804	0.0288	9.405	D 0.0001
	20	52.39	D 0.0053	D 0.0078	0.6927	1.044	0.0419	9.470	D 0.0000
1/40	10	54.26	D 0.0024	D 0.0000	0.6169	1.254	0.0378	8.537	D 0.0001
	20	37.98	D 0.0066	D 0.0000	0.5662	1.232	0.0466	8.448	D 0.0000

Note: 'D' indicates the stated value is below detection limits and the value stated is a system estimate.
'd' indicates the stated value is close to detection limits.

Table A1.70 ICP Data for Kaolinite and 2.5% Lime, Compacted on the 10/4/97 and Tested 7 days after Compaction for 24 Hours at 60 Revolutions per Minute. Filter only.

Solid to Liquid Ratio	Initial Cube Size (mm)	Concentration of Element in Solution in mg/kg (ppm)							
		Calcium (Ca)	Iron (Fe)	Lead (Pb)	Sodium (Na)	Silicon (Si)	Magnesium (Mg)	Aluminium (Al)	Manganese (Mn)
1/10	10	728.7	D 0.0039	D 0.0336	D 0.8376	0.5618	0.0132	D 0.3197	D 0.0005
	20	703.3	D 0.0025	D 0.0332	D 1.073	0.3225	0.0130	D 0.1050	D 0.0000
1/20	10	490.3	D 0.0027	D 0.0000	D 0.4525	0.3691	0.0141	0.7635	D 0.0002
	20	493.5	D 0.0034	D 0.0546	D 0.5944	0.4167	0.0121	0.8756	D 0.0005
1/40	10	255.3	D 0.0040	D 0.0214	D 0.2673	1.019	0.0170	2.765	D 0.0004
	20	279.6	d. 0.0036	D 0.0249	D 0.4205	1.190	0.0178	3.232	D 0.0004

Table A1.71 ICP Data for Kaolinite and 2.5% Lime, Compacted on the 10/4/97 and Tested 175 days after Compaction for 24 Hours at 60 Revolutions per Minute. Filter only.

Solid to Liquid Ratio	Initial Cube Size (mm)	Concentration of Element in Solution in mg/kg (ppm)							
		Calcium (Ca)	Iron (Fe)	Lead (Pb)	Sodium (Na)	Silicon (Si)	Magnesium (Mg)	Aluminium (Al)	Manganese (Mn)
1/10	10	327.9	D 0.0032	D 0.0000	0.9117	0.4941	0.0178	3.159	D 0.0000
	20	313.2	D 0.0020	D 0.0000	0.7921	0.5584	0.0155	3.904	D 0.0000
1/20	10	238.6	D 0.0048	D 0.0000	0.4954	0.7546	0.0144	7.297	D 0.0002
	20	232.2	d. 0.0100	D 0.0000	0.6281	0.9716	0.0292	7.860	d. 0.0002
1/40	10	151.7	D 0.0174	D 0.0000	0.4203	1.230	0.0271	8.732	D 0.0004
	20	152.0	D 0.0058	D 0.0000	0.3706	1.214	0.0175	9.094	D 0.0002

Note : 'D' indicates the stated value is below detection limits and the value stated is a system estimate.
'd' indicates the stated value is close to detection limits.

A1.2.8 English China Clay with 5000ppm Pb and 2.5% lime

Significantly at 7 days curing most Pb is released by the 1:20 solid to liquid ratio with a concentration of approximately 1.6ppm being typical. Increasing curing time effectively reduces the leachability of Pb to zero (see Tables A1.72, A1.73 and A1.74).

A1.2.8.1 Solid : liquid ratio

Figures A1.35 to A1.38 illustrate that as the solid to liquid ratio was increased, pH and conductivity increased. At 7 days curing the end of test conductivities of 6hr/30rpm tests with 20mm cube sizes (Figure A1.35) at the solid to liquid ratios 1:10, 1:20 and 1:40 were 7280µS/cm, 5170µS/cm and 2940µS/cm respectively whilst pH values were 12.64, 12.53 and 12.32 respectively. At 175 days curing the end of test conductivity values were 2170µS/cm, 1699µS/cm and 1201µS/cm respectively whilst pH values were 11.90, 11.81 and 11.69 respectively. At 301 days curing end of test conductivity values were 1662µS/cm, 1390µS/cm and 993µS/cm respectively whilst pH values were 11.84, 11.71 and 11.50. Increasing the solid to liquid ratio at 7 days curing from 1:40 to 1:20 therefore increased conductivity by a factor of 1.75 and pH by 0.21 pH divisions. Increasing solid to liquid ratio further from 1:20 to 1:10 increased conductivity by a factor of 1.41 and pH by 0.11 pH divisions. At 175 days curing, increasing solid to liquid ratio from 1:40 to 1:20 increased conductivity by a factor of 1.41 and pH by 0.12 pH divisions. Further increases in solid to liquid ratio from 1:20 to 1:10 increased conductivity by a factor of 1.28 and pH by 0.09 pH divisions. At 301 days increasing solid to liquid ratio from 1:40 to 1:20 increased conductivity by a factor of 1.40 and pH by 0.21 pH divisions. Further increasing solid to liquid ratio from 1:20 to 1:10 increased conductivity by a factor of 1.20 and pH by 0.13 pH divisions.

Analysis of data Tables A1.72 to A1.81 illustrate that as the solid to liquid ratio decreased and curing period increased Ca concentrations in leachates significantly decreased. For 6hr/30rpm tests with 20mm cube sizes at 7 days Table A1.72 clearly shows that increasing solid to liquid ratio from 1:40 to 1:20 resulted in an increase in concentration of Ca from 246ppm to 418ppm, a reduction in Si from 0.844ppm to 0.409ppm, Mg from 0.0175ppm to 0.0124ppm and Al from 3.70ppm to 1.59ppm. The similar increase in solid to liquid ratio from 1:20 to 1:10 resulted in an

increase in Ca from 418ppm to 695ppm, a reduction in Si from 0.409ppm to 0.239ppm, Mg from 0.0124ppm to 0,0147ppm and Al from 1.59ppm to 0.0211ppm. At 175 and 301 days curing all test produced increases in Ca and Na with increasing solid to liquid ratio whilst the solid to liquid ratio 1:20 produced the most Al. It was also clearly evident that the solid to liquid ratio 1:20 produced the least variability in pH and conductivity results between the two cube sizes.

A1.2.8.2 Cube Size

Generally by observation of Figures A1.35 to A1.38, 10mm cubes produce slightly higher final pH values. Where the resulting conductivity was higher, it was clear that Ca levels were also higher, with no apparent trends for the other elements. The exception to this was Al at 175 and 301 days curing where 20mm cubes tended to release more Al whilst at 7 days curing more Pb was released (Tables A1.73, A1.74, A1.78, A1.79).

A1.2.8.3 Rotation speed and test duration

Comparison of 6hr tests at 7 days curing (Figures A1.35 and A1.36) illustrates that at all solid to liquid ratios pH did not change significantly with increased rotation speed whilst conductivity values did slightly increase. At 175 days the high rotation speed produced significantly higher pH and conductivity. Comparison of Tables A1.72, A1.73 with A1.75, A1.76 illustrate that the Ca levels are again related to conductivity, particularly at the lower solid to liquid ratios. It was also clear that the higher rotation speed generally released less Pb, Na, Si, Mg and Al especially at 175 days curing

Comparison of 24hr tests at 7 and 175 days (Figures A1.37 and A1.38) illustrates that at all solid to liquid ratios pH values are slightly reduced at the higher rotation speed whilst conductivities remained unaffected. Tables A1.77 and A1.80 at 7 days curing clearly showed lower Ca release at the higher rotation speed along with reduced Pb, Si and Al particularly at the solid to liquid ratio 1:20. Tables A1.78 and A1.81 at 175 days curing showed lower Ca release at the higher rotation speed along with reduced Na, increased Si and Al, again particularly at the solid to liquid ratio 1:20.

Increasing test duration has varying effects. 30rpm tests (Figures A1.35 and A1.37) illustrate that at any curing period 24hr tests have higher final pH and

conductivity values particularly at the longer curing periods. With the exception of the 1: 10 solid to liquid ratio, at 7 days curing the higher conductivities were related to Ca concentration (Tables A1.72 to A1.74 and A1.77 to A1.79). At 7 days curing and specifically the 1:20 solid to liquid ratio, 24hr tests released more Pb, Ca and Si whilst other elements remained unaffected (Tables A1.72 and A1.77). At higher curing periods 24hr tests only appeared to release more Ca whilst other elements remained unaffected.

Comparison of 60rpm tests (Figures A1.36 and A1.38) showed lower pH and conductivity for 24 hr tests at 7 days curing with higher pH and conductivity at 175 days curing. Tables A1.75, A1.76 and A1.80, A1.81 explain this behaviour with varying Ca concentrations. 24hr tests release more Pb, Na and Si at any curing period and more Al only at the 1:40 solid to liquid ratio.

A1.2.8.4 Curing Time

At 7 days pH and conductivity values remained similar throughout a test at specific solid to liquid ratios whilst at 175 and 301 days there was a gradual increase in these values throughout the test duration. Increasing curing period from 7 days to 175 days resulted in large reductions in pH and conductivity with reduced although significant reductions in pH and conductivity from 175 days to 301 days. Tables A1.72 to A1.74 relate this to large reductions in Ca and Pb. Levels of Na and Al increase from 7 days curing to 175 days curing and remain relatively constant at these values at 301 days curing. Levels of Si tend to increase from 7 days curing to 175 days curing and decrease from 175 days curing to 301 days curing.

Figure A1.35 Conductivity and pH characteristics for English China Clay with 5000ppm Pb and 2.5% lime during 6hr/30rpm Batch Tests

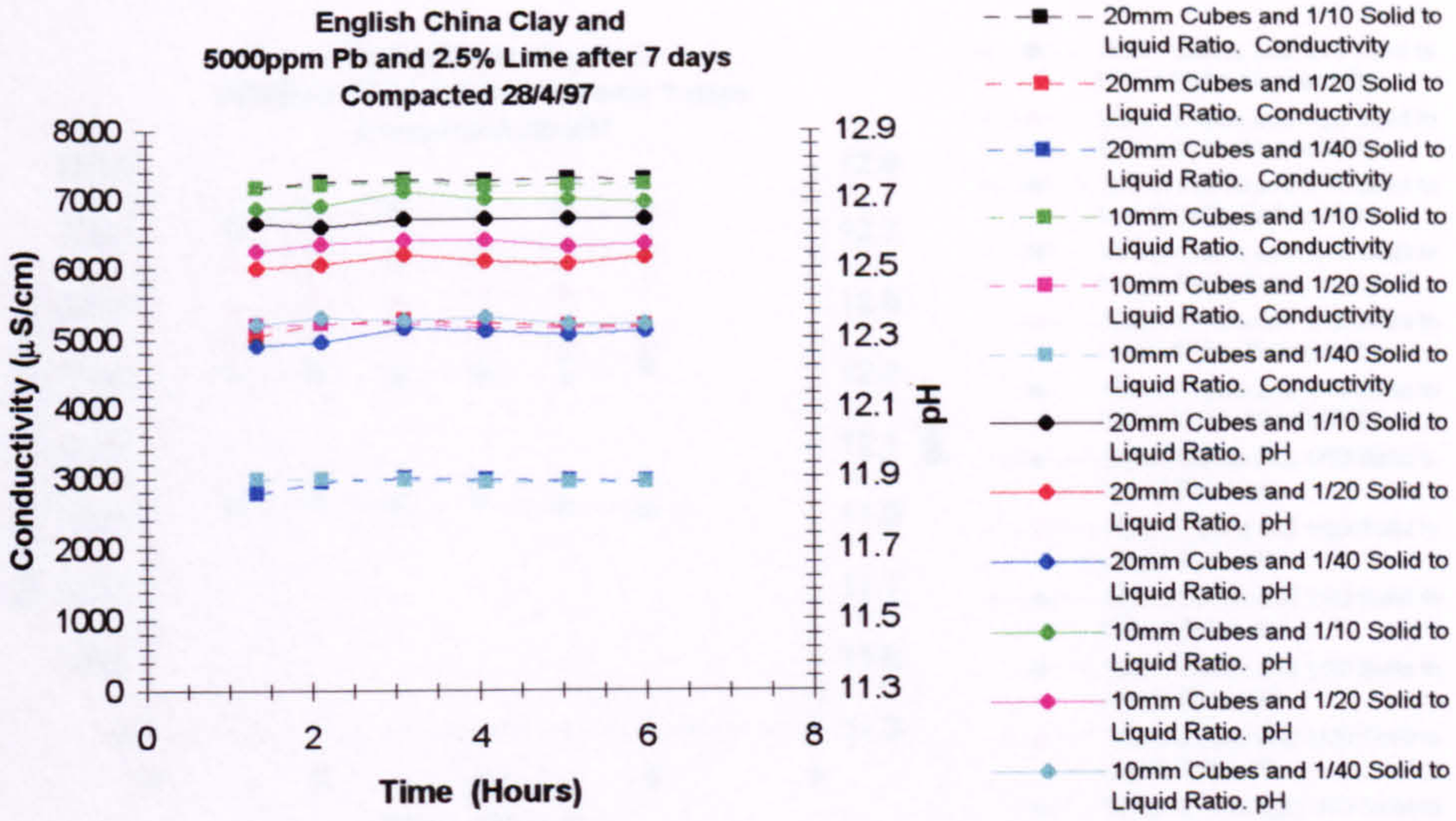

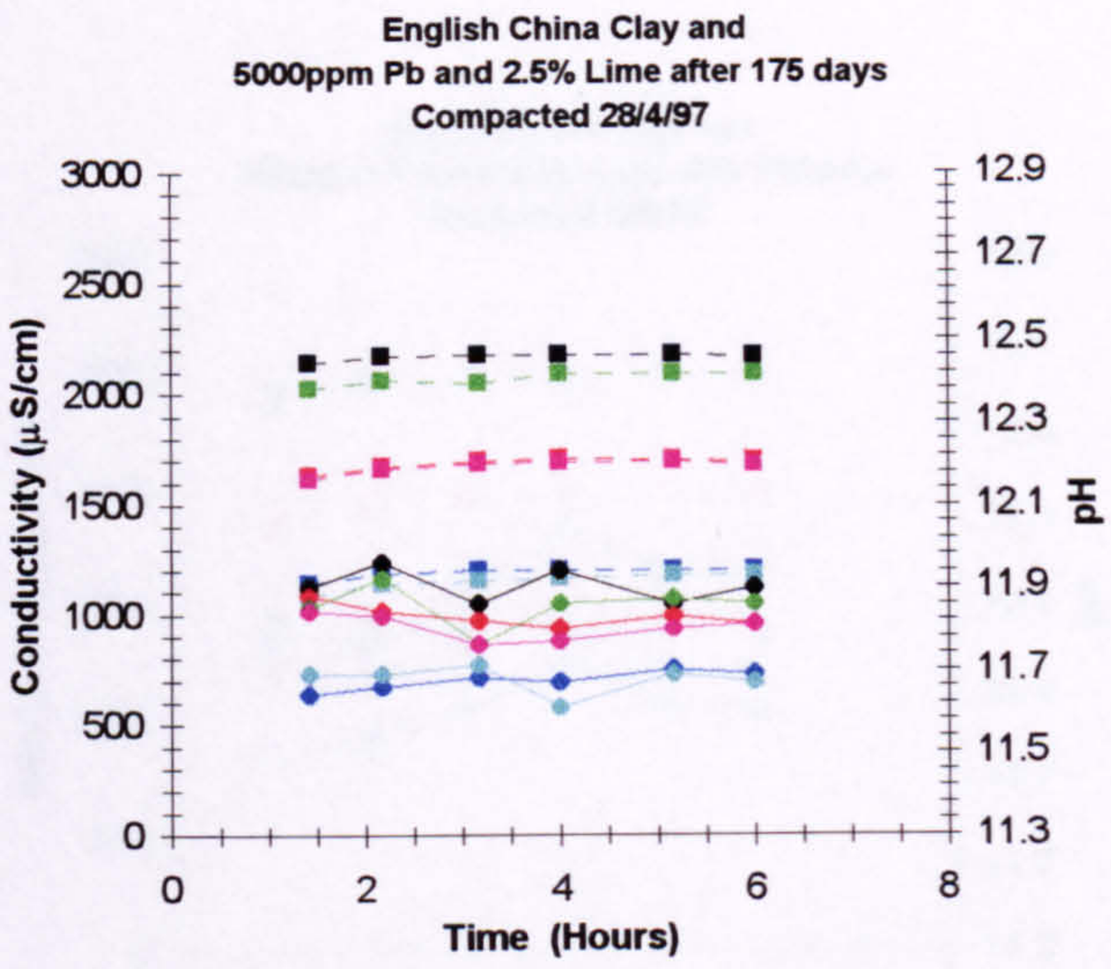

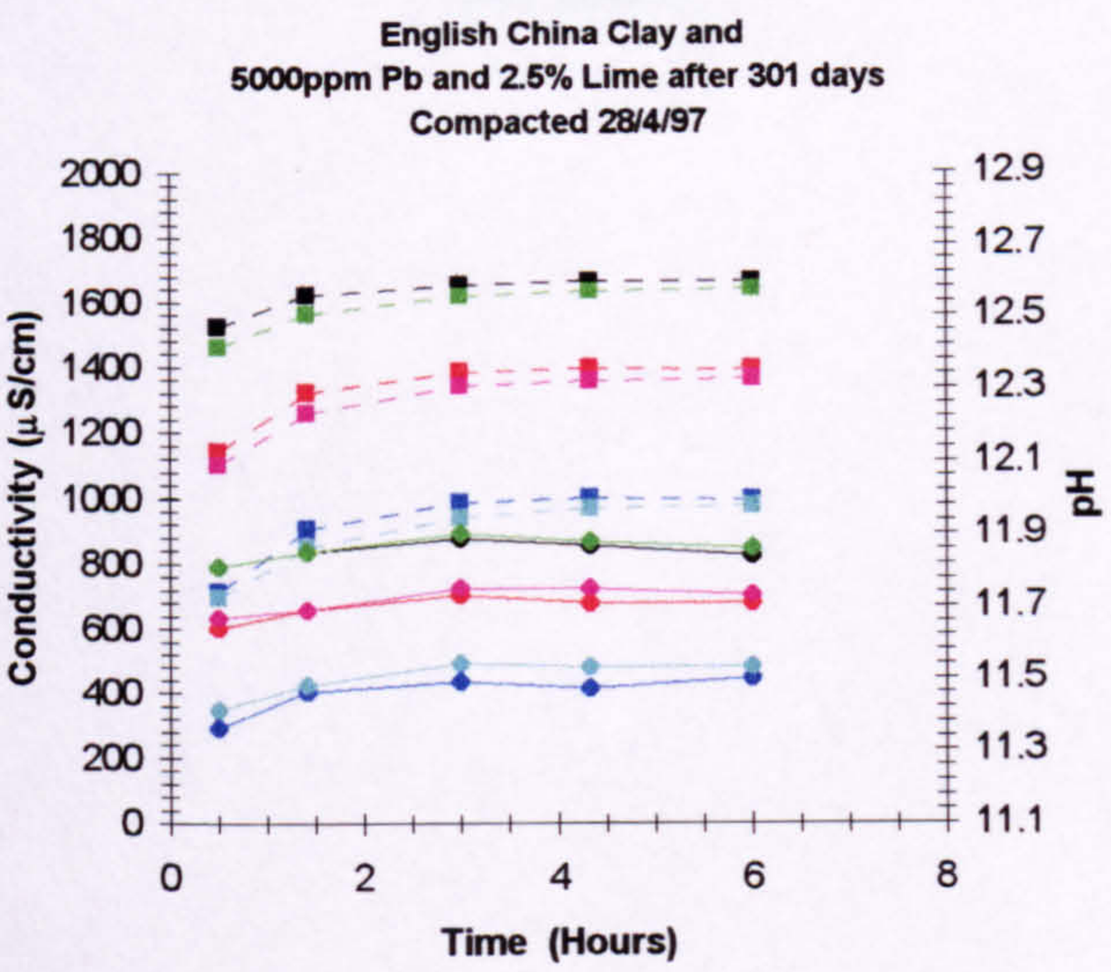

Figure A1.36 Conductivity and pH characteristics for English China Clay with 5000ppm Pb and 2.5% lime during 6hr/60rpm Batch Tests

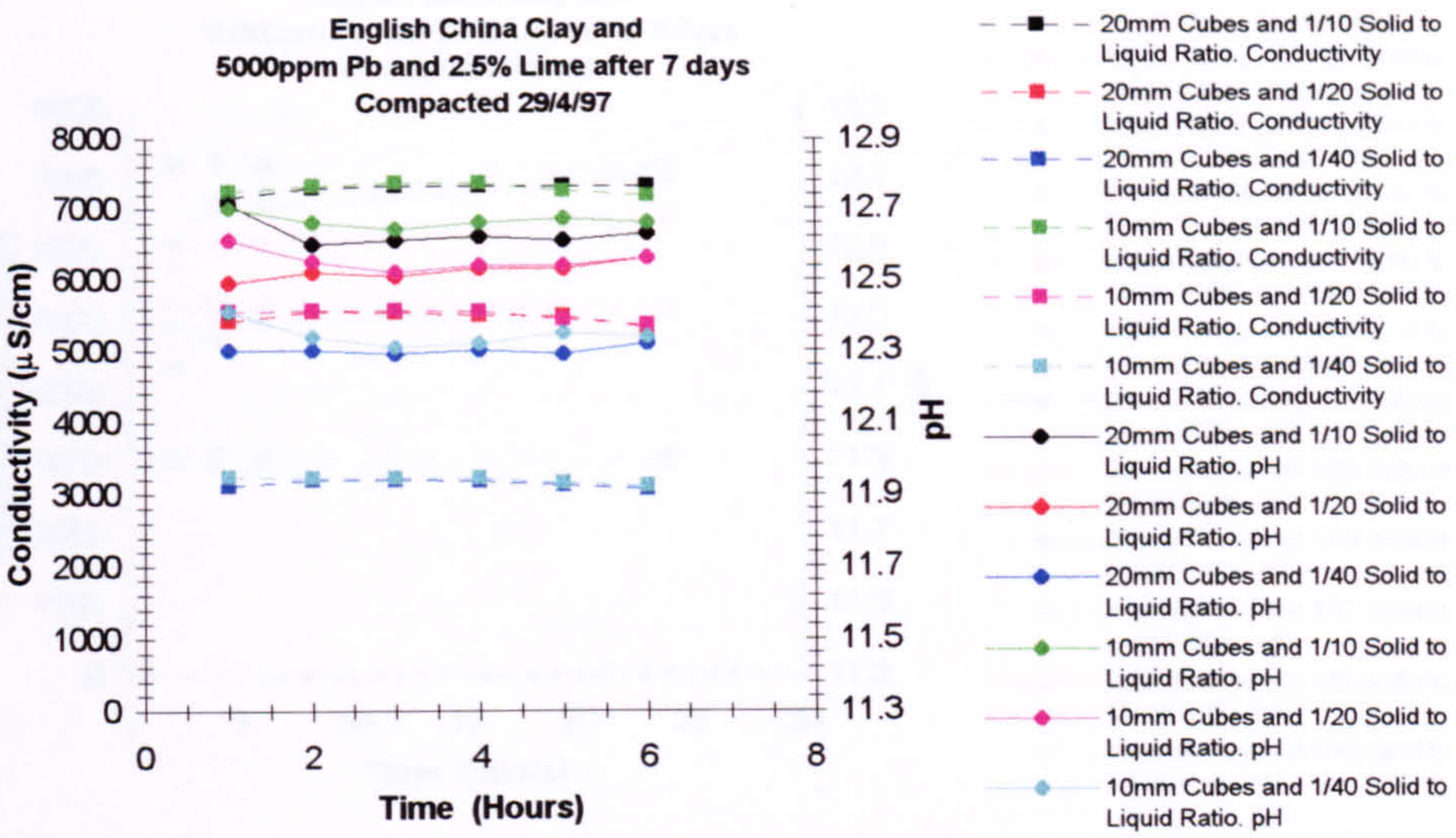

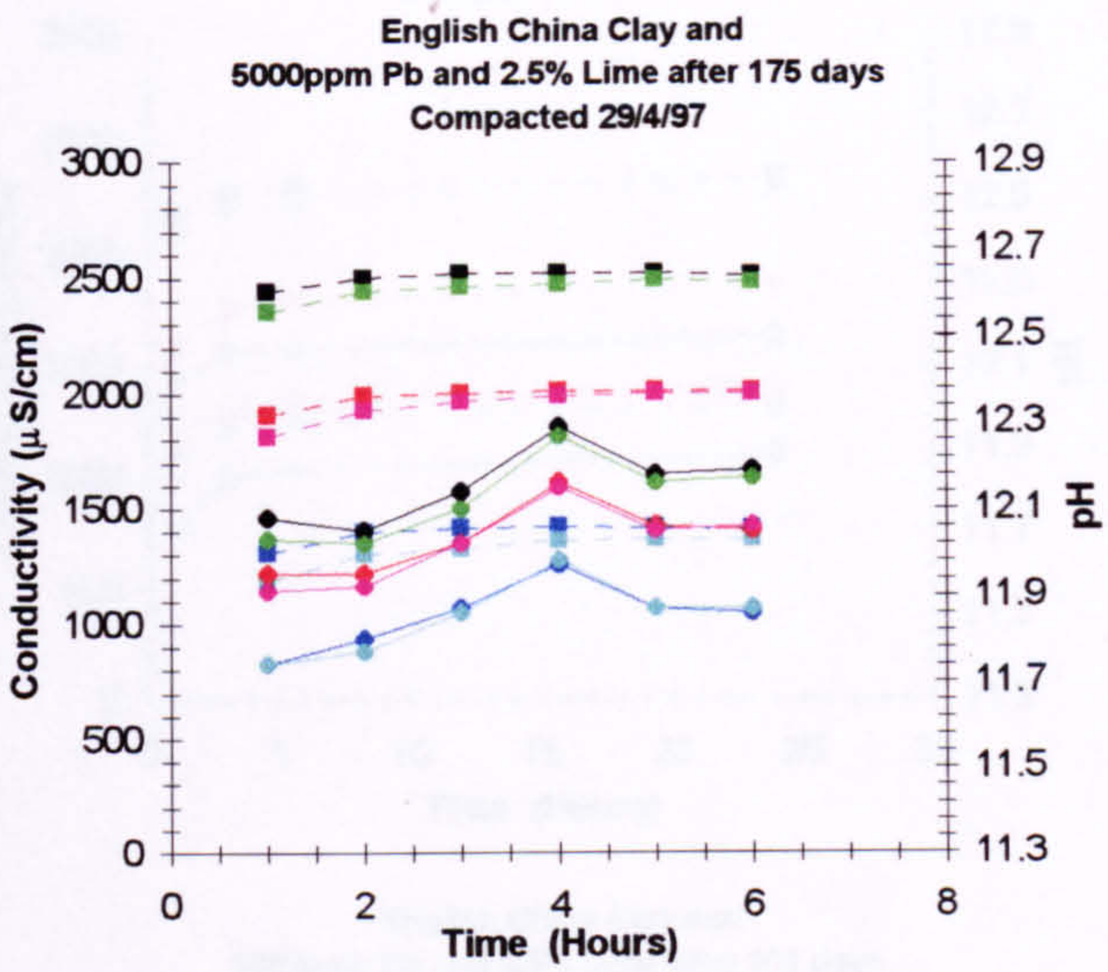

Figure A1.37 Conductivity and pH characteristics for English China Clay with 5000ppm Pb and 2.5% lime during 24hr/30rpm Batch Tests

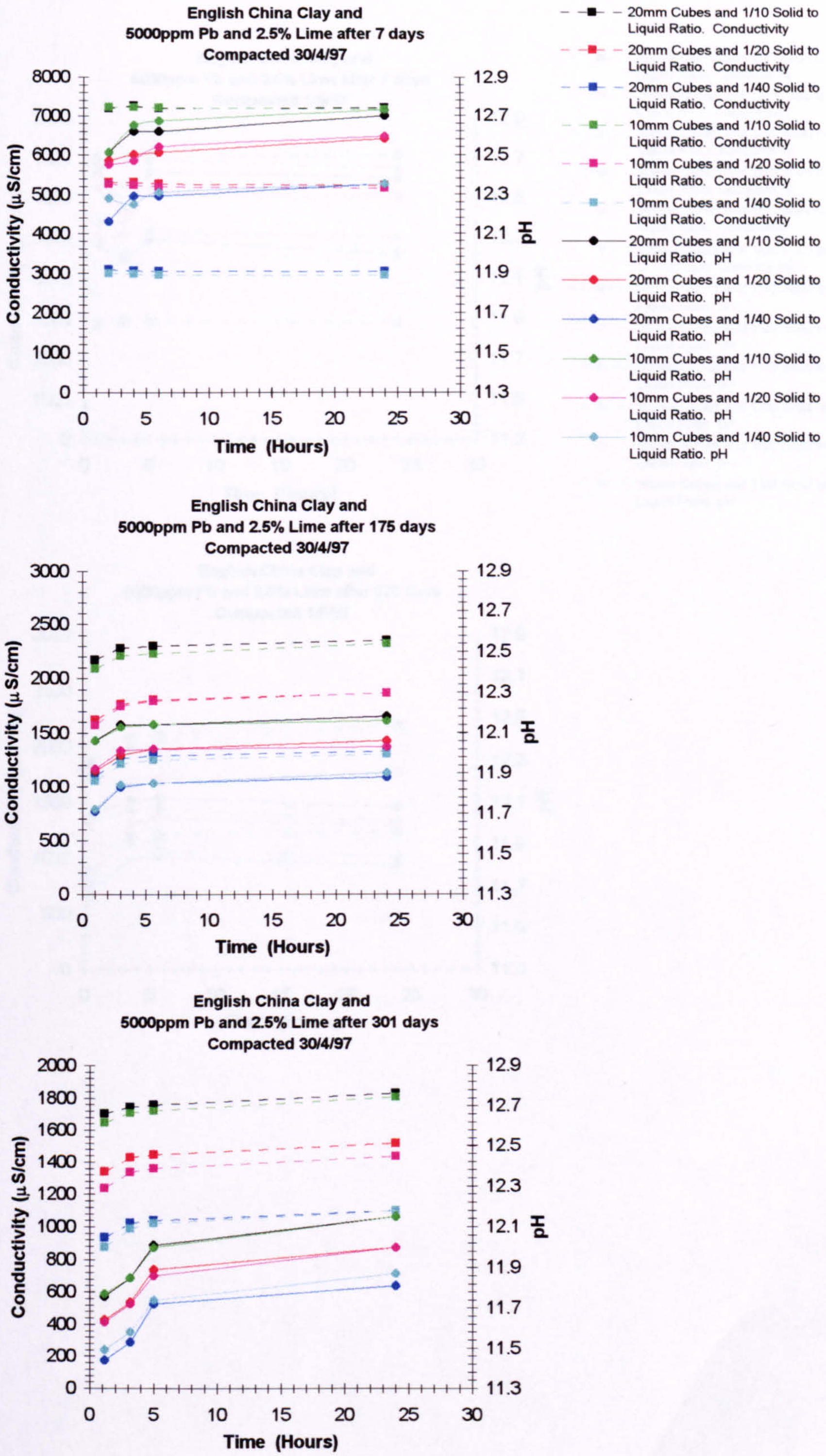

Figure A1.38 Conductivity and pH characteristics for English China Clay with 5000ppm Pb and 2.5% lime during 24hr/60rpm Batch Tests

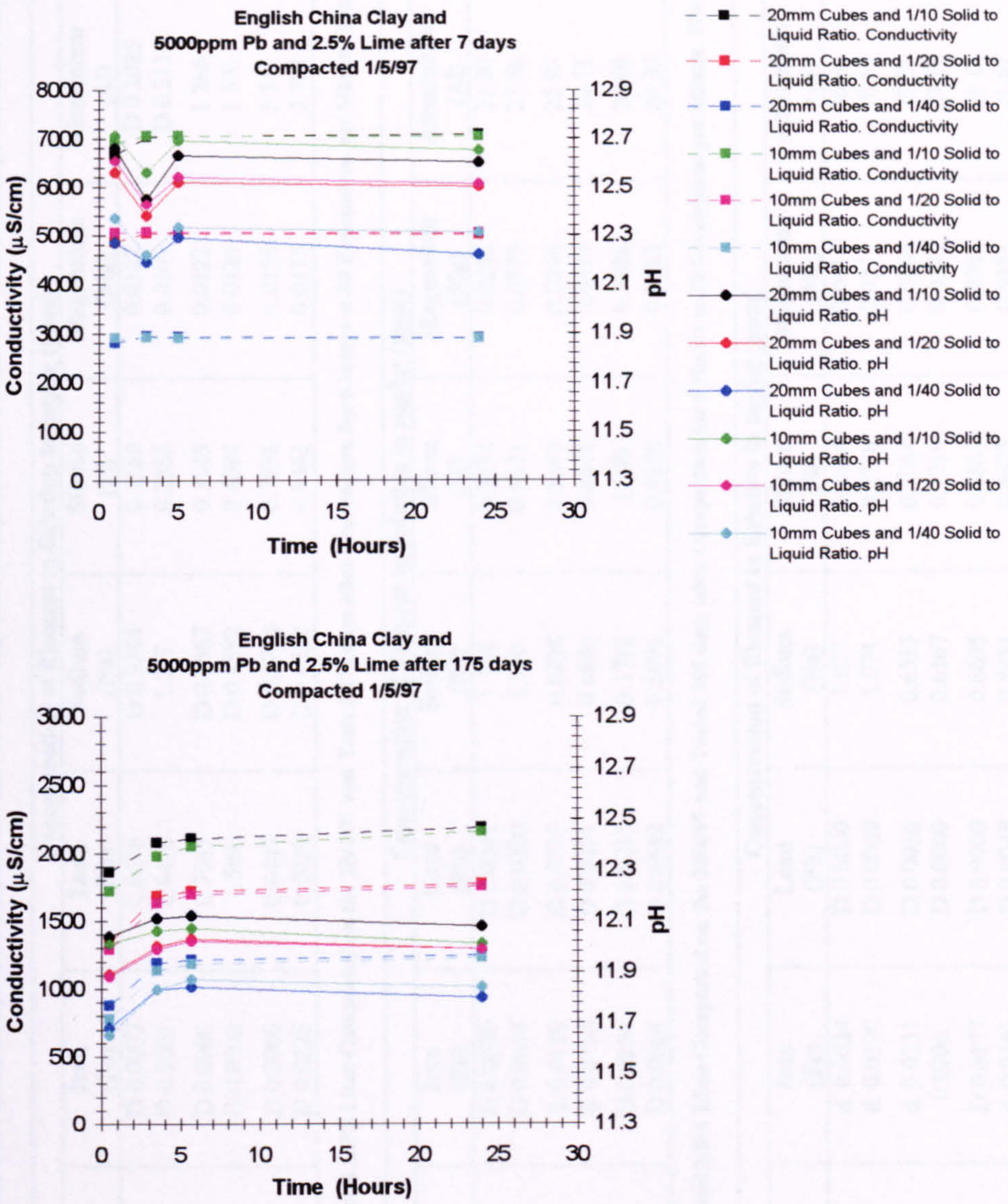

Table A1.72 ICP Data for Kaolinite and 5000ppm Lead and 2.5% Lime, Compacted on the 28/4/97 and Tested 7 days after Compaction for 6 Hours at 30 Revolutions per Minute. Filter only.

Solid to Liquid Ratio	Initial Cube Size (mm)	Concentration of Element in Solution in mg/kg (ppm)							
		Calcium (Ca)	Iron (Fe)	Lead (Pb)	Sodium (Na)	Silicon (Si)	Magnesium (Mg)	Aluminium (Al)	Manganese (Mn)
1/10	10	613.8	D 0.0007	0.6616	D 0.9244	0.1589	0.0122	D 0.2025	D 0.0002
	20	694.9	D 0.0001	0.8476	1.277	0.2386	0.0147	D 0.2114	D 0.0002
1/20	10	398.9	D 0.0000	0.7685	D 0.5567	0.3143	0.0122	1.266	D 0.0000
	20	418.4	D 0.0002	1.584	D 0.8582	0.4094	0.0124	1.595	D 0.0000
1/40	10	171.6	D 0.0000	0.4449	D 0.3756	0.7938	0.0156	3.331	D 0.0000
	20	246.8	D 0.0225	0.7420	D 0.6550	0.8441	0.0175	3.703	D 0.0000

Table A1.73 ICP Data for Kaolinite and 5000ppm Lead and 2.5% Lime Compacted on the 28/4/97 and Tested 175 days after Compaction for 6 Hours at 30 Revolutions per Minute. Filter only.

Solid to Liquid Ratio	Initial Cube Size (mm)	Concentration of Element in Solution in mg/kg (ppm)							
		Calcium (Ca)	Iron (Fe)	Lead (Pb)	Sodium (Na)	Silicon (Si)	Magnesium (Mg)	Aluminium (Al)	Manganese (Mn)
1/10	10	195.9	D 0.0030	D 0.0341	1.144	0.3974	0.0246	21.80	D 0.0000
	20	179.5	D 0.0044	D 0.0000	1.010	0.2931	0.0375	23.68	D 0.0000
1/20	10	154.1	d. 0.0120	D 0.0737	0.6298	0.8663	0.0246	25.85	D 0.0000
	20	136.7	d. 0.0158	D 0.0491	0.6636	0.8616	0.0379	26.71	D 0.0000
1/40	10	94.63	D 0.0234	D 0.0717	0.5712	1.070	0.0386	20.09	D 0.0000
	20	95.21	D 0.0064	D 0.0642	0.5091	0.9860	0.0385	20.30	D 0.0000

Table A1.74 ICP Data for Kaolinite and 5000ppm Lead and 2.5% Lime Compacted on the 28/4/97 and Tested 301 days after Compaction for 6 Hours at 30 Revolutions per Minute. Filter only.

Solid to Liquid Ratio	Initial Cube Size (mm)	Concentration of Element in Solution in mg/kg (ppm)							
		Calcium (Ca)	Iron (Fe)	Lead (Pb)	Sodium (Na)	Silicon (Si)	Magnesium (Mg)	Aluminium (Al)	Manganese (Mn)
1/10	10	139.2	d. 0.0024	D 0.0000	1.037	0.2644	0.0414	26.85	D 0.0000
	20	143.9	d. 0.0190	D 0.0000	1.074	0.2718	0.0335	28.57	D 0.0004
1/20	10	111.5	d. 0.0231	D 0.0050	0.6553	0.3064	0.0284	27.28	D 0.0002
	20	95.31	0.0206	D 0.0000	0.6167	0.2719	0.0347	27.79	D 0.0001
1/40	10	81.24	D 0.0177	D 0.0000	0.6605	0.4861	0.0744	21.17	D 0.0002
	20	81.49	d. 0.0141	D 0.0048	0.5231	0.4673	0.0353	21.61	D 0.0001

Note: 'D' indicates the stated value is below detection limits and the value stated is a system estimate.
'd' indicates the stated value is close to detection limits.

Table A1.75 ICP Data for Kaolinite and 5000ppm Lead and 2.5% Lime, Compacted on the 29/4/97 and Tested 7 days after Compaction for 6 Hours at 60 Revolutions per Minute. Filter only.

Solid to Liquid Ratio	Initial Cube Size (mm)	Concentration of Element in Solution in mg/kg (ppm)							
		Calcium (Ca)	Iron (Fe)	Lead (Pb)	Sodium (Na)	Silicon (Si)	Magnesium (Mg)	Aluminium (Al)	Manganese (Mn)
1/10	10	716.8	D 0.0000	0.5940	D 0.7633	0.1692	0.0095	D 0.1173	D 0.0000
	20	724.2	D 0.0000	0.9529	1.386	0.1849	0.0122	D 0.0799	D 0.0000
1/20	10	464.3	D 0.0424	1.219	D 0.4014	1.730	0.0146	2.090	D 0.0000
	20	463.6	D 0.0000	D 0.0438	D 0.5644	0.8916	0.0092	1.516	D 0.0000
1/40	10	163.0	D 0.0000	D 0.0349	D 0.2870	0.6824	0.0200	2.956	D 0.0000
	20	247.9	D 0.0000	D 0.3229	D 0.3537	0.7380	0.0163	3.118	D 0.0000

Table A1.76 ICP Data for Kaolinite and 5000ppm Lead and 2.5% Lime, Compacted on the 29/4/97 and Tested 175 days after Compaction for 6 Hours at 60 Revolutions per Minute. Filter only.

Solid to Liquid Ratio	Initial Cube Size (mm)	Concentration of Element in Solution in mg/kg (ppm)							
		Calcium (Ca)	Iron (Fe)	Lead (Pb)	Sodium (Na)	Silicon (Si)	Magnesium (Mg)	Aluminium (Al)	Manganese (Mn)
1/10	10	190.0	D 0.0013	D 0.0258	0.8157	0.4494	0.0227	19.31	D 0.0000
	20	115.3	D 0.0023	D 0.0017	0.7836	0.3063	0.0276	20.90	D 0.0000
1/20	10	65.73	D 0.0232	D 0.0000	0.5633	0.4295	0.0408	24.91	D 0.0000
	20	143.2	D 0.0019	D 0.0216	0.4905	0.4472	0.0232	25.14	D 0.0000
1/40	10	40.12	D 0.0017	D 0.0000	0.3822	0.1329	0.0491	11.51	d. 0.0002
	20	40.17	D 0.0000	D 0.0000	0.4830	d. 0.0556	0.0281	13.64	D 0.0000

Note: 'D' indicates the stated value is below detection limits and the value stated is a system estimate.
'd' indicates the stated value is close to detection limits.

Table A1.77 ICP Data for Kaolinite and 5000ppm Lead and 2.5% Lime, Compacted on the 30/4/97 and Tested 7 days after Compaction for 24 Hours at 30 Revolutions per Minute. Filter only.

Solid to Liquid Ratio	Initial Cube Size (mm)	Concentration of Element in Solution in mg/kg (ppm)							
		Calcium (Ca)	Iron (Fe)	Lead (Pb)	Sodium (Na)	Silicon (Si)	Magnesium (Mg)	Aluminium (Al)	Manganese (Mn)
1/10	10	690.0	D 0.0000	0.7526	D 0.8201	0.2161	0.0062	D 0.1593	D 0.0000
	20	694.9	D 0.0000	0.7319	D 0.9167	0.2224	0.0090	D 0.1141	D 0.0000
1/20	10	419.6	0.2000	3.019	D 0.5376	8.496	0.0898	7.820	D 0.0030
	20	480.5	d. 0.0599	4.208	D 0.4638	2.549	0.0275	3.185	D 0.0000
1/40	10	265.7	D 0.0000	0.4576	D 0.4054	0.7693	0.0205	2.336	D 0.0000
	20	246.9	D 0.0000	d. 0.4381	D 0.2789	0.7122	0.0144	3.199	D 0.0000

Table A1.78 ICP Data for Kaolinite and 5000ppm Lead and 2.5% Lime, Compacted on the 30/4/97 and Tested 175 days after Compaction for 24 Hours at 30 Revolutions per Minute. Filter only.

Solid to Liquid Ratio	Initial Cube Size (mm)	Concentration of Element in Solution in mg/kg (ppm)							
		Calcium (Ca)	Iron (Fe)	Lead (Pb)	Sodium (Na)	Silicon (Si)	Magnesium (Mg)	Aluminium (Al)	Manganese (Mn)
1/10	10	209.5	d. 0.0067	D 0.0248	0.9546	0.5276	0.0249	17.56	D 0.0000
	20	242.8	D 0.0118	D 0.0392	0.8099	0.3843	0.0188	19.56	D 0.0000
1/20	10	171.6	D 0.0043	D 0.1049	0.6988	0.7193	0.0250	22.08	D 0.0000
	20	136.0	d. 0.0148	D 0.0140	0.8317	0.4492	0.0394	23.00	D 0.0000
1/40	10	97.57	D 0.0025	D 0.0087	0.4120	0.7246	0.0413	18.79	D 0.0000
	20	91.09	D 0.0003	D 0.0000	0.4739	0.6636	0.0274	18.42	D 0.0000

Table A1.79 ICP Data for Kaolinite and 5000ppm Lead and 2.5% Lime, Compacted on the 30/4/97 and Tested 301 days after Compaction for 24 Hours at 30 Revolutions per Minute. Filter only.

Solid to Liquid Ratio	Initial Cube Size (mm)	Concentration of Element in Solution in mg/kg (ppm)							
		Calcium (Ca)	Iron (Fe)	Lead (Pb)	Sodium (Na)	Silicon (Si)	Magnesium (Mg)	Aluminium (Al)	Manganese (Mn)
1/10	10	197.1	D 0.0044	D 0.0000	1.191	0.2639	0.0285	24.64	D 0.0001
	20	195.2	d. 0.0053	D 0.0000	1.061	0.2441	0.0218	25.63	D 0.0001
1/20	10	146.1	D 0.0162	D 0.0000	0.8467	0.3489	0.0298	24.21	D 0.0002
	20	125.1	0.1089	0.1028	0.8394	2.771	0.0591	28.79	D 0.0014
1/40	10	89.05	D 0.0063	D 0.0000	0.4149	0.4669	0.0466	20.04	D 0.0000
	20	93.12	0.0226	D 0.0250	0.5428	0.9999	0.0245	21.20	D 0.0002

Note: 'D' indicates the stated value is below detection limits and the value stated is a system estimate.
'd' indicates the stated value is close to detection limits.

Table A1.80 ICP Data for Kaolinite and 5000ppm Lead and 2.5% Lime, Compacted on the 1/5/97 and Tested 7 days after Compaction for 24 Hours at 60 Revolutions per Minute. Filter only.

Solid to Liquid Ratio	Initial Cube Size (mm)	Concentration of Element in Solution in mg/kg (ppm)							
		Calcium (Ca)	Iron (Fe)	Lead (Pb)	Sodium (Na)	Silicon (Si)	Magnesium (Mg)	Aluminium (Al)	Manganese (Mn)
1/10	10	687.8	D 0.0000	0.5629	D 0.8023	0.2485	0.0144	D 0.1640	D 0.0000
	20	652.9	D 0.0021	0.5447	D 0.9408	0.1925	0.0174	D 0.2217	D 0.0006
1/20	10	486.5	D 0.0139	1.540	D 0.4266	1.273	0.0151	2.123	D 0.0004
	20	455.7	D 0.0029	1.269	D 0.4639	0.3769	0.0133	1.599	D 0.0001
1/40	10	228.3	D 0.0005	0.4611	D 0.2703	0.7280	0.0221	3.585	D 0.0001
	20	231.5	D 0.0000	D 0.2266	D 0.3782	0.7290	0.0204	3.843	D 0.0000

Table A1.81 ICP Data for Kaolinite and 5000ppm Lead and 2.5% Lime, Compacted on the 1/5/97 and Tested 175 days after Compaction for 24 Hours at 60 Revolutions per Minute. Filter only.

Solid to Liquid Ratio	Initial Cube Size (mm)	Concentration of Element in Solution in mg/kg (ppm)							
		Calcium (Ca)	Iron (Fe)	Lead (Pb)	Sodium (Na)	Silicon (Si)	Magnesium (Mg)	Aluminium (Al)	Manganese (Mn)
1/10	10	193.8	D 0.0009	D 0.0242	0.8752	0.4258	0.0202	18.18	D 0.0000
	20	221.7	D 0.0096	D 0.0165	0.8124	0.4898	0.0194	21.51	D 0.0000
1/20	10	135.3	0.0214	D 0.0607	0.4742	1.355	0.0322	23.37	D 0.0000
	20	166.5	D 0.0097	d. 0.1036	0.5205	1.055	0.0245	24.06	D 0.0000
1/40	10	73.07	D 0.0016	D 0.0043	0.4248	0.7380	0.0601	18.48	D 0.0000
	20	100.9	D 0.0012	D 0.0211	0.3616	0.7931	0.0335	18.26	D 0.0000

Note : 'D' indicates the stated value is below detection limits and the value stated is a system estimate.
'd' indicates the stated value is close to detection limits.

A1.2.9 English China Clay with 5000ppm Fe and 2.5% lime

Most importantly Tables A1.82 to A1.91 show that at all curing periods essentially no Fe was released into solution.

A1.2.9.1 Solid : liquid ratio

Inspection of Figures A1.39 to A1.42 illustrates that as solid to liquid ratio was increased pH and conductivity increased. In all tests there were very distinct increases in conductivity with increasing solid to liquid ratio. The most apparent behaviour related to solid to liquid ratio was the fact that the pH of 1:10 and 1:20 solid to liquid ratios were very similar in magnitude.

At 7 days curing the conductivities of 6hr/30rpm tests with 20mm cube sizes (Figure A1.39) at the solid to liquid ratios 1:10, 1:20 and 1:40 were 3520μS/cm, 2700μS/cm and 1685μS/cm whilst pH values were 11.90, 11.90 and 11.76. At 175 days curing the conductivity values were 3160μS/cm, 2470μS/cm and 1581μS/cm whilst pH values were 11.68, 11.68 and 11.44. Increasing the solid to liquid ratio at 7 days curing from 1:40 to 1:20 increased conductivity by a factor of 1.60 and pH by 0.14 pH divisions. Further increases in solid to liquid ratio from 1:20 to 1:40 increased conductivity by a factor of 1.30 and pH by 0.00 pH divisions. Increasing the solid to liquid ratio at 175 days curing from 1:40 to 1:20 increased conductivity by a factor of 1.56 and pH by 0.23 pH divisions. Further increases in solid to liquid ratio from 1:20 to 1:10 increased conductivity by a factor of 1.28 and pH by –0.01pH divisions.

Data Tables A1.82 to A1.91 illustrate that as solid to liquid ratio decreases and curing period increases Ca concentration only decreases by a small amount. Observation of Table A1.82 for 20mm cubes and 6hr/30rpm tests at 7 days curing illustrates that increasing solid to liquid ratio from 1:40 to 1:20 resulted in an increase in concentration of Ca from 205ppm to 368ppm. A similar increase in solid to liquid ratio from 1:20 to 1:10 resulted in an increase in Ca concentration from 368ppm to 528ppm. At 175 days curing and 301 days curing all tests produced increases in Ca and Na concentration with increasing solid to liquid ratio whilst the solid to liquid ratio 1:20 again produced the most Al. Mg and Si concentrations remained at similar magnitudes for all solid to liquid ratios and curing periods.

It is evident that the solid to liquid ratio 1:40 results in the highest pH and conductivity variability between the two cube sizes.

A1.2.9.2 Cube Size

Observation of Figures A1.39 to A1.42 illustrates again that 10mm cubes produced higher final pH values. Analysis of Tables A1.82 to A1.91 shows that Ca concentrations tended to increase with increased cube size whilst there were no clear trends at any curing period for differences in other element release between cube sizes at specific solid to liquid ratios.

A1.2.9.3 Rotation speed and test duration

Comparison of 6hr tests at 7 days curing (Figures A1.39 and A1.40) illustrate that at all solid to liquid ratios pH did not vary significantly with increasing rotation speed whilst conductivity did increase slightly. The latter fact is also evident in the higher Ca levels in solution at the higher rotation speed (Table A1.82 and A1.85). At 175 days both pH and conductivity were slightly higher at the higher rotation speed, again reflected in the Ca levels illustrated in Tables A1.83 and A1.86. Generally at the higher rotation speed more Na, Si, Mg and Al were released. Comparison of 24hr tests at 7 days curing (Figures A1.41 and A1.42) shows a slightly different result. The higher rotation speed tended to produce slightly lower pH and conductivity values whilst at 175 days pH values were higher and conductivity values were unchanged. Again variation in conductivity was reflected in Ca levels whilst generally other elements showed similar concentrations at both speeds. Al was the exception producing slightly higher concentrations at the higher rotation speeds.

Increasing test duration had varying effects. For 30rpm test at 7 days curing the longer test duration produced higher pH and conductivity values. At 175 days curing both test durations produced similar values whilst at 301 days the longer test duration produced higher pH and conductivity values. At 301 days with the exception of Ca, both durations released similar quantities of each element.

A1.2.9.4 Curing Time

Consideration of 30rpm tests (Figures A1.39 and A1.41) illustrates that increasing curing period from 7 days curing to 175 days curing generally resulted in small decreases in pH and conductivity. Between 175 days curing and 301 days

curing pH continued to drop with little change in conductivity. Between 7 days curing and 175 days curing 60 rpm tests (Figures A1.40 and A1.42) showed slight increases in pH whilst conductivity values reduced.

Generally Tables A1.87 to A1.91 indicate a reduction in Ca, Si and Mg whilst Al increases and Na fluctuates as curing period increases. Table A1.87, A1.88, A1.89 and A1.82, A1.83, A1.84 illustrate that Al reaches optimum at 175 days and retains this concentration level at 301 days.

Figure A1.39 Conductivity and pH characteristics for English China Clay with 5000ppm Fe and 2.5% lime during 6hr/30rpm Batch Tests

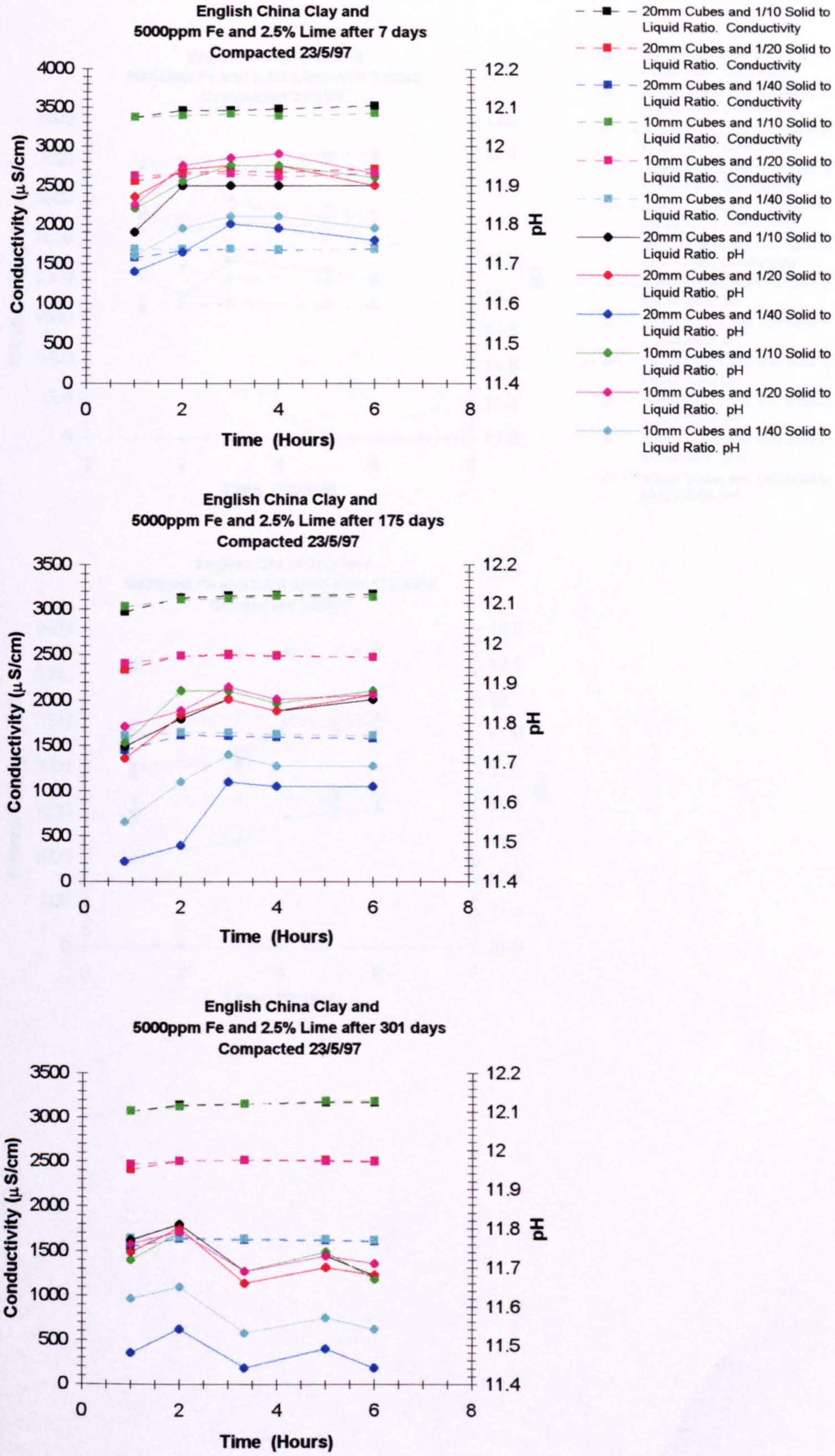

Figure A1.40 Conductivity and pH characteristics for English China Clay with 5000ppm Fe and 2.5% lime during 6hr/60rpm Batch Tests

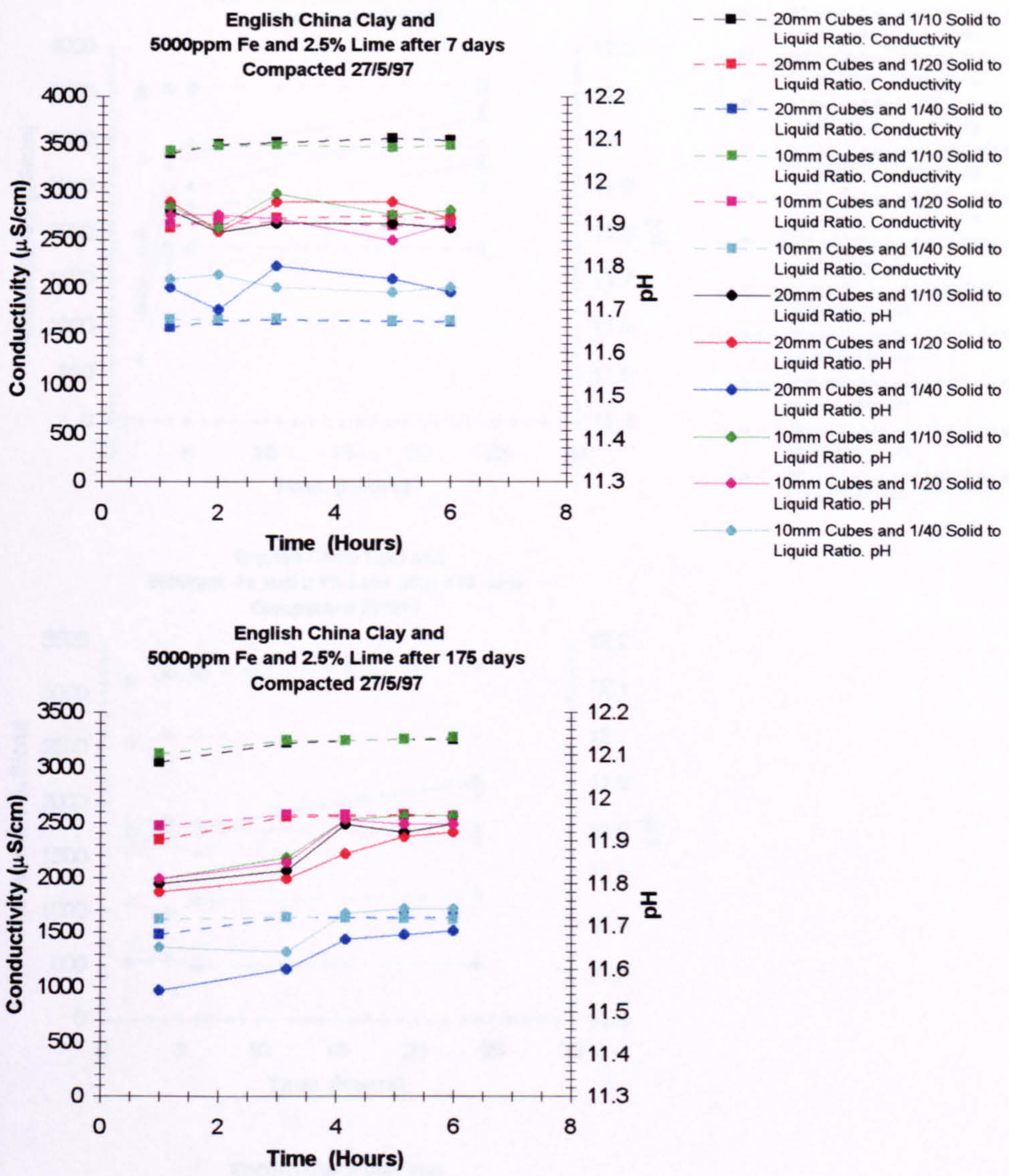

Figure A1.41 Conductivity and pH characteristics for English China Clay with 5000ppm Fe and 2.5% lime during 24hr/30rpm Batch Tests

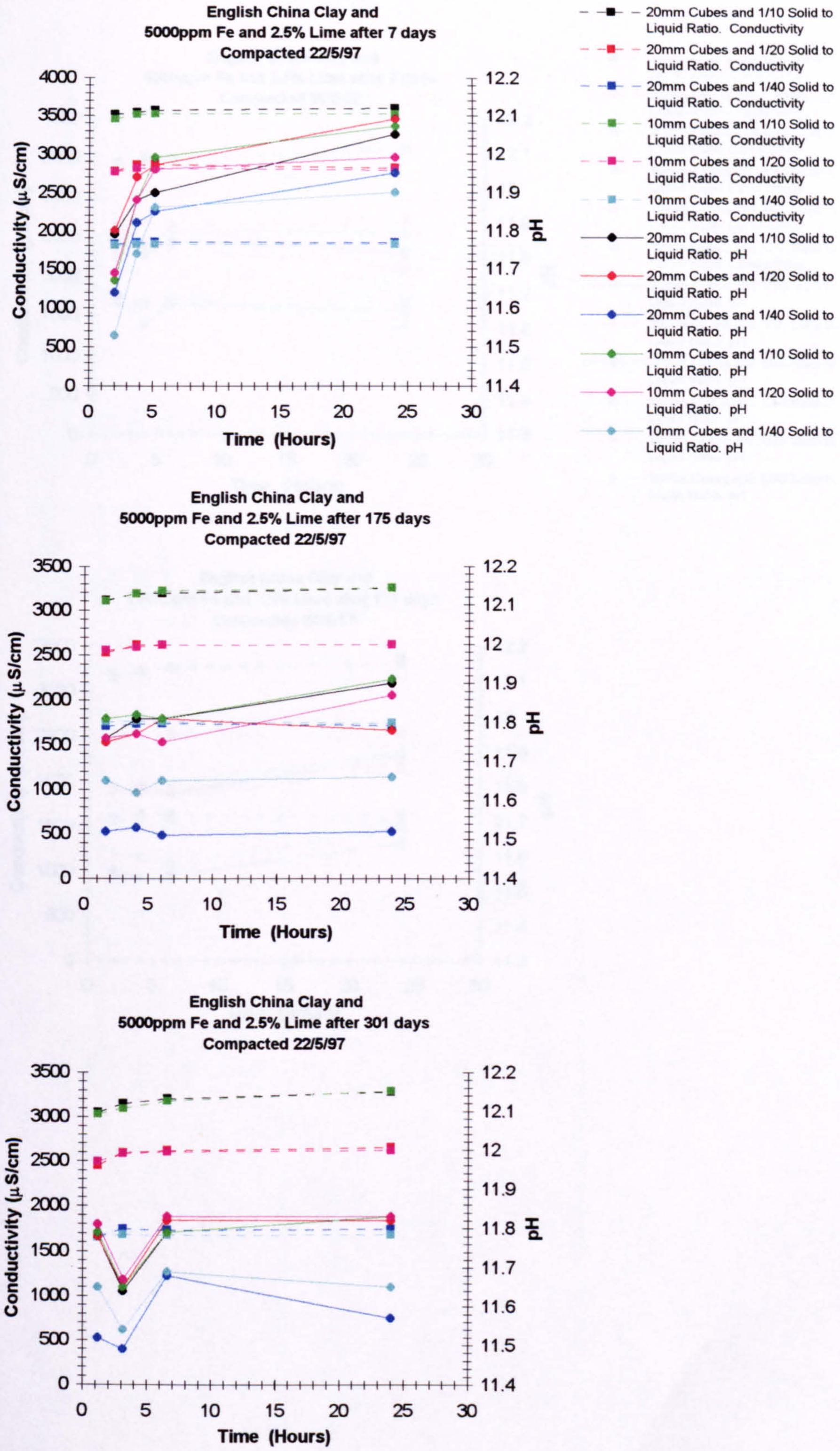

Figure A1.42 Conductivity and pH characteristics for English China Clay with 5000ppm Fe and 2.5% lime during 24hr/60rpm Batch Tests

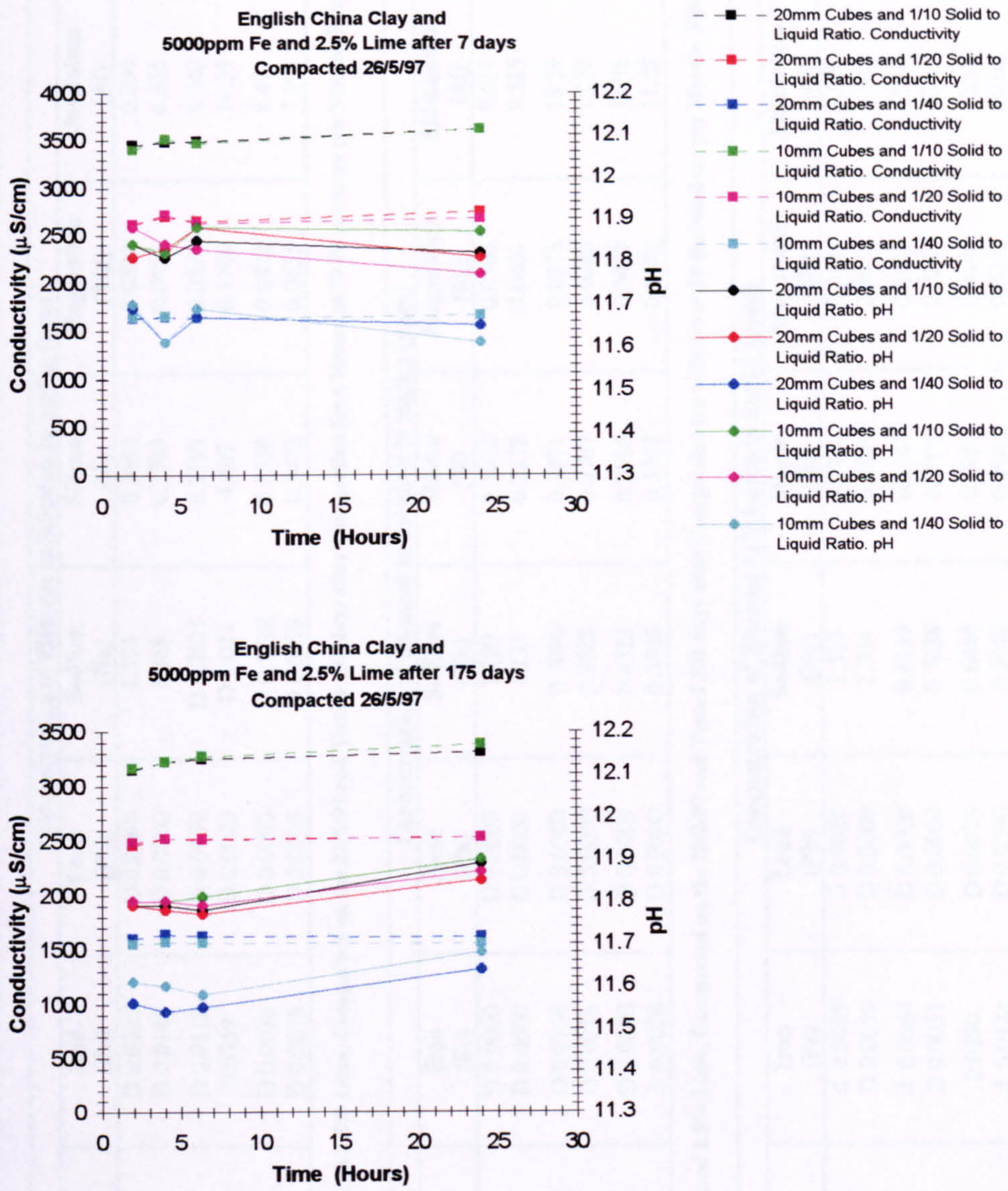

Table A1.82 ICP Data for Kaolinite and 5000ppm Iron and 2.5% Lime, Compacted on the 23/5/97 and Tested 7 days after Compaction for 6 Hours at 30 Revolutions per Minute. Filter only.

Solid to Liquid Ratio	Initial Cube Size (mm)	Concentration of Element in Solution in mg/kg (ppm)							
		Calcium (Ca)	Iron (Fe)	Lead (Pb)	Sodium (Na)	Silicon (Si)	Magnesium (Mg)	Aluminium (Al)	Manganese (Mn)
1/10	10	519.7	D 0.0220	D 0.0000	1.394	0.3694	0.0502	6.094	D 0.0018
	20	528.2	D 0.0141	D 0.0000	1.568	0.3709	0.0652	6.335	D 0.0000
1/20	10	345.2	D 0.0112	D 0.0179	D 0.7923	0.2199	0.0590	8.740	D 0.0001
	20	368.3	0.3759	D 0.0000	D 1.027	4.807	0.1740	14.53	D 0.0016
1/40	10	176.9	D 0.0038	D 0.0000	D 0.5718	0.3536	0.0442	8.472	D 0.0000
	20	205.4	D 0.0078	D 0.0103	D 0.6079	0.3472	0.0655	7.791	D 0.0000

Table A1.83 ICP Data for Kaolinite and 5000ppm Iron and 2.5% Lime, Compacted on the 23/5/97 and Tested 175 days after Compaction for 6 Hours at 30 Revolutions per Minute. Filter only.

Solid to Liquid Ratio	Initial Cube Size (mm)	Concentration of Element in Solution in mg/kg (ppm)							
		Calcium (Ca)	Iron (Fe)	Lead (Pb)	Sodium (Na)	Silicon (Si)	Magnesium (Mg)	Aluminium (Al)	Manganese (Mn)
1/10	10	519.0	D 0.0000	D 0.0000	1.229	0.3022	0.0506	9.614	D 0.0004
	20	529.6	D 0.0000	D 0.0000	1.235	0.2878	0.0401	9.523	D 0.0001
1/20	10	350.9	D 0.0156	D 0.0000	0.7090	0.3471	0.0375	13.39	D 0.0000
	20	358.0	D 0.0026	D 0.0000	0.7522	0.2767	0.0386	13.59	D 0.0001
1/40	10	198.5	D 0.0000	D 0.0000	0.4525	0.2935	0.0417	11.36	D 0.0000
	20	192.1	d. 0.0028	D 0.0000	0.5946	0.3733	0.0482	11.38	D 0.0000

Table A1.84 ICP Data for Kaolinite and 5000ppm Iron and 2.5% Lime, Compacted on the 23/5/97 and Tested 301 days after Compaction for 6 Hours at 30 Revolutions per Minute. Filter only.

Solid to Liquid Ratio	Initial Cube Size (mm)	Concentration of Element in Solution in mg/kg (ppm)							
		Calcium (Ca)	Iron (Fe)	Lead (Pb)	Sodium (Na)	Silicon (Si)	Magnesium (Mg)	Aluminium (Al)	Manganese (Mn)
1/10	10	534.6	d. 0.0089	D 0.0020	1.316	0.2766	0.0424	8.967	D 0.0001
	20	543.6	D 0.0059	D 0.0000	1.764	0.2804	0.0658	9.315	D 0.0000
1/20	10	388.2	d. 0.0064	D 0.0000	0.8159	0.2541	0.0301	13.34	D 0.0000
	20	367.5	D 0.0031	D 0.0000	0.7638	0.2101	0.0287	13.55	D 0.0002
1/40	10	216.5	0.0350	D 0.0079	0.6444	0.7451	0.0449	12.18	D 0.0003
	20	211.3	d. 0.0124	D 0.0000	0.5040	0.3063	0.0247	10.66	D 0.0000

Note. 'D' indicates the stated value is below detection limits and the value stated is a system estimate.
'd' indicates the stated value is close to detection limits.

Table A1.85 ICP Data for Kaolinite and 5000ppm Iron and 2.5% Lime, Compacted on the 27/5/97 and Tested 7 days after Compaction for 6 Hours at 60 Revolutions per Minute. Filter only.

Solid to Liquid Ratio	Initial Cube Size (mm)	Concentration of Element in Solution in mg/kg (ppm)							
		Calcium (Ca)	Iron (Fe)	Lead (Pb)	Sodium (Na)	Silicon (Si)	Magnesium (Mg)	Aluminium (Al)	Manganese (Mn)
1/10	10	553.3	0.3509	D 0.0000	2.219	3.146	0.2207	7.209	D 0.0027
	20	556.7	D 0.0170	D 0.0045	2.289	0.3045	0.1228	6.542	D 0.0004
1/20	10	366.5	D 0.0298	D 0.0000	D 1.104	0.4727	0.0810	10.62	D 0.0004
	20	384.9	D 0.0441	D 0.0000	1.365	0.6128	0.0809	10.13	D 0.0006
1/40	10	197.4	D 0.0116	D 0.0000	D 0.6484	0.4389	0.0549	8.457	D 0.0004
	20	176.5	D 0.0186	D 0.0000	D 0.7716	0.3749	0.0776	7.595	D 0.0004

Table A1.86 ICP Data for Kaolinite and 5000ppm Iron and 2.5% Lime, Compacted on the 27/5/97 and Tested 175 days after Compaction for 6 Hours at 60 Revolutions per Minute. Filter only.

Solid to Liquid Ratio	Initial Cube Size (mm)	Concentration of Element in Solution in mg/kg (ppm)							
		Calcium (Ca)	Iron (Fe)	Lead (Pb)	Sodium (Na)	Silicon (Si)	Magnesium (Mg)	Aluminium (Al)	Manganese (Mn)
1/10	10	537.4	D 0.0003	D 0.0000	1.421	0.2661	0.0586	9.577	D 0.0001
	20	533.5	D 0.0000	D 0.0000	1.482	0.2858	0.0629	9.654	D 0.0001
1/20	10	351.2	D 0.0099	D 0.0000	0.8950	0.3802	0.0344	13.49	0.0567
	20	342.4	D 0.0021	D 0.0000	0.8255	0.2540	0.0304	13.93	D 0.0001
1/40	10	201.0	D 0.0022	D 0.0000	0.7134	0.2920	0.0499	10.96	D 0.0000
	20	206.0	D 0.0019	D 0.0000	0.5598	0.3321	0.0407	11.20	D 0.0001

Note : 'D' indicates the stated value is below detection limits and the value stated is a system estimate.
'd' indicates the stated value is close to detection limits.

Table A1.87 ICP Data for Kaolinite and 5000ppm Iron and 2.5% Lime, Compacted on the 22/5/97 and Tested 7 days after Compaction for 24 Hours at 30 Revolutions per Minute. Filter only.

Solid to Liquid Ratio	Initial Cube Size (mm)	Concentration of Element in Solution in mg/kg (ppm)							
		Calcium (Ca)	Iron (Fe)	Lead (Pb)	Sodium (Na)	Silicon (Si)	Magnesium (Mg)	Aluminium (Al)	Manganese (Mn)
1/10	10	598.3	D 0.0226	D 0.0000	1.618	0.4854	0.0743	5.386	d. 0.0092
	20	597.7	D 0.0329	D 0.0000	3.665	0.3670	0.3253	5.286	D 0.0002
1/20	10	403.1	D 0.0103	D 0.0000	D 1.014	0.3538	0.0592	9.182	D 0.0000
	20	411.7	D 0.0166	D 0.0000	1.231	0.3460	0.1030	9.348	D 0.0003
1/40	10	236.5	D 0.0165	D 0.0000	D 0.6539	0.5009	0.0496	8.419	D 0.0001
	20	239.8	D 0.0167	D 0.0000	D 0.7499	0.4704	0.0705	8.399	D 0.0000

Table A1.88 ICP Data for Kaolinite and 5000ppm Iron and 2.5% Lime, Compacted on the 22/5/97 and Tested 175 days after Compaction for 24 Hours at 30 Revolutions per Minute. Filter only.

Solid to Liquid Ratio	Initial Cube Size (mm)	Concentration of Element in Solution in mg/kg (ppm)							
		Calcium (Ca)	Iron (Fe)	Lead (Pb)	Sodium (Na)	Silicon (Si)	Magnesium (Mg)	Aluminium (Al)	Manganese (Mn)
1/10	10	526.0	D 0.0087	D 0.0000	1.733	0.3433	0.0332	8.877	D 0.0000
	20	547.4	D 0.0027	D 0.0000	1.380	0.3507	0.0390	8.756	D 0.0000
1/20	10	366.0	d. 0.0014	D 0.0000	1.500	0.3073	0.0314	13.44	D 0.0000
	20	369.6	D 0.0010	D 0.0000	0.7672	0.2906	0.0337	13.39	D 0.0000
1/40	10	219.7	d. 0.0163	D 0.0000	1.448	0.4166	0.0351	11.82	D 0.0002
	20	207.0	D 0.0007	D 0.0000	0.6622	0.4049	0.0392	11.57	D 0.0000

Table A1.89 ICP Data for Kaolinite and 5000ppm Iron and 2.5% Lime, Compacted on the 22/5/97 and Tested 301 days after Compaction for 24 Hours at 30 Revolutions per Minute. Filter only.

Solid to Liquid Ratio	Initial Cube Size (mm)	Concentration of Element in Solution in mg/kg (ppm)							
		Calcium (Ca)	Iron (Fe)	Lead (Pb)	Sodium (Na)	Silicon (Si)	Magnesium (Mg)	Aluminium (Al)	Manganese (Mn)
1/10	10	580.7	0.0034	D 0.0000	1.372	0.2590	0.0347	8.693	D 0.0000
	20	584.6	d. 0.0119	D 0.0049	1.236	0.2871	0.0338	8.593	D 0.0003
1/20	10	400.6	d. 0.0026	D 0.0000	0.8006	0.2502	0.0267	13.01	D 0.0000
	20	383.4	D 0.0026	D 0.0000	0.8031	0.2198	0.0243	13.16	D 0.0002
1/40	10	232.9	D 0.0032	D 0.0000	0.5178	0.2733	0.0325	10.45	D 0.0003
	20	228.0	d. 0.0152	D 0.0000	0.5417	0.3188	0.0257	11.08	D 0.0000

Note: 'D' indicates the stated value is below *detection* limits and the value stated is a system estimate.
'd' indicates the stated value is close to detection limits.

Table A1.90 ICP Data for Kaolinite and 5000ppm Iron and 2.5% Lime, Compacted on the 26/5/97 and Tested 7 days after Compaction for 24 Hours at 60 Revolutions per Minute. Filter only.

Solid to Liquid Ratio	Initial Cube Size (mm)	Concentration of Element in Solution in mg/kg (ppm)							
		Calcium (Ca)	Iron (Fe)	Lead (Pb)	Sodium (Na)	Silicon (Si)	Magnesium (Mg)	Aluminium (Al)	Manganese (Mn)
1/10	10	601.6	D 0.0107	D 0.0000	1.298	0.3831	0.0363	6.479	D 0.0000
	20	588.4	D 0.0112	D 0.0156	1.644	0.3264	0.0456	6.790	D 0.0020
1/20	10	391.3	D 0.0065	D 0.0000	D 0.6853	0.3397	0.0227	9.754	D 0.0004
	20	396.0	D 0.0399	D 0.0000	D 0.8301	0.5309	0.0309	9.986	D 0.0008
1/40	10	223.6	D 0.0199	D 0.0000	D 0.4884	0.5242	0.0454	8.287	D 0.0002
	20	219.9	D 0.0131	D 0.0000	D 0.4283	0.4991	0.0364	8.087	D 0.0000

Table A1.91 ICP Data for Kaolinite and 5000ppm Iron and 2.5% Lime, Compacted on the 26/5/97 and Tested 175 days after Compaction for 24 Hours at 60 Revolutions per Minute. Filter only.

Solid to Liquid Ratio	Initial Cube Size (mm)	Concentration of Element in Solution in mg/kg (ppm)							
		Calcium (Ca)	Iron (Fe)	Lead (Pb)	Sodium (Na)	Silicon (Si)	Magnesium (Mg)	Aluminium (Al)	Manganese (Mn)
1/10	10	557.3	D 0.0070	D 0.0000	1.545	0.3132	0.0305	10.07	D 0.0001
	20	523.7	D 0.0025	D 0.0000	1.439	0.3211	0.0335	9.908	D 0.0000
1/20	10	367.5	D 0.0123	D 0.0000	0.9459	0.4301	0.0293	13.51	D 0.0001
	20	345.1	D 0.0084	D 0.0000	0.9507	0.3262	0.0329	13.90	D 0.0001
1/40	10	203.9	D 0.0102	D 0.0000	0.7858	0.4113	0.0401	10.52	D 0.0000
	20	215.0	0.0211	D 0.0000	0.7384	0.4859	0.0428	11.13	D 0.0001

Note : 'D' indicates the stated value is below detection limits and the value stated is a system estimate.
'd' indicates the stated value is close to detection limits.

A1.2.10 Wyoming Bentonite with no contaminants or lime

A1.2.10.1 Centrifugation

Due to the inherent nature of Wyoming Bentonite neither gravity nor vacuum filtration was possible. It was also not possible to fully centrifuge the samples to ensure completely satisfactory separation. As a result a standard speed and maximum duration of centrifugation was adopted allowing data to be considered relatively. Chemical data illustrated in Tables A1.92 to A1.101 therefore show very high levels of element concentrations that would not be present if filtration was possible. It should also be noted that the solid to liquid ratio 1:10 separated far better under centrifugation than all other solid to liquid ratios. Therefore when considering the chemical data of centrifuged material on a relative basis it is important to consider 1:20 and 1:40 solid to liquid ratios only. However later material will be considered where centrifugation and or filtration was carried out. In these cases the data from 1:10 solid to liquid ratio for the centrifuged samples provides a quantitative result which can be considered similar to the filtered samples.

A1.2.10.2 Solid : liquid ratio

Inspection of Figures A1.43 to A1.46 illustrates clearly that increased solid to liquid ratio results in a reduction in pH and an increase in conductivity. At 7 days curing the conductivity of 6hr 30rpm tests with 20mm cube sizes (Figure A1.43) at the solid to liquid ratio 1:10, 1:20 and 1:40 were 947µS/cm, 675µS/cm and 466 µS/cm respectively whilst pH values were 10.13, 10.24 and 10.27 respectively. At 175 days curing the conductivity values were 864µS/cm, 583 µS/cm and 367µS/cm respectively whilst pH values were 10.16, 10.21 and 10.13 respectively. At 301 days curing conductivity values were 845µS/cm, 620µS/cm and 443µS/cm respectively whilst pH values were 10.13, 10.14 and 10.06 respectively. Increasing solid to liquid from 1:40 to 1:20 at 7, 175 and 301 days curing therefore increased conductivity by factors of 1.45, 1.59 and 1.40 respectively whilst pH increased by -0.03, -0.11 and 0.08 pH divisions respectively. Further increasing solid to liquid ratio from 1:20 to 1:10 increased conductivity by a factors of 1.40, 1.48 and 1.36 respectively whilst pH increased by –0.11, -0.05 and –0.01 pH divisions respectively.

Clearly at all solid to liquid ratios there is a high degree of variability in pH and conductivity data. Consideration of the solid to liquid ratios 1:20 and 1:40 clearly

shows that the quantities of elements present after standard centrifugation were directly related to solid to liquid ratio. Analysis of Table A1.93 illustrates how elements were released in specific proportions after centrifugation. Therefore if 95ppm of Ca was released from one test this would also show fixed levels of the other elements. If another test released similar levels of Ca the levels of the other elements would also be similar. This is illustrated by comparison of the 1:10 solid to liquid ratio, 20mm cubes with the 1:20 solid to liquid ratio, 10mm cubes in Table A1.93.

A1.2.10.3 Cube Size

It was evident in all tests that 10mm cube sizes produced significantly lower final pH values and higher conductivities than 20mm cubes at the same solid to liquid ratios. These higher values represent the amount of breakdown of the cubes into the developing sludge. It was therefore expected that after centrifugation those cubes more readily broken down would produce higher elemental concentrations. This is clearly evident for most 10mm cube tests relative to 20mm cube tests (Tables A1.92 to A1.101)

A1.2.10.4 Rotation speed and test duration

During 6hr tests at 7 days curing (Figures A1.43 and A1.44) the 30rpm tests produced the higher pH and conductivity values. However at 175 days both 60rpm and 30rpm tests produced values within the same range. Analysis of data Tables A1.92, A1.93 and A1.95, A1.96 illustrates that both test speeds produce very similar at specific solid to liquid ratios data although 30rpm tests tend to be slightly elevated.

During 24hr tests at 7 days curing (Figures A1.45 and A1.46) the 30rpm tests generally produce slightly higher pH values and lower conductivities. At 175 days, although pH values are higher, conductivities are similar to those of the 60 rpm tests. Chemical data Tables A1.97, A1.98 and A1.100, A1.101 show that the 60 rpm tests generally break down more of the solid cubes therefore resulting in higher elemental concentrations after centrifugation.

Analysis of Figures A1.43, A1.44 and Figures A1.45, A1.46 highlight that both test durations result in a similar range of pH values whilst 24 hr tests have slightly elevated conductivities a specific solid to liquid ratios. It is clear that both 6hr and 24hr tests do not achieve equilibrium. However it is certain by the final pH and conductivity gradients of the tests that the 24hr tests are closer to equilibrium.

Analysis of data Tables A1.92, A1.93, A1.94 and A1.97, A1.98, A1.99 along with A1.95, A1.96 and A1.100, A1.101 illustrates that higher quantities of elements are released from the 24hr tests as expected.

A1.2.10.5 Curing Time

Observation of Figures A1.43 to A1.46 generally infers that as curing period increases pH and conductivity are reduced. For example Figure A1.43 illustrates reductions in pH of 10mm cubes at the 1:40 solid to liquid ratio from 10.26 to 10.22 to 10.11 and curing period was increased. Tables A1.95, A1.96 and A1.100, A1.101 also report increased centrifuged elemental release with increased curing period that suggests the samples are less easy to centrifuge which implies a chemical is change altering physical properties.

Figure A1.43 Conductivity and pH characteristics for Wyoming Bentonite with no contaminants or lime during 6hr/30rpm Batch Tests

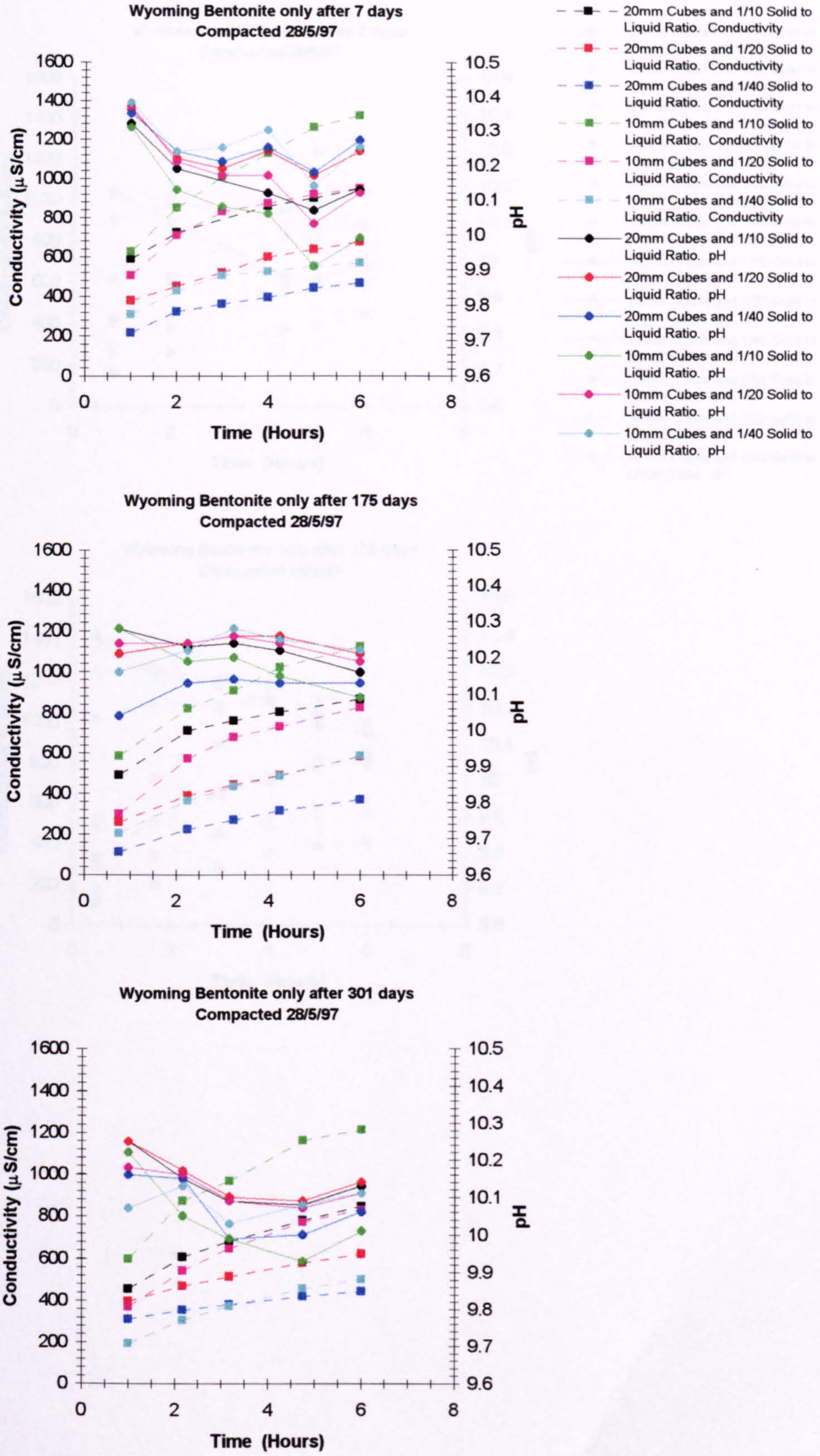

Figure A1.44 Conductivity and pH characteristics for Wyoming Bentonite with no contaminants or lime during 6hr/60rpm Batch Tests

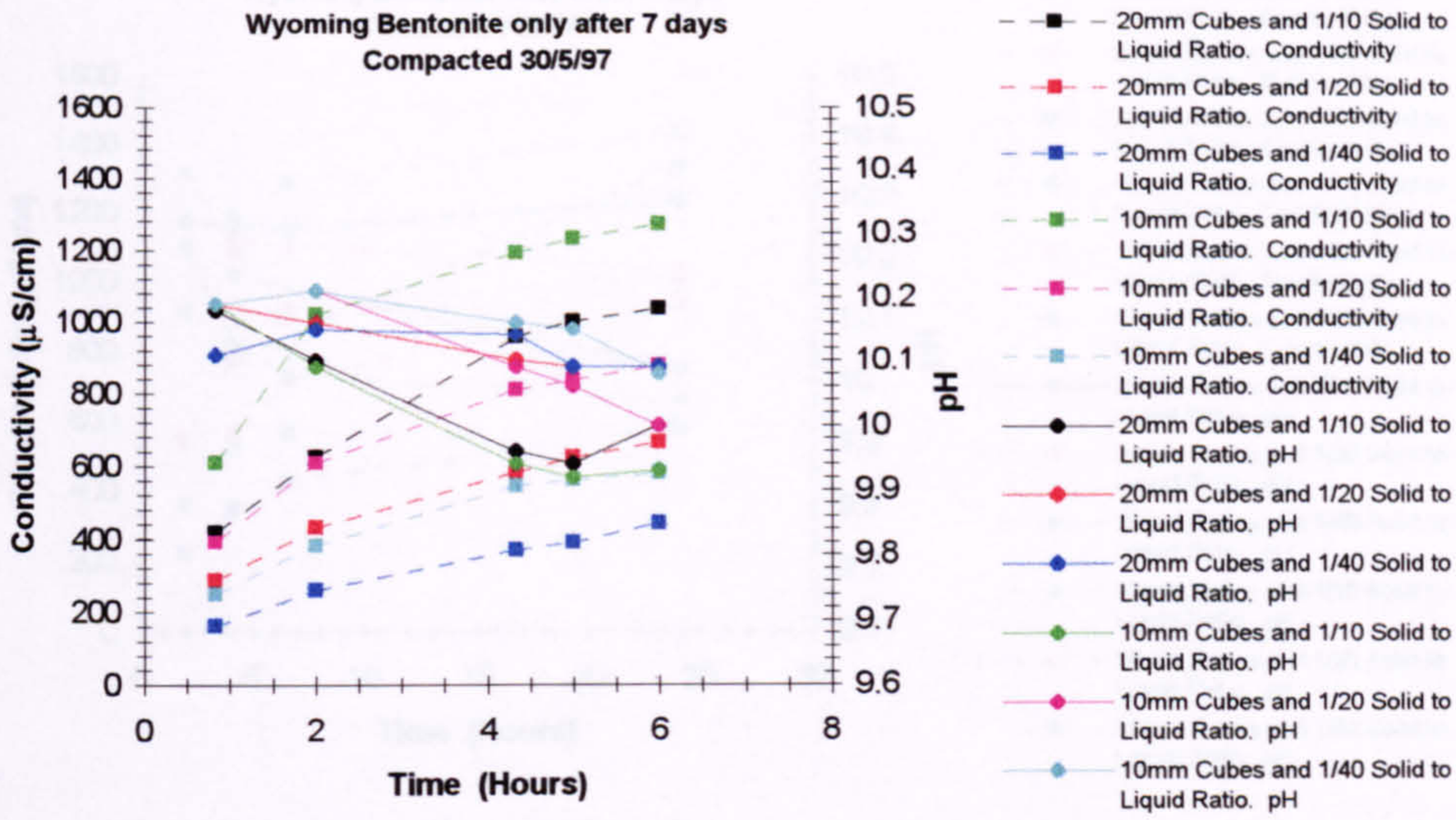

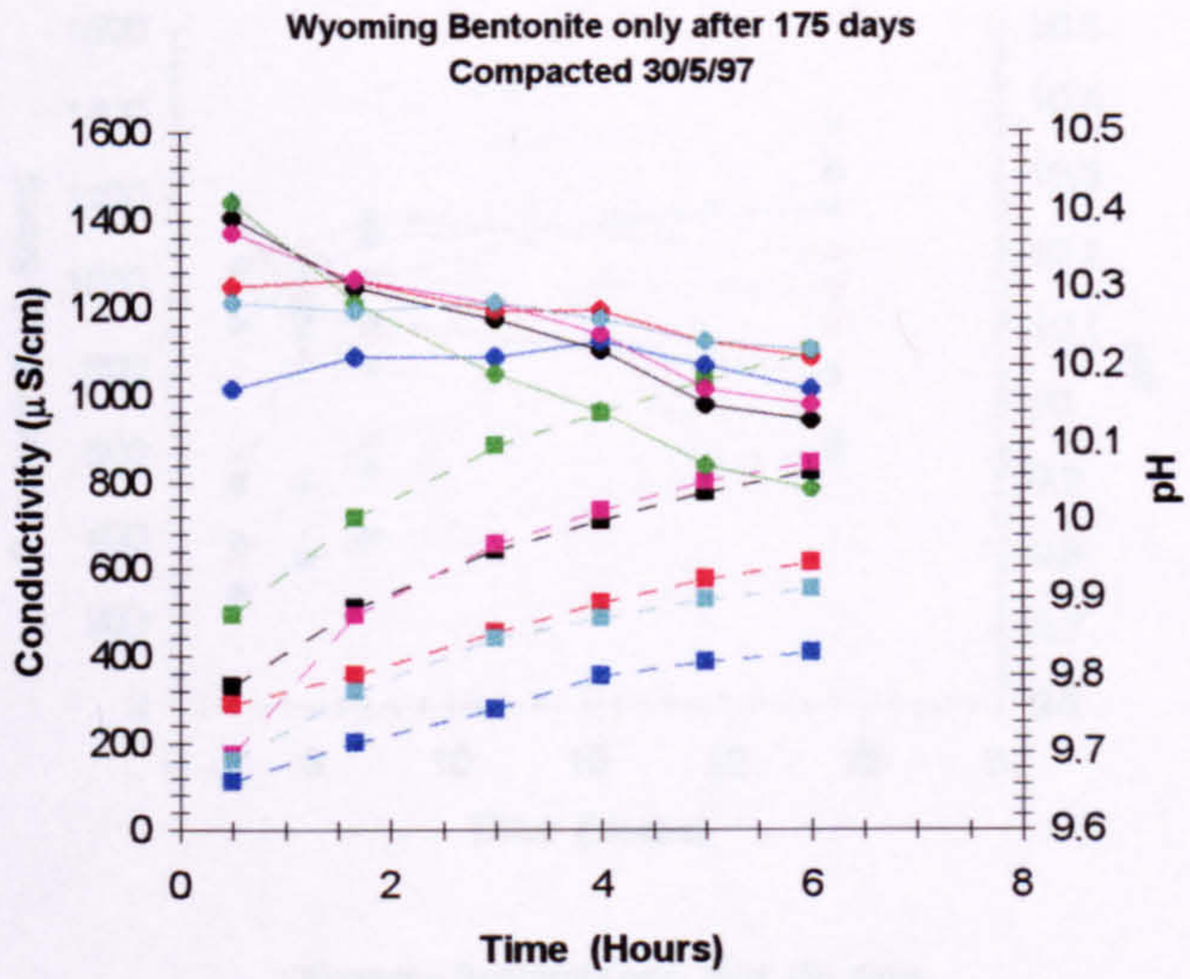

Figure A1.45 Conductivity and pH characteristics for Wyoming Bentonite with no contaminants or lime during 24hr/30rpm Batch Tests

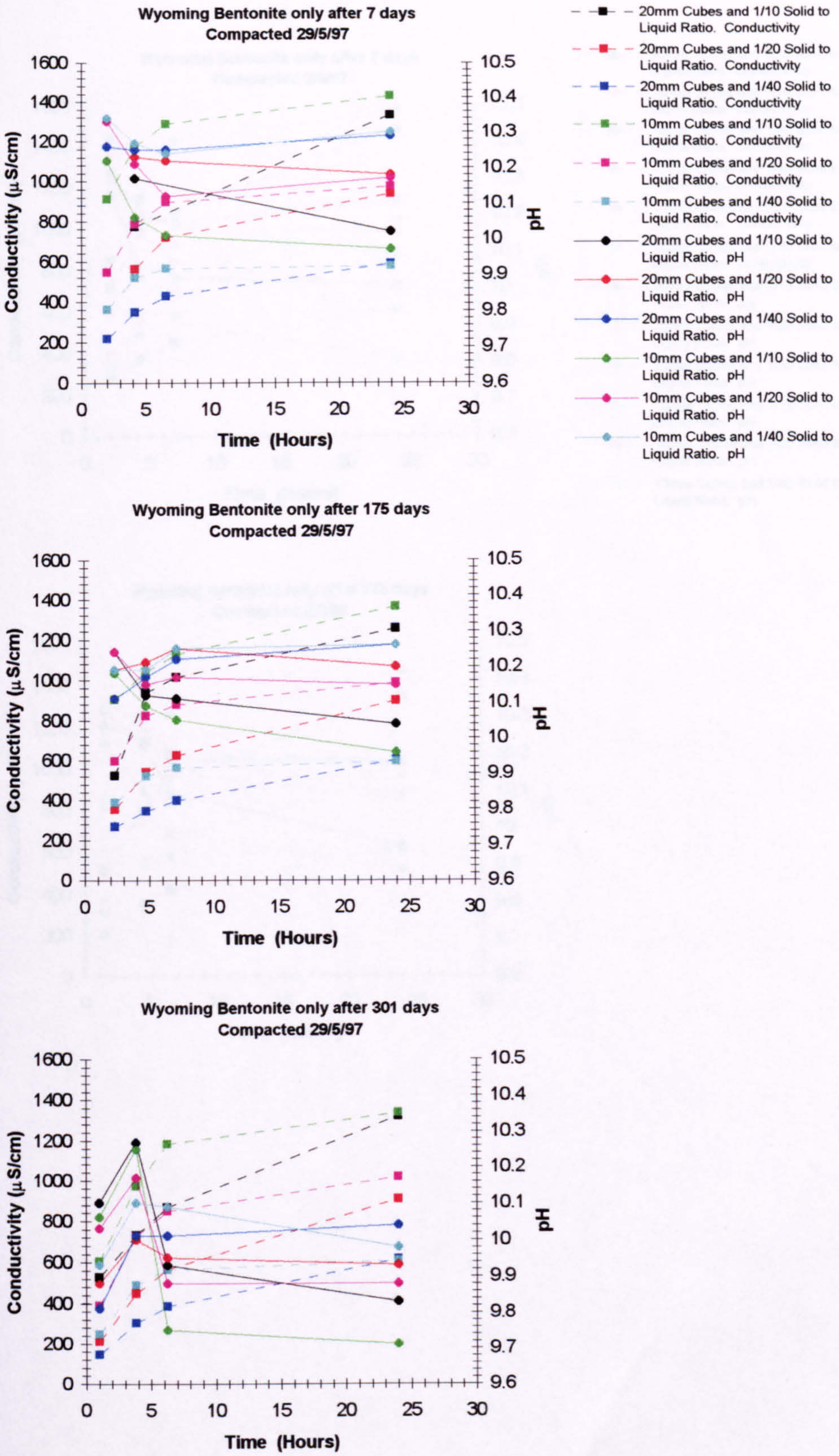

Figure A1.46 Conductivity and pH characteristics for Wyoming Bentonite with no contaminants or lime during 24hr/60rpm Batch Tests

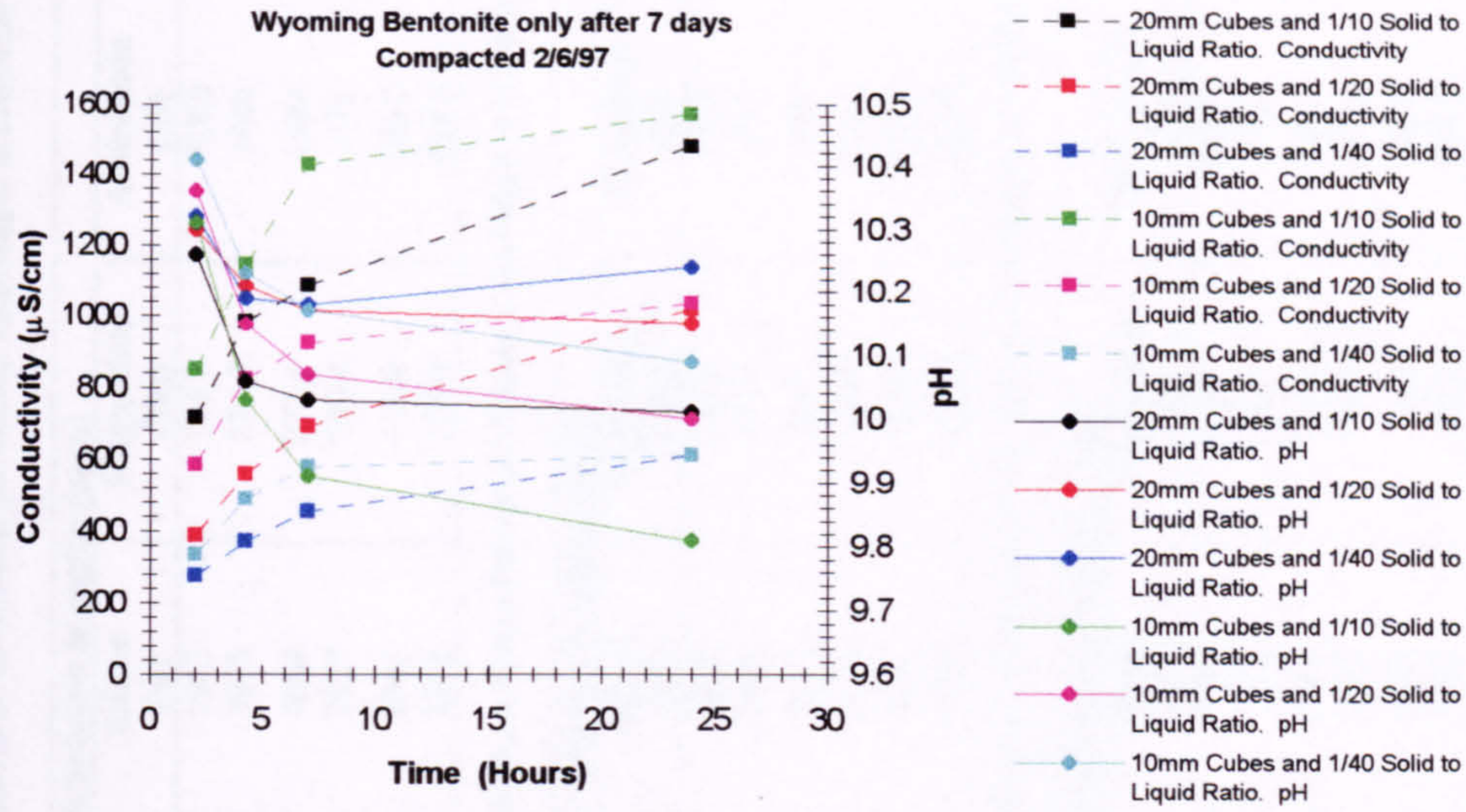

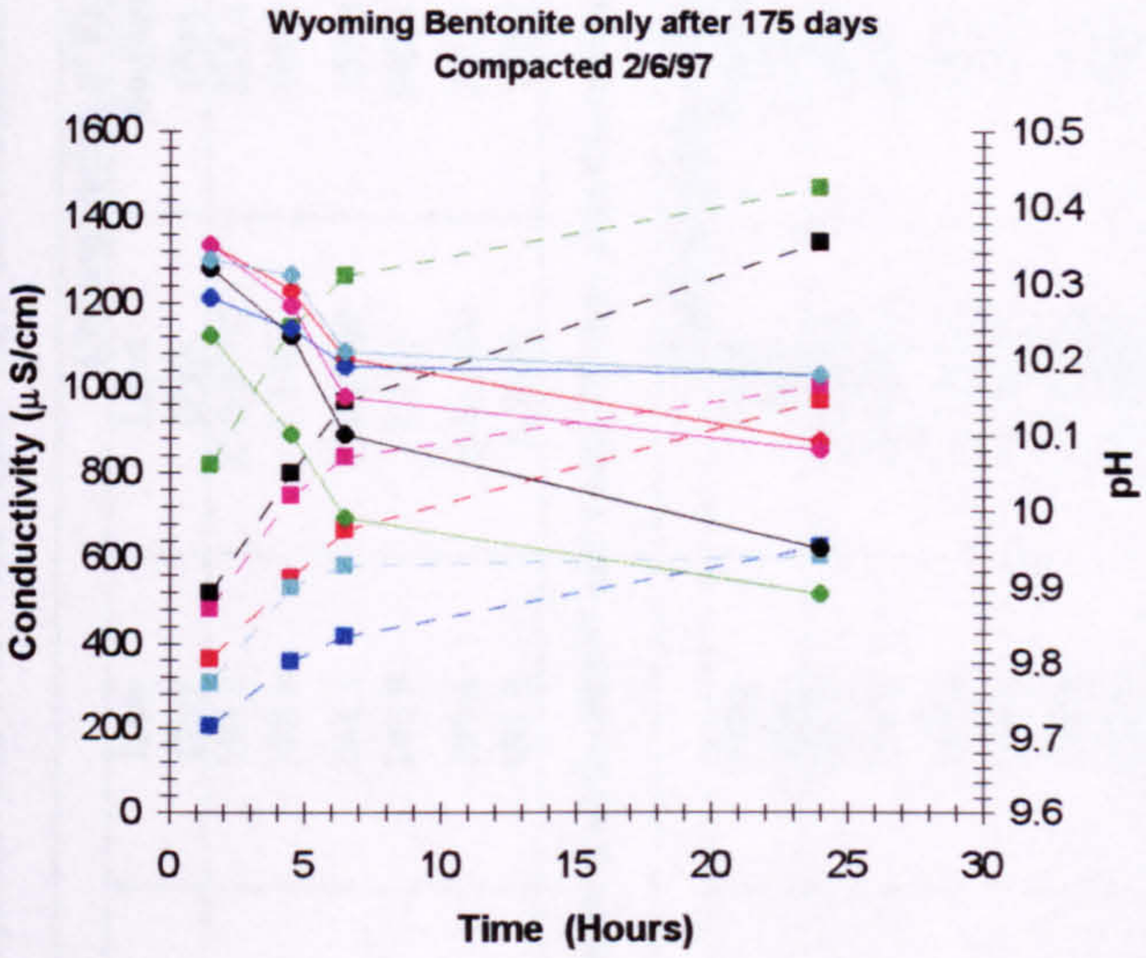

Table A1.92 ICP Data for Wyoming Bentonite only, Compacted on the 28/5/97 and Tested 7 days after Compaction for 6 Hours at 30 Revolutions per Minute. Centrifuged at 11000rpm for 30 minutes.

Solid to Liquid Ratio	Initial Cube Size (mm)	Concentration of Element in Solution in mg/kg (ppm)							
		Calcium (Ca)	Iron (Fe)	Lead (Pb)	Sodium (Na)	Silicon (Si)	Magnesium (Mg)	Aluminium (Al)	Manganese (Mn)
1/10	10	43.44	159.5	D 0.0000	235.4	1967	115.1	713.0	0.1600
	20	97.75	328.8	2.140	318.8	3975	234.7	1440	0.2850
1/20	10	108.85	384.3	D 0.0000	357.9	4669	275.6	1684	0.3200
	20	79.00	246.9	1.130	242.2	2957	180.4	1071	0.2650
1/40	10	66.15	190.4	D 0.0000	201.1	2365	140.8	842.0	0.2050
	20	79.45	181.4	0.9350	189.0	2246	139.8	814.0	0.2950

Table A1.93 ICP Data for Wyoming Bentonite only, Compacted on the 28/5/97 and Tested 175 days after Compaction for 6 Hours at 30 Revolutions per Minute. Centrifuged at 11000rpm for 30 minutes.

Solid to Liquid Ratio	Initial Cube Size (mm)	Concentration of Element in Solution in mg/kg (ppm)							
		Calcium (Ca)	Iron (Fe)	Lead (Pb)	Sodium (Na)	Silicon (Si)	Magnesium (Mg)	Aluminium (Al)	Manganese (Mn)
1/10	10	126.3	505.0	D 0.0000	420.9	5190	344.7	2115	0.4400
	20	94.25	354.6	D 0.0000	299.7	3618	244.0	1534	0.3300
1/20	10	95.35	353.4	D 0.0000	287.8	3622	243.4	1551	0.3150
	20	63.85	223.4	D 0.0000	196.2	2120	154.5	971.5	0.2000
1/40	10	53.80	181.8	D 0.0000	159.5	1846	124.3	774.5	0.1750
	20	36.46	119.0	D 0.0000	108.5	1008	81.85	508.0	0.1250

Table A1.94 ICP Data for Wyoming Bentonite only, Compacted on the 28/5/97 and Tested 301 days after Compaction for 6 Hours at 30 Revolutions per Minute. Centrifuged at 11000rpm for 30 minutes.

Solid to Liquid Ratio	Initial Cube Size (mm)	Concentration of Element in Solution in mg/kg (ppm)							
		Calcium (Ca)	Iron (Fe)	Lead (Pb)	Sodium (Na)	Silicon (Si)	Magnesium (Mg)	Aluminium (Al)	Manganese (Mn)
1/10	10	109.3	419.0	D 0.0000	379.1	4478	288.2	1675	0.3600
	20	95.55	337.3	D 0.0000	281.1	3548	228.4	1378	0.3000
1/20	10	100.7	353.5	D 0.0000	291.1	3771	246.4	1472	0.3350
	20	70.10	226.3	D 0.0000	193.8	2367	154.8	927.0	0.2200
1/40	10	57.95	171.1	D 0.0000	159.2	1807	118.6	708.5	0.1600
	20	47.75	150.3	D 0.0000	132.3	1075	104.2	617.0	0.1350

Note: 'D' indicates the stated value is below detection limits and the value stated is a system estimate.
'd' indicates the stated value is close to detection limits.

Table A1.95 ICP Data for Wyoming Bentonite only, Compacted on the 30/5/97 and Tested 7 days after Compaction for 6 Hours at 60 Revolutions per Minute. Centrifuged at 11000rpm for 30 minutes.

Solid to Liquid Ratio	Initial Cube Size (mm)	Concentration of Element in Solution in mg/kg (ppm)							
		Calcium (Ca)	Iron (Fe)	Lead (Pb)	Sodium (Na)	Silicon (Si)	Magnesium (Mg)	Aluminium (Al)	Manganese (Mn)
1/10	10	91.25	346.0	D 0.0000	397.1	4170	247.4	1559	0.3000
	20	65.20	327.9	D 0.0000	324.8	3766	230.8	1380	0.2900
1/20	10	88.95	320.0	D 0.0000	292.8	3842	226.4	1367	0.2700
	20	63.30	210.6	D 0.0000	207.8	2448	147.6	896.0	0.2350
1/40	10	58.70	193.2	D 0.0000	185.4	2268	135.1	835.5	0.1800
	20	55.05	140.3	0.5200	218.3	1583	103.0	593.5	0.2100

Table A1.96 ICP Data for Wyoming Bentonite only, Compacted on the 30/5/97 and Tested 175 days after Compaction for 6 Hours at 60 Revolutions per Minute. Centrifuged at 11000rpm for 30 minutes.

Solid to Liquid Ratio	Initial Cube Size (mm)	Concentration of Element in Solution in mg/kg (ppm)							
		Calcium (Ca)	Iron (Fe)	Lead (Pb)	Sodium (Na)	Silicon (Si)	Magnesium (Mg)	Aluminium (Al)	Manganese (Mn)
1/10	10	122.6	482.5	D 0.000	408.0	4946	335.1	2063	0.4150
	20	88.70	314.5	D 0.0000	282.2	3259	220.7	1393	0.2800
1/20	10	86.50	323.1	D 0.0000	281.0	3260	227.0	1429	0.2850
	20	58.55	199.9	D 0.0000	186.5	2044	140.7	884.5	0.2000
1/40	10	53.70	185.1	D 0.0000	166.6	1860	127.2	803.5	0.1550
	20	35.39	112.6	D 0.0000	110.8	959.5	80.05	497.0	0.1100

Note : 'D' indicates the stated value is below detection limits and the value stated is a system estimate.
'd' indicates the stated value is close to detection limits.

Table A1.97 ICP Data for Wyoming Bentonite only, Compacted on the 29/5/97 and Tested 7 days after Compaction for 24 Hours at 30 Revolutions per Minute. Centrifuged at 11000rpm for 30 minutes.

Solid to Liquid Ratio	Initial Cube Size (mm)	Concentration of Element in Solution in mg/kg (ppm)							
		Calcium (Ca)	Iron (Fe)	Lead (Pb)	Sodium (Na)	Silicon (Si)	Magnesium (Mg)	Aluminium (Al)	Manganese (Mn)
1/10	10	91.40	335.9	0.3600	421.5	4055	243.8	1464	0.3300
	20	81.50	287.9	D 0.0000	384.9	3313	200.6	1219	0.2450
1/20	10	103.65	387.4	D 0.0000	360.3	4621	279.2	1721	0.3400
	20	110.85	393.7	D 0.0000	352.4	4617	280.2	1689	0.3500
1/40	10	57.75	185.0	D 0.0000	183.5	2191	133.4	803.0	0.2050
	20	63.20	201.9	D 0.0000	196.9	2378	141.3	868.5	0.2200

Table A1.98 ICP Data for Wyoming Bentonite only, Compacted on the 29/5/97 and Tested 175 days after Compaction for 24 Hours at 30 Revolutions per Minute. Centrifuged at 11000rpm for 30 minutes.

Solid to Liquid Ratio	Initial Cube Size (mm)	Concentration of Element in Solution in mg/kg (ppm)							
		Calcium (Ca)	Iron (Fe)	Lead (Pb)	Sodium (Na)	Silicon (Si)	Magnesium (Mg)	Aluminium (Al)	Manganese (Mn)
1/10	10	64.10	200.5	D 0.0000	412.3	2086	142.3	871.5	0.8500
	20	113.6	450.7	D 0.0000	432.0	4731	310.5	1958	0.4050
1/20	10	105.6	413.8	D 0.0000	333.0	4318	286.3	1848	0.3550
	20	99.55	376.8	D 0.0000	317.3	3916	260.7	1651	0.3350
1/40	10	65.95	224.0	D 0.0000	190.9	2323	156.1	993.5	0.1850
	20	62.80	210.3	D 0.0000	186.5	2098	147.3	921.5	0.1950

Table A1.99 ICP Data for Wyoming Bentonite only, Compacted on the 29/5/97 and Tested 301 days after Compaction for 24 Hours at 30 Revolutions per Minute. Centrifuged at 11000rpm for 30 minutes.

Solid to Liquid Ratio	Initial Cube Size (mm)	Concentration of Element in Solution in mg/kg (ppm)							
		Calcium (Ca)	Iron (Fe)	Lead (Pb)	Sodium (Na)	Silicon (Si)	Magnesium (Mg)	Aluminium (Al)	Manganese (Mn)
1/10	10	143.0	513.0	D 0.0000	513.0	5355	341.9	1937	0.4650
	20	125.1	477.3	D 0.0000	401.9	5155	323.4	1860	0.4200
1/20	10	148.1	555.5	D 0.0000	418.7	5750	376.9	2080	0.5000
	20	114.0	402.1	D 0.0000	320.6	4338	276.3	1645	0.3700
1/40	10	81.80	233.2	D 0.0000	202.8	2433	161.1	960.0	0.2400
	20	78.95	245.5	D 0.0000	200.5	2465	166.5	985.0	0.2500

Note: 'D' indicates the stated value is below detection limits and the value stated is a system estimate.
'd' indicates the stated value is close to detection limits.

Table A1.100 ICP Data for Wyoming Bentonite only, Compacted on the 2/6/97 and Tested 7 days after Compaction for 24 Hours at 60 Revolutions per Minute. Centrifuged at 11000rpm for 30 minutes.

Solid to Liquid Ratio	Initial Cube Size (mm)	Concentration of Element in Solution in mg/kg (ppm)							
		Calcium (Ca)	Iron (Fe)	Lead (Pb)	Sodium (Na)	Silicon (Si)	Magnesium (Mg)	Aluminium (Al)	Manganese (Mn)
1/10	10	101.4	357.3	D 0.0000	500.5	4168	249.6	1581	0.4150
	20	100.4	420.0	D 0.0000	407.9	5290	287.8	1807	0.3650
1/20	10	106.9	406.2	D 0.0000	377.8	4638	283.6	1723	0.4050
	20	102.8	385.0	D 0.0000	364.8	4594	266.2	1681	0.3400
1/40	10	65.20	203.6	D 0.0000	205.2	2298	143.3	867.5	0.2050
	20	81.10	252.5	D 0.0000	259.9	2919	178.8	1099	0.2550

Table A1.101 ICP Data for Wyoming Bentonite only, Compacted on the 2/6/97 and Tested 175 days after Compaction for 24 Hours at 60 Revolutions per Minute. Centrifuged at 11000rpm for 30 minutes.

Solid to Liquid Ratio	Initial Cube Size (mm)	Concentration of Element in Solution in mg/kg (ppm)							
		Calcium (Ca)	Iron (Fe)	Lead (Pb)	Sodium (Na)	Silicon (Si)	Magnesium (Mg)	Aluminium (Al)	Manganese (Mn)
1/10	10	148.7	582.5	D 0.0000	596.0	6050	402.1	2393	0.5550
	20	141.9	561.5	D 0.0000	510.0	5970	385.3	2331	0.5100
1/20	10	137.8	533.5	D 0.0000	402.9	5405	367.0	2223	0.4600
	20	122.5	464.7	D 0.0000	371.4	4758	323.1	2022	0.4100
1/40	10	69.45	233.4	D 0.0000	194.8	2364	163.3	1026	0.2100
	20	72.75	241.6	D 0.0000	207.8	2306	166.9	1080	0.2300

Note : 'D' indicates the stated value is below detection limits and the value stated is a system estimate.
'd' indicates the stated value is close to detection limits.

A1.2.11 Wyoming Bentonite with 5000ppm Pb and no lime

A1.2.11.1 Solid : liquid ratio

Inspections of Figures A1.47 to A1.50 show a more constructed pattern of behaviour for pH and conductivity than for Wyoming Bentonite without Pb. Increasing solid to liquid ratio clearly increases conductivity and reduces pH.

At 7 days curing the conductivity of 6hr 30rpm tests with 20mm cube sizes (Figure A1.47) at the solid to liquid ratios 1:10, 1:20 and 1:40 were 950µS/cm, 573µS/cm and 438µS/cm respectively whilst pH values were 9.77, 9.92 and 9.93 respectively. At 175 days curing conductivity values were 1021µS/cm, 525µS/cm and 346µS/cm respectively whilst pH values were 9.64, 9.80 and 9.83 respectively. At 301 days curing conductivity values were 973µS/cm, 603µS/cm and 406µS/cm respectively whilst pH values were 9.72, 9.79 and 9.69. Increasing solid to liquid ratio from 1:40 to 1:20 at 7, 175 and 301 days curing therefore increased conductivity by factors of 1.31, 1.52 and 1.49 respectively whilst pH values increased by –0.01, -0.03 and 0.10 pH divisions respectively. Increasing solid to liquid ratio further from 1:20 to 1:40 increased conductivity by factors of 1.66, 1.94 and 1.61 respectively whilst pH increased by –0.15, -0.16 and –0.07 pH divisions respectively.

Generally it is clear that the higher solid to liquid ratios produce higher final conductivities and as Tables A1.102 to A1.103 illustrate, in the majority of cases higher final conductivities result in higher centrifuged elemental releases. It is also clear that these elemental releases are directly linked to the efficiency of solid and liquid separation as illustrated by the similarity of the results produced by the 1:10 solid to liquid ratio, 20mm cubes and the 1:20 solid to liquid ratio, 10mm cubes in Table A1.106. Other data table results show similar trends.

A1.2.11.2 Cube Size

Figures A1.47 to A1.50 illustrate that 10mm cube sizes produce lower final pH and higher final conductivities than 20mm cubes for the same solid to liquid ratio. Tables A1.102 to A1.112 also illustrate higher centrifuged final elemental compositions for 10mm cubes. Comparison of the solid to liquid ratio 1:40, 10mm cubes for uncontaminated Wyoming Bentonite (Table A1.101) and Pb contaminated Wyoming Bentonite (Table A1.111) shows very similar elemental releases, naturally

with the exception of Pb content, suggesting that the effects of centrifugation are measurable greater than the chemical effects of the Pb contamination.

A1.2.11.3 Rotation speed and test duration

Increasing rotation speed has no measurable effects on pH and conductivity for 6hr tests or 24hr tests.

Increasing test duration tends to have variable effects on pH for each rotation speed but certainly increases conductivity for both rotation speeds at all curing periods. It is also clear that at the 1:20 and 1:40 solid to liquid ratios which centrifuge similarly, the longer durations result in a higher release of elements as expected.

A1.2.11.4 Curing Time

With the exception of 6hr/30rpm tests (Figure A1.47) all tests show no significant reduction in final pH or conductivity as curing period increases from 7 days to 175 days. However, comparison of 7 days curing and 301 days curing (Figures A1.47 and A1.49) shows significant reductions in pH for the higher solid to liquid ratios. Tables A1.102 to A1.111 at the solid to liquid ratios 1:20 and 1:40 do not clearly illustrate any changes in the release of elements that could be linked to this pH variation. Based upon this analysis it cannot be certain that the addition of Pb has created any significant flocculation of the clay particles.

Figure A1.47 Conductivity and pH characteristics for Wyoming Bentonite with 5000ppm Pb and no lime during 6hr/30rpm Batch Tests

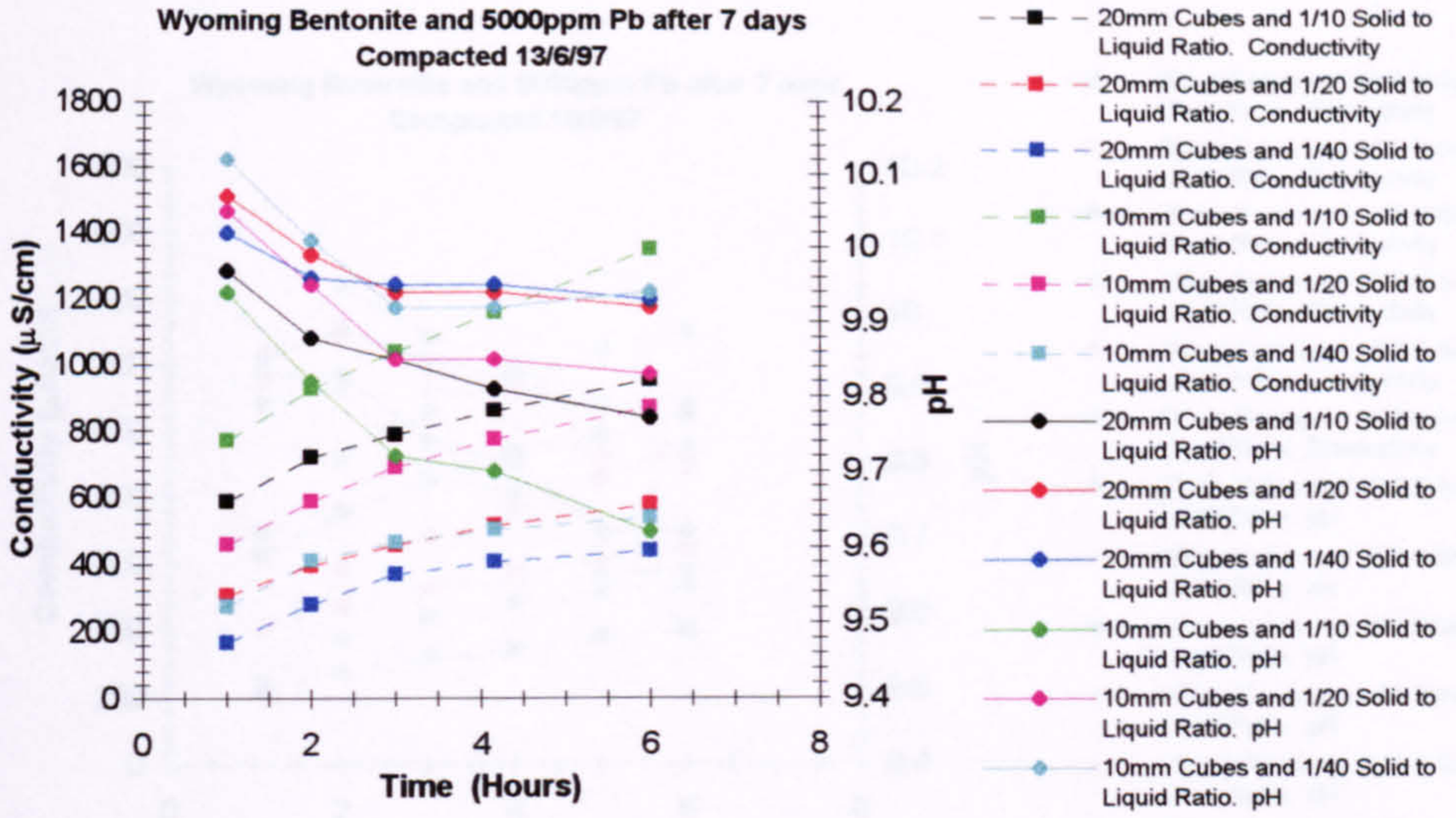

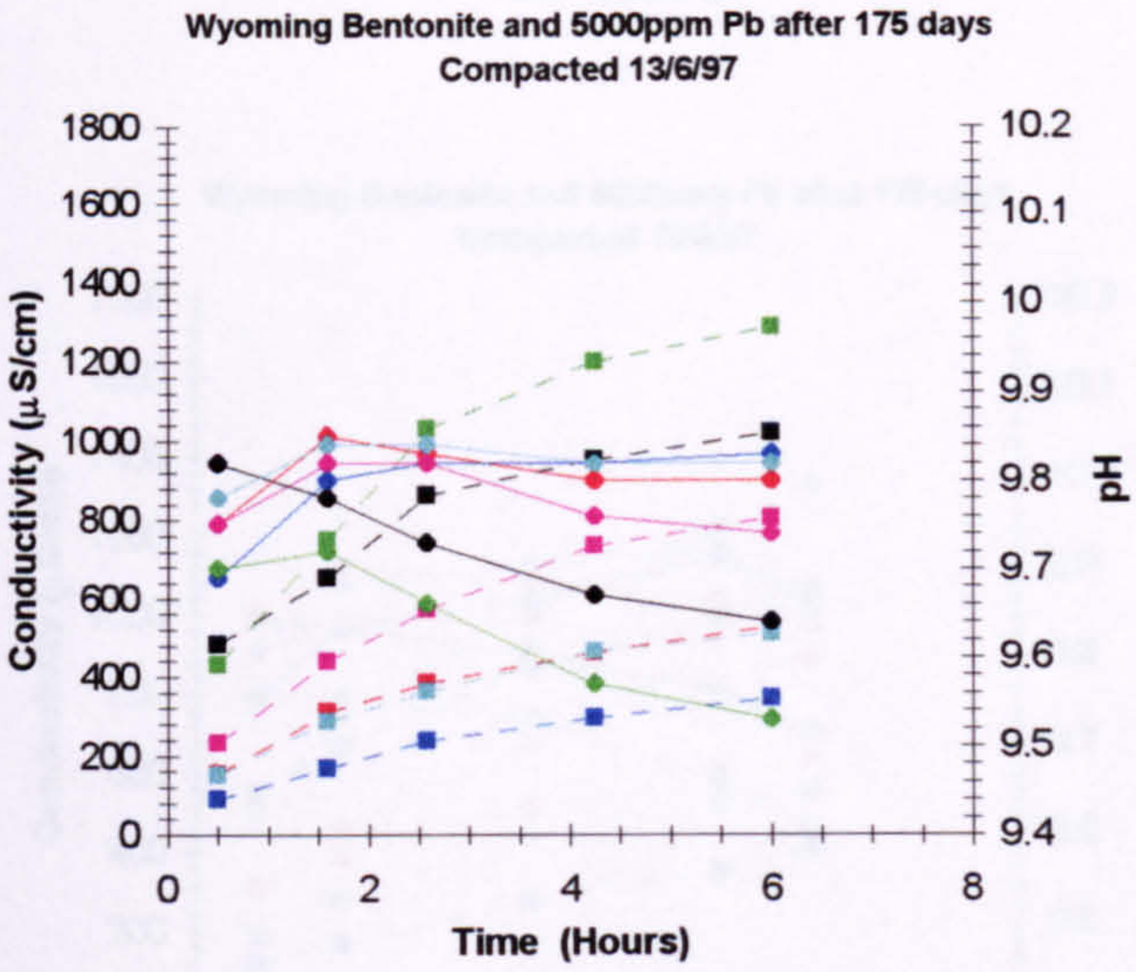

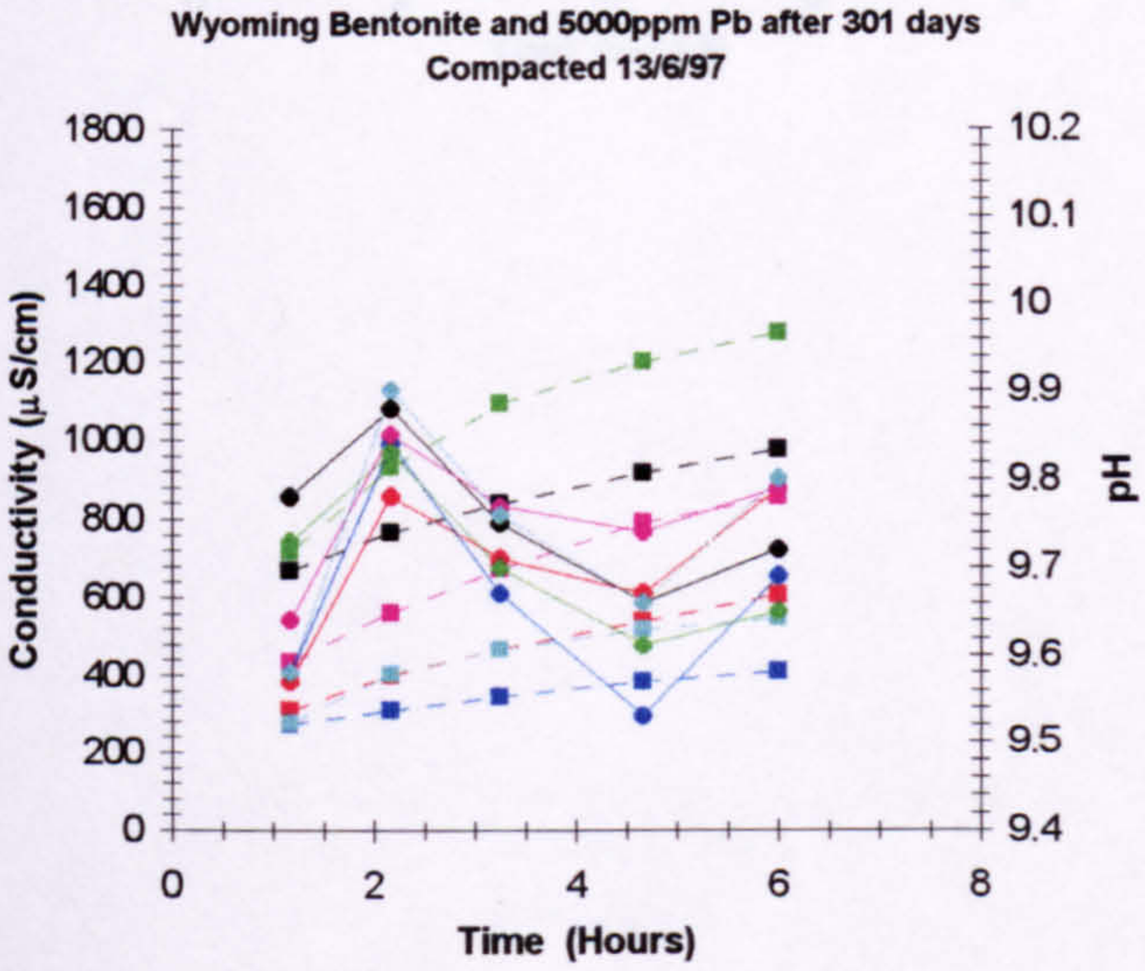

Figure A1.48 Conductivity and pH characteristics for Wyoming Bentonite with 5000ppm Pb and no lime during 6hr/60rpm Batch Tests

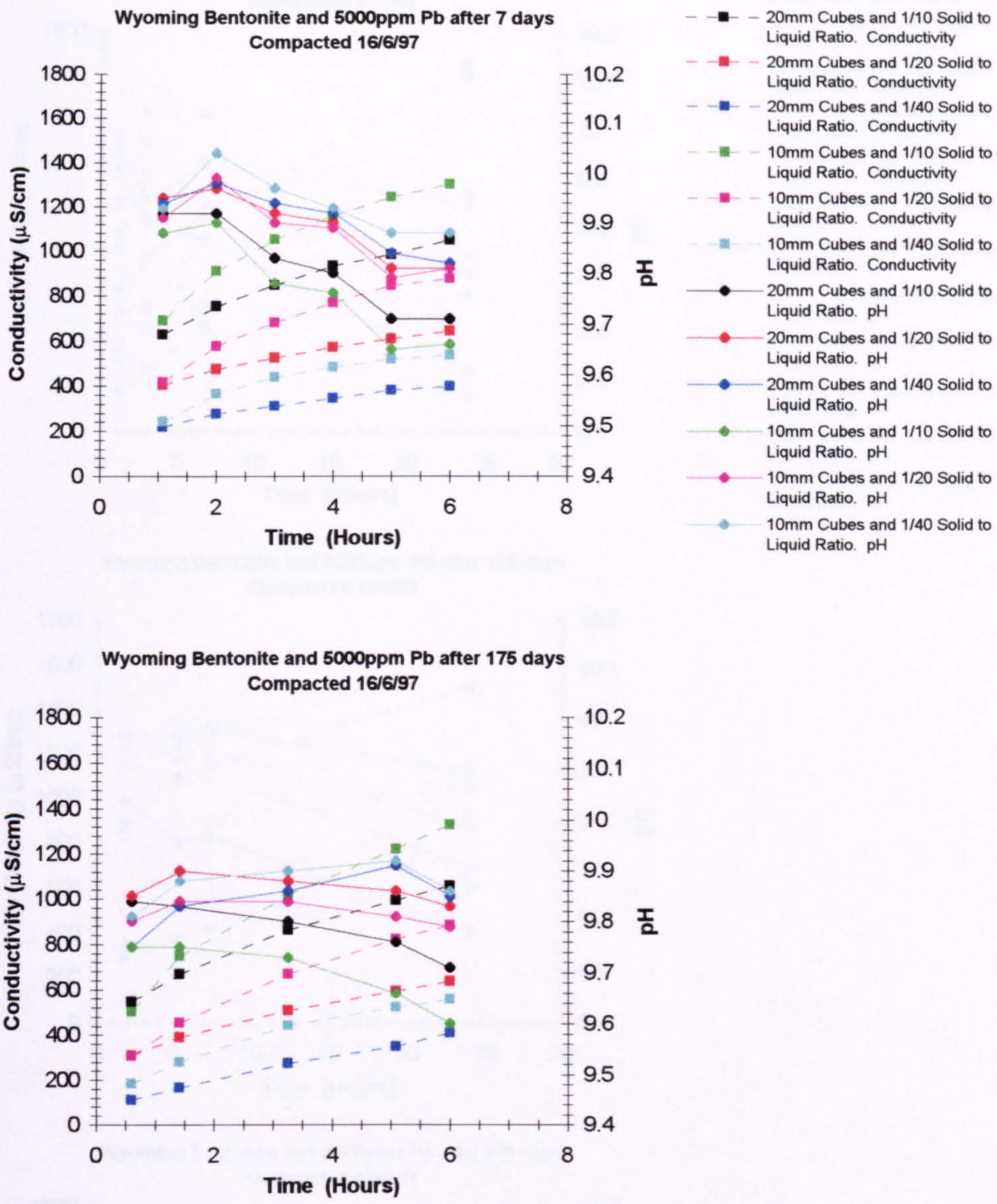

Figure A1.49 Conductivity and pH characteristics for Wyoming Bentonite with 5000ppm Pb and no lime during 24hr/30rpm Batch Tests

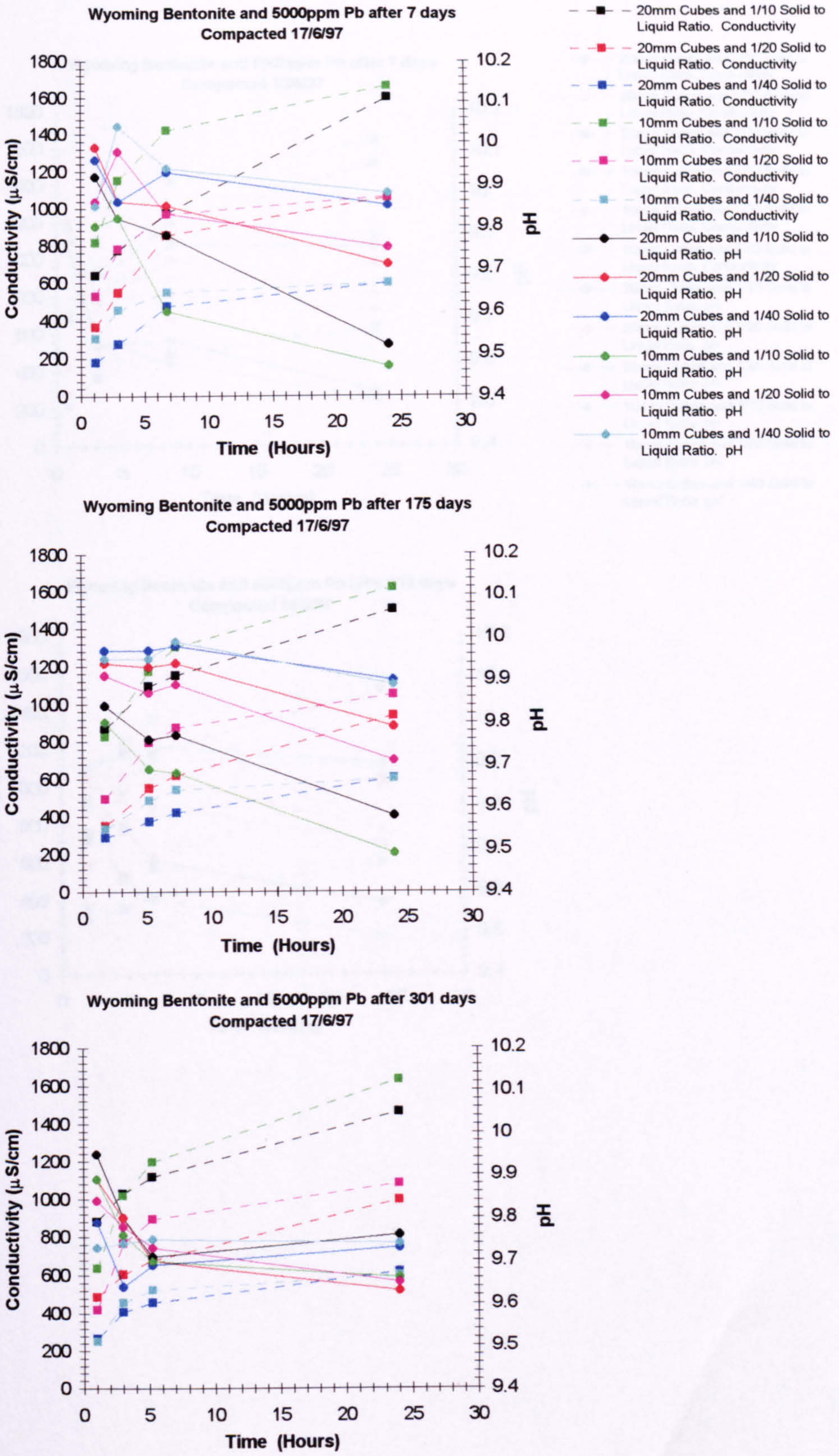

Figure A1.50 Conductivity and pH characteristics for Wyoming Bentonite with 5000ppm Pb and no lime during 24hr/60rpm Batch Tests

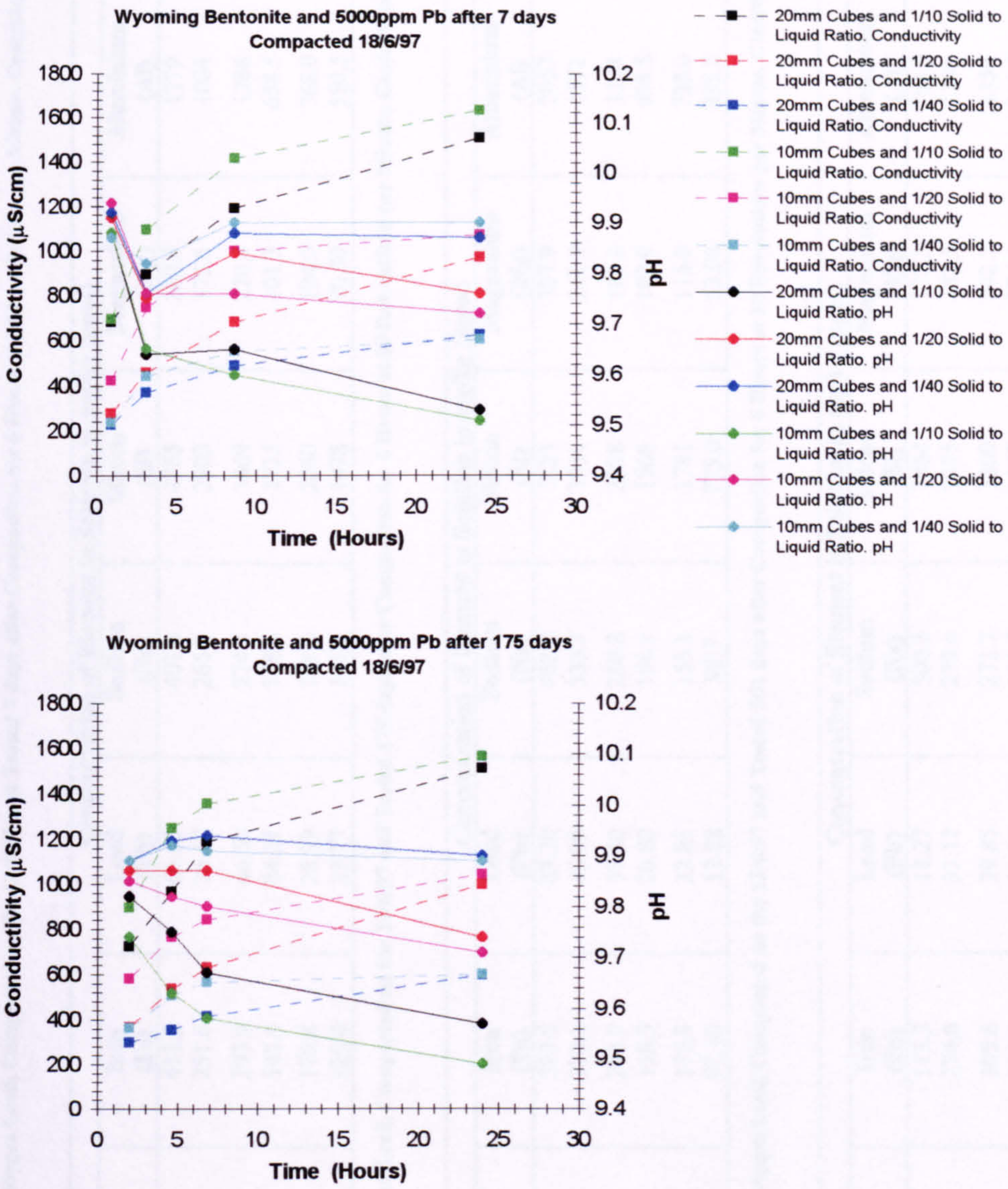

Table A1.102 ICP Data for Wyoming Bentonite and 5000ppm Lead, Compacted on the 13/6/97 and Tested 7 days after Compaction for 6 Hours at 30 Revolutions per Minute. Centrifuged at 11000rpm for 30 minutes.

Solid to Liquid Ratio	Initial Cube Size (mm)	Concentration of Element in Solution in mg/kg (ppm)							
		Calcium (Ca)	Iron (Fe)	Lead (Pb)	Sodium (Na)	Silicon (Si)	Magnesium (Mg)	Aluminium (Al)	Manganese (Mn)
1/10	10	114.55	411.3	66.55	401.6	4765	280.6	1779	0.4250
	20	73.90	251.6	36.17	265.7	2903	173.6	1084	0.2700
1/20	10	87.10	297.9	46.50	274.3	3469	210.4	1286	0.3200
	20	45.47	145.4	24.21	158.6	1725	101.3	638.5	0.2350
1/40	10	56.80	176.8	28.99	169.9	2060	124.0	768.0	0.2450
	20	42.82	129.4	23.77	131.6	1478	90.30	550.5	0.2150

Table A1.103 ICP Data for Wyoming Bentonite 5000ppm Lead, Compacted on the 13/6/97 and Tested 175 days after Compaction for 6 Hours at 30 Revolutions per Minute. Centrifuged at 11000rpm for 30 minutes.

Solid to Liquid Ratio	Initial Cube Size (mm)	Concentration of Element in Solution in mg/kg (ppm)							
		Calcium (Ca)	Iron (Fe)	Lead (Pb)	Sodium (Na)	Silicon (Si)	Magnesium (Mg)	Aluminium (Al)	Manganese (Mn)
1/10	10	137.3	510.5	83.30	462.7	5125	327.9	2057	11.98
	20	102.2	370.1	46.09	333.7	3714	241.9	1571	0.3700
1/20	10	82.05	294.9	37.40	260.8	2928	189.8	1228	0.3250
	20	48.41	158.5	20.80	154.5	1568	103.0	658.5	0.2150
1/40	10	43.04	175.5	22.83	155.1	1781	115.0	723.0	0.2250
	20	30.11	97.40	12.92	92.7	775.0	63.00	395.8	0.1400

Table A1.104 ICP Data for Wyoming Bentonite and 5000ppm Lead, Compacted on the 13/6/97 and Tested 301 days after Compaction for 6 Hours at 30 Revolutions per Minute. Centrifuged at 11000rpm for 30 minutes.

Solid to Liquid Ratio	Initial Cube Size (mm)	Concentration of Element in Solution in mg/kg (ppm)							
		Calcium (Ca)	Iron (Fe)	Lead (Pb)	Sodium (Na)	Silicon (Si)	Magnesium (Mg)	Aluminium (Al)	Manganese (Mn)
1/10	10	52.15	173.3	18.27	300.3	1864	118.3	764.0	0.1900
	20	79.55	274.0	33.12	279.4	2935	182.5	1208	0.3000
1/20	10	89.70	305.8	39.85	272.7	3200	202.2	1350	0.3450
	20	59.00	184.3	24.16	181.4	1963	124.4	811.5	0.2350
1/40	10	59.40	195.8	26.51	172.7	2088	130.8	853.5	0.2500
	20	38.88	121.2	17.71	115.3	876.5	80.75	528.5	0.1650

Note: 'D' indicates the stated value is below detection limits and the value stated is a system estimate. 'd' indicates the stated value is close to detection limits.

Table A1.105 ICP Data for Wyoming Bentonite and 5000ppm Lead, Compacted on the 16/6/97 and Tested 7 days after Compaction for 6 Hours at 60 Revolutions per Minute. Centrifuged at 11000rpm for 30 minutes.

Solid to Liquid Ratio	Initial Cube Size (mm)	Concentration of Element in Solution in mg/kg (ppm)							
		Calcium (Ca)	Iron (Fe)	Lead (Pb)	Sodium (Na)	Silicon (Si)	Magnesium (Mg)	Aluminium (Al)	Manganese (Mn)
1/10	10	108.0	375.3	60.05	383.4	4348	263.6	1611	0.4000
	20	88.25	299.9	45.77	305.3	3507	210.1	1288	0.3200
1/20	10	86.70	293.9	43.96	273.9	3435	204.2	1255	0.3550
	20	62.15	190.0	31.27	188.2	2228	134.5	832.5	0.2200
1/40	10	54.95	177.9	28.95	172.1	2073	123.3	763.5	0.1950
	20	36.14	112.5	21.87	117.2	1282	77.35	483.2	0.1800

Table A1.106 ICP Data for Wyoming Bentonite 5000ppm Lead, Compacted on the 16/6/97 and Tested 175 days after Compaction for 6 Hours at 60 Revolutions per Minute. Centrifuged at 11000rpm for 30 minutes.

Solid to Liquid Ratio	Initial Cube Size (mm)	Concentration of Element in Solution in mg/kg (ppm)							
		Calcium (Ca)	Iron (Fe)	Lead (Pb)	Sodium (Na)	Silicon (Si)	Magnesium (Mg)	Aluminium (Al)	Manganese (Mn)
1/10	10	123.1	454.4	70.30	437.6	4615	294.1	1922.5	0.4700
	20	89.10	324.1	40.07	317.0	3241	207.6	1376	0.3300
1/20	10	89.45	325.4	39.45	280.1	3287	210.3	1376	0.3400
	20	53.65	184.9	22.60	181.0	1850	119.6	770.0	0.2200
1/40	10	57.10	198.2	25.58	174.0	2029	128.1	832.5	0.2200
	20	31.31	103.8	13.42	108.7	843.0	66.95	433.4	0.1450

Note : 'D' indicates the stated value is below detection limits and the value stated is a system estimate. 'd' indicates the stated value is close to detection limits.

Table A1.107 ICP Data for Wyoming Bentonite and 5000ppm Lead, Compacted on the 17/6/97 and Tested 7 days after Compaction for 24 Hours at 30 Revolutions per Minute. Centrifuged at 11000rpm for 30 minutes.

Solid to Liquid Ratio	Initial Cube Size (mm)	Concentration of Element in Solution in mg/kg (ppm)							
		Calcium (Ca)	Iron (Fe)	Lead (Pb)	Sodium (Na)	Silicon (Si)	Magnesium (Mg)	Aluminium (Al)	Manganese (Mn)
1/10	10	188.4	694.0	137.5	600.0	8555	487.5	2983	0.7000
	20	156.7	585.0	109.3	498.3	6935	397.2	2454	0.5700
1/20	10	113.4	405.1	59.85	346.1	4774	281.5	1753	0.3800
	20	111.5	403.6	56.90	344.4	4750	279.6	1735	0.4150
1/40	10	59.75	192.2	31.17	178.8	2235	136.1	833.5	0.2550
	20	64.85	196.7	33.26	206.7	2192	147.5	917.0	0.4000

Table A1.108 ICP Data for Wyoming Bentonite 5000ppm Lead, Compacted on the 17/6/97 and Tested 175 days after Compaction for 24 Hours at 30 Revolutions per Minute. Centrifuged at 11000rpm for 30 minutes.

Solid to Liquid Ratio	Initial Cube Size (mm)	Concentration of Element in Solution in mg/kg (ppm)							
		Calcium (Ca)	Iron (Fe)	Lead (Pb)	Sodium (Na)	Silicon (Si)	Magnesium (Mg)	Aluminium (Al)	Manganese (Mn)
1/10	10	76.45	291.2	36.87	420.6	2989	189.7	1234	0.2650
	20	73.60	279.8	32.37	382.3	2836	180.3	1179	0.2600
1/20	10	131.5	493.3	72.2	392.9	5025	320.7	2056	0.4700
	20	96.35	347.9	45.59	300.8	3447	226.6	1469	0.3850
1/40	10	63.05	212.4	26.33	201.9	2146	138.7	896.0	0.2350
	20	61.75	208.2	26.68	188.4	2103	134.6	888.0	0.4900

Table A1.109 ICP Data for Wyoming Bentonite and 5000ppm Lead, Compacted on the 17/6/97 and Tested 301 days after Compaction for 24 Hours at 30 Revolutions per Minute. Centrifuged at 11000rpm for 30 minutes.

Solid to Liquid Ratio	Initial Cube Size (mm)	Concentration of Element in Solution in mg/kg (ppm)							
		Calcium (Ca)	Iron (Fe)	Lead (Pb)	Sodium (Na)	Silicon (Si)	Magnesium (Mg)	Aluminium (Al)	Manganese (Mn)
1/10	10	56.95	140.7	16.75	402.9	1492	96.3	624.5	0.1750
	20	81.05	257.6	34.14	383.8	2910	177.3	1176	0.2750
1/20	10	99.60	348.6	47.86	327.3	3680	237.0	1563	0.3400
	20	97.05	329.1	42.64	292.4	3616	222.9	1461	0.3500
1/40	10	72.95	236.6	31.36	206.0	2528	159.6	1060	0.2800
	20	74.05	225.6	29.52	197.6	2434	149.9	999.5	0.2850

Note: 'D' indicates the stated value is below detection limits and the value stated is a system estimate. 'd' indicates the stated value is close to detection limits.

Table A1.110 ICP Data for Wyoming Bentonite and 5000ppm Lead, Compacted on the 18/6/97 and Tested 7 days after Compaction for 24 Hours at 60 Revolutions per Minute. Centrifuged at 11000rpm for 30 minutes.

Solid to Liquid Ratio	Initial Cube Size (mm)	Concentration of Element in Solution in mg/kg (ppm)							
		Calcium (Ca)	Iron (Fe)	Lead (Pb)	Sodium (Na)	Silicon (Si)	Magnesium (Mg)	Aluminium (Al)	Manganese (Mn)
1/10	10	211.6	605.5	115.4	556.0	7630	417.1	2584	0.6000
	20	139.0	487.1	97.75	463.8	6320	341.1	2177	0.4850
1/20	10	116.8	414.4	68.05	364.1	4924	289.1	1796	0.4350
	20	95.35	321.8	50.10	302.3	3799	225.9	1373	0.3850
1/40	10	57.85	181.3	30.39	177.8	2138	127.1	796.5	0.2650
	20	59.75	186.8	30.93	178.4	2163	131.0	805.0	0.2600

Table A1.111 ICP Data for Wyoming Bentonite 5000ppm Lead, Compacted on the 18/6/97 and Tested 175 days after Compaction for 24 Hours at 60 Revolutions per Minute. Centrifuged at 11000rpm for 30 minutes.

Solid to Liquid Ratio	Initial Cube Size (mm)	Concentration of Element in Solution in mg/kg (ppm)							
		Calcium (Ca)	Iron (Fe)	Lead (Pb)	Sodium (Na)	Silicon (Si)	Magnesium (Mg)	Aluminium (Al)	Manganese (Mn)
1/10	10	16.30	47.55	6.290	154.4	381.5	31.41	196.4	0.0550
	20	45.70	163.5	22.65	191.1	1694	106.7	676.0	0.1450
1/20	10	141.7	522.5	84.15	396.5	5150	339.4	2127	0.5150
	20	118.6	431.7	64.90	349.7	4435	280.3	1795	0.4750
1/40	10	68.55	222.4	31.15	183.0	2289	143.5	925.0	0.2800
	20	70.25	224.2	32.00	187.9	2294	147.9	942.5	0.3300

Note: 'D' indicates the stated value is below detection limits and the value stated is a system estimate. 'd' indicates the stated value is close to detection limits.

A1.2.12 Wyoming Bentonite with 5000ppm Fe and no lime

A1.2.12.1 Centrifugation

Prior to consideration of the chemical data relating to Fe contaminated Wyoming Bentonite, it is important to discuss the effects of centrifugation. Initially an attempt was made to pressure filter samples through glass fibre filters. This only resulted in blocked filters after a few seconds without sufficient leachate for analysis. However, it was evident after batch tests that a physical change had occurred due to particle flocculation and clearly filtration over a long time period could be possible. Hence the chemical data obtained in Tables A1.112, A1.115, A1.122 and A1.123 were obtained by gravity filtration of samples for 24hrs in a room at $11.5^0C \pm 0.5^0C$ to limit evaporation. Comparison of Tables A1.122 with A1.118 and A1.123 with A1.120 illustrates the differences between filtered and centrifuged samples for the various solid to liquid ratios and cube sizes at specific curing periods. In both cases 1:10 solid to liquid ratios data obtained via centrifugation is very similar to that from filtered material. It could also be argued that data from the 1:20 solid to liquid ratios are acceptable, although very clearly that obtained from the 1:40 solid to liquid ratios are unacceptable.

Visual analysis of centrifuged samples showed clearly that at the 1:40 solid to liquid ratios, samples tended to be a clear yellow solution, indicating a high iron content in these samples. This was validated by the chemical analysis for example Table A1.122 relative to A1.119. Due to filtration time constraints and the limited resources to carry out filtration, samples were centrifuged. The conclusion of these considerations is that only samples at the 1:10 and 1:20 solid to liquid ratios should be considered unless the sample was filtered.

A1.2.12.2 Solid : liquid ratio

Inspection of Figures A1.51 to A1.54 shows yet more distinct variation in pH and conductivity than either uncontaminated Wyoming Bentonite or Wyoming Bentonite contaminated with 5000ppm Pb. Increasing solid to liquid ratio results in large reductions in pH and large increases in conductivity. At 7 days curing the conductivity of 6hr/30rpm tests with 20mm cube sizes at the solid to liquid ratios 1:10, 1:20 and 1:40 were 2460μS/cm, 1464μS/cm and 885μS/cm respectively whilst pH values were 8.25, 8.57 and 8.91 respectively. At 175 days curing conductivity

values were 2140μS/cm, 1371μS/cm and 697μS/cm respectively whilst pH values were 8.63, 8.90 and 9.15 respectively. At 301 days curing conductivity values were 2210μS/cm, 1145μS/cm and 992μS/cm respectively whilst pH values were 8.69, 9.05 and 9.18 respectively. Increasing solid to liquid ratio from 1:40 to 1:20 at 7, 175 and 301 days curing increased conductivity by factors of 1.65, 1.97 and 1.15 respectively whilst pH values increased by -0.34, -0.25 and -0.13 pH divisions respectively. Similarly increasing solid to liquid ratio further from 1:20 to 1:10 increased conductivity by factors of 1.67, 1.56 and 1.93 respectively whilst pH values increased by –0.32, -0.27, and –0.36 pH divisions respectively.

Table A1.112 for 6hr/30rpm tests shows typical levels of elements leached after batch tests at 7 days curing. 20mm cubes were shown to release 34.2ppm Ca, 0.101ppm Fe, 542ppm Na, 0.769ppm Si, 3.88ppm Mg and 0.0520ppm Mn with essentially no Pb or Al in final leachates. Clearly the large increases in Ca and Na are important and represent the exchanged fraction of the clay for the Fe contamination. Reducing the solid to liquid ratio from 1:10 to 1:20 reduced the concentration of Ca, Fe, Na, Mg and Mn whilst slightly increasing Si and Al. These trends were evident for all tests at the solid to liquid ratios 1:10 and 1:20 either filtered or centrifuged.

A1.2.12.3 Cube Size

Analysis of Figures A1.51 to A1.54 shows that the smaller cube size generally produces lower pH values and higher conductivity values at all solid to liquid ratios and especially for 6hr tests. These trends were also evident in the chemical data Tables A1.112 to A1.123 where 10mm cubes released more Ca, Na, Si and Mg as well as less Fe, Al and Mn. These trends were more apparent as the curing period increased (e.g. Tables A1.114 and A1.119) and may be related to reduced flocculation hence subsequently reduced effectiveness of centrifugation, although this was not evident from visual analysis of the leachate.

A1.2.12.4 Rotation speed and test duration

Comparison of 6hr tests at 7 days curing (Figures A1.51 and A1.52) illustrate that higher rotation speed produces higher pH values whilst conductivities remain unaffected. At 175 days neither pH nor conductivity appeared affected by increased

rotation speed. Analysis of Tables A1.112 and A1.115 at 7 days showed that the higher rotation speed tended to release less Ca, Na, Si, Mg and Mn.

Comparison of 24hr tests at 7 days curing (Figures A1.53 and A1.54) illustrate similar pH behaviour whilst at all curing periods although particularly high solid to liquid ratios the higher rotation speed produced lower conductivities. Comparison of Tables A1.117 and A1.120 relate this to reduced levels of Ca, Na and Mg with slightly increased Si at the higher rotation speed.

Comparison of 30rpm tests (Figures A1.51 and A1.53) illustrate that the longer test duration has no effect on pH at 7 days, although at lower solid to liquid ratios pH tends to reduce. Increasing test duration clearly increases conductivity at all curing periods and solid to liquid ratios. Consideration of the 1:10 solid to liquid ratio in Tables A1.112, A1.113, A1.114 and A1.117, A1.118, A1.119 illustrate that increasing test duration increases Na significantly whilst Ca and Mg increase moderately and other element fluctuate in level. Comparison of 60rpm tests (Figures A1.52 and A1.54) show no significant effects on pH or conductivity when test duration is increased with the exception that there is reduced variability in the behaviour of the two cube sizes during 24 hr tests. Analysis of Tables A1.115, A1.116 with Tables A1.123, A1.121 shows that at 7 days curing Mg, Si, Ca and Na levels increase whilst Mn levels reduce when test duration is increased. These trends were also similar at 175 days curing.

A1.2.12.5 Curing Time

As curing period increases all tests show slight increases in pH and reductions in conductivity especially during 24hr tests. Tables A1.112 to A1.123 for the 1:10 solid to liquid ratio shows significant reductions in Ca and Na whilst Si, Mg, Al and Fe slightly increased, suggesting continued chemical activity.

Figure A1.51 Conductivity and pH characteristics for Wyoming Bentonite with 5000ppm Fe and no lime during 6hr/30rpm Batch Tests

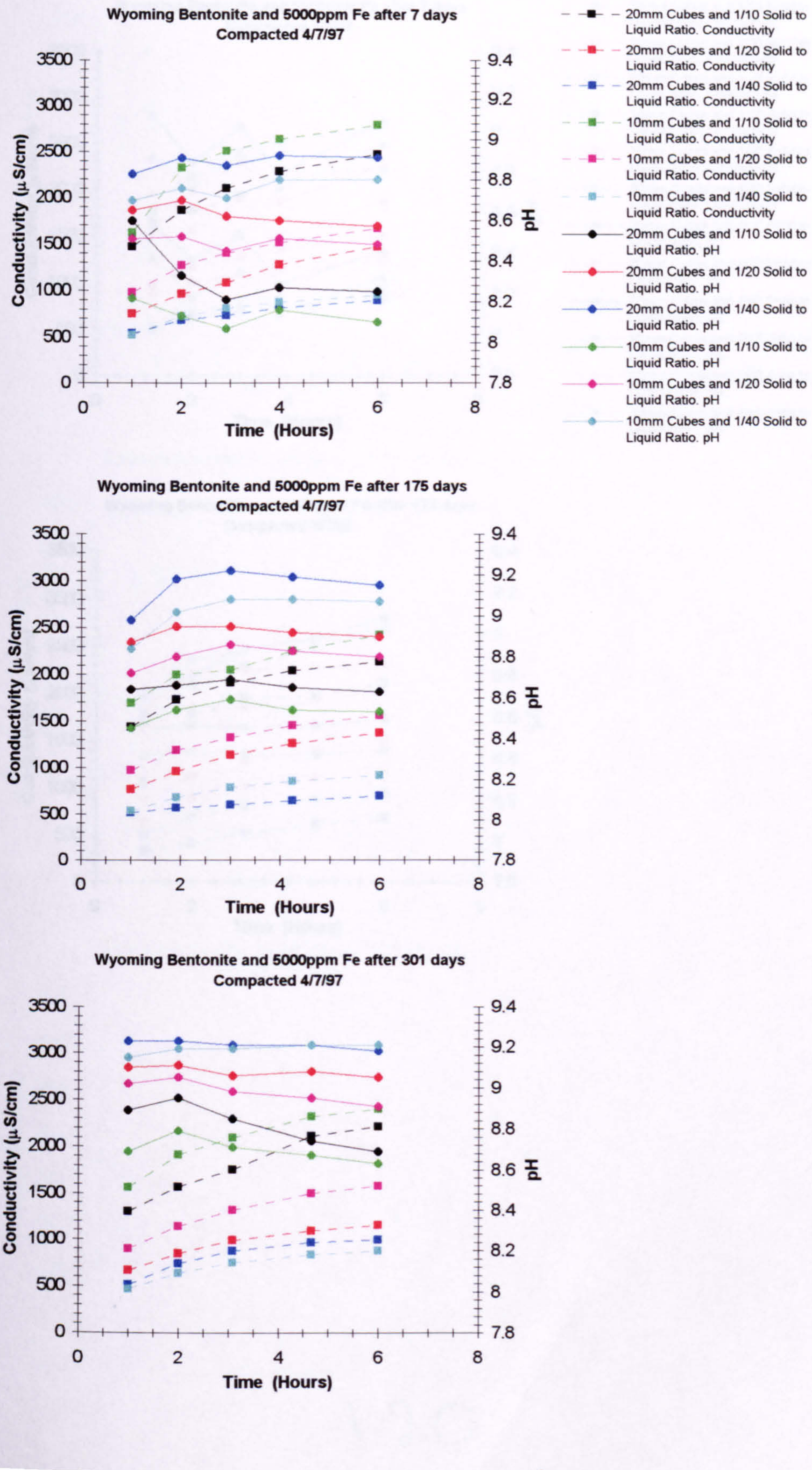

Figure A1.52 Conductivity and pH characteristics for Wyoming Bentonite with 5000ppm Fe and no lime during 6hr/60rpm Batch Tests

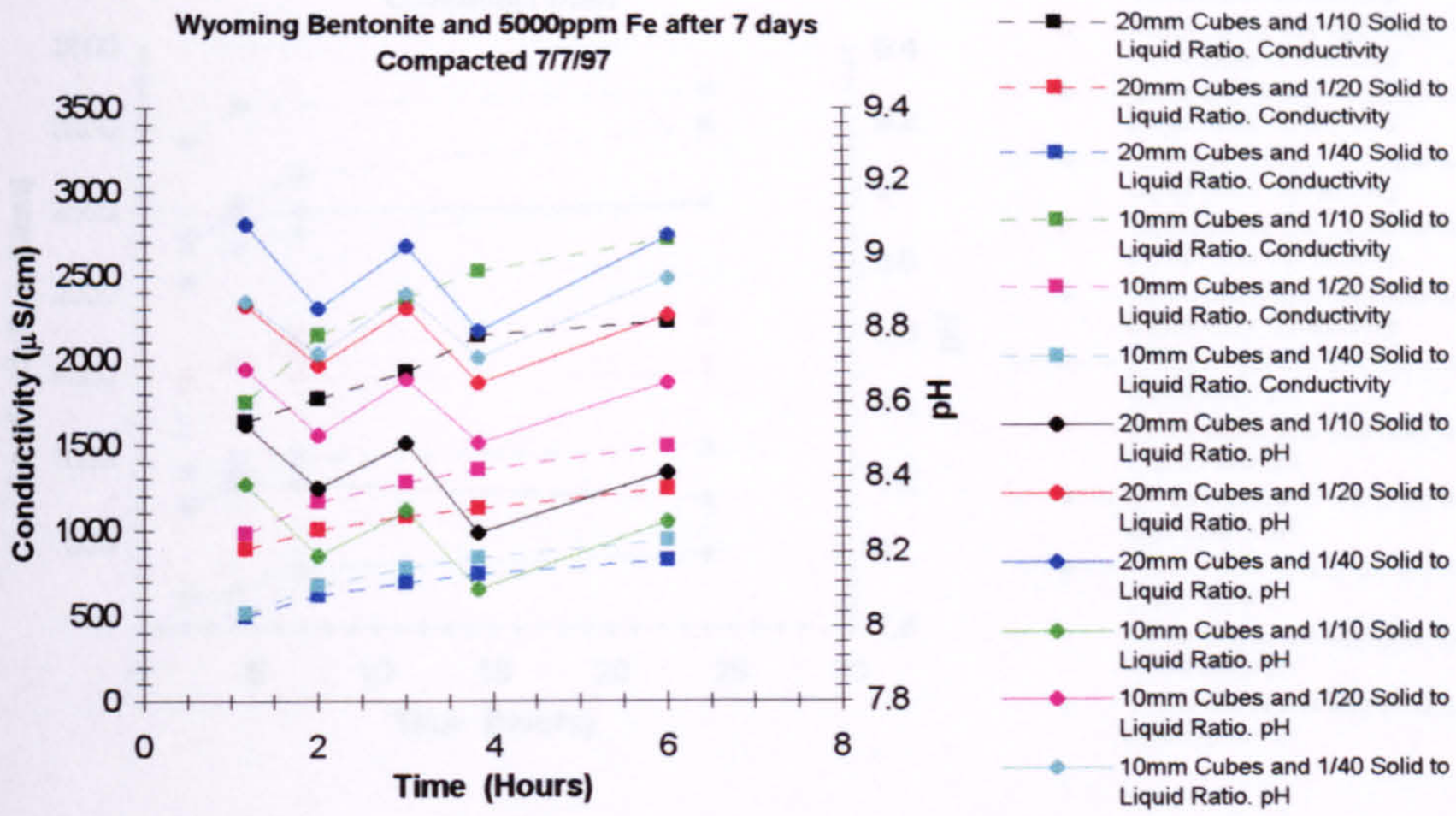

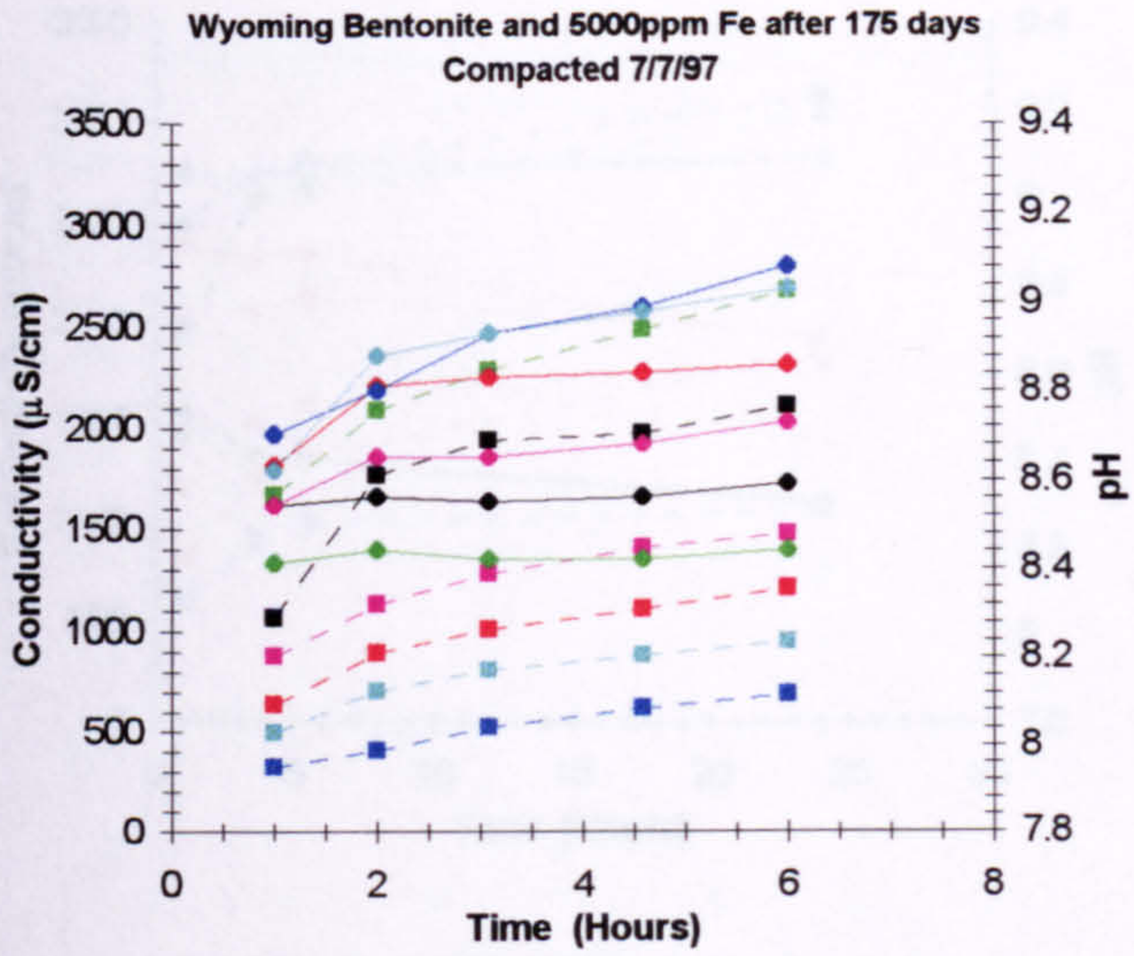

Figure A1.53 Conductivity and pH characteristics for Wyoming Bentonite with 5000ppm Fe and no lime during 24hr/30rpm Batch Tests

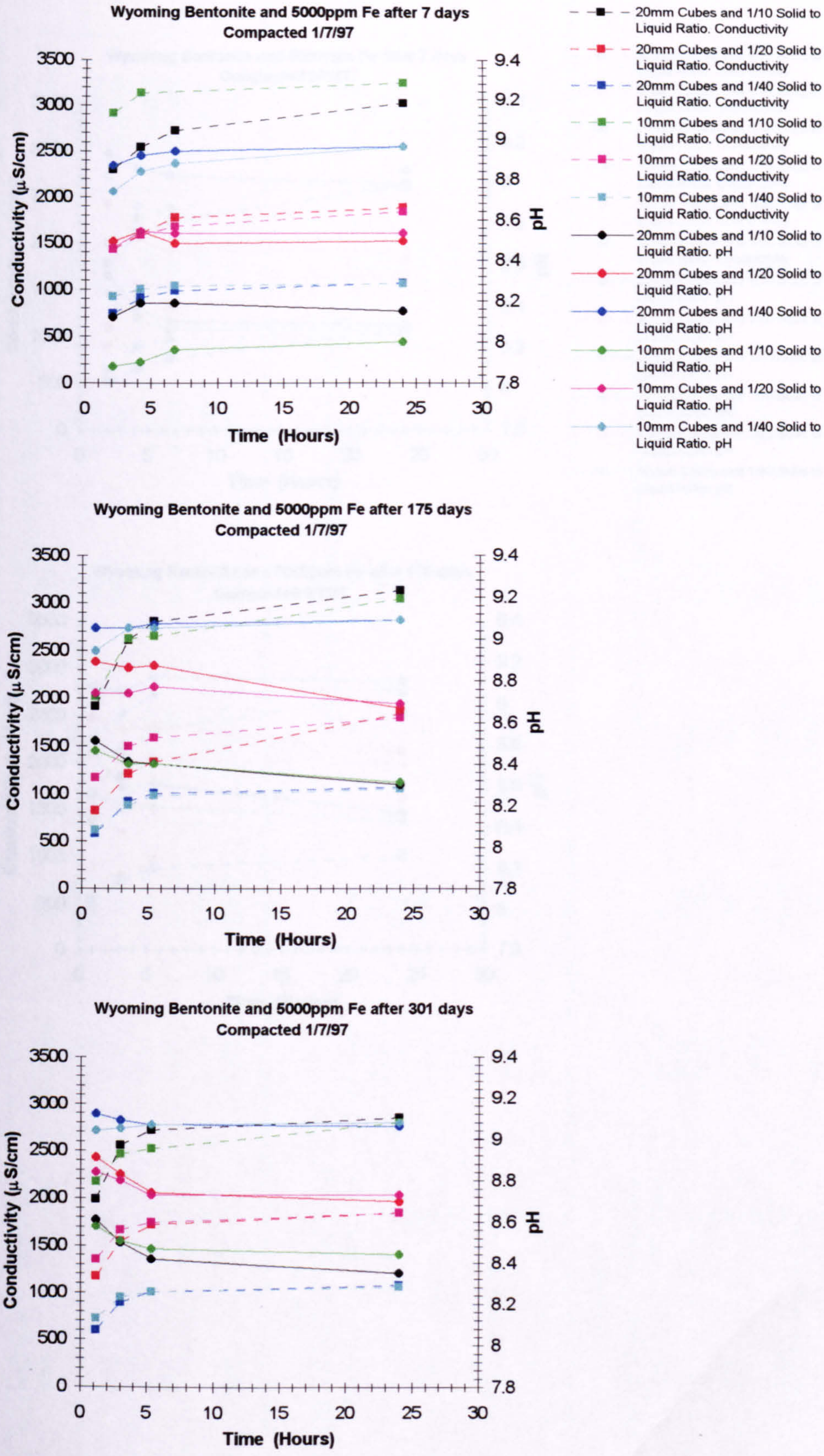

Figure A1.54 Conductivity and pH characteristics for Wyoming Bentonite with 5000ppm Fe and no lime during 24hr/60rpm Batch Tests

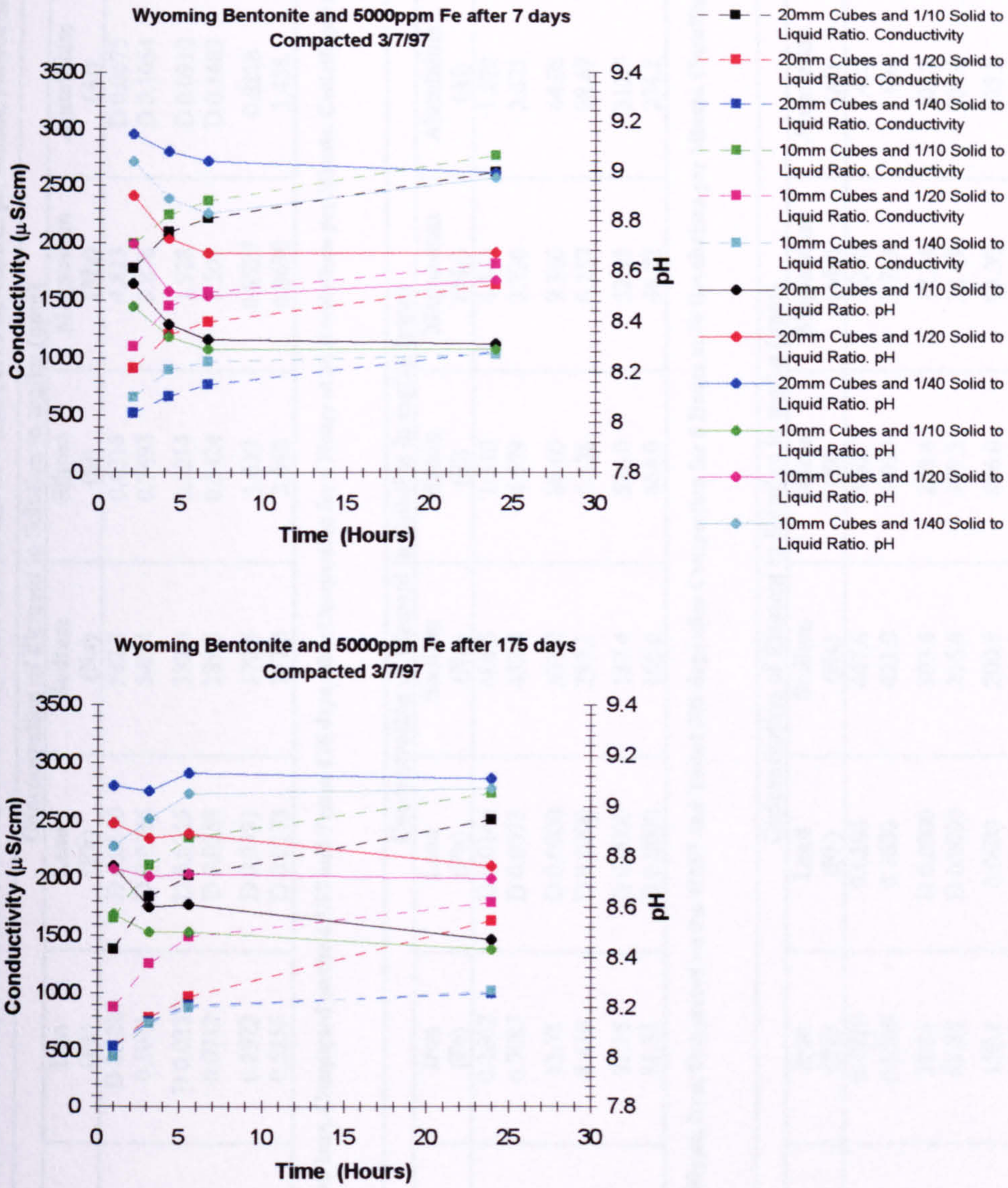

Table A1.112 ICP Data for Wyoming Bentonite and 5000ppm Iron, Compacted on the 4/7/97 and Tested 7 days after Compaction for 6 Hours at 30 Revolutions per Minute. Filtered only.

Solid to Liquid Ratio	Initial Cube Size (mm)	Concentration of Element in Solution in mg/kg (ppm)							
		Calcium (Ca)	Iron (Fe)	Lead (Pb)	Sodium (Na)	Silicon (Si)	Magnesium (Mg)	Aluminium (Al)	Manganese (Mn)
1/10	10	37.30	D 0.1209	D 0.0660	582.8	0.6318	4.813	D 0.0675	0.0731
	20	34.21	0.1011	D 0.0266	542.4	0.7693	3.876	D 0.1054	0.0520
1/20	10	15.39	D 0.0335	D 0.0225	332.4	0.5214	1.928	D 0.0910	0.0285
	20	14.05	0.0712	D 0.0259	289.5	0.6424	1.507	D 0.1483	0.0228
1/40	10	6.610	0.2972	D 0.0391	179.5	1.610	0.8727	0.8218	0.0130
	20	6.283	0.5256	D 0.0173	167.3	2.642	0.8630	1.438	0.0136

Table A1.113 ICP Data for Wyoming Bentonite 5000ppm Iron, Compacted on the 4/7/97 and Tested 175 days after Compaction for 6 Hours at 30 Revolutions per Minute. Centrifuged at 11000rpm for 30 minutes.

Solid to Liquid Ratio	Initial Cube Size (mm)	Concentration of Element in Solution in mg/kg (ppm)							
		Calcium (Ca)	Iron (Fe)	Lead (Pb)	Sodium (Na)	Silicon (Si)	Magnesium (Mg)	Aluminium (Al)	Manganese (Mn)
1/10	10	29.24	0.1667	D 0.0144	488.5	1.510	4.743	1.839	0.0282
	20	21.71	0.7087	D 0.0073	432.8	4.979	3.736	2.621	0.0259
1/20	10	17.87	13.75	D 0.0000	301.0	80.60	9.366	44.08	0.0505
	20	13.65	8.410	D 0.0000	287.1	5.138	6.257	28.67	0.026
1/40	10	39.88	92.15	D 0.0000	187.4	524.0	52.95	312.7	0.2719
	20	35.36	81.35	D 0.0000	166.6	464.0	46.72	274.2	0.2444

Table A1.114 ICP Data for Wyoming Bentonite and 5000ppm Iron, Compacted on the 4/7/97 and Tested 301 days after Compaction for 6 Hours at 30 Revolutions per Minute. Centrifuged at 11000rpm for 30 minutes.

Solid to Liquid Ratio	Initial Cube Size (mm)	Concentration of Element in Solution in mg/kg (ppm)							
		Calcium (Ca)	Iron (Fe)	Lead (Pb)	Sodium (Na)	Silicon (Si)	Magnesium (Mg)	Aluminium (Al)	Manganese (Mn)
1/10	10	25.10	0.4010	0.0280	447.6	3.927	5.040	1.425	0.0295
	20	17.97	0.6500	0.1600	421.0	4.990	3.763	1.994	0.0220
1/20	10	27.68	29.81	D 0.0000	303.6	238.4	18.14	101.2	0.0900
	20	33.56	62.85	D 0.0000	216.6	439.5	34.09	209.4	0.2100
1/40	10	69.15	158.1	0.0600	200.9	806.0	85.30	535.5	0.4900
	20	71.75	229.2	D 0.0000	219.5	2031	123.9	830.5	0.6840

Note: 'D' indicates the stated value is below detection limits and the value stated is a system estimate. 'd' indicates the stated value is close to detection limits.

Table A1.115 ICP Data for Wyoming Bentonite and 5000ppm Iron, Compacted on the 7/7/97 and Tested 7 days after Compaction for 6 Hours at 60 Revolutions per Minute. Filtered only.

Solid to Liquid Ratio	Initial Cube Size (mm)	Concentration of Element in Solution in mg/kg (ppm)							
		Calcium (Ca)	Iron (Fe)	Lead (Pb)	Sodium (Na)	Silicon (Si)	Magnesium (Mg)	Aluminium (Al)	Manganese (Mn)
1/10	10	33.64	D 0.0273	D 0.0269	566.6	0.5634	4.736	D 0.0314	0.0605
	20	24.47	D 0.0237	D 0.0232	480.8	0.6637	3.338	D 0.0587	0.0385
1/20	10	21.19	D 0.0534	D 0.0025	289.5	0.5989	1.897	D 0.0817	0.0239
	20	9.291	D 0.0418	D 0.0000	234.2	0.6579	1.304	D 0.1271	0.0159
1/40	10	5.528	0.4278	D 0.0000	176.4	2.323	0.9469	1.273	0.0121
	20	4.404	1.016	D 0.0268	150.1	5.370	1.116	3.147	0.0110

Table A1.116 ICP Data for Wyoming Bentonite 5000ppm Iron, Compacted on the 7/7/97 and Tested 175 days after Compaction for 6 Hours at 60 Revolutions per Minute. ***Centrifuged at 11000rpm for 30 minutes.***

Solid to Liquid Ratio	Initial Cube Size (mm)	Concentration of Element in Solution in mg/kg (ppm)							
		Calcium (Ca)	Iron (Fe)	Lead (Pb)	Sodium (Na)	Silicon (Si)	Magnesium (Mg)	Aluminium (Al)	Manganese (Mn)
1/10	10	32.30	0.0755	D 0.0134	524.6	0.8485	5.116	0.4616	0.0295
	20	20.41	0.4943	D 0.0039	431.4	3.653	3.385	2.047	0.0219
1/20	10	10.40	0.5119	D 0.0106	283.8	3.545	2.138	1.889	0.0128
	20	8.764	6.708	D 0.0000	230.0	41.36	5.030	23.51	0.0255
1/40	10	48.95	124.5	D 0.0000	260.5	681.0	70.10	414.0	0.3627
	20	25.26	51.60	D 0.0000	136.5	274.0	30.15	178.3	0.1700

Note: 'D' indicates the stated value is below detection limits and the value stated is a system estimate. 'd' indicates the stated value is close to detection limits.

Table A1.117 ICP Data for Wyoming Bentonite and 5000ppm Iron, Compacted on the 1/7/97 and Tested 7 days after Compaction for 24 Hours at 30 Revolutions per Minute. Centrifuged at 11000rpm for 30 minutes.

Solid to Liquid Ratio	Initial Cube Size (mm)	Concentration of Element in Solution in mg/kg (ppm)							
		Calcium (Ca)	Iron (Fe)	Lead (Pb)	Sodium (Na)	Silicon (Si)	Magnesium (Mg)	Aluminium (Al)	Manganese (Mn)
1/10	10	42.25	0.1430	D 0.0000	694.3	1.847	5.385	0.5379	0.0807
	20	37.83	0.0957	D 0.0000	628.5	1.419	4.858	d. 0.2902	0.0641
1/20	10	15.52	0.1250	D 0.0003	379.7	1.367	1.868	d. 0.4055	0.0220
	20	15.74	0.2016	D 0.0053	405.4	1.986	1.919	0.7596	0.0228
1/40	10	5.532	0.9561	D 0.0313	209.4	7.007	1.119	3.592	d. 0.0061
	20	5.205	0.5270	D 0.0000	208.1	3.955	0.8961	1.983	0.0079

Table A1.118 ICP Data for Wyoming Bentonite 5000ppm Iron, Compacted on the 1/7/97 and Tested 175 days after Compaction for 24 Hours at 30 Revolutions per Minute. Centrifuged at 11000rpm for 30 minutes.

Solid to Liquid Ratio	Initial Cube Size (mm)	Concentration of Element in Solution in mg/kg (ppm)							
		Calcium (Ca)	Iron (Fe)	Lead (Pb)	Sodium (Na)	Silicon (Si)	Magnesium (Mg)	Aluminium (Al)	Manganese (Mn)
1/10	10	37.97	0.1750	1.095	659.0	1.410	6.205	D 0.0000	0.0500
	20	41.15	0.2150	0.2350	668.5	1.620	6.845	0.4200	0.0500
1/20	10	15.30	0.7800	0.1500	364.2	4.960	2.870	2.400	0.0200
	20	12.49	0.8350	0.2150	352.6	5.640	2.575	2.670	0.0150
1/40	10	14.56	26.92	0.8550	198.7	173.4	15.36	91.15	0.0950
	20	27.54	63.20	0.3200	195.0	351.7	34.66	211.1	0.1750

Table A1.119 ICP Data for Wyoming Bentonite and 5000ppm Iron, Compacted on the 1/7/97 and Tested 301 days after Compaction for 24 Hours at 30 Revolutions per Minute. Centrifuged at 11000rpm for 30 minutes.

Solid to Liquid Ratio	Initial Cube Size (mm)	Concentration of Element in Solution in mg/kg (ppm)							
		Calcium (Ca)	Iron (Fe)	Lead (Pb)	Sodium (Na)	Silicon (Si)	Magnesium (Mg)	Aluminium (Al)	Manganese (Mn)
1/10	10	35.85	0.1797	0.0210	612.0	2.005	5.860	0.5917	0.0372
	20	41.20	0.1837	0.0260	657.0	2.468	6.805	0.8600	0.0467
1/20	10	12.39	4.715	0.0020	341.2	38.31	4.785	16.21	0.0270
	20	18.57	7.430	0.2300	369.1	59.20	6.610	25.79	0.0300
1/40	10	46.26	92.50	0.2000	204.2	557.5	51.20	311.8	0.2800
	20	35.7	78.45	D 0.0000	210.5	558.5	42.52	261.8	0.2350

Note: 'D' indicates the stated value is below detection limits and the value stated is a system estimate. 'd' indicates the stated value is close to detection limits.

Table A1.120 ICP Data for Wyoming Bentonite and 5000ppm Iron, Compacted on the 3/7/97 and Tested 7 days after Compaction for 24 Hours at 60 Revolutions per Minute. Centrifuged at 11000rpm for 30 minutes.

Solid to Liquid Ratio	Initial Cube Size (mm)	Concentration of Element in Solution in mg/kg (ppm)							
		Calcium (Ca)	Iron (Fe)	Lead (Pb)	Sodium (Na)	Silicon (Si)	Magnesium (Mg)	Aluminium (Al)	Manganese (Mn)
1/10	10	33.08	0.2048	D 0.0000	529.4	2.801	4.420	1.414	0.0404
	20	32.33	0.1678	D 0.0339	500.7	1.787	4.168	0.5438	0.0392
1/20	10	15.32	0.6393	D 0.0234	368.5	4.982	2.160	2.357	0.0188
	20	14.80	0.4040	D 0.0000	324.6	3.366	1.969	1.504	0.0156
1/40	10	64.70	160.4	D 0.0000	234.8	----	83.8	550.0	0.5537
	20	63.07	158.4	D 0.0000	230.0	----	86.6	607.0	0.5244

Table A1.121 ICP Data for Wyoming Bentonite 5000ppm Iron, Compacted on the 3/7/97 and Tested 175 days after Compaction for 24 Hours at 60 Revolutions per Minute. Centrifuged at 11000rpm for 30 minutes.

Solid to Liquid Ratio	Initial Cube Size (mm)	Concentration of Element in Solution in mg/kg (ppm)							
		Calcium (Ca)	Iron (Fe)	Lead (Pb)	Sodium (Na)	Silicon (Si)	Magnesium (Mg)	Aluminium (Al)	Manganese (Mn)
1/10	10	38.76	0.1300	0.2000	570.8	1.069	6.029	1.540	0.0370
	20	33.61	0.1660	0.0880	552.2	2.733	5.129	0.8100	0.0300
1/20	10	16.09	0.995	0.2000	342.9	6.867	2.956	4.084	0.0270
	20	16.93	9.030	0.0100	333.6	56.68	6.941	30.68	0.0350
1/40	10	20.09	36.56	0.0160	197.8	223.0	21.01	122.4	0.1130
	20	47.70	104.5	D 0.0000	202.1	555.6	58.39	351.3	0.3210

Note: 'D' indicates the stated value is below detection limits and the value stated is a system estimate. 'd' indicates the stated value is close to detection limits.

Table A1.122 ICP Data for Wyoming Bentonite 5000ppm Iron, Compacted on the 1/7/97 and Tested 175 days after Compaction for 24 Hours at 30 Revolutions per Minute. Filtered only.

Solid to Liquid Ratio	Initial Cube Size (mm)	Concentration of Element in Solution in mg/kg (ppm)							
		Calcium (Ca)	Iron (Fe)	Lead (Pb)	Sodium (Na)	Silicon (Si)	Magnesium (Mg)	Aluminium (Al)	Manganese (Mn)
1/10	10	37.01	0.0556	D 0.0260	673.5	0.6335	6.131	D 0.0695	0.0429
	20	45.33	0.0800	0.2200	674.5	1.155	7.370	1.035	0.2050
1/20	10	11.62	0.0193	D 0.0000	365.4	0.5625	2.410	D 0.1025	0.0204
	20	11.12	d. 0.0167	D 0.0000	419.9	0.7466	2.270	d. 0.2305	0.0163
1/40	10	5.535	0.1209	D 0.0159	199.1	1.111	0.9284	0.4015	D 0.0052
	20	4.893	0.1823	D 0.0000	206.5	1.439	0.9710	0.5795	0.0095

Table A1.123 ICP Data for Wyoming Bentonite and 5000ppm Iron, Compacted on the 3/7/97 and Tested 7 days after Compaction for 24 Hours at 60 Revolutions per Minute. Filtered only.

Solid to Liquid Ratio	Initial Cube Size (mm)	Concentration of Element in Solution in mg/kg (ppm)							
		Calcium (Ca)	Iron (Fe)	Lead (Pb)	Sodium (Na)	Silicon (Si)	Magnesium (Mg)	Aluminium (Al)	Manganese (Mn)
1/10	10	36.22	D 0.0382	D 0.0291	565.0	0.8619	4.832	D 0.0568	0.0532
	20	35.98	0.0890	D 0.0217	542.8	0.9861	4.417	D 0.0617	0.0475
1/20	10	18.29	0.0774	D 0.0376	358.1	0.8024	2.217	D 0.1044	0.0258
	20	20.07	D 0.0415	D 0.0382	320.0	0.8944	2.026	D 0.0797	0.0219
1/40	10	7.537	0.2235	D 0.0165	197.3	1.586	0.9847	0.6449	0.0113
	20	8.033	0.2184	D 0.0441	200.8	1.548	0.9844	d. 0.5824	0.0116

Note : 'D' indicates the stated value is below detection limits and the value stated is a system estimate. 'd' indicates the stated value is close to detection limits.

A1.2.13 Wyoming Bentonite with no contaminants and 2.5% lime

A1.2.13.1 Centrifugation

All samples for this design mix had to be centrifuged since at no curing period could sludges be gravity or vacuum filtered even over a period of days. However it was visually evident that samples centrifuged at 7 days curing produced clear colourless solutions with the exception of the 1:40 solid to liquid ratio which produced clear yellow solutions indicating a high Fe content. It was clearly evident that samples were undergoing a degree of flocculation. However at 175 and 301 days curing no samples showed any visual evidence of flocculation and visually appeared to have regained a level of plasticity. This was reflected in the difficulty with which solid and liquid could be separated via centrifugation. Tables A1.124 to A1.133 illustrate these changes chemically. Due to these changes, samples after 7 days curing behaved similarly to untreated uncontaminated Wyoming Bentonite and the chemical data is subject to the same analysis restrictions. Hence after 7 days curing only the 1:40 and 1:20 solid to liquid ratios will be considered further.

A1.2.13.2 Solid : liquid ratio

Inspections of Figures A1.55 to A1.58 show distinct changes in conductivity behaviour with increasing solid to liquid ratio although pH values showed high variability. At 7 days curing the conductivity of 6hr/30rpm tests with 20mm cube sizes of the solid to liquid ratios 1:40, 1:20 and 1:10 were 1639µS/cm, 1317µS/cm and 949µS/cm respectively whilst pH values were 11.69, 11.69 and 11.55 respectively. At 175 days curing the conductivity values were 1066µS/cm, 785µS/cm and 579µS/cm respectively whilst pH values were 11.30, 11.20 and 11.04 respectively. At 301 days curing conductivity values were 1106µS/cm 733µS/cm and 657µS/cm respectively whilst pH values were 11.17, 11.07 and 11.05 respectively. Increasing solid to liquid behaviour from 1:40 to 1:20 at 7, 175 and 301 days curing therefore increased conductivity by factors of 1.39, 1.36 and 1.12 respectively whilst pH values increased by 0.14, 0.16 and 0.02 pH divisions respectively. Increasing solid to liquid ratio further from 1:20 to 1:10 increased conductivity by factors of 1.24, 1.36 and 1.51 respectively whilst pH values increased by 0.00, 0.10 and 0.10 pH divisions respectively.

Inspection of Table A1.124 for 6hr/30rpm tests at the 1:10 solid to liquid ratio showed typical levels of elements released at 7 days. 20mm cubes released 4.73ppm Ca, 0.3273ppm Fe, 217ppm Na, 38.2ppm Si, 0.204ppm Mg and 1.227ppm Al. Table A1.124 also illustrates that as the solid to liquid ratio reduced levels of Ca, Fe, Si, Mg and Al increased whilst Na levels reduced. However Tables A1.125, A1.126 and A1.130, A1.131 illustrate that at 175 and 301 days curing decreasing solid to liquid ratio from 1:20 to 1:40 resulted in reduced levels of Ca, Fe, Na, Si, Mg and Al. This was clearly a result of the effects of centrifugation and essentially dilution obscuring variations brought about by chemical changes. However chemical change was clearly taking place as illustrated by the changing difficulty in solid and liquid separation.

Observation of Figures A1.55 and A1.57 clearly demonstrate that as curing period increased there was significant variation in conductivity between the solid to liquid ratios whilst pH values at different solid to liquid ratios tended towards one value.

A1.2.13.3 Cube Size

Analysis of Figures A1.55 to A1.58 shows that the smaller cube size generally produced higher pH and conductivity values at 7 and 175 days curing. These effects were less pronounced during 24 hr tests and this was probably due to more particle breakdown. At 7 days curing and especially at the solid to liquid ratios 1:40 and 1:20 (Tables A1.124, A1.129 and A1.127, A1.132) the 10mm cube sizes released more Ca, Mn and less Fe, Si, Mg, Al whilst Na was variable. The already observed changes illustrated by centrifugation at the curing periods 175 and 301 days curing were also evident here with the 10mm cube sizes at the solid to liquid ratios 1:40 and 1:20 releasing more of all elements than the 20mm cube sizes.

A1.2.13.4 Rotation speed and test duration

Comparison of 6hr tests at 7 days curing (Figures A1.55 and A1.56) show that higher rotation speed produces similar pH values although significantly higher conductivities particularly at the higher solid to liquid ratios. Comparison of Tables A1.124 and A1.127 relate this to much higher levels of Ca, Na and Si. Other elements including Fe, Mg and Al also showed an increase in level at the higher rotation speed. Comparison of 6hr tests at 175 days curing showed reduced pH at the

higher solid to liquid ratios and higher conductivity at the lower solid to liquid ratios for increased rotation speed.

Comparison of 24hr tests in Figures A1.57 and A1.58 showed similar trends although pH values at 7 days were significantly lower for the higher rotation speed.

Observation of Figures A1.55 and A1.57 for 30rpm tests showed that at 7 days curing, increasing test duration has no effect on pH or conductivity values. At 175 and 301 days increasing test duration resulted in higher final pH and conductivity values. Tables A1.124, A1.125, A1.126 and A1.129, A1.130, A1.131 relate this to increased Ca, Fe, Na, Si, Mg and Al. Consideration of 60rpm tests (Figures A1.56 and A1.58) showed no variation in pH as test duration increased at 7 days curing whilst conductivity values increased. At 175 days curing pH and conductivity values tended to increase with increasing test duration. Tables A1.127 and A1.132 at 7 days curing show as duration increased levels of Ca, Na, and Si increased whilst levels of Fe, Mg and Al decreased. At 175 days curing Tables A1.128 and Be show that all these elements increased in concentration.

A1.2.13.5 Curing Time

Figures A1.55 to A1.58 show clearly that pH and conductivity significantly reduces as curing period increases. A further interesting factor is that as curing period increases all pH values of all solid to liquid ratios tend towards a single value. Due to the large change in physical behaviour reducing the effectiveness of centrifugation it is not possible to fully interpret chemical changes with increasing curing period. It is however clear that there is a reduced level of flocculation a clear indicator of continuing chemical activity.

Figure A1.55 Conductivity and pH characteristics for Wyoming Bentonite with no contaminants and 2.5% lime during 6hr/30rpm Batch Tests

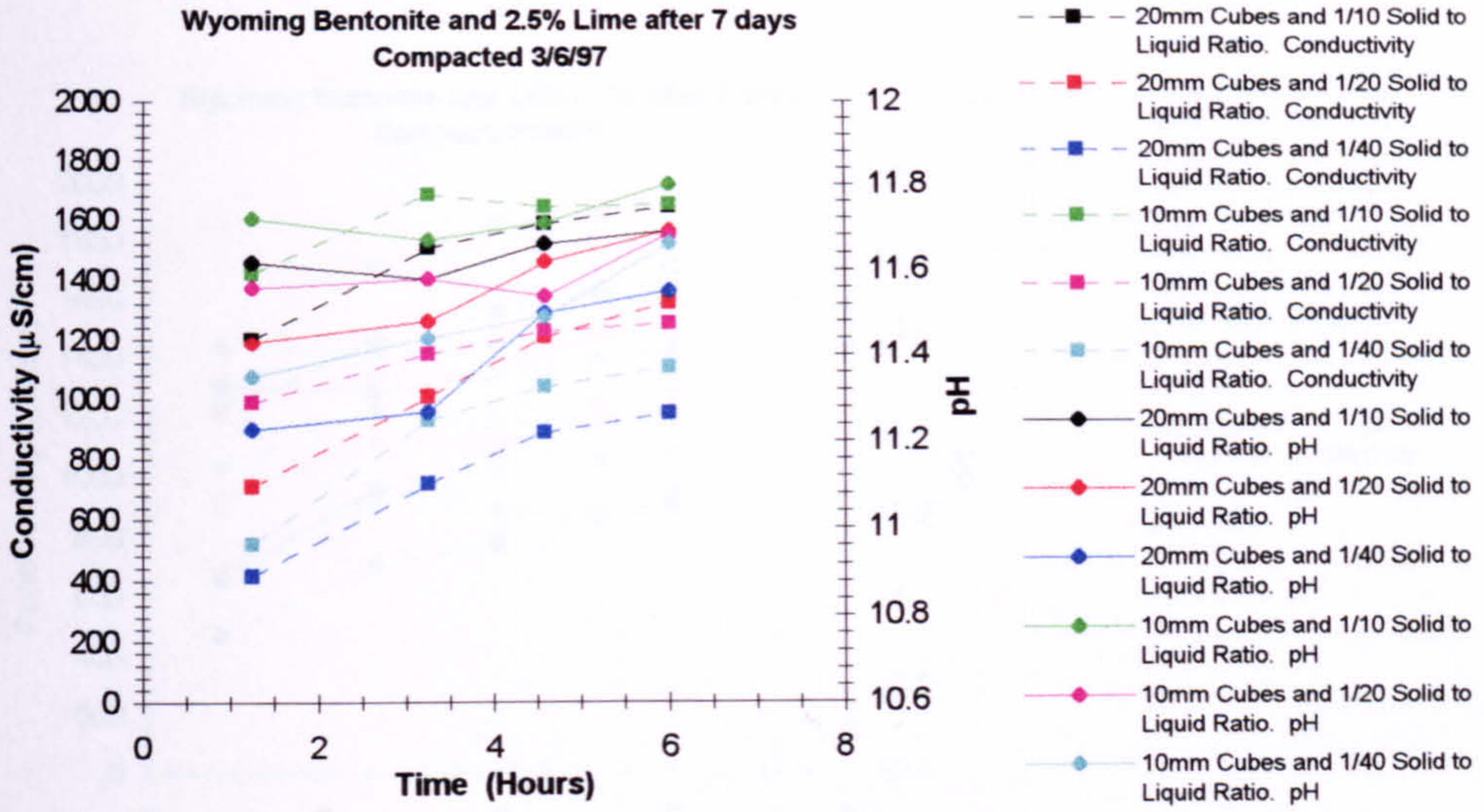

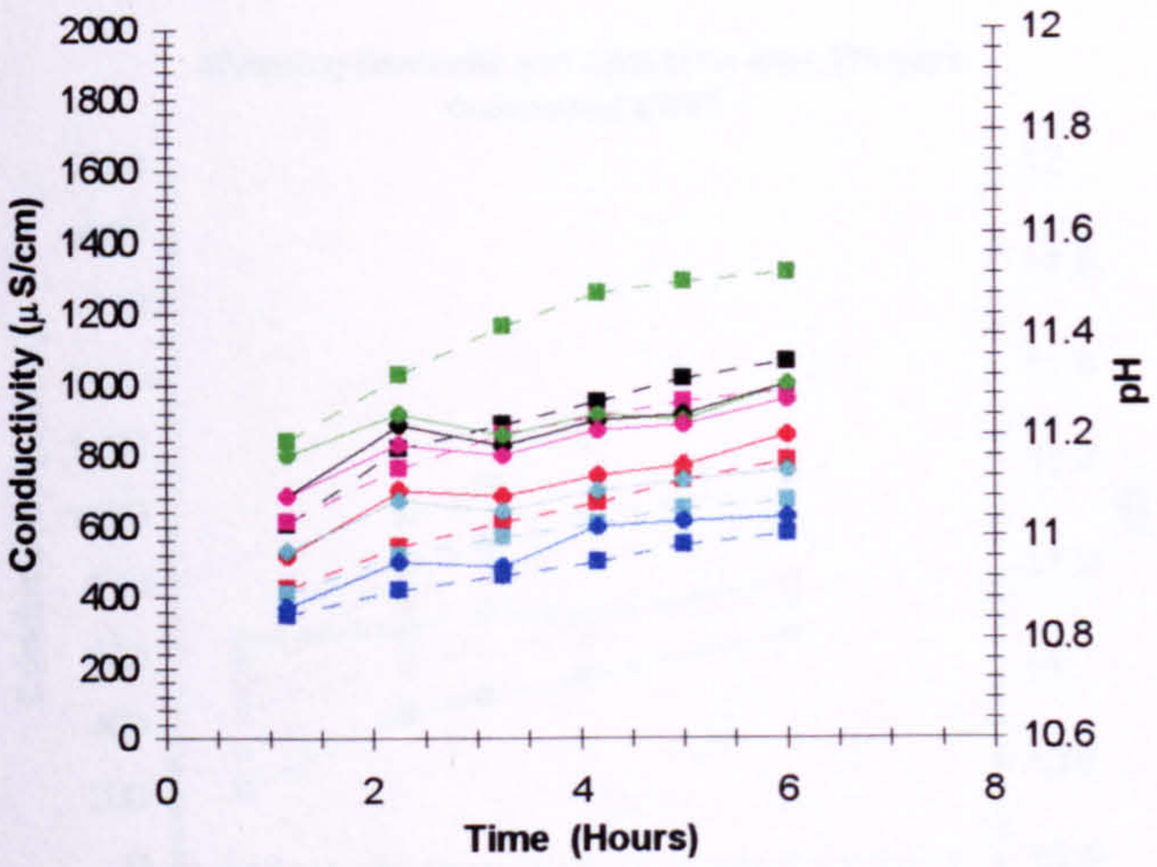

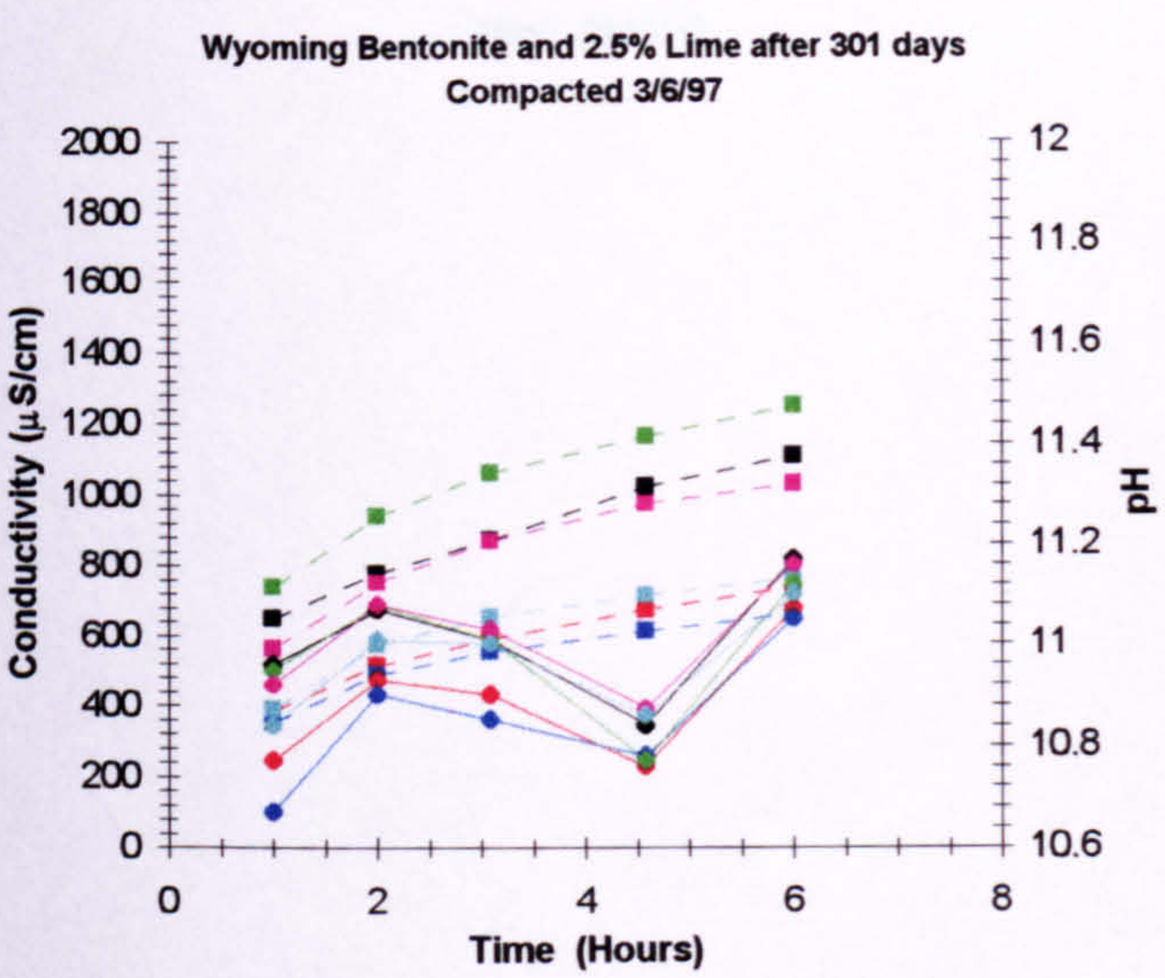

Figure A1.56 Conductivity and pH characteristics for Wyoming Bentonite with no contaminants and 2.5% lime during 6hr/60rpm Batch Tests

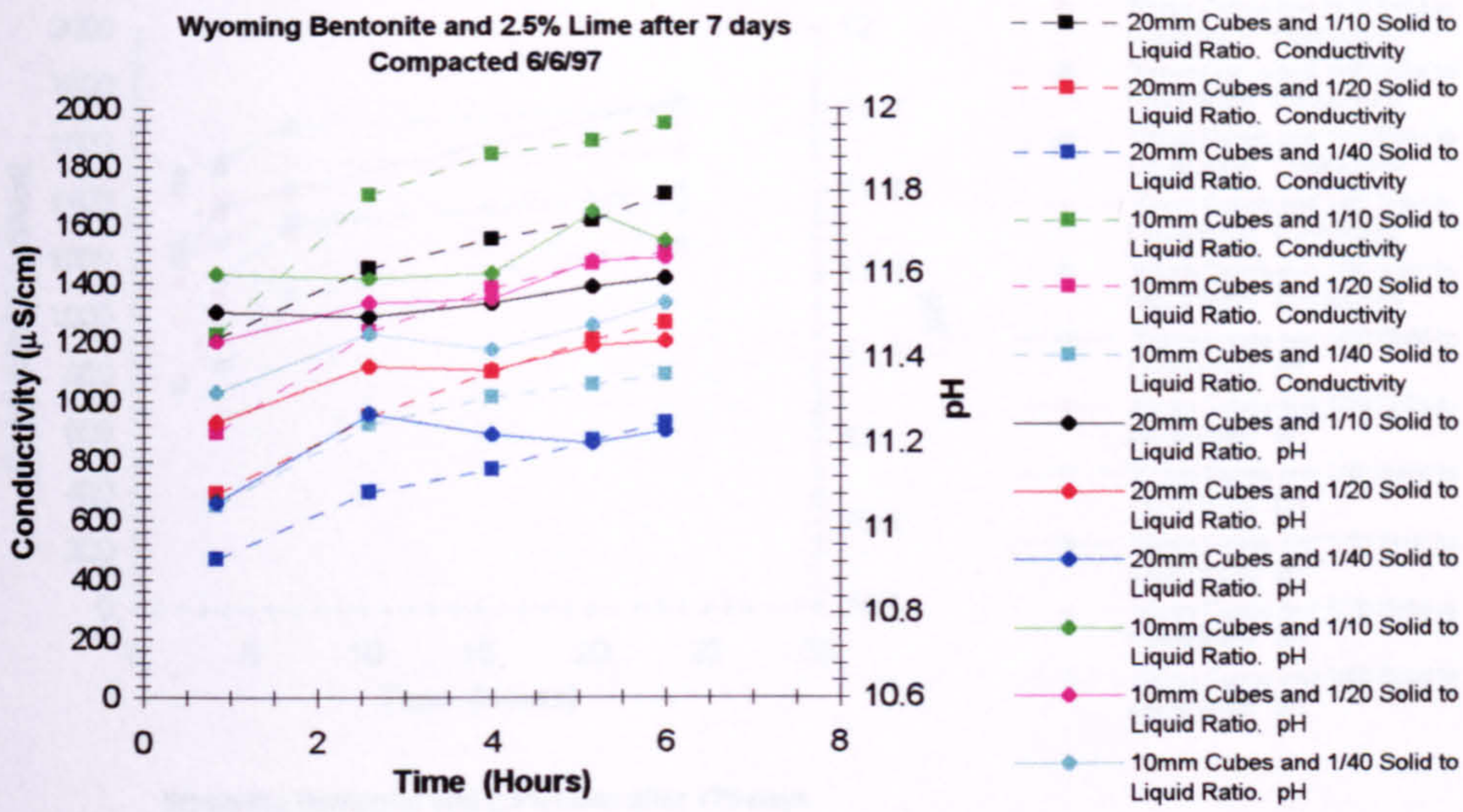

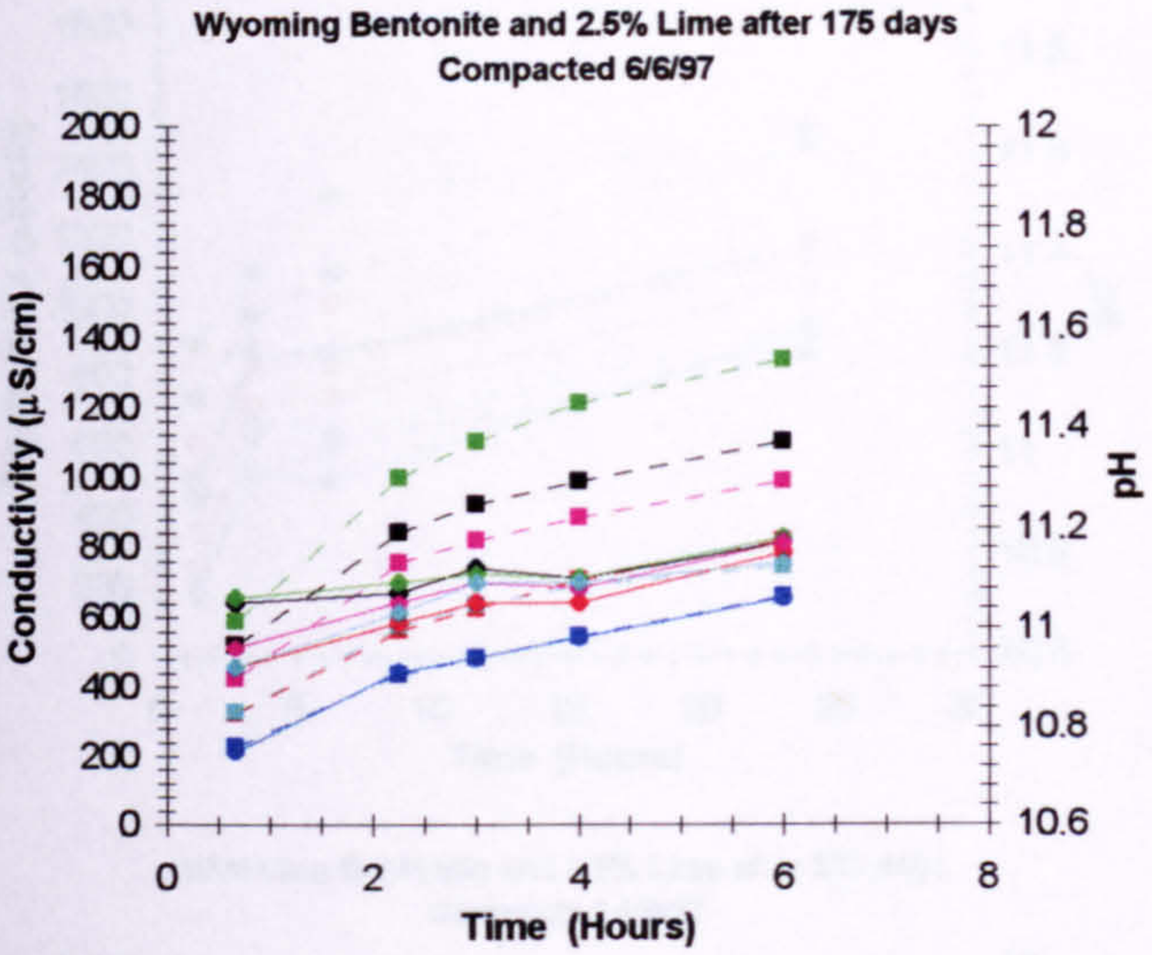

Figure A1.57 Conductivity and pH characteristics for Wyoming Bentonite with no contaminants and 2.5% lime during 24hr/30rpm Batch Tests

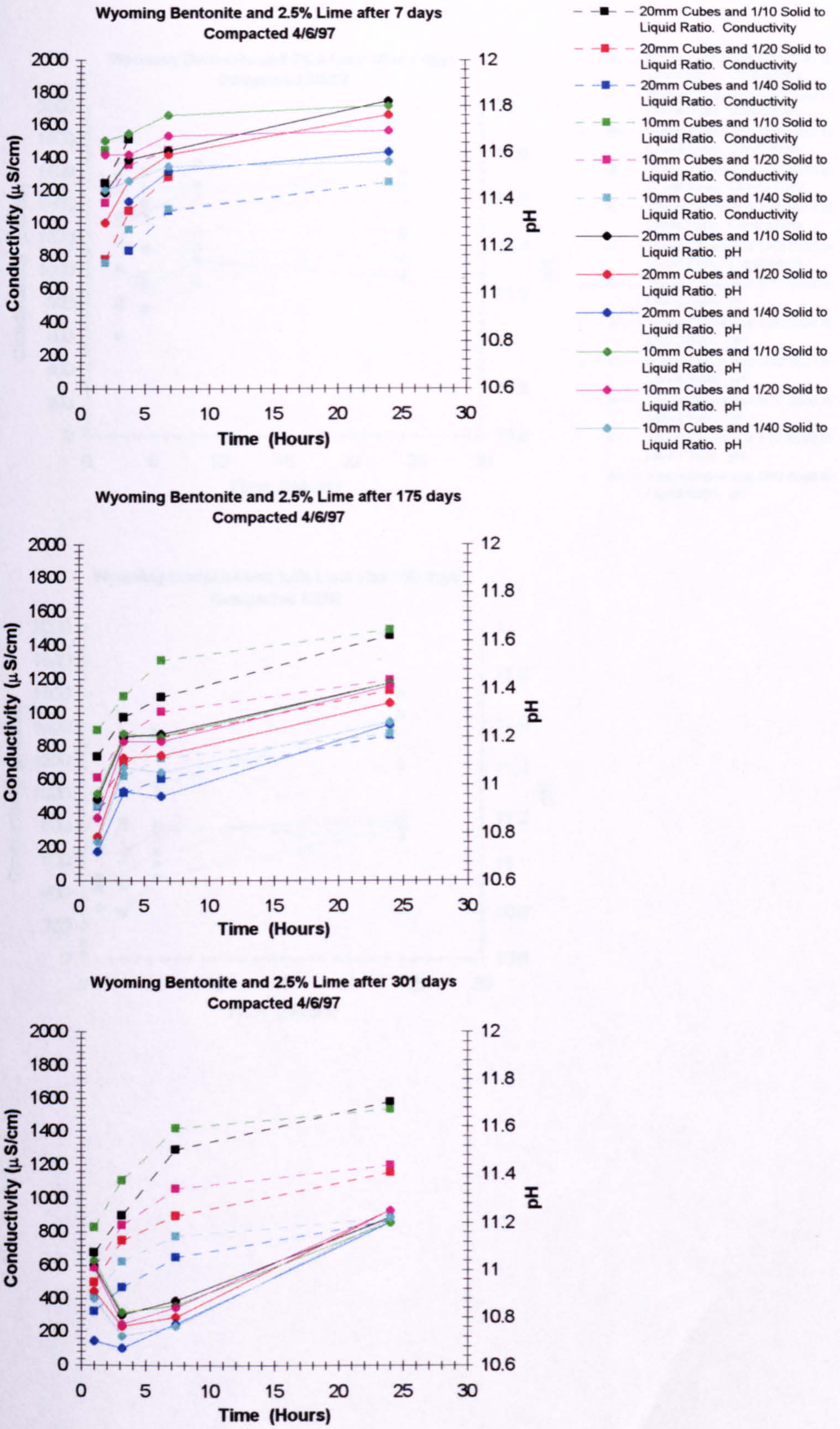

Figure A1.58 Conductivity and pH characteristics for Wyoming Bentonite with no contaminants and 2.5% lime during 24hr/60rpm Batch Tests

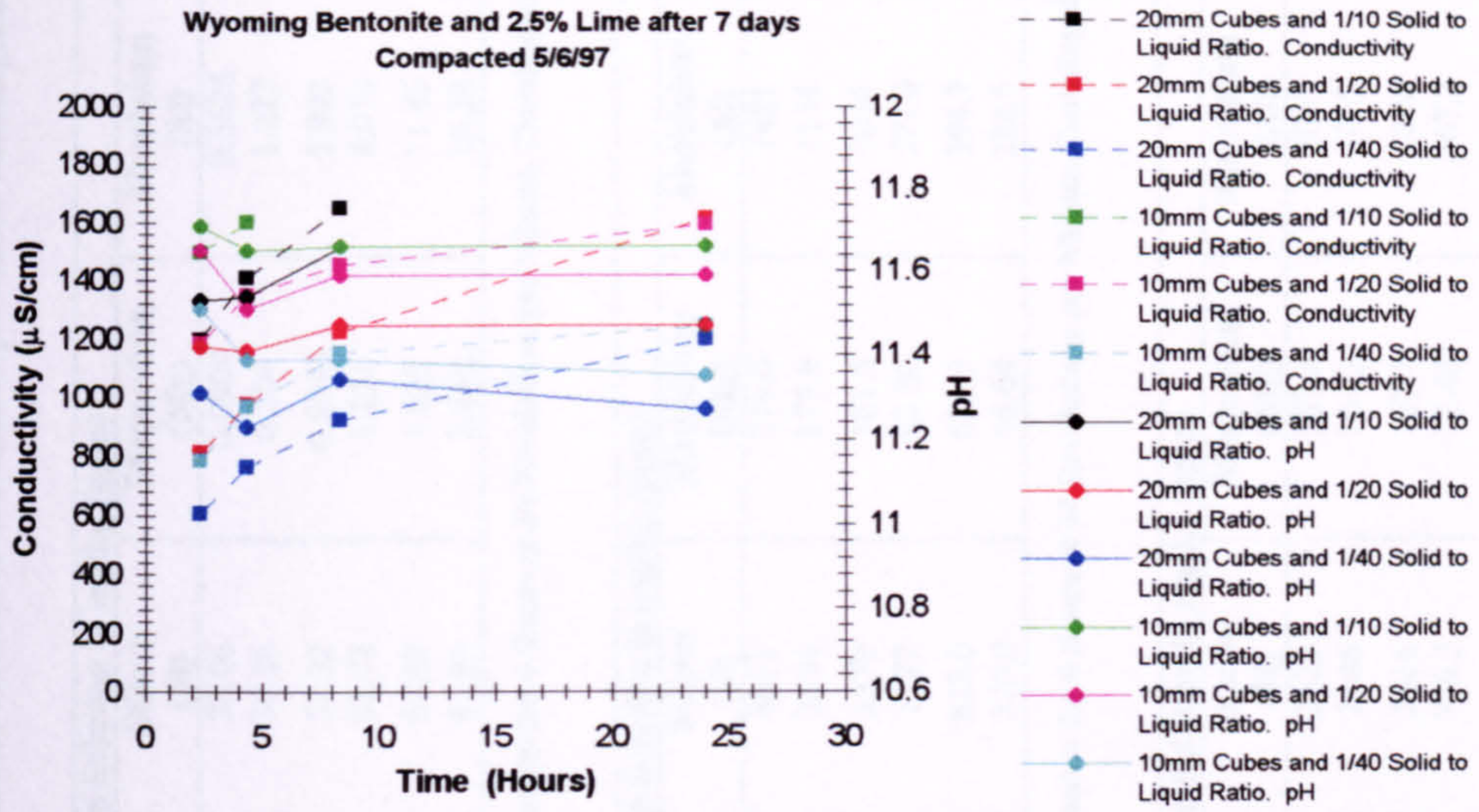

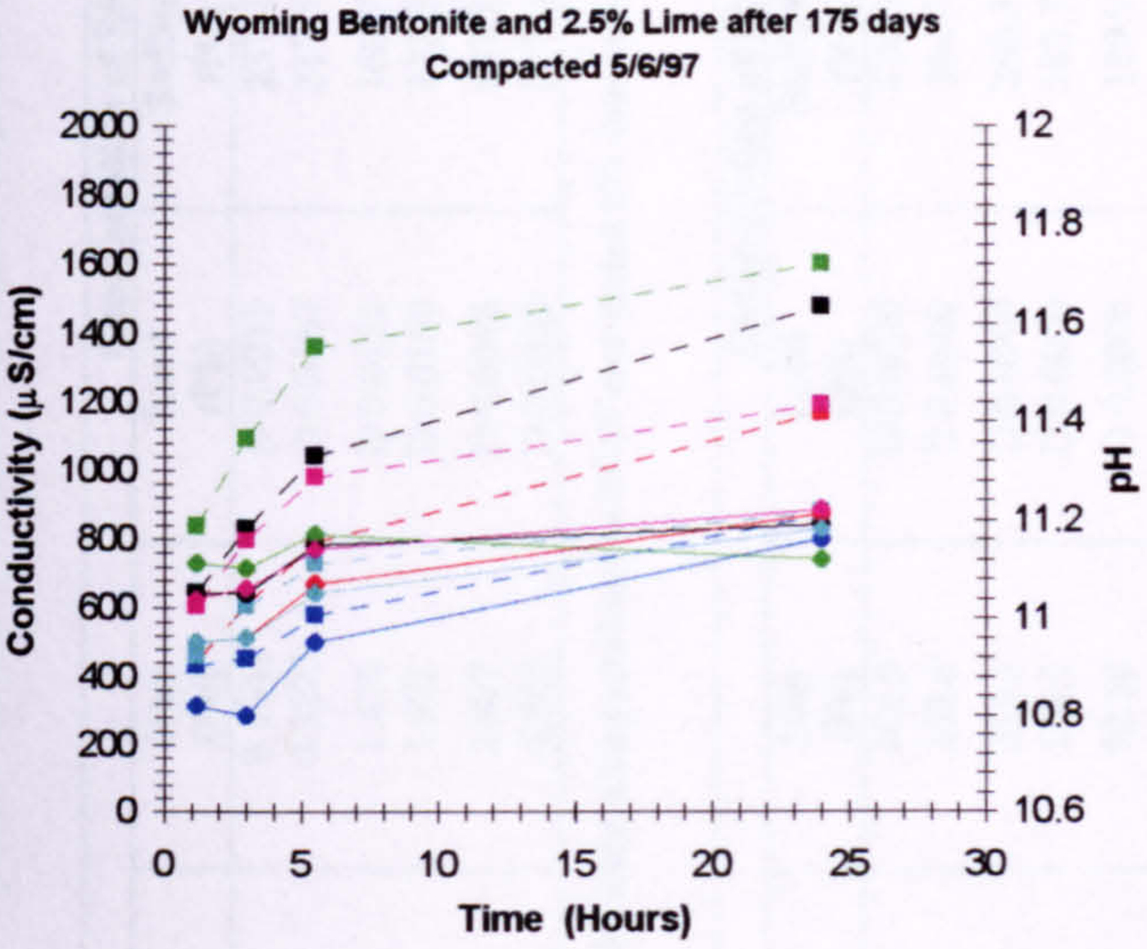

Table A1.124 ICP Data for Wyoming Bentonite and 2.5% Lime, Compacted on the 3/6/97 and Tested 7 days after Compaction for 6 Hours at 30 Revolutions per Minute. Centrifuged at 11000rpm for 30 minutes.

Solid to Liquid Ratio	Initial Cube Size (mm)	Concentration of Element in Solution in mg/kg (ppm)							
		Calcium (Ca)	Iron (Fe)	Lead (Pb)	Sodium (Na)	Silicon (Si)	Magnesium (Mg)	Aluminium (Al)	Manganese (Mn)
1/10	10	4.663	0.1541	D 0.0213	237.2	38.06	0.0909	0.5624	D 0.0015
	20	4.729	0.3273	D 0.0187	217.5	38.26	0.204	1.227	D 0.0016
1/20	10	4.420	1.478	D 0.0131	166.7	52.32	0.9093	5.990	D 0.0035
	20	4.009	1.972	D 0.0150	172.3	58.73	1.231	8.070	D 0.0026
1/40	10	4.951	2.877	D 0.0096	147.2	67.67	1.833	11.85	D 0.0030
	20	5.774	4.547	D 0.0000	127.0	81.89	2.888	18.24	d. 0.0058

Table A1.125 ICP Data for Wyoming Bentonite and 2.5% Lime, Compacted on the 3/6/97 and Tested 175 days after Compaction for 6 Hours at 30 Revolutions per Minute. Centrifuged at 11000rpm for 30 minutes.

Solid to Liquid Ratio	Initial Cube Size (mm)	Concentration of Element in Solution in mg/kg (ppm)							
		Calcium (Ca)	Iron (Fe)	Lead (Pb)	Sodium (Na)	Silicon (Si)	Magnesium (Mg)	Aluminium (Al)	Manganese (Mn)
1/10	10	486.0	465.9	D 0.0000	470.3	4811	319.0	1981	0.4850
	20	246.2	263.6	D 0.0000	304.7	2694	177.9	1134	0.2650
1/20	10	225.1	232.5	D 0.0000	268.3	2379	161.5	1014	0.2150
	20	121.4	134.1	D 0.0000	183.7	1377	92.80	571.0	0.1450
1/40	10	84.45	92.50	D 0.0000	139.9	823.0	63.85	394.7	0.1000
	20	59.25	67.50	D 0.0000	112.0	570.0	46.64	286.6	0.0600

Table A1.126 ICP Data for Wyoming Bentonite and 2.5% Lime, Compacted on the 3/6/97 and Tested 301 days after Compaction for 6 Hours at 30 Revolutions per Minute. Centrifuged at 11000rpm for 30 minutes.

Solid to Liquid Ratio	Initial Cube Size (mm)	Concentration of Element in Solution in mg/kg (ppm)							
		Calcium (Ca)	Iron (Fe)	Lead (Pb)	Sodium (Na)	Silicon (Si)	Magnesium (Mg)	Aluminium (Al)	Manganese (Mn)
1/10	10	224.0	250.0	D 0.0000	340.3	2523	167.5	1091	0.2650
	20	214.7	246.9	D 0.0000	302.3	2486	164.2	1065	0.2700
1/20	10	231.1	249.3	D 0.0000	298.1	2516	167.7	1094	0.2550
	20	93.60	107.2	D 0.0000	162.7	749.5	72.45	467.2	0.1150
1/40	10	125.1	137.0	D 0.0000	182.5	944.5	92.80	595.0	0.1600
	20	86.20	96.45	D 0.0000	141.1	672.0	65.35	420.7	0.1000

Note: 'D' indicates the stated value is below detection limits and the value stated is a system estimate. 'd' indicates the stated value is close to detection limits.

Table A1.127 ICP Data for Wyoming Bentonite and 2.5% Lime, Compacted on the 6/6/97 and Tested 7 days after Compaction for 6 Hours at 60 Revolutions per Minute. Centrifuged at 11000rpm for 30 minutes.

Solid to Liquid Ratio	Initial Cube Size (mm)	Concentration of Element in Solution in mg/kg (ppm)							
		Calcium (Ca)	Iron (Fe)	Lead (Pb)	Sodium (Na)	Silicon (Si)	Magnesium (Mg)	Aluminium (Al)	Manganese (Mn)
1/10	10	4.251	0.5444	D 0.0000	262.3	43.86	0.3474	2.354	D 0.0016
	20	4.552	2.288	D 0.0000	235.0	67.55	1.394	9.581	D 0.0051
1/20	10	15.84	19.44	D 0.0000	218.2	286.1	13.38	82.20	0.0191
	20	9.665	13.96	D 0.0000	180.6	204.5	8.975	58.23	0.0147
1/40	10	13.03	16.65	D 0.0000	156.3	244.4	10.77	69.03	0.0154
	20	18.24	20.35	D 0.0000	134.7	165.5	13.88	82.99	0.0232

Table A1.128 ICP Data for Wyoming Bentonite and 2.5% Lime, Compacted on the 6/6/97 and Tested 175 days after Compaction for 6 Hours at 60 Revolutions per Minute. Centrifuged at 11000rpm for 30 minutes.

Solid to Liquid Ratio	Initial Cube Size (mm)	Concentration of Element in Solution in mg/kg (ppm)							
		Calcium (Ca)	Iron (Fe)	Lead (Pb)	Sodium (Na)	Silicon (Si)	Magnesium (Mg)	Aluminium (Al)	Manganese (Mn)
1/10	10	314.9	383.4	D 0.0000	397.8	3899	251.1	1569	0.4000
	20	197.9	260.5	D 0.0000	304.0	2539	169.0	1067	0.2800
1/20	10	215.8	265.1	D 0.0000	279.8	2631	173.9	1075	0.2750
	20	110.5	143.7	D 0.0000	191.6	1430	94.10	572.0	0.1600
1/40	10	106.7	127.4	D 0.0000	170.9	1066	84.05	525.0	0.1650
	20	65.25	90.80	D 0.0000	139.8	753.0	60.00	367.9	0.1000

Note: 'D' indicates the stated value is below detection limits and the value stated is a system estimate. 'd' indicates the stated value is close to detection limits.

Table A1.129 ICP Data for Wyoming Bentonite and 2.5% Lime, Compacted on the 4/6/97 and Tested 7 days after Compaction for 24 Hours at 30 Revolutions per Minute. Centrifuged at 11000rpm for 30 minutes.

Solid to Liquid Ratio	Initial Cube Size (mm)	Concentration of Element in Solution in mg/kg (ppm)							
		Calcium (Ca)	Iron (Fe)	Lead (Pb)	Sodium (Na)	Silicon (Si)	Magnesium (Mg)	Aluminium (Al)	Manganese (Mn)
1/10	10	4.755	0.4957	D 0.0164	253.9	45.07	0.2994	1.997	D 0.0030
	20	5.098	0.5697	D 0.0051	263.6	51.39	0.3452	2.214	D 0.0016
1/20	10	4.889	1.090	D 0.0172	218.3	56.66	0.6795	4.399	D 0.0024
	20	4.254	1.287	D 0.0135	218.5	60.60	0.8166	5.231	D 0.0017
1/40	10	33.80	39.68	D 0.0000	176.6	447.6	25.65	158.6	0.0365
	20	28.94	30.47	D 0.0000	173.5	375.3	17.95	121.2	0.0299

Table A1.130 ICP Data for Wyoming Bentonite and 2.5% Lime, Compacted on the 4/6/97 and Tested 175 days after Compaction for 24 Hours at 30 Revolutions per Minute. Centrifuged at 11000rpm for 30 minutes.

Solid to Liquid Ratio	Initial Cube Size (mm)	Concentration of Element in Solution in mg/kg (ppm)							
		Calcium (Ca)	Iron (Fe)	Lead (Pb)	Sodium (Na)	Silicon (Si)	Magnesium (Mg)	Aluminium (Al)	Manganese (Mn)
1/10	10	263.7	260.4	D 0.0000	508.5	2735	179.4	1108	0.2850
	20	549.0	515.5	D 0.0000	496.4	5390	354.2	2148	0.5600
1/20	10	463.3	428.1	D 0.0000	364.5	4451	293.3	1852	0.4450
	20	323.3	320.0	D 0.0000	316.4	3329	217.2	1376	0.3250
1/40	10	181.7	182.6	D 0.0000	203.5	1897	125.7	790.0	0.1900
	20	171.7	173.4	D 0.0000	199.6	1799	119.4	746.5	0.1800

Table A1.131 ICP Data for Wyoming Bentonite and 2.5% Lime, Compacted on the 4/6/97 and Tested 301 days after Compaction for 24 Hours at 30 Revolutions per Minute. Centrifuged at 11000rpm for 30 minutes.

Solid to Liquid Ratio	Initial Cube Size (mm)	Concentration of Element in Solution in mg/kg (ppm)							
		Calcium (Ca)	Iron (Fe)	Lead (Pb)	Sodium (Na)	Silicon (Si)	Magnesium (Mg)	Aluminium (Al)	Manganese (Mn)
1/10	10	111.7	165.0	D 0.0000	404.8	1695	112.2	729.0	0.1600
	20	441.1	469.3	D 0.0000	517.0	4614	312.6	2025	0.5050
1/20	10	368.9	375.8	D 0.0000	381.5	3747	249.6	1631	0.4000
	20	346.3	343.2	D 0.0000	379.4	3395	235.2	1576	0.4050
1/40	10	194.2	196.1	D 0.0000	241.2	1960	134.3	871.0	0.2250
	20	179.1	192.0	D 0.0000	225.6	1994	129.4	831.5	0.2250

Note: 'D' indicates the stated value is below detection limits and the value stated is a system estimate. 'd' indicates the stated value is close to detection limits.

Table A1.132 ICP Data for Wyoming Bentonite and 2.5% Lime, Compacted on the 5/6/97 and Tested 7 days after Compaction for 24 Hours at 60 Revolutions per Minute. Centrifuged at 11000rpm for 30 minutes.

Solid to Liquid Ratio	Initial Cube Size (mm)	Concentration of Element in Solution in mg/kg (ppm)							
		Calcium (Ca)	Iron (Fe)	Lead (Pb)	Sodium (Na)	Silicon (Si)	Magnesium (Mg)	Aluminium (Al)	Manganese (Mn)
1/10	10	5.100	0.4859	D 0.0203	271.0	50.71	0.2983	1.903	D 0.0028
	20	4.670	0.5894	D 0.0317	266.3	51.39	0.3636	2.535	D 0.0032
1/20	10	4.460	1.569	D 0.0153	235.1	70.13	0.9579	6.312	D 0.0034
	20	4.419	2.030	D 0.0106	230.4	72.54	1.241	8.155	D 0.0037
1/40	10	13.37	14.03	D 0.0000	181.4	222.6	9.064	58.53	0.0132
	20	19.49	23.76	D 0.0000	172.4	312.3	14.36	93.51	0.0225

Table A1.133 ICP Data for Wyoming Bentonite and 2.5% Lime, Compacted on the 5/6/97 and Tested 175 days after Compaction for 24 Hours at 60 Revolutions per Minute. Centrifuged at 11000rpm for 30 minutes.

Solid to Liquid Ratio	Initial Cube Size (mm)	Concentration of Element in Solution in mg/kg (ppm)							
		Calcium (Ca)	Iron (Fe)	Lead (Pb)	Sodium (Na)	Silicon (Si)	Magnesium (Mg)	Aluminium (Al)	Manganese (Mn)
1/10	10	275.9	393.2	D 0.0000	490.2	3881	254.0	1595	0.4050
	20	329.6	401.5	D 0.0000	437.3	4160	263.7	1662	0.4250
1/20	10	284.6	345.7	D 0.0000	363.3	3488	229.6	1440	0.4150
	20	246.2	318.8	D 0.0000	345.6	3221	209.3	1305	0.3350
1/40	10	124.1	156.7	D 0.0000	208.2	1605	102.5	628.0	0.1900
	20	113.6	148.7	D 0.0000	196.7	1491	97.65	589.0	0.1800

Note : 'D' indicates the stated value is below detection limits and the value stated is a system estimate. 'd' indicates the stated value is close to detection limits.

A1.2.14 Wyoming Bentonite with 5000ppm Pb and 2.5% lime

A1.2.14.1 Centrifugation

The effects of centrifugation are again important for this design mix prior to analysis of the chemical data. At 7 days curing all samples could be filtered over a 24hr period in the cold room whilst at 175 and 301 days curing samples would not filter and had to be centrifuged. For comparison samples from one batch test at 7 days curing were centrifuged and chemically analysed and in parallel samples were filtered and analysed. The results of this analysis are shown in Tables A1.144 and A1.134. It is clear that for all solid to liquid ratios all Na values detected relate very well between centrifuged and filtered samples, however, only the 1:10 solid to liquid ratio centrifuged values for all elements are similar to the respective filtered values. This is particularly important when considering the leachability of Pb. Clearly for all filtered samples at 7 days curing (Tables A1.139, A1.137, A1.142 and A1.144) Pb is not detected, however after centrifugation Pb is present in high quantities which does not necessarily reflect the true chemical composition.

A1.2.14.2 Solid : liquid ratio

Inspection of Figures A1.59 to A1.62 shows variations in pH and conductivity that are a direct result of changing solid to liquid ratio. Increasing solid to liquid ratio results in large increases in both pH and conductivity. At 7 days curing the end of test conductivity values of 6hr/30rpm tests with 20mm cube sizes at the solid to liquid ratios 1:10, 1:20 and 1:40 were 2900µS/cm, 1931µS/cm and 1348µS/cm respectively whilst pH values were 11.98, 11.78 and 11.58 respectively. At 175 days curing conductivity values were 1814µS/cm, 1219µS/cm and 863µS/cm respectively whilst pH values were 11.42, 11.34 and 11.26 respectively. At 301 days curing conductivity values were 1737µS/cm, 1159µS/cm and 847µS/cm respectively whilst pH values were 11.39, 11.21 and 11.07 respectively. Increasing solid to liquid ratio from 1:40 to 1:20 at 7,175 and 301 days curing increased conductivity by factors of 1.43, 1.41 and 1.37 respectively whilst pH values increased by 0.20, 0.08 and 0.14 pH divisions respectively. Increasing solid to liquid ratio further from 1:20 to 1:10 increased conductivity by factors of 1.50, 1.49 and 1.50 respectively whilst pH increased by 0.20, 0.08 and 0.18 pH divisions respectively. Analysis of the chemical data from the filtered samples in Tables A1.139, A1.137, A1.142 and A1.144 illustrate that as solid

to liquid ratio decreased, levels of Si and Mg increased, Na decreased, Ca fluctuated and Pb, Fe, Al and Mn were generally below detection limits. At 175 and 301 days curing samples were centrifuged and as expected, as solid to liquid ratio decreased levels of Ca, Fe, Pb, Na, Si, Mg, Al and Mn decreased.

It is evident from the data tables that the addition of the Pb contaminant liberated more Na from the Wyoming Bentonite compared with the uncontaminated lime treated sample due to the increased cation exchange.

A1.2.14.3 Cube Size

Analysis of Figures A1.59 to A1.62 shows the smaller cube size generally produces higher pH and conductivity values especially at the lower solid to liquid ratios. Since Na concentrations of both filtered and centrifuged samples are similar in magnitude for specific solid to liquid ratios (e.g. Tables A1.144 and A1.134) and that Na concentrations are the highest of all elements it is not surprising that Na release changes similarly to conductivity. Hence where conductivity is higher for a specific cube size Na levels are also higher. The levels of other elements appear highly variable and not dependent on cube size. Observation of Figure A1.59 to A1.62 illustrates that the solid to liquid ratio 1:40 results in the highest degree of variability between cube sizes.

A1.2.14.4 Rotation speed and test duration

Comparisons of 6hr tests at 7 days curing (Figures A1.59 and A1.60) indicate slightly higher pH and conductivity values for the higher rotation speed. Tables A1.144, A1.135 and A1.137, A1.138 illustrate that this is in part due to significantly higher Na concentrations at 7 and 175 days curing. 7 day curing results for filtered samples in Tables A1.144 and A1.137 illustrate that levels of Fe and Mg reduce, Si remains unchanged and Ca varies with increasing rotation speed.

Comparison of 24hr tests at 7 days (Figures A1.61 and A1.62) indicate similar pH and conductivity for varying rotation speeds which is again illustrated in similar Na levels at specific solid to liquid ratios. At 175 days curing conductivity values are unaffected hence Na levels are similar in Tables A1.140 and A1.143, although pH values are significantly lower as the rotation speed increases.

Comparison of 30rpm tests (Figures A1.59 and A1.61) show that at 7 days curing the longer test duration increases pH and conductivity values whilst at 175 and

301 days curing this effect is reduced to insignificant at 301 days. These changes are again reflected in Na changes in Tables A1.134, A1.135, A1.136 and A1.139, A1.140, A1.141. It is also clear that the longer duration releases generally more Si, Mg and Al at any curing period, either filtered or centrifuged. Comparison of 60rpm tests (Figures A1.60 and A1.62) show no significant changes in pH or conductivity with increases test duration at 7 days or 175 days. Analysis of Tables A1.137, A1.138 and A1.142, A1.143 do however show similar behaviour to the 30rpm tests.

A1.2.14.5 Curing Time

It is evident from Figures A1.59 to A1.62 that as curing period increases pH and conductivity drop significantly from 7 to 175 days curing and continue to decrease by a reduced magnitude from 175 to 301 days curing. The chemical data shows highly variable behaviour although similarly to Wyoming Bentonite with no contaminants and 2.5% lime, as pH and conductivity drops with increasing curing period the degree of flocculation appears to reduce. It is also clear that as curing period increases the variation in pH due to changes in solid to liquid ratio is less significant.

Figure A1.59 Conductivity and pH characteristics for Wyoming Bentonite with 5000ppm Pb and 2.5% lime during 6hr/30rpm Batch Tests

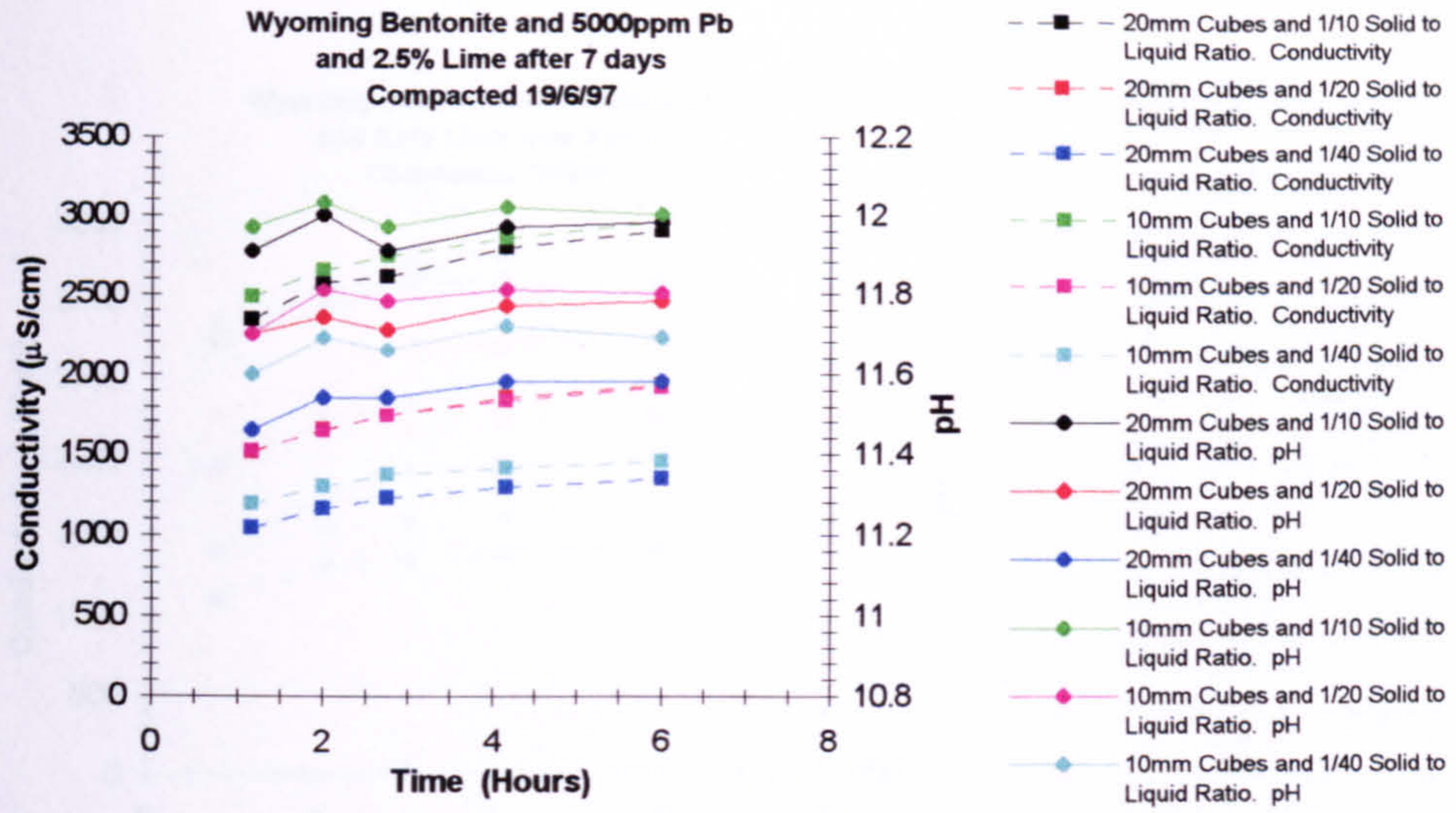

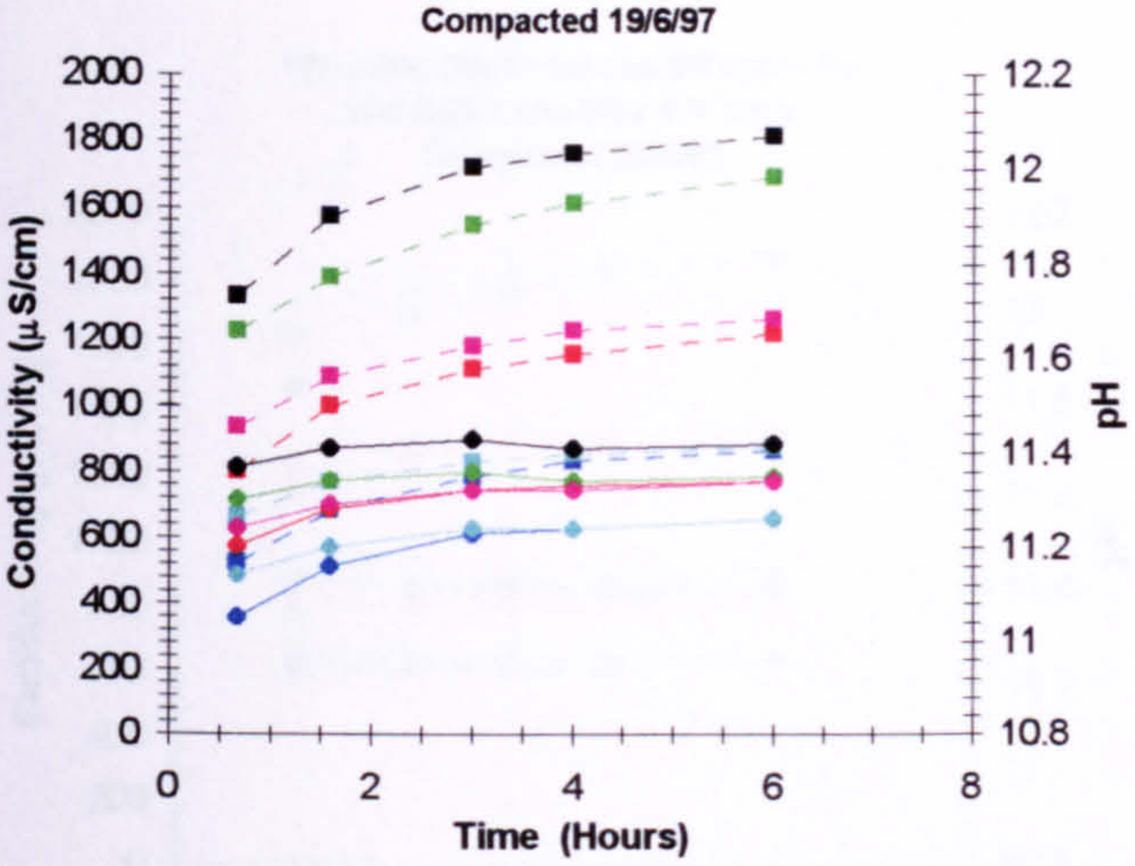

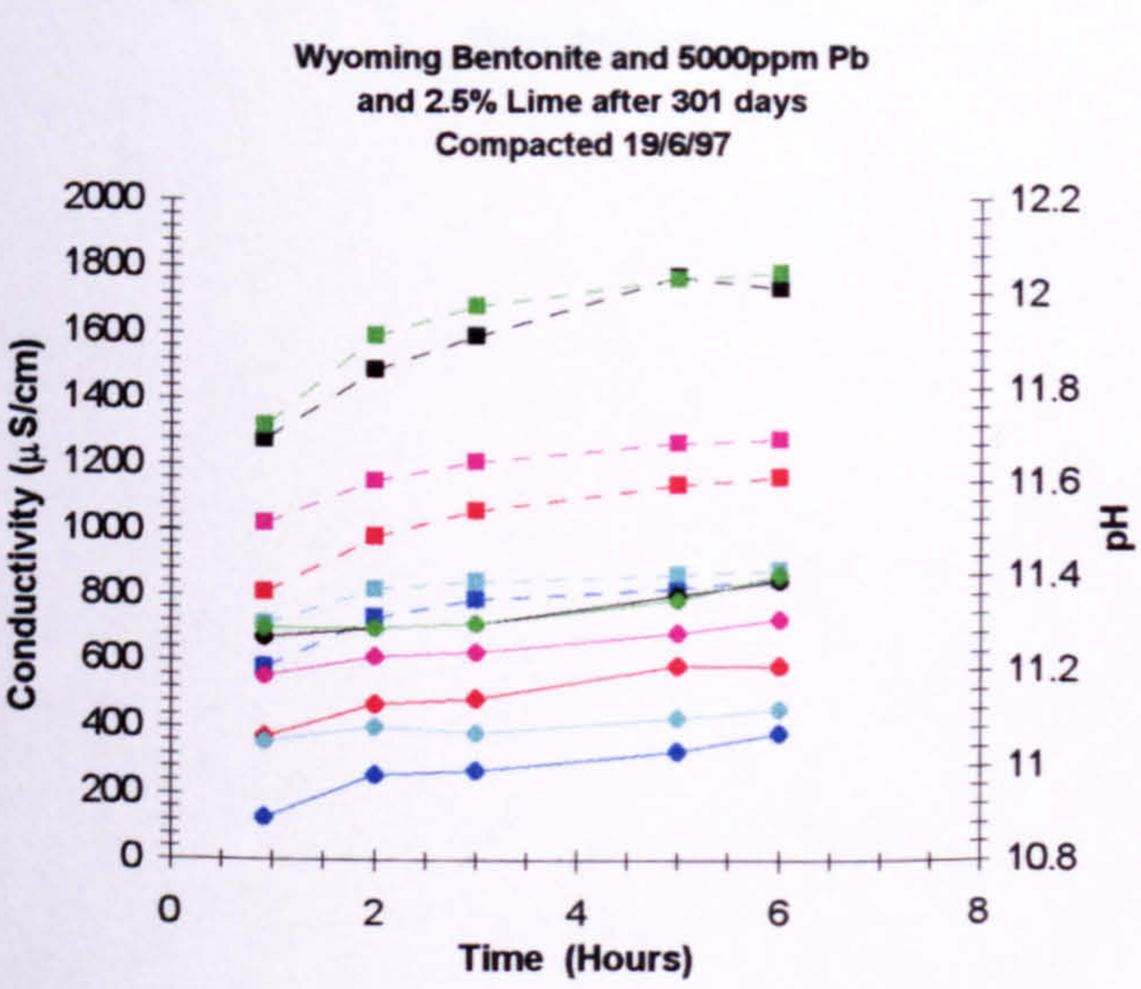

Figure A1.60 Conductivity and pH characteristics for Wyoming Bentonite with 5000ppm Pb and 2.5% lime during 6hr/60rpm Batch Tests

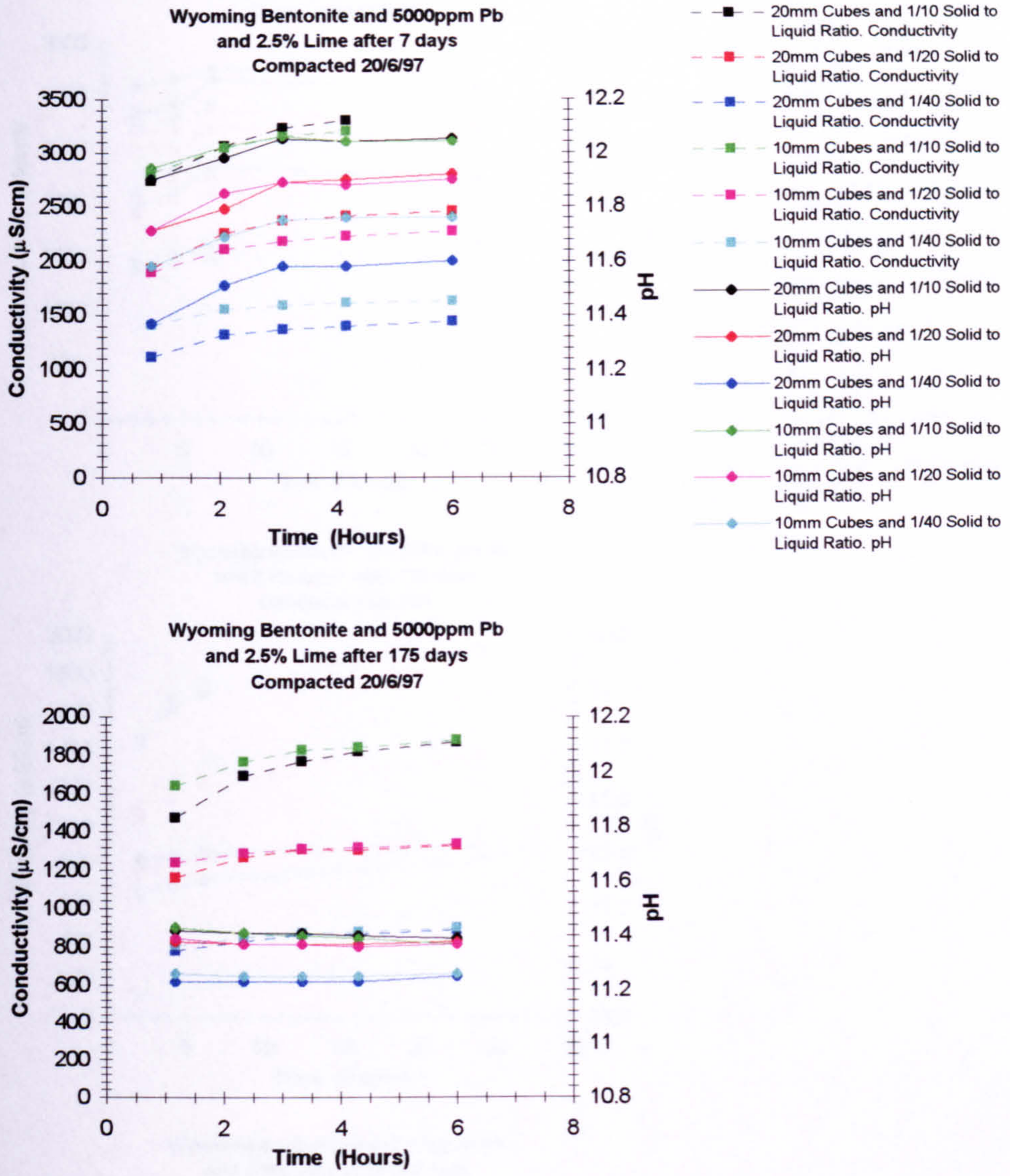

Figure A1.61 Conductivity and pH characteristics for Wyoming Bentonite with 5000ppm Pb and 2.5% lime during 24hr/30rpm Batch Tests

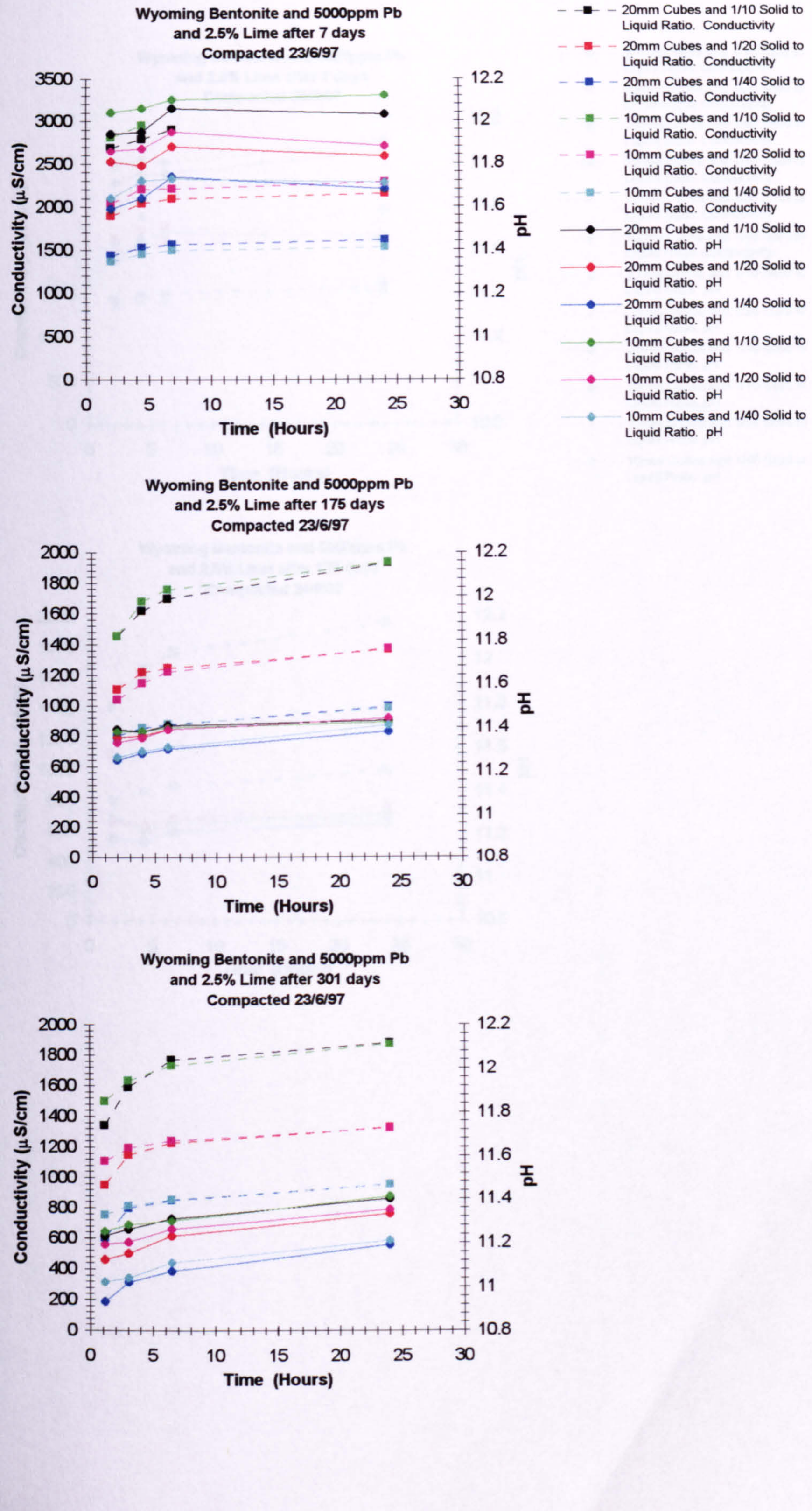

Figure A1.62 Conductivity and pH characteristics for Wyoming Bentonite with 5000ppm Pb and 2.5% lime during 24hr/60rpm Batch Tests

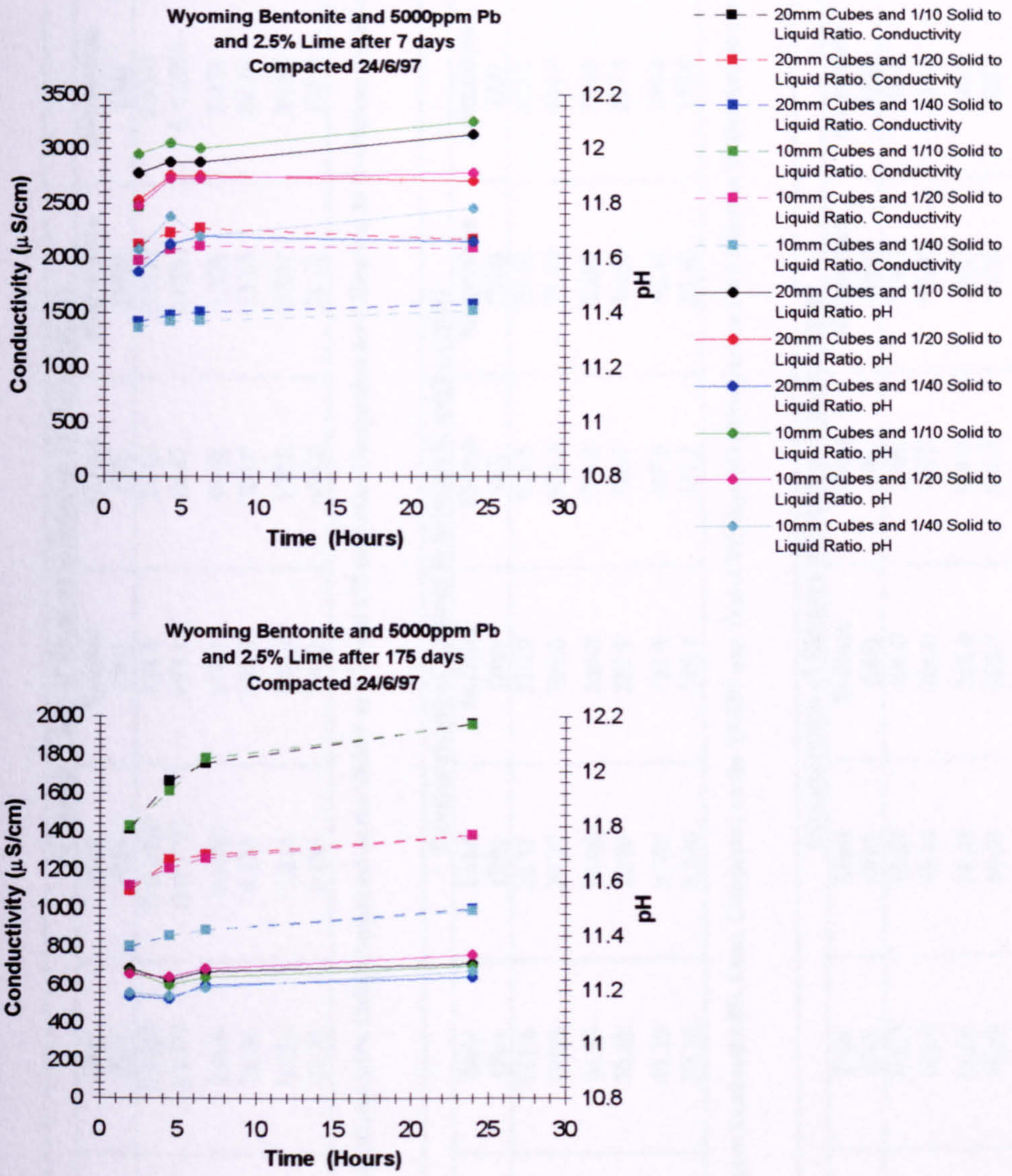

Table A1.134 ICP Data for Wyoming Bentonite and 5000ppm Lead and 2.5% Lime, Compacted on the 19/6/97 and Tested 7 days after Compaction for 6 Hours at 30 Revolutions per Minute. Centrifuged at 11000rpm for 30 minutes.

Solid to Liquid Ratio	Initial Cube Size (mm)	Concentration of Element in Solution in mg/kg (ppm)							
		Calcium (Ca)	Iron (Fe)	Lead (Pb)	Sodium (Na)	Silicon (Si)	Magnesium (Mg)	Aluminium (Al)	Manganese (Mn)
1/10	10	5.551	0.1224	D 0.2262	434.5	21.80	0.1122	0.9541	D 0.0000
	20	5.919	0.1479	D 0.1757	437.1	18.67	0.0863	d. 0.5056	D 0.0014
1/20	10	5.562	2.006	0.4688	271.3	48.32	1.223	8.171	D 0.0018
	20	16.44	21.36	4.131	288.0	303.0	13.63	86.16	0.0213
1/40	10	9.717	9.756	1.814	196.4	130.8	5.934	39.33	0.0083
	20	30.26	32.79	6.886	200.2	454.0	21.12	135.0	0.0345

Table A1.135 ICP Data for Wyoming Bentonite 5000ppm Lead and 2.5% Lime, Compacted on the 19/6/97 and Tested 175 days after Compaction for 6 Hours at 30 Revolutions per Minute. Centrifuged at 11000rpm for 30 minutes.

Solid to Liquid Ratio	Initial Cube Size (mm)	Concentration of Element in Solution in mg/kg (ppm)							
		Calcium (Ca)	Iron (Fe)	Lead (Pb)	Sodium (Na)	Silicon (Si)	Magnesium (Mg)	Aluminium (Al)	Manganese (Mn)
1/10	10	72.75	111.6	22.11	320.0	913.5	73.10	455.6	0.1050
	20	78.05	108.6	20.72	349.0	884.5	71.15	440.0	0.1200
1/20	10	58.00	94.55	18.06	246.2	778.0	62.60	390.9	0.0950
	20	45.12	70.20	12.80	225.9	570.5	46.66	287.3	0.0850
1/40	10	33.00	49.29	9.560	151.6	407.6	32.37	199.4	0.0550
	20	27.01	39.16	8.240	146.7	321.3	25.96	157.0	0.0400

Table A1.136 ICP Data for Wyoming Bentonite and 5000ppm Lead and 2.5% Lime, Compacted on the 19/6/97 and Tested 301 days after Compaction for 6 Hours at 30 Revolutions per Minute. Centrifuged at 11000rpm for 30 minutes.

Solid to Liquid Ratio	Initial Cube Size (mm)	Concentration of Element in Solution in mg/kg (ppm)							
		Calcium (Ca)	Iron (Fe)	Lead (Pb)	Sodium (Na)	Silicon (Si)	Magnesium (Mg)	Aluminium (Al)	Manganese (Mn)
1/10	10	104.9	160.7	33.29	406.0	1088	108.1	700.0	0.1950
	20	95.40	146.5	30.44	366.0	1093	98.50	636.5	0.2900
1/20	10	54.20	81.00	16.45	265.4	594.0	55.05	343.5	0.0950
	20	51.40	79.80	16.51	225.7	589.5	54.75	342.9	0.1350
1/40	10	26.97	37.48	7.335	153.7	384.9	25.47	159.35	0.0850
	20	31.60	45.00	9.585	148.2	440.0	31.06	189.1	0.1150

Note: 'D' indicates the stated value is below detection limits and the value stated is a system estimate. 'd' indicates the stated value is close to detection limits.

Table A1.137 ICP Data for Wyoming Bentonite and 5000ppm Lead and 2.5% Lime, Compacted on the 20/6/97 and Tested 7 days after Compaction for 6 Hours at 60 Revolutions per Minute. ***Filtered only.***

Solid to Liquid Ratio	Initial Cube Size (mm)	Concentration of Element in Solution in mg/kg (ppm)							
		Calcium (Ca)	Iron (Fe)	Lead (Pb)	Sodium (Na)	Silicon (Si)	Magnesium (Mg)	Aluminium (Al)	Manganese (Mn)
1/10	10	1.807	D 0.0087	D 0.0184	463.6	15.72	0.0312	D 0.0332	D 0.0007
	20	1.355	D 0.0221	D 0.0271	465.2	14.53	0.0441	D 0.1077	D 0.0000
1/20	10	1.479	D 0.0251	D 0.0000	279.9	23.22	0.0447	D 0.0978	D 0.0006
	20	1.337	D 0.0119	D 0.0020	292.0	17.91	0.0281	D 0.0581	D 0.0000
1/40	10	5.658	D 0.0215	D 0.0087	201.4	26.04	0.0479	D 0.0942	D 0.0009
	20	4.582	D 0.0293	D 0.0000	192.5	31.02	0.0460	D 0.1657	D 0.0006

Table A1.138 ICP Data for Wyoming Bentonite 5000ppm Lead and 2.5% Lime, Compacted on the 20/6/97 and Tested 175 days after Compaction for 6 Hours at 60 Revolutions per Minute. ***Centrifuged at 11000rpm for 30 minutes.***

Solid to Liquid Ratio	Initial Cube Size (mm)	Concentration of Element in Solution in mg/kg (ppm)							
		Calcium (Ca)	Iron (Fe)	Lead (Pb)	Sodium (Na)	Silicon (Si)	Magnesium (Mg)	Aluminium (Al)	Manganese (Mn)
1/10	10	96.05	113.4	21.38	372.6	936.0	74.95	466.8	0.1100
	20	88.85	101.2	18.98	360.0	831.0	66.40	418.6	0.0900
1/20	10	43.18	58.30	11.07	236.9	482.3	38.32	239.5	0.0500
	20	32.93	44.38	8.010	219.8	372.4	29.38	180.8	0.0500
1/40	10	25.87	32.25	5.885	153.5	274.9	21.68	129.7	0.0500
	20	28.82	36.81	7.090	154.8	313.3	24.95	151.0	0.0700

Note: 'D' indicates the stated value is below detection limits and the value stated is a system estimate. 'd' indicates the stated value is close to detection limits.

Table A1.139 ICP Data for Wyoming Bentonite and 5000ppm Lead and 2.5% Lime, Compacted on the 23/6/97 and Tested 7 days after Compaction for 24 Hours at 30 Revolutions per Minute. Filtered only.

Solid to Liquid Ratio	Initial Cube Size (mm)	Concentration of Element in Solution in mg/kg (ppm)							
		Calcium (Ca)	Iron (Fe)	Lead (Pb)	Sodium (Na)	Silicon (Si)	Magnesium (Mg)	Aluminium (Al)	Manganese (Mn)
1/10	10	1.304	D 0.0557	D 0.0316	502.5	17.71	0.0829	D 0.1188	D 0.0000
	20	1.990	D 0.0182	D 0.0290	480.2	19.90	0.0415	D 0.1159	D 0.0000
1/20	10	1.744	D 0.0121	D 0.0079	321.4	26.20	0.0522	D 0.0356	D 0.0000
	20	5.473	d. 0.0235	D 0.0175	331.9	30.84	0.0705	D 0.0885	D 0.0003
1/40	10	4.515	3.718	0.6821	209.8	77.43	2.395	15.07	D 0.0050
	20	1.444	0.1230	D 0.0180	209.1	32.77	0.0894	d. 0.4170	D 0.0000

Table A1.140 ICP Data for Wyoming Bentonite 5000ppm Lead and 2.5% Lime, Compacted on the 23/6/97 and Tested 175 days after Compaction for 24 Hours at 30 Revolutions per Minute. ***Centrifuged at 11000rpm for 30 minutes.***

Solid to Liquid Ratio	Initial Cube Size (mm)	Concentration of Element in Solution in mg/kg (ppm)							
		Calcium (Ca)	Iron (Fe)	Lead (Pb)	Sodium (Na)	Silicon (Si)	Magnesium (Mg)	Aluminium (Al)	Manganese (Mn)
1/10	10	138.1	173.5	32.09	415.2	1810	111.95	700.5	0.1900
	20	97.35	125.6	24.60	380.5	1057	82.65	517.0	0.1300
1/20	10	73.25	99.40	18.37	265.5	818.5	66.05	410.2	0.1300
	20	70.95	98.95	18.76	268.6	806.5	65.75	404.4	0.1200
1/40	10	42.06	52.00	9.565	167.8	445.7	34.37	214.1	0.0750
	20	39.42	48.63	9.245	169.5	418.6	33.04	200.7	0.0550

Table A1.141 ICP Data for Wyoming Bentonite and 5000ppm Lead and 2.5% Lime, Compacted on the 23/6/97 and Tested 301 days after Compaction for 24 Hours at 30 Revolutions per Minute.

Centrifuged at 11000rpm for 30 minutes.

Solid to Liquid Ratio	Initial Cube Size (mm)	Concentration of Element in Solution in mg/kg (ppm)							
		Calcium (Ca)	Iron (Fe)	Lead (Pb)	Sodium (Na)	Silicon (Si)	Magnesium (Mg)	Aluminium (Al)	Manganese (Mn)
1/10	10	30.66	40.05	6.690	387.5	309.5	27.21	164.0	0.0500
	20	96.35	133.4	26.17	410.2	975.0	89.15	559.0	0.2100
1/20	10	69.15	101.1	19.24	285.2	723.0	68.35	429.6	0.1150
	20	45.35	67.45	13.34	277.4	511.0	45.32	283.3	0.1150
1/40	10	42.58	54.20	10.55	192.3	400.6	36.22	231.2	0.0650
	20	39.26	51.35	11.08	173.3	395.0	34.29	217.2	0.0800

Note: 'D' indicates the stated value is below detection limits and the value stated is a system estimate. 'd' indicates the stated value is close to detection limits.

Table A1.142 ICP Data for Wyoming Bentonite and 5000ppm Lead and 2.5% Lime, Compacted on the 24/6/97 and Tested 7 days after Compaction for 24 Hours at 60 Revolutions per Minute. Filtered only.

Solid to Liquid Ratio	Initial Cube Size (mm)	Concentration of Element in Solution in mg/kg (ppm)							
		Calcium (Ca)	Iron (Fe)	Lead (Pb)	Sodium (Na)	Silicon (Si)	Magnesium (Mg)	Aluminium (Al)	Manganese (Mn)
1/10	10	6.412	D 0.0125	D 0.0302	482.4	18.36	0.0761	D 0.0708	D 0.0007
	20	4.225	d. 0.0747	D 0.0225	499.5	25.20	0.1152	D 0.1881	D 0.0004
1/20	10	6.676	D 0.0424	D 0.0000	326.9	28.24	0.0554	D 0.0486	D 0.0008
	20	2.922	D 0.0077	D 0.0000	332.2	24.88	0.0394	D 0.0500	D 0.0000
1/40	10	1.807	D 0.0086	D 0.0058	227.7	33.34	0.0619	D 0.0238	D 0.0000
	20	2.607	D 0.0108	D 0.0005	225.2	32.60	0.0607	D 0.0233	D 0.0000

Table A1.143 ICP Data for Wyoming Bentonite 5000ppm Lead and 2.5% Lime, Compacted on the 24/6/97 and Tested 175 days after Compaction for 24 Hours at 60 Revolutions per Minute. ***Centrifuged at 11000rpm for 30 minutes.***

Solid to Liquid Ratio	Initial Cube Size (mm)	Concentration of Element in Solution in mg/kg (ppm)							
		Calcium (Ca)	Iron (Fe)	Lead (Pb)	Sodium (Na)	Silicon (Si)	Magnesium (Mg)	Aluminium (Al)	Manganese (Mn)
1/10	10	133.7	161.5	31.43	416.2	1735	104.8	671.5	0.1700
	20	107.1	160.0	31.68	428.2	1703	103.7	664.5	0.1850
1/20	10	94.00	125.6	23.55	280.2	1054	82.85	515.0	0.1350
	20	79.40	109.9	20.81	267.9	914	71.05	452.3	0.1200
1/40	10	58.70	66.50	12.81	190.2	566.5	44.04	273.7	0.0950
	20	52.50	63.90	12.06	179.4	543.5	42.07	263.3	0.0850

Table A1.144 ICP Data for Wyoming Bentonite and 5000ppm Lead and 2.5% Lime, Compacted on the 19/6/97 and Tested 7 days after Compaction for 6 Hours at 30 Revolutions per Minute. Filtered only.

Solid to Liquid Ratio	Initial Cube Size (mm)	Concentration of Element in Solution in mg/kg (ppm)							
		Calcium (Ca)	Iron (Fe)	Lead (Pb)	Sodium (Na)	Silicon (Si)	Magnesium (Mg)	Aluminium (Al)	Manganese (Mn)
1/10	10	1.876	D 0.0260	D 0.0297	419.5	12.18	0.0680	D 0.1272	D 0.0033
	20	1.644	0.1463	D 0.0430	406.35	12.36	0.1323	0.7726	D 0.0006
1/20	10	2.945	D 0.0111	D 0.0048	257.5	29.13	0.0439	D 0.0604	D 0.0006
	20	1.431	0.6330	D 0.0860	265.6	37.75	0.4358	2.651	D 0.0010
1/40	10	2.068	D 0.0214	D 0.0338	197.0	31.24	0.0501	D 0.0957	D 0.0003
	20	12.48	16.71	2.884	189.3	228.5	10.92	68.67	0.0216

Note: 'D' indicates the stated value is below detection limits and the value stated is a system estimate. 'd' indicates the stated value is close to detection limits.

A1.2.15 Wyoming Bentonite with 5000ppm Fe and 2.5% lime

A1.2.15.1 Centrifugation

All tests at all curing periods for this design mix filtered easily due to flocculation of the clay particles. Significantly no Fe was released at any curing period from any filtered sample.

It was considered a good opportunity to assess the effects of centrifugation on samples easily gravity filtered. The assessment was made on sludges produced by 24hr/30rpm batch tests at 175 and 301 days curing at all solid to liquid ratios and cube sizes. Comparison of Tables A1.155, A1.156 and A1.151, A1.152 show clearly that the results are very similar for most elements. It was however clear that centrifuged samples release slightly less Ca and Na. At the lower solid to liquid ratios levels of Fe, Si, Mg and Al were all higher. However, at the solid to liquid ratio 1:10 and a lesser extent 1:20 there was essentially no difference between filtered and centrifuged samples.

A1.2.15.2 Solid : liquid ratio

Inspections of Figures A1.63 to A1.66 illustrate a number of trends relating to solid to liquid ratio. In every case at every curing period, as solid to liquid ratio increased conductivity increased. At 7 days curing, as solid to liquid ratio increased pH also increased whilst often at 175 days pH decreased with increasing solid to liquid ratio (e.g. Figures A1.64 and A1.66).

At 7 days curing the conductivity of 6hr/30rpm tests with 20mm cube sizes were, 4130µS/cm 2670µS/cm and 1680µS/cm respectively whilst pH values were 11.78, 11.69 and 11.51 respectively. At 175 days curing the values were, 3110µS/cm 1905µS/cm and 1160µS/cm respectively whilst pH values were 11.04, 11.09 and 11.07 respectively. At 301 days curing the values were, 3080µS/cm 1875µS/cm and 1140µS/cm respectively whilst pH values were 11.00, 11.05 and 10.99 respectively. Increasing solid to liquid ratio from 1:40 to 1:20 at 7, 175 and 301 days curing therefore increased conductivity by factors of 1.58, 1.64, and 1.64 respectively whilst pH increased by 0.18, 0.02, and 0.06 pH divisions respectively. Increasing solid to liquid ratio further from 1:20 to 1:10 increased conductivity by factors of 1.55, 1.63 and 1.64 respectively whilst pH increased by 0.09, -0.05 and –0.05.

It is very clear that there is little variation in conductivity values between cube sizes for specific solid to liquid ratios, although in the case of pH there is high variability.

Table A1.150 for 24hr/30rpm tests shows typical levels of elements leached at 7 days curing. 20mm cubes release 51.8ppm Ca, 0.0900ppm Fe, 744ppm Na, 15.8ppm Si and 0.0697ppm Mg whilst other elements remain below detection limits. Tables A1.145 to A1.154 all generally show reductions in Ca and Na when solid to liquid ratio is reduced whilst levels of Si and Mg were clearly variable. It is therefore certain that changes in conductivity were predominantly related to changes in Na and to a lesser extent Ca.

A1.2.15.3 Cube Size

Generally the smaller cube size produces higher conductivity values. However at 7days curing where the solid to liquid ratio 1:10 produced the highest pH of all the solid to liquid ratios, the 10mm cubes produced the higher pH of the two cube sizes (Figure A1.63). At 175 days curing where the solid to liquid ratio 1:10 produced the lowest pH of all the solid to liquid ratios, the 10mm cubes produced the lower pH of the two cube sizes (Figure A1.64). The effects on conductivity are reflected in the Na concentration variations in Tables A1.145 to A1.154.

A1.2.15.4 Rotation speed and test duration

Comparison of 6hr tests (Figures A1.63 and A1.64) show that at 7 and 175 days curing the higher rotation speed generally produced the lower pH values and similar conductivity values. Tables A1.145, A1.146 and A1.148, A1.149 show the higher rotation speed releases more Fe and Si whilst levels of Ca and Na show variable nature. Comparisons of 24hr tests (Figures A1.65 and A1.66, Tables A1.150, A1.151 and A1.153, A1.154) show similar behaviour to 6 hr tests, although the higher rotation speed also releases more Ca and Na after 24hr tests.

Comparison of 30rpm tests (Figures A1.63 and A1.65) show no change in final pH at any curing period due to the increased test duration although at 175 and 301 days curing conductivity levels are higher, particularly for the 1:10 and 1:20 solid to liquid ratios. This effect on conductivity is again reflected in Ca and particularly Na levels reported in Tables A1.146, A1.147 and A1.151, A1.152. Comparisons of

60rpm tests (Figures A1.64 and A1.66, Tables A1.153, A1.154 and A1.148, A1.149) show exactly the same behaviour as 30rpm tests for varying test duration.

A1.2.15.5 Curing Time

As curing period increased from 7 to 175 days, pH reduced significantly with moderate changes in conductivity. From 175 to 301 days curing pH slightly decreased with little change in conductivity. Tables A1.145 to A1.154 show generally small reductions in Ca as curing period increases. Levels of Na and Si generally increase with little variation in Mg whilst levels of Pb, Al and Mn remain below detection limits.

Figure A1.63 Conductivity and pH characteristics for Wyoming Bentonite with 5000ppm Fe and 2.5% lime during 6hr/30rpm Batch Tests

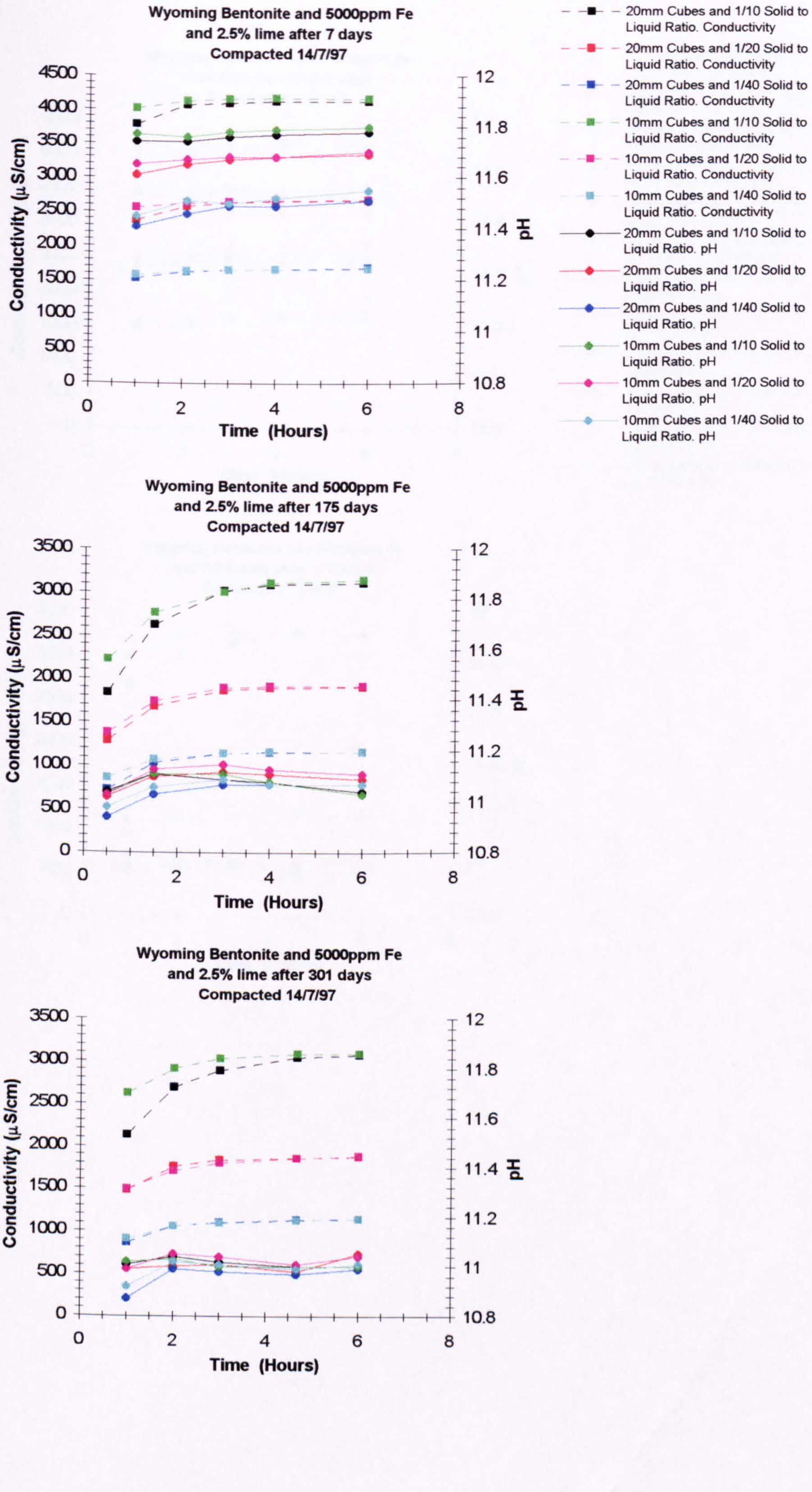

Figure A1.64 Conductivity and pH characteristics for Wyoming Bentonite with 5000ppm Fe and 2.5% lime during 6hr/60rpm Batch Tests

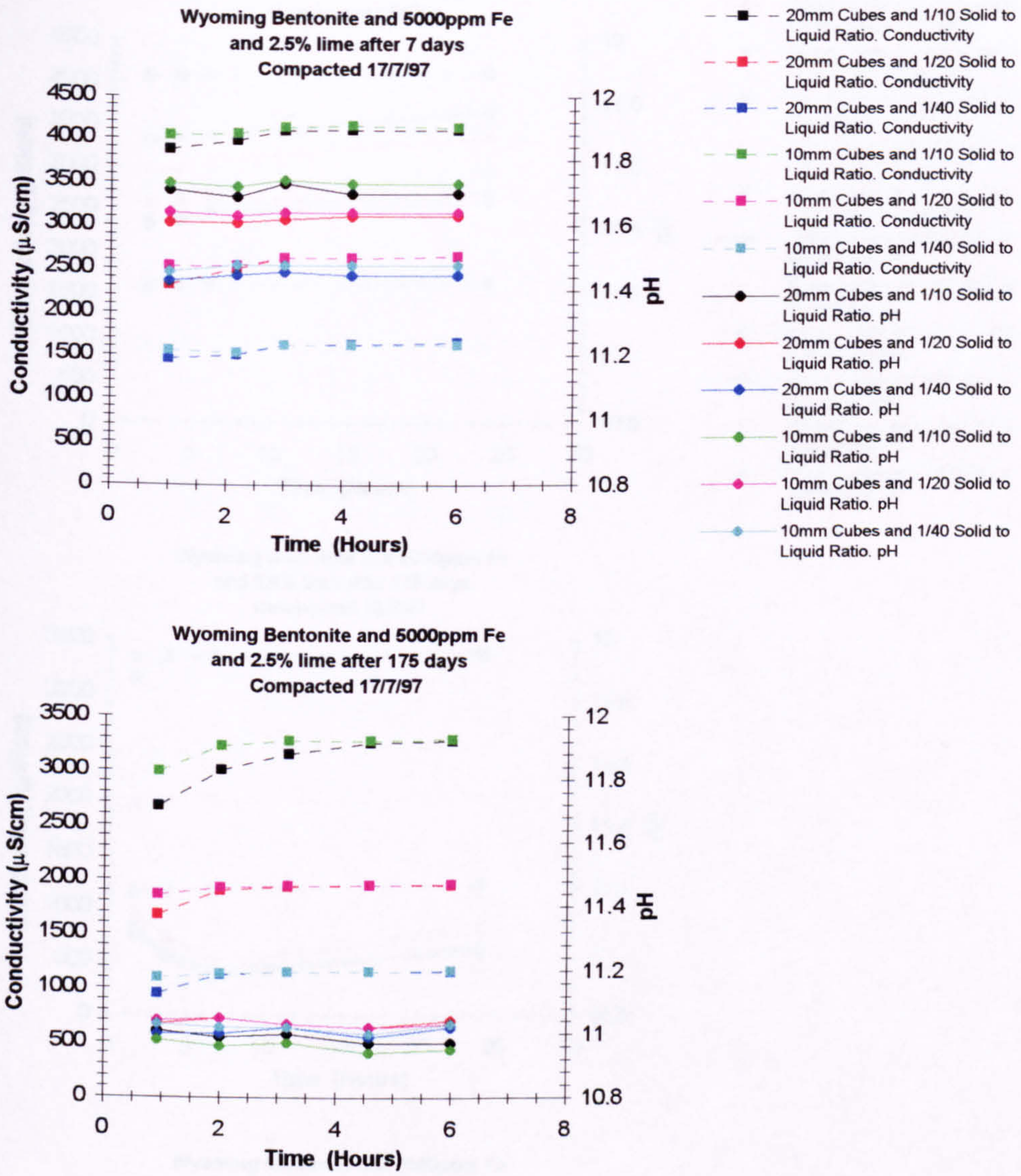

Figure A1.65 Conductivity and pH characteristics for Wyoming Bentonite with 5000ppm Fe and 2.5% lime during 24hr/30rpm Batch Tests

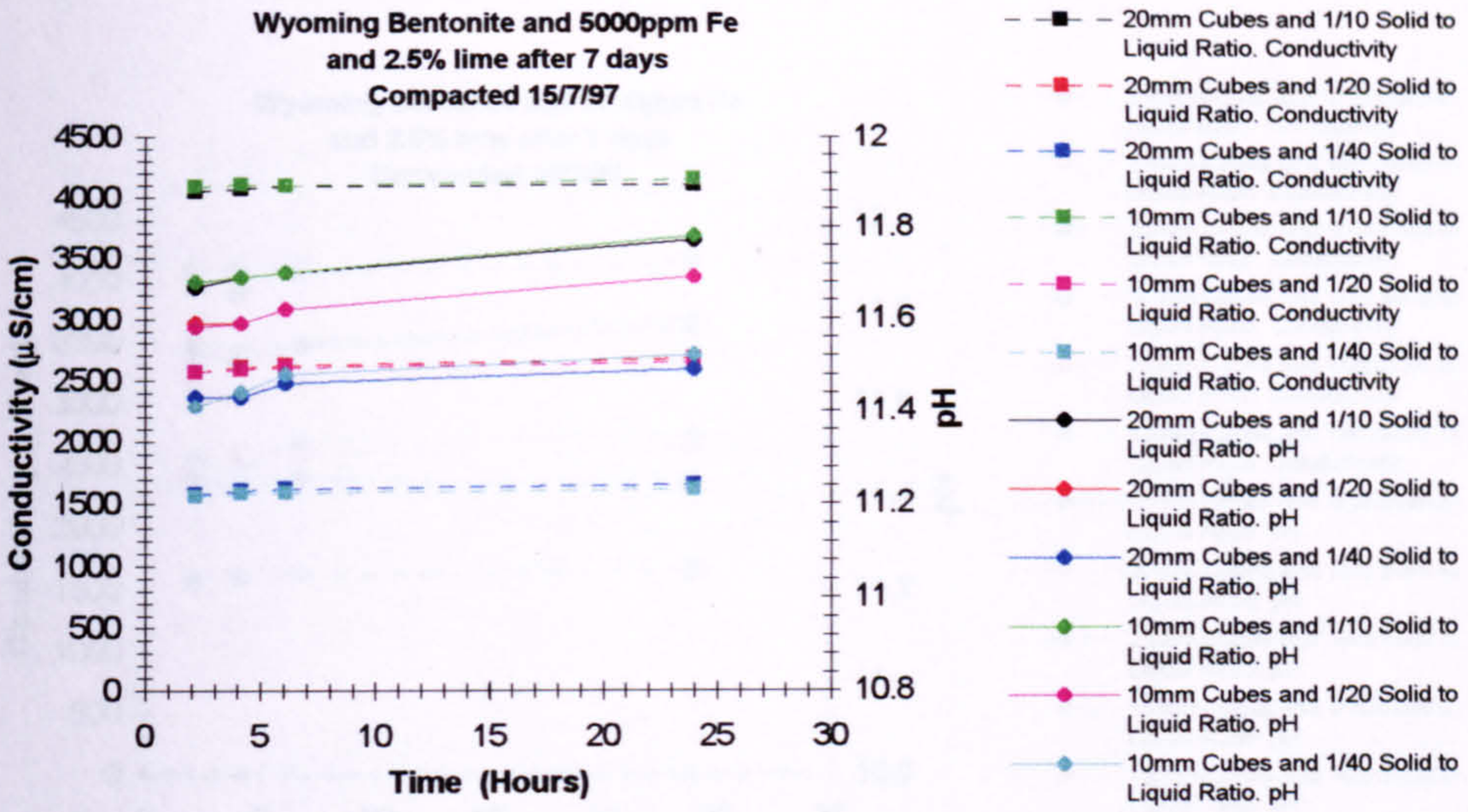

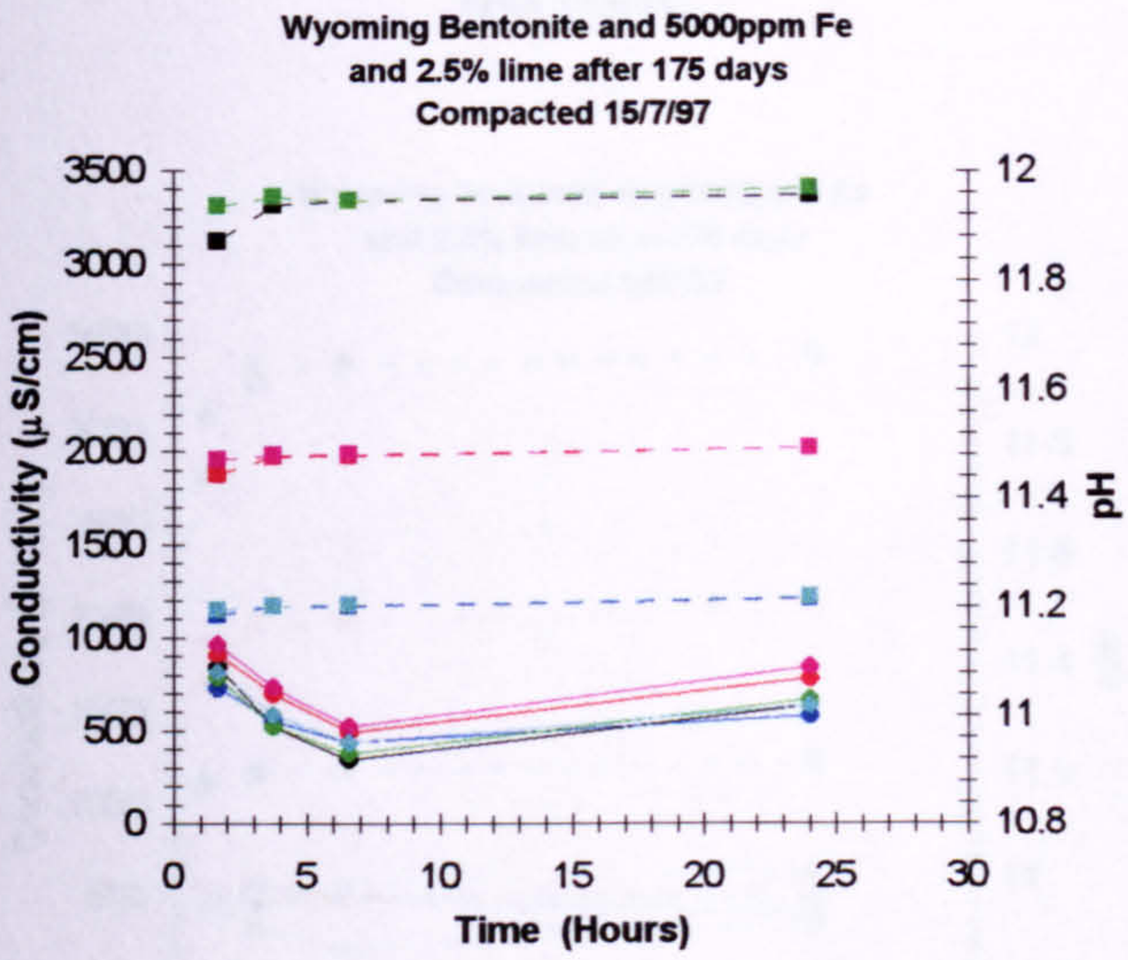

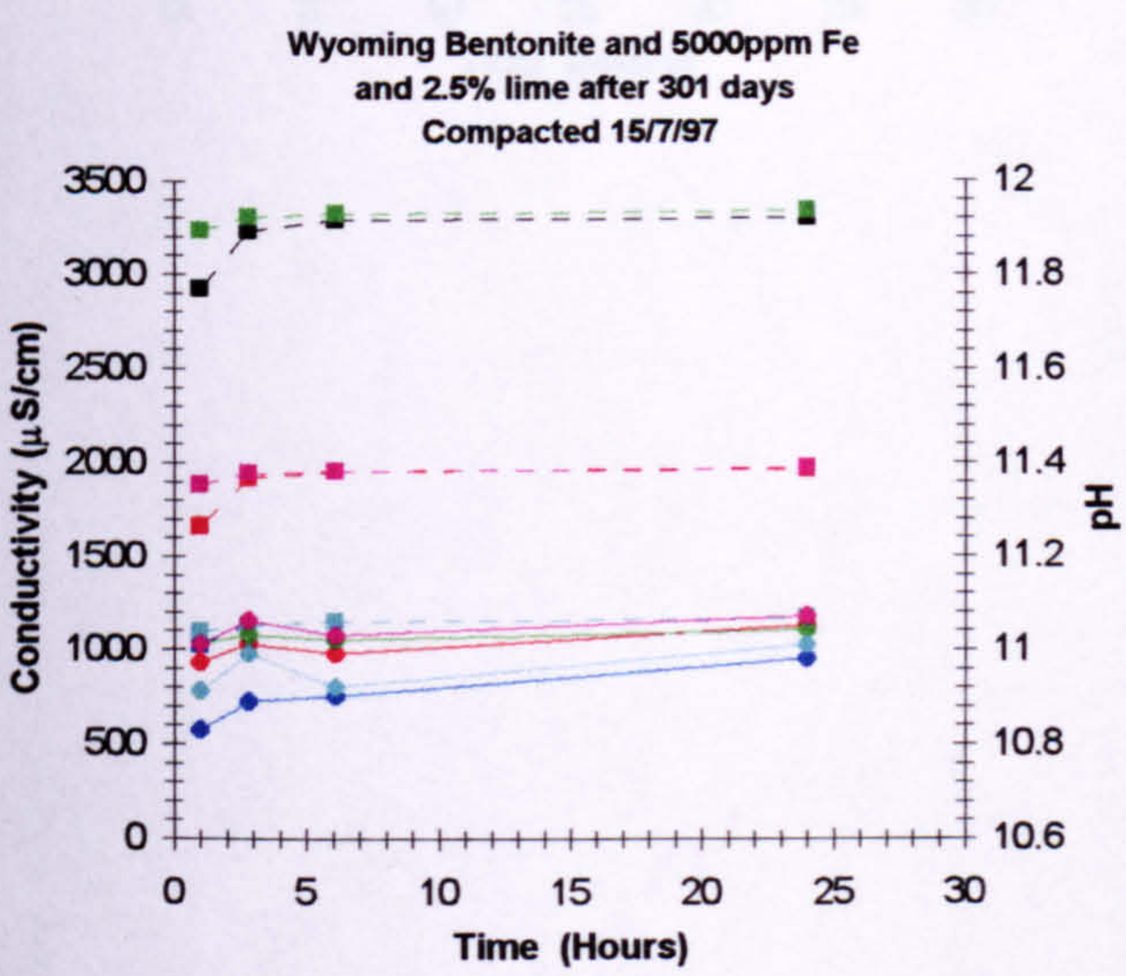

Figure A1.66 Conductivity and pH characteristics for Wyoming Bentonite with 5000ppm Fe and 2.5% lime during 24hr/60rpm Batch Tests

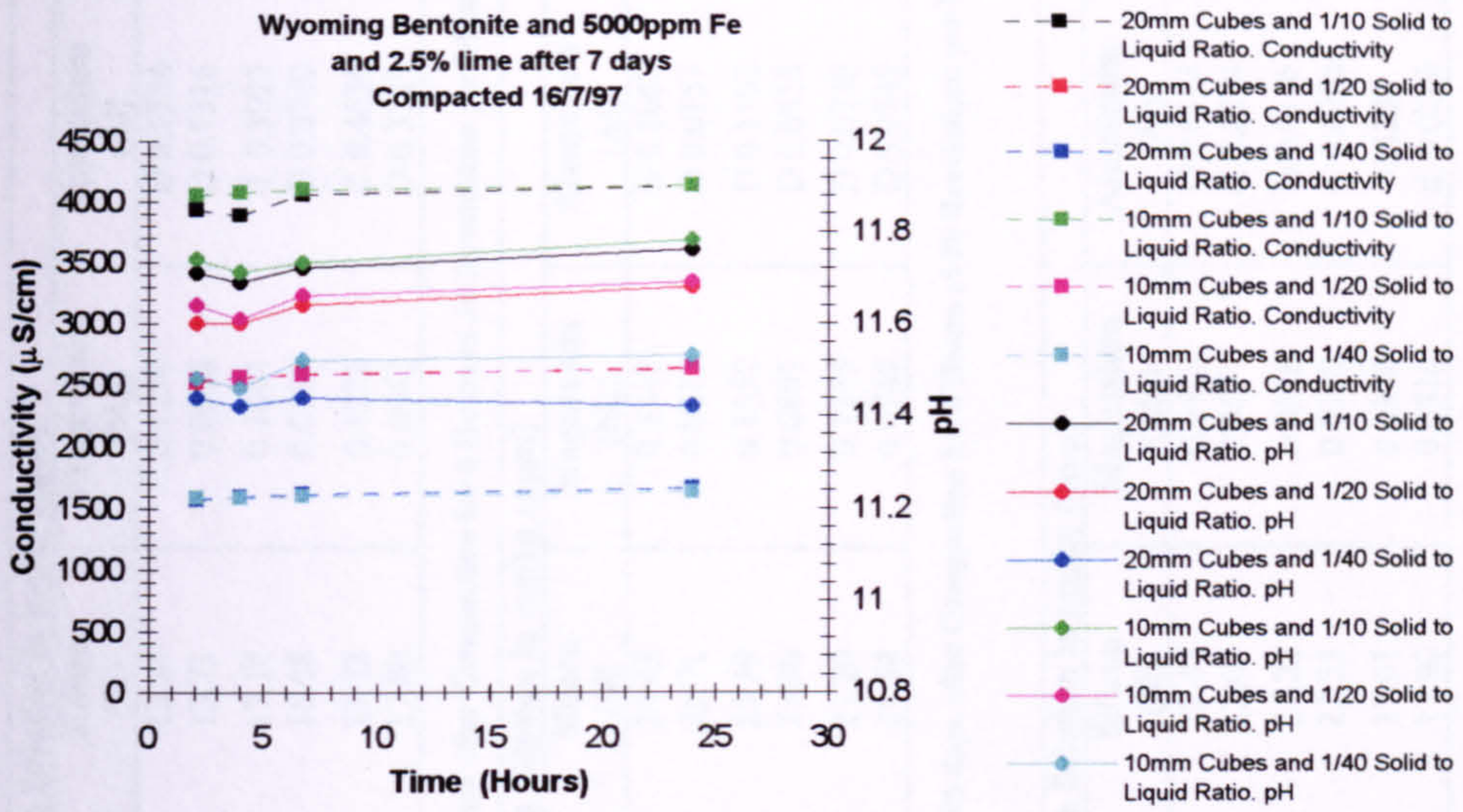

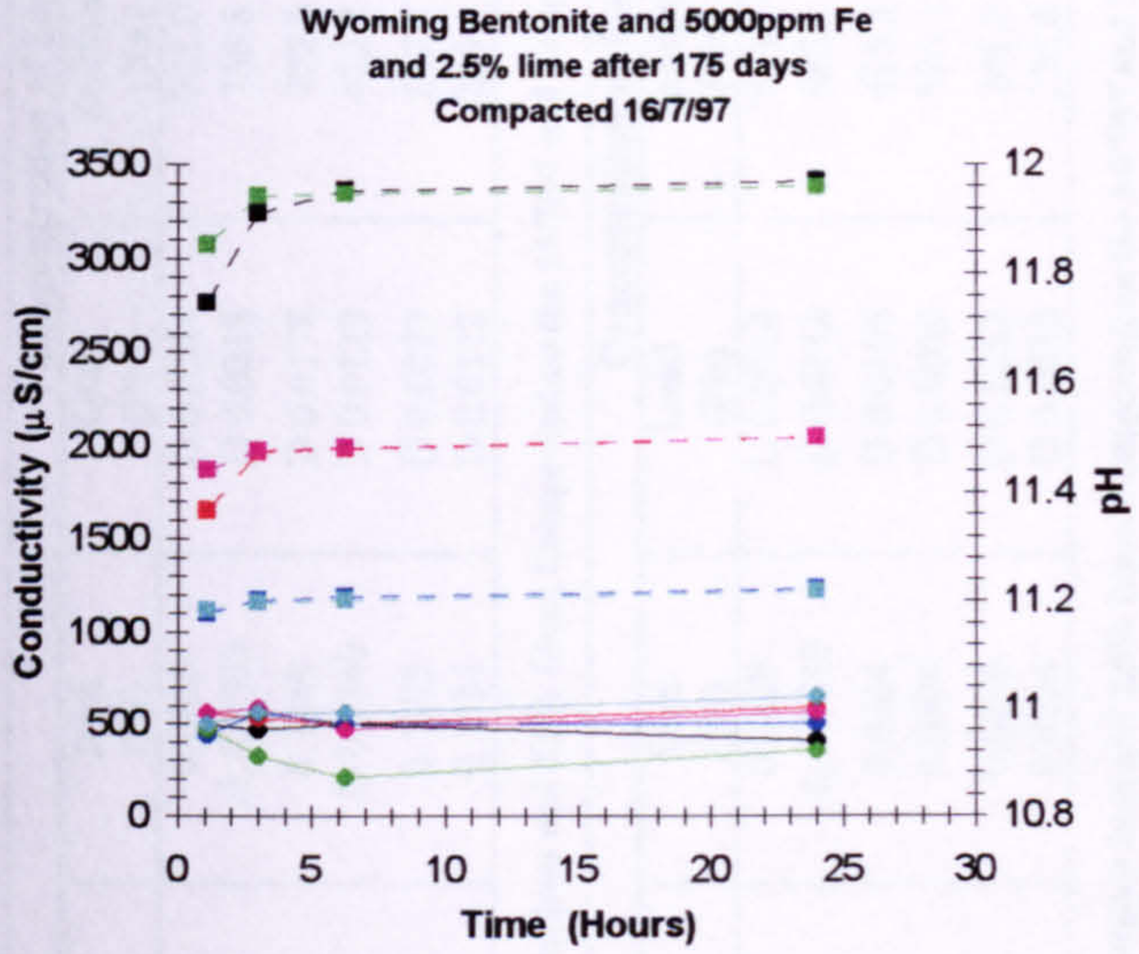

Table A1.145 ICP Data for Wyoming Bentonite and 5000ppm Iron and 2.5% Lime, Compacted on the 14/7/97 and Tested 7 days after Compaction for 6 Hours at 30 Revolutions per Minute. Filtered only.

Solid to Liquid Ratio	Initial Cube Size (mm)	Concentration of Element in Solution in mg/kg (ppm)							
		Calcium (Ca)	Iron (Fe)	Lead (Pb)	Sodium (Na)	Silicon (Si)	Magnesium (Mg)	Aluminium (Al)	Manganese (Mn)
1/10	10	13.90	0.0825	D 0.0244	721.0	13.34	0.1250	D 0.1384	D 0.0027
	20	35.80	d. 0.0585	D 0.0218	736.8	13.71	0.0928	D 0.1316	D 0.0011
1/20	10	15.67	0.1249	D 0.0178	402.9	17.18	0.1044	d. 0.3023	D 0.0014
	20	5.739	D 0.0340	D 0.0129	422.2	16.68	0.0589	D 0.0740	D 0.0009
1/40	10	8.640	0.1972	D 0.0037	227.7	17.72	0.1272	d. 0.4636	D 0.0020
	20	9.438	0.1334	D 0.0112	229.1	17.80	0.0842	D 0.3129	D 0.0010

Table A1.146 ICP Data for Wyoming Bentonite 5000ppm Iron and 2.5% Lime, Compacted on the 14/7/97 and Tested 175 days after Compaction for 6 Hours at 30 Revolutions per Minute. Filtered only.

Solid to Liquid Ratio	Initial Cube Size (mm)	Concentration of Element in Solution in mg/kg (ppm)							
		Calcium (Ca)	Iron (Fe)	Lead (Pb)	Sodium (Na)	Silicon (Si)	Magnesium (Mg)	Aluminium (Al)	Manganese (Mn)
1/10	10	49.19	0.0330	D 0.0014	673.7	24.43	0.1347	D 0.1063	D 0.0003
	20	47.93	d. 0.0019	D 0.0142	685.3	25.71	0.0475	D 0.0157	D 0.0004
1/20	10	24.03	0.0264	D 0.0105	415.3	25.59	0.1050	D 0.1102	D 0.0005
	20	24.64	0.0304	D 0.0020	386.5	25.00	0.0801	D 0.0555	D 0.0010
1/40	10	16.80	0.0959	D 0.0052	241.0	21.20	0.1255	D 0.0730	D 0.0017
	20	16.93	0.0254	D 0.0033	236.6	21.34	0.0740	D 0.0745	D 0.0005

Table A1.147 ICP Data for Wyoming Bentonite and 5000ppm Iron and 2.5% Lime, Compacted on the 14/7/97 and Tested 301 days after Compaction for 6 Hours at 30 Revolutions per Minute. Filtered only.

Solid to Liquid Ratio	Initial Cube Size (mm)	Concentration of Element in Solution in mg/kg (ppm)							
		Calcium (Ca)	Iron (Fe)	Lead (Pb)	Sodium (Na)	Silicon (Si)	Magnesium (Mg)	Aluminium (Al)	Manganese (Mn)
1/10	10	38.70	D 0.0024	D 0.0136	741.0	22.45	0.0458	D 0.0143	D 0.0002
	20	39.48	D 0.0038	D 0.0083	733.8	23.01	0.0671	d. 0.0224	D 0.0002
1/20	10	19.40	D 0.0034	D 0.0153	427.1	21.22	0.0316	D 0.0156	D 0.0001
	20	18.44	D 0.0027	D 0.0125	425.7	21.33	0.0380	d. 0.0066	D 0.0003
1/40	10	11.19	D 0.0302	D 0.0149	268.2	17.61	0.0398	0.1227	D 0.0004
	20	10.19	D 0.0066	D 0.0085	255.7	17.90	0.0316	d. 0.0286	D 0.0002

Note: 'D' indicates the stated value is below detection limits and the value stated is a system estimate.
'd' indicates the stated value is close to detection limits.

Table A1.148 ICP Data for Wyoming Bentonite and 5000ppm Iron and 2.5% Lime, Compacted on the 17/7/97 and Tested 7 days after Compaction for 6 Hours at 60 Revolutions per Minute. Filtered only.

Solid to Liquid Ratio	Initial Cube Size (mm)	Concentration of Element in Solution in mg/kg (ppm)							
		Calcium (Ca)	Iron (Fe)	Lead (Pb)	Sodium (Na)	Silicon (Si)	Magnesium (Mg)	Aluminium (Al)	Manganese (Mn)
1/10	10	48.69	0.2674	D 0.0076	682.4	15.29	0.1819	d. 0.3172	0.0081
	20	48.30	d. 0.0606	D 0.0215	681.9	14.23	0.1594	D 0.0824	D 0.0037
1/20	10	26.46	0.2806	D 0.0184	388.9	18.32	0.1913	D 0.2361	0.0186
	20	24.44	0.1127	D 0.0007	385.7	18.53	0.1373	D 0.0484	D 0.0027
1/40	10	15.83	d. 0.0758	D 0.0000	218.1	18.39	0.0859	D 0.0691	D 0.0017
	20	16.84	0.1046	D 0.0165	218.0	18.51	0.1177	D 0.0937	D 0.0023

Table A1.149 ICP Data for Wyoming Bentonite 5000ppm Iron and 2.5% Lime, Compacted on the 17/7/97 and Tested 175 days after Compaction for 6 Hours at 60 Revolutions per Minute. Filtered only.

Solid to Liquid Ratio	Initial Cube Size (mm)	Concentration of Element in Solution in mg/kg (ppm)							
		Calcium (Ca)	Iron (Fe)	Lead (Pb)	Sodium (Na)	Silicon (Si)	Magnesium (Mg)	Aluminium (Al)	Manganese (Mn)
1/10	10	46.53	D 0.0124	D 0.0308	769.7	26.41	0.0540	D 0.0155	D 0.0004
	20	46.58	D 0.0099	D 0.0181	755.5	27.66	0.0519	D 0.0017	D 0.0008
1/20	10	21.68	0.1091	D 0.0048	433.1	26.08	0.0888	0.3726	D 0.0007
	20	21.72	0.0161	D 0.0050	436.9	24.32	0.0510	D 0.0272	D 0.0007
1/40	10	9.442	0.0234	D 0.0117	251.5	22.42	0.0304	D 0.0612	D 0.0002
	20	10.90	0.0820	D 0.0155	253.8	22.55	0.0509	D 0.1931	D 0.0002

Note : 'D' indicates the stated value is below detection limits and the value stated is a system estimate.
'd' indicates the stated value is close to detection limits.

Table A1.150 ICP Data for Wyoming Bentonite and 5000ppm Iron and 2.5% Lime, Compacted on the 15/7/97 and Tested 7 days after Compaction for 24 Hours at 30 Revolutions per Minute. Filtered only.

Solid to Liquid Ratio	Initial Cube Size (mm)	Concentration of Element in Solution in mg/kg (ppm)							
		Calcium (Ca)	Iron (Fe)	Lead (Pb)	Sodium (Na)	Silicon (Si)	Magnesium (Mg)	Aluminium (Al)	Manganese (Mn)
1/10	10	48.60	0.0900	D 0.0000	712.7	15.81	0.0773	D 0.0964	D 0.0012
	20	51.78	0.0900	D 0.0000	744.8	15.83	0.0697	D 0.0907	D 0.0018
1/20	10	27.07	D 0.0586	D 0.0018	411.7	19.33	0.0521	D 0.0782	D 0.0012
	20	25.89	0.0935	D 0.0000	419.4	18.67	0.0585	D 0.0883	D 0.0012
1/40	10	17.17	d. 0.0619	D 0.0199	229.3	19.27	0.0604	D 0.1079	D 0.0011
	20	18.00	D 0.0574	D 0.0000	232.0	19.34	0.0649	D 0.0851	D 0.0007

Table A1.151 ICP Data for Wyoming Bentonite 5000ppm Iron and 2.5% Lime, Compacted on the 15/7/97 and Tested 175 days after Compaction for 24 Hours at 30 Revolutions per Minute. Filtered only.

Solid to Liquid Ratio	Initial Cube Size (mm)	Concentration of Element in Solution in mg/kg (ppm)							
		Calcium (Ca)	Iron (Fe)	Lead (Pb)	Sodium (Na)	Silicon (Si)	Magnesium (Mg)	Aluminium (Al)	Manganese (Mn)
1/10	10	46.89	D 0.0019	D 0.0000	721.5	28.06	0.0488	D 0.0000	D 0.0000
	20	47.13	d. 0.0172	D 0.0301	682.7	28.66	0.0877	D 0.0155	D 0.0022
1/20	10	22.27	D 0.0035	D 0.0235	413.5	28.33	0.0461	D 0.0000	D 0.0003
	20	22.41	0.0284	D 0.0000	419.3	27.20	0.0486	D 0.0331	D 0.0006
1/40	10	13.94	0.0212	D 0.0033	246.4	25.28	0.0386	D 0.0518	D 0.0001
	20	14.21	d. 0.0109	D 0.0146	237.8	24.50	0.0425	D 0.0344	D 0.0008

Table A1.152 ICP Data for Wyoming Bentonite and 5000ppm Iron and 2.5% Lime, Compacted on the 15/7/97 and Tested 301 days after Compaction for 24 Hours at 30 Revolutions per Minute. Filtered only.

Solid to Liquid Ratio	Initial Cube Size (mm)	Concentration of Element in Solution in mg/kg (ppm)							
		Calcium (Ca)	Iron (Fe)	Lead (Pb)	Sodium (Na)	Silicon (Si)	Magnesium (Mg)	Aluminium (Al)	Manganese (Mn)
1/10	10	43.26	d. 0.0069	D 0.0000	766.7	26.79	0.0475	d. 0.0221	D 0.0005
	20	43.15	D 0.0060	D 0.0000	764.6	26.63	0.0506	d. 0.0291	D 0.0005
1/20	10	19.48	D 0.0072	D 0.0001	427.5	25.28	0.0485	D 0.0244	D 0.0002
	20	22.35	d. 0.0164	D 0.0031	443.9	24.25	0.0793	D 0.0202	D 0.0002
1/40	10	12.88	0.3068	D 0.0037	261.4	22.54	0.2407	0.9487	D 0.0015
	20	9.649	0.2370	D 0.0012	257.1	22.54	0.1664	0.7932	D 0.0009

Note: 'D' indicates the stated value is below detection limits and the value stated is a system estimate.
'd' indicates the stated value is close to detection limits.

Table A1.153 ICP Data for Wyoming Bentonite and 5000ppm Iron and 2.5% Lime, Compacted on the 16/7/97 and Tested 7 days after Compaction for 24 Hours at 60 Revolutions per Minute. Filtered only.

Solid to Liquid Ratio	Initial Cube Size (mm)	Concentration of Element in Solution in mg/kg (ppm)							
		Calcium (Ca)	Iron (Fe)	Lead (Pb)	Sodium (Na)	Silicon (Si)	Magnesium (Mg)	Aluminium (Al)	Manganese (Mn)
1/10	10	50.50	0.1392	D 0.0000	709.8	16.88	0.1714	D 0.2888	D 0.0016
	20	51.69	D 0.0510	D 0.0000	701.5	15.83	0.1059	D 0.0770	D 0.0012
1/20	10	27.90	D 0.0500	D 0.0000	402.7	19.27	0.1614	D 0.0629	D 0.0008
	20	27.29	D 0.0536	D 0.0520	403.8	19.21	0.1092	D 0.0872	D 0.0012
1/40	10	19.56	D 0.0504	D 0.0050	229.5	19.76	0.2384	D 0.0520	D 0.0016
	20	17.02	D 0.0329	D 0.0240	224.4	19.34	0.0832	D 0.0518	D 0.0005

Table A1.154 ICP Data for Wyoming Bentonite 5000ppm Iron and 2.5% Lime, Compacted on the 16/7/97 and Tested 175 days after Compaction for 24 Hours at 60 Revolutions per Minute. Filtered only.

Solid to Liquid Ratio	Initial Cube Size (mm)	Concentration of Element in Solution in mg/kg (ppm)							
		Calcium (Ca)	Iron (Fe)	Lead (Pb)	Sodium (Na)	Silicon (Si)	Magnesium (Mg)	Aluminium (Al)	Manganese (Mn)
1/10	10	49.32	0.0153	D 0.0114	769.8	30.80	0.0531	D 0.0030	D 0.0004
	20	48.91	D 0.0907	D 0.0157	750.2	30.10	0.1379	D 0.0336	D 0.0004
1/20	10	23.32	d. 0.0104	D 0.0063	451.7	30.17	0.0666	D 0.0264	D 0.0004
	20	24.07	1.092	D 0.0002	433.7	35.95	0.5990	3.486	D 0.0031
1/40	10	14.79	0.0468	D 0.0078	258.6	26.96	0.0522	D 0.1116	D 0.0001
	20	16.76	0.0577	D 0.0000	262.5	27.54	0.0949	d. 0.1659	D 0.0006

Note: 'D' indicates the stated value is below detection limits and the value stated is a system estmate.
'd' indicates the stated value is close to detection limits.

Table A1.155 ICP Data for Wyoming Bentonite 5000ppm Iron and 2.5% Lime, Compacted on the 14/7/97 and Tested 175 days after Compaction for 24 Hours at 30 Revolutions per Minute. Centrifuged at 11000rpm for 30 minutes.

Solid to Liquid Ratio	Initial Cube Size (mm)	Concentration of Element in Solution in mg/kg (ppm)							
		Calcium (Ca)	Iron (Fe)	Lead (Pb)	Sodium (Na)	Silicon (Si)	Magnesium (Mg)	Aluminium (Al)	Manganese (Mn)
1/10	10	33.48	0.0865	D 0.0142	675.4	24.63	0.0960	0.3873	D 0.0000
	20	35.73	0.0895	D 0.0088	658.5	24.47	0.0779	0.3741	D 0.0004
1/20	10	16.14	0.3052	D 0.0024	371.2	23.82	0.2101	1.151	D 0.0009
	20	16.01	0.3475	D 0.0118	370.6	23.83	0.2281	1.302	D 0.0004
1/40	10	8.275	2.028	D 0.0096	219.7	31.30	1.216	7.275	D 0.0048
	20	7.937	2.179	D 0.0065	210.7	31.00	1.335	7.835	D 0.0050

Table A1.156 ICP Data for Wyoming Bentonite and 5000ppm Iron and 2.5% Lime, Compacted on the 14/7/97 and Tested 301 days after Compaction for 24 Hours at 30 Revolutions per Minute. Centrifuged at 11000rpm for 30 minutes.

Solid to Liquid Ratio	Initial Cube Size (mm)	Concentration of Element in Solution in mg/kg (ppm)							
		Calcium (Ca)	Iron (Fe)	Lead (Pb)	Sodium (Na)	Silicon (Si)	Magnesium (Mg)	Aluminium (Al)	Manganese (Mn)
1/10	10	35.03	0.0856	D 0.0000	759.1	25.43	0.0527	0.3090	D 0.0000
	20	33.09	0.0586	D 0.0000	742.7	25.37	0.0396	0.2250	D 0.0002
1/20	10	16.15	0.6320	D 0.0000	422.9	25.56	0.3640	2.337	D 0.0016
	20	16.07	0.6642	D 0.0000	445.6	26.21	0.3757	2.342	d. 0.0018
1/40	10	10.47	6.194	D 0.0000	248.6	52.15	3.425	22.45	0.0150
	20	9.306	5.455	D 0.0000	251.7	50.75	3.067	19.96	0.0133

Note: 'D' indicates the stated value is below detection limits and the value stated is a system estimate.
'd' indicates the stated value is close to detection limits.

A1.2.16 Wyoming Bentonite with no contaminants and 7.0% lime

A1.2.16.1 Centrifugation

All tests carried out at all curing periods for this design mix and all other contaminated mixes with 7.0% lime filtered easily due to highly flocculated clay particles. This result make it very straight forward to compare and contrast the chemical data sets.

A1.2.16.2 Solid : liquid ratio

Inspection of Figures A1.67 to A1.70 illustrates that at all curing periods as solid to liquid ratio increased both pH and conductivity increased in distinct increments. At 7 days curing the conductivity of 6hr/30rpm tests with 20mm cube sizes at 1:10, 1:20 and 1:40 solid to liquid ratios were 10050µS/cm, 7360µS/cm and 4820µS/cm respectively whilst pH values were 12.78, 12.60 and 12.32 respectively. At 175 days curing conductivity values were 3150µS/cm, 2180µS/cm and 1361µS/cm respectively whilst pH values were 12.18, 11.97 and 11.74 respectively. At 301 days curing conductivity values were 2920 µS/cm, 2040 µS/cm and 1348 µS/cm respectively whilst pH values were 12.05, 11.82 and 11.60 respectively. Increasing solid to liquid ratio from 1:40 to 1:20 at 7, 175 and 301 days curing therefore increased conductivity by factors of 1.53, 1.60 and 1.51 respectively whilst pH increased by 0.27, 0.23 and 0.22 pH divisions respectively. Further increasing solid to liquid ratio from 1:20 to 1:10 increased conductivity by factors of 1.37, 1.44 and 1.43 respectively whilst pH increased by 0.18, 0.21 and 0.23 pH divisions respectively.

It is very clear that all cube sizes produce similar pH and conductivity values at specific solid to liquid ratios.

Table A1.162 for 24hr/30rpm tests with a 1:10 solid to liquid ratio shows typical levels of elements leached at 7 days curing. 20 mm cubes produced leachate concentrations of 85.1ppm Ca, 842ppm Na, 1.05ppm Si and 0.0186 ppm Mg whilst other elements remained below detection limits. As solid to liquid ratio was increased at all curing periods from 1:40 to 1:20 to 1:10 Ca levels were seen to fluctuate, Na levels increased, Si, Mg and Al levels reduced whilst Mn, Fe and Pb were generally well below detection limits. In other tests however Al concentrations also increased slightly.

A1.2.16.3 Cube Size

Figures A1.67 to A1.70 surprisingly show that the 20mm cube size generally produced the higher pH and conductivity values at any curing period. The chemical data in Tables A1.157 to A1.166 relate this to the larger cube size releasing more Na into solution.

A1.2.16.4 Rotation speed and test duration

Comparison of 6hr tests (Figures A1.67 and A1.68) illustrates that at 7 days curing as rotation speed increased pH slightly reduced whilst conductivity remained relatively unaffected. However, at 175 days curing pH values were similar although conductivity was clearly higher. Tables A1.157, A1.158 and A1.160, A1.161 indicate variable behaviour. At 7 days curing the higher rotation speed resulted in higher concentrations of Ca, lower Mg and similar levels of Si and Na (reflected in the conductivity values) At 175 days curing Na concentrations reduced whilst levels of Ca, Si, Mg and Al were similar for the increased rotation speed.

Comparison of 24hr tests (Figures A1.69 and A1.70) illustrates that the higher rotation speed produced higher pH values and significantly higher conductivity values at all curing periods and solid to liquid ratios. Analysis of Tables A1.162, A1.163 and A1.165, A1.166 show that at 7 days curing the higher rotation speed releases significantly more Ca and Na whilst at 175 days curing Na levels were most likely to be the controlling factor with respect to conductivity since there was a large reduction in Ca concentration. Generally increasing rotation speed during 24 hr tests increases Ca, Na, Si, Mg whilst producing variable results for Al for different solid to liquid ratios.

Consideration of 30rpm tests (Figures A1.67 and A1.69 appear to suggest that as test duration was increased any curing period both pH and conductivity were reduced. Tables A1.157, A1.158, A1.159 and A1.162, A1.163, A1.164 suggest that increasing test duration has little obvious correlation to Ca concentrations due to highly variable behaviour at all curing periods. The 24hr test duration did however produce similar concentrations to the 6hr test duration for Na at 7 and 175 days curing, higher Na levels at 301 days curing, significantly higher Si at all curing periods, reduced Al and similar Mg at all curing periods.

Consideration of 60rpm tests (Figures A1.68 and A1.70) suggested that as test duration was increased at 7 and 175 days pH and conductivity increased significantly. Tables A1.160, A1.161 and A1.165, If show the longer duration produced significantly more Ca at 7 days and slightly more Ca at 175 days. Levels of Na were also higher whilst Si, Mg and Al were similar in magnitude to the shorter test duration.

A1.2.16.5 Curing Time

Figures A1.67 to A1.70 all illustrate that as curing period increases pH and conductivity were reduced significantly. Tables A1.157 to A1.166 all indicate large reductions in Ca and Na. Si and Mg levels increased continually from 7 to 175 to 301 days curing whilst Al increased from 7 to 175 days curing and remained stable at this level at 301 days curing.

Figure A1.67 Conductivity and pH characteristics for English China Clay with no contaminants and 7.0% lime during 6hr/30rpm Batch Tests

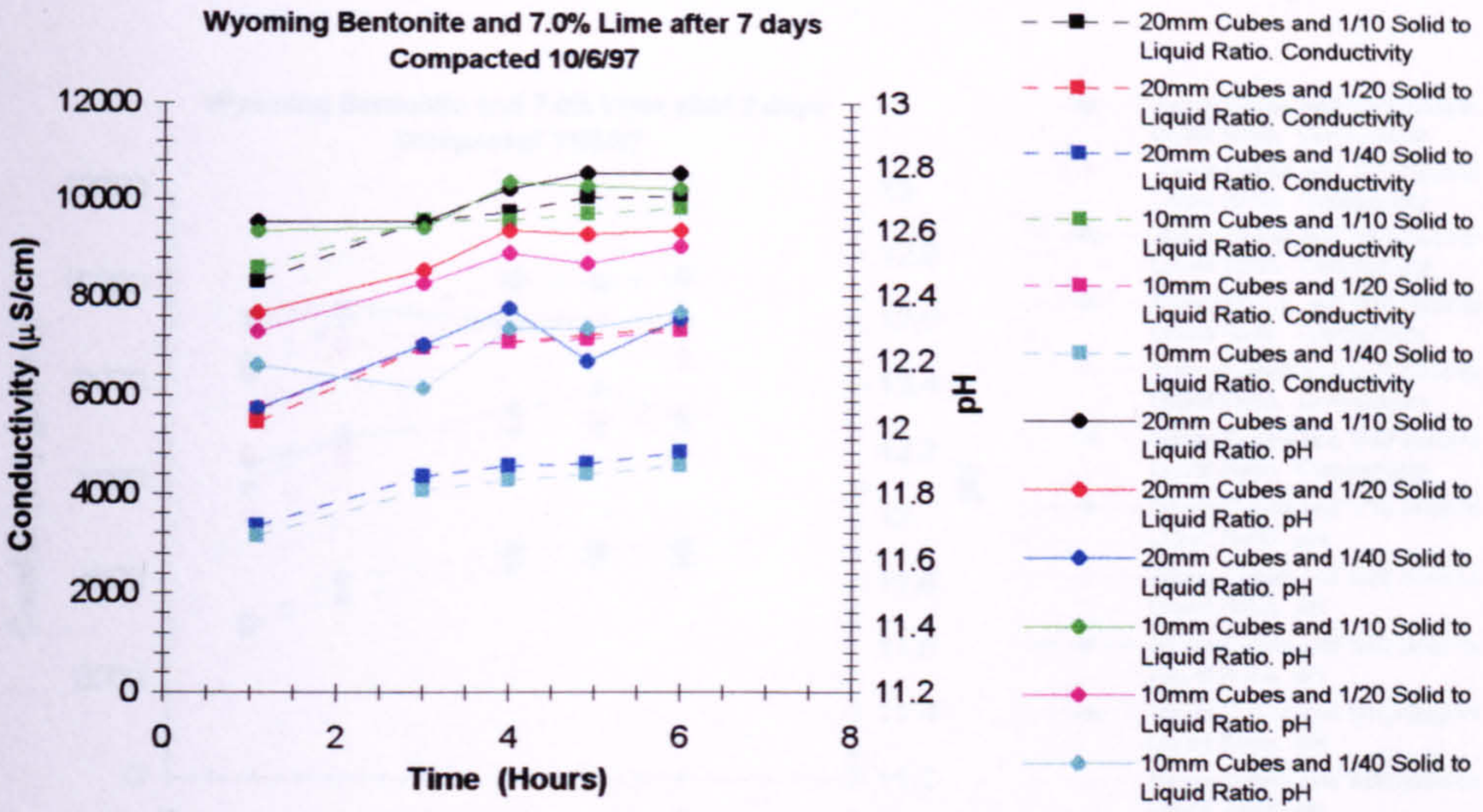

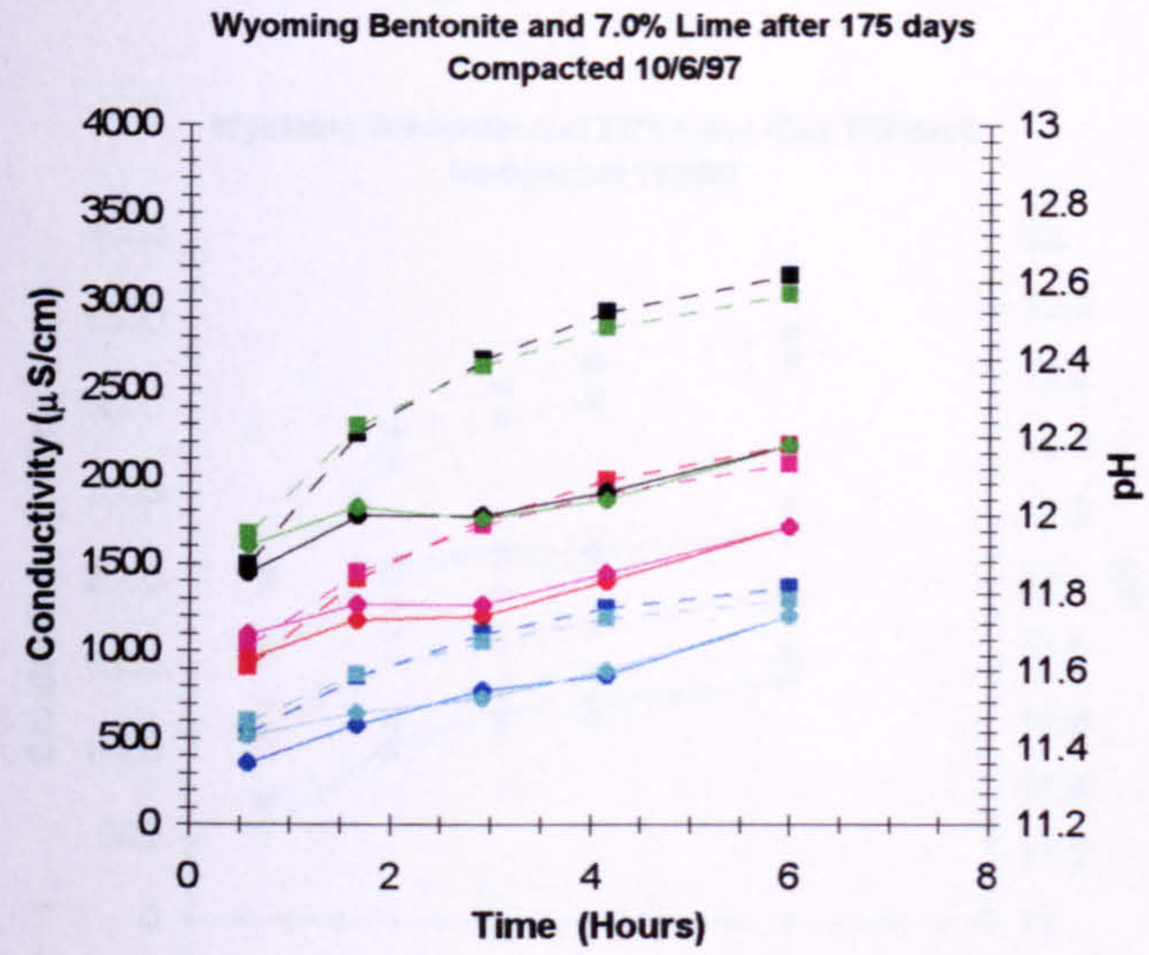

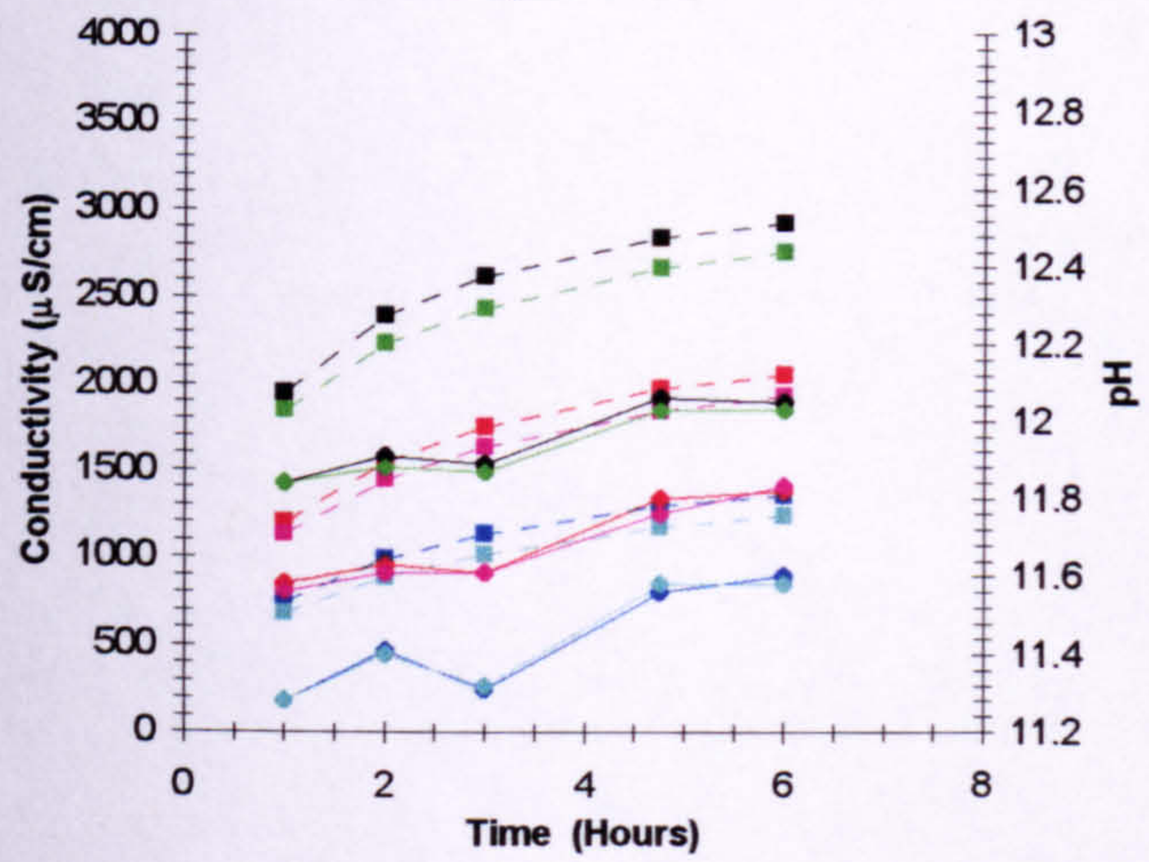

Figure A1.68 Conductivity and pH characteristics for English China Clay with no contaminants and 7.0% lime during 6hr/60rpm Batch Tests

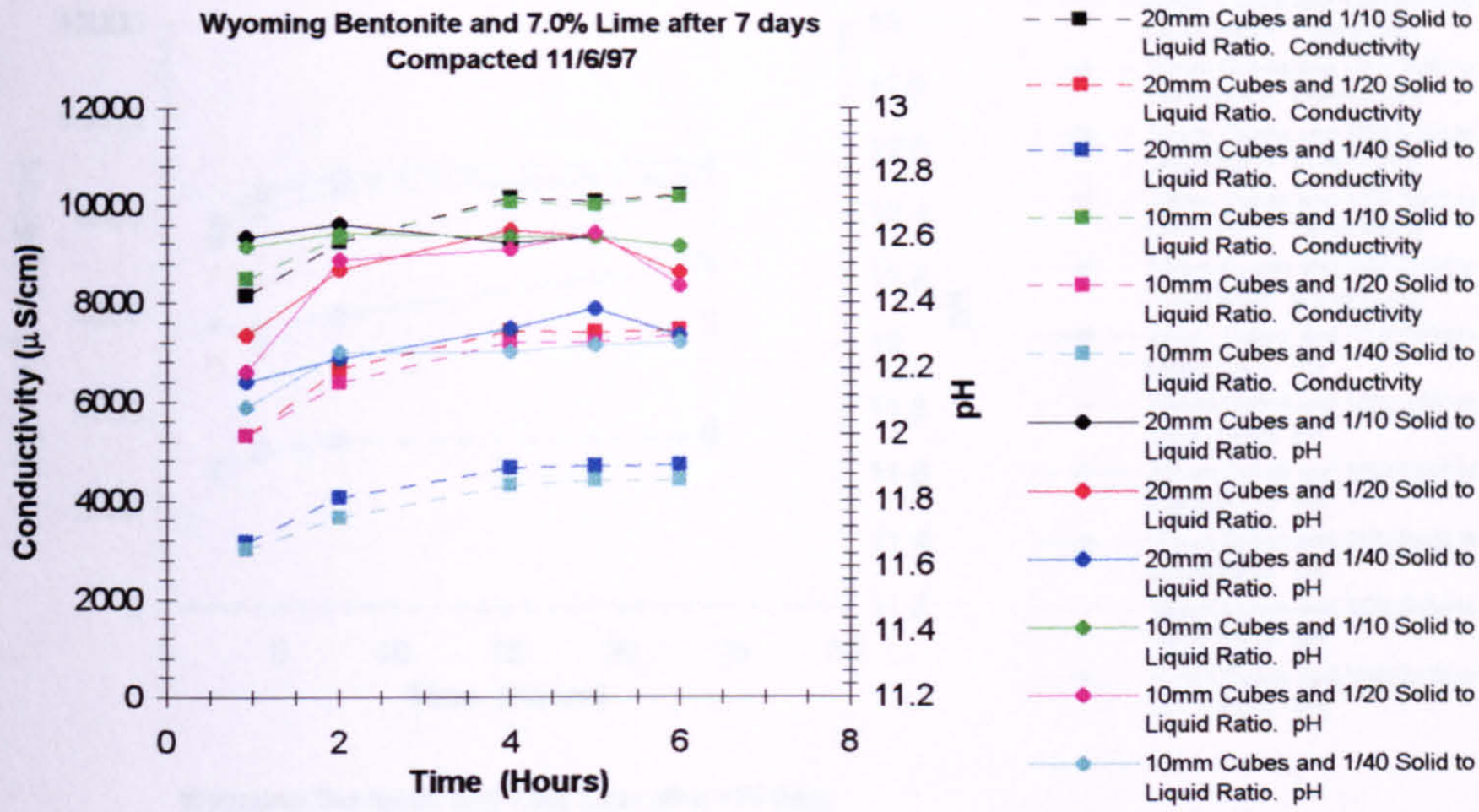

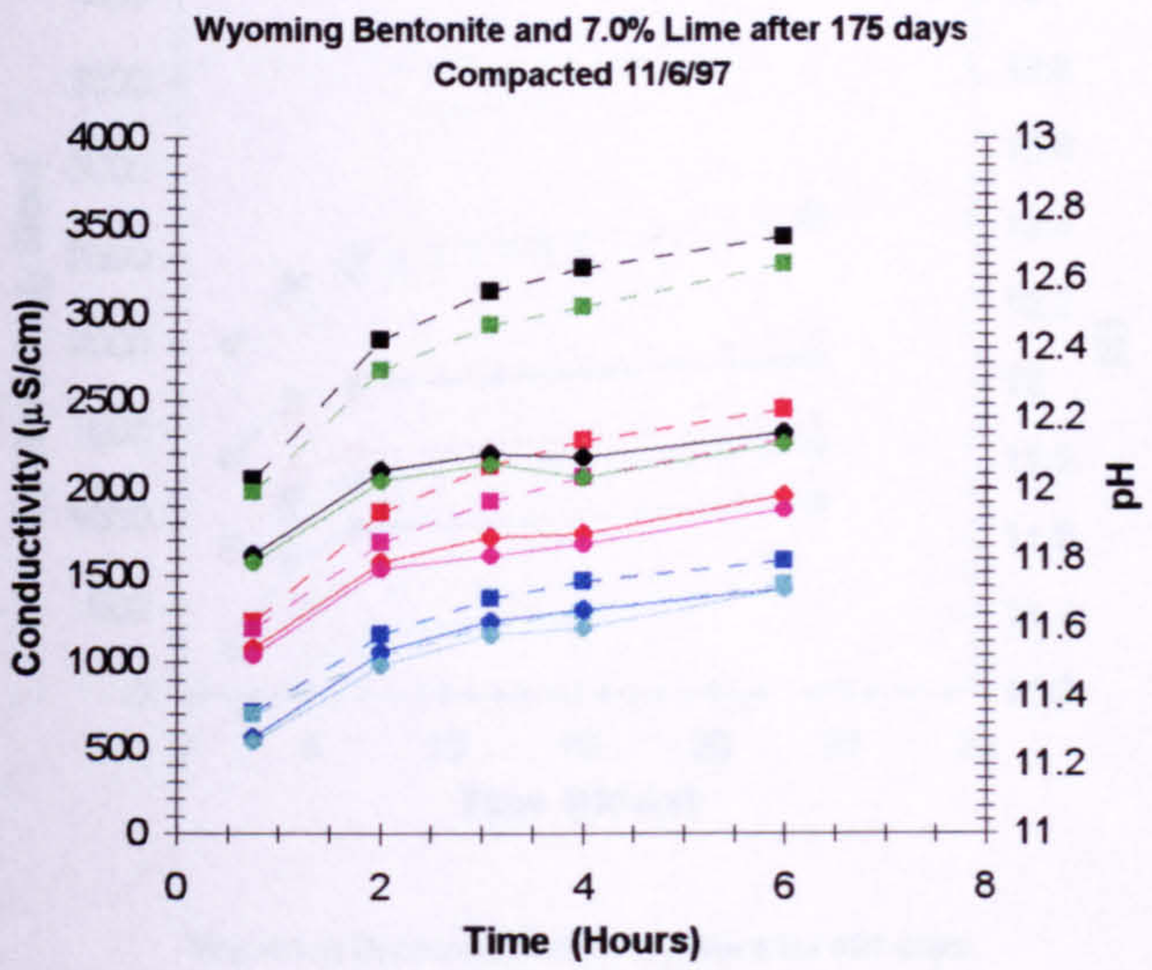

Figure A1.69 Conductivity and pH characteristics for English China Clay with no contaminants and 7.0% lime during 24hr/30rpm Batch Tests

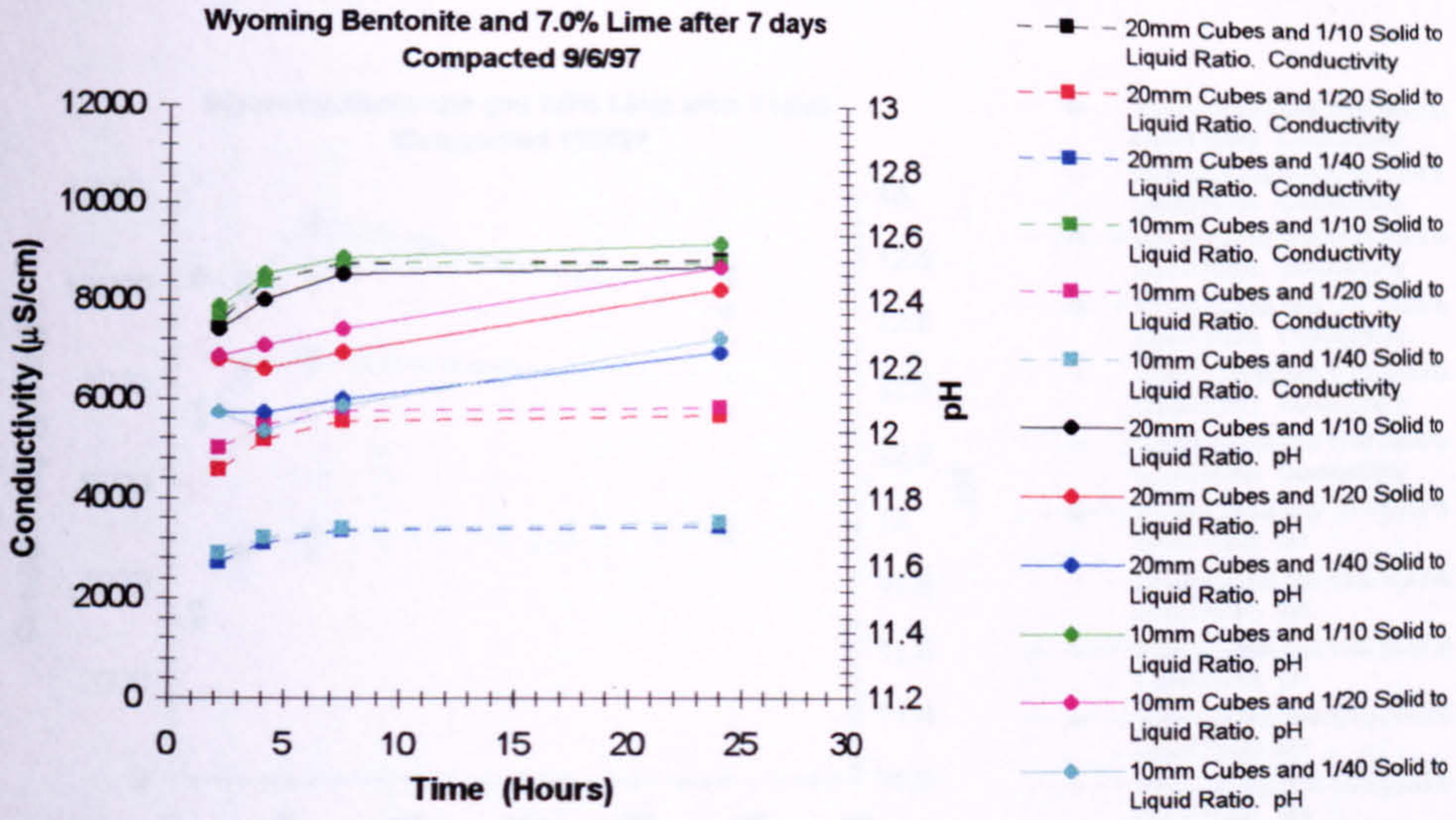

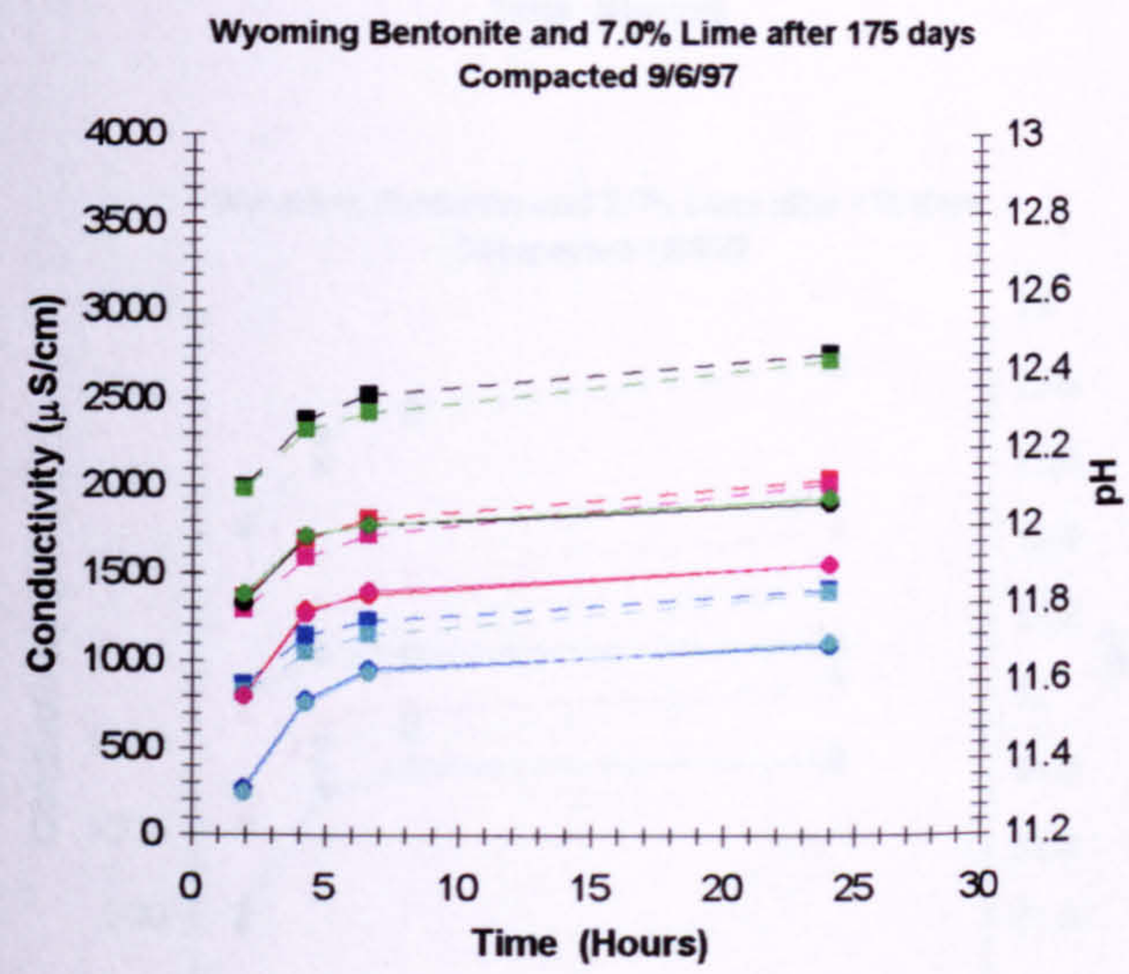

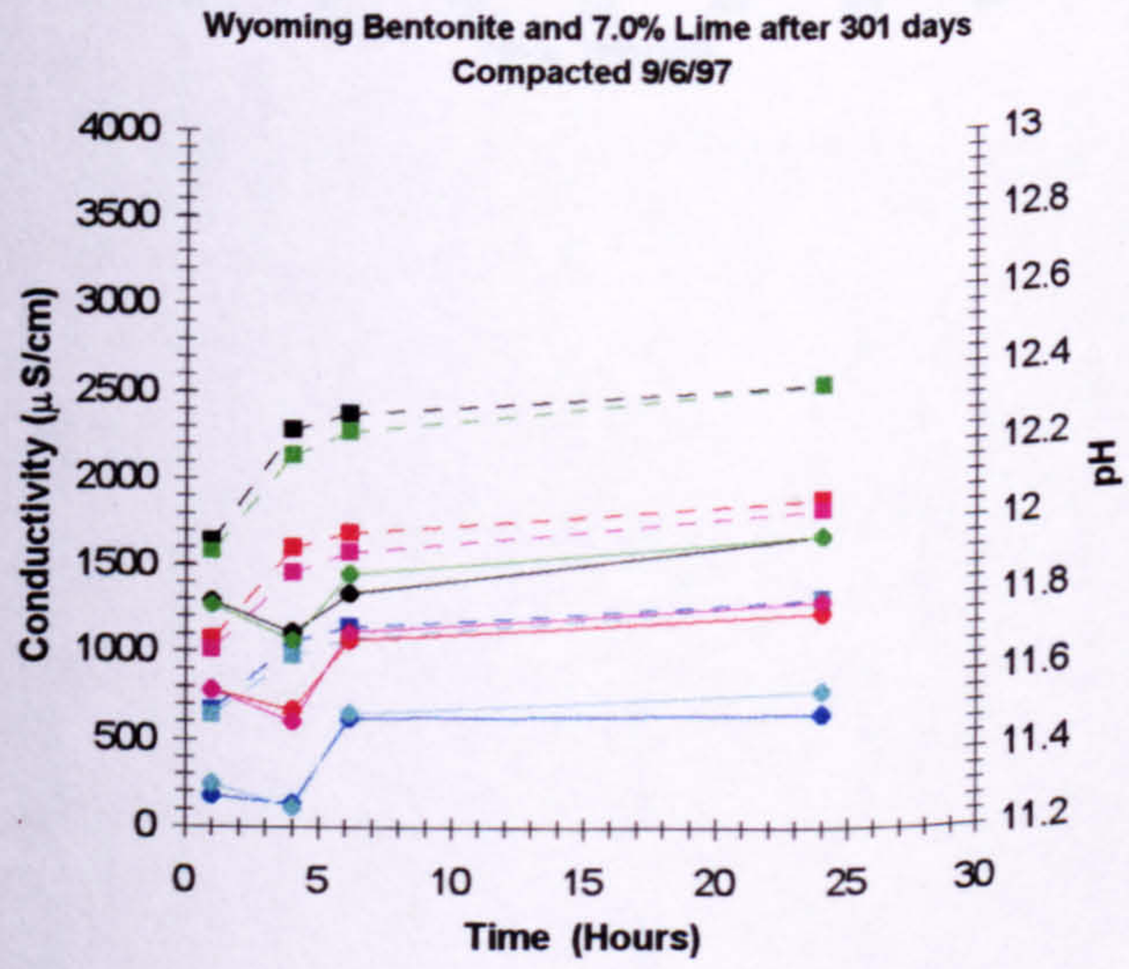

Figure A1.70 Conductivity and pH characteristics for English China Clay with no contaminants and 7.0% lime during 24hr/60rpm Batch Tests

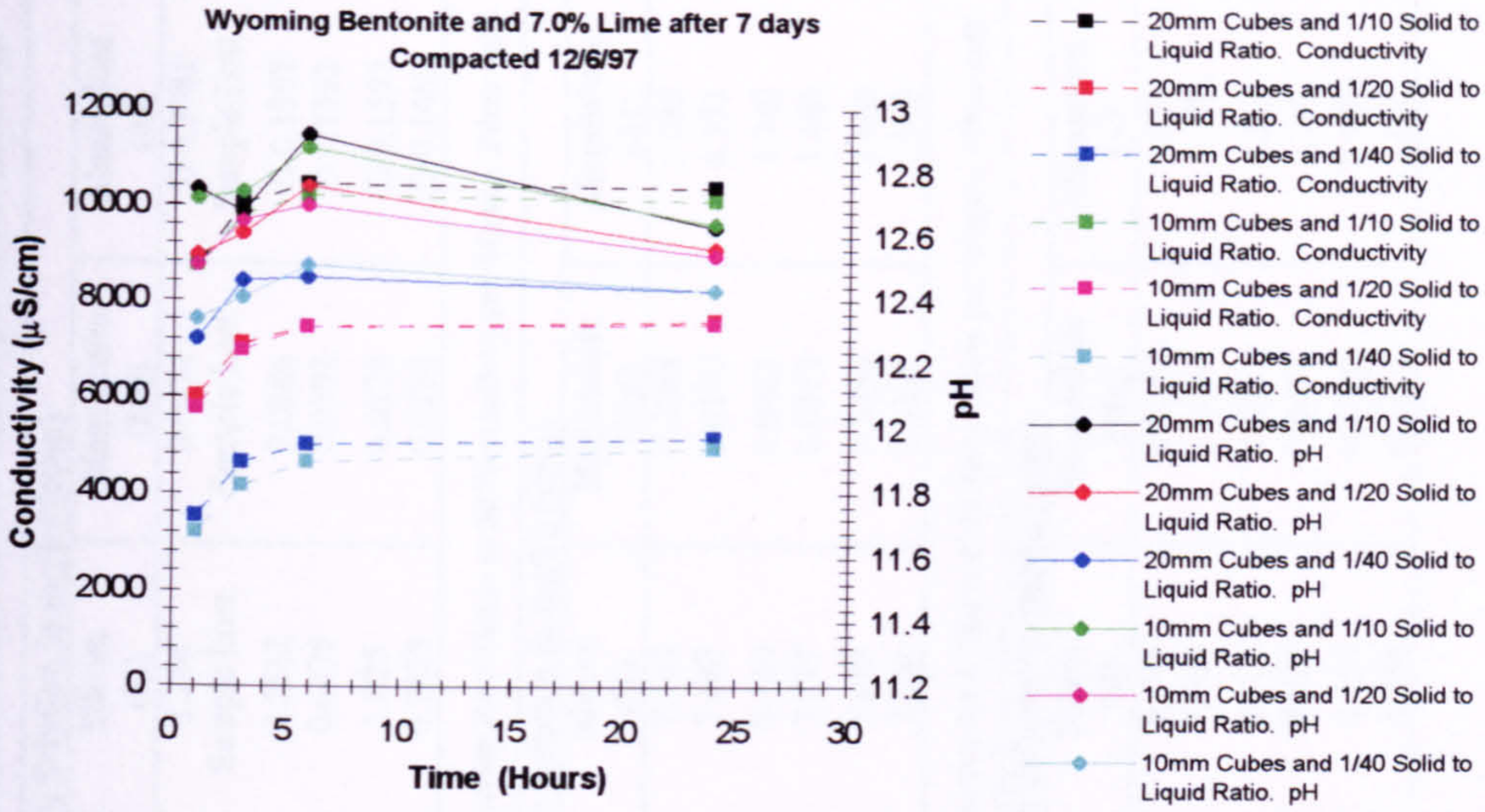

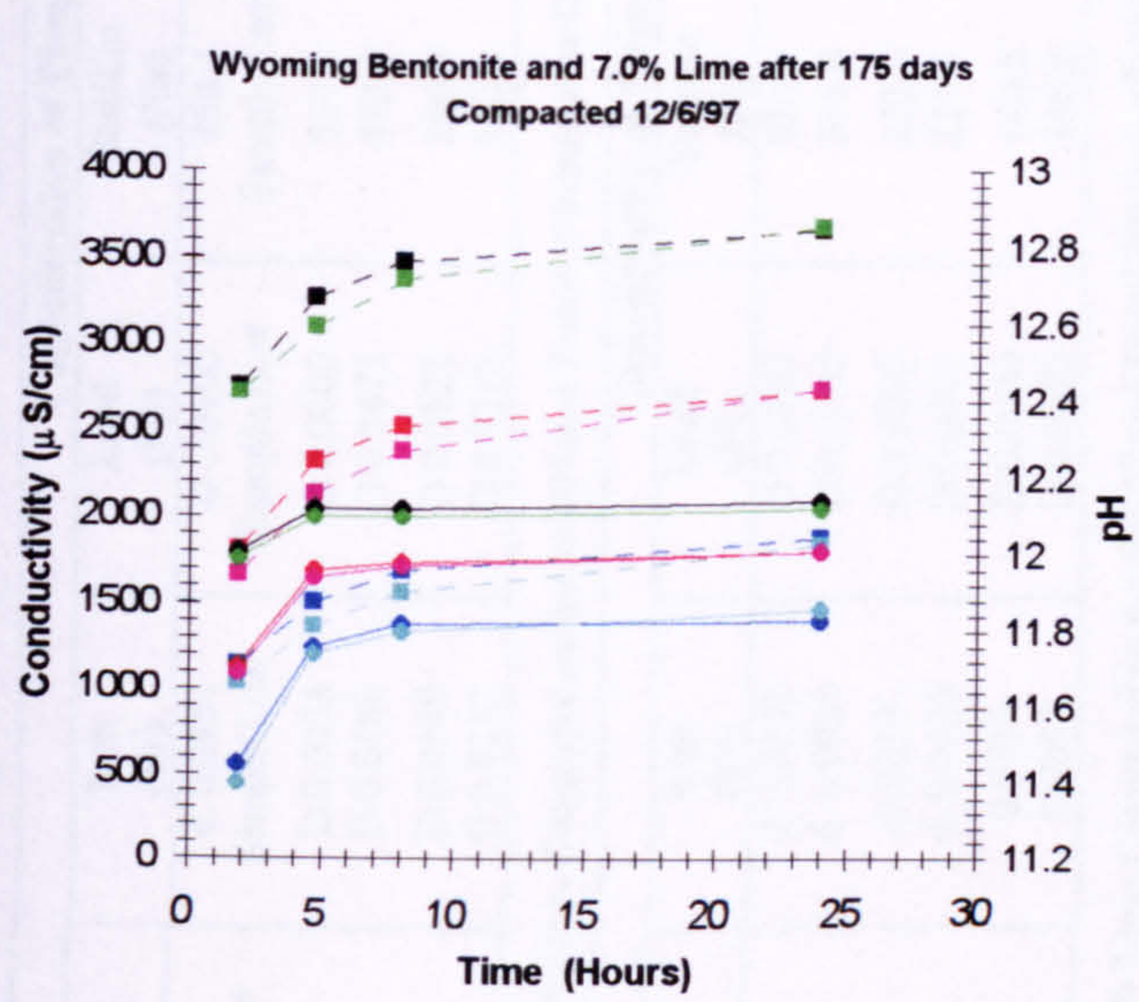

Table A1.157 ICP Data for Wyoming Bentonite and 7.0% Lime, Compacted on the 10/6/97 and Tested 7 days after Compaction for 6 Hours at 30 Revolutions per Minute. Filter only.

Solid to Liquid Ratio	Initial Cube Size (mm)	Concentration of Element in Solution in mg/kg (ppm)							
		Calcium (Ca)	Iron (Fe)	Lead (Pb)	Sodium (Na)	Silicon (Si)	Magnesium (Mg)	Aluminium (Al)	Manganese (Mn)
1/10	10	6.765	d. 0.0831	D 0.0100	858.4	1.294	0.0474	D 0.3981	D 0.0002
	20	Sample Lost	Sample Lost	Sample Lost	Sample Lost	Sample Lost	Sample Lost	Sample Lost	Sample Lost
1/20	10	55.13	D 0.0033	D 0.0000	537.0	0.5612	0.0186	D 0.1367	D 0.0000
	20	112.9	D 0.0180	D 0.0473	492.0	0.6476	0.0392	D 0.1392	0.0795
1/40	10	61.35	D 0.0149	D 0.0121	286.3	1.025	0.0278	D 0.1597	D 0.0000
	20	91.89	D 0.0212	D 0.0212	280.9	0.7853	0.0280	D 0.1469	D 0.0002

Table A1.158 ICP Data for Wyoming Bentonite and 7.0% Lime, Compacted on the 10/6/97 and Tested 175 days after Compaction for 6 Hours at 30 Revolutions per Minute. Filter only.

Solid to Liquid Ratio	Initial Cube Size (mm)	Concentration of Element in Solution in mg/kg (ppm)							
		Calcium (Ca)	Iron (Fe)	Lead (Pb)	Sodium (Na)	Silicon (Si)	Magnesium (Mg)	Aluminium (Al)	Manganese (Mn)
1/10	10	4.803	d. 0.0121	D 0.0000	350.5	7.733	0.0284	4.085	d. 0.0042
	20	6.350	d. 0.0035	D 0.0000	365.8	7.287	0.0100	4.391	D 0.0001
1/20	10	5.643	0.0213	D 0.0000	232.3	8.180	0.0401	3.740	D 0.0014
	20	2.454	d. 0.0126	D 0.0000	237.4	7.697	0.0319	3.486	D 0.0001
1/40	10	2.355	0.5734	D 0.0000	140.5	12.88	0.3694	3.865	D 0.0016
	20	5.271	0.0297	D 0.0000	148.3	7.241	0.0355	1.950	D 0.0001

Table A1.159 ICP Data for Wyoming Bentonite and 7.0% Lime, Compacted on the 10/6/97 and Tested 301 days after Compaction for 6 Hours at 30 Revolutions per Minute. Filter only.

Solid to Liquid Ratio	Initial Cube Size (mm)	Concentration of Element in Solution in mg/kg (ppm)							
		Calcium (Ca)	Iron (Fe)	Lead (Pb)	Sodium (Na)	Silicon (Si)	Magnesium (Mg)	Aluminium (Al)	Manganese (Mn)
1/10	10	6.934	D 0.0137	D 0.0000	365.1	8.178	0.0282	5.581	D 0.0004
	20	7.835	0.1217	D 0.0149	376.9	7.984	0.0630	5.687	D 0.0016
1/20	10	4.793	D 0.0302	D 0.0157	240.2	8.206	0.0272	4.215	D 0.0003
	20	5.764	D 0.0159	D 0.0141	268.4	8.056	0.0244	4.792	D 0.0002
1/40	10	3.500	0.1404	D 0.0054	149.9	8.520	0.0789	3.367	D 0.0004
	20	4.159	0.1556	D 0.0000	159.6	8.388	0.1427	3.666	D 0.0012

Note : 'D' indicates the stated value is below detection limits and the value stated is a system estimate.
'd' indicates the stated value is close to detection limits.

Table A1.160 ICP Data for Wyoming Bentonite and 7.0% Lime, Compacted on the 11/6/97 and Tested 7 days after Compaction for 6 Hours at 60 Revolutions per Minute. Filter only.

Solid to Liquid Ratio	Initial Cube Size (mm)	Concentration of Element in Solution in mg/kg (ppm)							
		Calcium (Ca)	Iron (Fe)	Lead (Pb)	Sodium (Na)	Silicon (Si)	Magnesium (Mg)	Aluminium (Al)	Manganese (Mn)
1/10	10	31.72	D 0.0102	D 0.0025	869.1	0.6566	0.0140	D 0.1255	D 0.0000
	20	24.79	D 0.0277	D 0.0162	866.4	0.6679	0.0138	D 0.1309	D 0.0000
1/20	10	137.9	D 0.0088	D 0.0000	551.0	0.5840	0.0141	D 0.0990	D 0.0000
	20	103.0	D 0.0086	D 0.0043	543.6	0.6016	0.0115	D 0.0939	D 0.0000
1/40	10	1.993	D 0.0384	D 0.0000	280.8	1.436	0.0240	D 0.2165	D 0.0000
	20	11.11	d. 0.0144	D 0.0090	303.4	1.001	0.0145	D 0.1287	D 0.0000

Table A1.161 ICP Data for Wyoming Bentonite and 7.0% Lime, Compacted on the 11/6/97 and Tested 175 days after Compaction for 6 Hours at 60 Revolutions per Minute. Filter only.

Solid to Liquid Ratio	Initial Cube Size (mm)	Concentration of Element in Solution in mg/kg (ppm)							
		Calcium (Ca)	Iron (Fe)	Lead (Pb)	Sodium (Na)	Silicon (Si)	Magnesium (Mg)	Aluminium (Al)	Manganese (Mn)
1/10	10	1.982	0.0134	D 0.0000	379.2	7.443	0.0273	3.526	D 0.0001
	20	2.435	d. 0.0115	D 0.0000	397.5	7.428	0.0300	3.888	D 0.0003
1/20	10	3.827	d. 0.0092	D 0.0000	243.0	7.476	0.0244	2.994	D 0.0000
	20	3.495	D 0.0112	D 0.0000	264.9	7.085	0.0313	3.090	D 0.0005
1/40	10	4.561	0.1343	D 0.0000	151.4	9.039	0.1086	2.955	D 0.0007
	20	3.550	0.0521	D 0.0020	164.4	7.487	0.0482	2.530	D 0.0004

Note: 'D' indicates the stated value is below detection limits and the value stated is a system estimate.
'd' indicates the stated value is close to detection limits.

Table A1.162 ICP Data for Wyoming Bentonite and 7.0% Lime, Compacted on the 9/6/97 and Tested 7 days after Compaction for 24 Hours at 30 Revolutions per Minute. Filter only.

Solid to Liquid Ratio	Initial Cube Size (mm)	Concentration of Element in Solution in mg/kg (ppm)							
		Calcium (Ca)	Iron (Fe)	Lead (Pb)	Sodium (Na)	Silicon (Si)	Magnesium (Mg)	Aluminium (Al)	Manganese (Mn)
1/10	10	86.49	D 0.0072	D 0.0096	828.7	0.8725	0.0128	D 0.1588	D 0.0000
	20	85.13	D 0.0201	D 0.0087	842.5	1.055	0.0186	D 0.2220	D 0.0000
1/20	10	4.961	D 0.0269	D 0.0000	492.5	1.615	0.0214	D 0.2776	D 0.0000
	20	56.40	D 0.0207	D 0.0062	532.9	1.598	0.0263	D 0.1578	D 0.0001
1/40	10	8.721	D 0.0446	D 0.0000	281.0	2.089	0.0239	D 0.2243	0.0779
	20	15.69	0.0873	D 0.0000	286.4	2.671	0.0622	D 0.4237	D 0.0000

Table A1.163 ICP Data for Wyoming Bentonite and 7.0% Lime, Compacted on the 9/6/97 and Tested 175 days after Compaction for 24 Hours at 30 Revolutions per Minute. Filter only.

Solid to Liquid Ratio	Initial Cube Size (mm)	Concentration of Element in Solution in mg/kg (ppm)							
		Calcium (Ca)	Iron (Fe)	Lead (Pb)	Sodium (Na)	Silicon (Si)	Magnesium (Mg)	Aluminium (Al)	Manganese (Mn)
1/10	10	5.398	d. 0.0076	D 0.0000	349.4	15.63	0.0251	1.968	D 0.0002
	20	5.073	d. 0.0084	D 0.0000	358.7	15.54	0.0451	2.019	D 0.0001
1/20	10	3.293	0.0359	D 0.0000	240.9	17.94	0.0378	1.471	D 0.0002
	20	3.371	D 0.0112	D 0.0000	246.3	17.05	0.0709	1.564	D 0.0001
1/40	10	6.323	1.876	D 0.0000	163.9	25.14	1.216	8.364	D 0.0035
	20	3.953	0.8028	D 0.0000	163.7	24.13	0.5448	4.144	D 0.0023

Table A1.164 ICP Data for Wyoming Bentonite and 7.0% Lime, Compacted on the 9/6/97 and Tested 301 days after Compaction for 24 Hours at 30 Revolutions per Minute. Filter only.

Solid to Liquid Ratio	Initial Cube Size (mm)	Concentration of Element in Solution in mg/kg (ppm)							
		Calcium (Ca)	Iron (Fe)	Lead (Pb)	Sodium (Na)	Silicon (Si)	Magnesium (Mg)	Aluminium (Al)	Manganese (Mn)
1/10	10	4.154	d. 0.0429	D 0.0083	420.3	16.42	0.0349	1.969	D 0.0004
	20	5.107	D 0.0141	D 0.0273	383.7	15.85	0.0398	1.981	D 0.0006
1/20	10	3.396	D 0.0119	D 0.0098	295.6	19.43	0.0243	1.431	D 0.0004
	20	3.919	d. 0.0385	D 0.0078	275.0	18.28	0.0333	1.356	D 0.0003
1/40	10	3.606	0.0954	D 0.0058	209.3	21.53	0.0837	1.333	0.0050
	20	3.313	0.0994	D 0.0109	174.4	20.01	0.0840	1.334	D 0.0006

Note: 'D' indicates the stated value is below detection limits and the value stated is a system estimate.
'd' indicates the stated value is close to detection limits.

Table A1.165 ICP Data for Wyoming Bentonite and 7.0% Lime, Compacted on the 12/6/97 and Tested 7 days after Compaction for 24 Hours at 60 Revolutions per Minute. Filter only.

Solid to Liquid Ratio	Initial Cube Size (mm)	Concentration of Element in Solution in mg/kg (ppm)							
		Calcium (Ca)	Iron (Fe)	Lead (Pb)	Sodium (Na)	Silicon (Si)	Magnesium (Mg)	Aluminium (Al)	Manganese (Mn)
1/10	10	137.8	D 0.0087	D 0.0089	903.7	0.5903	0.0087	D 0.1648	D 0.0003
	20	121.8	D 0.0295	D 0.0535	883.0	0.6293	0.0390	D 0.1257	D 0.0021
1/20	10	182.3	D 0.0056	D 0.0252	575.3	0.5670	0.0132	D 0.1321	D 0.0002
	20	156.2	D 0.0122	D 0.0552	565.6	0.5056	0.0149	D 0.1478	D 0.0000
1/40	10	131.0	D 0.0051	D 0.0258	318.6	0.7306	0.0189	D 0.0910	D 0.0000
	20	176.3	D 0.0000	D 0.0173	315.8	0.6135	0.0168	D 0.0622	D 0.0004

Table A1.166 ICP Data for Wyoming Bentonite and 7.0% Lime, Compacted on the 12/6/97 and Tested 175 days after Compaction for 24 Hours at 60 Revolutions per Minute. Filter only.

Solid to Liquid Ratio	Initial Cube Size (mm)	Concentration of Element in Solution in mg/kg (ppm)							
		Calcium (Ca)	Iron (Fe)	Lead (Pb)	Sodium (Na)	Silicon (Si)	Magnesium (Mg)	Aluminium (Al)	Manganese (Mn)
1/10	10	8.834	d. 0.0156	D 0.0047	438.3	7.905	0.0378	3.089	D 0.0001
	20	9.200	d. 0.0109	D 0.0000	443.2	7.446	0.0300	3.092	D 0.0001
1/20	10	8.067	0.0225	D 0.0000	312.9	8.114	0.0424	2.413	D 0.0004
	20	7.336	D 0.0118	D 0.0000	297.3	8.140	0.0204	2.578	D 0.0000
1/40	10	6.268	0.0367	D 0.0000	189.9	9.209	0.0458	2.090	D 0.0000
	20	6.518	0.0833	D 0.0000	192.6	9.295	0.0619	2.137	D 0.0004

Note: 'D' indicates the stated value is below detection limits and the value stated is a system estimate.
'd' indicates the stated value is close to detection limits.

A1.2.17 Wyoming Bentonite with 5000ppm Pb and 7.0% lime

A significant point of general note is that no Pb was released into any filtered leachate in any test at any curing period.

A1.2.17.1 Solid : liquid ratio

Inspection of Figures A1.71 to A1.74 shows that as solid to liquid ratio increases pH and conductivity values increase. At 7 days curing the conductivity of 6hr/30rpm tests with 20mm cube sizes at the solid to liquid ratios 1:10, 1:20 and 1:40 were 9460µS/cm, 7120µS/cm and 4450µS/cm respectively whilst pH and conductivity values were 12.72, 12.57 and 12.31 respectively. At 175 days curing the conductivity values were 3220µS/cm, 2260µS/cm and 1404µS/cm respectively whilst pH values were 12.22, 12.08 and 11.90 respectively. At 301 days curing the conductivity values were 2500µS/cm, 1629µS/cm and 1063µS/cm respectively whilst pH values were 11.94, 11.69 and 11.45 respectively. Increasing solid to liquid ratio from 1:40 to 1:20 at 7, 175 and 301 days curing therefore increased conductivity by factors of 1.60, 1.61 and 1.53 respectively whilst pH increased by 0.26, 0.18 and 0.24 pH divisions respectively. Increasing solid to liquid ratio further from 1:20 to 1:10 increased conductivity by factors of 1.33, 1.42, and 1.53 respectively whilst pH increased by 0.15, 0.14 and 0.25 pH divisions respectively.

It is clear that all cube sizes produce similar pH and conductivity values at the specific solid to liquid ratios.

Table A1.172 for 24hr/30rpm tests with 1:10 solid to liquid ratio shows typical concentrations of elements at 7 days curing. 20mm cubes released 96.3ppm Ca, 830ppm Na, 0.571ppm Si and 0.0119ppm Mg whilst other elements were below detection limits. Tables A1.167 to A1.176 show that as the solid to liquid ratio increased from 1:40 towards 1:10 at all curing periods Ca concentrations fluctuated, Na and Al concentrations increased, Si and Mg concentrations reduced whilst concentrations of Mn, Fe and Pb were generally well below detection limits. With the exception of the Al behaviour this was very similar to the Wyoming Bentonite with 7.0% lime design mix.

A1.2.17.2 Cube Size

There appears to be no obvious link between cube size and pH and conductivity. Observation of the data Table A1.167 to A1.176 also suggests no obvious trends relating cube size to the concentration of element release.

A1.2.17.3 Rotation speed and test duration

Comparison of 6hr tests (Figures A1.71 and A1.72) at 7 and 175 days curing illustrates that as the rotation speed was increased pH was unaffected whilst conductivity values were slightly higher. Tables A1.167, A1.168 and A1.170, A1.171 illustrate that the higher rotation speed released more Si whilst other elements appeared similar in concentration or fluctuated significantly highlighting no direct trends to rotation speed.

Comparison of 24 hr tests (Figures A1.73 and A1.74) at 7 days and 175 days curing shows the higher rotation speed resulting in slightly lower pH values and slightly higher conductivity values. At 7 days curing the results of each test at specific solid to liquid ratios appear very similar (Tables A1.172 and A1.175) whilst at 175 days (Tables A1.173 and A1.176) significantly more Ca and Na were released for the higher rotation speed. There were also slight increases in Al at this higher rotation speed.

Observation of Figures A1.71 to A1.74 illustrates that as the tests progressed pH and conductivity increased towards equilibrium values. 24hr tests were clearly closer to achieving the pH and conductivity equilibrium plateaux than 6hr tests although chemically the differences were not necessarily significant. Consideration of 30rpm tests (Figures A1.71 and A1.73) suggest that at 7 and 175 days curing the longer test duration resulted in slightly lower final pH values and slightly higher conductivity values. At 301 days curing the longer duration produced both higher pH and conductivity values. At 7 days curing Tables A1.167 and A1.172 show the longer duration producing significantly higher concentrations of Ca and slightly higher Na whilst the other elements were at similar levels between tests. At 175 days curing Tables A1.168 and A1.173 show the 24hr test duration producing similar levels relative to the 6hr test of Ca, Si and Mg and less Na. At 301 days Tables A1.169 and A1.174 show the 24hr test producing similar concentrations of concentrations of Ca and Si, higher concentrations of Na and lower concentrations of Al relative to 6hr tests.

Considerations of 60rpm tests (Figures A1.72 and A1.74) show the same pH and conductivity trends as the 30 rpm tests. At 7 days the chemical data in Tables A1.172 and A1.175 also show similar trends to the 30rpm tests. However at 175 days curing (Tables A1.173 and A1.176) the 24hr test duration produces significantly higher concentrations of Ca, Na and Al whilst Mg levels were similar to the 6hr tests.

A1.2.17.4 Curing Time

Figures A1.71 to A1.74 illustrate that as curing period increased both pH and conductivity reduced very significantly. Tables A1.167 to A1.176 illustrate huge reductions in Ca and Na whilst levels of Si, Al and Mg increase, Si most significantly.

Figure A1.71 Conductivity and pH characteristics for Wyoming Bentonite with 5000ppm Pb and 7.0% lime during 6hr/30rpm Batch Tests

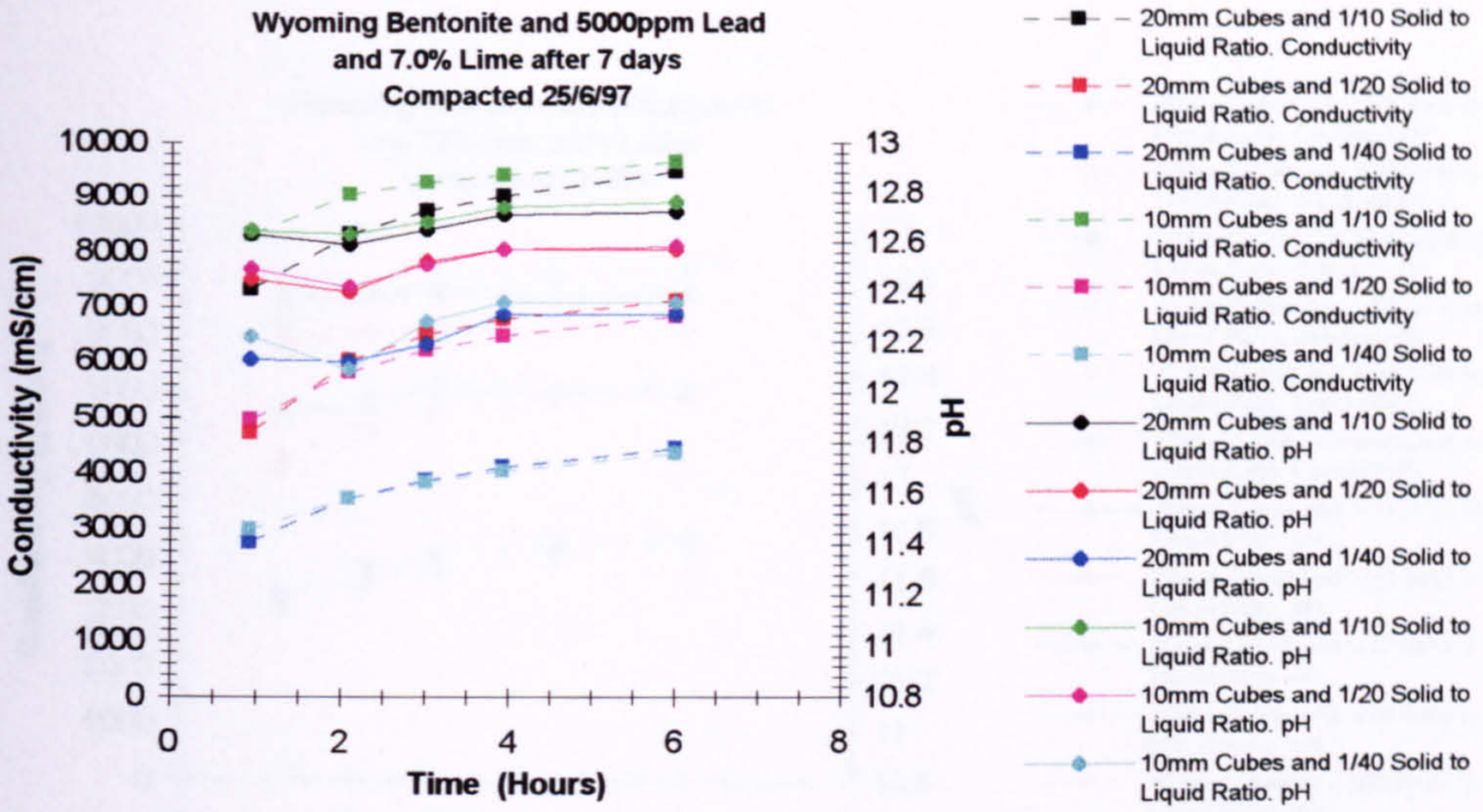

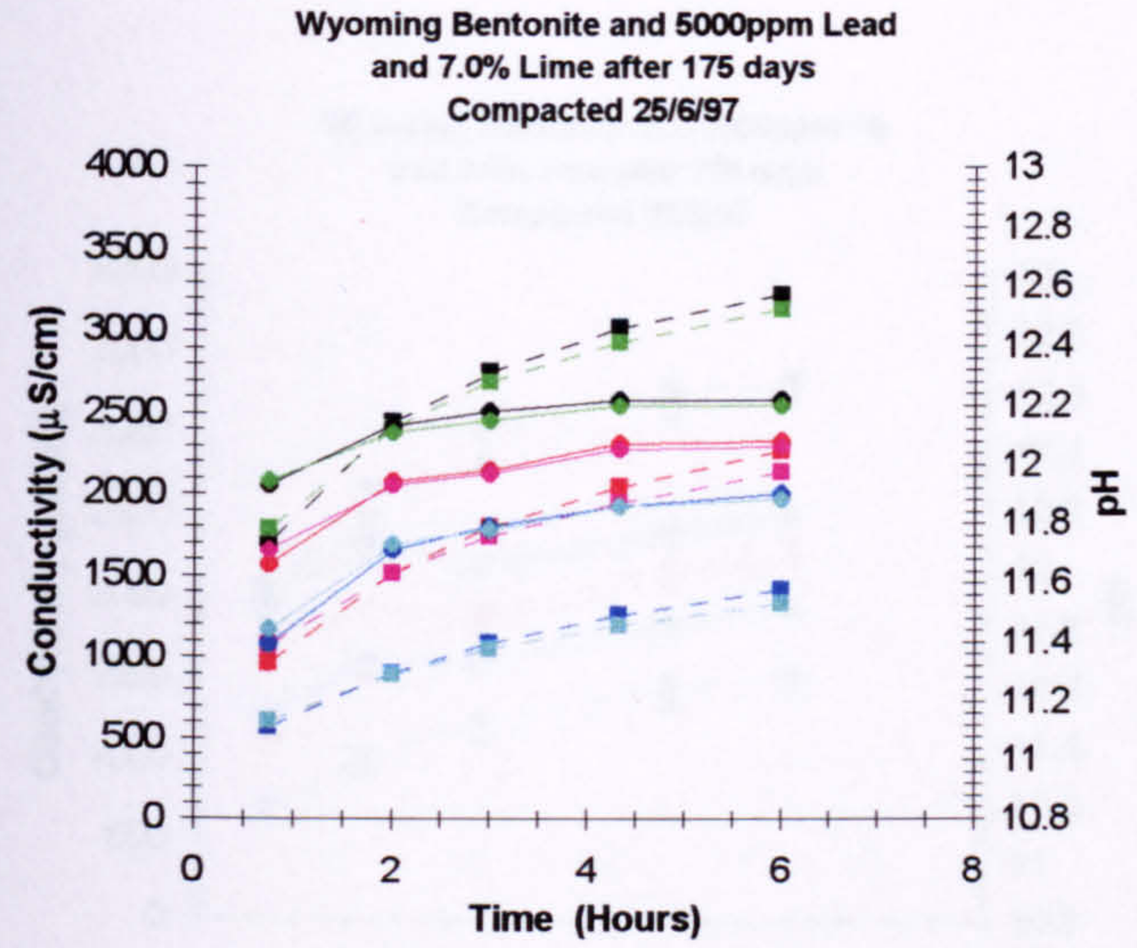

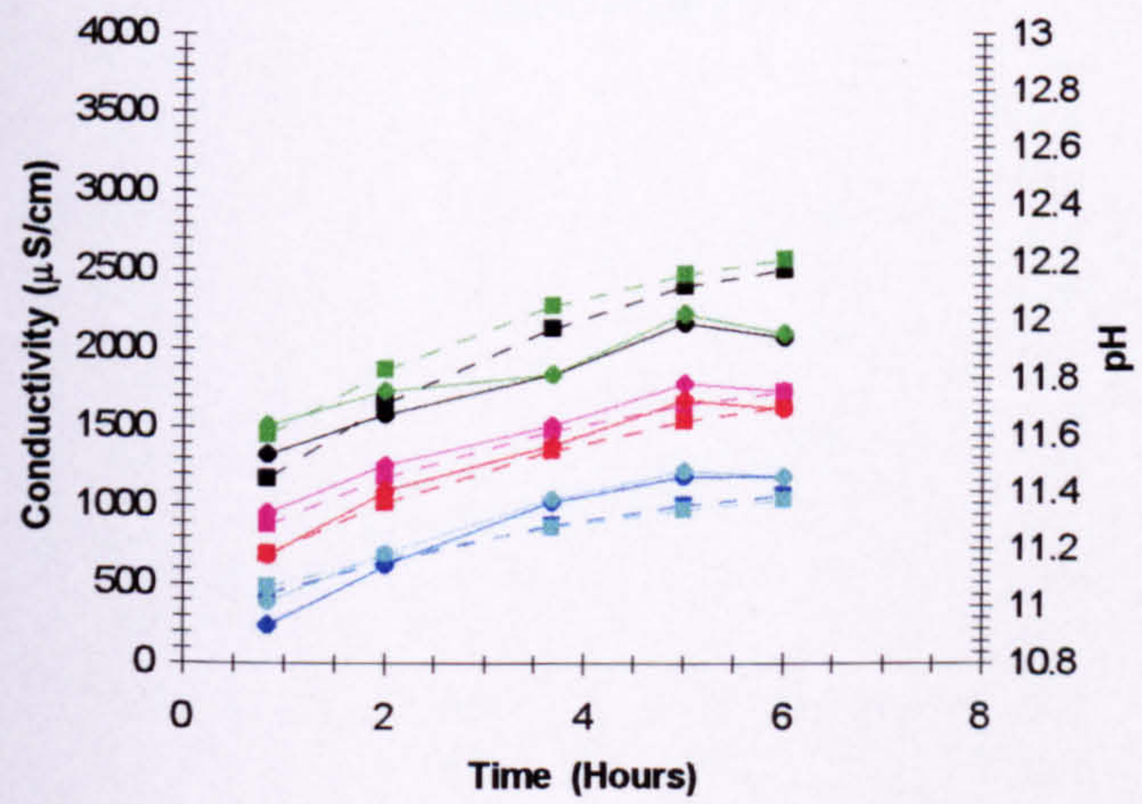

Figure A1.72 Conductivity and pH characteristics for Wyoming Bentonite with 5000ppm Pb and 7.0% lime during 6hr/60rpm Batch Tests

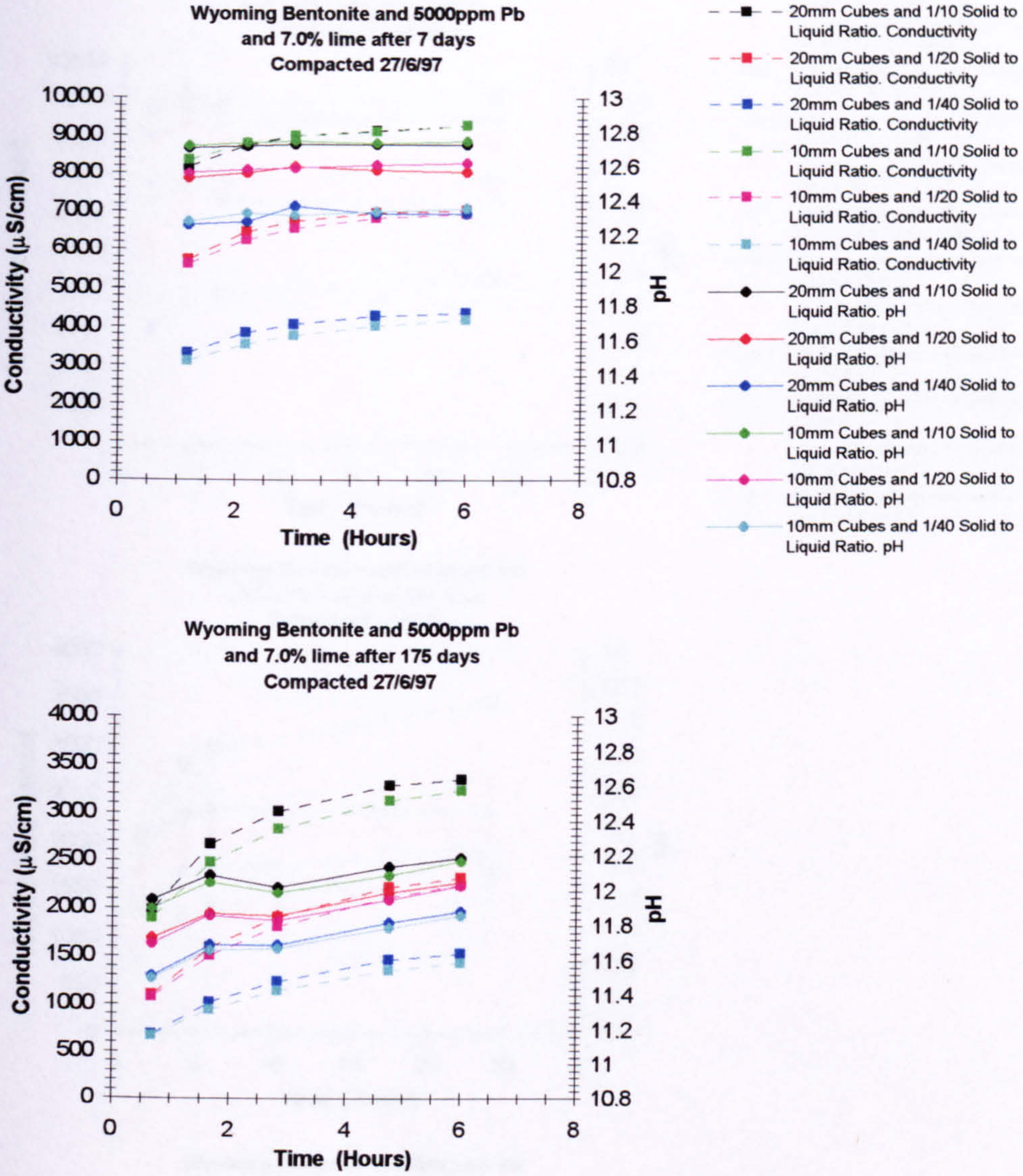

Figure A1.73 Conductivity and pH characteristics for Wyoming Bentonite with 5000ppm Pb and 7.0% lime during 24hr/30rpm Batch Tests

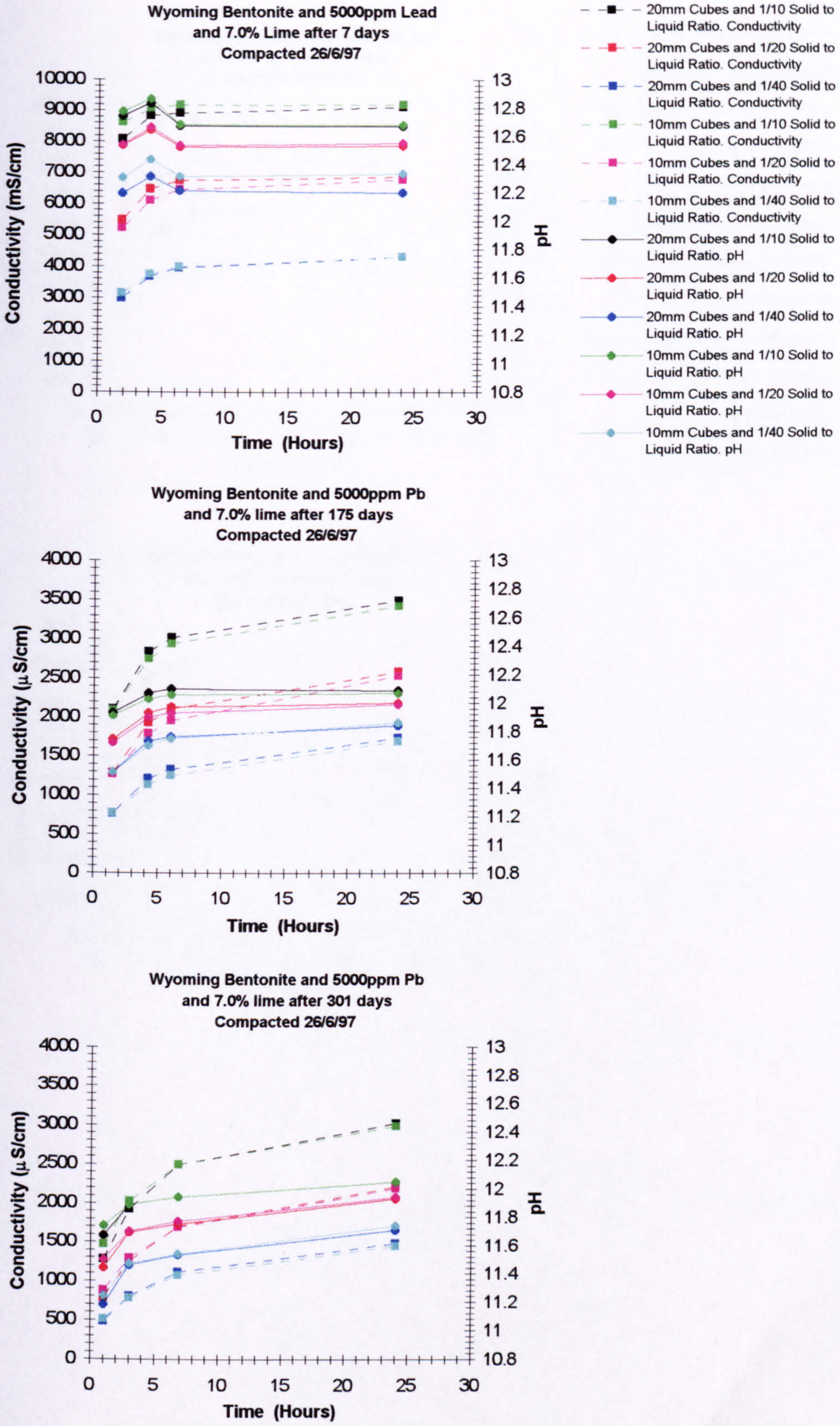

Figure A1.74 Conductivity and pH characteristics for Wyoming Bentonite with 5000ppm Pb and 7.0% lime during 24hr/60rpm Batch Tests

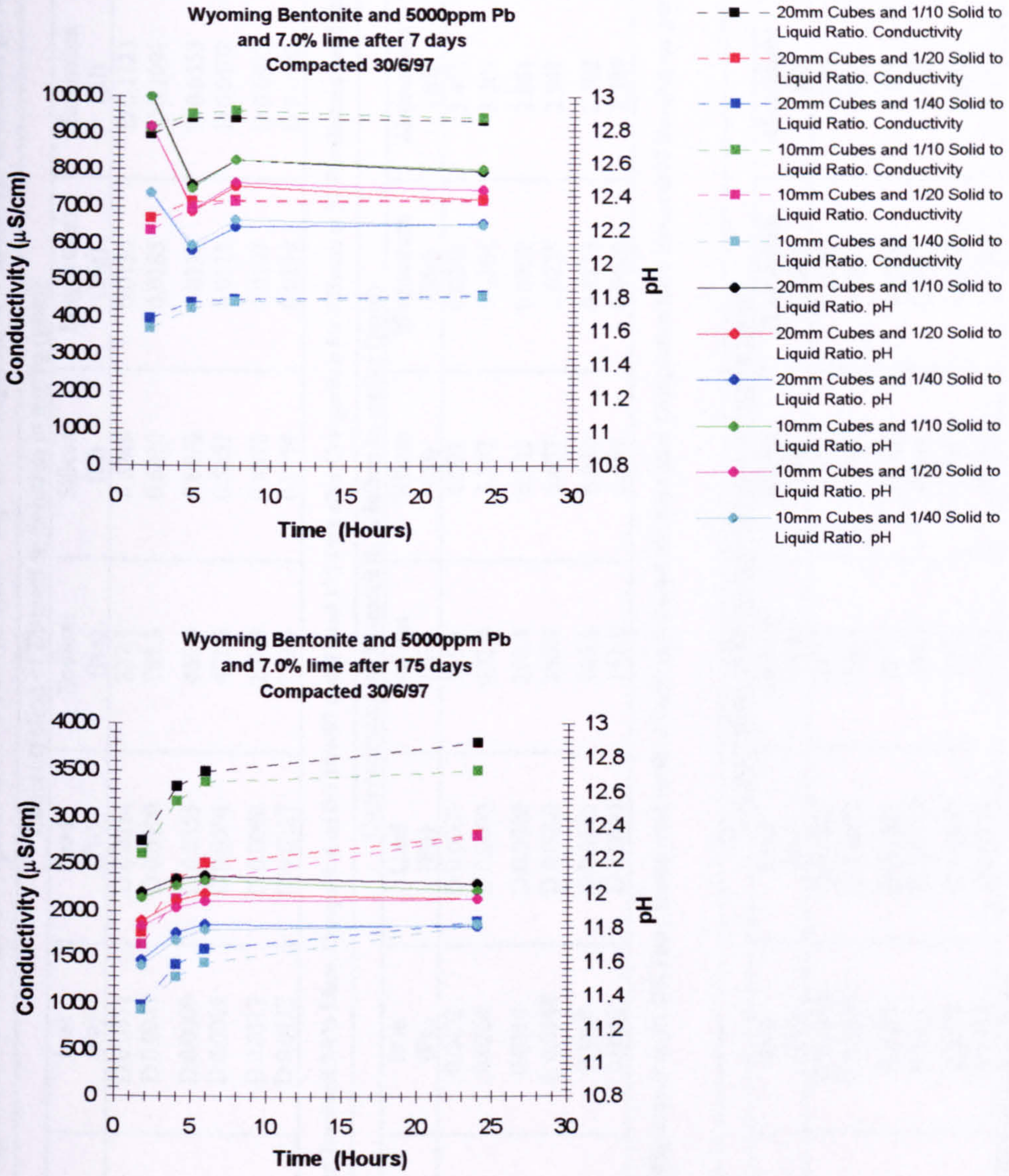

Table A1.167 ICP Data for Wyoming Bentonite and 5000ppm Lead and 7.0% Lime, Compacted on the 25/6/97 and Tested 7 days after Compaction for 6 Hours at 30 Revolutions per Minute. Filtered only.

Solid to Liquid Ratio	Initial Cube Size (mm)	Concentration of Element in Solution in mg/kg (ppm)							
		Calcium (Ca)	Iron (Fe)	Lead (Pb)	Sodium (Na)	Silicon (Si)	Magnesium (Mg)	Aluminium (Al)	Manganese (Mn)
1/10	10	4.946	D 0.0171	D 0.0314	827.1	0.6249	0.0130	D 0.1123	D 0.0005
	20	36.87	D 0.0047	D 0.0100	788.3	0.6330	0.0185	D 0.1091	D 0.0000
1/20	10	47.06	D 0.0009	D 0.0353	466.9	0.6970	0.0130	D 0.0553	D 0.0000
	20	88.73	D 0.0019	D 0.0504	472.5	0.5651	0.0111	D 0.0502	D 0.0000
1/40	10	1.460	D 0.0117	D 0.0000	262.3	0.8376	0.0107	D 0.0913	D 0.0003
	20	1.793	D 0.0137	D 0.0227	259.4	0.9454	0.0299	D 0.0985	D 0.0000

Table A1.168 ICP Data for Wyoming Bentonite 5000ppm Lead and 7.0% Lime, Compacted on the 25/6/97 and Tested 175 days after Compaction for 6 Hours at 30 Revolutions per Minute. Filtered only.

Solid to Liquid Ratio	Initial Cube Size (mm)	Concentration of Element in Solution in mg/kg (ppm)							
		Calcium (Ca)	Iron (Fe)	Lead (Pb)	Sodium (Na)	Silicon (Si)	Magnesium (Mg)	Aluminium (Al)	Manganese (Mn)
1/10	10	8.582	0.0452	D 0.0000	385.3	6.032	0.0248	3.459	D 0.0005
	20	10.51	0.0264	D 0.0000	402.8	5.787	0.0264	3.309	D 0.0003
1/20	10	7.349	0.0310	D 0.0000	250.4	6.112	0.0307	2.861	D 0.0004
	20	8.636	d. 0.0148	D 0.0000	260.8	5.657	0.0235	2.949	D 0.0005
1/40	10	4.769	0.1400	D 0.0165	145.8	6.630	0.1213	2.702	D 0.0003
	20	6.022	0.0581	D 0.0000	153.2	5.653	0.0440	2.389	D 0.0001

Table A1.169 ICP Data for Wyoming Bentonite and 5000ppm Lead and 7.0% Lime, Compacted on the 25/6/97 and Tested 301 days after Compaction for 6 Hours at 30 Revolutions per Minute. Filtered only.

Solid to Liquid Ratio	Initial Cube Size (mm)	Concentration of Element in Solution in mg/kg (ppm)							
		Calcium (Ca)	Iron (Fe)	Lead (Pb)	Sodium (Na)	Silicon (Si)	Magnesium (Mg)	Aluminium (Al)	Manganese (Mn)
1/10	10	9.575	D 0.0302	D 0.0000	407.1	7.650	0.0310	4.083	D 0.0005
	20	9.144	D 0.0204	D 0.0072	334.3	9.238	0.0331	4.087	D 0.0003
1/20	10	5.757	0.3011	D 0.0521	287.4	10.12	0.1952	4.525	D 0.0011
	20	4.843	0.1681	D 0.0142	209.7	8.809	0.1081	3.947	D 0.0005
1/40	10	4.928	0.6272	D 0.1017	177.0	11.91	0.3998	4.562	D 0.0023
	20	3.574	0.1958	D 0.0224	150.7	8.153	0.1289	2.895	D 0.0008

Note: 'D' indicates the stated value is below detection limits and the value stated is a system estimate.
'd' indicates the stated value is close to detection limits.

Table A1.170 ICP Data for Wyoming Bentonite and 5000ppm Lead and 7.0% Lime, Compacted on the 27/6/97 and Tested 7 days after Compaction for 6 Hours at 60 Revolutions per Minute. Filtered only.

Solid to Liquid Ratio	Initial Cube Size (mm)	Concentration of Element in Solution in mg/kg (ppm)							
		Calcium (Ca)	Iron (Fe)	Lead (Pb)	Sodium (Na)	Silicon (Si)	Magnesium (Mg)	Aluminium (Al)	Manganese (Mn)
1/10	10	1.694	D 0.0047	D 0.0260	811.8	0.8266	0.0082	D 0.1131	D 0.0004
	20	0.8438	D 0.0074	D 0.0000	841.0	0.9490	0.0153	D 0.1254	D 0.0004
1/20	10	0.9900	0.1540	D 0.0118	500.4	1.808	0.0964	d. 0.5267	D 0.0007
	20	79.80	D 0.0000	D 0.0410	491.9	0.5195	0.0121	D 0.0479	D 0.0000
1/40	10	0.6834	D 0.0065	D 0.0241	286.4	1.191	0.0166	D 0.0998	D 0.0003
	20	3.950	D 0.0051	D 0.0121	284.1	1.119	0.0095	D 0.1052	D 0.0002

Table A1.171 ICP Data for Wyoming Bentonite 5000ppm Lead and 7.0% Lime, Compacted on the 27/6/97 and Tested 175 days after Compaction for 6 Hours at 60 Revolutions per Minute. Filtered only.

Solid to Liquid Ratio	Initial Cube Size (mm)	Concentration of Element in Solution in mg/kg (ppm)							
		Calcium (Ca)	Iron (Fe)	Lead (Pb)	Sodium (Na)	Silicon (Si)	Magnesium (Mg)	Aluminium (Al)	Manganese (Mn)
1/10	10	3.000	d. 0.0066	D 0.0000	291.2	4.868	0.0472	3.246	D 0.0000
	20	9.944	d. 0.0095	D 0.0013	296.1	4.680	0.0224	3.204	D 0.0004
1/20	10	6.666	d. 0.0038	D 0.0000	182.2	4.510	0.0343	2.745	D 0.0001
	20	6.282	d. 0.0325	D 0.0000	197.5	4.318	0.0342	2.766	D 0.0002
1/40	10	4.825	0.2431	D 0.0362	116.8	5.696	0.1492	2.603	D 0.0009
	20	4.835	0.0372	D 0.0000	119.1	4.793	0.0530	2.289	D 0.0003

Note: 'D' indicates the stated value is below detection limits and the value stated is a system estimate.
'd' indicates the stated value is close to detection limits.

Table A1.172 ICP Data for Wyoming Bentonite and 5000ppm Lead and 7.0% Lime, Compacted on the 26/6/97 and Tested 7 days after Compaction for 24 Hours at 30 Revolutions per Minute. Filtered only.

Solid to Liquid Ratio	Initial Cube Size (mm)	Concentration of Element in Solution in mg/kg (ppm)							
		Calcium (Ca)	Iron (Fe)	Lead (Pb)	Sodium (Na)	Silicon (Si)	Magnesium (Mg)	Aluminium (Al)	Manganese (Mn)
1/10	10	95.26	D 0.0526	D 0.0000	832.0	0.6296	0.0123	D 0.1370	D 0.0002
	20	96.33	D 0.0043	D 0.0104	829.8	0.5710	0.0119	D 0.0997	D 0.0000
1/20	10	21.74	D 0.0020	D 0.0109	499.2	0.5999	0.0103	D 0.0824	D 0.0000
	20	135.2	D 0.0061	D 0.0247	494.2	0.5464	0.0139	D 0.0549	D 0.0000
1/40	10	80.24	D 0.0021	D 0.0442	290.9	0.7623	0.0236	D 0.0979	D 0.0000
	20	82.04	D 0.0074	D 0.0309	283.3	0.8435	0.0161	D 0.1182	D 0.0000

Table A1.173 ICP Data for Wyoming Bentonite 5000ppm Lead and 7.0% Lime, Compacted on the 26/6/97 and Tested 175 days after Compaction for 24 Hours at 30 Revolutions per Minute. Filtered only.

Solid to Liquid Ratio	Initial Cube Size (mm)	Concentration of Element in Solution in mg/kg (ppm)							
		Calcium (Ca)	Iron (Fe)	Lead (Pb)	Sodium (Na)	Silicon (Si)	Magnesium (Mg)	Aluminium (Al)	Manganese (Mn)
1/10	10	10.09	0.0280	D 0.0000	311.9	5.097	0.0285	3.077	D 0.0009
	20	10.54	0.0259	D 0.0056	314.3	4.704	0.0203	2.970	D 0.0003
1/20	10	7.461	d. 0.0399	D 0.0114	224.4	5.706	0.0191	2.667	D 0.0002
	20	9.041	0.0182	D 0.0000	238.7	5.480	0.0255	2.746	D 0.0002
1/40	10	5.694	0.1310	D 0.0000	141.9	7.041	0.0973	2.348	D 0.0001
	20	6.463	0.0439	D 0.0000	146.6	6.248	0.0513	2.166	D 0.0006

Table A1.174 ICP Data for Wyoming Bentonite and 5000ppm Lead and 7.0% Lime, Compacted on the 26/6/97 and Tested 301 days after Compaction for 24 Hours at 30 Revolutions per Minute. Filtered only.

Solid to Liquid Ratio	Initial Cube Size (mm)	Concentration of Element in Solution in mg/kg (ppm)							
		Calcium (Ca)	Iron (Fe)	Lead (Pb)	Sodium (Na)	Silicon (Si)	Magnesium (Mg)	Aluminium (Al)	Manganese (Mn)
1/10	10	9.852	D 0.0170	D 0.0064	441.9	7.884	0.0284	2.922	D 0.0013
	20	9.995	D 0.0219	D 0.0041	457.9	8.248	0.0271	2.863	D 0.0001
1/20	10	6.412	D 0.0128	D 0.0000	291.5	8.841	0.0233	2.576	D 0.0003
	20	6.827	D 0.0185	D 0.0186	312.6	8.747	0.0366	2.564	D 0.0002
1/40	10	3.652	D 0.0298	D 0.0112	192.7	9.850	0.0373	1.970	D 0.0002
	20	4.610	0.1824	D 0.0255	197.9	10.06	0.1458	2.621	d. 0.0003

Note : 'D' indicates the stated value is below detection limits and the value stated is a system estimate.
'd' indicates the stated value is close to detection limits.

Table A1.175 ICP Data for Wyoming Bentonite and 5000ppm Lead and 7.0% Lime, Compacted on the 30/6/97 and Tested 7 days after Compaction for 24 Hours at 60 Revolutions per Minute. Filtered only.

Solid to Liquid Ratio	*Initial Cube* Size (mm)	Concentration of Element in Solution in mg/kg (ppm)							
		Calcium (Ca)	Iron (Fe)	Lead (Pb)	Sodium (Na)	Silicon (Si)	Magnesium (Mg)	Aluminium (Al)	Manganese (Mn)
1/10	10	96.38	D 0.0014	D 0.0259	838.5	0.5853	0.0090	D 0.1104	D 0.0000
	20	94.15	D 0.0061	D 0.0560	848.3	0.5676	0.0071	D 0.0709	D 0.0000
1/20	10	34.42	D 0.0027	D 0.0282	517.2	0.4691	0.0081	D 0.0634	D 0.0000
	20	153.1	D 0.0019	D 0.0460	518.5	0.5124	0.0112	D 0.0965	D 0.0006
1/40	10	102.9	D 0.0023	D 0.0185	313.1	0.6700	0.0170	D 0.0389	D 0.0001
	20	116.5	D 0.0000	D 0.0220	307.3	0.7576	0.0172	D 0.0501	D 0.0000

***Table A1.176 ICP Data for Wyoming Bentonite 5000ppm Lead and 7.0% Lime*, Compacted on the 30/6/97 and Tested 175 days after Compaction for 24 Hours at 60 Revolutions per Minute. Filtered only.**

Solid to Liquid Ratio	*Initial Cube* Size (mm)	Concentration of Element in Solution in mg/kg (ppm)							
		Calcium (Ca)	Iron (Fe)	Lead (Pb)	Sodium (Na)	Silicon (Si)	Magnesium (Mg)	Aluminium (Al)	Manganese (Mn)
1/10	10	15.86	d. 0.0132	D 0.0000	436.9	5.961	0.0278	3.775	D 0.0001
	20	16.58	d. 0.0226	D 0.0118	310.3	3.704	0.0298	3.619	D 0.0001
1/20	10	12.30	d. 0.0207	D 0.0078	330.0	6.594	0.0295	3.211	D 0.0004
	20	13.57	d. 0.0103	D 0.0077	235.8	4.416	0.0216	3.366	D 0.0000
1/40	10	8.639	0.1668	D 0.0242	211.5	8.454	0.0997	3.109	D 0.0005
	20	9.211	0.6526	0.1318	169.1	8.856	0.3215	4.489	D 0.0010

Note: 'D' indicates the stated value is below detection limits and the value stated is a system estimate.
'd' indicates the stated value is close to detection limits.

A1.2.18 Wyoming Bentonite with 5000ppm Fe and 7.0% lime

A significant point of general note is that no Fe was released into any filtered leachate in any test at any curing period.

A1.2.18.1 Solid : liquid ratio

Inspection of Figures A1.75 to A1.78 illustrates that increasing solid to liquid ratio increases pH and conductivity. At 7 days curing the conductivity of 6hr/30rpm tests with 20mm cubes sizes at the 1:10, 1:20 and 1:40 solid to liquid ratios were 8690μS/cm, 6440μS/cm and 3870μS/cm respectively whilst pH values were 12.48, 12.36 and 12.13 respectively. At 175 days curing the conductivity values were 4250μS/cm, 2860μS/cm and 1828μS/cm respectively whilst pH values were 12.00, 11.91 and 11.74 respectively. At 301 days curing the conductivity values were 3700μS/cm, 2490μS/cm and 1602μS/cm respectively whilst pH values were 11.93, 11.82 and 11.64 respectively. Increasing the solid to liquid ratio from 1:40 to 1:20 at 7, 175 and 301 days curing therefore increased conductivity by factors of 1.66, 1.56 and 1.55 respectively whilst pH increased by 0.23, 0.17 and 0.18 pH divisions respectively. Increasing the solid to liquid ratio further from 1:20 to 1:10 increased conductivity by factors of 1.35, 1.49, and 1.49 respectively whilst pH increased by 0.12, 0.09 and 0.11 pH divisions respectively.

Tables A1.182 for 24hr/30rpm tests at the solid to liquid ratio 1:10 shows typical concentrations of elements produced at 7 days curing. 20mm cubes produced 314ppm Ca, 0.114ppm Fe, 1112ppm Na, 1.09ppm Si and 0.0554ppm Mg whilst other elements were below detection limits. Tables A1.177 to A1.186 highlight that the higher levels of conductivity coincide well with the higher Na concentrations in the leachates. However, generally the 1:20 solid to liquid ratio at 7 days curing produced the highest concentration of Ca followed by the 1:10 and then the 1:40 solid to liquid ratios. At 175 and 301 days curing Ca and Mg concentrations fluctuate whilst Na and Al continue to increase and Si decreases with increasing solid to liquid ratio.

A1.2.18.2 Cube Size

There are no obvious trends relating cube size to pH and conductivity variations. Analysis of the chemical data tables generally indicate that 10mm cubes

produce slightly higher concentrations of Si and Na., Mg and lower concentration of Al.

A1.2.18.3 Rotation speed and test duration

Similarly to the design mixes Wyoming Bentonite with 7.0% lime and Wyoming Bentonite with 5000ppm Pb and 7.0% lime, as the batch tests progress pH and conductivity clearly increase towards an equilibrium plateaux. Again it is clear from the gradients of the pH and conductivity graphs that the 24hr tests are probably closer to the equilibrium levels than the 6hr tests.

Comparison of 6hr tests (Figures A1.75 and A1.76) at 7 days curing illustrates that the higher rotation speed slightly increases the pH and conductivity values. At 175 days pH values were similar and conductivity values were higher for increased rotation speed. Tables A1.177, A1.178 and A1.180, A1.181 show that at both 7 and 175 days curing the higher rotation speed produced significantly higher concentrations of Ca and Al, higher levels of Ca and lower levels of Si. However, the higher rotation speed produced higher concentrations of Na at 7 days curing and lower concentrations at 175 days curing.

Comparison of 24hr tests (Figures A1.77 and A1.78) illustrates that the higher rotation speed at 7 days curing resulted in similar pH values and significantly higher conductivity values. At 175 days curing the higher speed produced lower pH values and only slightly higher conductivity values. Tables A1.182, A1.183 and A1.185, A1.186 illustrate that at 7 days curing the higher rotation speed produced higher concentrations of Ca, lower concentrations of Si and similar concentrations of Mg and Na. At 175 days curing the increased rotation speed resulted in higher Ca levels, significantly higher Al, higher Na and lower Si whilst Mg remained at similar levels.

Consideration of 30rpm tests (Figures A1.75 and A1.77) show that the longer test duration increased final pH and conductivity values at any curing period although the trend was less obvious at the longer curing periods. Tables A1.177, A1.178, A1.179 and A1.182, A1.183, Ag all generally show that the longer duration produced higher concentrations of Ca and Na, lower concentrations of Si and Al whilst similar concentrations of Mg.

Consideration of 60rpm tests (Figures A1.76 and A1.78) show that the longer test duration produced slightly high pH and significantly higher conductivity values particularly at 175 days curing. Tables A1.180, A1.181 and A1.185, A1.186 show at

7 days curing Ca concentrations were higher and Si concentrations were lower whilst at 175 days curing Ca concentrations fluctuated, Na concentrations were much higher, Si concentrations were lower whilst Mg and Al concentrations were unaffected by the increased test duration.

A1.2.18.4 Curing Time

Figures A1.75 to A1.78 all illustrate again very large reductions in pH and conductivity as curing period increases. Tables A1.177 to A1.186 relate this to very large reductions in Ca and Na concentrations, increases in Si concentration and no significant change in Mg concentration. Concentrations of Al increase from 7 to 175 days curing and then reduce from 175 to 301 days curing

Figure A1.75 Conductivity and pH characteristics for Wyoming Bentonite with 5000ppm Fe and 7.0% lime during 6hr/30rpm Batch Tests

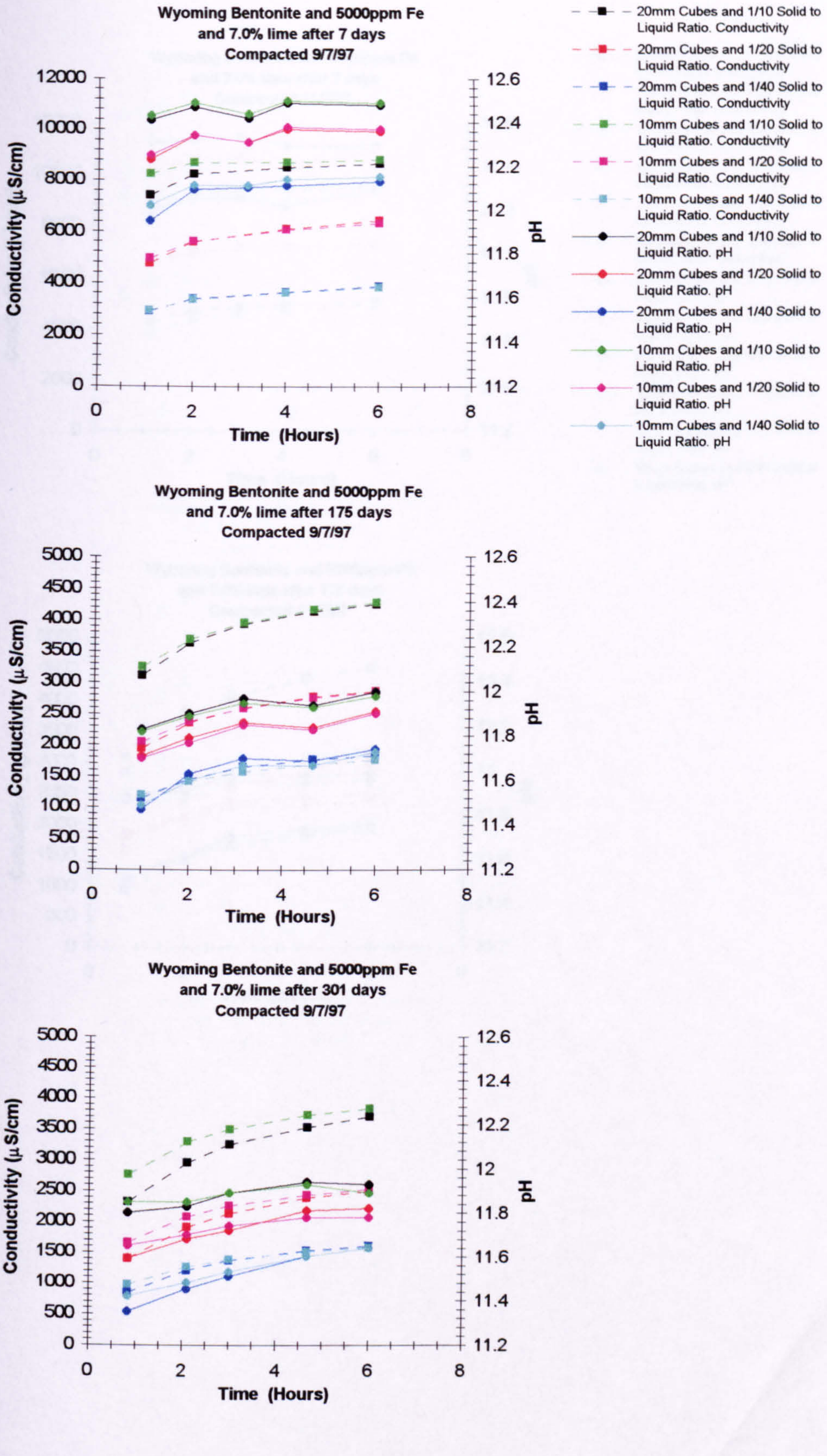

Figure A1.76 Conductivity and pH characteristics for Wyoming Bentonite with 5000ppm Fe and 7.0% lime during 6hr/60rpm Batch Tests

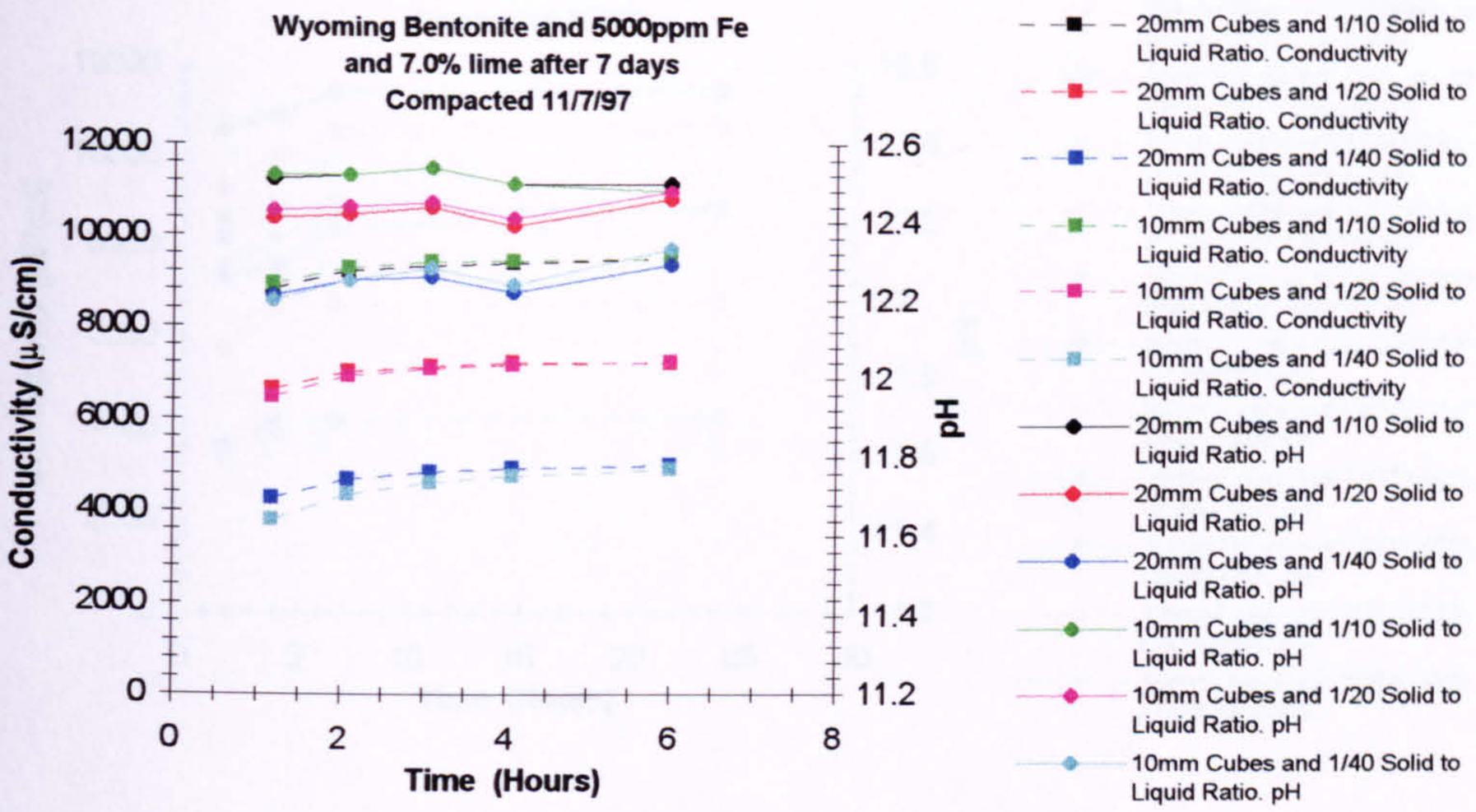

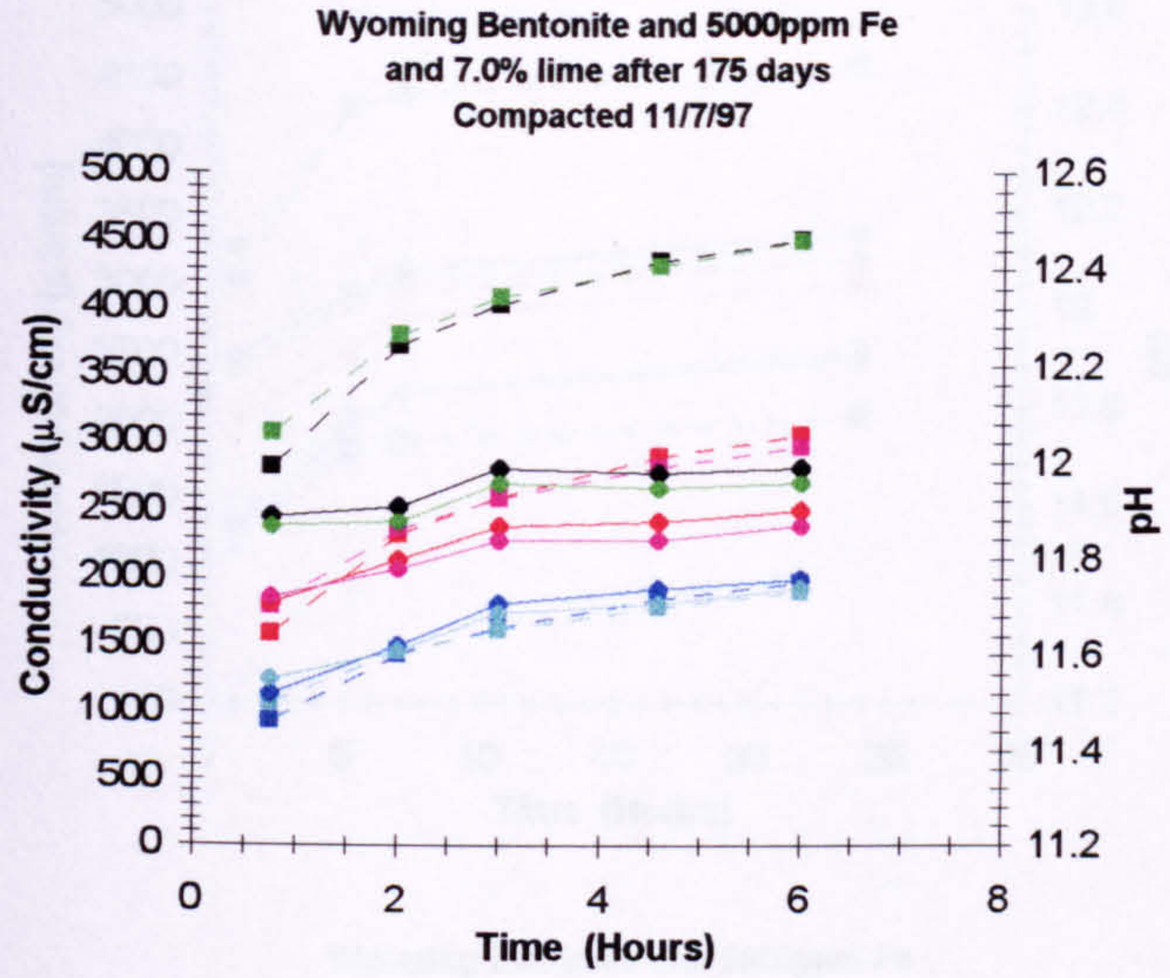

Figure A1.77 Conductivity and pH characteristics for Wyoming Bentonite with 5000ppm Fe and 7.0% lime during 24hr/30rpm Batch Tests

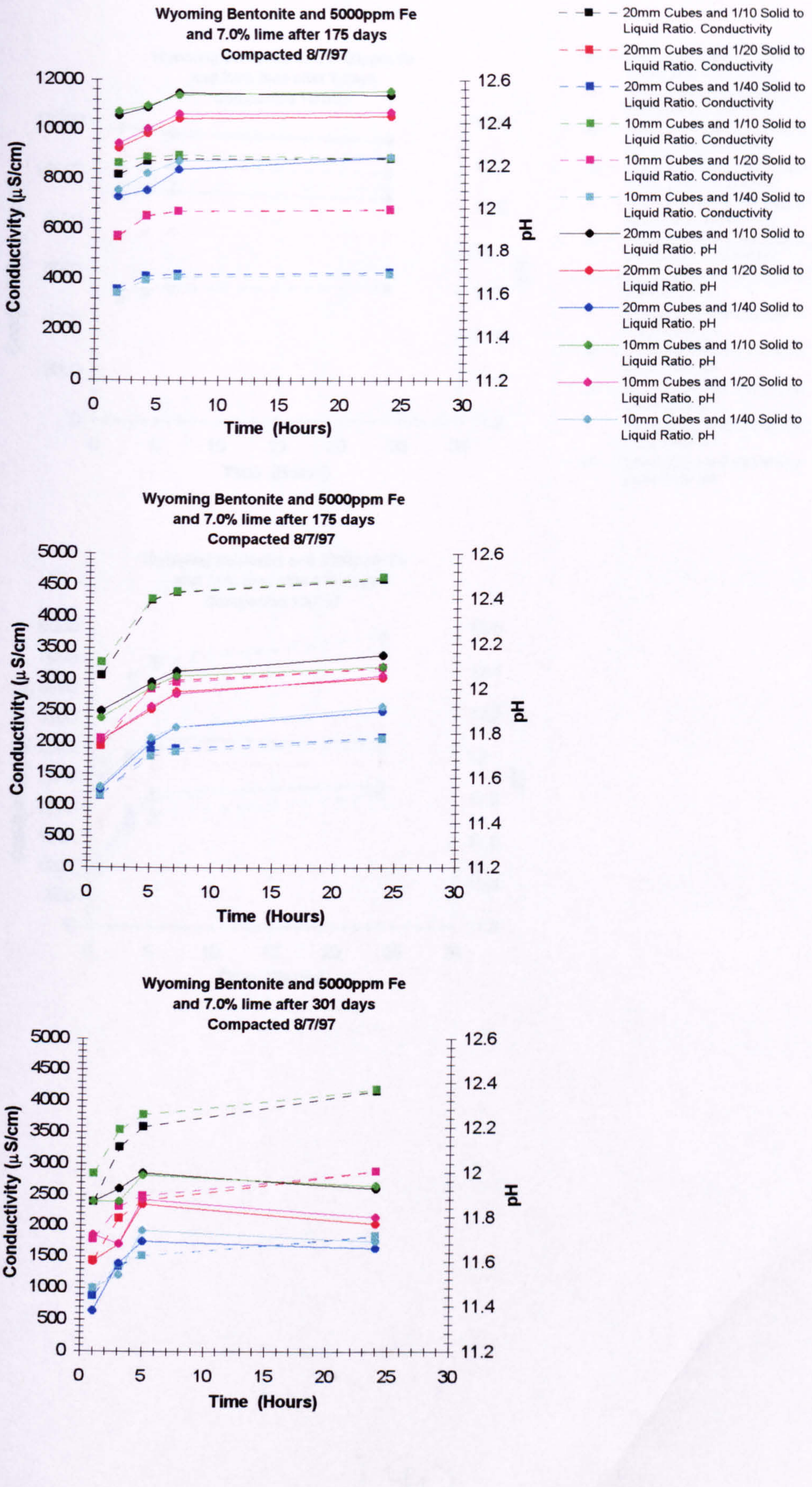

Figure A1.78 Conductivity and pH characteristics for Wyoming Bentonite with 5000ppm Fe and 7.0% lime during 24hr/60rpm Batch Tests

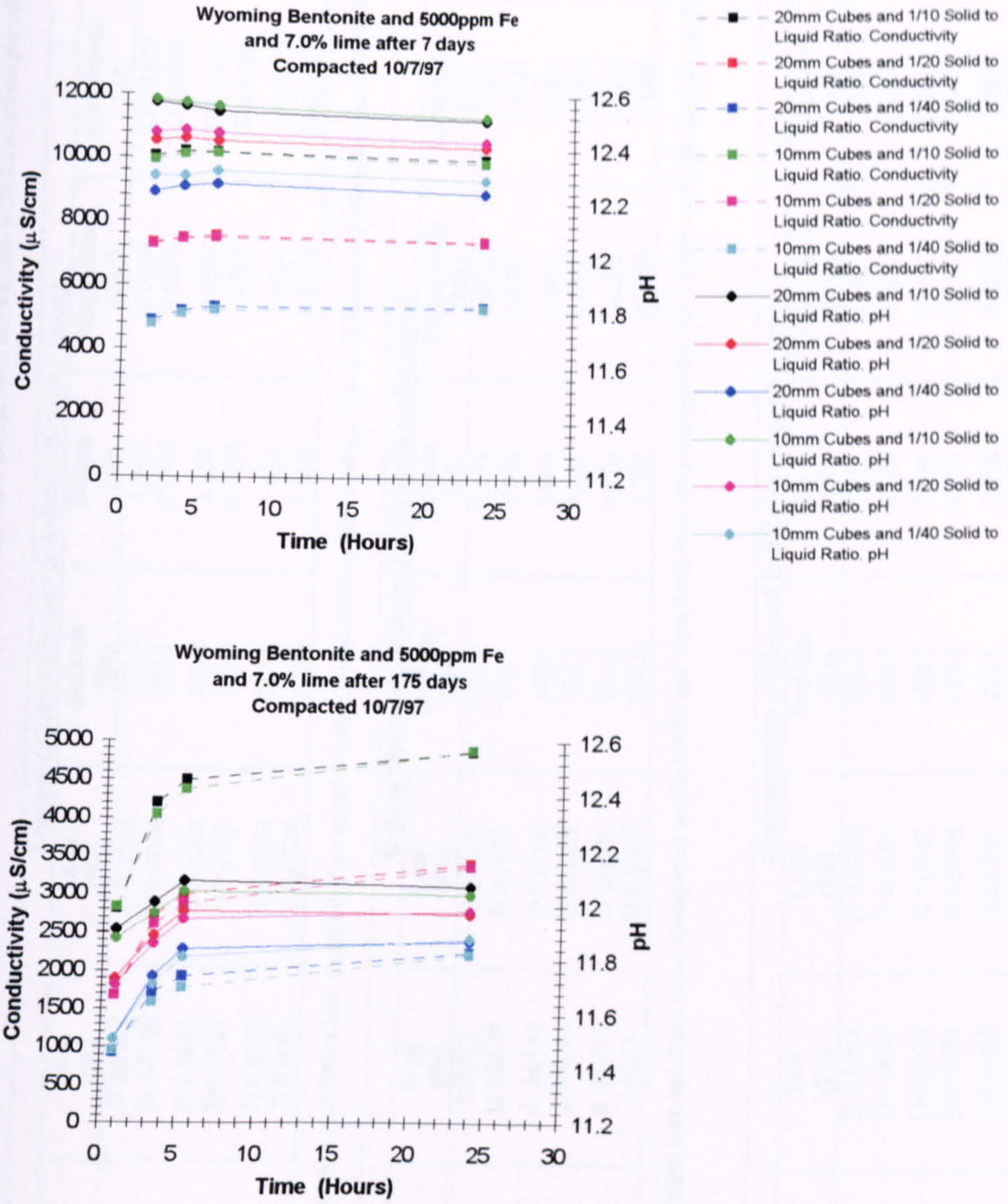

Table A1.177 ICP Data for Wyoming Bentonite and 5000ppm Iron and 7.0% Lime, Compacted on the 9/7/97 and Tested 7 days after Compaction for 6 Hours at 30 Revolutions per Minute. Filtered only.

Solid to Liquid Ratio	Initial Cube Size (mm)	Concentration of Element in Solution in mg/kg (ppm)							
		Calcium (Ca)	Iron (Fe)	Lead (Pb)	Sodium (Na)	Silicon (Si)	Magnesium (Mg)	Aluminium (Al)	Manganese (Mn)
1/10	10	180.0	D 0.0822	D 0.0306	928.5	1.082	0.0626	D 0.2129	D 0.0005
	20	268.3	D 0.0169	D 0.0048	907.5	0.7945	0.0258	D 0.0545	D 0.0010
1/20	10	188.9	D 0.0056	D 0.0000	498.8	1.056	0.0184	D 0.0481	D 0.0001
	20	235.3	D 0.0123	D 0.0305	563.9	0.9801	0.0181	D 0.0180	D 0.0004
1/40	10	163.5	D 0.0152	D 0.0220	273.0	1.671	0.0291	D 0.0507	D 0.0010
	20	128.2	D 0.0063	D 0.0124	265.9	1.665	0.0219	D 0.0571	D 0.0003

Table A1.178 ICP Data for Wyoming Bentonite 5000ppm Iron and 7.0% Lime, Compacted on the 9/7/97 and Tested 175 days after Compaction for 6 Hours at 30 Revolutions per Minute. Filtered only.

Solid to Liquid Ratio	Initial Cube Size (mm)	Concentration of Element in Solution in mg/kg (ppm)							
		Calcium (Ca)	Iron (Fe)	Lead (Pb)	Sodium (Na)	Silicon (Si)	Magnesium (Mg)	Aluminium (Al)	Manganese (Mn)
1/10	10	15.15	0.0317	D 0.0000	743.3	3.197	0.0356	0.5407	D 0.0001
	20	20.77	D 0.0074	D 0.0075	717.3	3.048	0.0211	0.4337	D 0.0004
1/20	10	1.528	d. 0.0141	D 0.0000	449.6	3.804	0.0261	0.5361	D 0.0028
	20	3.986	d. 0.0084	D 0.0239	431.7	3.432	0.0167	0.4500	D 0.0003
1/40	10	2.713	d. 0.0110	D 0.0000	264.2	4.176	0.0282	0.4210	D 0.0002
	20	1.900	0.0205	D 0.0000	256.8	3.709	0.0205	0.3868	D 0.0001

Table A1.179 ICP Data for Wyoming Bentonite and 5000ppm Iron and 7.0% Lime, Compacted on the 9/7/97 and Tested 301 days after Compaction for 6 Hours at 30 Revolutions per Minute. Filtered only.

Solid to Liquid Ratio	Initial Cube Size (mm)	Concentration of Element in Solution in mg/kg (ppm)							
		Calcium (Ca)	Iron (Fe)	Lead (Pb)	Sodium (Na)	Silicon (Si)	Magnesium (Mg)	Aluminium (Al)	Manganese (Mn)
1/10	10	18.63	D 0.0068	D 0.0126	696.9	4.152	0.0329	0.2833	D 0.0000
	20	9.487	D 0.0037	D 0.0183	662.3	4.126	0.0285	0.2578	D 0.0002
1/20	10	29.14	D 0.0023	D 0.0147	428.7	4.396	0.0337	0.3315	D 0.0001
	20	29.57	D 0.0033	D 0.0108	425.4	4.613	0.0219	0.3449	D 0.0001
1/40	10	18.85	D 0.0023	D 0.0165	256.4	4.605	0.0288	0.2586	D 0.0001
	20	19.61	D 0.0077	D 0.0152	259.4	4.548	0.0288	0.2695	D 0.0000

Note: 'D' indicates the stated value is below detection limits and the value stated is a system estimate.
'd' indicates the stated value is close to detection limits.

Table A1.180 ICP Data for Wyoming Bentonite and 5000ppm Iron and 7.0% Lime, Compacted on the 11/7/97 and Tested 7 days after Compaction for 6 Hours at 60 Revolutions per Minute. Filtered only.

Solid to Liquid Ratio	Initial Cube Size (mm)	Concentration of Element in Solution in mg/kg (ppm)							
		Calcium (Ca)	Iron (Fe)	Lead (Pb)	Sodium (Na)	Silicon (Si)	Magnesium (Mg)	Aluminium (Al)	Manganese (Mn)
1/10	10	229.7	D 0.0033	D 0.0125	968.7	0.6024	0.0197	D 0.0323	D 0.0001
	20	256.4	D 0.0039	D 0.0039	983.9	0.5903	0.0235	D 0.0632	D 0.0005
1/20	10	292.2	D 0.0577	D 0.0000	530.9	0.7855	0.0362	D 0.0474	D 0.0008
	20	240.9	D 0.0624	D 0.0077	515.1	0.7338	0.0237	D 0.0206	D 0.0001
1/40	10	247.0	D 0.0225	D 0.0114	279.6	1.090	0.0432	D 0.0643	D 0.0010
	20	210.5	D 0.0033	D 0.0029	273.0	0.9995	0.0292	D 0.0491	D 0.0001

Table A1.181 ICP Data for Wyoming Bentonite 5000ppm Iron and 7.0% Lime, Compacted on the 11/7/97 and Tested 175 days after Compaction for 6 Hours at 60 Revolutions per Minute. Filtered only.

Solid to Liquid Ratio	Initial Cube Size (mm)	Concentration of Element in Solution in mg/kg (ppm)							
		Calcium (Ca)	Iron (Fe)	Lead (Pb)	Sodium (Na)	Silicon (Si)	Magnesium (Mg)	Aluminium (Al)	Manganese (Mn)
1/10	10	49.93	D 0.0035	D 0.0000	733.2	3.042	0.0327	1.659	D 0.0002
	20	50.07	0.0214	d. 0.0037	750.3	2.808	0.0245	1.684	D 0.0001
1/20	10	31.10	0.0105	D 0.0168	414.0	3.310	0.0316	1.573	D 0.0005
	20	19.50	d. 0.0332	D 0.0186	444.7	3.026	0.0257	1.689	D 0.0003
1/40	10	42.93	d. 0.0194	D 0.0000	237.8	3.498	0.0491	1.281	D 0.0001
	20	17.54	0.0279	D 0.0000	253.8	3.235	0.0389	1.401	D 0.0002

Note : 'D' indicates the stated value is below detection limits and the value stated is a system estimate.
'd' indicates the stated value is close to detection limits.

Table A1.182 ICP Data for Wyoming Bentonite and 5000ppm Iron and 7.0% Lime, Compacted on the 8/7/97 and Tested 7 days after Compaction for 24 Hours at 30 Revolutions per Minute. Filtered only.

Solid to Liquid Ratio	Initial Cube Size (mm)	Concentration of Element in Solution in mg/kg (ppm)							
		Calcium (Ca)	Iron (Fe)	Lead (Pb)	Sodium (Na)	Silicon (Si)	Magnesium (Mg)	Aluminium (Al)	Manganese (Mn)
1/10	10	214.1	D 0.0176	D 0.0000	976.1	0.7149	0.0251	D 0.0037	D 0.0002
	20	314.5	0.1138	D 0.0000	1112	1.099	0.0554	D 0.1434	D 0.0011
1/20	10	189.7	D 0.0156	D 0.0000	525.2	0.7716	0.0189	D 0.0247	D 0.0000
	20	234.5	D 0.0131	D 0.0078	533.0	0.8630	0.0194	D 0.0000	D 0.0000
1/40	10	132.0	D 0.0407	D 0.0046	271.0	1.340	0.0336	D 0.0583	D 0.0004
	20	169.3	D 0.0118	D 0.0000	276.7	1.333	0.0256	D 0.0190	D 0.0005

Table A1.183 ICP Data for Wyoming Bentonite 5000ppm Iron and 7.0% Lime, Compacted on the 8/7/97 and Tested 175 days after Compaction for 24 Hours at 30 Revolutions per Minute. Filtered only.

Solid to Liquid Ratio	Initial Cube Size (mm)	Concentration of Element in Solution in mg/kg (ppm)							
		Calcium (Ca)	Iron (Fe)	Lead (Pb)	Sodium (Na)	Silicon (Si)	Magnesium (Mg)	Aluminium (Al)	Manganese (Mn)
1/10	10	34.74	0.0275	D 0.0244	761.9	3.220	0.0209	0.4687	D 0.0004
	20	24.00	0.0213	D 0.0069	754.5	3.173	0.0419	0.4436	D 0.0009
1/20	10	39.78	d. 0.0058	D 0.0148	456.2	3.558	0.0226	0.3582	D 0.0001
	20	41.19	D 0.0143	D 0.0000	442.9	3.415	0.0283	0.5245	D 0.0002
1/40	10	32.39	d. 0.0062	D 0.0066	278.8	3.838	0.0264	0.2878	D 0.0002
	20	31.56	d. 0.0102	D 0.0100	259.3	3.587	0.0432	0.4060	D 0.0000

Table A1.184 ICP Data for Wyoming Bentonite and 5000ppm Iron and 7.0% Lime, Compacted on the 8/7/97 and Tested 301 days after Compaction for 24 Hours at 30 Revolutions per Minute. Filtered only.

Solid to Liquid Ratio	Initial Cube Size (mm)	Concentration of Element in Solution in mg/kg (ppm)							
		Calcium (Ca)	Iron (Fe)	Lead (Pb)	Sodium (Na)	Silicon (Si)	Magnesium (Mg)	Aluminium (Al)	Manganese (Mn)
1/10	10	14.68	D 0.0066	D 0.0134	751.9	4.096	0.0389	0.2372	D 0.0001
	20	52.49	D 0.0062	D 0.0052	723.1	3.790	0.0293	0.2761	D 0.0003
1/20	10	5.837	D 0.0035	D 0.0164	449.9	4.237	0.0262	0.2916	D 0.0002
	20	35.16	D 0.0034	D 0.0078	440.1	4.132	0.0186	0.3136	D 0.0000
1/40	10	24.57	D 0.0042	D 0.0139	265.1	4.839	0.0198	0.2301	D 0.0002
	20	25.57	D 0.0040	D 0.0180	263.9	4.769	0.0208	0.2177	D 0.0002

Note: 'D' indicates the stated value is below detection limits and the value stated is a system estimate.
'd' indicates the stated value is close to detection limits.

Table A1.185 ICP Data for Wyoming Bentonite and 5000ppm Iron and 7.0% Lime, Compacted on the 10/7/97 and Tested 7 days after Compaction for 24 Hours at 60 Revolutions per Minute. Filtered only.

Solid to Liquid Ratio	Initial Cube Size (mm)	Concentration of Element in Solution in mg/kg (ppm)							
		Calcium (Ca)	Iron (Fe)	Lead (Pb)	Sodium (Na)	Silicon (Si)	Magnesium (Mg)	Aluminium (Al)	Manganese (Mn)
1/10	10	282.0	D 0.0058	D 0.0000	965.5	0.5015	0.0144	D 0.0112	D 0.0002
	20	329.7	D 0.0054	D 0.0231	989.5	0.4930	0.0137	D 0.0289	D 0.0002
1/20	10	287.7	D 0.0239	D 0.0000	539.5	0.7268	0.0304	D 0.0909	D 0.0004
	20	296.0	D 0.0062	D 0.0144	537.3	0.5493	0.0211	D 0.0248	D 0.0003
1/40	10	245.5	D 0.0049	D 0.0000	282.5	0.7443	0.0227	D 0.0713	D 0.0003
	20	254.4	D 0.0047	D 0.0002	273.2	0.7322	0.0236	D 0.0537	D 0.0001

Table A1.186 ICP Data for Wyoming Bentonite 5000ppm Iron and 7.0% Lime, Compacted on the 10/7/97 and Tested 175 days after Compaction for 24 Hours at 60 Revolutions per Minute. Filtered only.

Solid to Liquid Ratio	Initial Cube Size (mm)	Concentration of Element in Solution in mg/kg (ppm)							
		Calcium (Ca)	Iron (Fe)	Lead (Pb)	Sodium (Na)	Silicon (Si)	Magnesium (Mg)	Aluminium (Al)	Manganese (Mn)
1/10	10	22.77	d. 0.0038	D 0.0000	815.4	2.677	0.0222	1.704	D 0.0000
	20	52.86	0.0228	D 0.0129	820.5	2.760	0.0255	1.641	D 0.0002
1/20	10	31.35	d. 0.0091	D 0.0000	501.0	2.995	0.0211	1.481	D 0.0002
	20	22.99	d. 0.0331	D 0.0000	488.8	2.976	0.0281	1.513	D 0.0000
1/40	10	3.690	0.0610	D 0.0054	294.2	3.437	0.0444	1.315	D 0.0005
	20	32.50	d. 0.0098	D 0.0052	292.5	3.106	0.0274	1.177	D 0.0003

Note : 'D' indicates the stated value is below detection limits and the value stated is a system estimate.
'd' indicates the stated value is close to detection limits.

APPENDIX 2

CLAY-ION-INTERACTIONS:

ENERGY MODELS

A2.1 THE EISENMAN ENERGY MODEL OF CATION EXCHANGE

In order to predict selectivity and general ion behaviour it is useful to develop models. McBride (1994) explains a descriptive interpretation of cation exchange developed by Eisenman (1961) which provides a theory for the different behaviour of ions of different radius. The electrostatic attraction energy, E_{att}, between the adsorbed cation, A^+, and the surface charge site is inversely proportional to the sum of r_s, the effective radius of the charge site, and r_A, the radius of cation A^+. Hence Equation A2.1.

$$E_{att} \propto \frac{e^2}{(r_s + r_A)} \qquad \textbf{Equation A2.1}$$

Where:

e is the electronic charge unit

The exchange cation at the charge site is shown in Figure A2.1 below, but the direct contact shown here would require that energy be used to force aside water molecules separating the cation from the surface. This water is held by hydration of the site and the cation and hence the energy that must be expended should be proportional to the energy of hydration of the site, E_s, and of the cation, E_A. Hence the total energy E_{tot}, resulting from the movement of ion A^+ from solution into contact with the surface is given by Equation A2.2.

$$E_{tot} \propto \left\{ -\left(\frac{e^2}{r_s + r_A} \right) + E_s + E_A \right\} \qquad \textbf{Equation A2.2}$$

Figure A2.1 **Schematic depiction of the clay surface-exchange cation interaction in the case of (A) no water molecules present, (B) water present on a 'weak field' exchanger, and (C) water present on a 'strong field' exchanger (after McBride, 1994).**

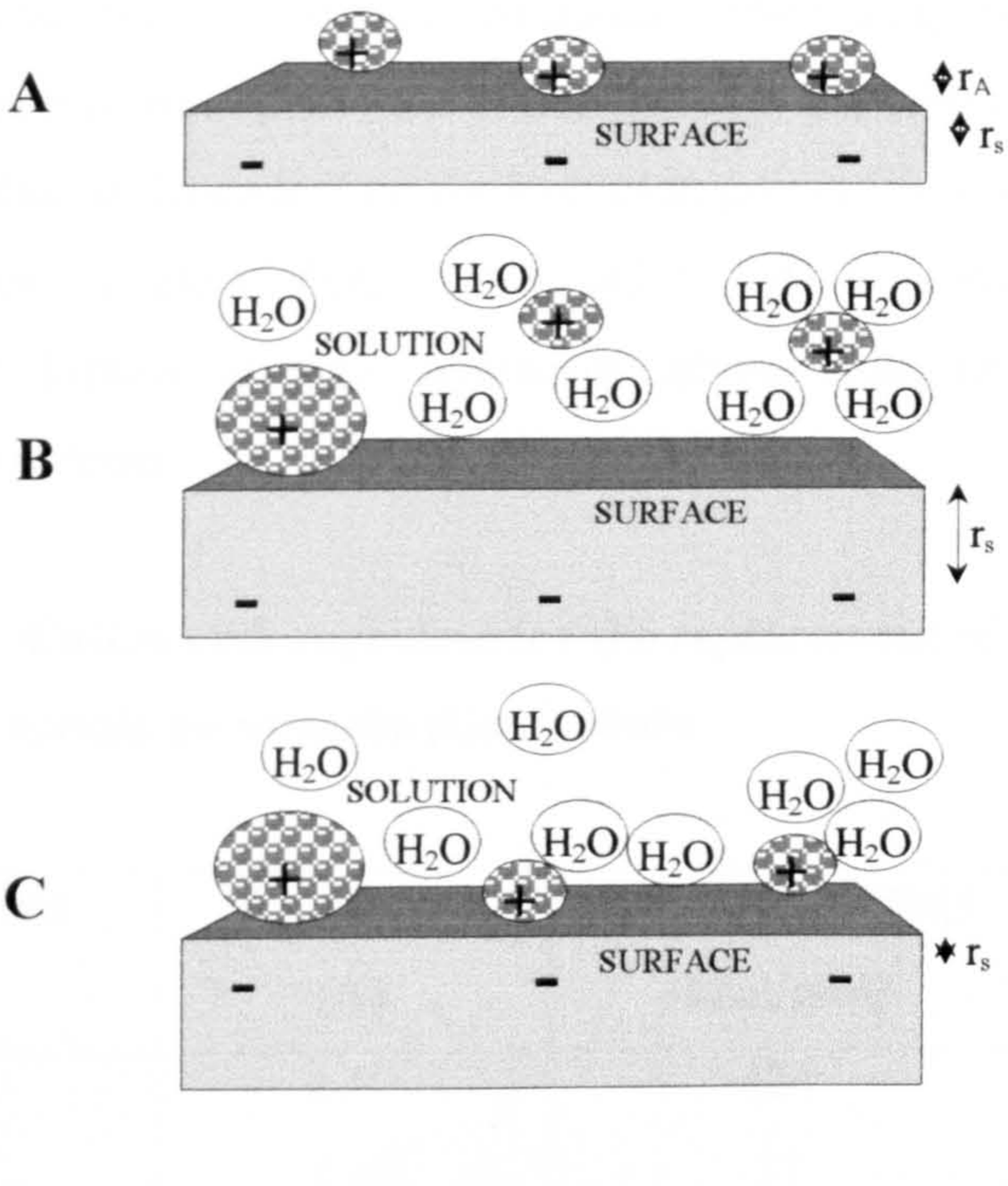

The adsorption of ion A^+ is inherently accompanied by the desorption of ion B^+, so that the overall change in energy for the exchange of ion B^+ by ion A^+ is given by Equation A2.3.

$$\Delta E_{tot} \propto \left\{ \left(\frac{e^2}{r_s + r_B} - \frac{e^2}{r_s + r_A} \right) - (E_B - E_A) \right\} \qquad \textbf{Equation A2.3}$$

Where:

r_B and E_B are the radius and hydration energy of ion B.

According to McBride (1994) this simple electrostatic model creates two limiting cases. When the structural charge is located well beneath the surface, which is the case for layer silicate clays after isomorphous substitution in the octahedral layer, then the distance between the exchange cation and the site of negative charge ($r_s + r_A$ or $r_s + r_B$) must be large, so that the electrostatic term in Equation A2.3

becomes small. The implication of this is that the energy of exchange, ΔE_{tot}, is largely dependent on the difference in hydration energies of ions A^+ and B^+. This weak field case is illustrated in Figure A2.1B where strongly hydrating cations such as Li^+, Ca^{2+}, and Mg^{2+} are not attracted strongly to the surface to overcome the forces of hydration. Only weakly hydrating cations such as K^+ and Cs^+ are expected to come into direct contact with the surface. McBride (1994) suggests that this behaviour of cation adsorption is appropriate for smectites, with the result that the energy of the exchange reaction is dependent on the hydration properties of the exchanging cations. This behaviour is clear from Table A2.1, where weakly hydrating cations spontaneously displace strongly hydrating cations from the clay, and energy is released in the process.

Table A2.1 Cation exchange data for the replacement of Na^+ by other alkali metals on smectite (Gast, 1969).

Replacing Ion (M^+)	Ion Radius (Å)	Hydration Energy (kcal/mol)	Reaction Heat (ΔH) (kcal/mol)
Li^+	0.60	124	+0.019 (endothermic)
K^+	1.33	77	-1.16 (exothermic)
Rb^+	1.48	72	-1.92 (exothermic)
Cs^+	1.69	66	-2.65 (exothermic)

A second possible limiting case for ion exchange based on the model occurs if the structural charge is at or near the solid surface, so that r_s is small relative to r_A and r_B. This results in the electrostatic term in Equation A2.3 being very significant and may contribute more to ΔE_{tot} than the hydration term. This is the strong field case illustrated in Figure A2.1C, where all cations are in direct contact with the clay surface. No permanent-charge clays are known to possess strong field behaviour, although Fe oxide minerals which develop negative charge by the dissociation of H_20 molecules have revealed a preference for smaller cations in the order $Li^+ > K^+ > Cs^+$, consistent with strong field exchanger behaviour. Clearly this order of selectivity is the opposite of that observed for permanent-charge layer silicate clays and according

to McBride (1994) may reflect the small effective radius (r_s) of the charged hydroxyl group at the oxide surface.

With ionic radius and charge being very important, a number of examples illustrating how these properties vary across the periodic table are illustrated as ionic potentials in Figure A2.2.

Figure A2.2 Ionic potentials (Z/r) of important ions found in soil (Loughnan, 1969)

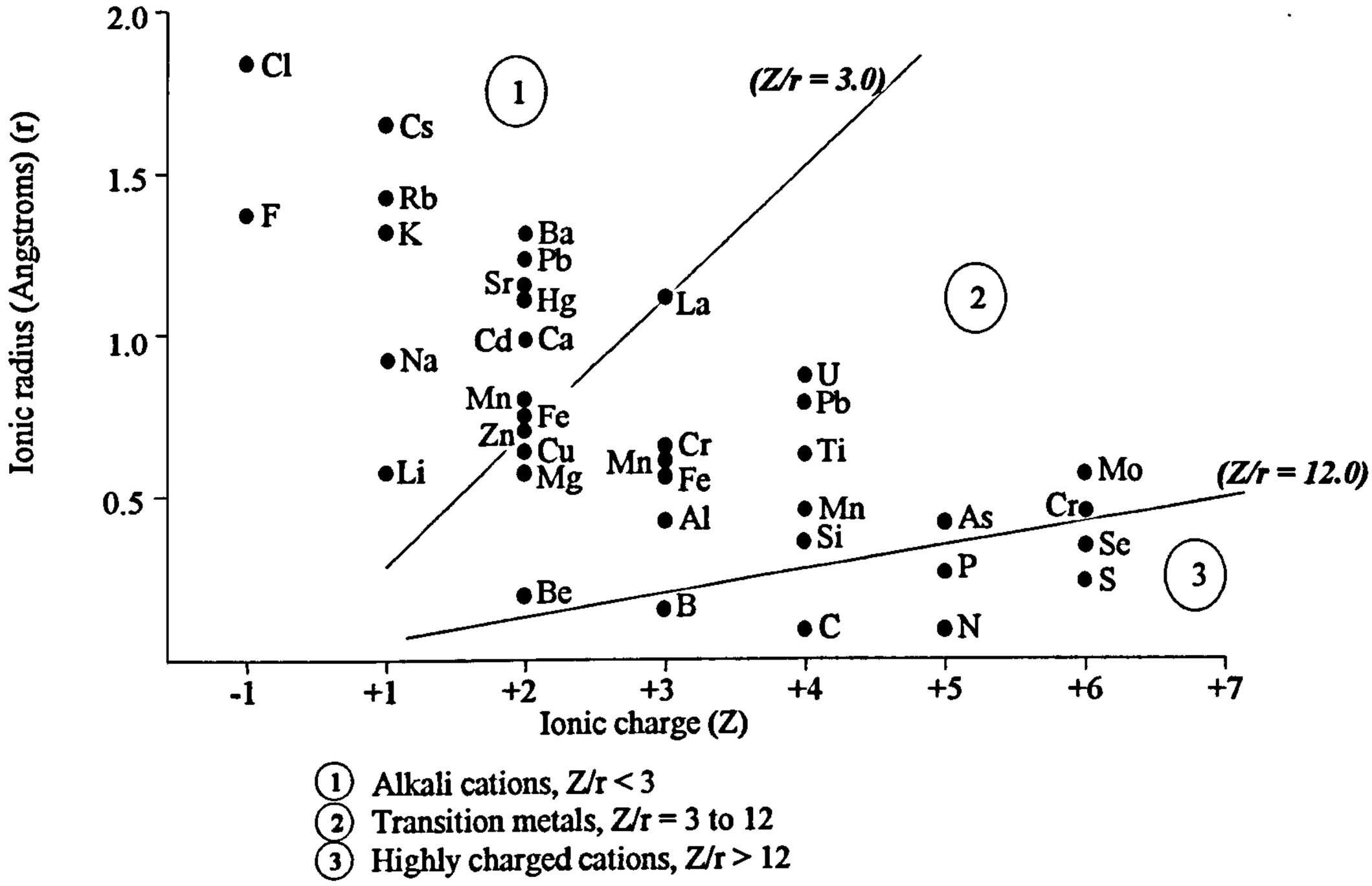

(1) Alkali cations, Z/r < 3
(2) Transition metals, Z/r = 3 to 12
(3) Highly charged cations, Z/r > 12

However conceptually useful, the Eisenman model is incomplete since it does no take into account entropy (disorder) changes associated with cation exchange. Entropy is calculated according to Equation A2.4 (Hill *et al*, 1989).

$$\text{Entropy } (JK^{-1}), \qquad S = k\ln W \qquad \textbf{Equation A2.4}$$

Where

k = Boltzmann Constant $= 1.38 \times 10^{-23} JK^{-1}$

W = The number of ways in which a change can occur.

For ions of equal charge, these entropy changes are quite small, however, for exchange between ions of different charge, the change in entropy may be substantial driving a reaction one way or the other. The sources of increased entropy in an

exchange reaction are changes in disorder of water molecules and cations, both adsorbed and in solution.

A2.2 CATION EXCHANGE BETWEEN IONS OF UNEQUAL CHARGE

At low salt concentrations, Ca^{2+} is a good competitor for exchange sites on clays occupied by monovalent ions but does not compete very well for sites occupied by cations of higher charge such as Al^{3+}. This is illustrated by Figure A2.3

Figure A2.3 Measured isotherms at low electrolyte concentrations for Ca^{2+} adsorption on K^{+}, Cu^{2+}, and Al^{3+} saturated smectites (McBride, 1994)

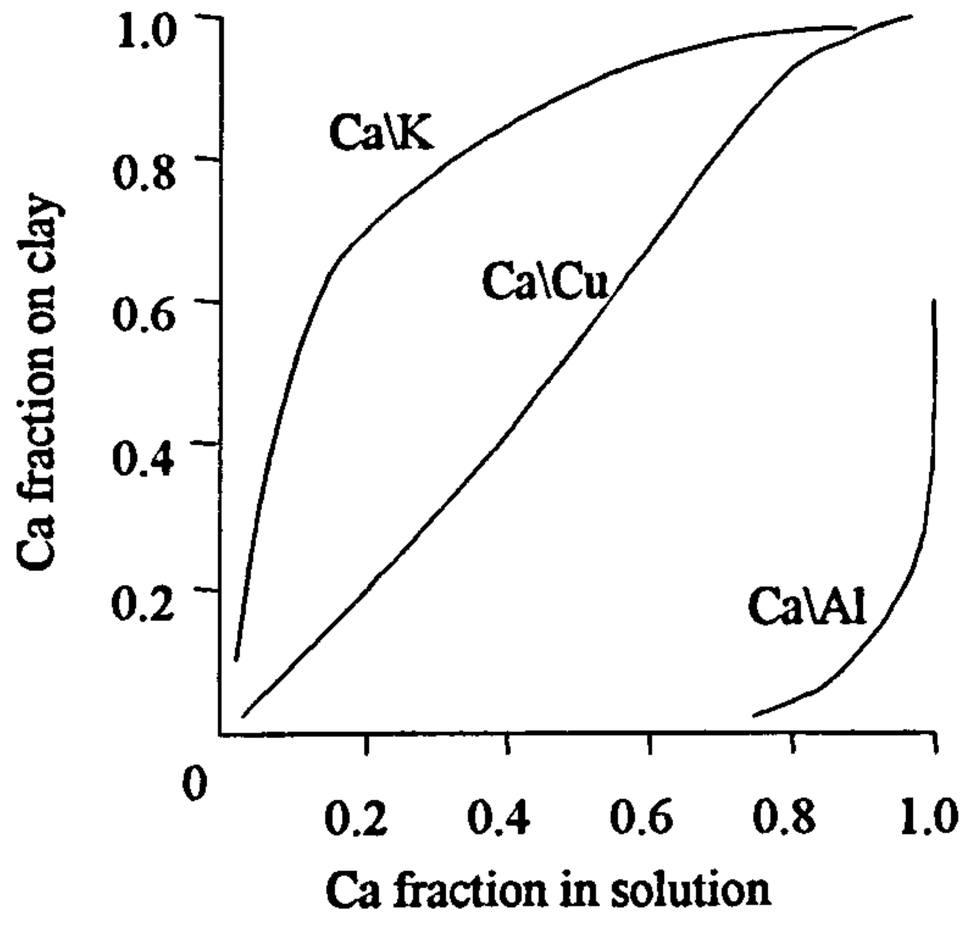

Results such as this could lead to the conclusion that electrostatic force only and hence cation valency governs selectivity as commonly observed for metal (M) on clays:

$$M^{3+} > M^{2+} > M^{+}$$

Surprisingly however thermodynamic studies of ion exchange have shown that the spontaneous exchange of low-charge by high-charge cations on clays is an endothermic process. Essentially this means that the reaction requires a net input of energy for the reaction to occur. Hence ΔH, the enthalpy change for the reaction is defined to be positive.

The trends associated with changing enthalpy (energy) and entropy(disorder) of the reaction are evident in Table A2.2.

Table A2.2 Thermodynamic data for the exchange of NH_4^+ and K^+ on smectite by alkaline earth metals (adapted from Gilbert *et al*, 1970)

Adsorbing Ion	Displaced Ion	Enthalpy Change ΔH^0 (kcal/mol)	Entropy Change ΔS^0 (cal/degree-mole)
Mg^{2+}	$2NH_4^+$	+2.79	+5.92
Mn^{2+}	$2NH_4^+$	+2.74	+5.83
Ca^{2+}	$2NH_4^+$	+2.70	+5.72
Sr^{2+}	$2NH_4^+$	+2.20	+4.13
Ba^{2+}	$2NH_4^+$	+1.92	+3.30
Ca^{2+}	$2K^+$	+3.87	+6.7

It has been hypothesised that the increase in entropy resulting from displacement of monovalent ions by divalent ions could arise from increased disorder of either cations or water molecules in the exchange reaction. The more strongly hydrating cations could have greater rotational mobility (disorder) at the clay surface than monovalent ions which may form ion pairs with the surface exchange sites. This is illustrated in Figures A2.4 and Figure A2.5.

Figure A2.4 Cations approaching a single smectite clay plate with octahedral layer charge (after McBride, 1994)

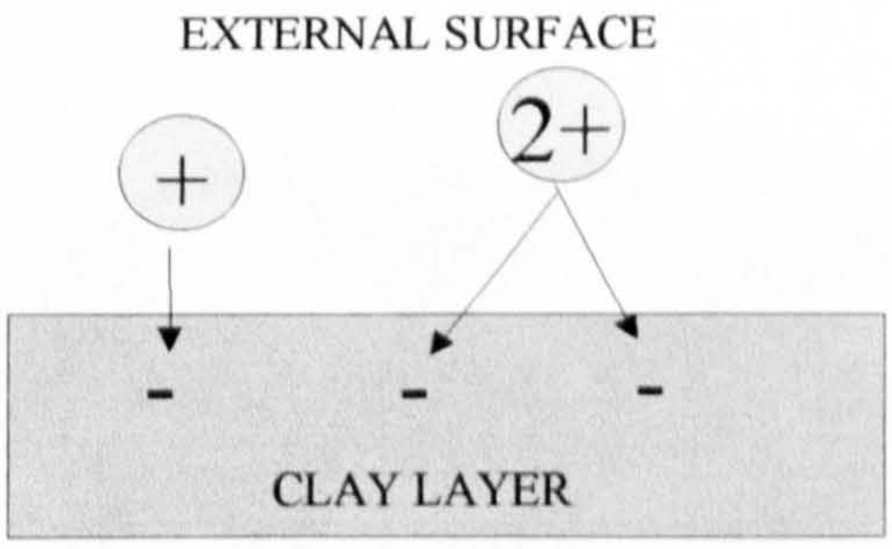

Figure A2.5 Monovalent and divalent cations between aligned smectite clay plates with octahedral layer charge (after McBride, 1994)

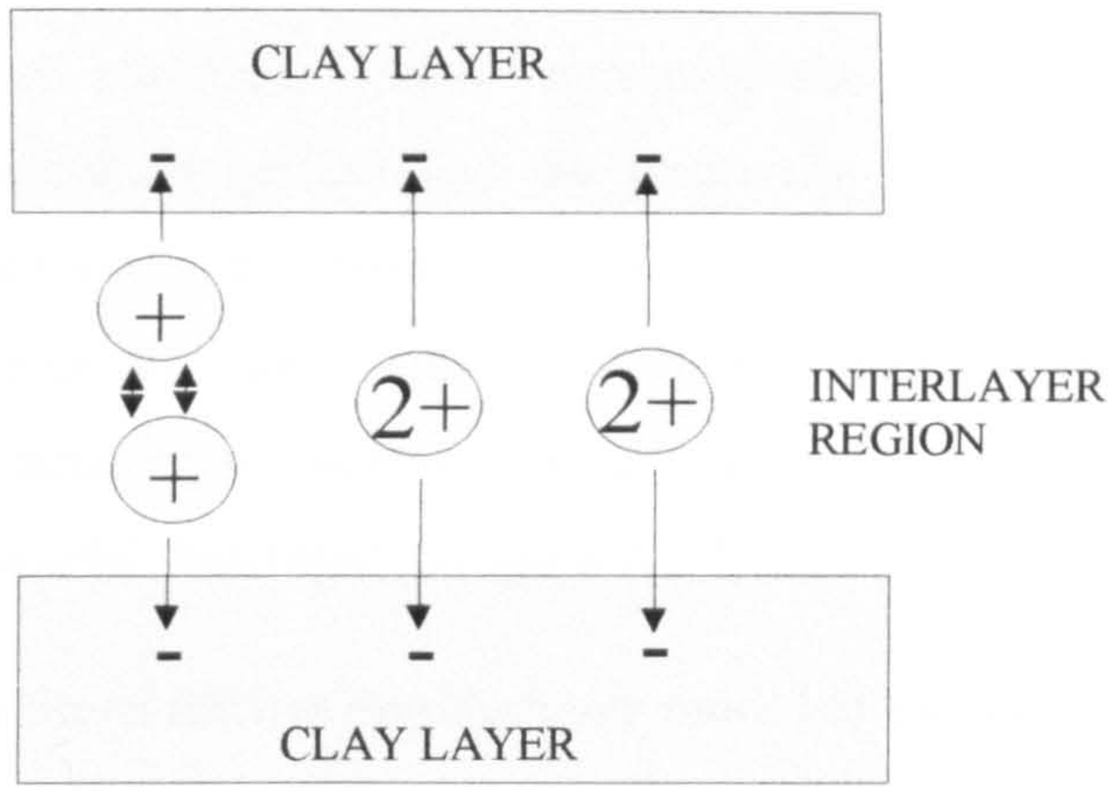

In Figure A2.4 the Na^+ ions can approach the surface charge quite closely, whereas the Ca^{2+} can not due to strongly held hydration shells. Thus electrostatically the Na^+ ion may be more stable thus explaining the endothermic nature of the Na^+ replacement by Ca^{2+} exchange reaction. Figure A2.5 illustrates what may occur if the clay plates become aligned and the ions situate between the plates. This geometry would prefer multivalent ions. Hence electrostatics and entropy considerations would result in the development of the system illustrated in Figure A2.6. Note the ions are in their most stable location with the calcium ions between the clay layers and the sodium ions on the outer surface of the clay layer.

Figure A2.6 Monovalent and divalent cations between multiple clay surfaces (after McBride, 1994)

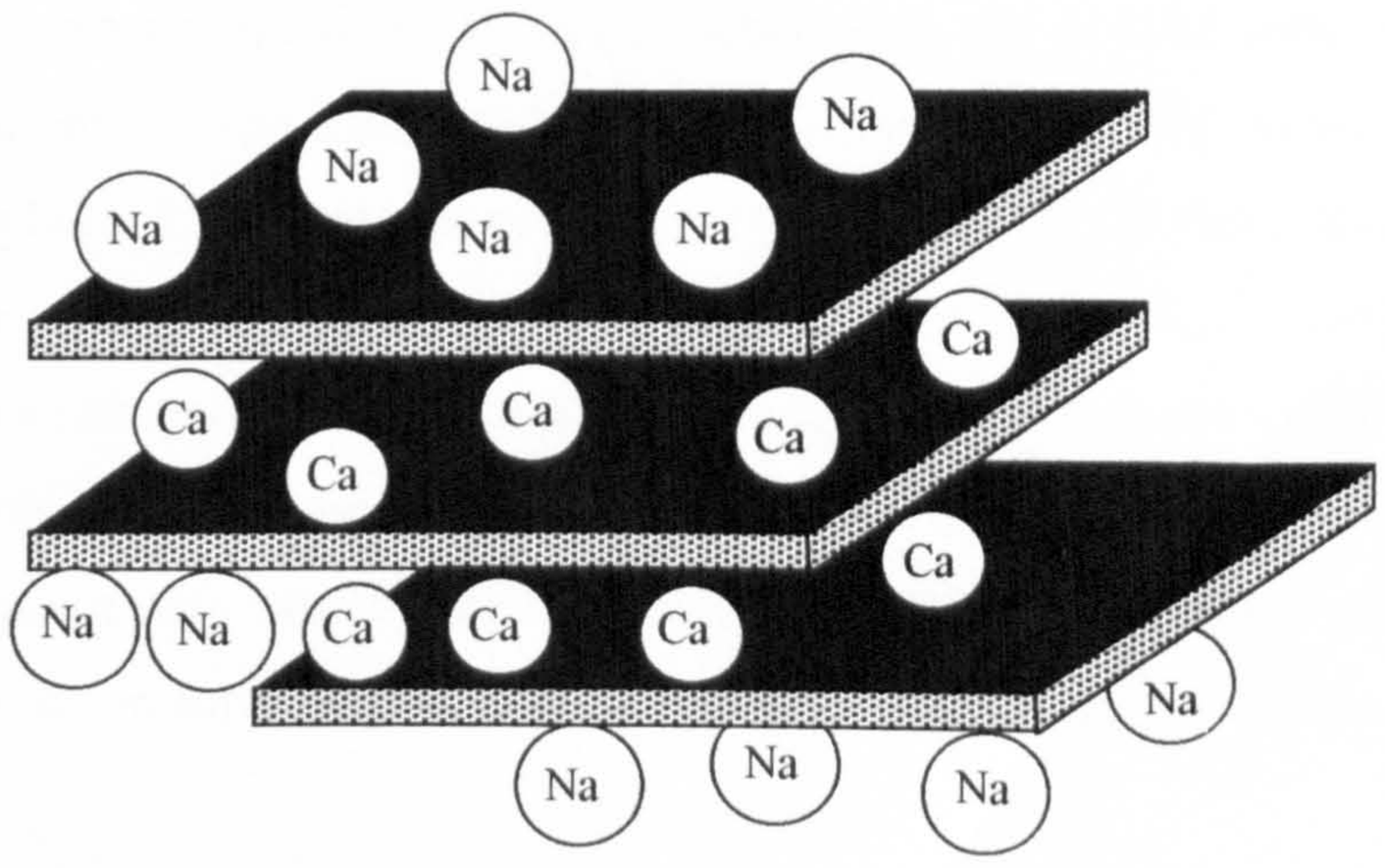

A2.3 THE STERN DIFFUSE DOUBLE LAYER MODEL OF CATION EXCHANGE

Many models of cation exchange at colloidal surfaces have incorporated a diffuse double-layer structure, which represents the parallel alignment of the negatively charged colloid surface and the positively charged layer. This model essentially explains the spatial distribution of ions relative to the charge surface since this cannot be determined experimentally. Arnold (1978) and White (1979) give a comprehensive introduction to the theory of these models. The most widely accepted model is the Stern model illustrated in Figure A2.7.

Figure A2.7 The Stern diffuse double layer model of cation exchange (Van Olphen, 1977)

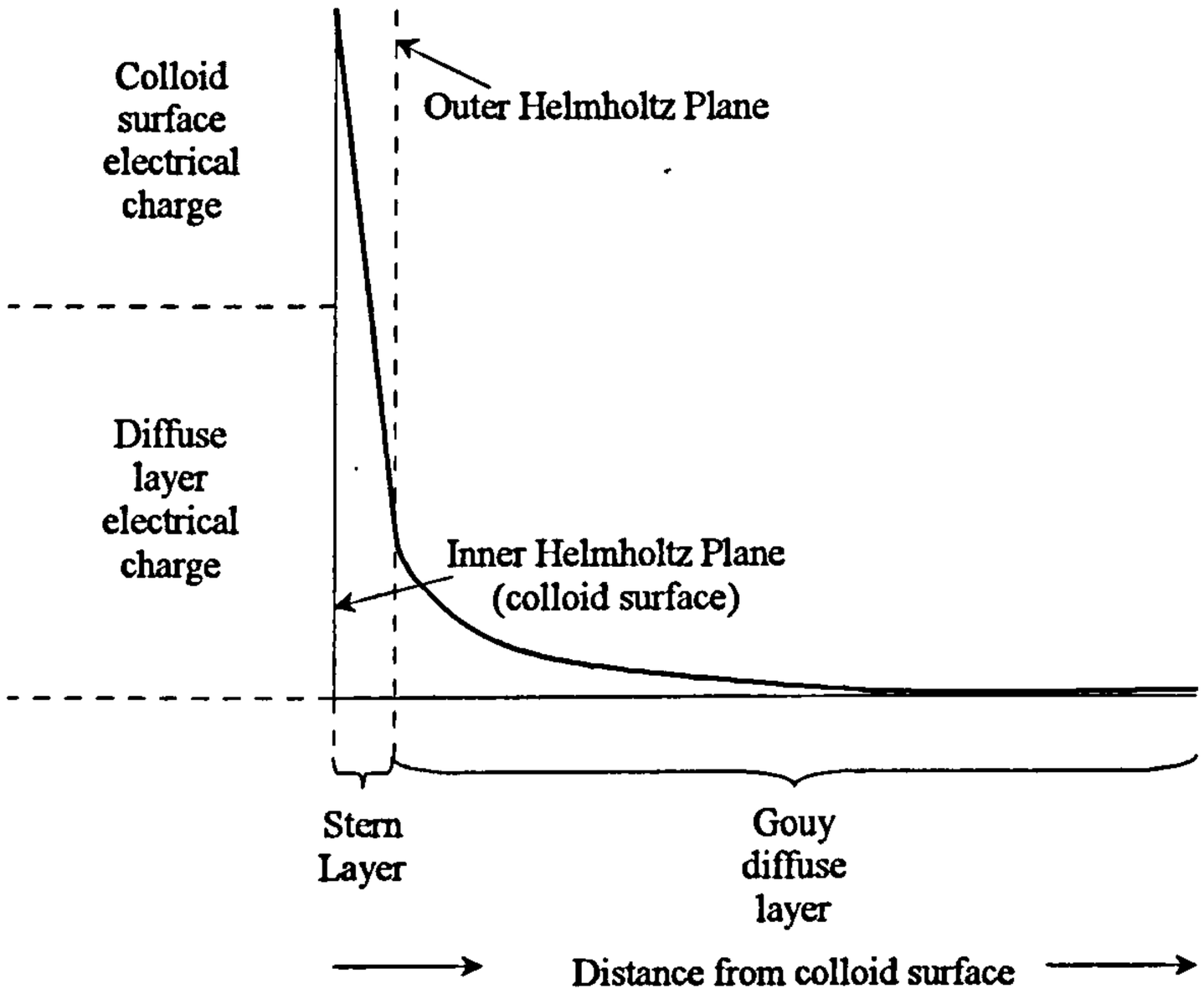

In the stern layer that lies immediately adjacent to the colloid surface, electrical charge decays linearly with distance from the colloid surface. The stern layer of cations is separated from the outer diffuse , or Gouy, layer by the outer Helmholtz plane. Electrical charge decays exponentially in the Gouy layer.

The colloidal properties of clays, such as dispersion, flocculation, and swelling, are influenced by the counter-ion distribution and as such it is an important theory. This model assumes that the surface can be visualised as a structurally featureless plane with evenly distributed charge, while counter-ions are assumed point charges in a uniform liquid continuum. Clearly simplified, the equilibrium

distribution of counter-ions in the Gouy-Chapman diffuse double-layer theory is represented by the Boltzmann equation, Equation A2.5:

$$n(x) = n_0 e^{\frac{-ze\psi(x)}{kT}} \qquad \textbf{Equation A2.5}$$

Where $n(x)$ and $\psi(x)$ are (respectively) the local concentration of counter-ions and the electrical potential at a distance, x, from the surface; n_0 is the concentration of counter-ions in bulk solution (i.e., at $x = \infty$); e is the unit of electronic charge; k is the Boltzmann constant; T is temperature (K); z is the charge of the counter-ion.

The equation therefore predicts a higher local concentration of cations near a negatively charged clay surface than in the bulk solution, and a lower concentration of anions near the surface than in solution (McBride, 1994) with concentrations tending towards that of the bulk solution as one move away from the colloid surface. However, McBride (1994) also states that modern statistical mechanical models of this clay interfacial region have predicted that ion-ion correlation (electrostatic) effects should cause deviations from this classical picture, such as positive adsorption of anions at intermediate distances from the surface when the cation is divalent or multivalent.

An important aspect of the diffuse double layer theory is, what occurs when concentration of the bulk solution is increased? Neilsen *et al.* (1972) illustrate in Figure A2.8 that the main effect of a higher bulk solution ionic concentration is to decrease the 'thickness' of the diffuse double. Reduction in the thickness of the diffuse double layer also occurs when the exchanging ion has a larger valency.

Figure A2.8 Distribution of monovalent cations and anions near the surface of a montmorillonite particle at three different concentrations in the bulk solution (original source: Neilson *et al.*, 1972)

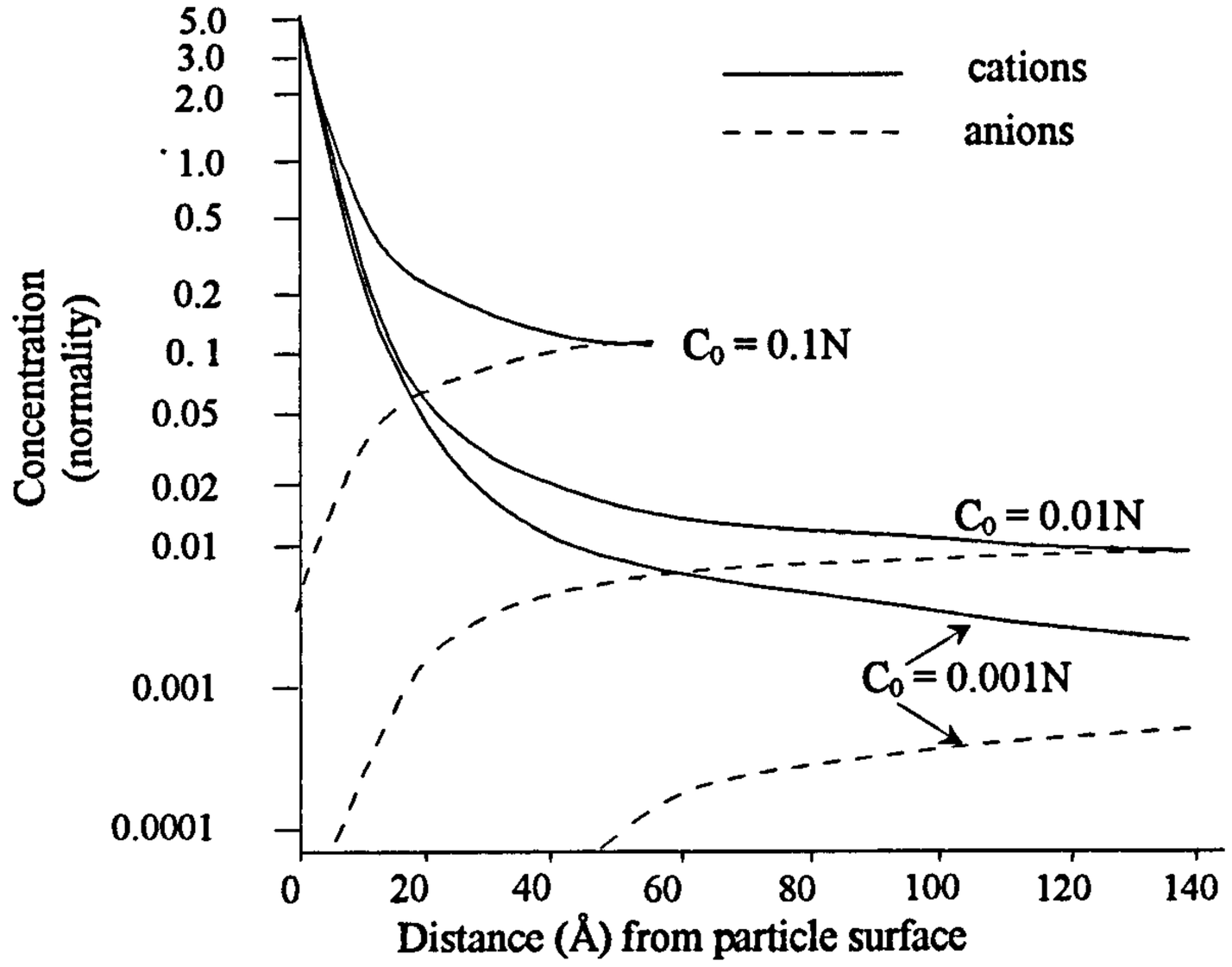

By combining the Boltzmann equation with other classical continuum equations that establish interrelationships among electrical potentials, charge imbalances and surface charge densities an equation describing the decrease in electrical potential with distance from the charged surface can be written (McBride, 1994). For clays with low charge densities, and assuming an electrolyte of monovalent ions ($z = 1$) Equation A2.6 is valid.

$$\psi(x) = \psi_0 e^{-kx} \qquad \textbf{Equation A2.6}$$

Where:

ψ_0 is the potential at surface ($x = 0$)

k can be thought of as the reciprocal of the double layer thickness.

k is controlled by the system described by the Equation A2.7.

$$k = A.z\left(\frac{n_0}{\in kT}\right)^{\frac{1}{2}} \qquad \textbf{Equation A2.7}$$

Where A is a constant, z is the counter-ion charge, n_0 is the electrolyte concentration, and $\in$ is the dielectric constant of the solvent. By inspection it is clear, exchange ions with low charge, solutions with low salt concentrations, and solvents with high dielectric constants (e.g. water) should expand the double layer of negatively charged clays. The significance of this is that an expanded double layer means that the negative electrical potential extends further away from the surface increasing the likelihood of electrostatic particle-particle repulsion, increasing the tendency of the particles to remain suspended in water as a stable colloidal dispersion.

Although the double layer theory was initially applied to clays of permanent charge, it was later used to describe the electrical potential at variable-charge (e.g., oxide) surfaces. McBride (1994) states that this application requires that the Nernst equation (Equation A2.8) be used first to determine the surface electrical potential, ψ_0, as a function of the solution pH.

$$\psi_0 = -2.303\frac{RT}{F}(pH - PZC) \qquad \textbf{Equation A2.8}$$

Where:

F is the Faraday constant

R is the ideal gas constant.

This model predicts that surface charge increases exponentially as the pH is adjusted away from the point of zero charge (PZC). Since surface charge, which governs adsorption on certain mineral structures, varies from positive to negative as the pH moves from acidic to alkaline, there exists a pH at which there is no charge developed on the mineral surface, the PZC. The pH at which this occurs is mineral dependent, an example of which is illustrated in Figure A2.9.

Figure A2.9 Surface Charge of Geothite (FeOOH) in Solutions of 1.0, 0.1 and 0.01 M NaCl during Acid Base Titrations

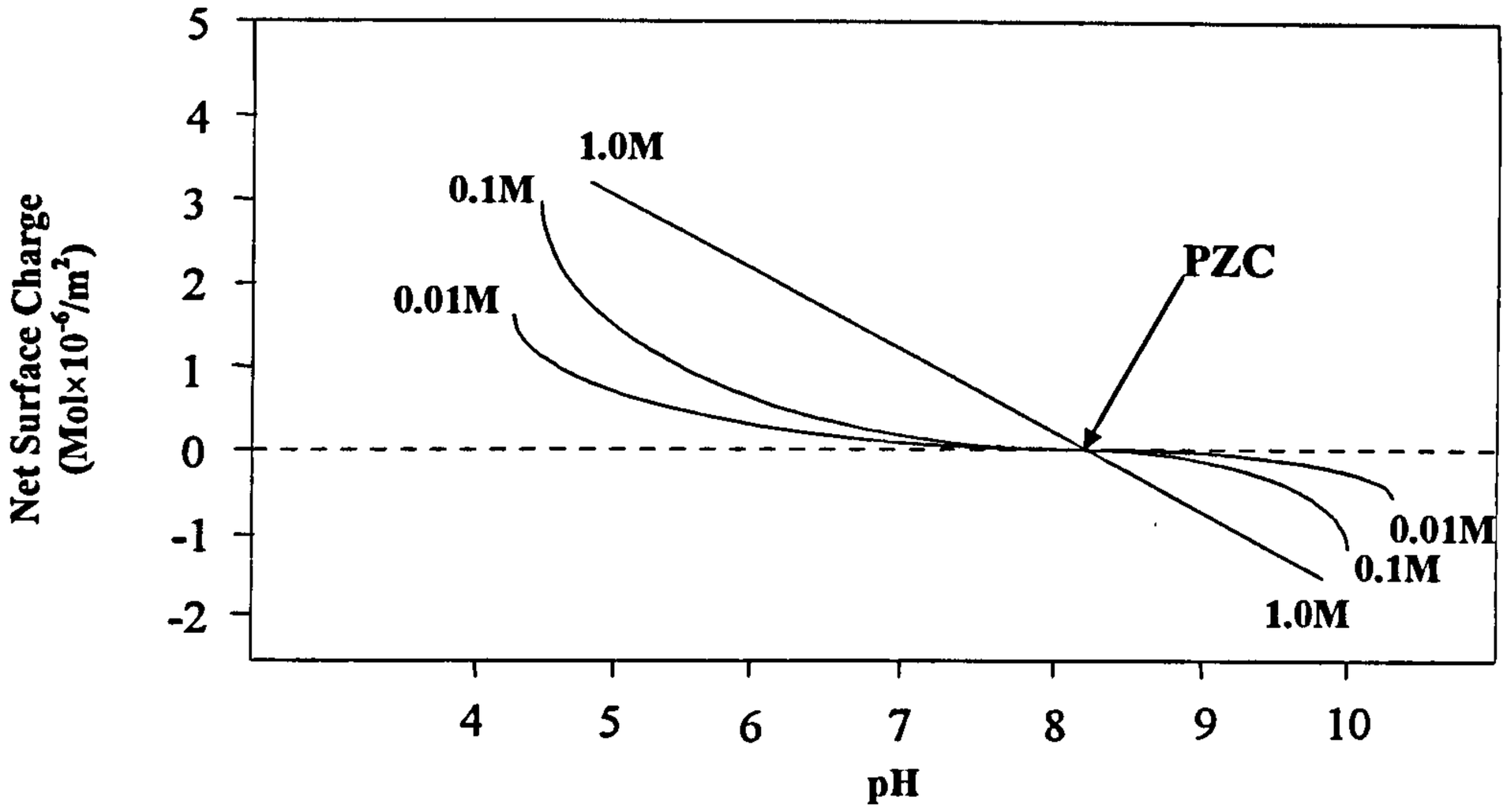

It is suggested by McBride (1994) that the use of the Nernst equation and diffuse double layer theory is not appropriate to surface adsorption since cations and anions may adsorb on oxides by direct co-ordination to the charged surface group. Consequently, the selectivity of metal ions for Fe oxides follows the order:

$$Li^+ > Na^+ > K^+$$

This order is the opposite of that expected for exchangeable cations that are separated from the surface by hydration water. The equation also assumes that the activity of H^+ at the surface does not change with pH. This cannot be the case since H^+ is also potentially adsorbed on the mineral surface.

A2.4 HYDROLYTIC EXCHANGE

Hydrolytic exchange is the process of cation exchange when the cation is a hydrogen ion H^+ or more precisely H_3O^+ ion. It should be noted that where permanent charge exchange sites are considered, only monovalent ions appear to be exchanged by hydrogen ions. Water dissociates into ions as shown by Equation A2.9. The exchange process of H^+ for Na^+ on a smectite mineral is shown in Equation A2.10.

$$2H_2O_{(l)} \Longleftrightarrow H_3O^+_{(aq)} + OH^-_{(aq)} \qquad \textbf{Equation A2.9}$$

$$H_2CO_3 + (Na^+\text{-SMECTITE}) \Longrightarrow Na^+ + HCO_3^- + (H^+\text{-SMECTITE}) \qquad \textbf{Equation A2.10}$$

The concentration of H_3O^+ ($[H_3O^+]$) and OH^- ions in solution in water is usually approximately the same and results in a pH of around 7. This occurs since equation A2.11 the ionic product for water K_w is always valid.

$$K_w = [H_3O^+] \times [OH^-] = 1 \times 10^{-14} \text{ moles}^2 \text{ dm}^{-6} \qquad \textbf{Equation A2.11}$$

Equation A2.12 shows how the pH of a solution is calculated mathematically.

$$pH = -Log_{10}[H_3O^+] \qquad \textbf{Equation A2.12}$$

Hence if the pH is known Equation A2.12 can be used to calculate hydrogen ion concentration and Equation A2.11 can be used to calculate hydroxide ion concentration

APPENDIX 3

CLAY, CONTAMINANT AND LIME MIX PREPARATION

A3.1 CONTAMINANT PREPARATION

In order to achieve a consistent level of mixing of clay and contaminant, the contaminant was added as a solution. Prior to mixing, the required contaminant solutions were created. In the case of the iron contaminant 403.999g $Fe(NO_3)_3.9H_20_{(s)}$ provides 55.847g Fe^{3+} ion. Therefore to add 1.000g Fe^{3+}, 7.234g $Fe(NO_3)_3.9H_20_{(s)}$ has to be added. Thus to achieve 5000ppm Fe^{3+} based on a dry mass of clay, 36170.18g of $Fe(NO_3)_3.9H_20_{(s)}$ has to be added to 1,000,000g of dry clay. Thus 144.680g of $Fe(NO_3)_3.9H_20_{(s)}$ has to be added to 4kg of dry clay. For convenience 144.6807g of $Fe(NO_3)_3.9H_20_{(s)}$ has been added to every 200ml of ICP water. Thus in a 1L volumetric flask 723.4036g of $Fe(NO_3)_3.9H_20_{(s)}$ has been added. This has been measured out in parts on a balance readable to 4 decimal places. Thus 200ml of solution provides 20g of Fe^{3+} ion. A similar calculation has been performed for $Pb(NO_3)_{2(s)}$ based on providing 20g of Pb^{2+} ion in 200ml of solution.

A3.2 CLAY, CONTAMINANT AND LIME MIX PREPARATION

The mixes have been carried out in a similar manner to those of the preliminary compaction tests described in Section 4.3.2. The mixes were carried out as follows :

1. Approximately 4kg of untreated clay was precisely measured and placed in a sealed polythene bag 24 hours prior to the mix. The water content of this clay was established in an oven at 105 ± 0.5^0C over 24 hours.

2. The clay from the sealed bag was placed in the mechanical mixer, the mass of clay residue in the plastic bag measured, and the precise mass in the mix calculated.

3. The mass of water to be added to achieve the required water content for compaction was calculated. If a contaminant was not to be added to the mix, this mass of ICP water was added to the mix in one pour evenly distributed over the clay and mixed for 20 minutes (see Figure 4.3). Where contaminant was added to the mix, the effective dry mass of clay in the mixer was calculated and the required mass of contaminant to be added to the effective dry mass of clay to achieve the required 5000ppm contaminant to dry clay ratio calculated. The contaminant

solutions created prior to the mix contain 20g of contaminant in 200ml of solution; hence the required volume of this solution to add to the clay was calculated. The volume of contaminant solution to be added was measured precisely using pipettes and burettes. Additionally the mass of extra ICP water to achieve the water content required for compaction was calculated. It was assumed that the density of the extra ICP water added and the densities of the contaminant solution were both equal to 1000kg/l. Although this is not precisely the case, in practice the difference has been shown to be insignificant in achieving the desired water content for compaction. The contaminant solution and the extra ICP water were mixed together and added evenly over the clay in the mechanical mixer in one pour and mixed thoroughly for 20 minutes. After this period a sample of the mixture was taken to measure water content and the remainder removed from the mixture and sealed in polythene bags for 24 hours at $11.5^0C \pm 0.5^0C$ to allow for any cation exchange or adsorption to occur. Where contaminant has not been added, these samples were also stored for 24 hours at $11.50^0C \pm 0.5^0C$ to ensure consistency in the methodology.

4. After 24 hours storage and cleaning of the mixer, the mass of the bag and clay was measured and the contents of the bag placed in the mixer again. Measuring the mass of the emptied bag allows the precise mass of the clay in the mixer to be calculated. Using the measured water content of the clay in the bag the effective dry mass of clay and contaminant in the mixer was calculated. Based on this effective dry mass of clay and contaminant, the required mass of lime to be added was calculated. This mass of lime was evenly distributed over the mixing clay mixture and allowed to mix for 20 minutes. In the event that lime was not added, the sample was still mixed for 20 minutes. Where contaminants were added the lime added to the mixture was based on the combined dry mass of clay and contaminant because in the field the precise mass of contamination may not be easily assessed from one region to another.

5. The sample was broken into pieces of 20mm or less. The resulting material was compacted into pre-weighed twin wall HDPE pipes with the same compactive effort per unit volume assessed in the initial compaction tests for each specific clay

and lime mix design. The initial proctor compaction tests utilised a 1L mould with a 2.5kg mass, falling 300mm, 27 times onto each of three layers of clay in the mould. Thus the energy supplied to the sample in the initial Proctor compaction tests E_P:

$$E_P = \frac{(2.5 \times 9.81 \times 300 \times 27 \times 3)}{1000} = 595.96J$$

Hence work done per unit volume of soil W_D:

$$W_D = \frac{596}{1000} = 0.596Jcm^{-3} = 596kJm^{-3}$$

The method of applying the same compactive effort in the final mix compactions was varied from the initial 'proctor' compaction tests due to the larger volume of the double walled plastic moulds and the required increase in the quantity of sample to be placed in the mould to fulfil the testing programme. The compaction specification for each sample actually used is shown in Table A3.1. A compaction hammer of greater mass and greater fall height was chosen to reduce the number of hammer drops per layer. Three layers were chosen since three samples from each plastic pipe were required to be tested at three time periods. Thus the consistency of compaction of each layer for each of the three tests was essentially independent and likely to be consistent. Considering the English China clay compaction specifications 1 to 3 in Table A3.1, the required number of hammer drops was calculated from the preliminary investigative compaction tests as follows :

$$\frac{(4.5 \times 9.81 \times 0.450 \times 3 \times \lambda)}{\left(\frac{\pi \times 0.150^2}{4}\right) \times 0.130} = 596000Jm^{-3}$$

Where λ = Compaction hammer drops per layer.

$596kJm^{-3}$ = compactive effort applied in preliminary proctor tests.

Thus $\lambda = 22.97 = 23$ Compaction hammer drops per layer.

The same method was applied to the Wyoming Bentonite specifications 4 to 6 in Table A3.1 for a compaction depth of 0.170m.

Table A3.1 Compaction specifications of mixes in twin-walled plastic pipes

SPECIFICATION	CLAY / CONTAMINANT / LIME MIX DESIGN					
	1. ECC Only	2. ECC +1.5% Lime	3. ECC +2.5% Lime	4. WB only	5. WB +2.5% Lime	6. WB +7.0% Lime
Required water content according to initial compaction tests (%)	29.30	34.45	35.65	46.00	58.30	60.60
Mould Diameter (m)	0.150	0.150	0.150	0.150	0.150	0.150
Total Compacted Depth (m)	0.130	0.130	0.130	0.170	0.170	0.170
Compaction Hammer Mass (kg)	4.5	4.5	4.5	4.5	4.5	4.5
Compaction Hammer Fall Height (m)	0.450	0.450	0.450	0.450	0.450	0.450
Number of Compacted Layers in Mould	3	3	3	3	3	3
Number of Compaction Hammer Drops per Layer	23	23	23	30	30	30
Energy per Unit Volume (kJm^{-3})	596	596	596	596	596	596

NB. : ECC = English China Clay **WB** = Wyoming Bentonite

The compaction specifications applied to contaminated samples are detailed below :

Compaction specification 1 was used to compact ECC+2500ppm Pb^{2+} and ECC+5000Fe^{3+}.

Compaction specification 2 was used to compact ECC+1.5%Lime+5000ppm Pb^{2+} and ECC+1.5%Lime+5000ppm Fe^{3+}.

Compaction specification 3 was used to compact ECC+2.5%Lime+5000ppm Pb^{2+} and ECC+2.5%Lime+5000ppm Fe^{3+}.

Compaction specification 4 was used to compact WB+5000ppm Pb^{2+} and WB +5000ppm Fe^{3+}.

Compaction specification 5 was used to compact WB+2.5%Lime+5000ppm Pb^{2+} and WB+2.5%Lime+5000ppm Fe^{3+}.

Compaction specification 6 was used to compact WB+7.0%Lime+5000ppm Pb^{2+} and WB+7.0%Lime+5000ppm Fe^{3+}.

6. The compacted samples were trimmed and the material density determined. The samples were sealed to the atmosphere by pouring molten paraffin wax at 40 ± 5.0^{0}C on each end of the sample in the mould and allowing it to solidify on cooling. The samples were stored at 11.5^{0}C ± 0.5^{0}C until required for testing at each of the three time-dependent curing periods, 7days, 175days and 301days. The process was repeated for the three other mixes of the same clay, contaminant and lime proportions and then for all other mix specifications. One sample preparation was carried out on each of 72 days to allow for consistency of curing period when samples were batch tested on 72 consecutive days for each of the three curing periods. Hence mixing occurred over 72 consecutive days and batch testing over 216 days.